Focussed Hydrothermal Alteration in Upper Crustal Oceanic Faults on Macquarie Island

Steven John Lewis, B. Sc. (Hons).

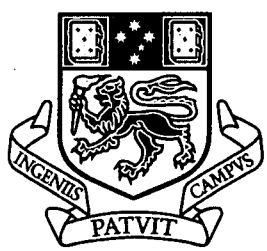

UNIVERSITY OF TASMANIA

Submitted in fulfilment of the requirements for the Degree of Doctor of Philosophy

University of Tasmania (April, 2007)

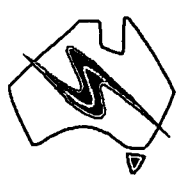

ARC Centre of Excellence in Ore Deposits

Dedicated to the native inhabitants of Macquarie Island

A bull elephant seal greets new arrivals to the tussock-fringed shores of Macquarie Island.

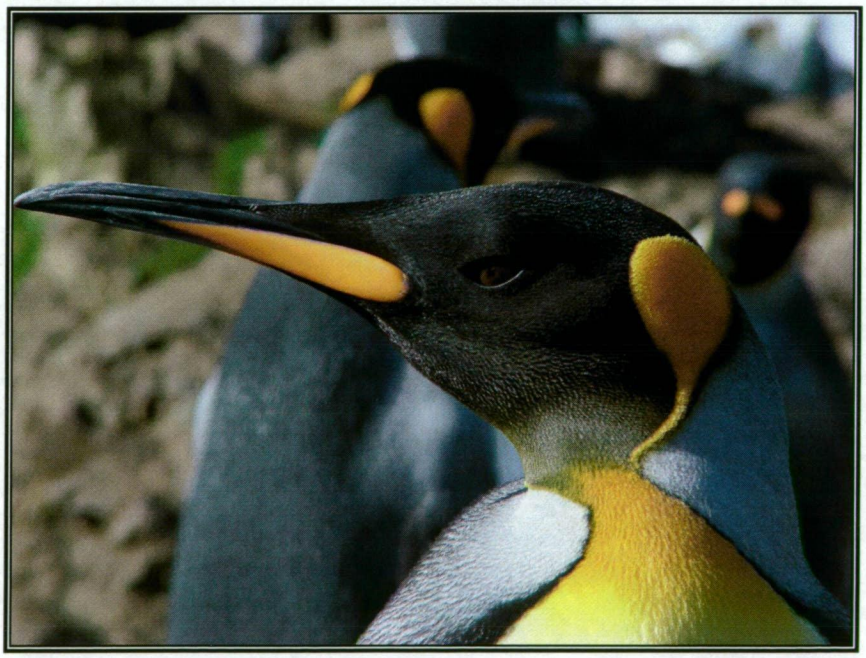

A majestic King penguin enjoys a rare sunny day on the pebbly beach at Green Gorge.

Thanks for the memories, one-and-all!

Declaration of Original Research

This thesis contains the results of an original research project undertaken at the Australian Research Council's Centre of Excellence in Ore Deposits (formerly the Centre for Ore Deposit Research) at the University of Tasmania between 2001 and 2005. It contains no material which has been accepted for a degree or diploma by this University or any other academic institution. To the best of my knowledge and belief this thesis also contains no material previously published or written by another person, except where due acknowledgment is made in the text.

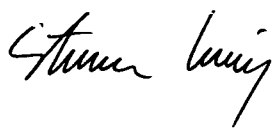

Steven Lewis

April, 2007

Authority of Access

I agree that this thesis may be made available for loan and limited copying in accordance with the relevant rules and regulations outlined in the *Copyright Act 1968.*

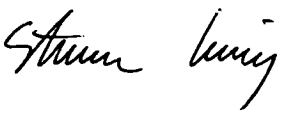

Steven Lewis

April, 2007

Introductory note on thesis structure

Because of its length, this PhD dissertation has been hard-bound into two separate volumes. Volume 1 contains all of the preliminary thesis information (i.e., the Abstract, Table of Contents, List of Figures and Tables, and the Acknowledgments), as well as Chapters 1 to 6. Volume 2 follows consecutively onwards (page numbers) from the previous tome and contains Chapters 7 to 10, the complete list of references and the six Appendices.

Abstract

Macquarie Island is an uplifted exposure of oceanic lithosphere lying deep within the Southern Ocean, less than ten kilometres east of the dextral transpressional boundary which separates the Indo-Australian and Pacific plates (54° 30' S, 158° 55' E). The island is a geological oddity; essentially an intra-oceanic ophiolite residing in its primary marine basin. Macquarie Island hosts a diverse spectrum of igneous rock types from all stratigraphic levels of the ocean crust, with pillow basalts and sheeted dolerite dykes most abundant. These upper crustal rocks were formed in the Late Miocene during slow crustal accretion and rifting (spreading rate ~ 20 mm per year) at the relict Proto-Macquarie Spreading Ridge (PMSR). Typical of many slow-spreading (magma-poor) mid-ocean ridges, tectonic activity played a dominant but episodic role in the geological evolution of Macquarie Island. Faults, fractures, and brittle shear zones are widespread across the island, and discrete igneous rock domains commonly have faulted margins. Many discontinuities were originally formed during amagmatic extension at the PMSR, although more recent transpressive tectonism (< 10 Ma) has further modified or reactivated most of these structures. An extensive array of neotectonic faults have also formed during ongoing uplift and deformation (post-spreading).

The Major Lake, Caroline Cove, and Sellick Bay Faults are prominent structural zones which cut sharply across upper crustal rocks in central and southern Macquarie Island. These steeply dipping fault systems are oriented subparallel (NW to NNE-strike) and are regularly spaced across the island (~ 10 km apart). Each fault forms a major geological boundary separating distinct lithologic domains which host disparate rock types (pillow basalts, sheeted dykes, and their transitional volcanic–intrusive packages) and regional alteration assemblages (recharge-related). Variably influenced by multiple episodes of extensional and strike-slip tectonic activity, all of these significant crustal discontinuities initially developed during seafloor-spreading at the PMSR. However, their orientations are largely oblique to the ENE trend of the palaeo-rift axis, suggesting that they may have formed structural accommodation zones during the waning stages of slow extension, or that they were related to active tectonism at a proximal ridge–transform intersection.

Structurally focussed zones of intensely altered volcanic rocks and sheeted dolerite dykes are intimately associated (spatially and genetically) with the Major Lake, Caroline Cove, and Sellick Bay Faults. Consistent geological and hydrothermal relationships attest to their critical role as crustal pathways and fracture conduits for hydrothermal systems. These major oceanic structures host highly distinctive hydrothermal assemblages which mainly consist of semi- to pervasively altered basaltic wall rocks, abundant hydrothermal veins and breccias, and patchy

domains of massive sulfide mineralisation. The alteration zones comprise (in total) six focussed hydrothermal facies, which are here defined as: (1) the vein and breccia, quartz-chlorite (VQC) facies; (2) the massive and veined, chlorite-quartz-pyrite (CQP) facies; (3) the vein-dominated, prehnite-zeolite (VPZ) facies; (4) the foliated, massive chlorite (FMC) facies; (5) the pervasive, Fe-oxyhydroxide overprint (PFO) facies; and (6) the narrow, focussed quartz vein (NQV) facies. The formation of a single diagnostic facies dominated peak hydrothermal conditions in each major structure; the VQC facies in the Major Lake Fault, the CQP facies in the Caroline Cove Fault, and the VPZ facies in the Sellick Bay Fault. In addition, both the VQC and CQP facies are partially overprinted by smaller-scale alteration assemblages that post-dated peak hydrothermal activity, i.e., the FMC and PFO facies.

The dominant fault-hosted alteration facies are highly anomalous, multi-component hydrothermal assemblages. They each have significantly different alteration minerals, hydrothermal textures, and physical attributes compared to regional igneous rock domains, i.e., non-fault zone crustal blocks. Multiple episodes of superimposed fluid–rock interaction produced these distinctive fault-hosted assemblages, with focussed hydrothermal activity mostly post-dating the main period of axial magmatism at the PMSR (crustal accretion). However, high-temperature fluid circulation was strongly influenced (initiated and sustained) by small-scale dyke pulses, mostly injected at deeper crustal levels than the present fault exposures. Rapid fluid discharge from the basement reservoir was probably also initiated (in part) by discrete tectonic events, such as oblique extension localised along specific fault segments. The physical manifestations of these relict fluid flow events are now well exposed at six key sites on Macquarie Island, where they afford an unparalleled opportunity to study the processes and products of structurally focussed hydrothermal activity in the ocean crust.

The Major Lake Fault Zone (MLFZ) is one of the best preserved and most extensive oceanic discontinuities on Macquarie Island. Mainly oriented NNW along its ~ 4 km-long strike, the MLFZ separates upper greenschist and lower amphibolite facies rocks of the Sandell Bay and Lusitania Bay Dyke Swarms (in the southern footwall) from zeolite facies pillow basalts in the northern hangingwall. The fault is the main structural host of quartz + chlorite-dominated alteration (VQC facies) and is also associated with late-stage foliated, massive 'chlorite' (FMC) facies. Furthermore, five planar alteration zones representing the narrow (< 1–2 m-wide), focussed quartz vein (NQV) facies are situated in the regional footwall package ~ 1–1.5 km south of the MLFZ. There are four discrete VQC facies sites at ~ 750 m-spaced intervals along the length of the Major Lake Fault, forming 1–15 m-wide and 80–150 m-long alteration zones. The distinctive spatial segmentation of VQC facies zones likely reflects small-scale hydrothermal upflow systems, locally controlled by basement structures such as obliquely intersecting faults or slight variations in the orientation of the MLFZ, e.g., structural step-overs, kinked zones or offsets. In contrast, the FMC facies is only well exposed at a single 10 m-wide and 55 m-long

outcrop segment in the central deformation corridor of the MLFZ (although its true strike extent and physical dimensions are uncertain due to the effects of surface cover and erosion).

The VQC facies comprises a multi-stage paragenetic association of hydrothermally derived alteration minerals. Quartz, chlorite and albite are dominant components, whereas epidote and pyrite occur sporadically in altered basalts and dolerites. The main VQC phases are reflected by moderate to strong enrichments in whole-rock Si and Fe concentrations, consistently depleted levels of Ca (due to igneous plagioclase alteration, e.g., the conversion of labradorite to albite), and highly elevated loss-on-ignition values (enhanced volatile contents). The earliest alteration stage is characterised by selectively pervasive chlorite alteration, which is widespread throughout the primary igneous groundmass. Chlorite also forms narrow veinlets and infills many vuggy cavities. Importantly, chlorites in the VQC facies are compositionally diverse and extend from Mg-rich to Fe-rich varieties (Fe # range = 0.29 to 0.64), with many also containing > 1 wt. % Mn (strongly suggestive of a fluid mixing origin). Hydrothermal fluids mostly ranged from 220°–260° C (mean = 237° C) during the precipitation of chlorite (paragenetic Stage I). In contrast, fluids were up to ~ 50° C hotter during the later formation of discrete quartz veins, intricate quartz stockwork arrays, and irregularly shaped patches of massive quartz alteration (Stage II). However, this diagnostic quartz-bearing stage precipitated across a much broader thermal range (176°–309° C), with fluid temperature variations of up to ~ 80° C occurring between discrete sites and different quartz sub-stages along the MLFZ. The distribution and abundance of pyrite trace elements in the VQC facies also varies at different outcrop sites, and are moderately well correlated with quartz precipitation temperatures. The most significant trace element enrichments are for Co, Ni, Cu, Zn, and Pb. Highly elevated levels of these elements mainly occur in pyrites associated with the lower temperature range of VQC quartz (≤ 220° C), whereas only Se concentrations are consistently enriched at higher temperature sites on the MLFZ. In contrast, sulfur isotope compositions of VQC facies pyrite are not site-specific. Their $\delta^{34}S$ values encompass the known range of seafloor-hosted sulfides (-1 ‰ to +11.9 ‰) although most are within +1 to +4 ‰, indicating that sulfur was mainly derived from leached magmatic crust.

The Caroline Cove Fault Zone (CCFZ) is variably exposed for ~ 1km along-strike at the south-western extremity of Macquarie Island. This NNW to NNE-oriented structure is dominated by abundant small-scale normal- and sinistral-oblique faults. Clay-bearing gouge and breccia zones (neotectonic) occur commonly in the central deformation corridor, clearly post-dating the main period of hydrothermal alteration. The CCFZ cuts across regional pillow basalts with zeolite and lower greenschist facies assemblages, and also partly forms the north-eastern boundary of the massive and veined, chlorite-quartz-pyrite (CQP) facies. The diagnostic CQP facies outcrops exclusively at Caroline Cove (northern end of the CCFZ), where it forms a fault-bound wedge of intensely altered volcanic rocks ~ 200 m-long and up to 80 m-wide (strike extent limited by neotectonic faulting and surface cover). Sporadic occurrences of the foliated, massive

chlorite (FMC) facies and the pervasive, Fe-oxyhydroxide overprint (PFO) facies also occur in the CCFZ. Both of these late hydrothermal assemblages are spatially restricted to the 1–2 m-wide, highly tectonised core of the fault zone (well exposed in the lower Caroline Creek valley), where they have partially overprinted intensely altered CQP facies basalts and some regional (less altered) volcanic rocks in the hangingwall package.

Similar to intensely altered rocks in the MLFZ, the CQP facies consists of a multi-stage paragenetic association with abundant chlorite, quartz, and albite. However, the CQP assemblage is more diverse; both pyrite and epidote are also dominant alteration minerals which form massive groundmass patches or interconnected vein arrays. Minor chalcopyrite is an important component of the sulfide-bearing assemblage, and late-stage barite infills some quartz vein cavities. The suite of alteration minerals strongly influences whole-rock geochemical compositions in the CQP facies. Moderate to strong enrichments in Si, Fe, S, Zn, Cu, Ba, and Mg are characteristic of these altered basalts, whereas only Ca is consistently depleted. Significant elemental additions are associated with net mass gains which range from 50–500 %, and the intense hydrothermal effects are further reflected by 5–30 % enrichments in the main volatile components, i.e., elevated loss-on-ignition values. Early stage chlorites are texturally comparable to those in the VQC facies, although all are Mg-rich (mean Fe # = 0.33) and have relatively lower Mn contents (mean Mn = 0.6 wt. %). Stage I CQP chlorites precipitated from slightly lower temperature hydrothermal fluids than those in the MLFZ (mean = 221° C), whereas massive and vein quartz in paragenetic Stage II formed between ~ 230–305° C (mostly ~ 300° C). Sulfides and epidote also precipitated during the peak quartz-forming stage, although the parent fluids of the CQP facies were not as highly enriched in trace elements as their VQC counterparts. Pyrites in the CQP facies have relatively low concentrations of metallic trace elements, with only Co, Ni, and Se consistently elevated above regional background levels. Pyrite sulfur isotope compositions are mostly +5 to +9 ‰, although some are highly $\delta^{34}S$–enriched (up to +11.9 ‰). The presence of Mg-rich chlorites and late-stage barite, the consistent addition (mass gain) of whole-rock Mg, the low pyrite trace element loads, and the $\delta^{34}S$–enriched sulfur isotope compositions all strongly suggest that significant volumes of entrained seawater (with relatively unmodified chemical compositions) played an important role in the evolution of the CQP facies. Variations in the volume of fault-entrained seawater between the Major Lake and Caroline Cove Faults were likely influenced by contrasting host rock permeabilities (pillow basalts versus sheeted dykes), different crustal depths, and heterogeneous fluid circulation patterns, i.e., differences in the mechanism of along-fault and up-fault focussed flow.

The diagnostic alteration facies in the NW-striking Sellick Bay Fault Zone (SBFZ) is highly distinctive, and differs significantly from those of fault-hosted rocks at Major Lake and Caroline Cove. The vein-dominated, prehnite-zeolite (VPZ) facies outcrops in a ~ 50 m-wide and ~ 200 m-long fault-parallel zone of strongly altered pillow basalts at a single locality in the upper Sellick

Bay escarpment. The structurally focussed alteration package is dominated by the heterogeneous development of Ca-rich zeolites (laumontite), prehnite, pumpellyite, and Fe-oxyhydroxides. These hydrothermal minerals, and their associated textural features, contrast sharply with those in the partly oxidised and relatively low grade volcanic rocks of surrounding regional domains. The VPZ facies comprises an unusual multi-component paragenesis (one of very few documented pumpellyite occurrences in oceanic crust) which formed during five main stages of focussed hydrothermal activity. The alteration minerals mainly occur as discrete veins > 10 mm-wide, intensive veinlet stockworks, and massively altered pillow basalt cores and inter-pillow margins. Relict hydrothermal fluid temperatures in the SBFZ were consistently < 200° C, and the low pressure conditions (0.5–1.0 kbar) suggest relatively shallow subseafloor depths (< 200 m) during pervasive fluid–rock interaction. Parent fluids of the VPZ facies were highly enriched in Ca and Fe, but contained lower concentrations of aqueous silica and H_2S compared to those which formed the VQC and CQP facies. In addition, the VPZ facies is not overprinted by late-stage, low temperature alteration assemblages (i.e., no FMC or PFO facies occur in the SBFZ), suggesting that hydrothermal activity was not as long-lived as in the Major Lake and Caroline Cove Fault Zones. The formation of the VPZ facies may be related to large-scale fluid recharge of the basement reservoir, or it may reflect the effects of compositionally diverse hydrothermal flow systems (discharge-related?) at the PMSR.

Subseafloor hydrothermal activity has clearly played an important role in the geological evolution of upper crustal rocks on Macquarie Island. The complex and dynamic palaeo-hydrothermal system was closely linked to episodic bouts of magmatism and tectonism during the waning stages of slow-spreading (crustal extension) at the PMSR. The most anomalous and intense fluid–rock interactions were strongly focussed in major oceanic fault zones, which provided highly permeable fluid pathways at these crustal levels. Pervasive hydrothermal processes mainly involved partial to complete wall rock (mineral) replacement, intense veining, and hydraulic brecciation of basalts and dolerites at depths of up to several hundred metres below the seafloor. Spatial and temporal differences in physico-chemical fluid parameters and host rock reactions characterise the discrete hydrothermal systems which formed each alteration facies. Rapidly discharging fluid upflow systems were segmented in some faults due to underlying structural influences in the basement, e.g., along the MLFZ. In addition, variations in the relative size, intensity, and crustal level of hydrothermal flow patterns are reflected by heterogeneous mineral and geochemical compositions; these are particularly influenced by chemically distinct fluid reservoirs, i.e., the variable influence of deep crustal fluids (evolved) and less modified seawater. The structurally focussed alteration zones have also been affected by episodic tectonic activity (syn- and post-rift) which further modified their distribution and architecture. Also, the sporadic and spatially restricted effects of late hydrothermal activity (FMC and PFO facies overprint zones) indicate that Macquarie Island's major oceanic faults were long-lived fluid conduits. However, the widespread precipitation of hydrothermal cements significantly decreased fracture

permeabilities over time, requiring ongoing structural renewal in each fault zone to maintain hydrothermal flow patterns and associated wall rock alteration processes in the upper crust.

Table of Contents

VOLUME 1

VOLUME 2

List of Figures

* Note that all of the thesis figures listed here are identified by a consecutive numbering scheme (chapter-specific), and the first sentence of the figure caption. Many thesis figures have multiple sentences for their captions but, for the sake of brevity, I have only included the initial sentence in this list (sufficient to easily identify each figure).

Chapter 4

Chapter 5

Chapter 6

Chapter 7

Chapter 8

Chapter 9

List of Tables

Chapter 7

Chapter 8

Chapter 9

Acknowledgments

As all who have undertaken the task are well aware, the completion of a doctoral research thesis is simply not possible without the assistance of an extensive support network. Although my name is the only one that graces the cover of this dissertation, a great many people have contributed towards its accomplishment. To one-and-all, I am truly grateful for your hard work and magnanimous efforts in the face of adversity.

The academic and administrative staff at the Centre for Ore Deposit Research (CODES) and the School of Earth Sciences (SES), University of Tasmania, provided incredible support and encouragement throughout the long PhD journey. Heartfelt thanks and gratitude must firstly go to my principal supervisor and academic mentor, Garry Davidson. Thanks Gaz for getting the project up and running, providing able and learned advice whenever required, and having eternal belief in my ability to see the project through until the very end. I would also like to thank my co-supervisor, Ron Berry, for his excellent advice, particularly regarding mineral chemistry and microprobe data. Other academic staff members at CODES, including Tony Crawford (thanks for the editing and corrections, Tony), Wally Hermann (excellent advice regarding uses and abuses of whole-rock geochemical data), Ross Large, Pat Quilty, Mike Roach, Khin Zaw, Leonid Danyushevsky, Dima Kamenetsky, Jocelyn McPhie, Anthony Harris and Andrew Rae, are also gratefully acknowledged for many helpful discussions, instructive insights, and thoughtful reviews throughout various stages of my research. Thanks also to Kate Godber, Bronwyn Kimber, and Andy Wakefield (CODES Honours students and volunteer field assistants) for collecting invaluable sample material and geophysical data that aided my project. Administrative and technical assistance at the CODES and SES was ably provided by Peter Comish, Simon Stephens, Phil Robinson, June Pongratz, Alastair Chilcott, Di Steffens, Sarah Gilbert, Christine Higgins, Lyn Starr, Katie McGoldrick, Nilar Hlaing, Lynne Vaudrey, Katrina Keep, and Kylie Kapeller. David Steele, Christine Cook, and Keith Harris at the Central Science Laboratory, University of Tasmania, are also acknowledged for their technical prowess and assistance with the electron microprobe and sulfur isotope analyses. I feel truly privileged to have enjoyed the aegis of the CODES and SES teams; the enthusiastic and creative academic environment significantly enhanced my overall PhD experience, provided access to myriad research facilities, and afforded me countless opportunities to enhance my geological skills and knowledge.

An equally important component of any PhD study is the technical and social support offered by fellow students. Having spent the last four years living and working in old Hobart Town, I've been fortunate to have made many fantastic acquaintances and lasting friendships among the local PhD student body. I would particularly like to thank my fellow office room-mates (the

guardians of M & P Room 310) James Cannell, Fiona Links, and Wallace Mackay (plus cameo roles from Steve Boden, Mike Buchanan, Vanessa Lickfold, and Reia Chmielowski) for their helpful assistance, good humour, and sense of fun (especially in the face of adversity). Thanks also to the office-bearers, committee members, and volunteers who've been associated with the student chapter of the Society of Economic Geologists, and the Geology Students Club at the University of Tasmania. Special mention among the PhD throng goes to Andrew Stacey, Bryan Bowden, Paul Cromie, Mawson Croaker, Rod Maier, Kate Bull, Alan Chester, and Sofia Tetroeva. Claire McMahon is especially thanked for allowing me access to some of her unpublished pyrite trace element results. I wish everyone the best for completing their studies, and then moving on with the rest of their lives; by all accounts, life sans-PhD does exist! Good luck to all of my friends and colleagues.

This project would certainly not have been possible without the kind and generous financial and logistical support offered by the Australian Antarctic Division (AAD). From providing transport to and from Hobart aboard the big orange taxi (*Aurora Australis*), to meeting my every need while stationed on Macquarie Island (except for underwear!), the AAD ensured the solid foundations of my geological fieldwork. In addition, the unparalleled opportunity to live and work in such a magical natural environment as Macquarie Island was truly a privilege that shall never forget. I would also like to acknowledge my fellow intrepid expeditioners, members of the 53rd and 54th Australian National Antarctic Research Expeditions (ANARE) to Macquarie Island. Although too numerous to mention individually the ANARE teams, ably commanded by station leaders Robb Clifton (2001-2002) and Joan Russell (2002-2003), were a credit to the professionalism of Australia's subantarctic endeavours. Lashings of helpful assistance were always at hand, ranging from medical, communications, and technical advice at VJM, through to the many willing 'mules' ready to help shift a few sample bags of rocks from one hut to another. I still vividly recall arriving cold, wet, and tired at Green Gorge after an exhaustive cross-island trek through driving sleet, and experiencing the wonders of field-cooked roast lamb and a bottle of home-brewed stout. Magical, memorable stuff; well done all!

Many other sources of financial, technical, and logistical assistance also aided my PhD quest. I would especially like to acknowledge the generous financial backing provided through competitive grants awarded from the Centre for Ore Deposit Research, University of Tasmania (travel grant for the 2004 SEG conference), the Society of Economic Geologists (2004 Hugh E. McKinstrey student research award), and the Australasian Institute of Mining and Metallurgy (2004 Gold 88 Endowment Fund award). Tony Brown and John Everard from Mineral Resources Tasmania are thanked for their initial help and enthusiasm with my project, and for providing me with access to unpublished whole-rock geochemical data. Ian Tapley from Horizon Geoscience Consulting is also acknowledged for allowing me to use detailed AIRSAR images in my thesis. The Tasmanian Parks and Wildlife Service is also thanked for granting access and sampling permits to live and work on Macquarie Island.

This project was established as a collaborative research effort between the University of Tasmania and Duke University in North Carolina. I would like to thank Jeff Karson at Duke for his assistance in conceptualising and developing this investigation, numerous helpful discussions while in the field and for on-going thoughts, ideas, and critical chapter reviews at various other times. Pete Rivizzigno from Duke University is also thanked for introducing me to aspects of Macquarie Island's geology, and providing able assistance during my first fieldwork season. Later collaborative links developed with Jeff Alt at the University of Michigan provided access and opportunity to undertake oxygen isotope analyses, and I thank Jeff for his assistance and generous offer to complete this exacting laboratory work. My project also benefited from discussions and field-time spent with researchers from the Southampton Oceanography Centre in the United Kingdom (Damon Teagle and Rosalind Coggon), the University of Texas in Austin (Karah Wertz and Nathan Daczko), and Curtin University in Western Australia (Arjan Dijkstra and Peter Cawood). I hope that the wonders of Macquarie Island's unique geology provide plenty of exciting new discoveries for each and every one of you.

Finally, I would like to thank my family and friends for their on-going support and eternal belief in my dream to complete a doctoral thesis; particularly Olga, Mum, Dad, Korn, and Vitchin – thanks for your confidence, love, and never-ending good humour. Thanks also to Victor and Thomas, two family additions that weren't around when I kicked things off many moons ago (nice work with the corrections Vic). Likewise, my two special little nieces; Olivia Mary and Eliza Patricia (with another boy/girl soon on the way!) – looking forward to watching you both grow and prosper over the coming years. Cheers to Pat, Jill, Grandma (and Grandpa - sadly missed since 2004) and everyone else at home in Avenel. And how could I ever forget the humble assistance and inspiration provided by Timmy and Tara during the final corrections phase at our beautiful new Burra home – those two little puppy dogs certainly know how to keep someone on the straight and narrow! Thanks to the many people in Hobart who've shared my trials and tribulations, especially the good folk at 35 Cromwell Street. I've been fortunate to experience the warmth and hospitality of a great home-away-from-home, and it's made a big difference to my sanity and ability to finish this project. Thus, special cheers to Frank, Bénédicte, Isabelle, Olivier, Holly, and Ed, plus the legions of other transient residents who've passed through the grand stone archway during my incumbency.

And lastly, to those that I may have accidentally overlooked or forgotten, please accept my humble and heartfelt gratitude. It's been a long and at times quite arduous journey, but just remember that, where there's a will, there's a way!

All the best

Steve

Chapter 1. – Introduction

1.1. Preamble

The circulation of hydrothermal fluids in the ocean crust is a complex and dynamic process that actively occurs at most segments of the mid-ocean ridge system. Combined with magmatic and tectonic activity, hydrothermal processes significantly influence the composition and evolution of the oceans and the oceanic crust (Alt, 1995; Honnorez, 2003). Hydrothermal circulation is a fundamental process in the transfer of energy and mass between the hydrosphere and the lithosphere, and is estimated to be directly responsible for ~ 20 % of the Earth's total heat loss (Stein and Stein, 1994; Staudigel, 2004). Hydrothermal systems are also important for the genesis of seafloor-hosted sulfide deposits and their ancient ore-bearing analogues (Hannington et al., 1995a; Herzig and Hannington, 1995). Recent research further indicates that hydrothermal activity helps to support an extensive biological community in the subseafloor, extending to depths at least 500 metres below the seawater–crust interface (Furnes and Staudigel, 1999; Takai et al., 2001; Kelley et al., 2002). These diverse and highly significant roles underline the global importance of hydrothermal processes in the Earth's oceanic crust, and the need for a comprehensive understanding of its myriad processes and products.

The interaction of hydrothermal fluids with the ocean crust is a dynamic and long-lived process that occurs in both the on- and off-axis (ridge-flank) tectonic environments. It causes progressive changes in the primary mineral and chemical composition of the igneous rocks (alteration), and is most extensive in the volcanic-dominated upper crust. The range of primary rock types and complex fluid pathways in this crustal section, coupled with the wide spectrum of fluid compositions, results in diverse and heterogeneous alteration assemblages. Numerous seafloor alteration facies have been defined from previous studies of the ocean crust and ophiolite terranes (e.g., Delaney et al., 1987; Gillis and Robinson, 1988; Alt and Teagle, 2003), and each consists of distinctive secondary minerals, paragenetic relationships, and textural features. As the hydrothermally derived facies are strongly influenced by the physical and chemical parameters of their parent fluids, the study and interpretation of altered ocean crust can directly contribute to our knowledge and understanding of seafloor hydrothermal systems.

Although hydrothermal fluids circulate pervasively in the upper oceanic crust, most fluid flow is preferentially focussed in highly permeable zones such as seafloor faults and fracture networks (Harper, 1999). Prolonged fluid–rock interaction in these conduits forms very distinctive but spatially restricted alteration facies. These intensely developed secondary assemblages are characterised by the pervasive replacement of primary wall rock minerals, complex and irregular vein networks, and unusual hydrothermal breccias. Most are derived from fluids that are

significantly hotter and more chemically evolved than those associated with regional or off-axis hydrothermal systems; these reactive fluids are commonly interpreted as the discharge (upflow) phase of subseafloor circulation (Delaney et al., 1987; Saccocia and Gillis, 1995). Focussed hydrothermal fluid discharge is also implicated in the formation of many seafloor sulfide deposits, based upon observations of active vent complexes and the nature of the underlying (and structurally controlled) alteration zones (Humphris and Tivey, 2000).

Many of the fundamental geological and geochemical attributes of structurally controlled alteration in the upper ocean crust are not well documented. Although our knowledge of hydrothermal processes and crustal alteration has substantially increased since the initial discovery of active seafloor vents (Edmond et al., 1979), most previous studies have focussed on relatively low temperature (regional) alteration assemblages, e.g., Gillis and Thompson (1993), Laverne et al. (1996), Alt and Teagle (2003). Comparatively few in-depth studies of focussed alteration zones have been undertaken, and most of these investigations were hampered by poor geological context, e.g., *in situ* samples were collected by dredge hauls or ocean drilling operations (commonly with poor core recoveries) (Delaney et al., 1987; Embley et al., 1988). Consequently, many fundamental aspects of fault-related alteration assemblages remain poorly understood especially their three-dimensional geometry, structural architecture, and spatial facies distribution. Although this knowledge gap has been supplemented by data from ophiolite field studies (Harper et al., 1988; Richards et al., 1989), the ambiguous tectonic origin of ophiolite terranes (back-arc, fore-arc, or mid-ocean ridge crust?), combined with the effects of emplacement metamorphism and deformation, limit the direct application and suitability of these findings to modern oceanic settings.

Macquarie Island is a globally unique exposure of oceanic lithosphere and arguably the most important ophiolite complex on Earth. This uplifted sliver of unsedimented seafloor still resides in its primary marine basin (Figure 1.1). It is the only known ophiolite that unequivocally formed at a mid-ocean ridge; recent evidence further indicates that crustal accretion occurred in a complex and tectonically active slow-spreading regime (Varne et al., 2000; Goscombe and Everard, 2001). Furthermore, the Middle to Late Miocene lithosphere of Macquarie Island hosts a diverse spectrum of igneous rock types that represent all stratigraphic levels of the ocean crust and upper mantle. These varied and exceptional attributes denote Macquarie Island as an unparalleled site for detailed geological studies of the ocean crust, and permit the application of standard fieldwork techniques.

Several geological researchers have previously recognised the scientific merits of Macquarie Island, and a number of investigative studies have been undertaken. Of special relevance to my project is the work of Griffin (1982) who, as part of his petrological research, conducted the first detailed study of regional alteration facies in the volcanic rock and sheeted dyke domains. A preliminary study of highly altered basalts near the Caroline Cove Fault Zone was also

incorporated in his work. Recent geological mapping and reconnaissance (Rivizzigno, 2002) identified several new locations on the island where intensely altered rocks, hosting abundant quartz- and sulfide-bearing veins and breccias, are intimately associated with other major seafloor faults. The recognition of these secondary (alteration) assemblages as the products of focussed hydrothermal fluid flow provided the opportunity to develop and implement my research project (J.A. Karson, 2001, pers. comm.).

Figure 1.1: A strong westerly wind sweeps relentlessly across the northern tip of Macquarie Island (North Head), draping the main research facility in a thin veil of misty haze. This north-facing view shows the narrow sandy isthmus which hosts Macquarie Island's base station (VJM), and also highlights the island's rugged morphology and abundance of low-lying vegetation.

This research thesis presents the results of a major investigation into an aspect of oceanic hydrothermal activity that remains considerably enigmatic. This is the first comprehensive study on the composition, distribution, and genetic relationships of structurally focussed alteration facies on Macquarie Island. Detailed field mapping and sample collection of *in situ* ocean crust provided a rare opportunity to constrain the spatial distribution, geometry, and structural architecture of secondary mineral assemblages from major seafloor faults. This work was further complemented by a range of micro-analytical, geochemical, and isotopic techniques that provided new data to interpret and analyse the hydrothermal systems. The research findings have broader implications for the evolution of Macquarie Island, and are also largely applicable to hydrothermal processes and alteration characteristics in other crustal sections formed at slow-spreading mid-ocean ridges.

1.2. Research aim

The major aim of my research project is to develop interpretative models to explain the geological and hydrothermal evolution of the Major Lake, Caroline Cove, and Sellick Bay Fault Zones on Macquarie Island.

1.3. Research objectives

The following research objectives were identified to fulfill the aim of my project:

i. Undertake an integrated geological and geochemical investigation of three relict seafloor faults that cut across rocks of the upper ocean crust on Macquarie Island, i.e., the Major Lake, Caroline Cove, and Sellick Bay Fault Zones. The fault systems selected for this study were identified and interpreted as NW- to N-striking*, rift axis accommodation structures formed during late-stage, slow and oblique oceanic spreading (Rivizzigno, 2002; Rivizzigno and Karson, 2004). Each fault zone hosts a different combination of hydrothermally derived alteration facies‡; these are defined, analysed, and interpreted to provide insight and understanding of the relict hydrothermal regime;

ii. Map and sample all fault zone outcrops in detail, with special emphasis on the spatial distribution, geographic dimensions, and structural architecture of the alteration facies;

iii. Based upon the initial fieldwork, further investigate the mineral, chemical, and isotopic attributes of the alteration assemblages using appropriate analytical methods. These consist of a comprehensive (microscopic) petrographic study, detailed mineral micro-analysis, whole-rock geochemistry of major and trace elements, and selected sulfur and oxygen isotope analyses;

iv. Determine the paragenesis and relative alteration timing of the secondary mineral assemblages in each facies, and the spatial and temporal relationship of the hydrothermal system to local magmatic and tectonic processes (and their products);

v. Determine the likely source of important elemental components in the hydrothermal system, such as sulfur and metals;

vi. Relate the observed alteration facies to hydrothermal system parameters and fluid conditions, including temperature, pressure, salinity, and redox;

vii. Compare and contrast the key features of the hydrothermal alteration facies from each fault-zone, to provide analysis and interpretation of the critical parameters that influence their similarities and differences; and

viii. Compare the data and interpretations of the structurally controlled alteration facies with research findings from other ocean crust and ophiolite studies. The results of this project will provide further scientific knowledge to complement and expand our current understanding of subseafloor hydrothermal systems.

---

* Note that compass directions are commonly abbreviated, e.g., NW refers to north-west.

‡ Refer to Appendix 1 – Glossary for definition of ambiguous or unfamiliar terms used in this thesis.

1.4. Research approach

A detailed geological and geochemical research agenda was developed and successfully implemented to address the key objectives and achieve the project aim. The research approach is reflected in the structure and organisation of my thesis, which is broadly subdivided into four major themes:

i. The **introduction** chapter (Chapter 1);

ii. The **background** chapters, which provide the necessary geological and research-specific context for my study (Chapters 2 to 4);

iii. The **results and data presentation** chapters, which outline the main research findings and provide initial interpretation of these data (Chapters 5 to 8); and

iv. The **synthesis** chapters (Chapters 9 and 10), in which the most significant outcomes and implications arising from this project are discussed and analysed, and the final conclusions presented.

The introduction chapter

The first chapter provides an overview of the project scope and outlines the nature of the research problem that I addressed. The project aim and key research objectives are also presented, along with a summary of the thesis content and structure.

The background chapters

The three chapters that follow the introduction provide the necessary background information and context for this project. Chapter 2 is devoted to Macquarie Island and its role as the research field laboratory. It includes details of the geography and physical characteristics of the island, in addition to information on access, logistics, and fieldwork conditions. A brief historical account is also provided, with special emphasis on the nature of previous (and other on-going) geological investigations. The final section of Chapter 2 is an overview of background information specific to my research project. It focusses on the project's origins and collaborative links, and also outlines the field and laboratory methods applied during this study.

Chapter 3 provides the geological context for the integrated research program. It presents a discussion of Macquarie Island's regional geology, combining summarised literature reviews and my field observations. The background geology chapter includes information on the regional tectonic setting and the evolution of the nearby Indo-Australian – Pacific plate boundary. Also discussed are the main igneous rock associations and important details relating to the island's igneous geochemistry, regional hydrothermal alteration, and structural architecture. This chapter

concludes with a review of the main evolutionary models proposed for Macquarie Island's origin at a palaeo mid-ocean ridge.

The final background chapter (Chapter 4) presents a review of current scientific knowledge and understanding of slow-spreading mid-ocean ridges, and identifies the most significant and high-impact aspects of my research work. It examines the structure and composition of ocean crust formed under slow-spreading conditions, and the main processes of crust formation. Hydrothermal processes and products, as documented from other studies of modern slow-spreading ridges and some ophiolites, are an important focus. Chapter 4 also reviews and assesses the main geological evidence which implicates a slow-spreading origin for Macquarie Island's oceanic crust.

The results and data presentation chapters

The background chapters are followed by four chapters that present the original research data and findings arising from this study. The initial results chapter (Chapter 5) defines and reviews the main rock types, hydrothermal alteration facies, and structural attributes of the Major Lake, Caroline Cove, and Sellick Bay Fault Zones. This chapter is based on geological field data obtained during reconnaissance and comprehensive site mapping, and includes outcrop and hand-specimen descriptions and structural data. It also contains detailed outcrop maps and sections of the main study locations. Many of the critical lithological and hydrothermal relationships, textures, and associations are illustrated with diagrams and photographs.

Chapter 6 presents the results of in-depth investigation of the mineralogy, paragenesis, and textural characteristics of the diagnostic alteration minerals in each hydrothermal facies. This chapter is based on microscopic petrographic analysis of thin- and polished-thin sections. Many of the important mineral textures and paragenetic relationships are also illustrated with detailed photomicrographs. The petrographic study is complemented by extensive electron microprobe data of the main alteration (silicate) minerals, and these results are also analysed and interpreted in detail.

The presentation and interpretation of whole-rock geochemical data is the main focus of Chapter 7. Major and trace element compositions derived from X-ray fluorescence (XRF) analysis of whole-rock samples are presented for the diagnostic fault zone facies. Limited ICP-MS* and fire assay analyses from the Caroline Cove area are also presented and discussed. This chapter also presents the results of whole-rock mass-balance and alteration index studies, which help to quantify major and trace element fluxes associated with hydrothermal activity.

The final results chapter (Chapter 8) is focussed on isotope and pyrite trace element geochemistry. Discrete pyrite grains in several alteration facies were analysed for their sulfur

* ICP-MS refers to geochemical data collected using inductively-coupled-plasma mass spectrometry.

isotope compositions, and many high-resolution trace element analyses were also performed using laser ablation methods. In addition, oxygen isotope ratios of quartz vein separates were analysed and interpreted. This chapter describes the application of these geochemical techniques, presents the important research findings, and provides discussion and analysis of these data.

The synthesis chapters

The final two chapters of my thesis provide a synthesis of the research findings in the context of Macquarie Island's regional tectonic setting, evolutionary history, and unique geology. Chapter 9 links all of the critical findings to present integrated geological and geochemical models of hydrothermal fluid flow and alteration in the Major Lake, Caroline Cove, and Sellick Bay Fault Zones. The broader implications of these research findings are considered for hydrothermal systems in other slow-spreading ocean crust environments. This chapter also outlines ideas for new and innovative research that could be undertaken on Macquarie Island, based on some initial thoughts and interpretations arising from my project.

The final chapter (Chapter 10) draws from the arguments which are discussed in the preceding chapter, and presents the main conclusions arising from my investigation. These focus on the most significant research findings and major project outcomes, and are directly linked to the key project aim and objectives.

Chapter 2. – Geological Research in a Subantarctic Wilderness

2.1. Introduction

Macquarie Island is a rare and stunning wilderness. Rugged, windswept, and remote; the island hosts an exceptional ophiolite complex and a diverse subantarctic ecosystem. Despite sporadic human occupation for nearly 200 years, its environment remains largely untouched by the influences of modern society. Widely recognised by the scientific community as a site of global significance, Macquarie Island's unique combination of natural features is also the foundation for its World Heritage status.

This chapter presents an introduction to Macquarie Island, and focusses on important background information related to this project. The first section gives an insight into the physical geography and administration of the island, and also provides an overview of its colourful history. The next section is a brief summary of previous geological studies and other contemporary research efforts. The final chapter theme reviews the origins and collaborative associations of my investigative research, and describes the field and laboratory methods used to achieve the key objectives. This section also pinpoints the main study locations (field sites) and provides general information about subantarctic fieldwork conditions.

2.2. Portrait of Macquarie Island

Geography and physical characteristics

Macquarie Island is one of eight subantarctic islands (or island groups) situated in the frigid expanse of the Southern Ocean. It lies approximately 1500 km SSE of Tasmania, and 1300 km N of the Antarctic continent (Figure 2.1). The nearest landfall is the New Zealand-administered Campbell and Auckland Island group, located over 600 km away to the NE.

Macquarie Island is situated in the Southern Ocean near a global marine boundary known as the Antarctic Convergence, where cold polar currents mix with warmer ocean waters from the north. The local climate is directly influenced by the Antarctic Convergence and cold, wet, and windy conditions prevail for most of the year. Snowfalls are common during winter, but there is no permanent ice cover. The annual temperature range varies slightly, with summer averages of 3°–7° C and 0°–5° C during the winter months. Strong W to NW wind is a persistent climatic force, and tempestuous gale-force storms, with wind-speeds up to 100 knots (180 km/h), also batter the

island. Annual rainfall exceeds 900 mm, and frequent cloud cover results in only 2 hours of average daily sunlight.

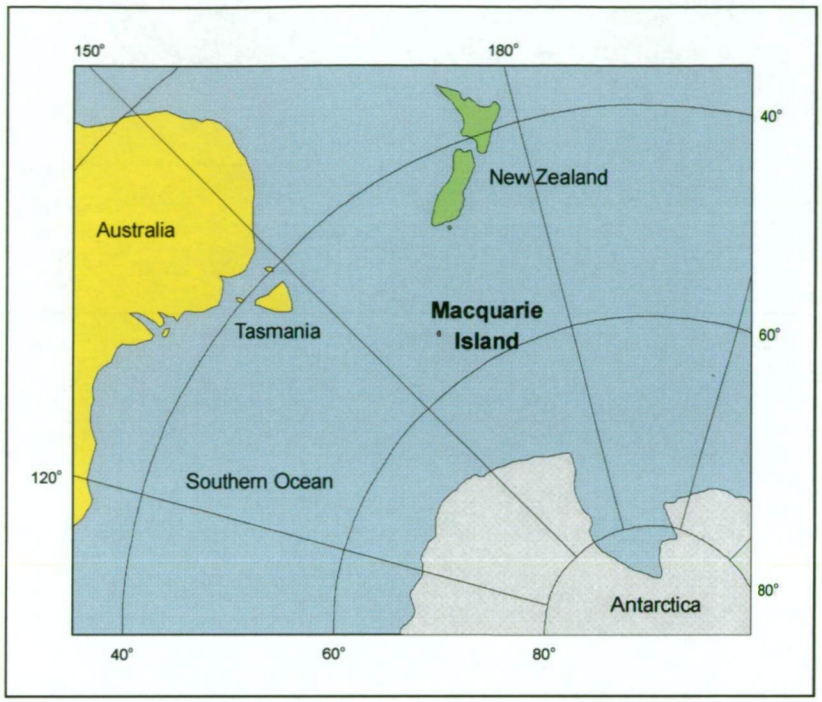

Figure 2.1: Map of the Southern Ocean between Australia, New Zealand and Antarctica. Macquarie Island is situated at 54° 30' S 158° 57' E, and is approximately half-way between Tasmania and Antarctica.

Macquarie Island is an elongated, NNE-trending landmass approximately 34 km-long and 3–5 km-wide (Figure 2.2). It comprises a total area of 12,785 hectares (~ 120 km^2), which includes a number of small offshore islets, sea-stacks, and rocky platforms. The island consists of an undulating central plateau, mostly 200–350 m above sea level, bounded on all sides by steep coastal escarpments (sloping at 20°–40°). A narrow, sandy isthmus occurs at the northern end of the island, joining the main landmass to a rocky knoll known as North Head. Flat-lying plains surround some coastal sections, and are most extensive around Handspike Point on the northwest coast (~ 1 km-wide). Several spire-like peaks are elevated above 350 m, with Mt Hamilton and Mt Fletcher the highest topographic points (both are 410 m above sea level). Freshwater lakes and tarns are widespread across the plateau, although active streams are rare and most are < 1 m-wide. Unlike other subantarctic islands, where glacial activity has previously been an important landscaping process, the rugged morphology of Macquarie Island has largely been shaped by marine erosion (Ledingham and Peterson, 1984; Selkirk et al., 1990; Adamson et al., 1996). Digital elevation models of Macquarie Island clearly show the elongated shape, steep coastal escarpments, and undulating plateau topography (Figure 2.3–2.6). The diverse ecosystem and stunning wilderness of Macquarie Island are illustrated in the scenic images shown in Figure 2.7–2.10. These photographs showcase the natural beauty of Macquarie Island, and ably support Sir Douglas Mawson's assertion that "this little island…is one of the wonder spots of the world" (Mawson, 1919).

Figure 2.2: Map of Macquarie Island showing the location of natural and man-made landmarks, and the main fieldwork sites investigated during this project. Site 1A is hosted by the Sellick Bay Fault, Sites 2A to 2D occur on the Major Lake Fault, and Site 3A occurs on the Caroline Cove Fault (Table 2.1).

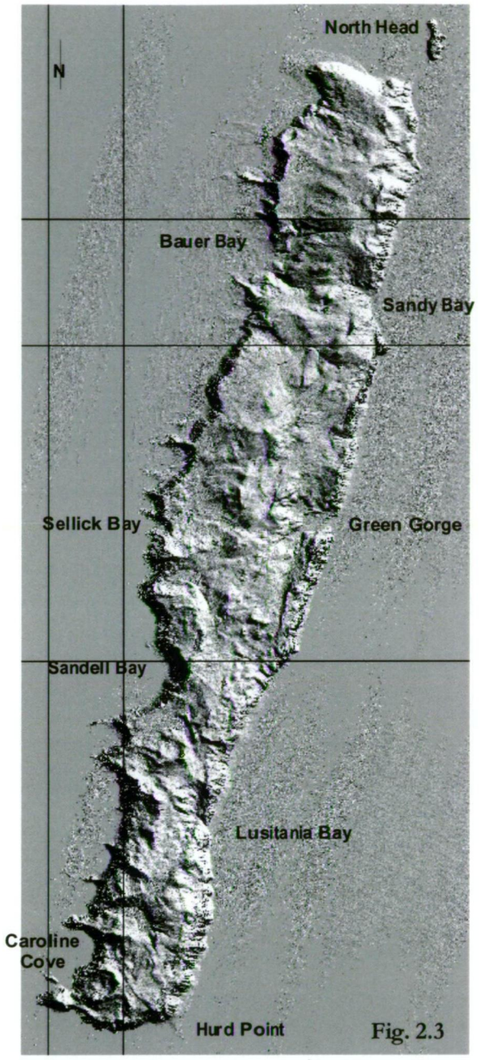

Fig. 2.3

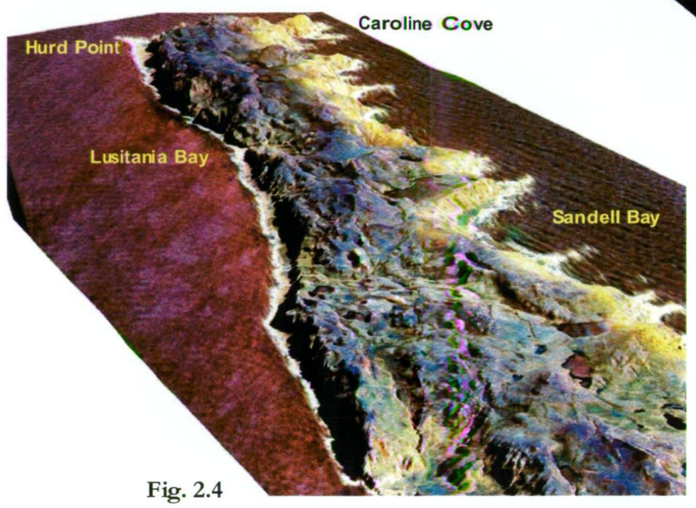

Fig. 2.4

Fig. 2.5

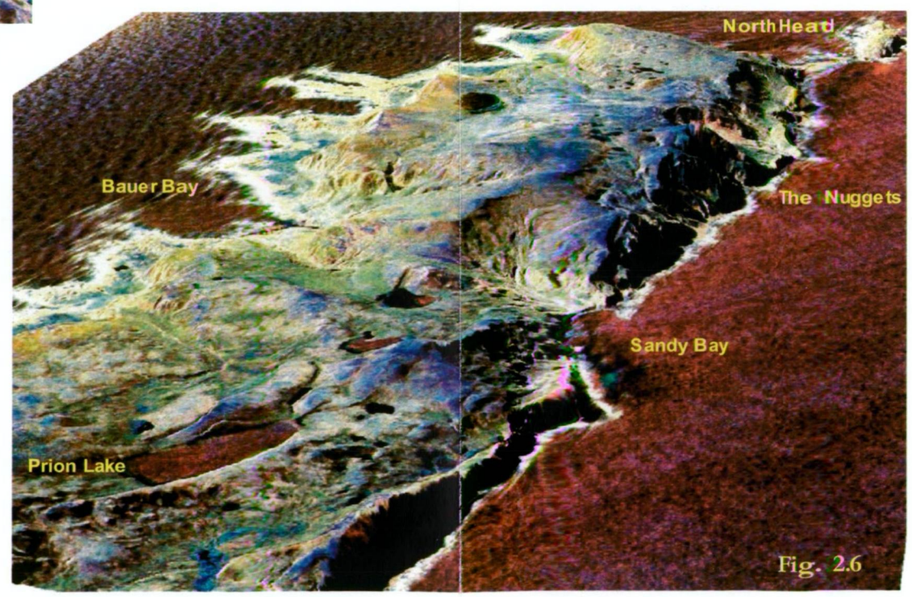

Fig. 2.6

Figure 2.3: A shaded digital elevation model (DEM) of Macquarie Island (illuminated from the NE). This model superbly illustrates the island's variable relief, steep coastal escarpments, and undulating central plateau. The DEM was created using interferometric radar data (TOPographic Synthetic Aperture Radar - TOPSAR) collected by the NASA-JPL AIRSAR instrument at an altitude of 8000 m.

Figure 2.4: An oblique 3-D perspective of the southern half of Macquarie Island (looking towards the SSW from above the Green Gorge region). This view, created by overlaying AIRSAR C-, L-, and P-band polarimetric data onto the DEM, highlights the steep escarpment slopes on the east coast, and the abundance of spire-like mountains in the south of the island.

Figure 2.5: An oblique 3-D image (view looking NNE) illustrating the elongated shape and rugged coastal morphology of Macquarie Island. This view was created using AIRSAR and DEM data as outlined above.

Figure 2.6: A 3-D perspective of the northern quarter of Macquarie Island (looking towards the NNW from the Sandy Bay region). Note the relatively undulating topography, which contrasts with the more mountainous southern half of Macquarie Island.

(All images kindly supplied courtesy of Ian Tapley (Horizon Geoscience Consulting), Arjan Dijkstra (Curtin University), and the Australian Antarctic Division).

Figure 2.7: The spire-like peak of Mt Fletcher rises above the Windy Ridge Lake on the central plateau. At an altitude of 410 m above sea-level, Mt Fletcher is the equal highest topographic point on Macquarie Island. The sparse vegetation and terrace-like slopes are characteristic of the plateaux feldmark terrain.

Figure 2.8: The Hurd Point beach, situated at the southern tip of Macquarie Island, is home to a small colony of Southern Elephant Seals and Royal Penguins during the summer months. Note the coastal fieldhut in the foreground, and the steep tussock-covered slopes that surround the narrow beach.

Figure 2.9: The Jesse Nichol Creek winds its ways towards Waterfall Bay, on the central east coast of Macquarie Island. Pyramid Peak, interpreted as a relict seafloor volcano, rises prominently in the background.

Figure 2.10: King Penguins soak up the sunshine on the rocky beach at Green Gorge during a rare sunny day. The steep coastal escarpment that surrounds this sheltered natural harbour is typical of the many fault-bounded ridgelines that occur commonly across Macquarie Island.

Administration and logistics

Macquarie Island is an Australian subantarctic territory administered by the state of Tasmania and managed by the Tasmanian Parks and Wildlife Service (TASPAWS). The island was officially declared a State Nature Reserve in 1933 (chiefly because of an influential campaign championed by Sir Douglas Mawson) and was listed as a World Heritage Area in 1997. The World Heritage listing recognised the unique geological composition and origin of Macquarie Island, and its superlative natural beauty. Management and protection of the island is also subject to many other international, national, and state conventions, e.g., Biosphere Reserve status.

Macquarie Island has no official residents and minimal infrastructure. The Australian Antarctic Division (AAD) maintains a research station on the northern isthmus that supports various scientific programs (Figure 2.2). This permanent station, known by its radio call sign VJM, is the main home for all long-term visitors. It is well equipped with modern communication, medical, and living facilities and can comfortably support up to 50 scientific and ancillary personnel. The island's annual population usually varies from ~ 15–20 during winter to ~ 30–40 over the summer months, when most scientific work is undertaken.

There are no formed roadways on Macquarie Island and the only vehicular transport is restricted to the immediate vicinity of VJM and the Isthmus. Pedestrian travel is the main mode of transport and is facilitated by a 92 km network of established walking tracks (Figure 2.2). A small fleet of inflatable rubber boats permits some near-shore sea transport along the relatively sheltered eastern coast, although boating activity is infrequent and highly dependent on calm weather conditions. At five coastal locations around the island, small self-contained huts permit field-based researchers to live near their work areas. Between 1998 and 2002, a further three huts were sited on the plateau (Windy Ridge, Mt Eitel, and Lake Tiobunga) to support TASPAWS rangers engaged in a feral cat eradication program.

Outside access to Macquarie Island is restricted to ship-borne travel. The research station is re-supplied with food and equipment on a once-yearly voyage commissioned by the AAD and usually undertaken by the P & O-line icebreaker, the *Aurora Australis*. Sporadic visits from tourist-chartered vessels occur over the summer months, but the island is situated well away from commercial air- and sea-lanes. Opportunities to visit and work on the island are rare and considerable planning and liaison is required with the AAD and the TASPAWS. All visitors to Macquarie Island require an authorised access permit and must adhere to strict quarantine procedures. In addition, scientific research proposals are subject to rigorous ethical and administrative scrutiny from both State and Federal government agencies, e.g., there is a strictly enforced 100 kg limit (per research group) placed on the collection of geological samples.

Historical background

The earliest historical record of Macquarie Island dates to 1810 when Frederick Hasselborough, captain of the sealing ship *Perseverance*, accidentally discovered the island en-route from Sydney to New Zealand. He claimed the island for the colony of New South Wales and named it after the incumbent governor, Lachlan Macquarie (Cox, 1999). Throughout most of the 19th and early 20th centuries Macquarie Island was used as a base for exploitation of the endemic seal and penguin populations. During this period several semi-permanent stations were established and at least 11 commercial ships were wrecked on the rocky coastline. By the time the last oil-gathering gangs had departed in 1919, much of the native fauna had been decimated, and a number of alien species were well established (Figure 2.11).

Figure 2.11: Rusted steam digesters rest forlornly among the coastal tussock grass on the Isthmus. Digesters were used to extract oil from the vast penguin population during the commercial operations of the late 19th and early 20th century. The double-spired coastal promontory in the left background is known as the Nuggets; it hosts an unusual occurrence of hydrothermally derived gypsum preserved in fault arrays that cut across sheeted dolerite wall rocks.

The importance of Macquarie Island as a location for multi-disciplinary scientific research has long been recognised. The earliest scientific collections were made during several Russian expeditions in the early 1820's. Small scientific parties from America and New Zealand visited in the late 19th century and made the first systematic collections (Cox, 1999). From 1911 to 1914 the Australasian Antarctic Expedition (AAE), led by Sir Douglas Mawson, established a research station on the northern isthmus. During this time a dedicated five-man team conducted detailed studies of the island's botany, zoology, and geology. Daily meteorological observations were also made, and an extensive map-making program was undertaken (Mawson, 1922).

In 1948 the Australian Commonwealth Government established a scientific research station on the northern isthmus under the aegis of the Australian National Antarctic Research Expeditions (ANARE). This station, which has been permanently maintained and upgraded several times since its inception, has hosted many scientific projects. Previous and on-going studies have included upper atmospheric physics research, monitoring of seabird and seal populations, and mapping of the *in situ* geology. A comprehensive meteorological dataset has also been compiled, with continuous records extending for over 50 years.

Current activity on Macquarie Island continues to focus on scientific research, management and monitoring of the ecosystem, and a limited amount of educational tourism. A new management plan, recently drafted by the TASPAWS, provides a policy framework for the future conservation and management of the nature reserve. This plan recognises the significance of Macquarie Island as a site for geological research, and future fieldwork should be viable. However, more stringent controls are likely to be implemented to ensure the long-term preservation of the delicate ecosystem, and the continued survival of the scientifically significant outcrops.

2.3. Previous geological research

Leslie Russell Blake, a surveyor assigned to the AAE of 1911–1914, undertook the first geological studies on Macquarie Island. Unfortunately Blake was killed during the Great War and considerable time elapsed before his work was published (Mawson, 1943). Blake compiled the first geological maps of Macquarie Island and divided the rocks into an Older Basic Group of intruded lavas, and a Younger Basic Group comprising pillow basalts and breccias unconformably overlying the older rocks (Duncan and Varne, 1988).

Macquarie Island was first identified as a subaerial exposure of oceanic crust by Varne et al. (1969). Subsequent reconnaissance mapping by Varne and Rubenach (1972) presented new geological data and showed that the island consists of numerous fault-bounded blocks from different (pseudo-stratigraphic) levels in the ocean crust. Quilty et al. (1973) identified poorly preserved nannoplankton from calcareous oozes at North Head and suggested an Early to Middle Miocene age. Recent palaeontology work, including the recognition of unusual phytoplankton species (bolboforms) from the south of the island, provides better constraints on the age of the sedimentary rocks and indicates a Late Miocene age (9.75–8.78 Ma) (Quilty et al., 2004). This age range is broadly consistent with 11.5–9.7 Ma radiometric dates (K-Ar and Ar-Ar methods) obtained from basaltic rocks (Duncan and Varne, 1988), and the 8.8–8.4 Ma interval from U-Pb dating of zircons in ultramafic pegmatites (Armstrong et al., 2004). However, other radiometric dates seemingly conflict with these data (e.g., zircon and apatite fission track dating) and suggest significantly younger ages of 6.5–4.2 Ma (Armstrong et al., 2004). These age discrepancies are further discussed in Chapter 3.4.

Most of the research conducted during the 1970's and 1980's involved studies of the igneous petrology and geochemistry. The results of these investigations confirmed the earlier interpretations of Macquarie Island as oceanic crust (Griffin and Varne, 1980; Griffin, 1982; Christodoulou, 1986). However, these studies also noted that some alkaline basaltic rocks have unusual and geochemically enriched compositions, such as relatively elevated levels of Nb and Sr. At the time, these E-MORB compositions were unknown from other mid-ocean ridge samples, although they have since been described, e.g., from some segments of the mid-Atlantic Ridge (Griffin and Varne, 1980). Palaeomagnetic data also supported a seafloor spreading origin for Macquarie Island, although these data suggested the island formed ~ 27 Ma (Williamson, 1979; Williamson, 1988). Varne et al. (1969) also used Macquarie Island as a possible example of magnetic striping in the ocean crust at the approximate time that this phenomenon was first identified. Subsequent studies of the regional tectonic setting have shown that the underlying geological assumptions supporting the palaeomagnetic data (and hence a Late Oligocene spreading age) are flawed (Lamarche et al., 1997; Massell et al., 2000; Daczko et al., 2003).

The nature and distribution of rock types on Macquarie Island were confirmed by several other reconnaissance studies. These presented field-based observations, rock descriptions, and the results of limited geological and geomorphological mapping (Christodoulou et al., 1984; Ledingham and Peterson, 1984; Crohn, 1986; Lees, 1987). An oxygen and carbon isotope study indicated that all of the oceanic rocks have been hydrothermally-altered to some extent (Cocker et al., 1982). Crohn (1986) undertook heavy metal trace element analyses on many volcanic and plutonic rocks, including intensely altered quartz-pyrite basalts from Caroline Cove. He concluded that most sulfide occurrences on Macquarie Island are the products of late-stage hydrothermal activity associated with magmatic volatiles (Crohn, 1986).

The first attempt to produce a detailed map of Macquarie Island and systematically classify the different volcanic and plutonic rocks was undertaken during the mid–1990's. Geologists from Mineral Resources Tasmania (MRT) mapped the entire island at a scale of 1:10,000. This work defined eight distinctive igneous rock associations (Goscombe and Everard, 1997, 1999; Goscombe and Everard, 2001) and led to the publication of the first tectonic model on the evolution of Macquarie Island (Goscombe and Everard, 2001). A series of map-sheets (incorporating 1:50,000, 1:25,000 and 1:10,000 scales) were also produced from this project (Goscombe and Everard, 1998).

The amount of geological research on Macquarie Island has significantly increased since the late 1990's. International attention has been prompted by recognition of Macquarie Island's origin at a slow-spreading mid-ocean ridge, and the potential for detailed ocean crust research in a subaerial setting. This focus has led to more in-depth investigations using cutting-edge technology and a range of geochemical techniques. Studies have included further work on the island's primary magmatic composition and mantle source (Bazylev and Kamenetsky, 1998;

Kamenetsky et al., 2000; Kamenetsky and Maas, 2002), the structural architecture and origin of major fault systems (Rivizzigno, 2002; Daczko et al., 2003; Wertz et al., 2003; Dijkstra and Cawood, 2004; Rivizzigno and Karson, 2004), and the geochemical and isotopic signatures of hydrothermal alteration in the upper crust (Alt et al., 2003; Davidson et al., 2004). A comprehensive review paper has also been published summarising the geology, structural history, and magmatic evolution of Macquarie Island (Varne et al., 2000). Data and interpretations from many of these recent studies are further reviewed in Chapter 3.

2.4. Overview of current research project

Project origins and collaborative associations

This doctoral project is a major component of a broader program of geological research, conducted under the aegis of Antarctic Science Advisory Committee (ASAC) project 1318. ASAC project 1318 was initiated as a collaborative research effort between the University of Tasmania (Dr Garry Davidson as chief investigator) and Duke University in North Carolina (Dr Jeffrey Karson). The project was designed to study the tectonic, magmatic, and hydrothermal evolution of Macquarie Island, and assess the wider implications for slow-spreading processes and products. The Australian Antarctic Division (AAD) provided funding to support both field- and laboratory-based work, including transportation and logistics for the project team members. Other competitive funding to support laboratory analyses was independently awarded by the Australasian Institute of Mining and Metallurgy (AusIMM), the Society of Economic Geologists (SEG) and the University of Tasmania's Centre for Ore Deposit Research (CODES).

During the life of this research project several new collaborations were forged between the University of Tasmania and other international research institutions. These expanded the scope of my project, and facilitated access to laboratory methods that were not originally proposed. Specific collaborations included oxygen isotope work with Dr Jeffrey Alt at the University of Michigan, and field studies (sample collection) with Dr Damon Teagle and Ms Rosalind Coggon of the Southampton Oceanography Centre. In addition, my project also benefited from newly acquired ground magnetic data (initial interpretations only) obtained in 2004 with funding from ASAC project 2409. This geophysical project (also developed by research staff at the University of Tasmania) aims to compile ground and airborne magnetic data to better resolve the complex geological structure and hydrothermal alteration assemblages of Macquarie Island.

Research methods

Fieldwork conditions

Geological fieldwork on Macquarie Island is a challenging experience that requires a high level of physical fitness and mental toughness. In terms of climatic conditions and physical isolation, it is comparable to working in areas such as Nepal, Siberia, and remote parts of northern Canada.

Steep and rugged terrain, frequent inclement weather, and poorly exposed outcrops hamper mapping efforts, and the collection of geological data and rock samples. Access in many areas of geological significance on Macquarie Island is also restricted by state legislation designed to minimise disturbance of penguin colonies and endangered seabirds, e.g., the albatross exclusion zone at Caroline Cove.

Despite these impediments, Macquarie Island is a unique geological laboratory and an unparalleled environment to study relatively young and pristine ocean crust. Standard mapping and sampling techniques can be successfully used to investigate the geology and overcome the usual technical and logistical problems that hinder exploration of the deep seafloor. Although considerable geological research has already been undertaken (as outlined in the previous section), great potential still exists for further studies of global significance. Future work in this environment will expand our existing knowledge of the tectonic, magmatic, and hydrothermal processes that form Earth's oceanic crust.

Fieldwork techniques

My doctoral research program involved two six-month fieldwork seasons; October to March of 2001–2002 and 2002–2003 (inclusive). Fieldwork was mostly undertaken in the central and southern regions of Macquarie Island, principally in the areas of Mt Martin–Major Lake, Caroline Cove, and Sellick Bay (Figure 2.2). Six key outcrop sites were studied and mapped in detail, and significant reconnaissance mapping was also undertaken in the surrounding districts (Table 2.1). These sites were selected because well preserved outcrops of hydrothermally altered rocks are intimately associated with major upper crustal faults (Figure 2.12–2.15). More in-depth descriptions and interpretations of these localities and their host faults are given in Chapter 5.

Geological mapping, field observations, and sample collection traverses were the main field techniques employed. Following broad-scale reconnaissance mapping (1:2500), the key outcrop localities were mapped in greater detail (1:500 or 1:1000) using a combination of pegged grids and a Garmin e-trex GPS (with a reproducible accuracy of $\pm$ 10 m). All maps were hand-drawn on waterproof graph paper, and field notes and data were recorded in waterproof notebooks. Approximately four hundred rock samples were collected and described (Appendix 2), and magnetic susceptibility data was also measured for each sample (Appendix 3).

Fieldwork was conducted on the steep upper-escarpment slopes that surround the coast, and at several plateau-based sites (Figure 2.2). During fieldwork I mainly took nightly refuge at the Lake Tiobunga and Mt Eitel huts (now removed from the island following the success of a TASPAWS feral cat eradication program), and the coastal villas of Hurd Point and Waterfall Bay. Standard field days involved 3–8 km round-trip hikes across rugged topography, carrying a heavy backpack laden with essential geological and safety equipment.

Table 2.1: Main site details of focussed hydrothermal alteration zones associated with oceanic fault systems in Macquarie Island's upper crust.

Site	Site name	Fault	Easting	Northing	Comments
1A	**Sellick Bay escarpment**	Sellick Bay Fault Zone	489200	3946000	Situated in the upper escarpment slope overlooking southern Sellick Bay. Well exposed outcrop at the scarp edge is proximal to a narrow creek valley. Intense veining occurs in ~ 50 m wide, NW-trending zone that crosscuts altered and deformed pillow and massive basalt (Figure 2.12).
2A	**Sandell Bay creek**	Major Lake Fault Zone	489050	3940650	This site occurs in the upper escarpment slope above southern Sandell Bay. A steep NNW-trending creek valley erodes the slope and variably exposes the Major Lake Fault Zone. Basalt & sheeted dykes are well exposed in the local vicinity. A 10–20 m wide zone of highly altered rocks forms a 100 m, fault-parallel ridgeline in the footwall slope.
2B	**Major Lake foreshore**	Major Lake Fault Zone	489300	3939820	This site occurs on the SE foreshore of Major Lake (Figure 2.13). The steep lake wall coincides with the NNW-trending Major Lake Fault, although it is mostly obscured by soil and debris. A narrow (1–2 m) ridgeline of intensely altered dolerite is sporadically exposed for 60–70 m in the upper grassy slope. The low-lying altered outcrop runs subparallel to the fault trend, and minor ***in situ*** outcrop occurs along the shoreline.
2C	**East Mt Martin**	Major Lake Fault Zone	489860	3939130	Situated on the lower E slope of Mt Martin ~ 100 m E of the Overland Track. Highly altered pillow basalt is exposed in a 5–10 m wide, elongate zone parallel to a narrow valley. Three main outcrops are prominent in a NNW-orientation (fault-parallel), and the surrounding area is mostly obscured by cover (Figure 2.14).
2D	**Lusitania Bay escarpment**	Major Lake Fault Zone	490290	3937580	This site occurs at the upper escarpment slope above north Lusitania Bay. A 10–20 m, NNW-trending outcrop of altered dolerite is well exposed along-strike for ~ 80 m. Less altered basalt also crops out sporadically in the nearby escarpment, although most slopes are scree-covered.
3A	**Caroline Cove**	Caroline Cove Fault Zone	486600	3931500	Intensely altered basalt is exposed for ~ 100 m in the steep valley walls of the Caroline Creek (Figure 2.15). Outcrop is sporadic, although a continuous 50 m section occurs south of the Caroline Cove beach. Several 10–20 m-wide outcrops of highly altered basalt also occur in the steep coastal zone.

Note: In addition to the main study sites along the Major Lake Fault Zone (Site 2A–2D), there are also five small-scale sites (Sites 2E–2J) with similar alteration minerals and hydrothermal textures in the regional Mt Martin – Major Lake district, i.e., not directly situated on the Major Lake Fault. Further details of these locations are discussed in Chapter 5.3.

Figure 2.12: The main field site at the Sellick Bay escarpment (Site 1A). Intensely veined and altered pillow basalt is well preserved in the upper slope adjacent to the narrow NW-trending creek valley, which coincides with the Sellick Bay Fault Zone. The steep, scree-covered terrain surrounding the site is typical of most escarpment sections on Macquarie Island.

Figure 2.13: Low-lying outcrop at Major Lake foreshore (Site 2B). This narrow ridgeline runs parallel with the adjacent Major Lake Fault Zone, ~ 10 m to the right (east) of view, and is variably exposed along-strike for 70–80 m. This view looks towards the NW, with Major Lake and the Sandell Bay escarpment prominent in the background.

Figure 2.14: The central outcrop of intensely altered basalt at East Mt Martin (Site 2C), looking south towards the Overland Track. Three main outcrops occur at this locality, forming a ~ 100 m-long, elongated zone parallel to the narrow creek valley. The steep and well vegetated slopes of Mt Martin occur at the right of view.

Figure 2.15: View looking north along the steep and narrow confines of the Caroline Creek valley towards Caroline Cove. The valley here coincides with the strike of the Caroline Cove Fault Zone; intensely altered pillow basalts with abundant quartz and sulfide alteration are well exposed in the western wall (left of view).

Laboratory work

The rock samples collected on Macquarie Island were transported to the University of Tasmania at the end of each field season aboard the *Aurora Australis* (Antarctic research vessel). These samples were used for laboratory work aimed at elucidating the mineral, chemical, and isotopic characteristics of the focussed alteration facies (Appendix 2). The sample preparation procedures, operating conditions and data for the main laboratory techniques are outlined in Appendices 4–6, and further discussed and interpreted in Chapters 6–8. The analytical procedures included:

i. Petrographic analysis of approximately one hundred and ten polished thin-sections, to identify the main secondary minerals and paragenetic relationships, describe their textural features and associations, and assist in further defining each alteration facies;

ii. Electron microprobe studies of selected alteration (silicate) minerals from polished thin-sections, to determine their chemical and structural compositions and assist with interpreting hydrothermal fluid conditions (e.g., chlorite geothermometry) and processes of fluid–wall rock interaction;

iii. X-ray fluorescence (XRF) analysis of seventy-two milled whole-rock samples, to determine the major and trace element compositions of hydrothermal facies and help to quantify mass-balance exchange between fluids and wall rocks during alteration, and characterise alteration indices;

iv. Integrated (solution) ICP-MS and fire-assay analysis of ten highly altered, sulfide-rich whole-rock samples, to assess a broader range of trace element compositions than the XRF method can perform (including Au);

v. Conventional sulphur isotope analysis of sixty-six sulfide minerals from the Major Lake and Caroline Cove districts, to help interpret hydrothermal fluid parameters and the likely source of sulfur;

vi. Oxygen isotope analysis of eighteen quartz vein separates to assist with estimating fluid temperatures during hydrothermal alteration (geothermometry); and

vii. Laser ablation-ICPMS analysis of pyrite grains (one hundred and fifty-one spot analyses) from sulfide-bearing alteration zones, to determine their trace element compositions and provide further evidence for interpreting the relict hydrothermal systems.

Chapter 3. – The Geology of Macquarie Island

3.1. Introduction

Macquarie Island is a unique geological environment, the only location on Earth where all stratigraphic levels of the oceanic lithosphere are exposed above sea-level in their original marine basin (Goscombe and Everard, 2001). The island hosts a diverse igneous rock association, complex structural relationships, and an extensive suite of hydrothermally derived mineral assemblages; all are characteristic of the ocean crust. Macquarie Island also represents the sole ophiolite terrane that unequivocally formed at a slow-spreading mid-ocean ridge (spreading rate < 30 mm/year; Karson, 2002). In contrast to most ophiolites, the geometry and history of this relict spreading system are moderately well constrained by tectonic reconstructions and comprehensive geophysical data, e.g., Sutherland (1995), Lamarche (1997), Massell et al. (2000). These attributes denote Macquarie Island as a site of major geological significance, and an ideal location to study the composition and evolution of slow-spreading ocean crust.

This chapter provides a synthesis of existing knowledge on the geology of Macquarie Island. It is compiled from an extensive literature review and further supplemented by my field observations. The purpose of this chapter is to:

i. Present an overview of the regional tectonic setting;

ii. Summarise the important geological characteristics of Macquarie Island, including the rock types, structural architecture, and the regional alteration assemblages;

iii. Review the main tectonic models proposed for the evolution of Macquarie Island; and

iv. Provide the background geological context for the data, observations, and interpretations arising from my research project.

3.2. Regional tectonic setting

The dextral transform boundary that separates the oceanic Indo-Australian and Pacific plates south of New Zealand is known as the Macquarie Ridge Complex (MRC) (Hayes and Talwani, 1972; Massell et al., 2000). This is a complex, arcuate suture zone that extends ~ 1600 km from continental New Zealand (the Alpine Fault) to the Indo-Australian – Antarctic – Pacific triple junction (Figure 3.1).

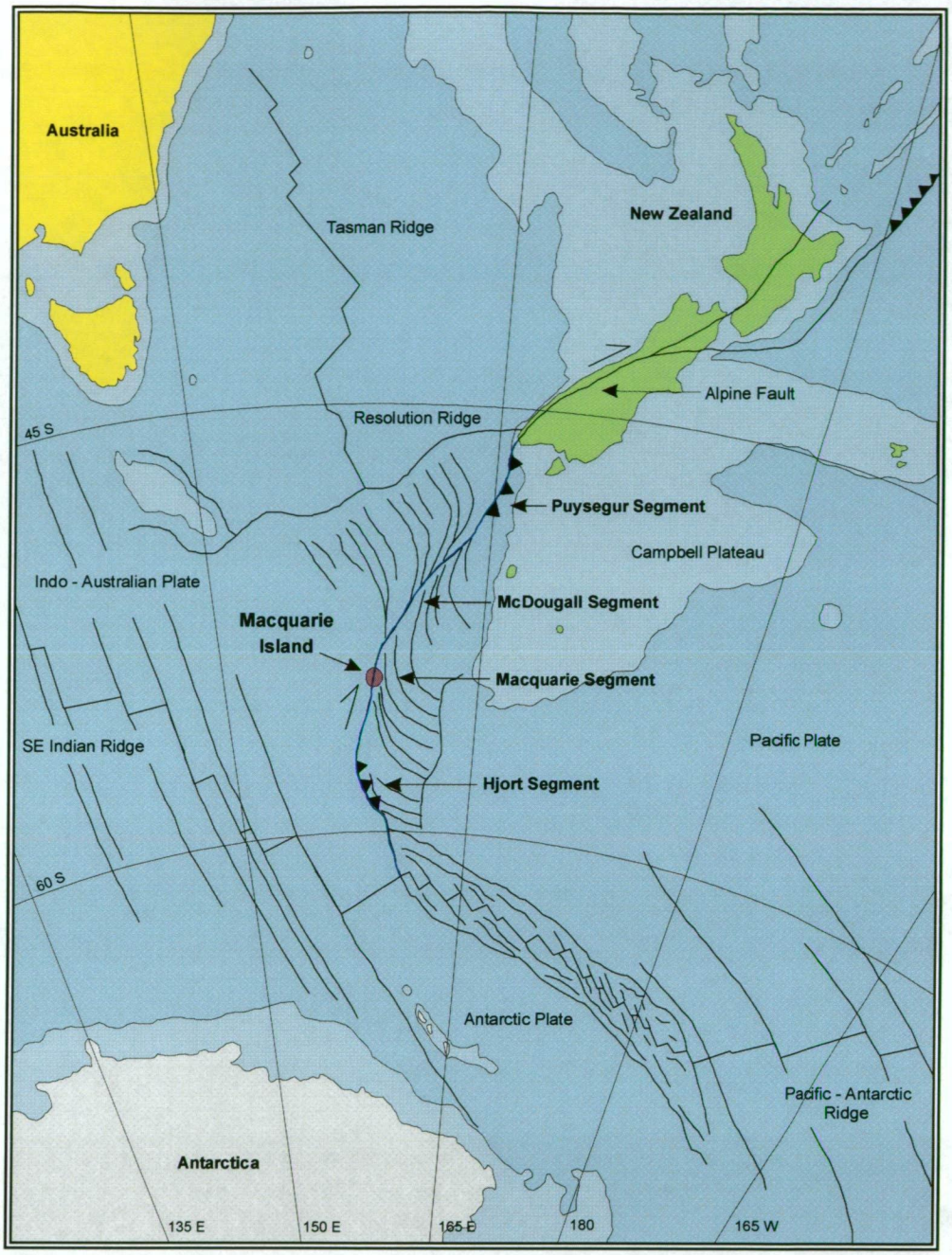

Figure 3.1: The Macquarie Ridge Complex (MRC) extends over 1600 km from the Alpine Fault in New Zealand to the triple point junction between the Antarctic – Pacific – and Indo-Australian plates. This regional tectonic map of the Southern Ocean highlights the location of the four discrete ridge-trough segments that comprise the MRC. Note the characteristic bend in the geometry of broad-scale fractures and spreading segments proximal to the active ridge system. The warped seafloor fracture zones reflect the dominance of dextral strike-slip motion along the MRC since the cessation of spreading about 10 Ma (post-spreading structures formed during neotectonic activity). Areas of pale blue ocean shown on this map mark the 2000 m bathymetric contour (map modified after Daczko et al., 2003).

Striking predominantly NNE, the Macquarie Ridge Complex is subdivided into four geographically distinct ridge and trough segments. The individual segments of the MRC, known from north to south as the Puysegur, McDougall, Macquarie, and Hjort ridges (Massell et al., 2000), vary in their orientation, morphology, and tectonic framework (Table 3.1). Macquarie Island occurs in the central (Macquarie) segment of the MRC (Figure 3.1); it represents the emergent apex of a 5 km-high and 50 km-wide ridge and trough system that comprises two

parallel ridges separated by a median valley (Daczko et al., 2003). Macquarie Island occurs on the eastern ridge, and is situated ~ 4.5 km east of the active deformation zone associated with the present Indo-Australian – Pacific plate boundary. Most of this ridge segment lies at shallow bathymetric depths (< 50 m), and seismic imaging shows a pronounced flat-topped morphology that suggests previous marine planation (Massell et al., 2000). Further to the east, a deep (5000–6000 m) and steep-sided ocean trench (the Macquarie Trench) flanks the uplifted ridgeline.

In the Macquarie segment of the MRC, the Indo-Australian – Pacific plate boundary is marked by a highly deformed shear zone ~ 5–15 km-wide (Daczko et al., 2003). This active structural corridor hosts a series of closely spaced, ridge-parallel lineaments interpreted as active fault escarpments (Daczko et al., 2003). The faults form a right-stepping, *en echelon* array characterised by extensional relay zones and pull-apart basins that propagate between discrete fault terminations. The prevailing tectonic reconstruction indicates mostly dextral strike-slip motion along the Macquarie Ridge Complex, with at least 200 km of displacement during the past 10 million years (Varne et al., 2000b). The fault zone remains seismically active and shallow crustal earthquakes with magnitudes > 6.2 occur annually (Jones and McCue, 1988). Teleseismic and motion studies indicate that most earthquakes involve shallow strike-slip movement, consistent with regional dextral tectonism (Frohlich et al., 1997).

3.3. Evolution of the Macquarie Ridge Complex

The Macquarie Ridge Complex coincides with the inferred position of a palaeo-mid-ocean ridge that formed the oceanic lithosphere of Macquarie Island (Massell et al., 2000). This relict spreading centre, known as the Proto-Macquarie Spreading Ridge (PMSR), generated new ocean crust during Middle Eocene (~ 40 Ma) to Late Miocene (< 10 Ma) rifting of the Indo-Australian and Pacific plates (Goscombe and Everard, 2001). Seafloor spreading along this extensional plate boundary separated existing ocean crust of the Tasman basin (formed 80–55 Ma) from the continental Campbell Plateau (Figure 3.1).

Plate motion modelling and tectonic reconstructions have been used to interpret the spreading history and evolution of the Macquarie Ridge Complex (Sutherland, 1995; Lamarche et al., 1997b; Massell et al., 2000). These models are based on the relative movement of each tectonic plate's rotational pole, and the preserved sea-floor fracture zones and spreading fabric (e.g., faulted abyssal hills) imaged on the seafloor during marine geophysical surveys. The prevailing tectonic interpretation suggests that the Indo-Australian – Pacific plate boundary progressively evolved from an Eocene mid-ocean ridge (initiated ~ 40 Ma), to a system of large-offset transform faults (10's to 100's of km-long) separated by short (< 50 km) spreading segments (Middle to Late Miocene), before eventually forming the present dextral transform boundary (post Late Miocene) (Varne et al., 2000b).

The interpretation of seafloor magnetic anomalies, combined with plate motion reconstructions, has also been used to model variations in the spreading rate and ridge geometry of the Proto-Macquarie Spreading Ridge (Sutherland, 1995; Massell et al., 2000). The rate of seafloor spreading progressively diminished from ~ 30 mm/year (39–30 Ma), to ~ 25 mm/year (30–20 Ma), and eventually to ~ 20 mm/year (20–10 Ma)* (Varne et al., 2000a). Clockwise rotation of the spreading axis also accompanied the waning spreading rate, and resulted in progressive re-orientation of the ridge geometry (Daczko et al., 2003). Original NNE-striking segments evolved into a series of shorter E-trending ridges (25–40 km-long) off-set by major transform faults (Lamarche et al., 1997a). The reorganisation of the plate boundary reflects asymmetric spreading rates (between the Indo-Australia – Antarctic plates and the Pacific – Antarctic plates) and the progressive migration of the Pacific plate pole of rotation (Massell et al., 2000; Varne et al., 2000a). The rotational pole of the Pacific plate, situated ~ 2500 km east of the Macquarie Ridge Complex, migrated over 1000 km (southwards) during the prolonged spreading history of the Proto-Macquarie Spreading Ridge, and eventually caused shear stress to supersede extension (Massell Symons and Mosher, 2004). This transformation resulted in the coalescence of the major transform faults, and led to the formation of the present dextral strike-slip boundary.

The Macquarie Ridge Complex has continued to evolve since the cessation of spreading, with underthrusting and crustal shortening of the Indo-Australian plate resulting in transpression (Meckel et al., 2004). This has caused extensive uplift and deformation, and led to the formation of the steep and narrow submarine ridge that defines the MRC. Thermoluminescence dating of raised beach deposits on Macquarie Island suggested an average uplift rate of 0.8 mm/year, implying that Macquarie Island was first exposed above sea-level about 600 Ka (Adamson et al., 1996).

3.4. Age of the Macquarie Island crust

The proximity of Macquarie Island to the present Macquarie Ridge Complex (and hence the Proto-Macquarie Spreading Ridge) implies that most *in situ* rocks formed during the final stages of seafloor spreading. Tectonic reconstructions (as previously outlined) estimated a model spreading age of ~ 12–9.5 Ma for the Macquarie Island crust. This age range is supported by radiometric data obtained from basaltic rocks (K-Ar and Ar-Ar dating), which gave probable crystallisation ages of 11.5–9.7 Ma (Duncan and Varne, 1988). Planktonic foraminifera and calcareous nannoplankton in sedimentary oozes (inter-pillow deposits) from North Head also suggested Middle to Late Miocene ages (Quilty et al., 1973).

* Note that the spreading rate for the 20–10 Ma period is inferred from data that is independent of the Indo-Australia – Pacific plate boundary. However, the model rate is assumed to be a good approximation and is consistent with the (earlier) well constrained Eocene and Oligocene rates of spreading (Lamarche et al., 1997).

Table 3.1: Summary of important features associated with discrete segments of the Macquarie Ridge Complex.

Ridge segment	Latitude	Length	Mean orientation	Intersection angle of the plate vectors	Comments
Puysegur	46°30' S to 50°30' S	~ 330 km	045°	30° to 45°	★ Two subparallel ridges occur, flanked by a trough to the west; ★ The western ridge is continuous with the MacDougall segment to the south; ★ The eastern ridge terminates at ~ 50°30' S; ★ The Indo-Australia plate under-thrusts the Pacific plate in the northern segment; and ★ No underthrusting is interpreted for the southern segment (strike-slip only).
McDougall	50°30' S to 53°30' S	~ 410 km	030°	8° to 12°	★ The MacDougall Ridge is continuous with the western Puysegur Ridge; ★ A deep, flanking trench occurs east of the ridge; ★ The ridge axis is bisected by a steep valley (with a maximum depth of 700 m); and ★ Most interpretations suggest that pure strike-slip motion predominates.
Macquarie	53°30' S to 56°30' S	~ 350 km	015°	14° to 23°	★ The ridge-trough polarity is similar to the MacDougall segment; ★ A very deep trench occurs to the east (with a maximum depth of ~ 6 km); ★ The strike of the MRC varies significantly between the MacDougall and Macquarie segments, and the transition zone coincides with a deep trough (~ 4000 m); ★ This segment hosts the only subaerial exposure of the MRC (Macquarie Island); and ★ Tectonic activity is dominantly transpressional.
Hjort	56°30' S to 58°30' S	~ 300 km	000°	35° to 45°	★ The main trench occurs west of the MRC in the Hjort segment; ★ Twin subparallel troughs occur in ~ 25 km section at the ridge transition zone; ★ The Hjort segment is unlikely to have ever been an active spreading ridge; and ★ Multiple lines of evidence suggest previous underthrusting and the possible initiation of a subduction zone.

Table compiled from data in Massell et al. (2000), Daczko et al. (2003), and Meckel et al. (2004).
Refer to Figure 3.1 for the geographic distribution of each ridge segment.

The prevailing view on the age of Macquarie Island has recently been challenged by several studies. The discovery and analysis of enigmatic microfossils (bolboforms) in sedimentary rocks from the southern half of Macquarie Island has provided tightly constrained Late Miocene ages (9.75–8.78 Ma) (Quilty et al., 2004). U-Pb dating of zircon grains from phlogopite-bearing ultramafic pegmatites closely correlates with these palaeontology data (8.8–8.4 Ma +/- 0.2 Ma) (Armstrong et al., 2004). However, fission track dating produced significantly younger ages, with intrusive rocks from the north of the island respectively dated at 5.2–4.2 Ma (apatite) and 6.5–5.5 Ma (zircon). A tabular basalt flow from the Sandell Bay region was also fission track dated at 4.7 Ma (+/- 0.7 Ma) (Armstrong et al., 2004). In addition, preliminary age dating (unpublished) of volcanic glasses from several localities across Macquarie Island indicates that some extrusive rocks may have formed ~ 6 Ma (K. L. Wertz, 2004, pers. comm.).

Radiometric and palaeontology data, combined with tectonic reconstructions and plate evolution models, clearly imply that Macquarie Island crust formed during the waning stages of seafloor spreading at the Proto-Macquarie Spreading Ridge. This conflicts with earlier age estimates obtained from palaeomagnetic data, which suggested that Macquarie Island formed ~ 27 Ma during the Oligocene (Williamson, 1979). However, the underlying assumptions in support of the palaeomagnetic constraints have since been discredited (Varne et al., 2000b) and, although some ambiguity still exists, it seems likely that most rocks formed during the Middle or Late Miocene (~ 9–6 Ma). Further radiometric dating planned by several research groups may provide more rigorous data and better age constraints in the future.

3.5. Rock types of Macquarie Island

Macquarie Island hosts a diverse assemblage of igneous rock types comprising all stratigraphic levels of the typical ocean crust profile (see review in Chapter 4.2). These rocks are similar to *in situ* material dredged from the nearby Macquarie Ridge Complex (Summerhayes, 1969; Watkins and Gunn, 1970), and are also typical of many continental ophiolites, such as the Josephine ophiolite in north-western USA (Alexander and Harper, 1992) and the Lizard complex in Cornwall, UK (Roberts et al., 1993). The igneous assemblages include various extrusive rocks, sheeted dolerite dykes, and compositionally diverse mafic and ultramafic plutonic rocks. Basalt and dolerite are the most abundant rock types and comprise the entire southern and central regions of Macquarie Island (~ 75 % of the total land-mass; Figure 3.2). In contrast, the island's northern quarter is dominated by fault-bounded units of gabbro and a spectrum of ultramafic rock types (Figure 3.3).

The oceanic crust of Macquarie Island has been subdivided into eight lithological associations; each has a characteristic suite of igneous rock types and structural attributes (Table 3.2 and Figure 3.4; Goscombe and Everard, 1997). These rock associations formed at different crustal depths, and the various groups broadly correlate with the main units comprising idealised ocean crust profiles (Penrose, 1972).

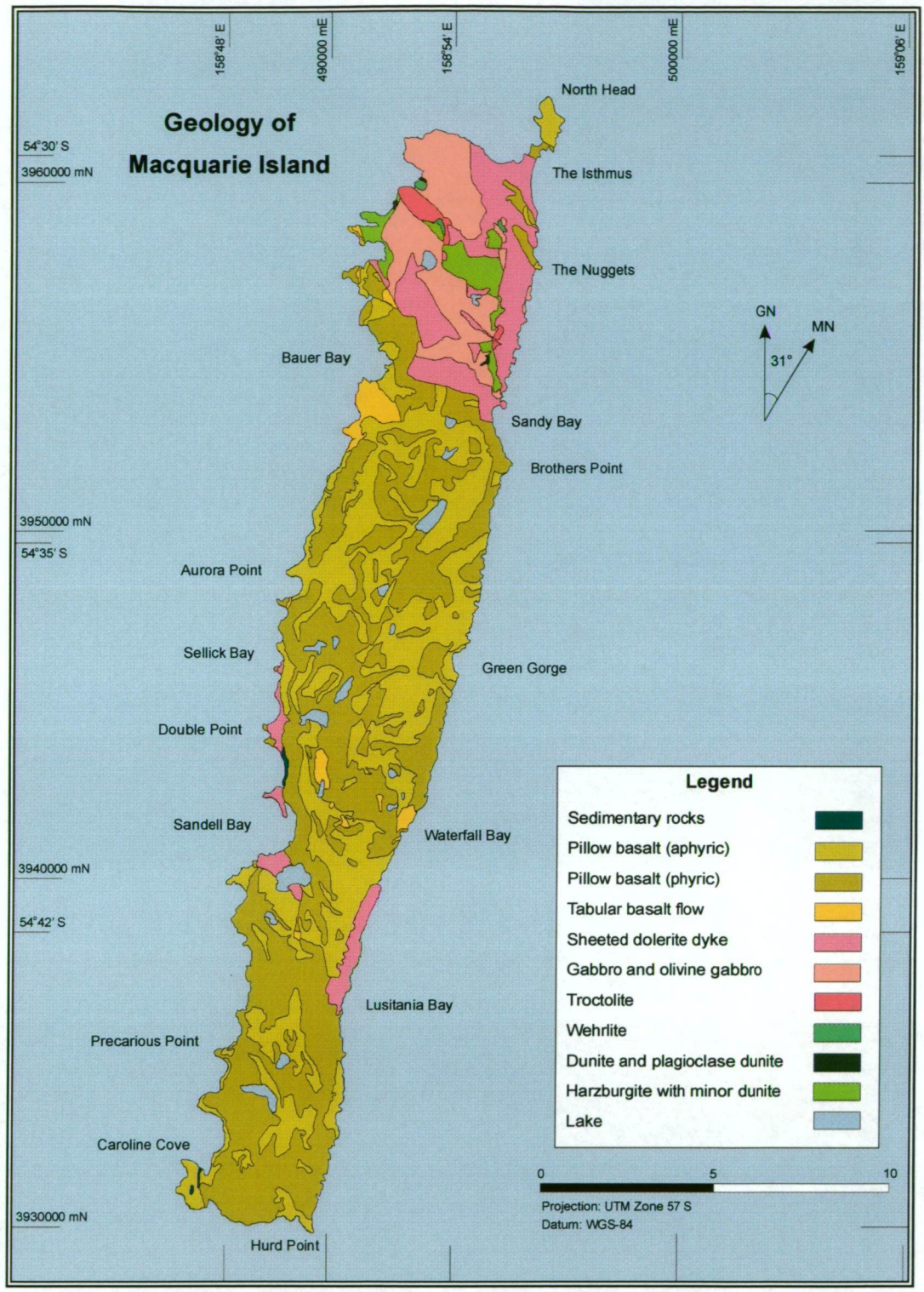

Figure 3.2: Geological map of Macquarie Island showing the regional distribution of the various rock types that comprise this section of oceanic lithosphere (minor surficial deposits have been omitted). Pillow basalt is the most abundant rock type and occurs widely throughout the central and southern districts. In contrast, the northern quarter of the island hosts a wide range of discrete, fault-bounded units; many were formed at deep plutonic levels (map modified after Goscombe and Everard, 1998).

However, unlike intermediate- and fast-spreading ocean crust and most continental ophiolites, e.g., the Samail ophiolite in Oman (Einaudi et al., 2000), the exposed section of lithosphere on Macquarie Island does not preserve a typical 'layer-cake' sequence. Geological relationships

indicate an unusual and complex structural architecture, and most discrete rock domains are fault-bound. Many fault margins (especially in the northern quarter of the island) juxtapose rock types from disparate crustal levels, e.g., an exposed geological boundary near the Overland Track at Boot Hill shows oxidised pillow basalt in direct contact with serpentinised harzburgite.

The eight rock associations are:

i. Extrusive basalts with minor sedimentary rocks;

ii. Sheeted dolerite dykes;

iii. A micro-gabbro transition zone;

iv. A massive to layered gabbro assemblage;

v. A troctolite unit;

vi. A mixed plagioclase-wehrlite and dunite group;

vii. A mixed dunite and harzburgite association; and

viii. A harzburgite association.

Based on the eight rock associations defined by Goscombe and Everard (1997) Macquarie Island is further subdivided into discrete lithological domains (Figure 3.4). The domain nomenclature associated with the mapping scheme is consistently used in this thesis, although some aspects of the classification have been modified. In general, the eight rock associations of Goscombe and Everard (1997) can be simplified into four main lithologic groups. These represent the main stratigraphic levels in the idealised ocean crust profile, and consist of volcanic and sedimentary rocks formed at or near the seafloor, sheeted dolerite dykes, gabbroic rocks, and the various ultramafic rocks of the lower crust and upper mantle (Table 3.2).

Seafloor volcanic and sedimentary rocks

Volcanic rocks are very common on Macquarie Island and comprise ~ 60–70 % of the total outcrop area (Figure 3.2). Pillow basalt is the most abundant extrusive rock (Figure 3.5 and 3.6), and coherent massive flows (Figure 3.7), hyaloclastite zones (Figure 3.8), and volcanic breccia deposits also occur. Small exposures of picrite (probably forming plug-like intrusive bodies) and unusual hornblende-bearing basalt flows crop out at several localities near the centre of the island (Everard and Crawford, 2004).

Table 3.2: Summary of important geological features for the main rock associations that comprise the Macquarie Island ophiolite.

Rock association name	Number of domains	Characteristic rock types	Igneous and structural components	Estimated max. thickness of total crustal zone
Extrusive basalt and sedimentary rocks	6	★ Abundant pillow basalt; ★ Minor massive flow basalt, hyaloclastite, and volcaniclastic breccias; ★ Rare picrite and hornblende-bearing basalt; ★ Thin mudstone, sandstone, and conglomerate horizons inter-bedded with volcanic rocks; ★ Small pods of inter-pillow sedimentary ooze (calcareous and siliceous) are common; and ★ Discrete, late-stage dolerite dykes have intruded all domains (<10 %).	★ Primary volcanic and sedimentary layering (bedding) is common; ★ Abundant brittle vein and gouge faults; ★ Hydrothermal veins and fracture-filled faults are also common; ★ Alteration minerals are mainly zeolite, prehnite, and clays; and ★ Volcanic unconformities (hiatus) are rare.	1000 m
Sheeted dolerite dykes	8	★ Subparallel dolerite dyke intrusions comprise 70 to 100 % of each dyke complex; ★ Rare pillow basalt transition zones occur at some locations; and ★ Gabbro screens vary in abundance in the deeper crustal levels (locally 30 to 70 % in these lower-most transition zones).	★ Multiple intrusive stages are recognised; most post-date formation of the deeper plutonic rocks; ★ Minor localised cleavages; ★ Brittle faults and fractures are common; and ★ Zeolite, prehnite, quartz, epidote, actinolite, and gypsum veins are the main alteration minerals.	1500 m
Micro-gabbro transition	3	★ Micro-crystalline gabbro is the main rock type; and ★ Minor sheeted dolerite dykes occur locally.	★ A narrow lithological zone separating gabbro and dolerite domains; and ★ Contains abundant vein and gouge-filled faults.	200 m
Gabbro	4	★ Massive and layered, medium to coarse-grained gabbro is abundant; ★ Minor discrete dolerite dykes; and ★ Rare ultramafic screens.	★ Minor gabbro xenoliths and micro-gabbro dykes; ★ Vein and gouge-filled faults and actinolite-filled fractures are common; and ★ Rare ductile shear zones and flaser mylonite.	1200 m
Troctolite	1	★ Coarse-grained and well-layered troctolite is most abundant; ★ Discrete dolerite dykes are common (20 to 40 %); and ★ Minor layered gabbro and plagioclase-wehrlite also occurs.	★ Compositional layering is well developed at fine- (1–5 cm) to medium-scales (12–50 cm); ★ Layered anorthosite and plagioclase-wehrlite are common; ★ Minor semi-ductile shear zones occur locally; and ★ Rare primary igneous scour surfaces.	255 m
Plagioclase-wehrlite and dunite	1	★ Massive plagioclase-wehrlite (rarely layered) is the main rock type; ★ Dunite and plagioclase-dunite are relatively minor; ★ Abundant discrete dolerite dykes (locally up to 50 %); and ★ Rare troctolite and gabbro screens, and also minor gabbro veins and dykes.	★ Tabular to elongate dunite and plagioclase-dunite lenses (2–25 cm-wide); ★ A compositionally diverse igneous assemblage; ★ Commonly associated with the troctolite domain; ★ Prehnite, actinolite, talc, and wollastonite-filled veins are common; and ★ Serpentine-filled fault planes also occur.	325 m
Dunite-harzburgite	1	★ Massive dunite and plagioclase-dunite are common; ★ Plagioclase-wehrlite is a minor component; ★ Discrete dolerite dykes sporadically intrude all units (30 to 50 % locally); and ★ Minor harzburgite and gabbro veins or dykes.	★ Compositional layering is common; ★ Steep gabbro veins are widespread; and ★ Serpentine-filled veinlets and faults also occur.	215 m
Harzburgite	3	★ Massive to layered harzburgite; ★ Abundant gabbro veins and dykes; ★ Troctolite, dunite, and wehrlite occur rarely; and ★ Minor discrete, late-stage dolerite intrusions.	★ Tensional serpentine veinlets and foliated magnetite seams occur; ★ Ductile shear zones are preferentially partitioned into gabbro units; ★ Hydrothermal veins are common; talc, chlorite, actinolite, phlogopite, plagioclase, and serpentine are all abundant; and ★ Minor lenses and pods of dunite occur.	700 m

Notes:

1. Table compiled from information in Goscombe and Everard (1998), Goscombe and Everard (2001), and Varne et al. (2000).
2. Figures 3.2–3.4 show the geographic distribution of the different rock domains and their major geological relationships.

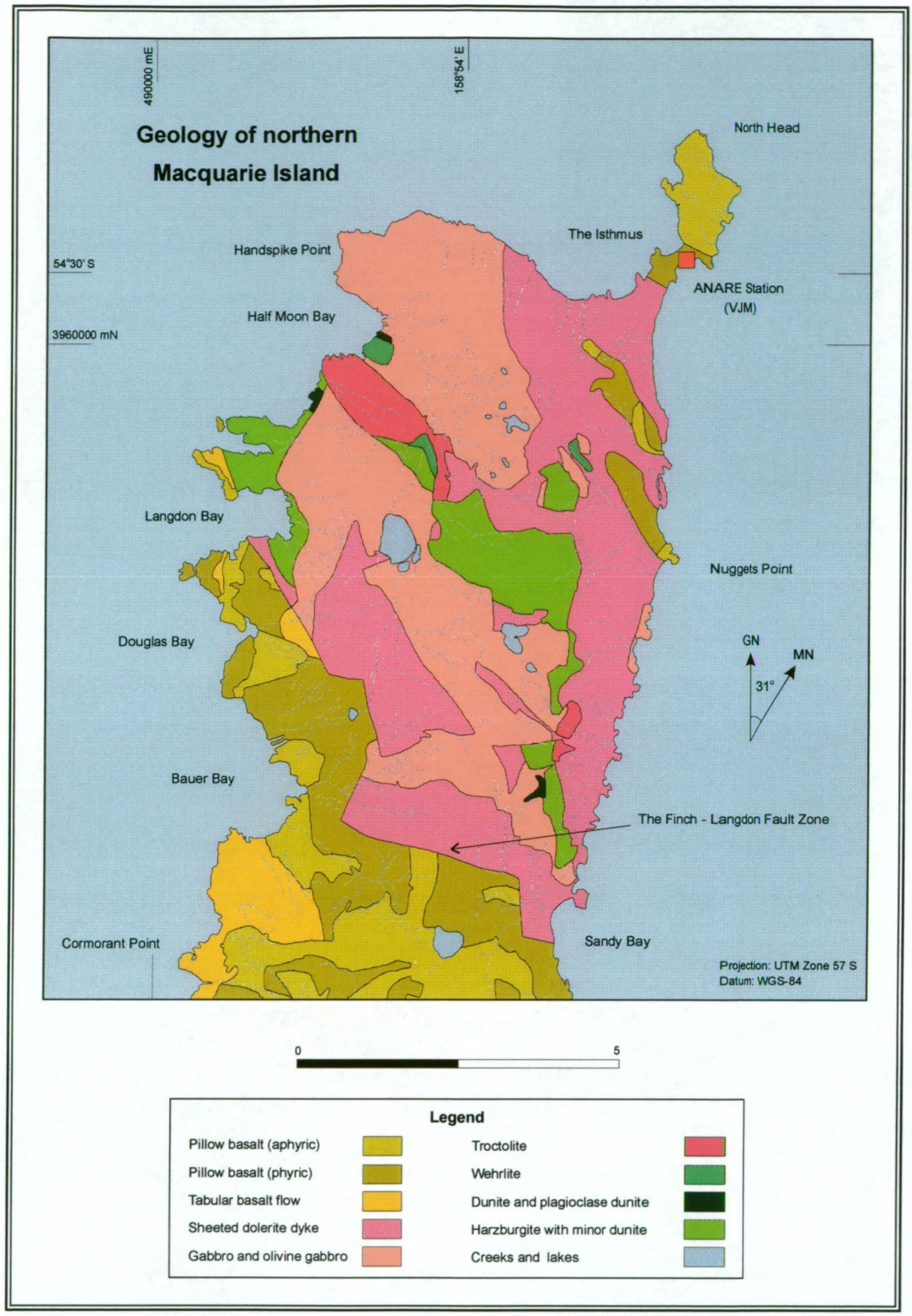

Figure 3.3: Geological map of the northern quarter of Macquarie Island, showing the distribution of rock types mainly formed in the mid to deep crust and upper mantle (surficial deposits such as sand and soil omitted for clarity). Sheeted dolerite dykes and gabbros are the most abundant rock units in this region, although minor extrusive and sedimentary rock associations occur at several locations. Most of the geological boundaries are sharp and well defined sublinear margins (although they rarely outcrop), mainly interpreted as faulted contacts (map modified after Goscombe and Everard, 1998).

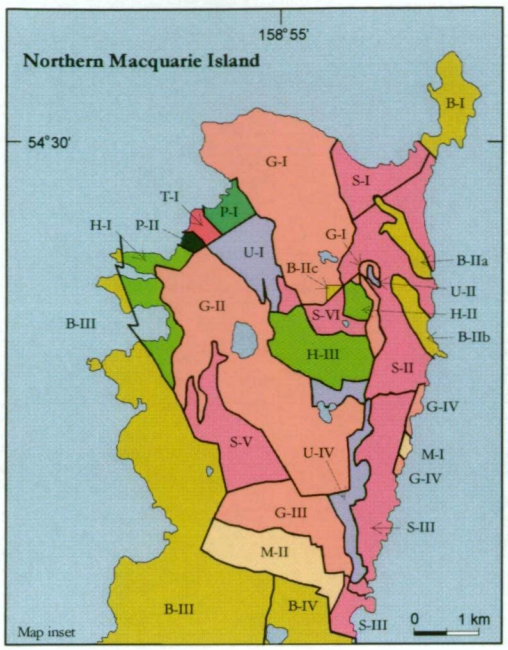

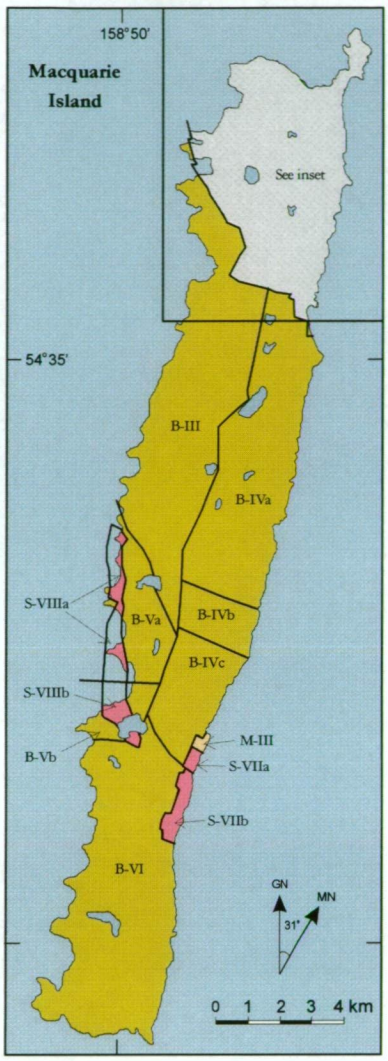

Rock association domains

Basalt and sedimentary rocks

North Head	B-I
Nuggets graben zone A	B-IIa
Nuggets graben zone B	B-IIb
Northern block outliers	B-IIc
Aurora Point	B-III
Brothers Point	B-IV
Sandell Bay	B-V
Hurd Point	B-VI

Sheeted dolerite dyke complexes

Western swarm	S-I
Eastern swarm	S-II
Sandy Bay swarm	S-III
Northeast Bauer swarm	S-V
Central swarm	S-VI
Waterfall Bay swarm	S-VII
Sandell Bay swarm	S-VIII

Micro-gabbro transition zones

Eastern coast	M-I
Southern swarm	M-II
North Waterfall Bay swarm	M-III

Gabbro associations

Northern gabbro	G-I
Island Lake gabbro	G-II
Bauer gabbro	G-III
Eastern coast gabbro	G-IV

Troctolite association

Western troctolite	T-I

Plagioclase - wehrlite and dunite

Half Moon Bay domain	P-I

Dunite and harzburgite association

Eagle Bay domain	P-II

Undifferentiated ultramafic rocks

Half Moon Bay ultramafic domain	U-I
North Mountain wehrlite domain	U-II
Plateau ultramafic domain	U-III
Mount Blair ultramafic sheet	U-IV

Harzburgite associations

West coast harzburgite	H-I
Boot Hill harzburgite	H-II
Plateau harzburgite	H-III

Figure 3.4: Map of Macquarie Island showing the distribution and abundance of the many different rock associations and structural domains proposed by Goscombe and Everard (2001). Textural variations in the basaltic domains (e.g., different phenocryst populations) are not differentiated on this map (refer to Figure 3.2).

Basaltic textures vary from aphyric to densely-phyric. Most extrusive rocks are porphyritic and contain medium- to coarse-grained plagioclase phenocrysts in crypto-crystalline or very fine-grained groundmass (minor olivine and clinopyroxene phenocrysts also occur; Griffin, 1982). Variable phenocryst abundances provide useful field-based criteria to distinguish individual volcanic units (basalt domains), and this technique was successfully applied by Goscombe and Everard (1997) during regional mapping (Figure 3.2). Basalt is typically greyish-brown or purplish-brown and many are sparsely to moderately vesicular. Vesicles (mostly ~ 1–3 mm-wide) are commonly infilled (amygdules) with pale, fine-grained secondary minerals such as prehnite, calcite, and zeolites.

Diverse pillow basalt morphologies occur across Macquarie Island and include flattened ellipsoids, elongated lobes, and other irregular or bulbous shapes (Figure 3.6). The average diameter of individual pillow shapes varies from ~ 10 cm to 1 m-across (up to a maximum of ~ 3–4 m-wide), although pillow size is relatively uniform in most individual outcrops. In some volcanic rock packages, such as the 850 m-thick Mt Waite section on the central west coast, massive basaltic flows transition upwards into 1–3 m-long mega-pillows (Davidson et al., 2004). Common lithologic features in volcanic rock domains include radial cooling fractures, chilled basalt flow margins (upper and lower boundaries), ropy surface wrinkles, and multiple flow crusts (Figure 3.9).

Most basaltic sequences comprise moderately or tightly packed pillow lobes separated by thin selvages (~ 5–20 mm) of altered volcanic glass. Volcanic glass is common in most basaltic domains, and also forms the groundmass in the matrix-dominated hyaloclastite and volcanic breccia (Figure 3.8). However, because nearly all volcanic glass is highly altered, glassy breccias are typically very friable and poorly exposed (highly weathered and eroded).

Sedimentary rocks are spatially widespread but volumetrically minor within most extrusive rock associations. In contrast to many ophiolite terranes Macquarie Island lacks a well developed sedimentary carapace atop the volcanic rocks, implying that the Proto-Macquarie Spreading Ridge received low sediment input. Thinly laminated mudstone, siltstone, and sandstone lenses (typically < 1 m-thick) are sporadically interbedded with the volcanic succession, although some sedimentary horizons are laterally persistent for several kilometres and provide excellent marker beds for mapping, e.g., the west coast escarpment between Sellick Bay and Sandell Bay (Figure 3.2). Many sedimentary rocks contain fragments of volcaniclastic material, and probably formed as proximal turbidite flows and small debris fans at the base of active fault scarps (Daczko et al., 2005). Minor clast-supported conglomerates and talus breccias also occur (Goscombe and Everard, 2001). Clasts are generally angular and include fragments of locally derived basalt, dolerite, and gabbro; the diverse clast spectrum suggests that many different rock types were exposed on the palaeo-seafloor and subjected to submarine erosion (Daczko et al., 2005).

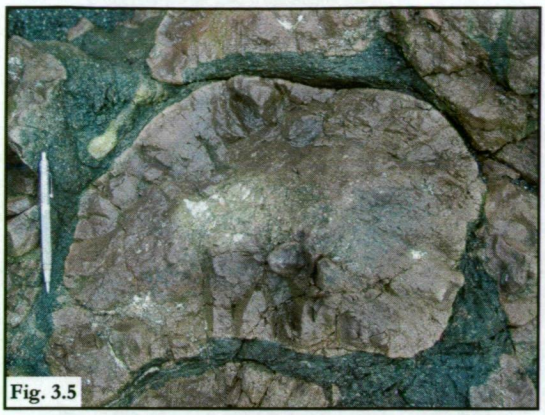
Fig. 3.5


Fig. 3.6


Fig. 3.7

Fig. 3.8

Figure 3.5: Cross-section exposure of an eroded pillow basalt on the north-eastern coastline of Macquarie Island, near the Nuggets promontory. The purplish-brown basalt is moderately oxidised and contains irregular alteration patches with abundant pale zeolite and prehnite (as seen in the pillow core). Discrete pillow shapes are prominent and surrounded by dark green, pervasively altered volcanic glass. The elongated, pale green pod (upper left of view) in the glassy matrix consists of very fine-grained and siliceous sedimentary material. Similar pods of siliceous ooze are widespread, but volumetrically minor, in most volcanic rock associations (the total length of the scriber included for scale is 13 cm).

Figure 3.6: Outcrops of greenish-grey, moderately plagioclase-phyric pillow basalt are prominent on the central plateau near Lake Tiobunga; these rocks are characteristic of the Zone BVI extrusive association. Individual lobes are commonly ~ 1–2 m-long and most have distinctly elongated and sinuous pillow shapes. The local volcanic package is tightly packed, and discrete basaltic lobes are separated by narrow selvage zones (most are < 2 cm-wide) (the hammer shown for scale here is 35 cm-long).

Figure 3.7: Subvertical columnar joints are well developed in many massive and coherent basaltic flow units. The moderately oxidised rocks shown here outcrop in the upper escarpment slope surrounding Sellick Bay on the central west coast. Massive basalt flows are not common in most extrusive rock domains on Macquarie Island, although they are locally abundant south of Bauer Bay. The coherent basalt units are typically less eroded than pillow basalts, and most are surrounded by very angular *in situ* scree and talus.

Figure 3.8: This weathered outcrop of matrix-dominated, basaltic hyaloclastite is situated in the Sellick Bay escarpment. The volcanic glass matrix is pervasively altered and replaced by dark greenish clay minerals and irregular, patchy domains of Fe-oxyhydroxide minerals. Isolated fragments of angular to subrounded basalt, including small and partly spalled pillow lobes, are sporadically distributed in the glassy matrix. In contrast to the eroded groundmass, most basaltic fragments are relatively pristine and outcrop prominently on the exposed weathering surface.

Small (< 30 cm-across), isolated pods of green or reddish-brown, fine-grained mudstone or sedimentary ooze (siliceous and calcareous) occur in some pillow basalt sequences (Figure 3.5 and 3.10). Many pod-like sedimentary deposits have formed within glass-rich inter-pillow selvages, and are best preserved in volcanic domains that have undergone relatively low-grade hydrothermal alteration. Sedimentary oozes contain a diverse micro-fossil assemblage that consists of various foraminifera, calcareous nannoplankton, and several unusual bolboform species (Quilty et al., 2004).

Sheeted dolerite dykes

Sheeted dolerite dykes occur mainly in the northern quarter of Macquarie Island, and are closely associated with gabbro and ultramafic rocks. In the south-central region two sheeted dyke units form isolated, fault-bounded domains at Cape Toutcher – Sandell Bay and Lusitania Bay (Figure 3.4). These intrusive complexes, respectively termed the Sandell Bay Sheeted Dyke Swarm and the Waterfall Bay Sheeted Dyke Swarm, are important lithological domains that form the footwall of the Major Lake Fault Zone (Chapter 5). Most sheeted dyke domains are highly faulted and structurally dismembered, and there are no complete crustal sections that preserve a continuous and transitional sequence from underlying gabbro to overlying extrusive rocks (J.A. Karson, 2003, pers. comm.). However, multiple 100–300 m-wide dolerite-gabbro transition zones are recognised in the north of the island (Varne and Rubenach, 1973), and several isolated dyke-basalt transition zones in the Double Point (Davidson et al., 2004) and Sandell Bay regions (central Macquarie Island) are not extensively faulted.

The sheeted dyke complexes consist of multiple subparallel dolerite intrusions, with individual dykes commonly recognised by variations in igneous textures and the presence of chilled margins (Figure 3.11 and 3.12). Dolerite is typically fine-grained and equigranular, and varies from greenish-blue to bluish-grey. Sparsely plagioclase-phyric and fine- to medium-grained crystalline dykes also occur. Goscombe and Everard (2001) proposed a temporal framework for the sheeted dykes (broadly verified during my fieldwork), with relatively wide (~ 2–3 m) and early-formed plagioclase-phyric dykes progressively evolving to form late, narrow (< 50 cm-wide) aphyric dykes (Figure 3.13). Dyke orientations are mostly consistent in discrete fault-bounded domains (~ 10 % strike variation), but commonly vary for different intrusive complexes.

Several sheeted dyke – gabbro transition zones occur in the northern quarter of Macquarie Island, comprising 30–70 % dolerite dykes intruding massive gabbro (Goscombe and Everard, 1997). Gabbro screens and enclaves also occur at lower levels of many sheeted dyke complexes (locally up to 30 % gabbro screens), but are less abundant higher in the crust (~ 5–10 %). Field relationships in the transition zones, such as chilled dyke margins and gabbro xenoliths in dolerite (Figure 3.14), suggest that the sheeted dykes and gabbroic rocks are not mutually intrusive. The sheeted dykes are largely interpreted to post-date gabbro, with temporally distinct magmatic episodes separated by deformation and cooling events (Dijkstra and Cawood, 2004).


Fig. 3.9

Fig. 3.10

Fig. 3.11

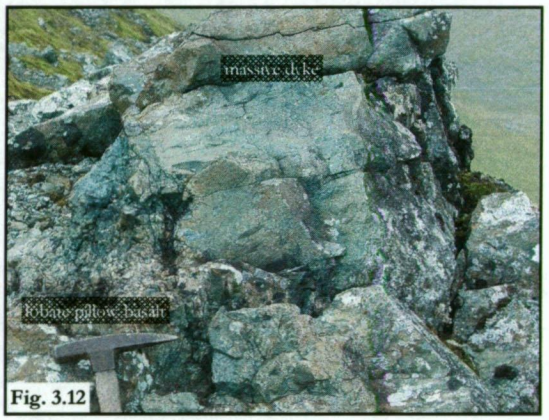

Fig. 3.12

Figure 3.9: The extrusive rock domains on Macquarie Island contain many unusual and highly distinctive pillow basalt phenomena that attest to submarine volcanism. The multiple, overlapping crusts on this ropy pillow basalt are relatively uncommon, and probably formed from successive flows.

Figure 3.10: Irregular, pod-like deposits of fine-grained, brownish-red mudstone commonly occupy narrow selvages between pillow lobes. The small (most are ~ 10–30 cm-wide) inter-pillow pods are especially common in volcanic rock associations affected by relatively low-grade regional alteration, although they are not ubiquitous. These sedimentary rock deposits formed during non-eruptive periods (each representing a short volcanic hiatus) at the palaeo-spreading ridge, and provide good evidence of ephemeral magmatic activity.

Figure 3.11: Multiple, subparallel dolerite intrusions are typical of sheeted dyke domains on Macquarie Island. The outcrop shown here contains two temporally distinct dyke generations, recognised by variations in physical and textural attributes such as colour, grain size, and phenocryst populations. At least four different intrusive stages occur in this local area of the Sandell Bay Sheeted Dyke Swarm, near the southern margin of Major Lake. All of these intrusive rocks dip moderately (40–45°) towards the NNW and are commonly surrounded by *in situ* scree.

Figure 3.12: The subvertical dolerite dyke shown here intruded tightly packed lobate pillow basalt in the crustal transition zone. The margins of the fine-grained, aphyric dyke are slightly sinuous and irregular, reflecting preferential dyke intrusion along glassy inter-pillow selvages, i.e., commonly zones of weakness in the volcanic rock package. Intrusive relationships such as this are common in the sheeted dyke and extrusive rock domain in the Mt Martin district (Sandell Bay Sheeted Dyke Swarm).

Fig. 3.13

Fig. 3.14

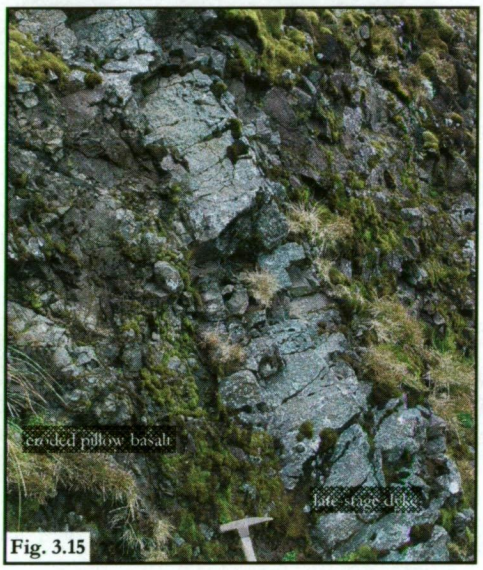

Fig. 3.15

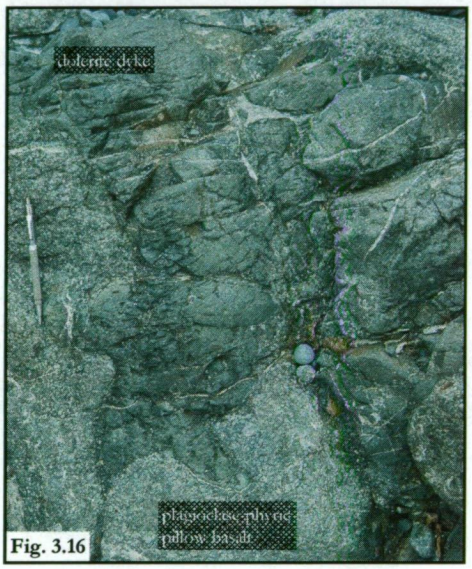

Fig. 3.16

Figure 3.13: Subparallel micro-dykes occur sporadically in the Sandell Bay Sheeted Dyke Swarm, but are difficult to recognise in outcrop because of their small size, limited strike extent, and restricted spatial distribution. These greenish-blue, fine-grained crystalline rocks are generally aphyric and have sinuous orientations. Dolerite micro-dykes represent the final intrusive phase in most sheeted dyke complexes on Macquarie Island.

Figure 3.14: Macro-view of an irregular, coarse-grained gabbro xenolith hosted in fine-grained, bluish-grey dolerite typical of the sheeted dyke complex near North Mountain (in the northern quarter of Macquarie Island). Gabbroic fragments of variable size and shape occur sporadically in the sheeted dyke associations north of the Finch-Langdon Fault Zone, although they are rare in the Sandell Bay and Waterfall Bay intrusive complexes (south-central Macquarie Island). These lithologic relationships provide relative evidence of igneous timing relationships, and imply that gabbro crystallisation pre-dated intrusion of the sheeted dykes.

Figure 3.15: Discrete, late-stage dolerite dykes occur widely in most igneous rock associations, and are especially common in the extrusive domains of central and southern Macquarie Island. This steep, NW-dipping dyke (< 1 m-wide) intruded oxidised, zeolite facies pillow basalts exposed around the south-eastern foreshore of Major Lake. In contrast to many intrusive rocks (sheeted dykes), this discrete dyke has relatively sharp and subplanar boundaries in the surrounding host-rocks.

Figure 3.16: Pillow basalts on the northern isthmus near VJM station host isolated dolerite dykes. Most are dark bluish-grey rocks and have fine-grained, aphyric textures that significantly contrast with the surrounding plagioclase-phyric pillow basalt. Thin, chilled contact margins are common, and narrow slivers and irregular protrusions of dolerite also anastomose around the relatively coherent pillow lobes. Fine veinlets of pale prehnite and zeolite cut across the groundmass of both rock types, providing clear evidence that local hydrothermal activity post-dated dyking events.

Discrete dykes variably intrude all igneous associations and are especially abundant in the volcanic rock domains. These dykes are not considered part of the sheeted dyke association, and most are probably late-stage intrusives that significantly post-date their host rock sequences (Goscombe and Everard, 1997). The discrete dykes are steeply dipping and subplanar (~ 0.5–1.5 m-wide), and most have dark bluish-grey, very fine-grained groundmass (Figure 3.15). Contact margins are commonly irregular in the volcanic rock units, as many dykes were preferentially intruded along glassy selvages that separate individual pillows (Figure 3.16).

Massive and layered gabbros

Gabbroic rocks are common in northern Macquarie Island, with an estimated crustal thickness of ~ 1200 m (Goscombe and Everard, 1997). Five fault-bounded domains were recognised by Goscombe and Everard (1997), although subsequent ground magnetic work revealed greater structural complexity than originally mapped (Godber, 2003). The spatial distribution and geological boundaries of several gabbroic associations were redefined as a result of this recent geophysical investigation, especially in the vicinity of the Finch-Langdon Fault Zone (Figure 3.3).

The gabbroic rocks on Macquarie Island are mostly massive and coarse-grained (Figure 3.14), and range in composition from pyroxene-gabbro to gabbro-norite (Dijkstra and Cawood, 2004). Layered gabbros are relatively uncommon, although a small exposure with distinctive leucocratic- and melanocratic-layering crops out near Handspike Point (Varne et al., 2000). Gabbroic rocks at Elizabeth and Mary Point on the north-western coastline (Figure 3.3) have distinctive modal layering, with olivine-gabbro and troctolite grading upwards to plagioclase-rich gabbro (Dijkstra and Cawood, 2004).

The gabbroic rocks do not intrude adjacent sheeted dyke domains. These (consistent) field associations imply that gabbro-related magmatism largely pre-dates formation of dolerite (A.H. Dijkstra, 2004, pers. comm.). Screens and enclaves of steeply dipping peridotite occur in all gabbroic domains, and are especially common in the gabbro–ultramafic rock transition zones. These relationships suggest that most gabbroic rocks formed as a series of mega-dykes (50–300 m-wide) that intruded pre-existing peridotite (Goscombe and Everard, 2001; Dijkstra and Cawood, 2004).

Ultramafic rocks

The deep crust to upper-mantle peridotites that occur in the northern quarter of Macquarie Island (Figure 3.3) are subdivided into three lithologic associations (Goscombe and Everard, 1997). These distinctive ultramafic units consist of variable amounts of wehrlite, dunite, and harzburgite (Figure 3.17). Individual ultramafic domains are fault-bounded; many peridotites also occur as subplanar and laterally continuous screens (relict slivers) in gabbroic intrusions (Goscombe and Everard, 2001). Most ultramafic rocks are massive and isotropic, although some wehrlite and harzburgite units are compositionally layered (Varne et al., 2000). Discrete dolerite

and gabbro dykes are also common and comprise up to 50 % of some ultramafic rock associations.

Figure 3.17: Isolated boulders of harzburgite crop out on the scree-covered central plateau of Macquarie Island near Boot Hill and the Overland Track. The angular outcrop appearance and orange-brown weathering rind are typical of most upper mantle rock exposures in the local area. The enlarged outcrop view (right) shows pervasively altered, coarse-grained groundmass (rich in serpentine and talc) cross-cut by abundant magnetite-bearing veinlets.

Macquarie Island peridotites are coarse- to very coarse-grained rocks with adcumulate or orthocumulate textures (Christodoulou, 1986). Some very coarse-grained ultramafic rocks form distinctive pegmatites, and these contain trace zircon crystals that have been dated using U-Pb and fission track methods (Armstrong et al., 2004). Most igneous minerals in the ultramafic rocks (e.g., olivine, orthopyroxene, and Cr-spinel) are strongly altered and replaced by a diverse hydrothermal assemblage that comprises serpentine, actinolite, chlorite, tremolite, and magnetite (Christodoulou, 1986). Serpentine is especially common, and is characterised by partial vein-style replacement of olivine and texturally destructive (pervasive) alteration of the crystalline groundmass (Godber, 2003).

3.6. Regional hydrothermal alteration of the upper crust

Mineral assemblages of unequivocal hydrothermal (non-igneous) origin are common in all volcanic and intrusive rock domains on Macquarie Island. The secondary minerals variably replace and overprint igneous phases, partially to completely infill primary voids and cavities, and form discordant vein networks and breccia cements. The alteration minerals, hydrothermal textures, and paragenetic relationships are similar to those noted from other upper crustal rocks recovered from the seafloor, e.g., drill-core from ODP Hole 504B (Alt et al., 1986; Ishizuka, 1989), and from many ophiolite terranes, e.g., the Del Puerto ophiolite in California (Evarts and Schiffman, 1983) and the Josephine ophiolite in Oregon (Harper et al., 1988).

Griffin (1982) undertook a comprehensive study of upper crustal regional alteration on Macquarie Island and defined four alteration mineral assemblages (facies). Griffin's work showed that all volcanic rocks and sheeted dykes have interacted with seafloor hydrothermal fluids, although the intensity and extent of the alteration assemblages is highly variable. Each alteration

facies comprises a characteristic suite of secondary minerals that broadly correlates with variations in crustal depth and peak hydrothermal conditions (Griffin, 1982). The alteration facies are interpreted to have formed during semi-pervasive and pervasive fluid-rock interaction in the on- and near-axis spreading environment. Minor off-axis and uplift-related hydrothermal activity and alteration probably also occurred during the geological evolution of Macquarie Island (Daczko et al., 2003).

The four regional alteration facies identified by Griffin (1982) (Table 3.3 and Figure 3.18) are:

i. A seafloor-weathering facies characterised by abundant smectite and calcite (mainly restricted to North Head), formed mainly from low-temperature (< 50° C) and strongly oxidised fluids;

ii. A complex zeolite mineral facies with a diverse assemblage of Ca- and Na-rich zeolites;

iii. A widespread but heterogeneous prehnite to lower-greenschist assemblage that contains abundant albite, chlorite, epidote, prehnite, and titanite; and

iv. An upper-greenschist to lower-amphibolite facies that occurs exclusively in the lower segments of the sheeted dykes, and is indicative of peak hydrothermal conditions in the regional hydrothermal system (upper-crust).

The spatial distribution of these four groups broadly defines discrete regional alteration domains on Macquarie Island (Figure 3.18). However, because hydrothermal processes are heterogeneous in the ocean crust, alteration intensity is highly variable across a wide scalar range, including hand-samples, outcrops, and regional domains. Commonly, the most intensely altered rocks are spatially associated with regions of high crustal permeability, such as brittle faults, fracture networks, and zones of enhanced primary (igneous) permeability, e.g., dyke margins. These crustal discontinuities are commonly the locus of chemically evolved, high-temperature hydrothermal fluids that cause pervasive wall rock alteration and the precipitation of secondary veins and breccia cements (Saccocia and Gillis, 1995; Alt, 1999). The characteristics and processes of high intensity, structurally focussed hydrothermal alteration are the central themes of my research project. The main data presentation chapters of my thesis significantly expand upon this topic and provide new results and interpretations for the alteration assemblages from the Major Lake, Caroline Cove, and Sellick Bay Fault Zones (Chapter 5).

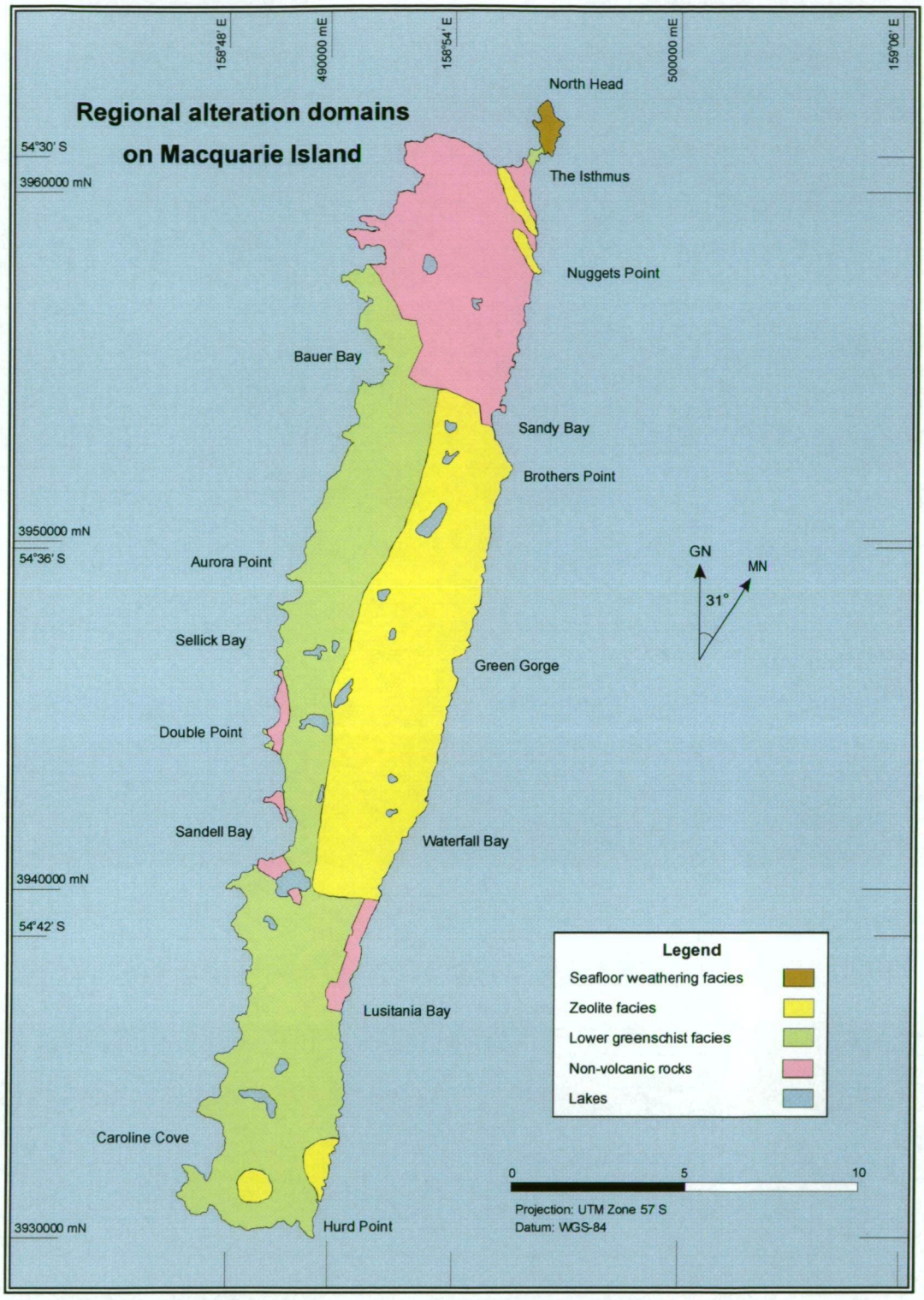

Figure 3.18: Regional alteration map of Macquarie Island showing the broad spatial distribution of hydrothermal mineral facies in the upper crustal rock units, i.e., volcanic rock and sheeted dyke domains (after Griffin, 1982). The lower-greenschist facies forms the most abundant hydrothermally derived group, and these mineral assemblages are common in the host-rocks that surround the major oceanic faults investigated during this project, e.g., the Caroline Cove Fault.

Table 3.3: Summary of the main features associated with regional alteration facies in upper crustal rocks on Macquarie Island.

Regional facies	Main minerals	Minor minerals	Main locations	Interpretation	Comments
Seafloor weathering (oxidation)	★ Calcite; and ★ smectite.	★ Celadonite; ★ phillipsite; ★ saponite; and ★ Fe-oxyhydroxides.	★ Mainly around North Head; and ★ minor sporadic distribution in some zeolite facies domains.	★ Low-temperature assemblages (< 50° C); ★ oxidising fluids; and ★ restricted to the upper-most 200 m of the volcanic pile.	★ Only affects primary olivine and volcanic glass; and ★ alteration is preferentially developed along grain boundaries and internal crystal fractures.
Zeolite	★ A variety of Na- and Ca-rich zeolites are common, such as thomsonite, mesolite, phillipsite, and natrolite.	★ Smectite; ★ calcite; ★ sericite; and ★ K-feldspar.	★ The eastern half of central Macquarie Island, especially around Green Gorge and Pyramid Peak; and ★ also occurs in the NW graben zones between the Nuggets and Hasselborough Bay.	★ Low to moderate temperature range (~ 50° to 200° C); ★ low-pressure assemblages (< 0.5–1 kb); ★ low abundance of CO_2 in the fluid; and ★ fluid chemistry varies.	★ Similar to seafloor weathering; ★ pervasive alteration of primary olivine and volcanic glass; ★ plagioclase phenocrysts are variably altered and commonly have clay-rich turbidity; and ★ plagioclase groundmass crystals have only minor alteration.
Prehnite to lower-greenschist	★ Chlorite; ★ titanite ★ prehnite; and ★ albite.	★ Epidote; ★ K-feldspar; and ★ sericite.	★ The most abundant alteration facies on Macquarie Island; and ★ especially common in the western-central and southern regions.	★ Moderate to high temperatures (~ 200° to 320° C); ★ low-pressure (~ 1 kb); and ★ formed in the mid- to lower-extrusive pile.	★ The alteration intensity is highly variable in this facies domain; ★ a wide range of Fe- and Mg-rich chlorite compositions; and ★ alteration of plagioclase varies from patchy to complete pseudomorphic replacement.
Upper-greenschist to lower-amphibolite	★ Common amphibole minerals are actinolite, hornblende, and tremolite (after cpx).	★ Titanite; ★ quartz; ★ chlorite ★ talc; and ★ epidote.	★ Only affects the sheeted dyke complexes such as the Sandell Bay Dyke Swarm.	★ High temperature facies (450° C); ★ low-pressure (~ 1.5 kb); and ★ reduced fluid chemistry.	★ Alteration intensity and mineral assemblages vary in different areas; and ★ this facies is relatively uncommon and has a patchy spatial distribution.

Note: Table modified from information in Griffin (1982).

3.7. Igneous geochemistry and petrogenesis

Rocks of the upper crust

The extrusive rocks and sheeted dykes of Macquarie Island have mineral compositions, major element abundances, and radiogenic isotope signatures consistent with mid-ocean ridge basaltic magmatism (MORB) (Kamenetsky et al., 2004). Basalt ranges in composition from tholeiitic to alkaline, and Mg-numbers* vary between 0.51 and 0.72 (Griffin and Varne, 1980). Tholeiites are the most abundant type of basalt and commonly occur in the southern and northern districts (excluding North Head). Basaltic rocks of alkaline composition are mainly confined to North Head and the central regions of the island, although they occur sporadically in all extrusive domains (Griffin, 1982). Most of the alkaline rocks are associated with low-grade regional metamorphic assemblages and, by inference, with relatively shallow crustal depths.

The major and trace element composition of Macquarie Island's upper crustal rocks have many similarities with 'normal' mid-ocean ridge basalt (N–MORB) (Griffin, 1982). However, some of Macquarie Island's basaltic rocks are geochemically enriched E–MORB variants, and are characterised by elevated abundances of K, Sr, Rb, and Nb (Griffin and Varne, 1980). These rocks are compositionally similar to basalt recovered from some segments of the mid-Atlantic Ridge, such as the FAMOUS area (Bryan and Moore, 1977). Recent geochemical analyses on basaltic glasses from Macquarie Island have provided further evidence of the complexity and spectrum of MORB compositions (Kamenetsky et al., 2000). These new data complement and expand on the earlier whole-rock analyses, and have many significant implications for the island's petrogenesis. Two distinct compositional groups, respectively known as Group I and Group II glasses, were defined by Kamenetsky et al. (2000), based mainly on the relationship between Mg-number and highly incompatible element abundances (best expressed by the ratios of K_2O/TiO_2 and La/Sm) (Figure 3.19). Group I glasses have relatively unfractionated compositions and are characterised by elevated Mg-numbers (0.63 to 0.69) and primitive forsterite and Cr-spinel. In contrast, the Group II (fractionated) glasses contain more compositionally evolved olivine and Cr-spinel, and have lower Mg-numbers and less abundant alkaline elements. Radiogenic isotopes also show well correlated trends with the major and trace element compositions of the volcanic glasses (Kamenetsky et al., 2004).

Group I glasses are characterised by an unusual seriate variation of MORB compositions. These range from typical N–MORB to E–MORB, and include highly enriched compositions that define a new end-member of the E–MORB suite. The most primitive E–MORB glasses are extremely enriched in alkaline elements and have highly radiogenic Sr and Pb isotope compositions (Kamenetsky et al., 2000). The enriched Group I glasses have no counterpart in the fractionated Group II suite (Kamenetsky et al., 2004).

* Mg number = $[Mg/(Mg + Fe^{2+})]$; where $Fe^{2+} = 0.9\ Fe_{total}$

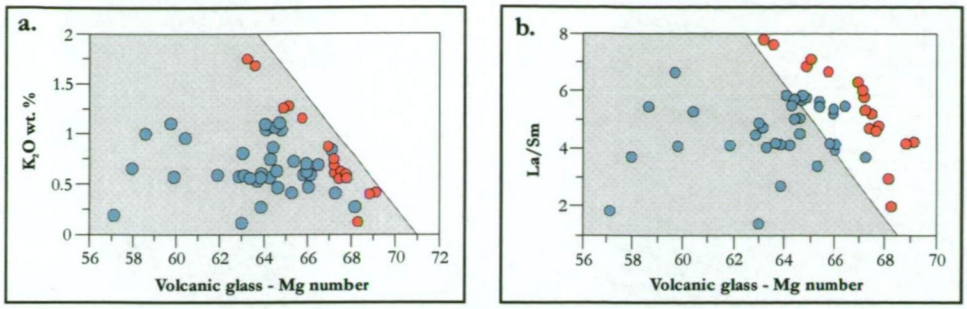

Figure 3.19: Relationship between Mg number and incompatible elements (K_20 – Figure a.) and element ratios (La/Sm – Figure b.) for Macquarie Island Group I (red circles) and Group II (blue circles) glasses. The shaded plot regions represent the field of typical MORB glass compositions (existing analyses from the literature). These diagrams clearly show that Group I glasses (arbitrarily defined as samples with the highest Mg-number) are highly enriched and have relatively primitive compositions compared to Group II (modified after Kamenetsky et al., 2000).

The compositional diversity of Macquarie Island's basaltic suite (both whole-rock and volcanic glass data) provides evidence to interpret geochemically enriched and heterogeneous mantle sources (Griffin and Varne, 1980; Kamenetsky et al., 2000). Varne et al. (2000) considered the unusual and diverse compositions to be the result of waning magmatic activity at the Proto-Macquarie Spreading Ridge. They proposed a model with two mantle sources, each with characteristic geochemical and isotopic signatures. These mantle reservoirs survived as discrete melts because of inefficient mixing during the waning stages of slow-spreading extension (Varne et al, 2000). These atypical mantle processes are unlikely to occur at magmatically robust mid-ocean rifts (intermediate- and fast-spreading ridges) and are probably indicative of the slow-spreading environment (see Chapter 4.3 for further discussion of slow-spreading mid-ocean ridges).

Kamenetsky at al. (2004) suggested that the consistent and well correlated geochemical trends between Group I and Group II glasses provide evidence to interpret possible genetic links. Simple mixing of enriched and depleted melts is considered unlikely, as it does not account for many of the unusual and highly distinctive geochemical attributes (Kamenetsky et al., 2004). These workers proposed a possible explanation for the genesis of Macquarie Island melts, involving the concomitant evolution of a spinel-lherzolite mantle source (at low degrees of partial melting) and another (subsidiary) mantle-derived partial melt (Kamenetsky et al., 2004).

Rocks of the lower crust and upper mantle

Prior to 2003, most geochemical studies suggested that gabbro and peridotite were genetically related to the overlying extrusive rocks and sheeted dykes (Griffin and Varne, 1980; Christodoulou, 1986). The similarity of major element compositions and phenocryst assemblages (e.g., clinopyroxene in both troctolite and tholeiitic basalt), coupled with close spatial relationships and apparent transitional assemblages between gabbro and dolerite, were all cited as strong evidence for their evolutionary links. However, recent geochemical analyses of upper mantle rocks provide evidence in conflict with the earlier interpretations and suggest that the

volcanic and ultramafic rocks are not cogenetic (Wertz et al., 2004). Trace element analyses of orthopyroxene, clinopyroxene, and Cr-spinel obtained from residual mantle peridotites (plagioclase-free rocks) shows spoon-shaped rare-earth element patterns (i.e., depletion of heavy rare-earth elements and enrichment of light rare-earth elements) and anomalous levels of Sr enrichment. Most Cr spinel grains have relatively high Cr-numbers* (0.39 to 0.46) and low amounts of Ti, and clinopyroxene crystals also have very low Ti and Na compositions (Wertz et al., 2004). These geochemical data are significantly different from those of the extrusive rocks and the sheeted dykes. In contrast to the highly depleted residual mantle peridotites, the upper crustal rocks span a range of N–MORB to highly enriched E–MORB compositions. The disparity of these compositional data suggests that the lower crust and upper mantle units crystallised from a distinct magmatic source that was not genetically related to the volcanic rocks and dykes.

3.8. Structural geology of Macquarie Island

The uplifted oceanic lithosphere of Macquarie Island is a structurally complex mosaic of fault-bounded rocks that spans a broad range of crustal depths (seafloor to the upper-mantle). Most lithological boundaries are faulted, and brittle structural discontinuities are very common in all rock associations (Figure 3.20). Faults and fractures are moderately to steeply dipping and kinematically diverse; normal, oblique, and strike-slip (mainly dextral) structures are widespread. Most structural discontinuities strike north to north-east, reflecting the dominant influence of the nearby Macquarie Ridge Complex (major dextral plate boundary). However, despite the relatively consistent fault orientations, considerable variations exist in the width, length, and amount of displacement for different fault and fracture systems. Structural displacement has also played an important role in shaping the rugged topography of Macquarie Island. Linear to curvi-linear fault scarps and ridges are very common (Figure 3.21), and active faulting continues to influence the island's morphology and landscape (Ledingham and Peterson, 1984).

The high concentration of faults on Macquarie Island is not surprising considering its evolution at a slow-spreading mid-ocean ridge, and its current proximity to the active Indo-Australian–Pacific plate boundary (Figure 3.20). The origin of all faults, and their associated structural components, are directly related to these dominant tectonic regimes; hence, most discontinuities can conveniently be subdivided into two associations. The separate structural groups, which have significant differences in terms of fault styles and orientations, are:

* Cr number = [Cr/(Cr + Al)]

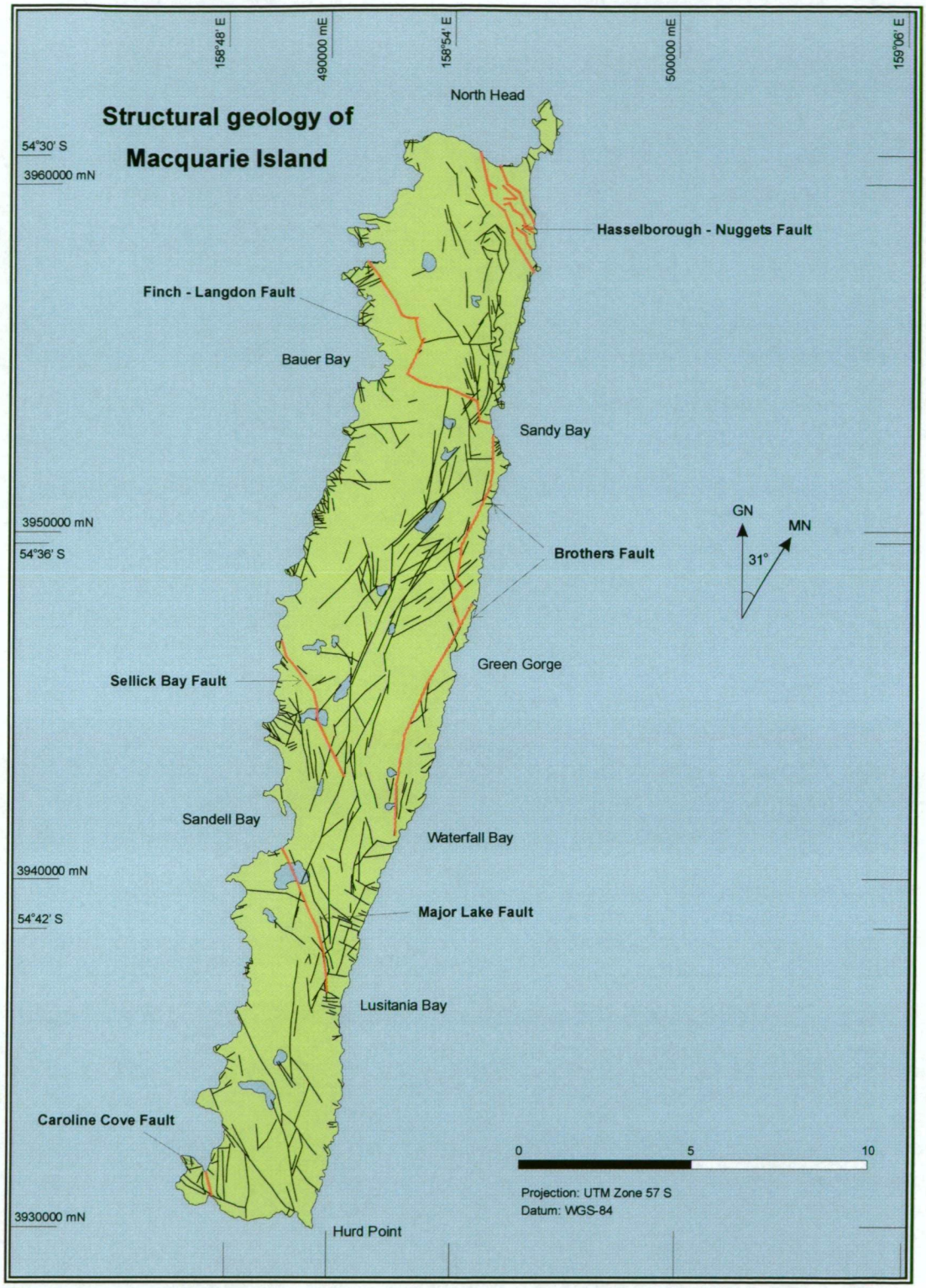

Figure 3.20: Regional structural geology map of Macquarie Island showing the spatial distribution of major fault systems. Most faults shown here strike NNW to NE and were formed during uplift-related transpression and transtension at the post-spreading Indo-Australian – Pacific plate margin (the Macquarie Ridge Complex). These neotectonic faults commonly have highly pronounced and well defined topographic expression at the surface, and typically form linear to curvi-linear ridges and valleys (although the faults rarely outcrop). The most significant fault zones on Macquarie Island are highlighted on this map, and each of these structures formed during complex and multi-stage deformation processes (long-lived tectonism). The Sellick Bay, Major Lake, and Caroline Cove Faults (the three southern-most fault systems highlighted) were the main focus of my research (map modified after Goscombe and Everard, 1998).

i. ***Seafloor-spreading structures,*** which developed during on- or near-axis tectonic extension at the Proto-Macquarie Spreading Ridge; and

ii. ***Neotectonic structures,*** which post-dated spreading and formed during (dextral) transform or transpression at the Macquarie Ridge Complex.

Figure 3.21: This well defined linear ridgeline occurs on the central plateau at Red River, about 3 km north-west of Green Gorge. Many neotectonic faults (as shown here) have significant topographic expression and form distinctive ridges or valleys across Macquarie Island's undulating plateaux.

Seafloor-spreading faults

Seafloor-spreading structures formed during extension in the on- or near-axis environment of the Proto-Macquarie Spreading Ridge. Many extensional faults have acted as permeable conduits for hydrothermal fluids, and are now spatially associated with intense wall rock alteration zones or vein assemblages, e.g., Chapter 5.3. Seafloor faults commonly have delicate mineral slickenlines (single or multiple orientations) preserved on discrete fault planes. In addition, many spreading-related faults are associated with foliated cataclasite zones (some with brecciated fragments of hydrothermally altered wall rocks or secondary cements) that are cross-cut by late-stage vein arrays. These geological relationships provide good evidence for multiple episodes of tectonic and hydrothermal activity in the axial environment, and the temporal and spatial overlap of these dominant crust-forming processes (Wertz et al., 2003).

Most of the major seafloor-spreading faults are steeply dipping, north-west- to north-striking extensional structures. These faults are generally poorly exposed in outcrop, and most lack significant topographic expression. Significant seafloor fault systems on Macquarie Island include the Finch-Langdon, Major Lake, Caroline Cove, and Sellick Bay Fault Zones (Figure 3.20). The latter three faults listed here are the main structural systems investigated in this research project (Chapter 5). The Finch-Langdon Fault Zone (FLFZ) occurs in the northern quarter of Macquarie Island and forms the main crustal boundary that separates the upper-mantle and deep crustal domains (dominated by mafic and ultramafic plutonic rocks) from the extrusive rock associations in the central and southern areas of the island. It has a complex geometric arrangement and structural architecture that comprises seven discrete segments of variable north-

west to north-east trend that obliquely intersect at high-angles. The Finch-Langdon Fault Zone was the main focus of several recent research efforts (Wertz et al., 2000; Wertz et al., 2003), including a comprehensive ground magnetics survey undertaken by the University of Tasmania. The magnetic mapping provided new and detailed information on the distribution of the lithological units that surround the FLFZ, and also re-interpreted many geological boundaries and fault orientations that were originally mapped (Godber, 2003). Consequently, no further work was carried out on the Finch-Langdon Fault Zone during this project.

Extensional structures are also evident in the lower-crust and upper-mantle rocks that occur in the north of the island (Figure 3.3). Brittle faults and fractures are abundant, and have similar orientations and characteristics to those in the volcanic rocks. In addition, a range of dilational fabrics, including actinolite-filled fractures and serpentine foliations, have also been identified (Goscombe and Everard, 2001). Semi-ductile shearbands and ductile mylonites occur in gabbroic rocks that intrude the ultramafics, although there are no regionally pervasive ductile fabrics in the peridotites (Goscombe and Everard, 2001; Dijkstra and Cawood, 2004).

Neotectonic faults

Faults which post-dated seafloor-spreading were formed during uplift-related tectonic activity (transform and transpressive movement) at the Macquarie Ridge Complex. Neotectonic faults are widespread throughout all lithologic domains, and are most abundant in the volcanic rock associations on the central and southern plateaux. In these areas steep, linear to curvi-linear fault scarps and ridges are commonly separated by elongated valleys (horst and graben blocks, Figure 3.22). Prominent neotectonic fault scarps have probably formed since Macquarie Island first emerged above sea-level (Goscombe and Everard, 2001). Many faults remain seismically active, and on-going tectonism associated with movement at the Macquarie Ridge Complex continues to affect the morphology of topographic features.

Recent fault scarps vary in length from several hundred metres to ~ 7 km, with most 500–1000 m-long (Daczko et al., 2003). Distinctive fault scarps and ridges with different orientations commonly intersect and terminate at oblique junctions. The amount of displacement along neotectonic fault scarps is generally < 20 m, although several major ridge-forming faults have 100–200 m of throw, e.g., segments of the Brothers Fault along the central east coast (Daczko et al., 2003). Neotectonic faults are poorly exposed on Macquarie Island because of extensive erosion, burial (soil cover), and mass-wasting. However, rare outcrops occur between Brothers Point and Green Gorge; these have narrow zones of fragmented fault rock (cataclasite) that mainly consist of moderately friable, clay-rich breccias with well defined (closely spaced) subvertical foliations. Fault zone breccias are commonly matrix-supported and contain abundant small (< 1–2 mm), subangular to angular fragments. Some breccia zones overprint seafloor faults and host altered wall rock or hydrothermal vein material (Figure 3.23).

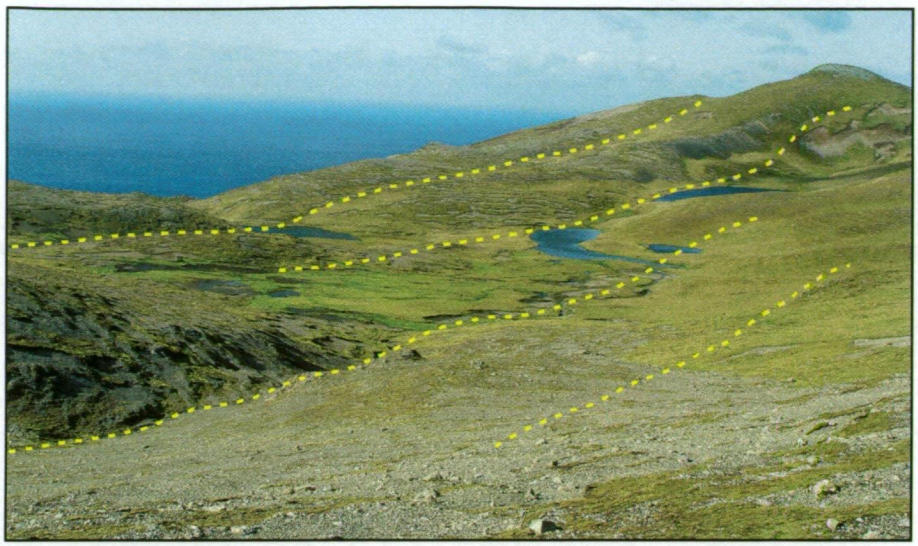

Figure 3.22: View looking south-east from the Overland Track near Mt Martin, on the central plateau of Macquarie Island. A series of subparallel NNW- to N-striking neotectonic faults (highlighted by the dotted lines) clearly show the pronounced influence of neotectonic faulting in shaping the island's rugged topography.

Figure 3.23: This finely foliated neotectonic fault zone reactivated (overprinted) an earlier-formed seafloor fault. The fractured basaltic groundmass is strongly clay-altered and oxidised, and cross-cut by abundant pale zeolite veins. These localised alteration minerals formed during hydrothermal fluid-rock interaction in the ocean crust, indicating that the fault zone initially formed during rifting.

Neotectonic faults have a wide range of orientations that vary from WNW to NE, although the most significant faults (in terms of total length and amount of displacement) consistently strike NNE to NE (Figure 3.24). In the central districts of Macquarie Island the major neotectonic fault systems have significantly influenced the steep and sublinear topography. A series of left- and right-stepping *en echelon* faults form relatively narrow (< 500 m-wide) pull-apart basins and uplifted ridgelines (Figure 3.22) (Daczko et al., 2003).

According to Goscombe and Everard (2001), most neotectonic faults preserve evidence of strike-slip or reverse shear. However, fieldwork undertaken during this project, combined with other contemporary studies (Daczko et al., 2003; Wertz et al., 2003), conflicts with their interpretation

and indicates that recent faults mainly have normal or normal-oblique (dextral) kinematic indicators. Pure strike-slip motion is not common, and is mostly recognised in relatively small fault zones (< 1–2 m) that overprint or reactivate earlier spreading-related structures. Reverse faults are even less abundant, and mainly form minor outcrop-scale discontinuities.

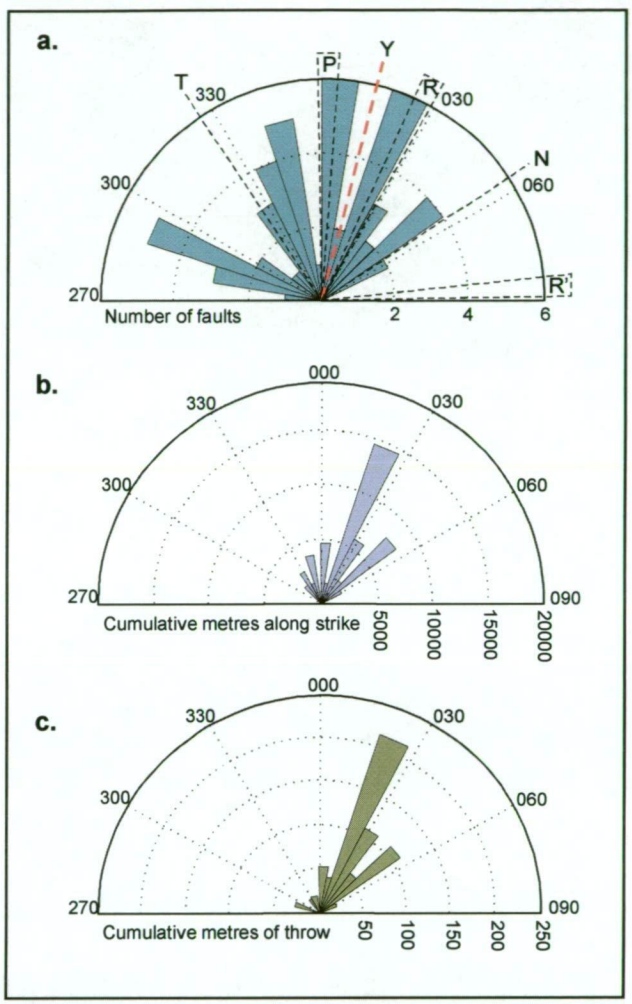

Figure 3.24 (a): Rose diagram of neotectonic fault orientations on Macquarie Island, showing the abundance of NNW- to NE-oriented structures. Overlayed on this diagram is the trend of the nearby plate boundary (Y), and the secondary fault orientations expected for classical wrenching models (R and R' are the Riedel shear set, P is the primary shear, N is normal, and T is thrust). Macquarie Island's neotectonic fault arrays do not precisely match the expected orientations.

Figure 3.24 (b) and (c): Neotectonic fault data weighted for along-strike length and amount of displacement. These diagrams show that the NNE-striking faults are the most significant group of neotectonic structures that occur on Macquarie Island (modified after Daczko et al., 2003).

A model that accounts for the abundance of normal and oblique neotectonic faults on Macquarie Island was proposed by Daczko et al. (2003). Although post-spreading faults formed under regional transpression, the Macquarie Island segment is inferred to lie within a zone of localised extension (Daczko et al., 2003). Similar local extensional zones are also interpreted from seafloor geophysical data obtained from other sections of the Macquarie and McDougall segments along the Macquarie Ridge Complex (MRC) (Massell et al., 2000). These structures are thought to represent extensional relay zones and pull-apart basins that propagated between the terminating

edges of major dextral faults (Daczko et al., 2003). This model accounts for many observed fault characteristics on Macquarie Island, and is currently preferred to other interpretations, such as Goscombe and Everard's (2001) D3 stage (outlined in the following section).

3.9. Geological models for the evolution of Macquarie Island

The oceanic crust that forms Macquarie Island comprises a varied assemblage of fault-bounded igneous rocks. The island's complex structural architecture and diverse range of (juxtaposed) rock types differs significantly from the classic model of a 'layer-cake' ocean crust (Penrose, 1972), and from most other ophiolite terranes. The observed field relationships and unusual geochemical data provide evidence of complicated and multi-phase crust-forming processes, consistent with Macquarie Island's well established slow-spreading origin (Chapter 4.3).

The primary rock types and many structural components are thought to have formed at or near the slow-spreading Proto-Macquarie Ridge during the waning stages of extension (< 10 Ma) (Goscombe and Everard, 1999; Massell et al., 2000; Wertz and Mosher, 2004). Relatively short, E-striking ridge segments (~ 25–40 km-long) were likely separated by large off-set, N-striking transform faults (Massell et al., 2000). However, considerable ambiguity exists for many features of this relict divergent boundary, such as the local extensional setting, the detailed ridge structure, and the interplay (and relative importance) of separate magmatic and tectonic events.

Three main hypotheses are currently proposed by different research groups to explain the evolution of Macquarie Island. These are:

i. The three-stage geodynamic model (Goscombe and Everard, 2001);

ii. The ridge–transform intersection model (Wertz et al., 2003; Wertz and Mosher, 2004); and

iii. The oblique-spreading model (Rivizzigno and Karson, 2004).

In addition to these models, other evolutionary interpretations based on evidence from specific areas (and localised geological relationships) on Macquarie Island have also been ventured by Davidson et al. (2004) and Dijkstra and Cawood (2004). The final section of this regional geology chapter briefly reviews the main tectonic models, and provides some relevant comments based on my field observations.

The three-stage geodynamic model

The first detailed study of the structural architecture and composition of Macquarie Island was undertaken by Goscombe and Everard (2001). They presented a comprehensive structural dataset (comprising field observations and oriented measurements of faults, veins, cleavages, intrusive rock orientations, ductile deformation fabrics, and various kinematic indicators), and

suggested that all rock types and structural components were formed during three distinct tectonic periods (D1, D2, and D3).

The evolution of most igneous rock types and their associated structures (e.g., extensional faults) occurred during D1 (Goscombe and Everard, 2001). This is interpreted as a protracted period of N-S extension and crust formation, and is associated with a wide range of seafloor-spreading structures such as:

i. Abundant normal and normal-oblique faults. These vary from hand-sample and outcrop-scale features (mm-, cm-, and m-scale structures) to major crustal fractures that transect the island and extend off-shore (10's to 100's of kilometres). Extensional faults on Macquarie Island are mainly brittle structures with a variety of styles, e.g., vein-faults and fracture-faults. They have a maximum spatial density of ~ 650 faults / km^2 in some volcanic domains (Goscombe and Everard, 2001);

ii. A variety of deformation fabrics and structures intimately associated with faulting, such as brittle fractures, cleavages, veins, and breccias. Many of these structural features were permeable zones in the ocean crust that acted as conduits for seafloor hydrothermal fluids. Thus, a common relationship exists between extensional faults and hydrothermally derived alteration minerals and veins;

iii. Dolerite dykes, which intruded most rock domains in varying abundance, and gabbro dykes and veins that only occur in the plutonic rock associations;

iv. Semi-ductile shear zones, serpentine-filled fractures and veins, and ductile mylonites in the rock units of the lower crust; and

v. Uplift and tilting of fault-bounded blocks from different crustal levels, resulting in the juxtaposition of exotic rock associations. Normal growth faulting at the spreading ridge is interpreted as the main cause of differential block uplift, and the associated seafloor exposure of lower-crust and upper-mantle rocks (Goscombe and Everard, 2001).

Goscombe and Everard (2001) proposed that a relatively short-lived episode (D2) of off-axis, NE-directed extension followed the main period of crust formation. Magmatic, tectonic, and hydrothermal activity associated with the D2 event is interpreted to have formed off-axis dyke swarms (e.g., the Sandell Bay Sheeted Dyke Swarm), various late-stage extrusive rocks devoid of dolerite dykes, palaeo-seafloor volcanos (e.g., Pyramid Peak), and minor hydrothermal veins. However, much of the evidence for the D2 stage proposed by Goscombe and Everard (2001) is equivocal, and many other research groups remain unconvinced of spatially and temporally distinct episodes of off-axis magmatism. The processes and effects of magmatic activity along a spreading ridge are highly variable and complicated, rendering the identification of discrete stages

of crust formation highly problematic (J.A. Karson, 2003, pers. comm.). Multiple magmatic and tectonic episodes (for which much evidence exists on Macquarie Island) during protracted spreading and crustal growth in the on- and near-axis environment (i.e., during D1) could readily account for the range of structures interpreted as D2 in origin.

The final tectonic phase proposed by Goscombe and Everard (2001) accounts for all neotectonic structures formed during dextral transcurrent motion along the Macquarie Ridge Complex (D3). The neotectonic structures significantly influence the morphology of Macquarie Island, and include many major fault scarps and ridge- or valley-forming faults. Goscombe and Everard (2001) suggested that most neotectonic structures are strike-slip or reverse faults. They also interpreted differential block rotations during neotectonic activity (varying from 6°–68°) to have significantly modified the orientation of the primary spreading fabric, e.g., dyke orientations. However, several aspects of the Goscombe and Everard (2001) D3 event are also disputed by other researchers, and are not consistent with more recent structural models (Rivizzigno, 2002; Daczko et al., 2003). For example, fieldwork undertaken during this research project (and supported by evidence obtained from K.L. Wertz and N.R. Daczko, 2003, pers. comm.) has shown that neotectonic faults have predominantly normal to normal-oblique kinematics. Although evidence of strike-slip and reverse faulting occurs in some oceanic faults (e.g., the Major Lake Fault Zone at Sandell Bay creek, as discussed in Chapter 5), most post-spreading faults were clearly not formed under these structural conditions. In addition, differential block rotation is generally not compatible with the local extensional regime interpreted for this segment of the Macquarie Ridge Complex, and is considered unlikely to have significantly modified many primary structures (Daczko et al., 2003).

The ridge–transform intersection model

A detailed investigation of the Finch-Langdon Fault Zone (FLFZ) provided the basis for the interpretive models of Wertz et al. (2003) and Wertz and Mosher (2004). The FLFZ obliquely cuts across the northern quarter of Macquarie Island, and is one of the most significant seafloor-spreading structures (Figure 3.20). It forms the boundary between the northern plutonic rock associations, and the basaltic domains that comprise most of the remaining landmass. The Finch-Langdon Fault Zone consists of seven discrete fault segments that intersect at high-angles and have variable NW-, NNW-, and NE-directed orientations. Although most of the fault is poorly exposed and lacks significant topographic expression, some outcrop-scale fault planes preserve delicate mineral slickenlines (hydrothermal mineral growth fibres) and mainly indicate dextral-oblique motion. The orientation, shear sense, and associated structural features of the Finch-Langdon Fault Zone are consistent with formation in the near-axis environment, and suggest that it has not undergone significant neotectonic reactivation (Wertz et al., 2003).

The complex geometry, range of structural features, and proximity with deep crust and upper mantle rocks suggests that the Finch-Langdon Fault Zone formed on the inside-corner high of a

ridge–transform intersection (RTI) (Wertz et al., 2000). Deep oceanic lithosphere is commonly exhumed by major detachment faults at ridge-transform intersections (Severinghaus and MacDonald, 1988). Significant fault scarps ~ 400–2500 m-high (Tucholke and Lin, 1994) bound the uplifted blocks, and many seafloor exposures are draped by extensive talus breccia deposits. Crustal discontinuities at RTI inside-corners have a variety of preferred orientations that form in response to the interaction of extensional and transform motion. Structural orientations are typically parallel and oblique to both the ridge and the transform axis, reflecting the relative influence of normal, oblique, and strike-slip faulting (Fox and Gallo, 1984; MacLeod et al., 1990).

Macquarie Island crust is thought to have formed at the inside-corner high of a ridge–transform intersection, where a short-spreading segment of the east-striking Proto-Macquarie Spreading Ridge was intersected by an orthogonal transform fault (Figure 3.25) (Wertz et al., 2003). The Finch-Langdon Fault Zone preserves the range of structural geometries and fault kinematics that are typically associated with these complex spreading regimes. Most of the structural features associated with the FLFZ are also consistent with the seafloor-spreading fabric and (orthogonal) transform fault arrays interpreted from swath reflectivity and bathymetric data in the surrounding marine basin (Massell et al., 2000).

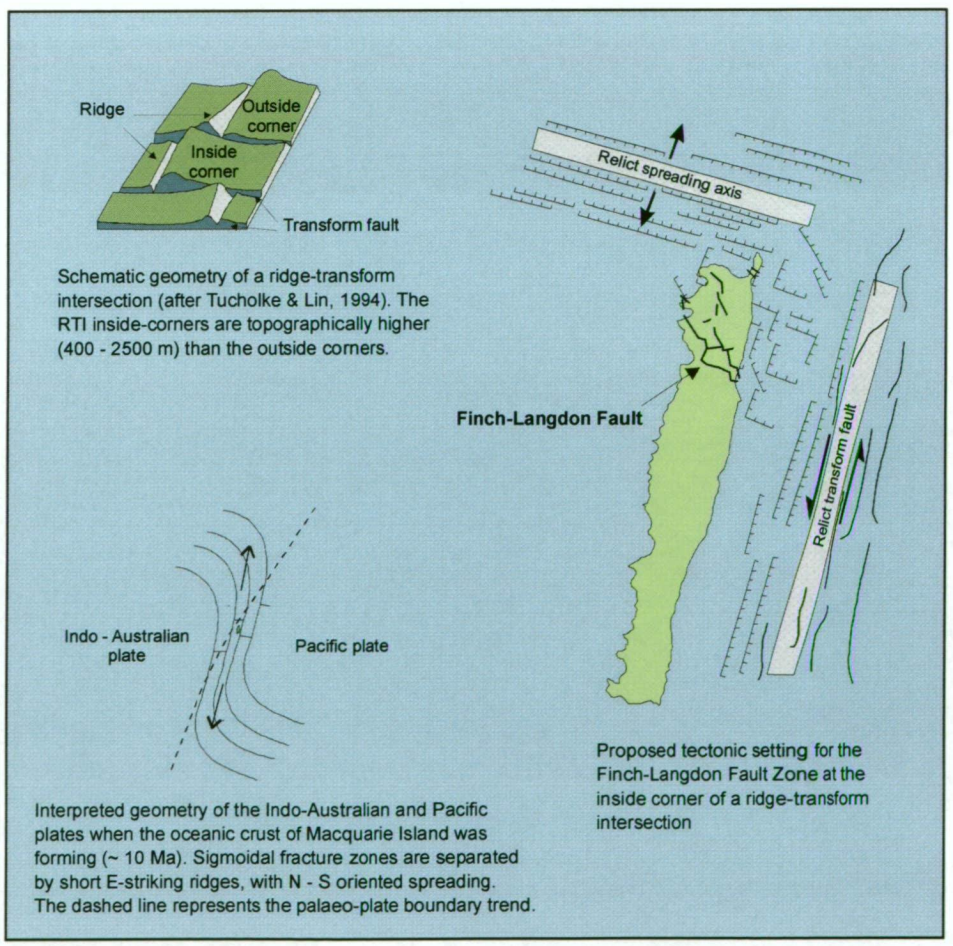

Figure 3.25: Schematic diagram highlighting the main components of the ridge – transform inside-corner model proposed by Wertz et al. (2003) for the origin of Macquarie Island.

Wertz and Mosher (2004) further expanded their initial ridge–transform intersection model and suggested that multiple episodes of magmatic activity had formed the oceanic crust of Macquarie Island. The updated model suggested that discrete ridge segments during the waning stages of extension were inherently unstable, and that a new spreading ridge propagated through the existing RTI inside-corner. The new ridge segment tapped a different melt source from its predecessor, and subsequent magmatic extension produced the sheeted dykes and volcanic rocks of the upper crust (Wertz and Mosher, 2004). The ridge propagation model accounts for significant geochemical variations that occur between the depleted mantle peridotites and the relatively enriched extrusive rocks (as discussed in Chapter 3.7).

The tectonic model proposed by Wertz et al. (2003) and Wertz and Mosher (2004) accounts for many complex structural and lithologic relationships on Macquarie Island. It combines a comprehensive set of field and laboratory data from the Finch-Langdon Fault Zone with marine geophysical data (spreading fabric) from the nearby seafloor. The RTI model accounts for a range of structural orientations, fault-related attributes, and kinematic data interpreted to form at the inside-corner high of a ridge–transform intersection. The model is also largely consistent with the prevailing model for the evolution of the Proto-Macquarie Spreading Ridge, and its progression from an extensional boundary to the current dextral transform system (Chapter 3.2).

In general, the ridge–transform intersection model proposed by Wertz et al. (2003) and Wertz and Mosher (2004) presents a plausible and coherent interpretation for the local spreading regime during the formation of Macquarie Island. However, some aspects of the model are not easily reconciled with the geological data, and many important field relationships cited as evidence for an inside-corner origin are likely over-interpreted. There are numerous geological features of ridge – transform intersections that remain poorly understood and inadequately defined, including detailed information relating to their inherent structural, kinematic, and lithological associations. Most of our current ideas and knowledge of ridge–transform intersections are largely based on limited geological evidence obtained from a few isolated sites along the global mid-ocean ridge chain. In addition, many geological features of the Finch-Langdon Fault Zone, such as its dog-leg fault orientations, high-angle structural intersections, fault-scarp breccia deposits (draped talus), and plutonic rock exposures, are not unique to RTI inside-corners (J.A. Karson, 2003, pers. comm.). The existence of active oblique-slip faults at RTI inside-corners has also not been unequivocally observed. Furthermore, other common features of ridge – transform intersections, including deep-seated detachment faults, are not part of the FLFZ's complex structural architecture. Therefore, although the tectonic models of Wertz et al. 2003 and Wertz and Mosher (2004) are consistent with some geological features and relationships at the Finch-Langdon Fault Zone, several of their critical (hypothetical) components require further research and modification.

The oblique-spreading model

The spatial distribution, structural orientation, and many other geological relationships associated with several of Macquarie Island's major seafloor-spreading faults provided the basis for the evolutionary interpretation of Rivizzigno and Karson (2004). A series of NW- to N-striking fault zones (with predominantly dextral-normal shear sense) structurally segment Macquarie Island at 10–15 km intervals (Figure 3.26). These structural discontinuities, which mimic the orientation of most off-shore bathymetric lineaments (Massell et al., 2000), are intimately associated with high temperature, hydrothermal alteration assemblages and localised subparallel dyke swarms.

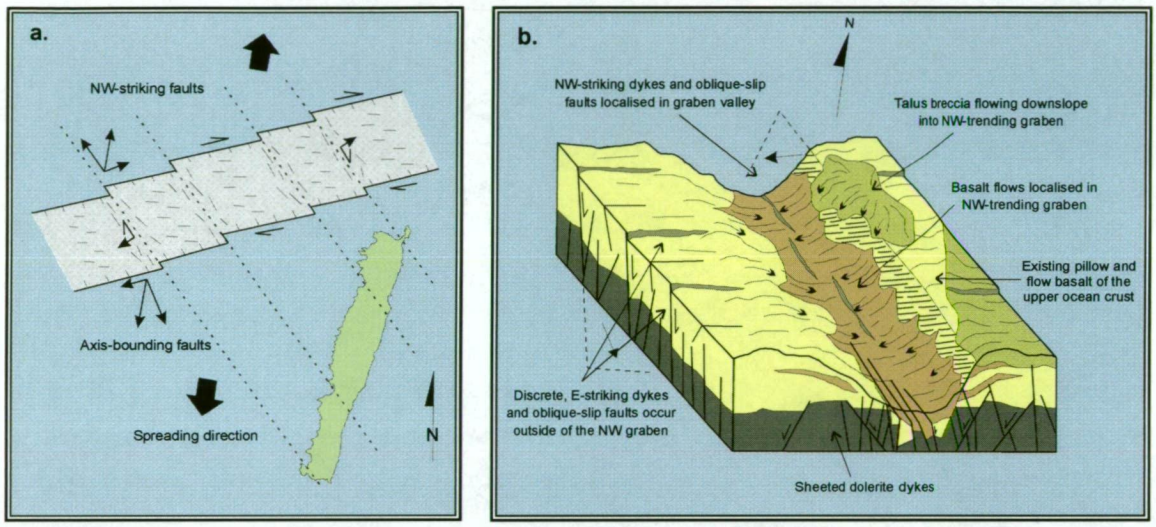

Figure 3.26 (a): Schematic diagram illustrating the main features of the oblique-spreading model proposed for Macquarie Island (Rivizzigno and Karson, 2004). The ENE-striking axis of the Proto-Macquarie Spreading Ridge is systematically off-set along its length by NW-striking accommodation zones (dotted lines) correlated with major faults on the island. NW-oriented dykes and oblique-slip faults are intimately associated with these local structural zones, but most other intrusive rocks and structural breaks run parallel to the main ridge direction.

Figure 3.26 (b): A schematic representation of the sea-floor geology in the NW- to N-striking accommodation zones, showing the graben-like depression and variable orientation of discrete dykes and faults on the palaeo-seafloor.

The complex igneous and structural attributes of the NW- to N-striking fault zones are not consistent with simple orthogonal-spreading, and are also not predicted for most slow-spreading ridges (Chapter 4). Rivizzigno and Karson (2004) proposed that the NW-oriented structural breaks represent a characteristic tectonic component associated with obliquely spreading mid-ocean ridges. These well defined structural zones, commonly known as non-transform offsets (NTO's) or transfer zones (MacDonald et al., 1991), helped to accommodate along-strike variations in the rate of seafloor extension and the supply of magma at the Proto-Macquarie Spreading Ridge. The major crustal discontinuities host structurally distinct (orientations) and localised intrusive rocks, faults, and fractures, and also contain unique hydrothermally derived alteration assemblages; all are interpreted to have formed in the on- and near-axis (oblique-spreading) environment. Geological features observed near the margins of the NW- to N-striking fault zones, such as highly elongated and steeply plunging pillow basalt lobes and

extensive talus breccia deposits, further indicate that they probably formed local seafloor depressions (Figure 3.26) (Rivizzigno, 2002).

The oblique-spreading ridge model of Rivizzigno and Karson (2004) suggested that discrete spreading segments of the E-striking Proto-Macquarie Spreading Ridge (PMSR) were relatively short (~ 50 km maximum length) and off-set by large-displacement transform faults (Figure 3.26). The pattern of ridge segmentation was highly irregular (this aspect of the model is similar to the interpretation of Goscombe and Everard, 2001), and many local magmatic and tectonic processes varied between different segments, e.g., the amount of volcanic activity and the scale and intensity of faulting. Although most magmatic activity along the PMSR (e.g., dyke intrusions) formed subparallel to the strike of the ridge axis (ENE), the accommodation zones were localised sites of magmatism oblique to the main trend. Over time, as active crust formation and rifting waned, the spreading direction became progressively more oblique to the ridge axis, and the individual segment lengths continued to shorten until spreading was eventually superseded by dextral transcurrent motion (Rivizzigno and Karson, 2004).

The presence of local and spatially restricted dykes, faults, and hydrothermal assemblages, combined with the regular-spacing (segmentation?) and subparallel orientation of the major NW- to N-striking faults, provides the main evidence for the interpretation of oblique-spreading (Rivizzigno and Karson, 2004). However, several geological features and relationships cited in support of this model are not consistent with field-based data obtained during my project. For example, the four major fault zones (Figure 3.26) are not consistently subparallel (i.e., the Caroline Cove Fault strikes N to NNE, the Major Lake Fault strikes mainly NNW, and the FLFZ comprises multiple orientations); depressed topographic fault-zone expressions are also uncommon at the present surface. Most of these faults are not associated with extensive sedimentary or talus breccia deposits, and I found no unequivocal evidence of basaltic flows in discordant contact (overlying) with the main fault corridors. Furthermore, multiple lines of geological evidence strongly suggest that several fault zones were modified during post-spreading uplift, and thus may not preserve their original seafloor architecture and structural geometries (Chapter 5). Kinematic indicators are also more complex (than indicated), and dextral-normal displacement is not as widespread or dominant as proposed in the oblique-spreading model. Finally, discrete dykes with NW strike orientations have a wider spatial distribution on Macquarie Island than indicated by Rivizzigno and Karson (2004); they are not restricted solely to the NW-striking fault (accommodation) zones.

Similar to the ridge–transform intersection model of Wertz et al. (2003), the oblique-spreading model also suffers from the over-interpretation of some geological relationships. Furthermore, this model relies on several geological relationships and phenomena for which little or no evidence could be validated during my fieldwork. Thus, as for the other two models previously discussed, several problems caution against the widespread application and suitability of the

oblique-spreading ridge model, and suggest that further targeted research is needed to better constrain the evolution of Macquarie Island's oceanic lithosphere.

Results arising from other geological investigations, with further implications for the evolution of Macquarie Island

A detailed study of hydrothermal alteration at the sheeted dyke to volcanic rock transition zone was undertaken by Davidson et al. (2004). During fieldwork at Double Point (central west coast of Macquarie Island, Figure 3.2) unequivocal evidence for multiple, ridge-parallel magmatic events was observed and interpreted (Davidson et al., 2004). Many intrusive relationships in this area clearly indicate that late-stage on-axis dykes intruded (subparallel) older and slightly rotated basaltic crust. This localised sheeted dyke swarm also supplied magma to an overlying extrusive pile of younger pillow basalt associated with the Zone B-Va domain (Figure 3.4). These relationships conflict with the Goscombe and Everard (2001) interpretation for off-axis injection of sheeted dykes (their D2 stage). The evolutionary model proposed by Davidson et al. (2004) implied that multiple periods of on- or near-axis magmatic and tectonic activity formed the oceanic crust of Macquarie Island. This is largely consistent with other tectonic models (e.g., Wertz et al., 2003; Dijkstra and Cawood, 2004) which also recognised temporally distinct phases of magmatic and amagmatic extension in the on-axis environment.

Multiple stages of on-axis crust formation at the Proto-Macquarie Spreading Ridge were also proposed by Dijkstra and Cawood (2004) for the evolution of Macquarie Island. They recognised that 'layer-cake' ocean crust profiles of the Penrose type-section are not common, and that many geological field relationships preclude a genetic link between the upper crust (volcanic and sheeted dyke associations) and the rocks of the lower crust and upper mantle. This interpretation is also supported by markedly different geochemical signatures (whole-rock compositions and various ratios), providing further evidence that the disparate crustal segments are not co-magmatic (Wertz et al., 2004). According to Dijkstra and Cawood (2004), Macquarie Island's crust probably formed from the base up and involved alternating periods of magmatic and tectonic extension, typical of most slow-spreading mid-ocean ridges (Chapter 4). This interpretation recognises that simple crustal accretion and top-down cooling models are incompatible with many field relationships, and are thus unlikely to be applicable for Macquarie Island. The gabbro-peridotite suite (plutonic association) formed initially, and cooled to amphibolite-greenschist facies conditions prior to being uplifted in the ridge environment (on- or near-axis). Subsequent magmatism (geochemically distinct) intruded sheeted dyke swarms into the pre-existing peridotite and gabbro, and led to the later eruptive episodes that formed the volcanic rock packages (Dijkstra and Cawood, 2004). Although different crust-forming phases and processes are explicitly discussed by Dijkstra and Cawood (2004), their model does not provide further details for the orientation or structure of the Proto-Macquarie Spreading Ridge or other progressive evolutionary stages.

3.10. Conclusions

Sir Douglas Mawson, famed Antarctic explorer and renowned Australian geologist, was captivated by the natural beauty and geological complexity of Macquarie Island. Although not fully aware of its remarkable origins, he aptly described Macquarie Island as "...a mountain range rising abruptly from the sea..." and "...a true wonder spot of the world" (Mawson, 1943). These assertions have subsequently been validated by the geological community and the World Heritage committee; Macquarie Island is now widely recognised as one of Earth's premier subaerial ocean crust exposures.

This chapter has presented an overview of Macquarie Island's significant geological attributes and relationships. Important information on the regional tectonic setting and the evolution of the Indo-Australian–Pacific plate boundary in the local area (the Macquarie Ridge Complex) provides critical background for my project. A detailed summary of the main igneous rock associations, including their regional alteration assemblages, geochemical signatures, and structural attributes, has clearly shown that Macquarie Island comprises a complex, *in situ* mosaic of oceanic lithosphere. Finally, a concise review of several recent structural models confirmed that the island's origin and evolution is still the subject of on-going geological debate. Further targeted research is needed to better constrain its geodynamic history, which may help to resolve some of the major geological uncertainties and refine the current interpretative models.

Chapter 4. – Slow-Spreading Mid-Ocean Ridges and Seafloor Hydrothermal Systems

4.1. Introduction

The final background chapter is based on an extensive literature review that complemented my research, and focussed on the processes and products of slow-spreading mid-ocean ridges and subseafloor hydrothermal circulation. A comprehensive understanding of these critical themes greatly assisted in:

i. Outlining the key concepts, terminologies, and models associated with slow-spreading crust and hydrothermal systems. This study also showed how ideas have progressively evolved with the advent of new and more detailed data and observations;

ii. Planning and implementing my research program. Many techniques and methods that have successfully been used for other ocean crust and ophiolite studies were reviewed, modified, and then applied to suit my investigation;

iii. Identifying the highly significant scientific themes of my study. By recognising the potential benefits afforded by this project, especially in terms of site access, geological exposure and analytical technology, I was able to target specific aspects of focussed hydrothermal alteration that remain poorly defined or understood, e.g., the spatial distribution of physical and geochemical anomalies associated with altered upflow zones in the ocean crust;

iv. Compiling an extensive dataset of published observations and analytical results obtained from previous alteration studies in ocean crust and ophiolite settings. Detailed and diverse petrographic, mineralogical, geochemical, and isotopic data provided extremely useful information to compare with the outcomes of this project; and

v. Recognising some of the limitations and potential problems associated with my research plan, and learning how other workers have addressed these issues.

This review chapter focusses on the core themes of my literature study. The first section (Chapter 4.2) outlines important characteristics of slow-spreading ocean crust, including the dominant spreading mechanisms, unusual seafloor rock exposures, and common ridge morphologies. This information provides important context for Chapter 4.3, which reviews the geological evidence for Macquarie Island's palaeo-spreading regime. Given that its primary

spreading rate is mainly inferred from plate motion modelling and tectonic reconstructions (Chapter 3), this critique outlines the case for Macquarie Island's slow-spreading origin based on the available geological data (sourced from published work and my field observations). Several ambiguous geological features which may be inconsistent with this interpretation are also reviewed.

Chapter 4.4 addresses the oceanic hydrothermal system, and this section provides further important background information and project context. The prevailing conceptual model of subseafloor hydrothermal circulation is initially presented, including a review of its relationship to spreading rate variations. This section also includes a detailed synthesis of previous research into focussed hydrothermal discharge and related alteration assemblages. Examples from a number of seafloor and ophiolite investigations are cited, along with details of the study locations, research themes, and analytical techniques. The major findings and interpretations arising from these studies are also presented, with special emphasis on the relationship between hydrothermal fluid chemistry and wall rock alteration. In the final section, I identify the most significant benefits and limitations of this research project, and discuss their potential impact on our current understanding of discharge-related alteration systems in the ocean crust.

4.2. Structure and composition of slow-spreading ocean crust

Our understanding of the internal structure and composition of the ocean crust has significantly increased in the past thirty years. New data and observations from ocean drilling and submersible operations, complemented by on-going research in ophiolite terranes, have dramatically revised the classic model of a simple 'layer-cake' oceanic crustal sequence (Figure 4.1) (Penrose, 1972). A diverse range of unusual rock associations and structural relationships has been documented at many mid-ocean ridge segments. Crustal profiles that differ most significantly from the Penrose model commonly occur at slow-spreading ridges*, where rifting is accommodated by the complex interplay between magmatic accretion and tectonic extension. The study of these heterogeneous segments of oceanic lithosphere has led to many important insights into the products and processes of seafloor spreading.

General characteristics

Slow-spreading ridges have highly variable magma budgets, although most are relatively magma-poor and lack a permanent melt supply (Detrick et al., 1990; Phipps Morgan and Chen, 1993).

* Seafloor spreading rates vary greatly along different segments of the global mid-ocean ridge system. Slow-spreading ridges have full extension rates < 30 mm / year (Karson, 2002), and some ultraslow-spreading segments along the Southwest Indian and mid-Atlantic Ridges are opening at < 10 mm / year (Dick et al., 2000; Vogt and Jung 2004). Intermediate-spreading ridges are defined as those with spreading rates between 30–60 mm / year (Karson, 2002). Fast-spreading ridges have annual spreading rates > 60 mm; some segments of the East Pacific Rise are opening at > 150 mm / year (Hey et al., 2004).

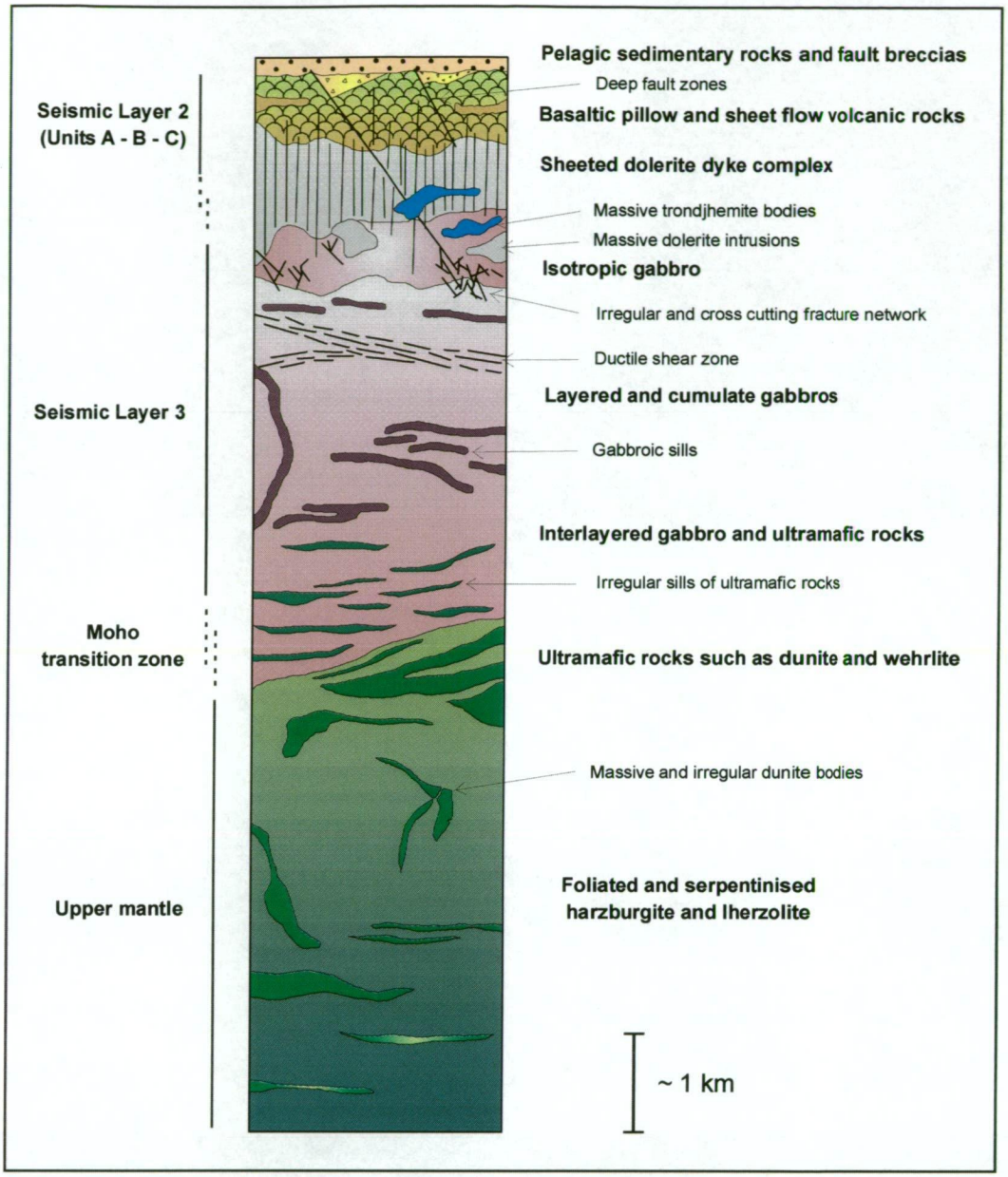

Figure 4.1: Composite cross-section (Penrose model) of oceanic lithosphere showing the classic profile for its internal structure, and the distribution of the main rock units. This section is based on seafloor observations and reconstructed ophiolite terranes, and is most applicable to crustal sections formed at magmatically robust spreading ridges, i.e., mainly intermediate- and fast-spreading ridges. The generalised, layer-cake model assumes subhorizontal contacts between the major rock units and subvertical sheeted dyke intrusions, and is correlated with the main seismic boundaries that occur in the ocean crust (shown in the left-hand column). In contrast to this model, significant differences in structural architecture and lithologic relationships are observed along many slow-spreading ridges (magmatically poor). Major vertical and lateral variations (up to kilometre-scale) commonly occur in slow-spreading crustal sections, and many of these oceanic profiles lack the complete sequence of rock units shown here (modified after Karson, 1998).

Ephemeral volcanic eruptions and dyke intrusions involve relatively small volumes of magma compared to those of most fast-spreading ridges. Seafloor spreading is accommodated by a combination of magmatic accretion and tectonic extension, and the relative dominance and intensity of these processes alternates spatially and temporally. Brittle and plastic deformation, isostatic uplift, and crustal exhumation are important tectonic mechanisms that facilitate on-going rifting (Thy and Dilek, 2000). Karson (1998) suggested that mechanical extension is the likely

'default mechanism' of plate separation for most slow-spreading ridges, and is only interrupted by relatively short-lived periods of magmatic accretion (which may last from tens of thousands to a few million years).

Slow-spreading ridges with low and infrequent magmatic input commonly have heterogeneous crustal profiles, and a range of unusual physical and geological characteristics. The relatively simple and horizontally layered Penrose type-section shown in Figure 4.1 (which is more typical of crust formed at intermediate- and fast-spreading ridges) is rarely developed at slow-spreading systems, except for a few (relatively) magmatically robust ridges, e.g., the Reykjanes segment of the mid-Atlantic Ridge (Bell and Buck, 1992; Jones, 2003). On-going amagmatic extension is interspersed with episodes of ephemeral volcanic activity and dyke intrusion, and results in many complex structural and igneous relationships. Extensive, subvertical fault scarps along axial valley walls (many with > 1 km relief) commonly expose anomalous lithologic associations (Figure 4.2). These 'tectonic windows' (Fox et al., 1980) typically occur near ridge axis offsets and segment discontinuities such as transform faults and major shear zones. Tectonic windows are uncommon along fast-spreading ridges because magmatic accretion is the dominant spreading process, although rare examples occur at the Hess Deep Rift on the East Pacific Rise (Karson and Christeson, 2003), and the Blanco Fracture Zone on the Juan de Fuca Ridge (Karson, 1998).

Structural exhumation of highly deformed oceanic crust, combined with large-displacement normal faulting (some major axial faults extend from the seafloor into the upper mantle), are important seafloor spreading processes that form tectonic windows (Dilek et al., 1998; Karson, 1998). Low-angle detachment faults also exhume dome-like massifs of lower crust and upper mantle rocks at some slow-spreading ridges. These occur in segments of thin and structurally extended crust, and are known as oceanic core complexes (analogous to similar structural assemblages formed by extreme extension in continental terranes) (Karson, 1998). Fault scarp exposures are also subjected to mass-wasting and seafloor weathering, and many talus or breccia deposits contain a diverse assemblage of eroded rock fragments (Mitchell, 2001).

Morphology of slow-spreading ridges

Mechanical extension is the dominant spreading process at most slow-spreading ridges. Extensive faulting and fracturing of the crust, coupled with low and intermittent magmatic accretion, forms a distinctive structure and morphology along the ridge axis. Wide axial valleys (most are > 10 km, with some ~ 40 km across) are major seafloor depressions flanked by steep, fault escarpments (Gracia et al., 2000; Sloan and Patriat, 2004). Some axial valleys are bound by fault scarps with up to 5 km vertical relief, although most average ~ 1–2 km (Karson, 1998). The valley floor is topographically rugged and hosts a complex, ridge-parallel network of spaced and step-like normal faults. Most valley lineaments are planar, inward-dipping faults that form low relief scarps and fissures, although minor listric faults also occur (Mutter and Karson, 1992). Active neovolcanic zones are uncommon and widely spaced; however, localised volcanic flows

(comprising small volumes of lava) may bury some ridge axis structures. The rough and undulating topographic expression of most slow-spreading ridges contrasts with the relatively smooth and elevated seafloor profiles which are typical of intermediate- and fast-spreading ridges (Karson, 2002).

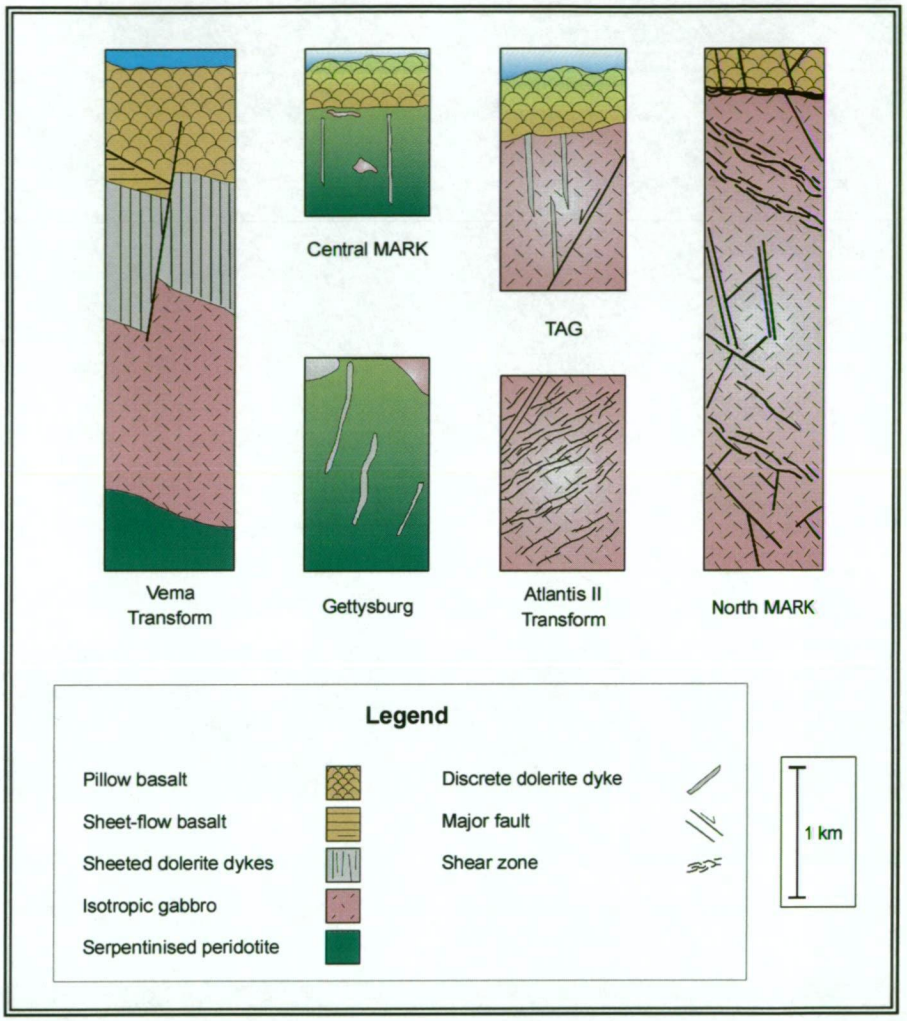

Figure 4.2: Profiles of oceanic lithosphere reconstructed from seafloor observations of major fault scarps at slow-spreading ridges. The diverse range of igneous rock associations illustrates the structural and lithological complexity that characterises 'tectonic windows'. Most crustal sections were compiled from submersible traverses across kilometre-scale survey areas. The examples shown here are mainly from the Atlantic Ocean (e.g., the MARK profiles occur at the Kane Fracture zone on the mid-Atlantic Ridge), except for the Atlantis II Transform which occurs on the Southwest Indian Ridge (modified after Karson (1998) and references therein).

Slow-spreading ridges are morphologically segmented* by major discontinuities that cut across the ridge axis trend every 20–50 km (Mutter and Karson, 1992). Transform faults, oblique shear zones, and non-transform offsets form rugged bathymetric depressions which are focal points for

* These mainly correspond to 1st–and 2nd–order ridge axis discontinuities, as defined in the hierarchical scheme of ridge segmentation (Macdonald et al., 1991). Mid-ocean ridges are partitioned into discrete axial segments of varying length by different types of discontinuities. Major 1st-order structures are commonly transform faults; these are widely spaced along the ridge axis (~ 200–500 km apart) but are relatively long-lived (> 5 x 10^6 years) and have large amounts of offset (> 50 km average). Oblique shear zones and rift axis jogs are examples of 2nd–order discontinuities. Smaller-scale 3rd– and 4th–order structures include inter-volcano gaps and ridge devals. These are spaced at intervals < 20 km apart, have minimal offsets (< 1 km), and are relatively short-lived structures (100's–1000's of years) (Macdonald et al., 1988; Macdonald et al., 1991).

brittle oblique-slip deformation and detachment faulting (Dilek et al., 1998). In contrast, many central ridge segments are topographically smooth and occur at higher seafloor elevations, i.e., similar to intermediate- and fast-spreading ridges (Figure 4.3).

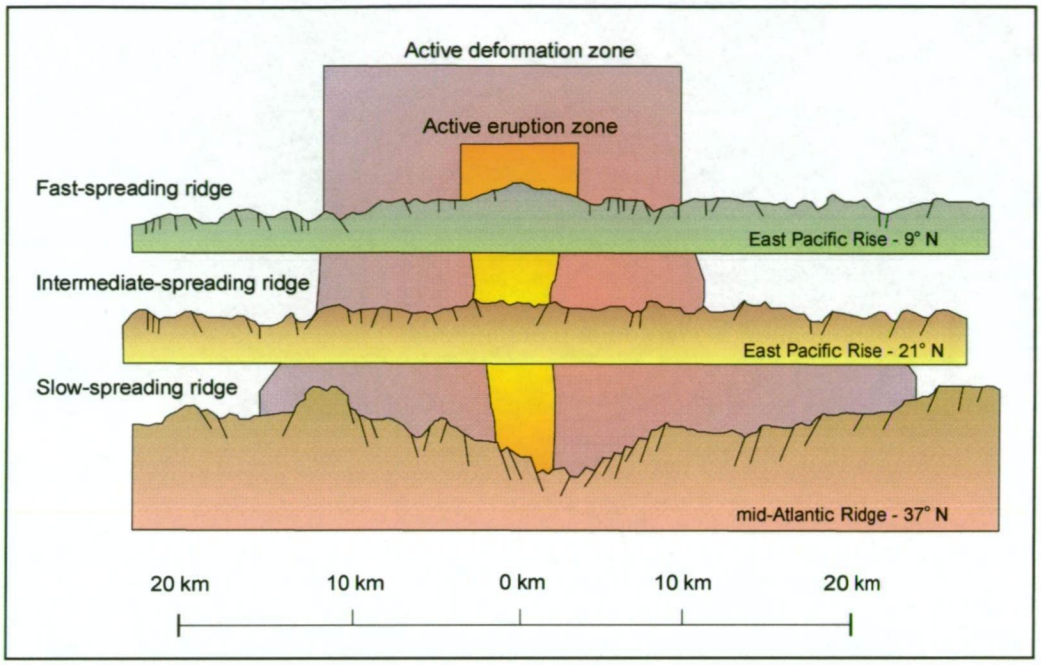

Figure 4.3: The morphology and structure of mid-ocean ridges commonly varies with spreading rate. These ridge-normal profiles show the relatively wide and rugged axial valleys commonly associated with slow-spreading ridges. The width of the active volcanic and deformation zones also varies with spreading rate. Note that the vertical profiles are schematic representations and are not drawn to scale (modified after Kelley et al., 2002).

There are also significant structural, compositional, and topographic variations at different areas of ridge-transform intersections (Tucholke and Lin, 1994). In particular, many inside-corner blocks consist of thin and structurally extended crust with extensive and complex (irregular) fault arrays. Major detachment faulting and sparse volcanic activity influences the morphology and structure of inside-corner blocks, and deep crust and upper mantle rocks are commonly exposed at the seafloor (Tucholke and Lin, 1994). The opposing outside-corner segment of the ridge-transform intersection typically hosts a thicker and less-deformed crustal sequence.

Along-strike variability of slow-spreading ridges

Geophysical studies of the mid-Atlantic Ridge have shown considerable along-strike variations in the thickness and internal structure of the oceanic crust and lithosphere, e.g., Detrick et al. (1990); Lin et al. (1990) (Figure 4.4). Similar ridge-parallel variations are observed and interpreted at other spreading segments and ridge systems, and imply that segment-scale processes play an important role in determining the composition and architecture of slow-spreading ocean crust. For example, most magmatic activity at slow-spreading ridges (which typically occurs as ephemeral injections of small-volume dykes and sills, and minor volcanic eruptions) is focussed at central ridge segments (Cannat, 1996; Thy and Dilek, 2000). Consequently, the oceanic crust is

relatively thick at segment centres (~ 5–6 km), and typical layered crustal profiles comprising gabbros, sheeted dykes, and basaltic lavas have similarities with the Penrose model (Figure 4.1). In contrast, many segment margins (i.e., near major ridge axis discontinuities) are composed of thin and structurally dismembered crust (Cannat, 1996). Magmatic events are rare and extensive tectonism results in a highly deformed and complex lithologic melange; diverse volcanic and plutonic rock associations (including ultramafic rocks) are commonly exposed in fault scarps and tectonic windows (Figure 4.2 and 4.4).

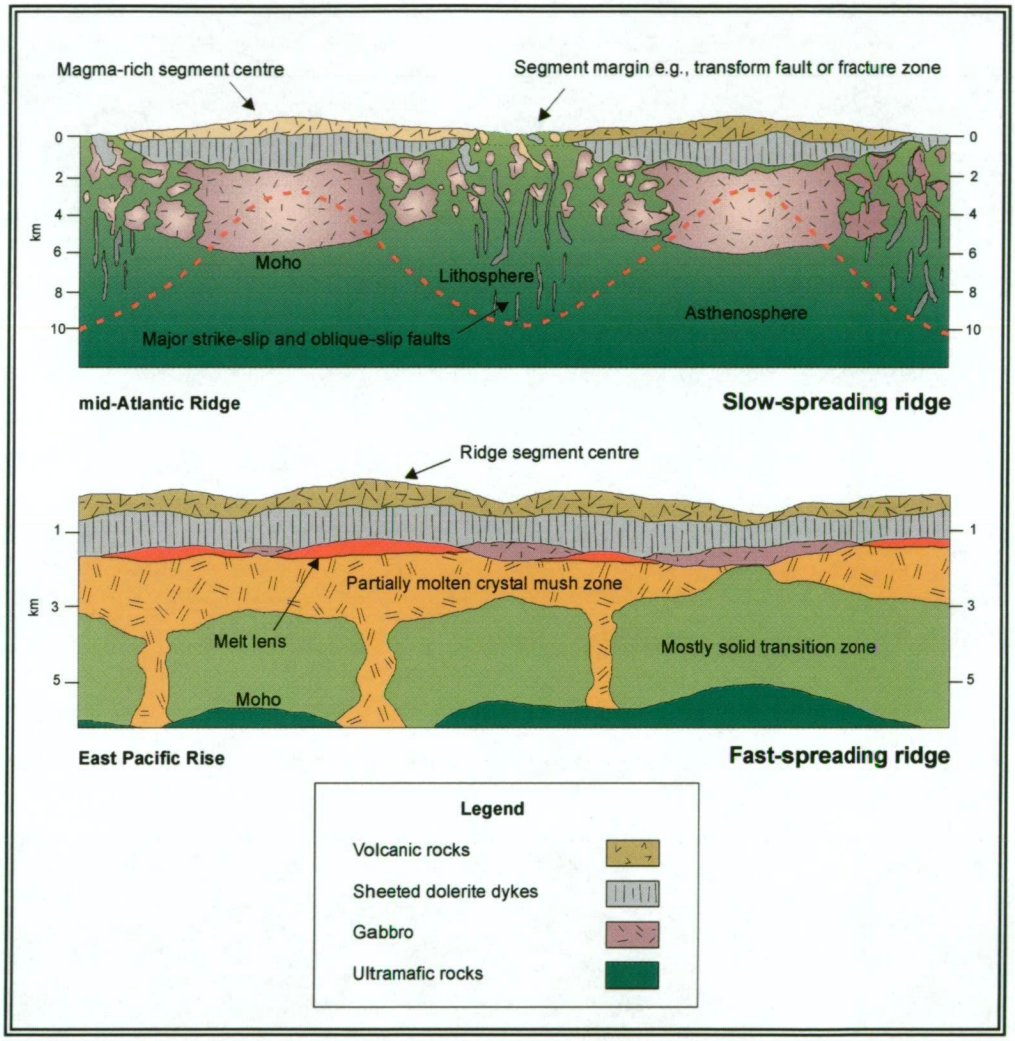

Figure 4.4: Ridge-parallel profiles highlighting the main variations in structural architecture, crustal thickness, and the spatial distribution of rock units at slow- and fast-spreading mid-ocean ridges. Significant along-strike variations are interpreted for slow-spreading ridges, with segment margins characterised by thin and disrupted crust, and low volumes of magmatic activity. Major subvertical faults have fragmented and deformed the layered crustal profile and, in many cases, led to the formation of extensive 'tectonic windows'. In contrast, most fast-spreading ridges have a steady-state melt lens that promotes robust magmatic activity. On-going magmatic accretion forms layer-like crustal profiles that closely resemble the idealised Penrose model (modified after Dilek et al., 1998).

Although many ridge axis profiles conform to the generalised model of along-strike variability (Figure 4.4), recent oceanographic studies (using submersible vehicles) have documented further complexities and variations (Karson, 1998). Thick gabbroic packages at the eastern Kane Transform Fault (situated on the slow-spreading mid-Atlantic Ridge) provide evidence of deep-

seated magmatism on a larger-than-expected scale for this tectonic environment (Karson and Winters, 1992). Unusually high volumes of volcanic activity have also been observed at some ridge-transform intersections, such as the Vema Transform Fault (also on the mid-Atlantic Ridge) (Auzende et al., 1989). In addition, seafloor fault scarp exposures of deep crust and upper mantle rocks are not solely restricted to ridge segment margins or major axial discontinuities (Karson, 1998). These anomalous occurrences attest to the inherent variability of slow-spreading ridges, and confirm that simple ocean crust profiles are not widely applicable. Although many axis-normal structures and spreading-related processes consistently vary for different ridge segments, the documented segment-scale heterogeneities emphasise the complexity of slow-spreading systems and caution against the use of generalised interpretative models (Table 4.1).

Oblique extension in slow-spreading systems

Slow-spreading mid-ocean ridges influenced by oblique extension have been described for segments of the Southwest Indian Ridge (Grindlay et al., 1998), the Mohns Ridge in the Norwegian Sea (Dauteuil and Brun, 1996), and the mid-Atlantic Ridge south of the Oceanographer Fracture Zone (Sempere et al., 1990). Along these ridge systems, patterns of axial segmentation (MacDonald et al., 1991) are more irregular than at ridges affected by orthogonal (normal) extension. Major rift zone discontinuities are characterised by relatively short offsets (e.g., commonly < 10 km displacement) and have indistinct off-axis expressions on the seafloor (Rivizzigno and Karson, 2004). The distribution, intensity, and relative importance of magmatic and tectonic processes may vary significantly between adjacent ridge segments, e.g., their rates of spreading and volcanic activity, and their angles of obliquity. Ridge axis discontinuities in these obliquely spreading systems, which are widely referred to as non-transform offsets or transfer zones (MacDonald et al., 1991), are interpreted to act as 'accommodation' zones for the segment-scale variations (Dauteuil and Brun, 1996). Oceanic accommodation zones are sites of intense structural deformation and localised (small volume) magmatic and hydrothermal activity. Discrete structures within these zones, such as oblique-slip normal faults and narrow dykes, are commonly oriented suborthogonal to the dominant axial trend (Rivizzigno and Karson, 2004).

As discussed in Chapter 3.9, Rivizzigno and Karson (2004) interpreted geological evidence from several major fault zones (such as the Major Lake and Caroline Cove Faults) to suggest that Macquarie Island formed at an oblique slow-spreading mid-ocean ridge. Although I consider some of their evidence and interpretations to be equivocal (Chapter 3.9), there is no doubt that these fault zones were localised sites of hydrothermal and structural activity in the on-axis environment (Chapter 5). Thus, regardless of the tectonic regime at the time of formation (and the wider implications that this may have for the evolution of the Proto-Macquarie Spreading Ridge), the initial recognition of these anomalous faults by Rivizzigno and Karson (2004) provided the important foundations for developing my research project.

Table 4.1: Generalised criteria for discriminating physical and geological characteristics of slow- and fast-spreading mid-ocean ridges.

	Slow-spreading ridges	Fast-spreading ridges
Spreading rate	< 30 mm / year	> 60 mm / year
Sspreading mechanism	Combination of tectonic extension and magmatic accretion. Tectonic-induced spreading is more widespread and important than for fast-spreading ridges.	Extensive magmatic activity, with frequent injection of sheeted dykes the main process driving crustal growth.
Ridge morphology	'Rough' – wide axial valleys (> 10 km) with extensive high relief, major fault scarps and draped talus deposits. Substantial variations in seafloor topography.	'Smooth' – Broad axial high with relatively minor depression in active neovolcanic zone. No major topographic contrast or large variations in relief.
Axial magma chamber	Ephemeral and discontinuous magma chamber, mainly situated (if present) beneath thicker crustal sections at central ridge segments. Low volume magma budget, with sporadic and relatively short-lived volcanic episodes.	Nearly steady-state axial melt lens able to support almost continuous magmatic accretion. However, magma chambers are unlikely to occur near major (large offset) ridge axis discontinuities.
Structural style	Large-scale extensional (normal) faults with significant displacement (up to 6–8 km). Some deep-rooted faults may extend into the upper mantle, and expose deep-level plutonic rocks (e.g., ultramafics) at shallow crustal depths or on the seafloor.	The extent, intensity, and spatial distribution of structural activity are comparatively limited. Most extensional faulting occurs near major axial discontinuities, such as propagating rift tips or overlapping spreading centres (Macdonald et al., 1991).
Seismic profile	Seismic layers 1 and 2 are commonly rotated. Deep-seated, shallow- to moderate-dipping seismic reflectors coincide with normal fault scarps in the basement.	Seismic reflectors are not significantly inclined.
Common rock types	Pillow basalts and heterolithic fault-scarp talus deposits are common on the seafloor. Sheeted dyke complexes are comparatively rare. Exposures of deep crust and upper mantle rocks occur in 'tectonic window' fault scarps, and may be locally significant.	Massive volcanic flow units and sheeted dyke complexes are extensive. Plutonic rock exposures are rare.
Geological variability	Inherently heterogeneous. The generalised Penrose model (1972) of systematically layered ocean crust is not widely applicable. Common along-strike variations in ridge axis geology, structure, composition, and crustal thickness between adjacent segments. Also common segment-scale variations between discrete segment margins (near major axial discontinuities) and centres, e.g., spreading rates and extensional mechanisms.	Relatively consistent crustal structure and composition, with layered ocean crust sections commonly forming Penrose-style (1972) profiles. Spreading-related processes are not as variable along-strike, and there are also considerably less segment-to-segment scale variations (Figure 4.4).
Hydrothermal processes	See review in Chapter 4.4 and Table 4.3	See review in Chapter 4.4 and Table 4.3

Sources: Penrose (1972), Norrell and Harper (1988), Macdonald et al. (1991), Alexander and Harper (1992), and Karson (2002).

4.3. Macquarie Island – a slow-spreading origin?

Tectonic reconstructions of the Proto-Macquarie Spreading Ridge (PMSR), combined with the interpretation of seafloor magnetic anomalies, have been used to constrain the spreading rate during the formation of Macquarie Island (Sutherland, 1995; Massell et al., 2000; Varne et al., 2000). These models suggested slow-spreading occurred along the PMSR from the Late Oligocene to the Middle Miocene, prior to the on-set of transcurrent tectonic activity (Chapter 3). Calculated rates implied that spreading progressively waned from ~ 30 mm/year (39–30 Ma) to ~ 20 mm/year (20–10 Ma) (Lamarche et al., 1997). However, the spreading rate when Macquarie Island formed (~ 12–8 Ma) has only been inferred from plate motion models that may not be widely applicable for the Macquarie segment of the Indo-Australian–Pacific plate boundary (Varne et al., 2000). Although the interpretation is based on valid tectonic predictions and is consistent with the well established rates for the 39–20 Ma period (i.e., the progressive shut-down of the palaeo-rift system), there are no definitive and locally specific model data to support slow-spreading at the time of Macquarie Island's formation.

In the absence of definitive rate markers, this section outlines the geological case for acceptance of Macquarie Island's slow-spreading origin. Many of the island's lithologic relationships and structural features are most compatible with ocean crust formed at a slow-spreading (magma-poor) ridge. Important geological evidence to support this interpretation includes:

i. The Macquarie Island ophiolite does not consist of Penrose-style ocean crust. Most geological boundaries separating different crustal units (especially in the northern plutonic rock domain) are complex and extensively faulted; simple and horizontally layered transitional boundaries are rare;

ii. Large-scale oceanic structures with significant amounts of displacement occur commonly on Macquarie Island, e.g., the Finch-Langdon and Major Lake Faults. The abundance and widespread distribution of major oceanic fault systems provides evidence for extensive mechanical extension during the formation of Macquarie Island's crust;

iii. Many areas of Macquarie Island's northern crustal block have similarities with 'tectonic window' exposures at slow-spreading ridges. The spectrum of oceanic rock types (seafloor extrusives, sheeted dykes, gabbros, and peridotites) occurs in this relatively small geographic region (~ 30 km^2), and most have complex structural and igneous relationships. These unusual and diverse lithologic mosaics are uncommon at intermediate- and fast-spreading ridges;

iv. A wide variety of cross-cutting and intrusive igneous relationships, volcanic unconformities, and complex brittle and ductile structures attest to distinct temporal episodes of magmatic construction and tectonic deformation, e.g., relatively low

(alteration) grade volcanic rocks unconformably overlie sheeted dykes containing lower amphibolite facies mineral assemblages and fragmented gabbroic screens (Davidson et al., 2004). These diverse structural and lithologic features imply that multiple crust-forming phases were variously dominated by magmatic- and amagmatic processes, consistent with slow-spreading models;

v. The presence of angular dolerite and gabbro clasts in sedimentary breccia and talus deposits on Macquarie Island indicates that deep crustal rocks were exposed in fault scarps on the seafloor, and subjected to seafloor erosion and mass-wasting (Goscombe and Everard, 2000; Wertz et al., 2003; Daczko et al., 2005). Seafloor outcrops of gabbro and other plutonic rocks have previously been noted in slow-spreading crust (e.g., Mitchell, 2001; John et al., 2004), but are rarely associated with fast-spreading ridges;

vi. Medium- and coarse-grained plagioclase phenocrysts are common in many basaltic rocks on Macquarie Island. Their widespread distribution and abundance suggests extended crystallisation periods in an axial magma chamber, with relatively infrequent episodes of magmatic input to disrupt the growth of large igneous crystals; and

vii. Many igneous rocks on Macquarie Island have highly unusual geochemical signatures (Kamenetsky et al., 2000; Everard and Crawford, 2004). For example, some volcanic glasses are extremely primitive and geochemically enriched (Chapter 3.7); these define a new end-member of the E–MORB compositional spectrum which correspond to very low degrees of partial (mantle) melting (Kamenetsky et al., 2000). The crystalline equivalents of the enriched glasses form a suite of hornblende-bearing basalts, and some fractionated counterparts are also significantly enriched in incompatible elements (Everard and Crawford, 2004). Although many of these anomalous MORB compositions and basaltic rock types are unknown from other spreading ridges (irrespective of spreading rate), Varne at al. (2000) suggested that the heterogeneous compositions could only have survived in a slow-spreading (magma-poor) environment. Long-lived and magmatically robust ridges (fast-spreading) would likely have obliterated the small volume (geochemically distinct) melt fractions implied by the diverse compositional range (Varne et al., 2000).

The geological evidence cited above strongly suggests that Macquarie Island formed at a slow-spreading ridge segment. The various structural and lithologic relationships imply that tectonic extension was the dominant spreading mechanism, and that magmatic accretion was episodic. However, some aspects of Macquarie Island's geological architecture and composition are atypical of slow-spreading ridges. Sheeted dyke complexes are rare in slow-spreading crust and have only been documented from a few locations, such as the Vema Fracture Zone (Auzende et al., 1989), and the Kings Trough area in the eastern Atlantic Ocean (Karson, 1998). However, sheeted dyke complexes are widespread on Macquarie Island, and at least five discrete crustal

blocks are defined (Goscombe and Everard, 2001). The Macquarie Island dykes intruded both plutonic (gabbro) and volcanic rock packages, although there are no continuous (transitional) sections which consist of all three rock types. Multiple temporal stages of dyke injection are also recognised on the basis of cross-cutting relationships, igneous textures, and chilled dyke margins. Clearly, the intrusion of sheeted dolerite dykes was an integral component of Macquarie Island's formation, despite the relative paucity of dyke complexes associated with other slow-spreading ridges.

The highly faulted and lithologically diverse terrane comprising northern Macquarie Island has many similarities with 'tectonic window' exposures (fault scarp) documented from other slow-spreading environments. However, tectonic windows are not restricted solely to slow-spreading ridges. Extensive fault scarps have also been described from the Hess Deep Rift on the fast-spreading East Pacific Rise (Lonsdale, 1988; Karson and Christeson, 2003), and the Blanco Fracture Zone on the Juan de Fuca Ridge (intermediate-spreading rate) (Juteau et al., 1995). Though, in contrast to many slow-spreading ridge segments, both the Hess Deep Rift and Blanco Transform exposures have crustal profiles that are more consistent with the classic ocean crust model (Penrose section). Relatively simple, layered igneous profiles occur at both localities, comprising upper-most pillow and massive-flow basalts underlain by sheeted dykes and gabbros. Complex lithologic associations and structural relationships, and exposures of serpentinised ultramafic rocks, do not occur at the Hess Deep Rift or Blanco Fracture Zone (Karson, 2002). Therefore, although 'tectonic windows' and major fault scarps are not unique and diagnostic features of slow-spreading crust, the unusual and diverse range of rock types exposed in the northern quarter of Macquarie Island is most consistent with a slow-spreading origin.

The structure and composition of Macquarie Island's crust is highly complex and unusual, and most geological features are consistent with a slow-spreading mid-ocean ridge origin. The diverse magmatic and tectonic characteristics strongly imply that the island formed during multiple periods of crustal growth. Amagmatic processes were the dominant spreading mechanism, interspersed with episodic dyking and extrusive events originating from an ephemeral axial magma chamber (Chapter 3.9). Most geological evidence supports the independent evolutionary model for the Proto-Macquarie Spreading Ridge (and Macquarie Island), which has mainly been inferred from tectonic plate reconstructions and seafloor magnetic anomalies. Although some of Macquarie Island's geological attributes have rarely been described from other slow-spreading ridges, the intrinsic heterogeneity of these anomalous crust-forming environments probably accounts for the unusual range of rock compositions and structural relationships. Clearly, these diverse features further expand the spectrum of geological phenomena that must be expected in slow-spreading oceanic environments.

4.4. Hydrothermal systems in the ocean crust

A comprehensive understanding of subseafloor hydrothermal systems, and their key role in altering the primary igneous composition of the ocean crust, is fundamental to my research project. Given its critical importance, this section outlines the main concepts, terms, and models associated with oceanic hydrothermal circulation. Chapter 4.4 has a strong emphasis on alteration assemblages formed by hydrothermal fluid discharge, and also provides discussion of hydrothermal system variations relative to spreading rate, i.e., slow-spreading versus fast-spreading. An overview of previous research into focussed hydrothermal upflow zones, with examples from mid-ocean ridge and ophiolite settings, provides further useful context and background information for the results of this study (Chapters 5 to 8). The final theme of Chapter 4 presents a discussion of the most significant and beneficial aspects of my project, and reviews potential study limitations.

Convective hydrothermal regimes and heat sources

Hydrothermal fluid circulation convectively cools the ocean crust for ~ 65 million years following its creation at a mid-ocean ridge (Stein and Stein, 1994). After this time, the crust is effectively sealed from widespread fluid circulation due to the combined effects of accumulated sediment cover (which restricts seawater recharge), and the precipitation of secondary minerals (which reduces crustal permeability) (Alt, 1999). However, crustal sealing rates are not uniform throughout the oceanic basins because of local variations in sedimentation rates, and the relative influence of tectonic and magmatic activity (which affects crustal permeability); these are relatively common and widespread (Alt, 1999).

Fluid convection in the ocean crust is driven by thermal energy derived from the lithosphere. Convective regimes are broadly classified as either 'active' or 'passive' systems (Lister, 1982), depending on the nature of the heat engine, the crustal location, and the extent of fluid circulation (both lateral and vertical) (Table 4.2 and Figure 4.5). Although this classification is relatively simplistic and does not account for complex variables in the oceanic hydrothermal system (e.g., active, high temperature fluid circulation around off-axis intrusions), it clearly differentiates the main convective regimes and their dominant processes.

Table 4.2: Comparison of 'active' and 'passive' hydrothermal circulation regimes in the ocean crust.

	'Active' convection regime	'Passive' convection regime
Oceanic location	Mainly restricted to the immediate **ridge axis** environment, i.e., within 1–5 km of the active spreading centre; but possibly localised around off-axis intrusions and hot-spots.	Widespread in all **off-axis areas**, including the ridge flanks and the stable abyssal plains of the oceanic basins.
Main sources of thermal energy	1. An **axial magma chamber** on fast-spreading ridges, with discrete dyke events providing local and transient heat sources; and 2. Prolonged **cooling and cracking** of deep plutonic rocks at slow-spreading ridges.	Steady-state thermal cooling and contraction of the oceanic lithosphere.
Temperature range	**High temperature** conditions (250°–400° C).	**Moderate to low temperature** conditions (< 100° C and mostly 5°–50° C).
Rate of fluid circulation	**Rapid and active** circulation of hydrothermal fluids commonly channelled in major structural conduits.	Hydrothermal fluid circulation is **slow, sluggish, and usually diffuse** (non-focussed) in both "open" and "closed" passive systems (Figure 4.5).
Depth of fluid penetration	1. At fast-spreading ridges the fluid penetration depth is limited by the underlying magma chamber, and probably reaches a **maximum of 1–2 km**; and 2. Deeper convective systems **(~ 3–4 km)** may penetrate the lower crust at slow-spreading ridges, because major crustal faults provide deep fluid pathways and there is no permanent magma chamber to disrupt flow patterns.	Maximum penetration depths of 1–2 km are theoretically possible, but most circulation occurs in the highly permeable upper-volcanic pile (**100–200 m below the seafloor**).
Total heat loss from the global oceanic lithosphere	Difficult to quantify, but estimated at ~ **8–20 %.**	Accounts for **most global heat loss** from oceanic lithosphere (~ 80–92 %).
Residence time in the convective regime	Situated only at the ridge axis, so most activity occurs in **< 1 million years.**	May persist for **10's of millions of years** until crustal permeability is sufficiently diminished (e.g., clogged or sealed by precipitation of secondary minerals), or until convective heat loss terminates at ~ 65 Ma.

Sources: Lister (1982), Alt (1999), and Staudigel (2004).

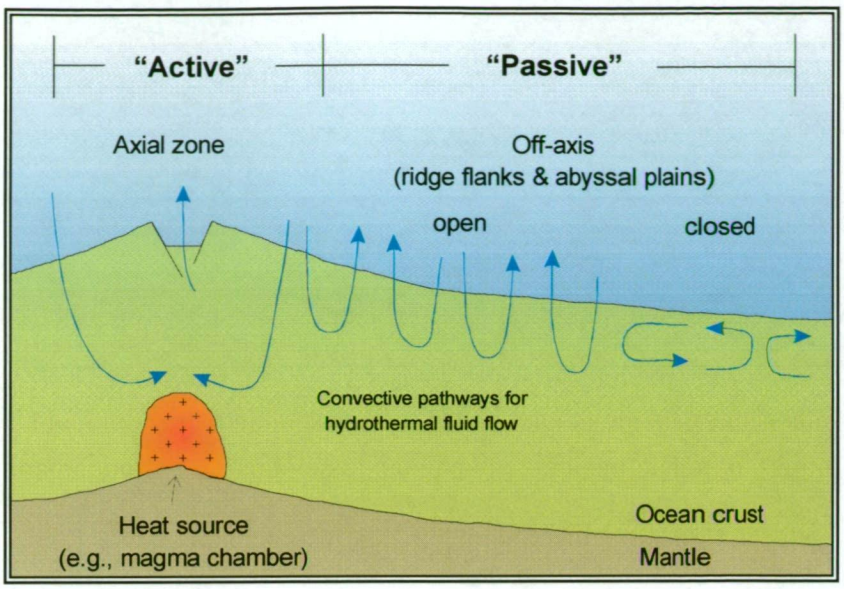

Figure 4.5: A schematic diagram distinguishing the 'active' and 'passive' convection regimes in the ocean crust. In this model, 'active' circulation is restricted to the axial ridge environment where vigorous, high temperature hydrothermal convection is driven by the proximal heat source. In contrast, the 'passive' regime involves relatively shallow fluid penetration and low temperature convection in the off-axis environment. The ocean crust is affected by passive fluid circulation for up to 65 million years; off-axis flow is also spatially extensive and probably account for > 80 % of total heat loss from the oceanic lithosphere (refer to Table 4.2) (modified after Alt, 1999).

Active and passive fluid convection is driven by three main heat sources, although the relative influence and extent of each source varies (Table 4.2) (Alt, 1995). The most important hydrothermal heat sources are:

i. **An axial magma chamber.** This is the main heat source for active (axial zone) hydrothermal systems, especially along ridges where steady-state magma chambers exist, e.g., fast-spreading segments. Heat is extracted across a narrow conductive boundary layer above the melt lens, and the high heat flux is capable of sustaining prolonged fluid circulation in the active regime (Lowell et al., 1995; Kelley et al., 2002) . Discrete dyke and eruptive events also produce relatively short-lived bursts of intense hydrothermal activity, with life-spans that vary from weeks to months (Butterfield et al., 1999; Seewald et al., 2002). These transient events have a dramatic effect on local (specific vent fields) circulation patterns and fluid compositions in the active hydrothermal regime (Haymon, 1996), e.g., as observed and recorded during submersible investigations along the 9°–10° N segment of the East Pacific Rise (Haymon et al., 1993);

ii. Prolonged thermal flux provided by **the cooling and solidification of hot crust and mantle rocks.** This is an important source of long-term heat for ridge segments that lack a steady-state axial magma chamber (i.e., slow-spreading ridges), and is also the main driver of passive, off-axis hydrothermal circulation (Alt, 1995). During periods of low magmatic flux in the axial environment, heat is extracted along a downward-penetrating 'cracking' front that cools the entire crust and provides a deep-seated energy

source for the hydrothermal system (Wilcock and Delaney, 1996). Tectonic extension, the main seafloor-spreading process at slow-spreading ridges, creates a complex and extensive network of highly permeable fractures in the crust; these allow fluids to circulate to greater depths with time, possibly penetrating to the upper mantle prior to the renewal of magmatic activity (Wilcock and Delaney, 1996); and

iii. **Non-magmatic heat derived from exothermic alteration reactions.** Recent seafloor investigations have shown that hydrothermal venting at some slow-spreading ridge segments lacks an obvious heat engine. The Lost City hydrothermal field is situated ~ 15 km west of the mid-Atlantic Ridge, and is hosted in seafloor exposures of serpentinised peridotite which have been tectonically exhumed (Blackman et al., 2002). Several workers have proposed that exothermic reactions during the alteration of ultramafic rocks* may provide sufficient heat flux to drive hydrothermal circulation, and thus account for the active, low temperature vents (~ 40°–75° C) at this site (Gracia et al., 1997; Baker et al., 2004). Many serpentinisation reactions are strongly exothermic (Lowell and Rona, 2002), and associated vent fluids are commonly enriched in dissolved gases predicted from such reactions, e.g., methane and hydrogen (Charlou et al., 1991). However, German and Parson (1998) indicated that considerable uncertainty exists regarding the efficiency and timing of serpentinisation reactions to support long-lived convection. Recent heat balance modelling has also shown that these reactions are unlikely to have a major impact on hydrothermal convection (Allen and Seyfried, 2004). Although these models experimentally confirmed the exothermic nature of many reactions, the total thermal output was insufficient to sustain prolonged hydrothermal circulation, e.g., a relatively short-lived 50° C temperature rise was produced at optimal fluid temperatures and fluid-rock ratios. However, Allen and Seyfried (2004) also noted that further research is required to fully assess the impact of alteration reactions as a potential hydrothermal heat source.

In addition to the main heat sources outlined above, localised and spatially restricted thermal activity may also drive limited volumes of fluid circulation in the oceanic crust, e.g., secondary crustal heating may result from insulated fluid discharge in focussed structural conduits (G.J. Davidson, 2005, pers. comm.). Geological evidence for these thermal processes is derived from sulfur isotope patterns identified in altered wall rocks surrounding some volcanic-hosted sulfide deposits, e.g., the Hellyer deposit in western Tasmania (Davidson, 2005). However, the relative extent and importance of this thermal mechanism remains speculative in modern seafloor environments (especially at mid-ocean ridges), and further research (beyond the scope of this project) is required to assess its efficiency and influence relative to the main heat sources.

---

* Examples of exothermic reactions in ultramafic rocks (after Allen and Seyfried, 2004) include:

2forsterite + $3H_2O$ = serpentine + brucite

3fayalite + $2H_2O$ = 2magnetite + $3SiO_{2\,(aq)}$ + $2H_{2\,(aq)}$

The conceptual hydrothermal model

The active hydrothermal regime is a complex and dynamic system that consists of five main components (Figure 4.6) (Honnorez, 2003). These are:

i. **A heat source** (which, as discussed in the previous section, provides the energy required to initiate and sustain hydrothermal flow);

ii. **The oceanic crust.** Crustal permeability is an important variable that influences many hydrothermal parameters, such as the geometry and rate of fluid flow, and the extent of water–rock interaction (and thus also affects alteration reactions and the formation of secondary mineral assemblages) (Fisher, 1998). Permeability is relatively high in the volcanic rocks of the upper crust (e.g., 10–100 mD*), but decreases rapidly with depth into the lower extrusive and sheeted dyke sections (e.g., < 0.1–0.5 mD) (Honnorez, 2003). Thus, most fluid circulation is restricted to the upper 100–200 m of the ocean crust, except where highly permeable faults cut across the igneous pile and provide a pathway for deep and focussed fluid flow (Alt, 1999). The ocean crust also plays a critical role as the hydrothermal fluid reservoir, providing a sufficient source of water to permit sustained convective cooling (essentially an unlimited fluid supply according to Honnorez, 2003);

iii. **The seawater recharge zone.** Cold (< 2° C), oxygen-rich seawater percolates downwards into the permeable upper crust (mainly due to gravity) and continually replenishes the oceanic (crustal) reservoir. Seawater recharge mainly occurs off-axis (the passive regime), especially in areas of relatively young crust (high permeability) that have not been sealed by sediment cover, e.g., bare ridge flanks or exposed seamounts (Alt and Teagle, 2000). Seawater temperatures progressively increase as fluids descend into the crust, undergoing various hydrothermal reactions that modify both fluid and rock compositions. The main crustal alteration processes during hydrothermal recharge are low temperature chemical reactions that include oxidation, fixation of alkalis and Mg, and precipitation of anhydrite (Figure 4.7) (Alt, 1999);

* Permeability measured in millidarcys (mD).

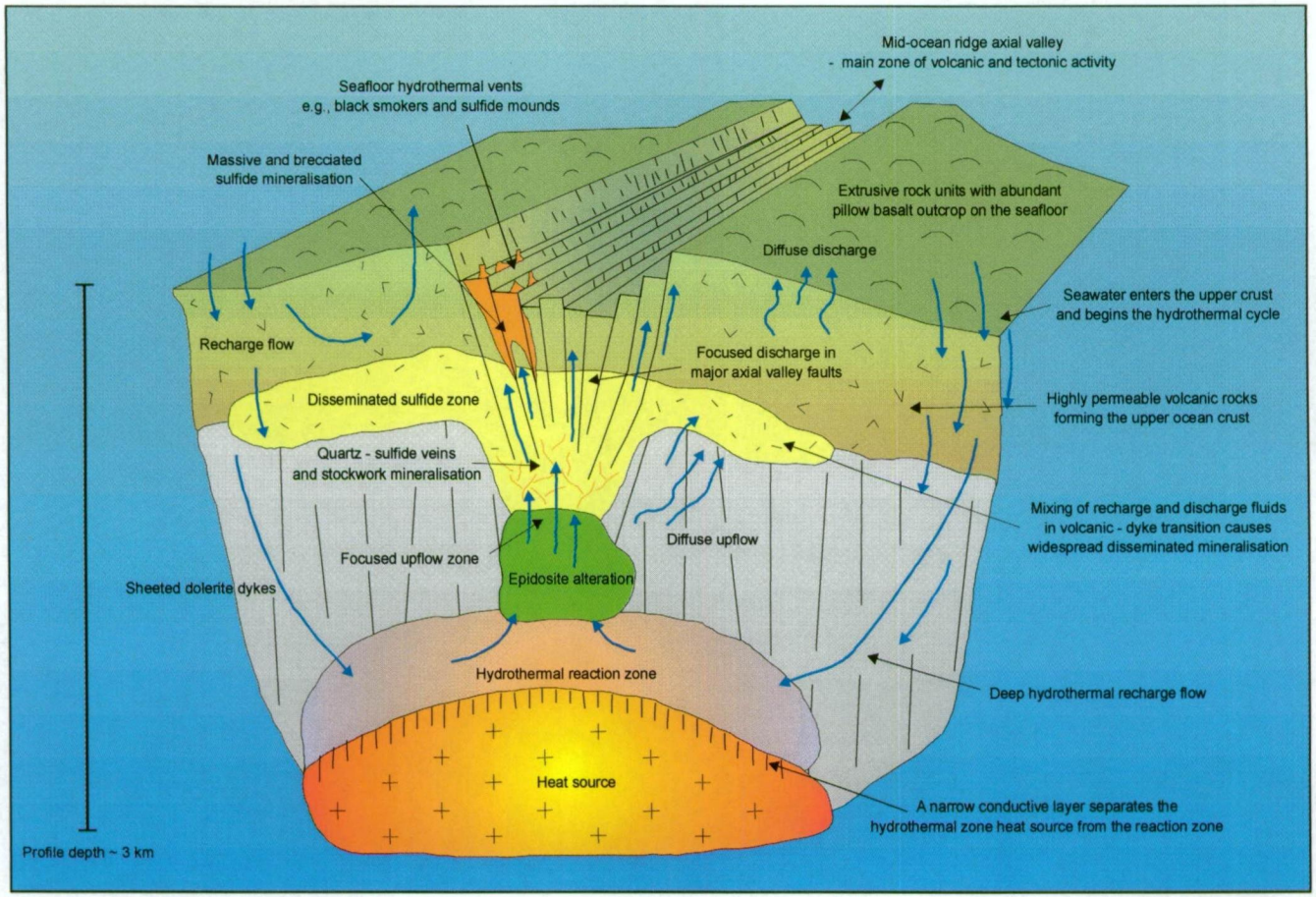

Figure 4.6: Schematic representation of subseafloor hydrothermal fluid circulation at an intermediate- to fast-spreading mid-ocean ridge. The hydrothermal system is driven by the axial magma chamber, and seawater initially enters the crust in the widespread ridge-flank recharge zones. Deep hydrothermal flow is hindered by low permeability of the sheeted dyke complex, although some recharge fluids eventually reach the reaction zone. Near-critical reaction zone conditions result in rapid fluid discharge, with turbulent upflow focussed in deep-seated structural conduits. This diagram also illustrates the main crustal alteration zones formed during hydrothermal upflow; these include deep epidosites above the hydrothermal reaction zone, and quartz-sulfide vein networks near the dyke-basalt transition. Discharge fluids that vent at the seafloor may form black smoker chimneys or sulfide-rich mounds, and these are commonly underlain by extensive stockworks and breccia zones (modified after Alt, 1999; Honnorez, 2003).

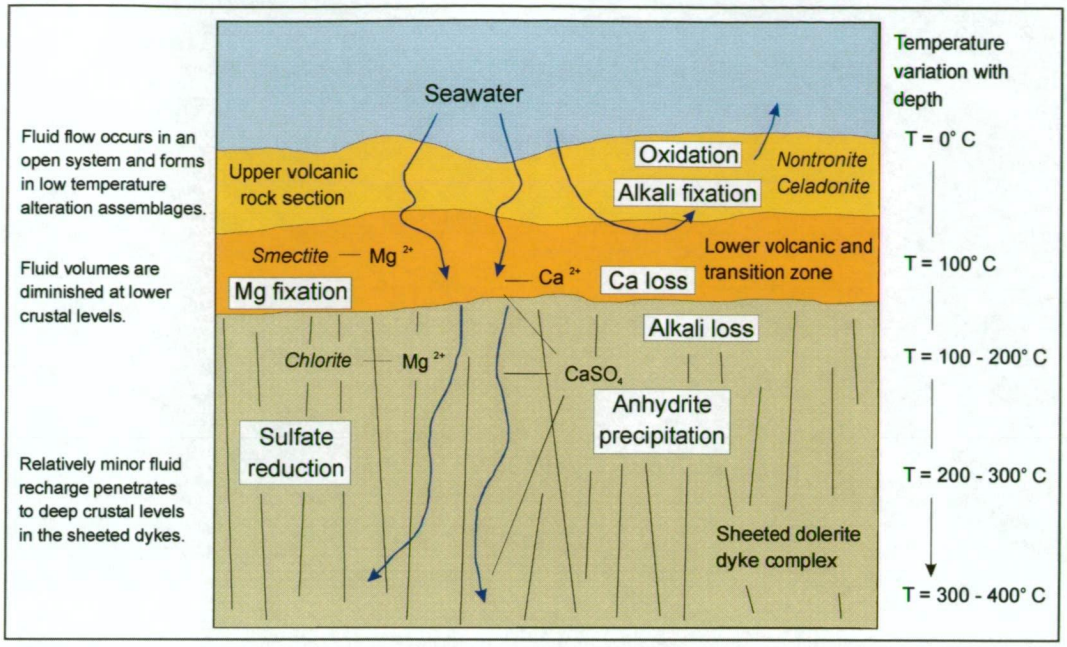

Figure 4.7: Schematic diagram showing the main fluid-rock interactions (alteration processes) and flow paths during hydrothermal recharge (seawater-sourced) in the upper crust. Water-rock ratios progressively diminish with depth, and most fluid circulation is restricted to the upper-most crust (< 200 m) where permeable volcanic rocks are abundant. The main secondary minerals formed at different crustal depths during recharge reactions are shown in italics (modified after Alt, 1995).

iv. **The deep crust reaction zone.** The base of oceanic hydrothermal convection is a zone of steep temperature and pressure gradients situated above the main heat source, e.g., the melt lens below a fast-spreading ridge axis (Figure 4.6). This occurs in the 'active' (on-axis) regime, and mainly corresponds to the lithologic transition zone between the lower sheeted dykes and upper gabbros (Nehlig, 1993). High temperature reactions dramatically affect fluids in the reaction zone, resulting in distinctive changes to their chemical composition and physical properties. Many researchers have suggested that the composition of venting seafloor fluids is 'fixed' in the reaction zone under these extreme conditions (Sleep, 1991; Nehlig, 1993). Based on the wide range of dissolved chlorine and aqueous metal concentrations in vent fluids (see review in German and Von Damm, 2004), the physical conditions of the reaction zone are estimated to approach the critical point for seawater, i.e., ~ 375°–420° C and 0.3–0.5 kb (Saccocia et al., 1994). Highly efficient hydrothermal reactions leach metals and sulfur from the wall rocks, and also cause significant recrystallisation and oxygen isotope ($\delta^{18}O$) depletion (Alt, 1995). Upper greenschist and amphibolite facies mineral assemblages are commonly formed in this environment, and consist mainly of secondary amphiboles (e.g., actinolite and Mg-hornblende), anorthite, and talc (Honnorez, 2003); and

v. **The zone of hydrothermal fluid discharge.** The near-critical temperature and pressure in the reaction zone drastically alters many hydrothermal fluid parameters (German and Von Damm, 2004). Significant decreases in fluid density and viscosity combined with increasing thermal expansion and heating capacity coefficients, cause

rapid adiabatic upflow. Theoretical flow rates are estimated at 0.5–5 m/s (Alt, 1995), and these interpretations are supported by limited geological evidence, e.g., Delaney et al. (1987) suggested fluid velocities of ~ 1 m/s based on the occurrence of partly rounded rock fragments in a hydrothermal breccia from the Kane Fracture Zone on the mid-Atlantic Ridge. Discharge fluids are significantly hotter and more chemically evolved than pristine seawater; most are strongly reduced, moderately to highly acidic (pH < 4), enriched in H_2S and dissolved metals (e.g., Fe, Mn, and Cu), and significantly depleted in Mg and SO_4 ,e.g., Tivey et al., 1995; James and Elderfield, 1996.

There are two distinct styles of hydrothermal discharge, with significant variations in crustal permeability and fluid conduit architecture (Figure 4.8) (Harper, 1999).

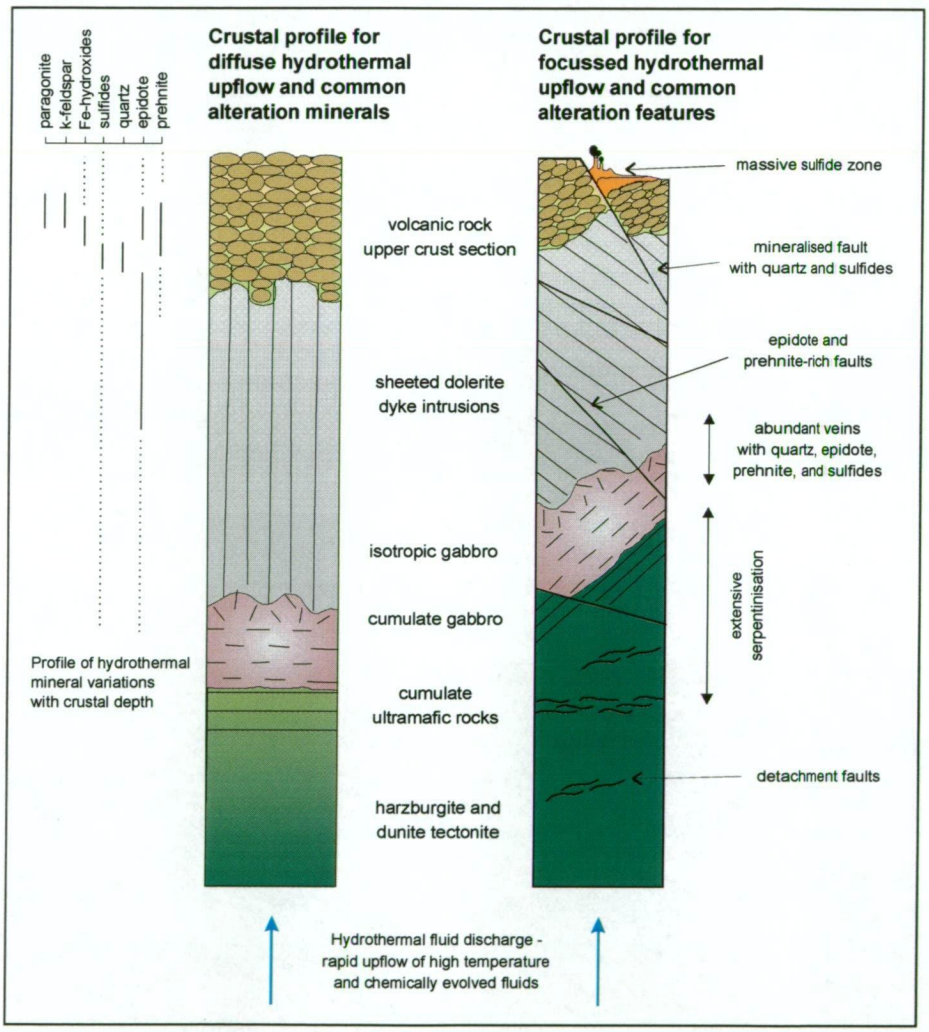

Figure 4.8: Comparison of secondary mineral assemblages associated with different styles of discharge alteration. Diffuse hydrothermal upflow (regional scale) results in a vertical crustal zonation with various secondary minerals at different depths (left of view). Most assemblages formed by diffuse flow are heterogeneously distributed (patchy and sporadic) in outcrop. Epidote-rich assemblages (local epidosites) occur at deeper crustal levels, and disseminated quartz-sulfide alteration is common in the sheeted dyke to volcanic rock transition zone. In contrast, focussed upflow is channelled in permeable crustal fault and fracture networks, and water–rock ratios in these conduits are considerably higher than for most diffuse systems. The characteristic alteration assemblages are intimately associated with their host structures (right-hand profile). Hydrothermal fluids penetrate to deeper crustal levels, and may cause serpentinisation of lower crust and upper mantle ultramafic rocks (modified after Harper, 1999).

'Focussed' upflow occurs when high temperature fluids are channelled from the reaction zone to the seafloor in relatively narrow structural conduits (Hannington et al., 1995). Active seafloor vents, e.g., black and white smoker chimneys (dominated respectively by pyrite + Cu-Pb-Zn sulfides and barite-silica mineral assemblages), and volcanic-hosted massive sulfide deposits, are the most obvious and spectacular manifestations. Focussed discharge occurs at high water–rock ratios, and the permeable fault and fracture conduits commonly extend to deep crustal levels (> 1 km vertical extent). In contrast, 'diffuse' discharge occurs when upflow fluids are poorly channelled and fail to rapidly vent on the seafloor (Harper, 1999). This process results in low temperature seafloor vent systems (5°–50° C) and causes widespread subseafloor mineralisation, e.g., disseminated sulfides in the sheeted dyke to extrusive rock transition zone (Figure 4.10).

Prolonged fluid–rock interaction in focussed upflow conduits forms very distinctive secondary mineral assemblages in the ocean crust. These are mainly precipitated from solution when ascending hydrothermal fluids are conductively cooled (wall rock conduction) or mixed with relatively unevolved seawater (entrained into shallow crustal levels). Extensive stockwork systems, hydrothermal breccias, and pervasively altered wall rocks (volcanic and sheeted dyke units) commonly underlie seafloor vent fields and mineralised zones. The most highly altered wall rocks are centred about the main structural conduit. Concentric, pipe-like alteration haloes, with laterally and vertically zoned secondary mineral assemblages, also surround the upflow structures. Focussed hydrothermal discharge systems and related alteration zones have been documented from modern seafloor settings, such as the Trans-Atlantic Geotraverse (TAG) mound on the mid-Atlantic Ridge (Humphris and Tivey, 2000), and the Galapagos Fossil Hydrothermal Field (Galapagos Rift) (Ridley et al., 1994). Geological evidence of highly altered upflow zones has also been documented below (stratigraphically) many ophiolite-hosted sulfide deposits, e.g., the Turner-Albright deposit in the Josephine ophiolite (Zierenberg et al., 1988), and the volcanic-hosted Ivanovka deposit in the southern Ural Mountains (Nimis et al., 2004).

The secondary mineral assemblages associated with focussed discharge conduits directly reflect the chemical composition of their parent hydrothermal fluid, and the main alteration processes and chemical reactions. In the deeper upflow zone high temperature reactions, estimated at 350–440° C (Alt and Bach, 2003), remove calcium from solution, enhance metal solubility, and result in the widespread precipitation of epidote. Geochemical constraints and experimental models have shown that extensive quartz precipitation occurs as rising hydrothermal fluids are conductively cooled (from ~ 400° to 250° C and pressures of 0.5 to 0.25 kb) in the subseafloor environment (Seyfried et al., 1999). The geological evidence for these reactions is observed in the lower sheeted dyke complexes of some ophiolites, such as the Troodos ophiolite in Cyprus (Richardson et al., 1987; Bettison-Varga et al., 1995). Extensive epidosite* domains (> 100 m wide) are interpreted as deep-level hydrothermal discharge zones (Figure 4.6) (Alt, 1995). Smaller

* Epidosites are highly altered, coarse-grained rocks with a distinctive granoblastic texture. They contain abundant epidote, quartz and titanite, and are highly depleted in metallic elements such as Mg, Na, Zn, and Cu (Harper et al., 1988).

areas of patchy epidosite alteration, interpreted as evidence for diffuse upflow, have also been documented from some ophiolites, including the Josephine ophiolite (Alexander et al., 1993), and the Samail ophiolite in Oman (Nehlig and Juteau, 1988).

Focussed discharge pathways at higher crustal levels (extrusive rock package) are also sites of intense hydrothermal alteration. Pervasive recrystallisation of the basaltic wall rocks is common, although alteration intensity and spatial distribution are considerably heterogeneous. Quartz-rich stockworks and hydrothermal breccias are abundant, and widespread chlorite, pyrite, and epidote are diagnostic components of the paragenesis (Figure 4.6 and 4.9). The secondary mineral assemblages and hydrothermal textures imply elevated water–rock ratios and prolonged interaction of high temperature, chemically evolved fluids (and a minor component of entrained seawater) with the host rocks. Multiple hydrothermal events are probably common for long-lived systems such as the TAG mound (episodically active for ~ 140 thousand years), and may result in a complex sequence of vein-forming stages, on-going precipitation and dissolution reactions, and cross cutting alteration phases (Humphris and Tivey, 2000).

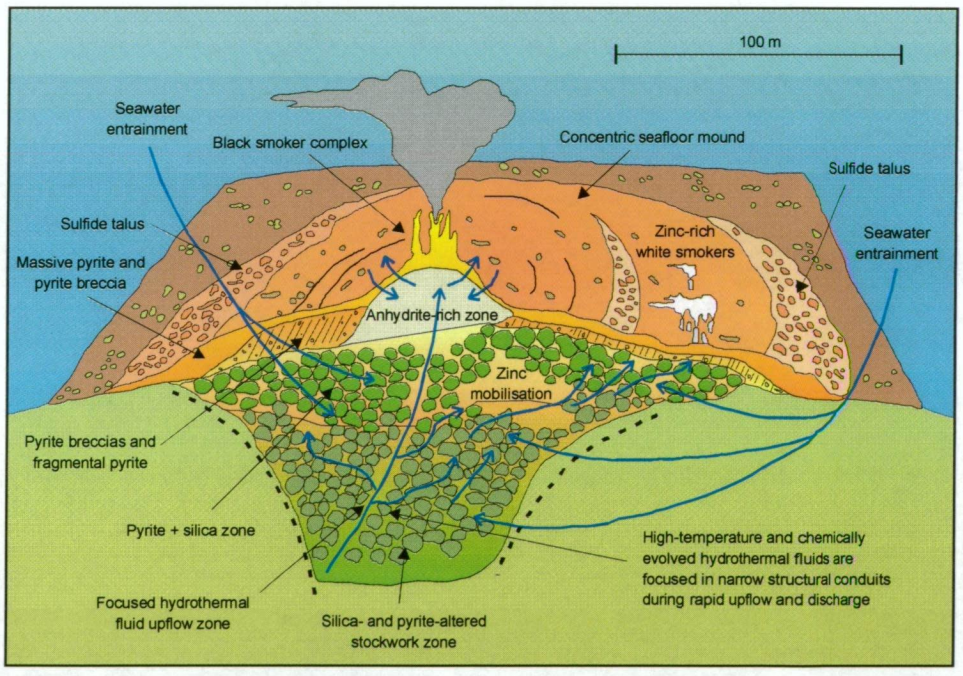

Figure 4.9: The long-lived Trans-Atlantic Geotraverse (TAG) mound is situated near the mid-Atlantic Ridge at 26°08' N, 44°49' W. Subseafloor fluid flow is strongly channelled in a major, deep-seated fault system, and multiple episodes of hydrothermal activity have formed a relatively narrow, pipelike alteration zone underlying the mound. The secondary mineral assemblages in the alteration pipe are zoned both vertically and laterally; the most intensely altered rocks are intimately associated with highly permeable (structural) conduits. Large volumes of cold, oxygenated seawater are entrained into the upper levels of the TAG mound, vigorously mixing with the chemically evolved and high temperature hydrothermal (upflow) fluids. Fluid mixing is an important process that initiates precipitation of many hydrothermally derived minerals (modified after Humphris and Tivey, 2000).

The conceptual model of the seafloor hydrothermal system (outlined above) provides a key framework to evaluate and interpret the alteration products that form during seawater–rock interaction. Multiple parameters vary considerably between the major components of the

hydrothermal system (e.g., hydrothermal flow rates and pathways, and fluid residence times), and these significantly impact upon the characteristic alteration assemblages. However, it is also critical to realise that the conceptual boundaries which demarcate the recharge, reaction, and discharge zones are not always clearly defined in oceanic rocks. In reality, the different components of the hydrothermal system may form a complex and dynamic continuum, whereby the definition of each zone is arbitrarily theoretical.

Along-axis variations in hydrothermal activity

In addition to the above caveat, the basic conceptual model for oceanic hydrothermal systems overly simplifies the pattern of axial flow, as it fails to consider along-strike variations (ridge-parallel) in the fluid circulation regime (Figure 4.10). Many oceanographic studies have shown that the spatial and temporal distribution of hydrothermal activity, and its relative intensity and volume, varies dramatically along different ridge segments. German and Parson (1998) investigated axis-parallel variations along three segments of the mid-Atlantic Ridge, and showed significant differences in the distribution and vigour of hydrothermal activity between each site. The most active hydrothermal vent fields were spatially associated with central ridge segments (magmatically robust), and with broad, segment-end discontinuities, e.g., non-transform offsets. Their study also showed that, on a regional-scale, there is an almost positive linear relationship between the abundance of vents and the rate of spreading, although this correlation is not consistent at the (smaller) scale of discrete sites (German and Parson, 1998). Fine-scale (3rd– and 4th–order) segmentation of hydrothermal systems (along-strike) has also been noted from the East Pacific Rise, with the predominance of focussed magmatic heat sources in central ridge segments interpreted as the main cause of localised fluid upflow zones (Haymon, 1996; Haymon and White, 2004). Further evidence of axis-parallel variations in hydrothermal activity has also been provided by geophysical data (ship-borne magnetics survey) collected along the Endeavour segment of the Juan de Fuca Ridge. Tivey and Johnson (2002) documented multiple magnetic anomalies along the ridge axis, and interpreted these data as evidence for systematically spaced zones (~ 200 m apart) of hydrothermal upflow and associated wall rock alteration.

The studies outlined above have provided evidence that the spatial distribution and flux capacity of oceanic hydrothermal systems (along-axis) are strongly influenced by the location, volume, and timing of magmatic activity (Haymon, 1996) (Figure 4.10). These fundamental controls are especially critical for magmatically robust ridges (i.e., fast-spreading), where the near steady-state magma lens and frequent dyke injections provide a consistent source of thermal energy to focus hydrothermal patterns. In contrast, vigorous hydrothermal activity along many slow-spreading ridges (where magmatic activity is mostly sporadic) is commonly associated with major structural discontinuities, e.g., non-transform offsets (German and Parson, 1998).

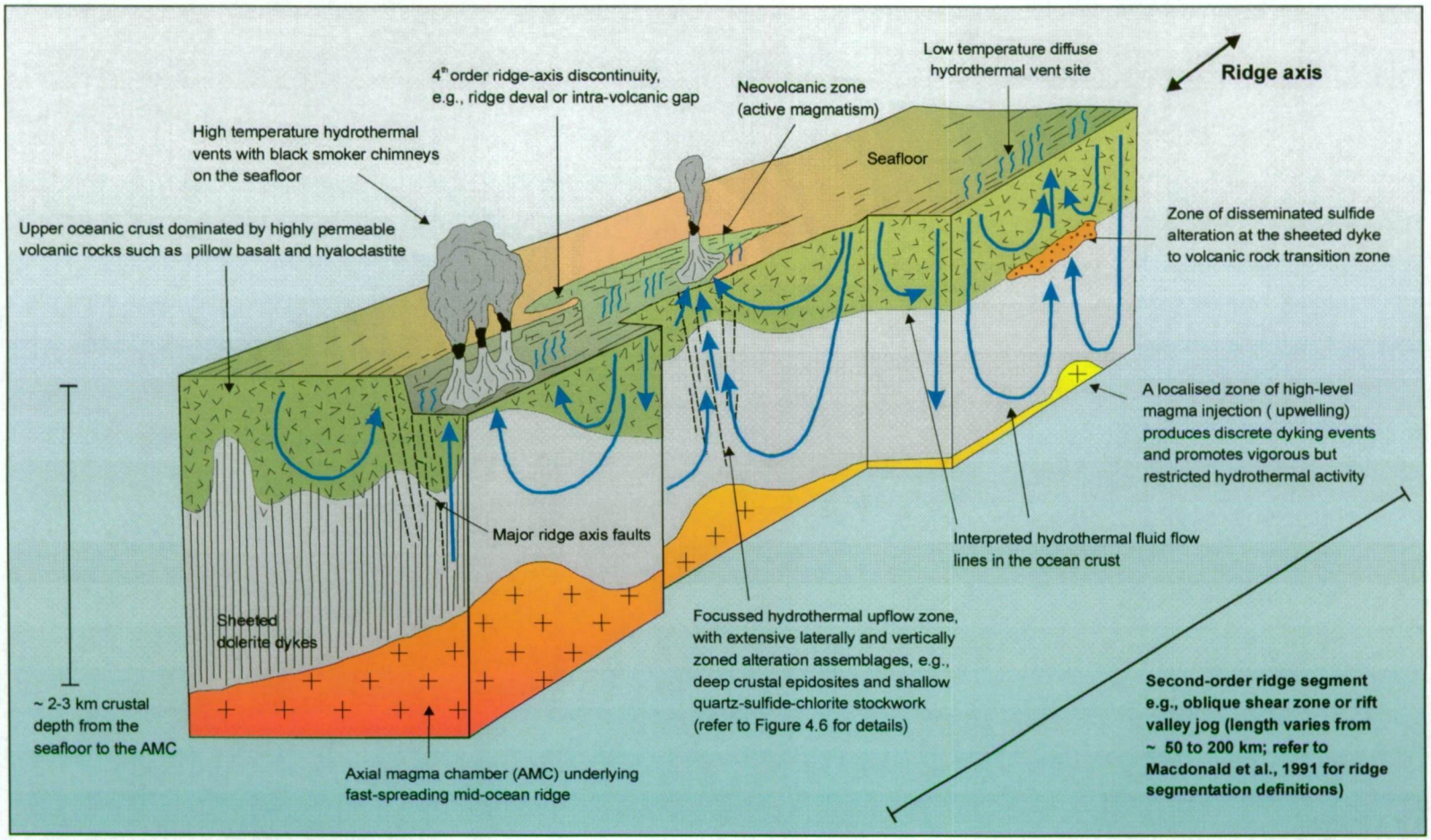

Figure 4.10: Schematic (cut-away) diagram illustrating three-dimensional variations in the pattern of hydrothermal fluid flow at a mid-ocean ridge. The second-order ridge segment shown here is underlain by a high-level magma chamber (typical of a magmatically robust fast-spreading ridge) that provides sufficient heat to promote vigorous hydrothermal circulation. This model integrates ridge-normal and ridge-parallel fluid flow patterns, and specifically emphasises the strong relationship between sites of fluid upflow and high-level heat sources, e.g., upwelling magma injections. A significant component of hydrothermal circulation occurs parallel to the ridge axis, with upflow fluids (both focussed and diffuse flow) sourced from deep within the crust. Most hydrothermal circulation is restricted to the highly permeable volcanic rocks in the upper crust; fluid flow is also preferentially channelled in structural conduits at these levels and forms focussed alteration assemblages that underlie many seafloor vent fields (diagram modified after Haymon, 1996).

Many of the highly fractured structural breaks along slow-spreading ridges are rooted deep within the crust and upper mantle, and provide access to relatively long-lived heat sources (e.g., cooling plutonic rocks) capable of sustaining hydrothermal activity in the absence of consistent ridge magmatism. Further discussion of the influence of spreading rate on oceanic hydrothermal activity is provided in the next section of Chapter 4.4.

In summary, numerous investigations of mid-ocean ridges have clearly shown significant ridge-parallel variations in the distribution and intensity of oceanic hydrothermal activity. These variations reflect regional- and local-scale segmentation of hydrothermal systems along the spreading ridge, and are directly related to the (ridge-axis) segmentation of magmatic and structural activity. Recognition of segmented hydrothermal activity on mid-ocean ridges provides strong evidence that hydrothermal circulation patterns in the ocean crust vary both along- and across the ridge axis. Thus, it is critical for the basic conceptual model of oceanic hydrothermal circulation to emphasise the multi-dimensionality of subseafloor flow patterns at spreading ridges, and also consider the effects of segmentation on the distribution and abundance of associated zones of hydrothermally altered rocks.

Influence of spreading rate on hydrothermal activity

Active hydrothermal circulation at mid-ocean ridges is closely linked to the magmatic and tectonic processes that control seafloor spreading. Significant differences in the nature of their dominant spreading mechanisms causes many hydrothermal processes and products to vary relative to spreading rate (Table 4.3) (Wilcock and Delaney, 1996). Consistent variations in the physical distribution and spatial extent of hydrothermal circulation patterns, and in the location of active vent sites (both along- and across-strike), have been documented for the slow-spreading mid-Atlantic Ridge and many of the intermediate- to fast-spreading ridges in the Pacific basin, e.g., the East Pacific Rise and the Costa Rica Rift (Haymon, 1996; German and Parson, 1998; Haymon and White, 2004). The timing and duration of hydrothermal heat fluxes also varies in space and time between fast- and slow-spreading ridges (Figure 4.11). In addition, there are significant differences in the morphology and structure of seafloor vent deposits, e.g., slow-spreading ridges host relatively large and long-lived (mound-like) deposits compared to those on fast-spreading ridges (which are commonly spindly chimneys) (Table 4.3) (Nehlig, 1993; Wilcock and Delaney, 1996). Hydrothermal fluid compositions and incipient alteration assemblages (especially in the deeper segments of the crust) are also influenced by spreading rate, although these parameters are relatively more difficult to quantify and assess (Gillis, 1995; Humphris and Tivey, 2000; Gillis et al., 2001).

Table 4.3: Discussion and analysis of the influence of mid-ocean ridge spreading rates on critical components and features associated with subseafloor hydrothermal systems.

	Slow-spreading ridges (< 30 mm per year)	Fast-spreading ridges (> 60 mm per year)
How does the dominant extensional process affect the hydrothermal system?	Prolonged periods of tectonic extension are episodically punctuated by relatively short magmatic events. Waxing and waning cycles of magmatic and tectonic activity promote greater variability in the vigour and efficiency of the hydrothermal system than at fast-spreading ridges (Figure 4.11). The location, size, and structure of vent sites are also strongly influenced by cyclic variations in the dominant spreading mechanism.	A stable axial magma chambers supports robust magmatic activity and continual accretion of new ocean crust. The high magma budget also plays a vital role in initiating and sustaining hydrothermal systems, with on-going intrusive events generating many small and relatively short-lived hydrothermal systems (Figure 4.11) (Haymon, 1996).
What is the size and spacing of hydrothermal systems along a spreading segment?	Hydrothermal systems are generally larger and have a wider spatial distribution at slow-spreading ridges (German and Von Damm, 2004). During episodic magmatic events hydrothermal circulation patterns are similar to those at fast-spreading ridges, i.e., commonly focussed in magma-rich areas and formed in response to discrete intrusive events. However, extensive hydrothermal systems also form at magma-poor ridge segments, especially proximal to major crustal structures, e.g., non-transform offsets and oblique shear zones. These provide an effective pathway to long-lasting thermal energy, such as the prolonged cooling and contraction of deep plutonic rocks (German and Parson, 1998).	Hydrothermal activity is strongly focussed at magma-rich ridge segments, e.g., central portions of 3rd order ridge segments (Haymon and White, 2004), and is commonly absent from magma-poor areas, such as ridge segment margins. Hydrothermal activity is also relatively widely spaced, and large vent fields are rare because of small and localised hydrothermal heat fluxes (Figure 4.11).
What is the duration and relative timing of hydrothermal activity?	Hydrothermal systems may exist for relatively long periods of time (Figure 4.11), because deep crustal faults provide direct pathways to a prolonged source of thermal energy, e.g., the TAG sulfide mound on the mid-Atlantic ridge has been episodically forming for ~ 140 thousand years (Humphris and Tivey, 2000). However, hydrothermal events are relatively infrequent along spreading segments that lack access to a deep-seated heat source, because of the ephemeral magma supply.	The high number of discrete dyke and eruptive events generates many small-scale and localised hydrothermal cells, especially along magma-rich ridge segments. Most hydrothermal activity is relatively vigorous but short-lived, as the heat generated during each intrusive event rapidly diminishes, e.g., some fast-spreading hydrothermal systems persist for only ~ 1–10 years (German and Von Damm, 2004).
To what depth do hydrothermal fluids penetrate into the oceanic crust?	Large-scale hydrothermal systems may penetrate to the plutonic level of the oceanic crust (~ 3–4 km below the seafloor) because extensive tectonic activity generates multiple, long-lived (and commonly deep-seated) fluid pathways (German et al., 1996). The absence of a steady-state magma chamber also permits deeper fluid penetration and circulation than at fast-spreading ridges.	Fluid flow occurs along a relatively uniform network of crustal micro-fractures that are mainly restricted to the most permeable rocks in the upper crust. Deeper fluid penetration is highly focussed in fractures and faults, which are less abundant than at slow-spreading ridges. The maximum depth of fluid penetration is ultimately restricted by the crustal depth of the steady-state magma chamber, and rarely exceeds 1–2 km (Gillis, 1995).
What is the typical morphology and structure of seafloor hydrothermal vents?	Large seafloor exhalative mounds commonly form on slow-spreading ridges (e.g., the TAG sulfide mound) due to long-lived hydrothermal systems sustained by prolonged crustal heat extraction. Large seafloor deposits are also favoured by infrequent and low volume eruptions (i.e., vent sites are not smothered by lava), and by the maintenance of high crustal permeability (i.e., abundant tectonic activity ensures that fluid pathways are not permanently sealed following mineral precipitation).	Discrete, spindly chimneys (some up to 10 m-high) are common. Larger vent deposits rarely occur because abundant volcanism and transient hydrothermal activity are not conducive to their formation (Gillis et al., 2001).
What rock types commonly host hydrothermal cells and active vent sites?	A diverse range of host rocks are possible, because rock units from many crustal levels are commonly exposed at or near the seafloor in 'tectonic windows', e.g., the Rainbow and Lost City hydrothermal fields on the mid-Atlantic Ridge are hosted in serpentinised ultramafic rocks (Gracia et al., 2000; Kelley et al., 2001). Host rock variations may directly influence the hydrothermal fluid composition.	Most hydrothermal vent fields are hosted in young sheet flow basalts in the neovolcanic zone, as the constant magmatic activity promotes vigorous hydrothermal circulation (Hey et al., 2004).
How does the chemical composition of the hydrothermal fluids vary along the ridge?	Vent fluid compositions along individual ridge segments are generally more uniform than at fast-spreading ridges, reflecting the influence of a stable and deep-seated fluid source. Longer-lived, slow-spreading hydrothermal systems also entrain greater volumes of seawater, which mixes and dilutes evolved hydrothermal fluids. Seawater dilution may generate relatively oxidised fluids that have lower concentrations of potassium (relative to sodium) and boron (German and Von Damm, 2004).	A diverse range of fluid compositions may exist in a relatively small vent field area on a particular spreading segment, e.g., hydrothermal vents spaced ~ 10–100 m apart have significantly different fluid compositions on several fast-spreading ridge segments. This reflects the highly localised and relatively shallow fluid source region (German and Von Damm, 2004).

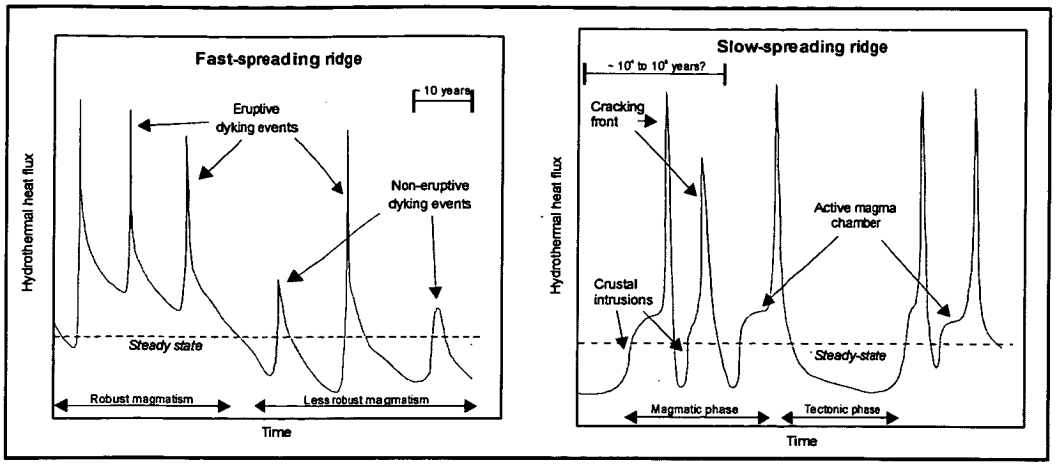

Figure 4.11: The hydrothermal heat flux at a mid-ocean ridge is interpreted to vary in space and time relative to the spreading rate. High heat fluxes at fast-spreading ridges are associated with discrete dyking events, producing vigorous but relatively short-lived hydrothermal cells that rapidly decay over weeks and months. Dyking events are common during periods of robust magmatism, but hydrothermal fluxes diminish during less intense magmatic accretion. Discrete hydrothermal systems at slow-spreading ridges exist for longer temporal periods. Prolonged heat spikes occur when magmatic activity wanes and tectonic extension generates deep-seated crustal permeability. Access to the deep lithosphere supports long-lived fluid convection, until crustal permeability is diminished and the deep thermal energy source is sealed, e.g., by the precipitation of secondary minerals. Subsequent episodic magmatism may renew the heat flux, and ephemeral dyke events produce small-scale fluxes (modified after Wilcock and Delaney, 1996).

Previous research into focussed hydrothermal discharge systems

The discharge phase of seafloor hydrothermal systems has a dramatic impact on the composition of the ocean crust (Staudigel, 2004). However, despite the presence of highly distinctive mineral assemblages and substantial sulfide-rich deposits (as previously outlined), subseafloor alteration zones (formed during focussed fluid discharge) have not been widely studied at modern ridges*. This partly reflects the inherent technical and logistical difficulties involved in seafloor exploration, and the reliance on observations and sample collections obtained from ocean drilling, dredge-hauls, and submersibles. In addition, the restricted distribution of focussed upflow conduits, and the relative inaccessibility of their subseafloor root zones, has ensured that many geological features remain poorly understood, e.g., the detailed spatial distribution of mineral and textural features, and the geochemical variations within discrete zones and between proximal structures.

Although many impediments hamper the *in situ* study of seafloor alteration assemblages, several important and well integrated projects have successfully investigated active and fossil hydrothermal systems. These have examined seafloor vent deposits (e.g., the TAG mound), fault scarp and mound-like exposures of underlying stockworks, and highly altered rock fragments collected during mid-ocean ridge dredge-hauls (Table 4.4). Most previous work has focussed on describing the mineral assemblages and textures, and collecting geochemical data, e.g., mineral, whole-rock, and isotope analyses. Data collected during laboratory studies have assisted in the

* Although subseafloor alteration zones have not received extensive study, many aspects of seafloor hydrothermal vent systems (e.g., their composition, structure, and associated biological communities) have been relatively well investigated.

interpretation of hydrothermal conditions (e.g., water-rock interactions) and the formational processes associated with the mineral assemblages. The study results and interpretations from the major investigations shown in Table 4.4 are further referenced and compared to the Macquarie Island hydrothermal system in Chapter 9.

Scientific understanding of hydrothermal upflow zones has also been complemented by a number of studies in ophiolite terranes (Table 4.5). These (potential) terrestrial analogues of ocean crust provide relatively accessible exposures and allow for the detailed observation of many geological and hydrothermal features. Research conducted in ophiolite settings remains one of the best ways to understand the spatial distribution and structural architecture of alteration assemblages and fracture conduits (German and Von Damm, 2004). Previous detailed mapping and sampling work has provided observations and insights that are currently beyond the scope of submersible or ocean drilling programs. However, several important caveats apply to ophiolite studies. Although the structure and composition of ophiolites implicates some style of seafloor spreading, most have igneous rock compositions (geochemical signatures) that imply back-arc or fore-arc settings, i.e., not formed at a mid-ocean ridge environment. In addition, the structural framework and alteration characteristics of most ophiolites are further complicated by emplacement-related tectonism and metamorphism, which commonly disrupts and overprints spreading-related features. Consequently, continuing research which integrates *in situ* ocean crust and ophiolite studies is required to further increase our knowledge of focussed hydrothermal upflow zones, and their impact on the composition and structure of the ocean crust.

4.5. Scientific impact of my research project

Benefits

An important outcome of this literature review was recognising existing knowledge gaps related to focussed hydrothermal systems. My work addresses some of these issues by providing new geological data and insights from Macquarie Island; a unique terrestrial exposure of oceanic crust. The most significant benefits arising from this project included:

i. The opportunity for detailed geological fieldwork at different stratigraphic levels of the ocean crust. Of particular importance was the opportunity for mapping the size, geometry, and spatial distribution of subseafloor alteration systems, and observing their *in situ* paragenetic associations, hydrothermal textures, and structural compositions;

Table 4.4: An overview of previous alteration studies from focussed hydrothermal discharge zones at modern mid-ocean ridges.

Reference	Study location	Focus of study	Sampling technique	Main study methods	Important research conclusions
Delaney *et al.* (1987)	The **Kane Fracture Zone** on the slow-spreading mid-Atlantic Ridge (commonly referred to as the **MARK** area).	A detailed laboratory study of unusual quartz-cemented, 'greenstone' breccias (basaltic) recovered from major ridge axis faults.	Samples collected during dredge haul and submersible operations.	1. Detailed hand-specimen and thin-section observations of alteration minerals and textures; 2. Microprobe analyses of secondary chlorite and sulfide minerals; and 3. A fluid inclusion study of the quartz cement.	The assemblages formed during multiple stages of high salinity and high temperature hydrothermal fluid flow. The discharge fluids were focussed in major ocean fault conduits and attained high fluid velocities (0.5–1 m/s). The alteration reactions proceeded at elevated water-rock ratios, and mineral precipitation likely occurred during fluid mixing (with seawater) or conductive cooling.
Embley *et al.* (1988) and Ridley *et al.* (1994)	The **Galapagos Fossil Hydrothermal Field** on the fast-spreading Galapagos Rift.	An investigation of the upper-most stockwork underlying a relict vent field. The highly altered and mineralised zone is exposed at the seafloor by oceanic faulting and weathering. The collected samples were subjected to rigorous laboratory analyses.	Collection of *in situ* samples (with limited geological context) during submersible operations.	1. Hand-sample and thin-section petrography of altered rocks; 2. Microprobe analyses of secondary minerals (mainly chlorite); and 3. Whole-rock geochemistry (major and trace elements) and isotope (Sr and O) analyses.	The highly altered stockwork zone has many mineral, textural, and structural similarities with the upper parts of ophiolite-hosted massive sulfide deposits. The intensity and distribution of alteration is very heterogeneous and strongly correlated with macro- and micro-permeability. Multiple lines of evidence (e.g., the Fe–Mg ratio of chlorite and Sr isotope data) suggest variable amounts of mixing between hydrothermal fluids and entrained seawater.
Saccocia and Gillis (1995)	The **MARK** area (slow) and the **Hess Deep** on the fast-spreading East Pacific Rise.	An in-depth laboratory study of highly altered hydrothermal breccias. The main focus is the link between the alteration mineral compositions and the physico-chemical fluid parameters.	Hydrothermal breccia samples collected by dredge haul and submersible operations.	1. Detailed study of alteration petrography; 2. Microprobe analyses of chlorite and epidote; and 3. A fluid inclusion study of quartz cements.	The physical and tectonic setting of the recovered samples, combined with the distinctive mineral suite, implies these breccias formed in a focussed upflow zone. Variations in the alteration mineral assemblages and chemical compositions, and the fluid inclusion data, are used to define two breccia types (Type I and II). High temperature fluids with variable salinities and compositions (especially the relative abundances of H_2S, Fe, and Mg) are inferred from these data.
Zierenberg *et al.* (1995)	The **Gorda Ridge** (an intermediate-rate spreading rift south of the Juan de Fuca Ridge).	Outlines the discovery of an off-axis, diffuse hydrothermal vent field during a submersible research study, and complemented by laboratory analyses of the hydrothermal assemblages.	Submersible-based discovery and sample collection of silica-rich, hydrothermal assemblages in basaltic hyaloclastite.	1. Detailed hand-specimen and petrographic study; 2. XRD analyses of bulk mineralogy; 3. Microprobe analyses of secondary silica and layer-silicate minerals; and 4. Whole-rock geochemical (using ICP-ES) and isotope (Sr and O) analyses;	The diffuse hydrothermal field occurs in an unusual location, i.e., off-axis and 300 m above the rift valley floor. Focussed discharge sites are rare. Comparison of the alteration features with ophiolite-hosted massive sulfide deposits indicates many similarities, such as the structural setting, secondary mineralogy and chemistry, hydrothermal textures, and the depositional environment. The abundance of Mg-rich chlorite is interpreted as evidence of mixing between hydrothermal fluids and entrained seawater.
Humphris and Tivey (2000)	The **TAG sulfide mound** on the slow-spreading mid-Atlantic Ridge.	Provides a synthesis of results from investigations of one of the largest and best studied seafloor vent deposits. This includes a review of the alteration characteristics and a well-constrained model for the mound's formation.	A review of the geology and geochemistry of the TAG mound, using data from various submersible, dredge, and Ocean Drilling Program operations, e.g., ODP 158.	1. Describes the morphology and structure of the mound; 2. Provides details of the vent fluid chemistry; and 3. Describes the mineralogy, textures, and distribution of alteration minerals.	The TAG mound has a long (~ 140 thousand years) and complex evolutionary history and preserves evidence for active and relict hydrothermal activity. The multi-stage, episodic hydrothermal activity reflects variations in the dominance of magmatic and tectonic spreading processes. The mound is underlain by intensely altered and sulfide-veined basaltic wall rocks, and these form a ~ 90-m-wide, concentric alteration pipe. The hydrothermal assemblages are zoned both laterally and vertically in the upflow conduit (Figure 4.9)
Gillis *et al.* (2001)	The **Hess Deep** on the fast-spreading East Pacific Rise.	A submersible-based study along a 4-km-wide fault scarp segment. This study documented and sampled the alteration assemblages in the upper volcanic rock and sheeted dyke units, and also recognised a zone of fault-hosted mineralisation.	Seafloor observations and sample collection during submersible operations.	1. Detailed petrographic analyses of altered rock samples to document the mineralogy, paragenesis, textures, alteration intensity, and secondary mineral relationships; 2. Microprobe analyses of secondary minerals and application of chlorite geothermometry; and 3. Whole-rock geochemistry (major and trace elements) and O isotope analyses.	A zone of high temperature hydrothermal fluid flow was identified from a small, faulted outcrop area in the upper sheeted dykes. This zone hosts quartz-, chlorite-, and sulfide-altered rocks and is interpreted as a focussed discharge zone based on similar mineral assemblages from other seafloor localities. However, the alteration intensity is less pervasive, and calculated water-rock ratios are lower than other ocean crust and ophiolite examples. This may reflect relatively short episodes of hydrothermal activity due to the frequent volcanism at this fast-spreading ridge.
Teagle and Alt (2004)	The **Bent Hill deposit** on the intermediate- to fast-spreading Endeavour segment of the Juan de Fuca Ridge.	This study examines a sediment-hosted massive sulfide deposit, based mainly on samples collected during an extensive drilling campaign. The study focusses on the hydrothermal alteration characteristics of the igneous ocean crust that underlies the deposit.	Documents the results of two Ocean Drilling Program legs (ODP 856 and ODP 1035) at the 35 m-high Bent Hill Massive Sulfide (BHMS) Mound.	1. Detailed petrographic descriptions of fresh and altered rocks; 2. Microprobe analyses of chlorite; and 3. Whole-rock geochemistry and isotope (Sr and O) analyses.	The basaltic crust underlying the BHMS deposit is variably recrystallised, and contains abundant secondary quartz, chlorite, sulfides, and epidote. The alteration assemblages reflect large-scale hydrothermal upflow at elevated fluid temperatures (~ 320°–370° C). Alteration involved ~ 20 % mass loss, and was strongly channelled along discrete igneous-sediment contacts. The sediments are also highly altered and contain abundant hydrothermal quartz and chlorite.

Table 4.5: Important published studies of hydrothermal processes and products in ophiolite terranes.

Ophiolite location and age	References
The **Troodos** ophiolite in Cyprus (Cretaceous)	Richards et al. (1989) Gillis and Robinson (1990) Bickle and Teagle (1992) Gallahan and Duncan (1994) Bettison-Varga et al. (1995) Bickle et al. (1998)
The **Josephine** ophiolite in NW California and SW Oregon, USA (Jurassic)	Harper et al. (1988) Zierenberg et al. (1988) Alexander and Harper (1992) Alexander et al. (1993)
The **Samail** ophiolite in Oman (Cretaceous)	Haymon et al. (1989) Nehlig et al. (1994) Juteau et al. (2000) Kawahata et al. (2001) Bosch et al. (2004)

The three ophiolite terranes listed here have arguably been the focus of the most detailed hydrothermal alteration studies. Further examples of ophiolite-hosted mineralisation and alteration are documented in the reviews of Galley and Koski (1999) and Harper (1999).

ii. The direct interpretation of spatial and temporal relationships between magmatic – tectonic – and hydrothermal activity (based on robust geological field evidence). These relationships provide better constraints for the relative timing and duration of hydrothermal activity on Macquarie Island, and have wider implications for the evolution of the Proto-Macquarie Spreading Ridge. Potentially, these ideas may also be applicable to other slow-spreading ridges;

iii. The strong emphasis and focus on subseafloor alteration assemblages from major spreading-related faults. Previous *in situ* studies of oceanic hydrothermal systems and their altered rocks were largely restricted to seafloor deposits, e.g., the TAG mound (Humphris and Tivey, 2000), and rare fault scarp exposures or ocean drilling intersections of upper stockwork zones (Table 4.3). However, this project investigates the effects of focussed hydrothermal flow at deeper crustal levels, e.g., lower volcanic rock units and sheeted dyke transition zones. The characteristics of alteration assemblages at these depths are documented only from sporadic ODP drill-holes and a few ophiolite studies (Table 4.4–4.5). Consequently, many of their geological features and relationships are poorly understood from modern ocean crust settings, e.g., spatial dimensions and fault-zone distribution; and

iv. The application of diverse analytical and interpretative methods closely integrated with geological fieldwork. Employing this wide-ranging investigative strategy generates extensive field, mineral, chemical, and isotopic data for assessing diverse alteration parameters, e.g., collecting well constrained (1–10 m scale) altered rock samples from

around the major fault zones permits the spatial distribution of geochemical and isotopic tracers (alteration haloes) to be mapped and interpreted at hand- and outcrop-scale. Innovative analytical techniques also yield new geochemical data, rarely obtained for other seafloor alteration systems at modern spreading ridges, e.g., the laser ablation-ICPMS system permits fine spatial analysis of pyrite trace element compositions at low detection limits. These detailed analyses provided further information to help constrain and interpret relict fluid conditions and element source areas in each fault zone.

Limitations

In addition to recognising the most significant aspects of this project, the literature review also highlighted potential limitations. These limitations recognise the inherent heterogeneity of tectonic, magmatic, and hydrothermal processes at slow-spreading ridges, and caution against the widespread application of the study data and results. Many unusual geological features documented on Macquarie Island, and the mechanisms that formed them, may essentially be unique to this small segment of ocean crust.

A final consideration relates to the effects of uplift-related tectonic activity, and its potential impact on the distribution and architecture of hydrothermally altered rocks on Macquarie Island. Although Macquarie Island has not undergone major tectonic collision or continental obduction, its internal structure and composition has been influenced by ~ 10 million years of strike-slip and transpressional displacement (Chapter 3). Post-spreading tectonism may have disrupted, overprinted, or reactivated many faults and fractures, and thus rearranged their associated hydrothermal mineral assemblages. Chapter 5 presents further discussion on the effects of uplift-related tectonism observed during my field-based studies, including useful methods to discriminate oceanic faults from neotectonic (post-spreading) structures.

Chapter 5. – Geology of Focussed Hydrothermal Alteration Facies on Macquarie Island

5.1. Introduction

Faults, fractures, and brittle shear zones are common structural components of Macquarie Island's volcanic rock and sheeted dyke domains. Their widespread distribution reflects the complex, multi-stage evolution of this ophiolite terrane, and its proximity to the Indo-Australian–Pacific plate boundary. Many structural discontinuities, which encompass a broad scalar range, were formed during slow-spreading crustal growth and extension at the Proto-Macquarie Spreading Ridge (PMSR) (Goscombe and Everard, 2001). Several major fault zones, interpreted as accommodation structures which formed during late-stage oblique spreading (Rivizzigno and Karson, 2004), host very distinctive and localised occurrences of intensely altered rocks. The intimate spatial relationship between faults and alteration zones indicates that these early (oceanic) fault systems were permeable conduits for hydrothermal fluids in the ocean crust (Harper, 1999). Intense water–rock interactions produced the focussed alteration facies, which mainly consist of pervasively altered wall rocks, abundant hydrothermal veins and breccias, and minor sulfide mineralisation.

This chapter presents the main geological data and results obtained during detailed field studies of three NW- to NNE-striking faults and their surrounding host rocks. The Major Lake, Caroline Cove, and Sellick Bay Fault Zones, situated in central and southern Macquarie Island, are intimately associated with anomalous occurrences of hydrothermally altered basalt and sheeted dolerite dykes. The most intensely altered rocks outcrop sporadically along-strike in each fault, and are well exposed at six key locations (refer to Chapter 2, Figure 2.2 and Table 2.1). In addition, five small-scale alteration zones also occur in the proximal footwall domain of the Major Lake Fault Zone, i.e., the Sandell Bay Sheeted Dyke Swarm. Regional reconnaissance and detailed site mapping of the best preserved outcrops led to the classification of six focussed hydrothermal facies; these are intimately associated with the major structural conduits and do not occur elsewhere on Macquarie Island.

The purpose of this chapter is to:

i. Define the structurally controlled alteration facies identified during fieldwork;

ii. Outline the geographic distribution of the main fault zones and their associated alteration facies, and the geological features of their regional host rocks;

iii. Describe the characteristic secondary minerals, textural features, and other important outcrop attributes of the altered rocks, including their intimate structural relationships;

iv. Compare the main geological and alteration characteristics of each major fault zone; and

v. Provide initial analysis of the most significant themes arising from this field study, focussing on the geological evidence which can help to interpret the complex relationships between the hydrothermal, magmatic, and tectonic systems.

5.2. Focussed, fault zone alteration facies

All of the extrusive rocks and sheeted dykes on Macquarie Island are hydrothermally altered, although there is considerable variation in the scale and intensity (Chapter 3.6). Most of the secondary minerals are interpreted to have formed during regional alteration processes allied with seawater-dominated hydrothermal recharge (Griffin, 1982). These alteration assemblages formed across a continuum of metamorphic conditions, ranging from seafloor oxidation to upper greenschist and lower amphibolite facies (Griffin and Varne, 1980). However, despite the effects of widespread regional alteration, many igneous mineral compositions and textures are well preserved; in varying abundances they coexist (in disequilibrium) with the secondary assemblages.

The fieldwork data and observations collected during this project largely support the classification schemes and genetic interpretations of regional alteration assemblages proposed by Griffin (1982) (Chapter 3.6). However, my field studies have unequivocally shown that the most intensely altered upper crustal rocks on Macquarie Island are intimately associated with major structural discontinuities. Although the focussed alteration zones are not abundant, they have many highly anomalous and distinctive features such as characteristic outcrop patterns, unique secondary mineral assemblages, and diverse hydrothermal textures. These criteria, which are the main components recommended for the classification of **alteration facies** (Appendix 1), clearly distinguish the structurally controlled alteration zones from lithological domains affected by widespread regional alteration. In addition, these variations are further interpreted as evidence for significantly different genetic processes associated with the regional and focussed hydrothermal systems.

Based upon the main field criteria outlined above, six structurally focussed alteration facies are recognised on Macquarie Island (Table 5.1). Each represents an anomalous, multi-component facies that formed during hydrothermal alteration of the primary fault zone wall rocks. In varying proportions, the focussed alteration facies consist of:

i. A disequilibrium mineral assemblage that has partly to completely replaced the igneous minerals (and volcanic glass) in the host rocks. Alteration intensity mostly ranges from moderate to strong (Appendix 1), although localised patches of very intense recrystallisation and replacement also occur. Distinctive alteration textures include

selective (partial) to complete grain replacement, and semi-pervasive or pervasive alteration in groundmass domains of irregular (and variable) size and shape;

ii. Vughs, vesicles, and other primary rock cavities now infilled by secondary minerals. These amygdules contain both mono-mineral and finely intergrown, multi-phase crystal aggregates; most are massive or have very fine, concentric layering; and

iii. Well defined veins and veinlets that sharply cut across and overprint the igneous phenocryst and groundmass minerals. Vein assemblages are commonly dominated by a single hydrothermal mineral phase (e.g., quartz), although minor accessory minerals are intergrown with many vein segments, e.g., pyrite and epidote. Hydrothermal breccias, comprising angular fragments of altered wall rock hosted in the vein cement, are also widespread. Multiple vein stages occur in several alteration facies and are recognised by angular cross-cutting relationships or crack-seal vein textures.

The Major Lake, Caroline Cove, and Sellick Bay Fault Zones are intimately associated with five of the focussed alteration facies defined during this study (Table 5.1 and Table 5.2). The distribution and abundance of each facies varies significantly between individual faults and outcrop sites, and none of the fault zones hosts the complete facies spectrum. Instead, the main faults are each characterised by a distinctive hydrothermal association that comprises two or three discrete facies, and the key outcrop sites provide evidence of their mutual relationships (both spatial and evolutionary). In contrast to the five main hydrothermal associations, the narrow, focussed quartz vein (NQV) facies only occurs in small-scale structures such as minor fault arrays and local dyke margins (Table 5.2). The NQV facies has a limited spatial distribution, and *in situ* exposures are restricted to the Sandell Bay Sheeted Dyke Swarm (SBSD) and Zone BVI extrusive rock domain* in the Major Lake–Mt Martin district (Figure 5.1).

The alteration mineral assemblages and hydrothermal textures of the vein and breccia, quartz-chlorite (VQC) facies, the massive and veined, chlorite-quartz-pyrite (CQP) facies, and the narrow, focussed, quartz vein (NQV) facies, share several important characteristics. These include the high proportion of quartz-cemented veins and breccias, and widespread chlorite alteration of the primary host rocks. However, distinctive variations in the spatial distribution and physical appearance of the altered outcrop zones, and in the relative abundances of other hydrothermal minerals such as epidote, pyrite, chalcopyrite, and barite, clearly warrant the definition of the separate alteration facies presented here (adhering to the facies nomenclature guidelines proposed by Gifkins et al., 2005). The spatial and genetic relationships for each focussed alteration facies, and the evolutionary implications of this geological evidence, are further discussed in Chapter 5.6.

* Using Goscombe and Everard's (2001) regional domain nomenclature (Chapter 3.5).

Table 5.1: Summary of focussed alteration facies associated with upper crustal fault zones on Macquarie Island.

Alteration facies	Abbreviation	Main sites	Intensity	Main minerals	Minor minerals	Comments
Vein and breccia, quartz-chlorite facies	**VQC**	2A. Sandell Bay creek 2B. Major Lake foreshore 2C. East Mt Martin 2D. Lusitania Bay	moderate to strong	quartz + chlorite	± pyrite ± epidote	Intimate spatial association with the footwall of the **Major Lake Fault Zone**.
Foliated, massive chlorite facies	**FMC**	2A. Sandell Bay creek 3A. Caroline Cove	moderate to intense	chlorite	± prehnite	Poorly preserved and highly susceptible to weathering and erosion. Only occurs in the central deformation zone of the **Major Lake** and **Caroline Cove Faults**.
Massive and veined, chlorite-quartz-pyrite facies	**CQP**	3A. Caroline Cove	strong to intense	chlorite + quartz + pyrite	± epidote ± chalcopyrite ± barite	The best outcrops occur in a highly altered, fault-bound wedge at **Caroline Cove**. Some similarities with the VQC facies.
Pervasive, Fe-oxyhydroxide overprint facies	**PFO**	3A. Caroline Cove	moderate	Reddish-brown and purplish-red Fe-oxyhydroxide minerals		Spatially restricted facies that partly overprints the main deformation zone in the **Caroline Cove Fault**.
Vein-dominated, prehnite-zeolite facies	**VPZ**	1A. Sellick Bay escarpment	strong to intense	prehnite + zeolite minerals	± pumpellyite ± clay minerals ± Fe-oxyhydroxide minerals	Extensively developed in a 50-m-wide outcrop zone of the **Sellick Bay Fault** (upper escarpment slopes).
Narrow, focussed, quartz vein facies	**NQV**	2E. Mt Martin west 2F. Tio south 2G. Tio east 2H. Major Lake south 2J. Sandell Bay escarpment	moderate to strong	quartz + chlorite	± epidote ± pyrite	Small-scale zones of focussed alteration occur sporadically in regionally altered basalts and sheeted dykes ~ 1-2 km west of the **Major Lake Fault Zone**. A variant of the VQC facies, but with different structural hosts and outcrop features.

Notes:
1. The field site locations, outcrop features, and geological characteristics for each facies are presented throughout Chapter 5.
2. The detailed alteration paragenesis and hydrothermal textures are discussed in Chapter 6.3.
3. Refer to Appendix 1(Glossary) for definitions relating to alteration intensity.
4. Refer to Figure 2.2 and Figure 5.1 for site location details.

Geology of the Major Lake and Mt Martin district

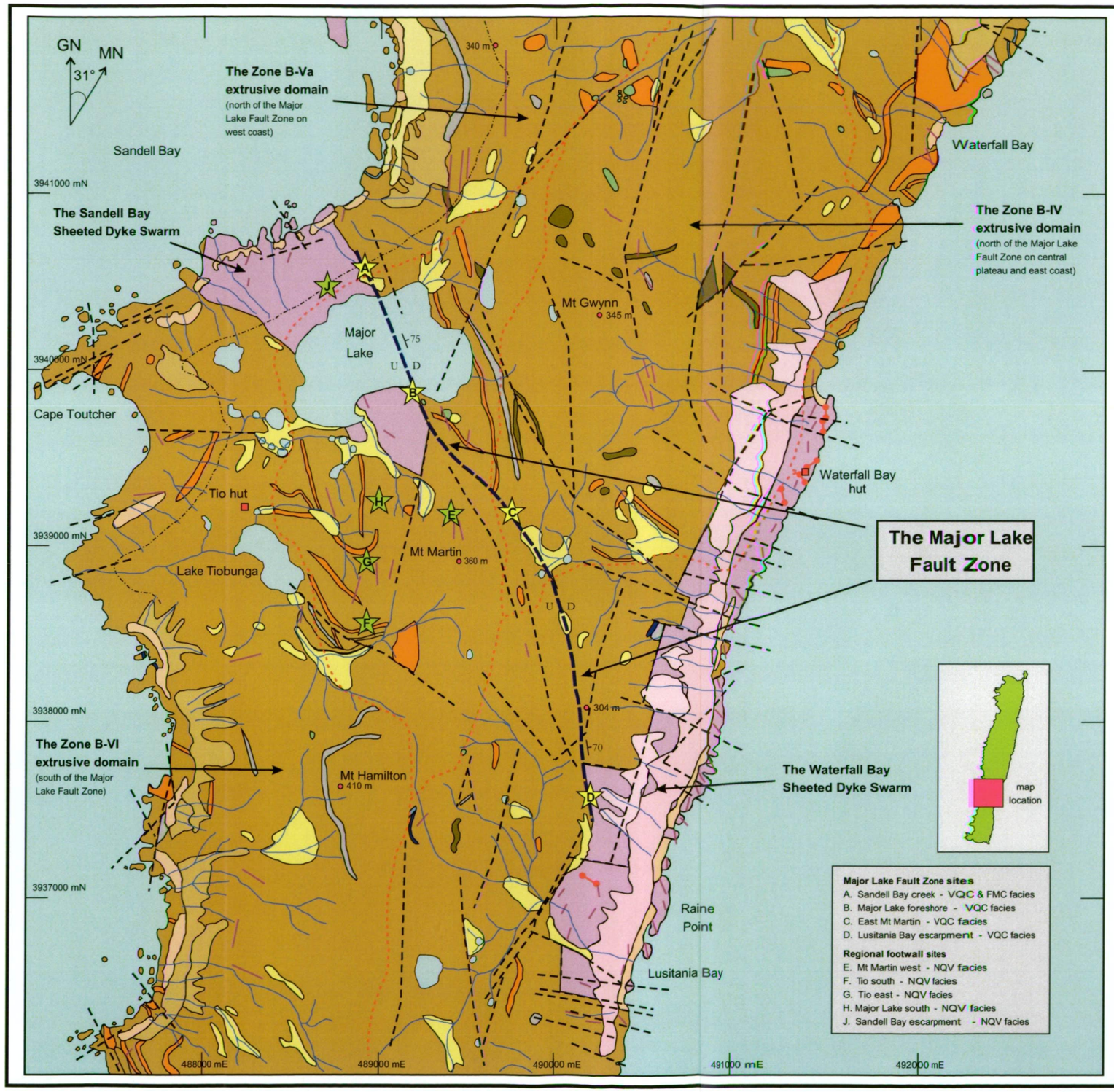

Major Lake Fault Zone sites
A. Sandell Bay creek - VQC & FMC facies
B. Major Lake foreshore - VQC facies
C. East Mt Martin - VQC facies
D. Lusitania Bay escarpment - VQC facies

Regional footwall sites
E. Mt Martin west - NQV facies
F. Tio south - NQV facies
G. Tio east - NQV facies
H. Major Lake south - NQV facies
J. Sandell Bay escarpment - NQV facies

Legend

- Alluvium
- Beach deposits
- Coastal "featherbed"
- Basalt scree
- Dolerite scree
- Dolerite alluvial fan
- Mudstone
- Conglomerate
- Hyaloclastite
- Volcanic breccia
- Pillow basalt
- Massive flow basalt
- Picrite
- Sheeted dolerite dyke
- Discrete dolerite dyke
- Gabbro screen
- Fault
- Lake
- Creek
- Walking track
- Hut
- Spot height
- Escarpment edge
- Major Lake Fault Zone site
- Regional footwall site

Scale 1:25,000

0 meters 1,000

Projection: UTM Zone 57 S
Datum: WGS-84
Contours: Not shown

This map is modified from map sheet 5 in the 1:10,000 Macquarie Island map series produced by Mineral Resources of Tasmania (1998). Geological data based on original field mapping by Ben Goscombe & John Everard (Tasmanian Geological Survey), and supplemented by detailed reconnaissance and site mapping undertaken during my fieldwork.

Figure 5.1: Geology map of the Mt Martin - Major Lake region, showing the location of the main study sites on the Major Lake Fault Zone and in the regional footwall domain.

Table 5.2: Summary of the outcrop sites that host structurally focussed alteration facies in the Major Lake – Mt Martin region.

Site name	Alteration facies	Location	AMG East	AMG North	Structural host	Local rock type	Outcrop length	Outcrop width	Comments
Sandell Bay creek (Site 2A)	1 VQC 2 FMC	Upper to mid-level west coast escarpment at south Sandell Bay	489050 mE	3940650 mN	**Major Lake Fault** – NNW to N orientation	Sheeted dolerite dykes and transitional pillow basalt of the Sandell Bay Sheeted Dyke swarm (SBSD)	150 m	av. = 10–15 m min. = 5 m max. = 30 m	The largest and most significant outcrop of structurally controlled alteration on the Major Lake Fault Zone (MLFZ). The alteration system is subparallel and adjacent to the creek valley exposure of the MLFZ (FMC outcrop zone), and is terminated at the mid-scarp level by a NNE-striking cross-fault.
Major Lake foreshore (Site 2B)	VQC	South-east foreshore of Major Lake	489300 mE	3939820 mN	**Major Lake Fault** – NNW to N orientation	Sheeted dolerite and transition zone pillow basalt of the SBSD	80 m	1–3 m	A small alteration zone sited on the upper slope of a prominent linear ridgeline. A narrow, elongated outcrop is discontinuously exposed in an 80 m segment subparallel to the MLFZ.
East Mt Martin (Site 2C)	VQC	~ 600 m east of Mt Martin, on the central plateau	489860 mE	3939130 mN	**Major Lake Fault** – NNW orientation	Pillow basalt with common discrete dykes (Zone BVI domain)	110 m	5–10 m	The alteration zone consists of three main outcrop exposures evenly distributed along a 110 m fault-parallel section. The main deformation zone is not exposed in the coincident creek valley.
Lusitania Bay escarpment (Site 2D)	VQC	Upper level of east coast scarp at north Lusitania Bay	490290 mE	3937580 mN	**Major Lake Fault** – NNW to N orientation	Transition zone pillow basalt to sheeted dolerite dykes of the Lusitania Bay Sheeted Dyke swarm	75 m	av. = 10–15 m min. = 5 m max. = 25 m	The alteration zone occurs in the upper escarpment slope and is subparallel to the trend of the ridgeline. The very steep slope hosts highly fractured outcrops with abundant faults and breccias.
Mt Martin west (Site 2E)	NQV	~ 200 m north-west of Mt Martin summit	489550 mE	3939135 mN	Local 2 m wide dyke margin (358° / 50° E)	Pillow basalt and discrete dykes (Zone BVI)	4 m	2 m	A narrow alteration zone is focused on the east margin of a discrete N-striking dyke. A 50 cm zone of oxidised, fractured dolerite suggests post-hydrothermal structural disruption.
Tio south (Site 2F)	NQV	~ 400 m south-east of Lake Tiobunga on the central plateau	488895 mE	3938545 mN	Unknown - no margins (038° / 54° W)	Pillow and massive flow basalt and discrete dolerite dykes (Zone BVI)	1.5 m	15–20 cm	A discrete quartz vein is exposed *in situ* but lacks exposed contact margins with the host rock. The massive quartz vein hosts minor angular wall rock breccia fragments.
Tio east (Site 2G)	NQV	~ 200 m east of Lake Tiobunga on the central plateau	488900 mE	3938875 mN	Local, small-scale fault (345° / 75° W)	Pillow basalt and discrete dolerite dykes (Zone BVI)	5 m	50–70 cm	The subplanar alteration zone occurs near a small fault that cross-cuts the pillow basalt host-rock. Irregular patches of massive and vein quartz are abundant and contain many breccia fragments.
Major Lake south (Site 2H)	NQV	~ 500 m south of Major Lake on the central plateau	489000 mE	3939265 mN	Local 1 m wide dyke margin (005° / 65° W)	Pillow basalt and discrete dolerite dykes (Zone BVI)	4 m	70 cm	Alteration zone developed at margins of discrete, narrow dyke in pillow basalt. Abundant massive and vein quartz with dark green, chloritised wall rock. Common orange-red oxidation staining.
Sandell Bay escarpment (Site 2J)	NQV	Small regional scarp outcrop ~ 100 m south-west of MLFZ	488980 mE	3940535 mN	Small, localised fault (350° / 80° E)	Sheeted dolerite dykes and transition zone pillow basalt (Zone BVI)	1 m	1 m	A small, localised zone of quartz-rich altered basalt in the upper escarpment slope of the Sandell Bay Sheeted Dyke swarm. Abundant jigsaw-fit hydrothermal breccia occurs here.

Notes:

1. VQC = vein and breccia, quartz-chlorite facies; FMC = foliated, massive chlorite facies; and NQV = narrow, focussed quartz vein facies.
2. Sites 2A to 2D are situated on the Major Lake Fault Zone, and sites 2E to 2J occur in the regionally altered footwall block of the Sandell Bay Sheeted Dyke Swarm.
3. The structural data indicate strike direction and amount of dip; the alteration zone dimensions are approximate.
4. Easting and northing coordinates are AMG Zone 57 S (WGS-84 datum), with ± 10 m resolution.
5. Refer to Figure 5.1 for site locations and Chapter 3 for definitions of the regional geology domains and local rock types.

5.3. Altered rocks from the Major Lake Fault Zone

Geographic distribution and regional context

The Major Lake Fault Zone (MLFZ) is one of the longest (~ 4 km strike extent) and best preserved oceanic faults on Macquarie Island (Rivizzigno and Karson, 2004). The MLFZ cuts across south-central Macquarie Island between Lusitania Bay and Sandell Bay, striking predominantly NNW (Figure 5.1). It further extends offshore, and is correlated with seafloor lineaments that are interpreted as spreading-related fracture zones (Massell et al., 2000; Daczko et al., 2003). Well preserved outcrops of the Major Lake Fault's central deformation zone, and the focussed alteration facies that are intimately associated with it, occur at Sandell Bay creek (Site 2A) (Figure 5.1 and 5.2). This site, situated in the upper escarpment slope at the southern end of Sandell Bay, is one of the key project field localities. Most other central segments of the MLFZ are highly eroded and covered (obscured) with abundant soil, scree, and vegetation.

Figure 5.2: This steep valley coincides with the central deformation corridor of the Major Lake Fault Zone (Site 2A – Sandell Bay creek). The prominent rocky ridgeline south-west of the creek (left of view) comprises a fault-parallel zone that hosts strongly altered basalt and dolerite of the vein and breccia, quartz-chlorite (VQC) facies. The deeply incised creek bed exposes a weathered, friable outcrop of altered volcanic rocks from the foliated, massive chlorite (FMC) facies. This view looks down-slope (towards the west) from the upper edge of Macquarie Island's ~ 200-m-high west coast escarpment, with the southern coastline of Sandell Bay in the background.

The Major Lake Fault Zone is an important geological boundary that, in many places along-strike, juxtaposes disparate volcanic rock and sheeted dyke domains (Figure 5.1) (Goscombe and Everard, 2001). Reconnaissance fieldwork further showed that the MLFZ separates igneous rock packages that have significantly different regional alteration assemblages, e.g., zeolite facies pillow basalts (Zone BVa domain) abut greenschist facies sheeted dykes (the SBSD) in the

vicinity of Major Lake foreshore (Site 2B). Critically, the MLFZ is also the main structural host for two of the focussed hydrothermal facies identified during this project. The vein and breccia, quartz-chlorite (VQC) facies is intimately associated with the MLFZ and, although most fault segments are poorly exposed, prominent outcrops of VQC facies rocks occur at four locations (Figure 5.1 and Table 5.2). These outcrop sites are restricted to the immediate structural footwall of the MLFZ (i.e., the Sandell Bay Sheeted Dyke Swarm and Zone BVI volcanic rock domain) and are absent from the adjacent volcanic rock package on the northern side of the fault (Zone BIV and BVa domains). Preservation and exposure of the main VQC facies sites is clearly enhanced by the high abundance of hydrothermally derived quartz.

The Major Lake Fault Zone is also the host structure for altered basalts of the foliated, massive chlorite (FMC) facies. However, these rocks are highly susceptible to weathering and erosion and, consequently, there is only one main field occurrence (Site 2A; Figure 5.2). The five regional outcrop sites of the narrow, focussed quartz vein (NQV) facies (Sites 2E to 2J) also occur < 1.5 km west of the MLFZ. This hydrothermal facies is hosted within the transitional package of sheeted dolerite dykes and pillow basalts associated with the Sandell Bay Sheeted Dyke Swarm and Zone BVI domain (Figure 5.1 and Table 5.2).

Host rocks of the Major Lake Fault Zone

Sheeted dolerite and pillow basalt in the footwall

The structural footwall of the Major Lake Fault Zone (MLFZ) consists of the Sandell Bay and Waterfall Bay Sheeted Dyke Swarms (termed the SBSD and WBSD respectively), and the Zone BVI extrusive rock association (Hurd Point group; Figure 5.1) (Goscombe and Everard, 2001). The footwall domain, situated south-west of the MLFZ, contains most focussed alteration zones in the Major Lake – Mt Martin district, including all outcrop sites of the VQC and NQV facies. Typically, the boundaries between discrete lithological domains in this region are poorly exposed and rarely outcrop, although limited field relationships provide evidence that most contacts are faulted.

The rocks of the SBSD and WBSD are best exposed in the coastal foreshore and steep escarpment slopes; they form only sporadic and low-lying outcrops on the plateau. Most outcrops consist of moderately to steeply dipping sheeted dolerite dykes that consistently strike NNW to NNE (Figure 5.3). Multiple, subparallel intrusive phases are mainly recognised by textural features such as grain size variations, distinct phenocryst populations, and the presence of chilled (aphanitic) dyke margins. A 200–300 m-wide outcrop segment composed of pillow basalts and discrete dykes occurs adjacent to the MLFZ in both the western (Sandell Bay) and eastern (Lusitania Bay) coastal escarpments (near Sites 2A and 2D respectively). These mixed rock packages, which have not previously been documented, are interpreted here as part of the extrusive to hypabyssal transition zone that occurs in the ocean crust (Chapter 4.2).

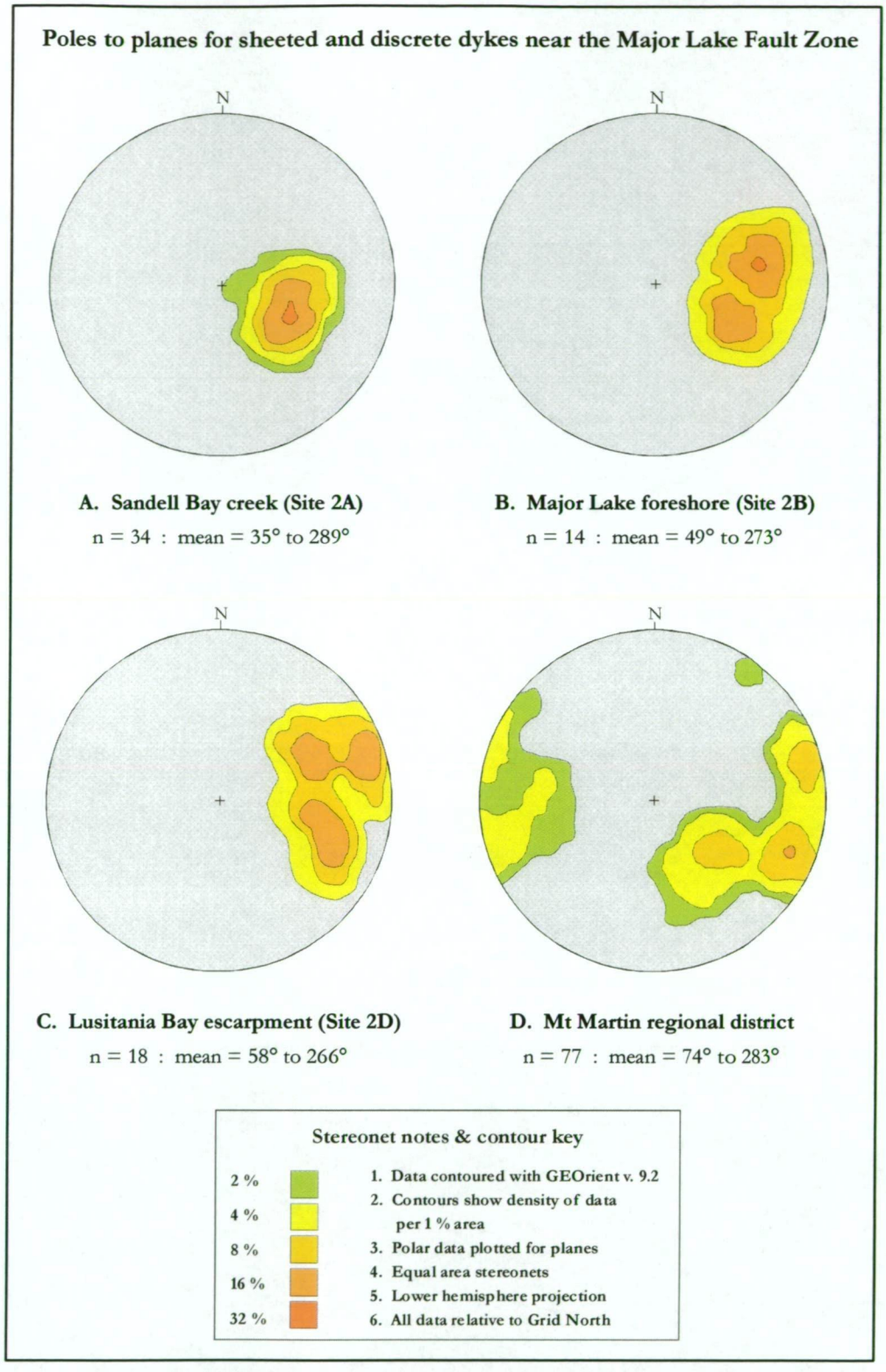

Figure 5.3: Contoured stereographic projections (poles to planes) of sheeted (A to C) and discrete (D) dolerite dykes in the Major Lake – Mt Martin district, highlighting the consistent NNW- to NNE-strike of most intrusive rocks. Narrow, isolated dykes occur widely in both the hangingwall and the footwall domains of the Major Lake Fault Zone, and the sheeted dykes form part of the Sandell Bay Sheeted Dyke Swarm (Site 2A and 2B) and Waterfall Bay Sheeted Dyke Swarm (Site 2D). Discrete dykes have a broader range of orientations, although the majority trend is similar to the sheeted dyke complexes.

The sheeted dolerite dykes are bluish-green to greenish-grey and vary from fine-grained, aphyric to moderately plagioclase-phyric rocks. Most outcrops are blocky and angular; narrow, brittle joints and fractures are abundant. Irregular patches (< 3–5 cm-across) or discontinuous veinlets of chlorite, actinolite, albite, and epidote occur widely in the groundmass, and fine-grained pyrite is sparsely disseminated. Most dykes in the SBSD and WBSD have moderate to low magnetic susceptibilities, typically < 100 x 10^{-5} SI units (Figure 5.4 and Appendix 3). The secondary mineral assemblages of these rocks, combined with their low magnetic signatures and distinctive textural features, suggests that widespread (regional) hydrothermal alteration occurred under greenschist facies conditions (Griffin, 1982).

Small, localised faults and brittle fracture zones (~ 0.5–2.0 m-wide) occur commonly in the footwall rocks; most are closely associated with moderately to steeply dipping, subparallel vein networks (Figure 5.5). Discrete veins typically have well defined margins and a width range of 1–5 mm. Pale orange-white to greyish-white prehnite is the most abundant cement, and extensive vein networks are commonly surrounded by bleached wall rock selvages (Figure 5.6).

Pillow basalts in Zone BVI occur widely on the central plateau in the Mt Martin – Major Lake – Lake Tiobunga district (Figure 5.1) (Goscombe and Everard, 2001). These basaltic rocks are sparsely to moderately porphyritic and, similar to the sheeted dykes, are also bluish-green to greenish-grey (Figure 5.7). Tabular and elongate plagioclase laths are abundant (< 1–5 mm-long), and many contain irregular patches and fine veinlets of pale green and dark greenish-black alteration (partial chlorite replacement). Irregular-shaped aggregates of fine-grained quartz and epidote also occur sporadically in the altered groundmass. These delicate intergrowths partly replace 2–5 cm-wide zones of the inter-pillow matrix or discrete pillow cores (Figure 5.8). Most Zone BVI basaltic rocks have low to moderate magnetic susceptibilities (Figure 5.4) which, combined with the observed secondary mineral assemblages and hydrothermal textures, suggests lower greenschist facies regional alteration, akin to the adjacent sheeted dyke domains (Griffin, 1982).

Volcanic rock outcrops in Zone BVI consist mainly of tightly packed pillow basalts separated by narrow selvages (most are < 10 mm-wide) of dark bluish-green volcanic glass (highly chloritised). Discrete, well formed pillow shapes are prominent and include elongated and subrounded lobes ~ 0.5–1.5 m-long and < 1 m in diameter. Elongate pillow axes in the Zone BVI extrusive domain consistently trend ENE to NE and have shallow or moderate plunges (most are < 30°). Individual dykes have sporadically intruded the pillow basalt package, and most are similar in textural appearance and orientation to rocks from the adjacent sheeted dyke complexes (the SBSD and WBSD).

Figure 5.4: Frequency histogram of magnetic susceptibility data from upper crustal rocks in the Mt Martin - Major Lake region.

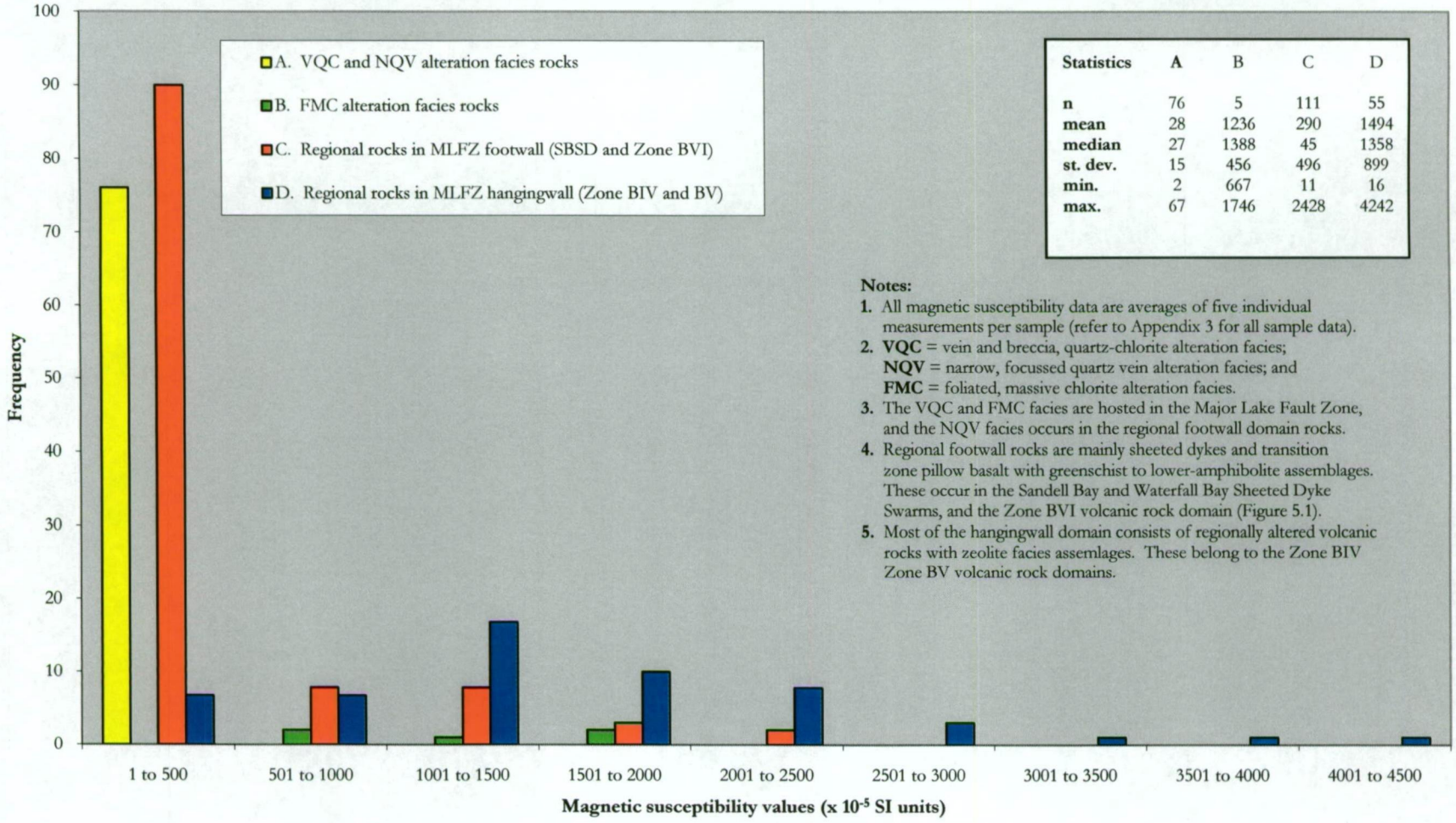

Statistics	A	B	C	D
n	76	5	111	55
mean	28	1236	290	1494
median	27	1388	45	1358
st. dev.	15	456	496	899
min.	2	667	11	16
max.	67	1746	2428	4242

Notes:

1. All magnetic susceptibility data are averages of five individual measurements per sample (refer to Appendix 3 for all sample data).
2. **VQC** = vein and breccia, quartz-chlorite alteration facies; **NQV** = narrow, focussed quartz vein alteration facies; and **FMC** = foliated, massive chlorite alteration facies.
3. The VQC and FMC facies are hosted in the Major Lake Fault Zone, and the NQV facies occurs in the regional footwall domain rocks.
4. Regional footwall rocks are mainly sheeted dykes and transition zone pillow basalt with greenschist to lower-amphibolite assemblages. These occur in the Sandell Bay and Waterfall Bay Sheeted Dyke Swarms, and the Zone BVI volcanic rock domain (Figure 5.1).
5. Most of the hangingwall domain consists of regionally altered volcanic rocks with zeolite facies assemlages. These belong to the Zone BIV Zone BV volcanic rock domains.

Extrusive rocks and discrete dykes in the hangingwall

The rock types, tectonic structures, and regional alteration assemblages in the hangingwall of the Major Lake Fault Zone (geographically situated to the north and north-east of the fault) are significantly different to those in the footwall domain at Sandell Bay creek (Site 2A), Major Lake foreshore (Site 2B), and East Mt Martin (Site 2C). At these locations the hangingwall rocks comprise an extrusive-dominated sequence of fine-grained, purplish-grey pillow basalt, minor zones of hyaloclastite, discrete dolerite dykes, and rare picrite plugs. The rocks, which belong to the Zone BIV and BVa volcanic rock associations (Goscombe and Everard, 2001), lack the focussed quartz-bearing alteration facies (VQC and NQV) that occur in the footwall. The local hangingwall rocks are brittle and very susceptible to erosion (especially the hyaloclastite units), and most are poorly exposed near the Major Lake Fault Zone. Less weathered outcrops are restricted to minor low-lying occurrences in the upper escarpment slope or around the foreshore of Major Lake (Figure 5.9). Unlike Site 2A, 2B, and 2C, the alteration zone at Lusitania Bay (Site 2D) is completely surrounded by the transitional pillow basalt and sheeted dyke complex of the Waterfall Bay Sheeted Dyke Swarm (Figure 5.1).

The hangingwall basaltic rocks are aphyric to moderately plagioclase-phyric and have purplish-grey groundmass (Figure 5.10). The pillow basalt is sparsely vesicular; vesicles comprise < 2 % of the total rock and mostly occur within pillow rims. Vesicles are 1–3 mm in diameter and are mainly infilled with pale, very fine-grained zeolite minerals. Hydrothermal veins are commonly associated with small fractures and faults (most are < 5 cm-wide), and are variably cemented with fine-grained prehnite and zeolite minerals, reddish-brown Fe-oxyhydroxide minerals (e.g., goethite), and dark brownish-green clays. These distinctly coloured alteration phases also commonly occur in the fractured and brecciated matrix of discrete fault zones. Small-scale and localised faults are sporadically distributed in Zone BIV and BVa, e.g., three subparallel faults were mapped in a 150 m-long x 50 m-wide section of abundant pillow basalt outcrop in the upper Sandell Bay escarpment. Most of these faults are steeply dipping and consistently strike NNW to NNE.

In contrast to the sheeted dykes and pillow basalts in the SBSD and Zone BVI, the hangingwall volcanic rocks are highly magnetic. Average magnetic susceptibilities are ~ 1500 x 10^{-5} SI units, and many rocks in Zone BIV have values > 2000 x 10^{-5} SI units (Figure 5.4). These basaltic rocks also lack most of the common secondary minerals that occur in the footwall domain; quartz, epidote, and pyrite are all absent. The alteration mineral assemblages and regional hydrothermal attributes are indicative of relatively low grade alteration under zeolite facies conditions (Griffin, 1982).


Fig. 5.5

Fig. 5.6

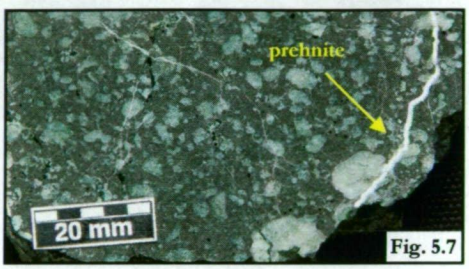

Fig. 5.7

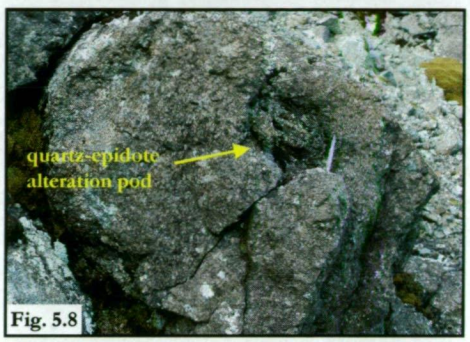

Fig. 5.8


Fig. 5.9

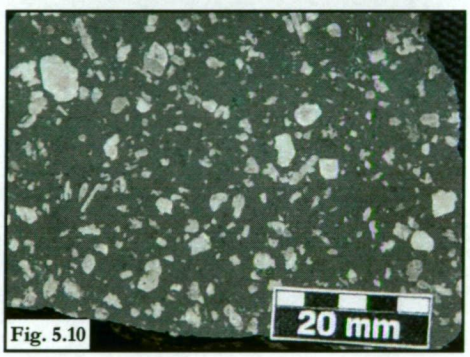

Fig. 5.10

Figure 5.5: Subparallel prehnite veins occur in a small fault within the Sandell Bay Sheeted Dyke complex (near Site 2J in the Sandell Bay escarpment). Vuggy cavities are common in thick, massive prehnite veins, such as the central vein segment shown here (the total scribe length is ~ 13 cm).

Figure 5.6: Massive prehnite-rich veinlets cross-cut the bleached and altered groundmass of this fine-grained, fault-hosted dolerite. This sample was collected from the fault-zone outcrop shown in Figure 5.5 (sample MCQ-080 from the Sandell Bay Sheeted Dyke Swarm).

Figure 5.7: A typical Zone BVI pillow basalt from the pillow-dyke transition zone in the upper escarpment above Lusitania Bay (Site 2D). Distinctive pale green alteration (chlorite-rich) is common in the plagioclase crystals and the aphanitic groundmass. Several pale, narrow prehnite veins cut across this sample, but lack any obvious alteration haloes (sample MCQ-383 from the Waterfall Bay Sheeted Dyke Swarm).

Figure 5.8: Cross-section view of a ~ 1 m-wide, discrete pillow basalt lobe on the western flank of Mt Martin (near Site 2E). The subrounded cavity (near the scriber) contains the eroded remnants of an intergrown quartz-epidote aggregate that has partly replaced the primary groundmass.

Figure 5.9: Purplish, fine-grained pillow basalt around the south-eastern shoreline of Major Lake (near Site 2B) is typical of the extrusive rocks in the hangingwall of the Major Lake Fault Zone. Radial fractures and dark green, inter-pillow volcanic glass are prominent in this outcrop.

Figure 5.10: A moderately plagioclase-phyric pillow basalt from the hangingwall domain of the Major Lake Fault Zone. The purplish-grey groundmass and high magnetic susceptibility of these rocks contrast markedly with the footwall volcanic and sheeted dyke package (sample MCQ-128 collected near the Sandell Bay creek (Site 2A)).

At several locations in the Sandell Bay escarpment a previously unrecognised volcanic unconformity was mapped in the hangingwall package north of the MLFZ (Zone BVa). This local unconformity separates underlying hyaloclastite from a prominent, ridge-crest exposure of pillow basalt. In places, the unconformity is marked by thin and discontinuous pods of fine-grained, pinkish-brown mudstone. Unconformable extrusive contacts are not common on Macquarie Island, e.g., Goscombe and Everard (1997) recognised only seven local unconformities during their island-wide mapping project; none were observed in the local footwall domain of the MLFZ. The presence of this volcanic unconformity suggests that temporally distinct and localised magmatic events produced the different extrusive rock packages, and provides further geological evidence to distinguish lithological domains around the MLFZ.

Geological and hydrothermal characteristics of alteration facies from the Major Lake Fault Zone

The Major Lake Fault Zone (MLFZ) and the surrounding footwall rocks host outcrops of three focussed alteration facies recognised and defined during this field study (Table 5.1 and Table 5.2). The vein and breccia, quartz-chlorite (VQC) facies and the narrow, focussed quartz vein (NQV) facies are recognised only from this local area; the foliated, massive chlorite (FMC) facies also occurs in the Caroline Cove Fault Zone (Chapter 5.4). This section summarises the important outcrop and hand-specimen characteristics of the VQC and NQV facies. Based on the well preserved exposure in the Sandell Bay creek (Site 2A), a comprehensive overview of the FMC alteration facies, and its intimate structural relationship with the central deformation zone of the Major Lake Fault, is also presented. The alteration mineral paragenesis and the micro-textures of each facies are detailed in Chapter 6 (petrographic study results).

Vein and breccia, quartz-chlorite (VQC) facies

The vein and breccia, quartz-chlorite (VQC) facies is the most common style of focussed hydrothermal alteration associated with the Major Lake Fault Zone (MLFZ). The four VQC outcrop sites (i.e., Sandell Bay creek, Site 2A; Major Lake foreshore, Site 2B; East Mt Martin, Site 2C; and Lusitania Bay escarpment, Site 2D) are characterised by similar and highly distinctive alteration mineral assemblages and hydrothermally derived textures. The spatial distributions and structural relationships of these altered rocks with the MLFZ are also relatively consistent for each site, although their absolute outcrop dimensions and fracture intensities vary (Table 5.2). These diagnostic geological features contrast with the main characteristics of the regionally altered footwall rocks (SBSD and Zone BVI), and differ even more significantly with the hangingwall basalts (Zone BIV and BVa).

At each key outcrop site on the MLFZ, the VQC facies rocks form discrete and elongated, fault-parallel zones with a consistent NNW orientation (Figure 5.11 and 5.12).

Geology of the Major Lake foreshore (Site 2B)

GN MN
31°
Magnetic north is shown for 2005
It moves 3.6' east each year

View looking south-east across Major Lake at the foreshore study site and fault scarp.

Direction of view shown for the inset photograph.

Major Lake

3939900 mN

3939800 mN

3939700 mN

MCQ-321 40
MCQ-320
MCQ-322 46
MCQ-323
MCQ-319
MCQ-324
MCQ-318
MCQ-329
MCQ-328
MCQ-327
MCQ-325
MCQ-326
MCQ-330
MCQ-317
MCQ-316
MCQ-331
MCQ-315
MCQ-332
MCQ-314
MCQ-333
MCQ-313
MCQ-312
MCQ-311
MCQ-310
MCQ-309

The Major Lake Fault Zone
Interpreted position based on the trend of the steep fault escarpment (as shown in the inset photograph).

MCQ-334
MCQ-335
23°
20°
MCQ-336
MCQ-337
MCQ-338
MCQ-339
MCQ-340

Zone BV-b (Sandell Bay) volcanic rock association
(Using the nomenclature of Goscombe and Everard, 2001).

Sandell Bay Sheeted Dyke Swarm
(Using the nomenclature of Goscombe and Everard, 2001).

VQC facies outcrop zone

This elongated, fault-parallel ridge contains several (~ 1-2 m-wide) outcrops of the vein and breccia, quartz-chlorite alteration facies.

The fault zone scarp slopes steeply to the E (see photo inset).

78

75
Fault zone orientation

75
75

Structural footwall domain of the MLFZ (SBSD)

Sheeted dolerite dykes and minor transition zone basalt with distinctive greenschist to lower-amphibolite facies assemblages and textures (regional alteration assemblages).

Interpreted up-thrown block (footwall)
(Actual sense of fault displacement not evident in outcrop).

Interpreted down-thrown block (hangingwall)

43
58
46
245 m

The central deformation corridor of the Major Lake Fault Zone is mostly obscured by soil and scree in this slope, although minor subcrop exposures of the foliated, massive chlorite alteration facies sporadically occur. However, no detailed structural data or samples were collected here because of extensive weathering, abundant soil cover, and considerable access problems on the steep escarpment.

Structural hangingwall domain of the MLFZ (Zone BV-b)

The dominantly pillow basalt sequence (with minor discrete dykes) contains low grade regional alteration assemblages (zeolite facies) and lacks the vein and breccia, quartz-chlorite facies.

map location

489000 mE
489100 mE
489200 mE
489300 mE
489400 mE

Legend

- Vein and breccia, quartz-chlorite alteration facies - outcrop
- Foliated, massive chlorite alteration facies (location mostly interpreted)
- Sheeted dolerite (footwall domain) - outcrop & scree
- Pillow basalt (hangingwall domain) - outcrop & scree
- Elongated pillow basalt - with axial trend & plunge (20°)
- Picrite (hangingwall domain) - outcrop & scree
- Discrete dolerite dyke - dip & direction shown (75)
- Vegetation cover - mainly low grass & moss
- Inferred fault (topographic feature)
- Lake
- Lake shoreline
- Creek
- Spot height (245 m)
- Sample site (rock specimen)
- Sample number (MCQ-340)

Scale 1 : 2000

0 meters 100

Projection: UTM Zone 57 S
Datum: WGS-84
Contours: Not shown
Survey control: Garmin E-trex GPS unit
Mapping & drafting: Steven Lewis

Figure 5.11: Outcrop geology and sample locality plan for the Major Lake foreshore (Site 2B). A narrow ridge of the vein and breccia, quartz-chlorite (VQC) facies outcrops in a ~ 75 m-long elongated corridor subparallel to the Major Lake Fault Zone. The strong structural control and intimate relationship between the VQC facies and the Major Lake Fault Zone is clearly evident. A distinctive change in rock type and regional alteration grade occurs across the deformation zone, and the VQC facies is absent from the pillow basalt sequence in the hangingwall. Although most of the steep escarpment slope is inaccessible and covered with soil, small subcrop exposures of highly weathered basalt with probable foliated, massive chlorite alteration (FMC) facies assemblages were observed in several locations (refer to Figure 5.1 for the relative location of Site 2B on the MLFZ).

Geology of East Mt Martin (Site 2C)

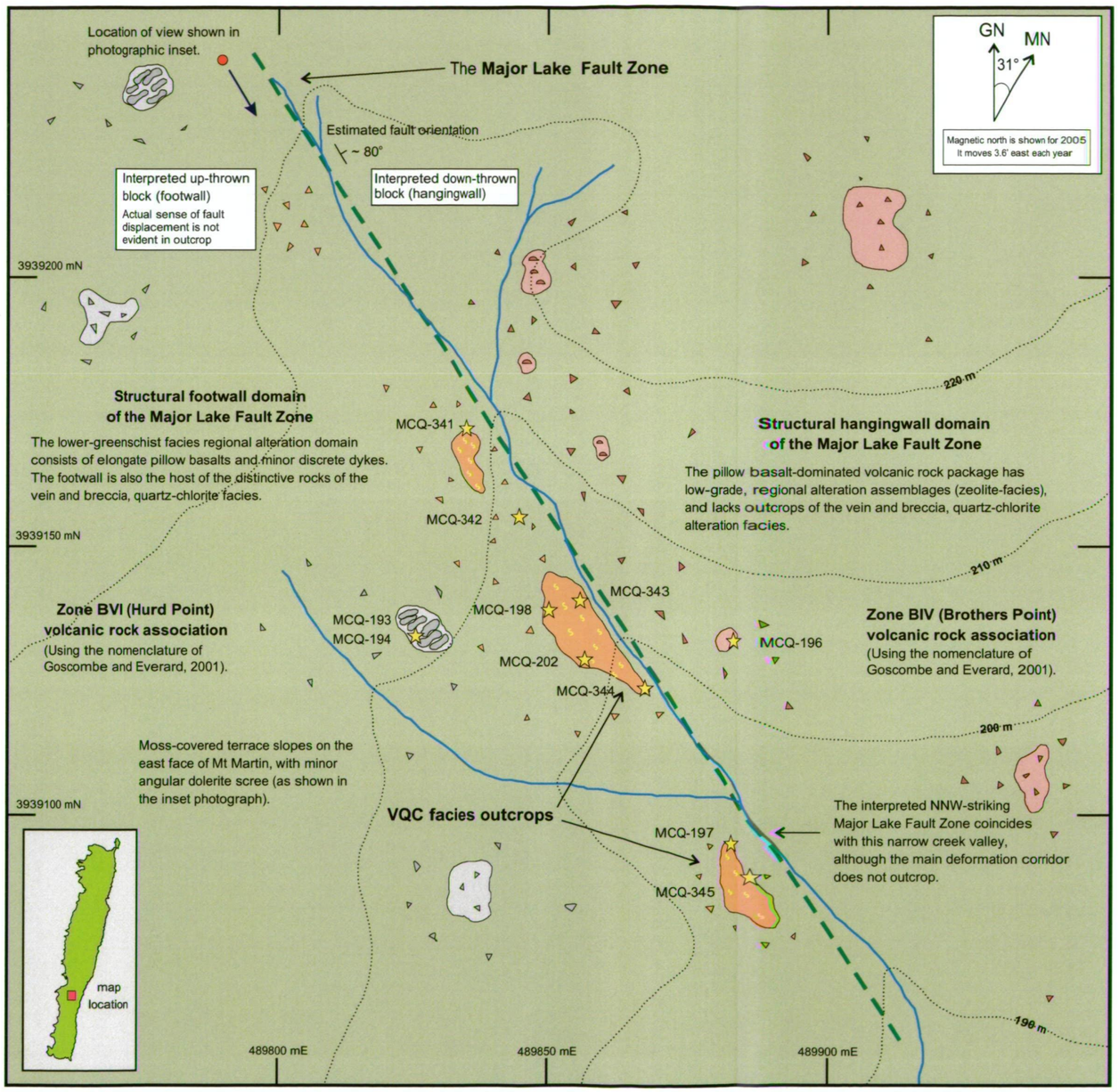

Legend

- Altered basalt with the vein and breccia, quartz-chlorite alteration facies - outcrop & scree
- Pillow basalt and sheeted dykes with regional lower-greenschist assemblages (footwall domain) - outcrop & scree
- Pillow basalt with regional zeolite facies assemblages (hangingwall domain) - outcrop & scree
- Interpreted trend of the Major Lake Fault Zone
- Vegetation cover - mainly low grass & moss
- Creek valley
- Contours (metres above sea-level) — 200 m
- Sample site (rock specimen)
- Sample number — MCQ-343

Scale 1 : 1000

0 meters 50

Projection: UTM Zone 57 S
Datum: WGS-84
Contours: 10 m interval
Survey control: Garmin E-trex GPS & tape and compass survey grid
Mapping & drafting: Steven Lewis

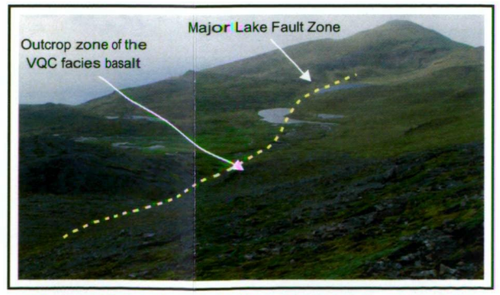

View looking SE along the projected trend of the Major Lake Fault Zone (as shown in this plan). The three altered basalt outcrops with typical vein and breccia, quartz-chlorite facies assemblages occur on the right (west) of the small valley, which coincides with the main deformation corridor of the Major Lake Fault Zone (not exposed).

Figure 5.12: Outcrop geology and sample locality plan for East Mt Martin (Site 2C). Three outcrops of altered basalt occur in a 110 m-long zone, and these exposures have mineral assemblages and textures which are characteristic of the vein and breccia, quartz-chlorite (VQC) facies. This focussed alteration domain is parallel and adjacent to the NNW-striking Major Lake Fault Zone, although the main deformation corridor is not exposed; hence, the foliated, massive chlorite (FMC) facies does not outcrop at this locality. Similar to all of the sites that host altered rocks of the VQC facies, there is a strong spatial association between the focussed hydrothermal assemblages and their primary structural conduit.

The irregular VQC facies outcrops are blocky and angular; abundant brittle faults, fractures, and joints extensively dissect most exposures. Rusty, orange-brown staining and surface oxidation is semi-pervasive at all sites, and is especially well developed along subplanar fracture zones and joint surfaces. However, most outcrops are prominently exposed, and their significant positive relief markedly contrasts with the eroded wall rocks that surround each site (Figure 5.13).

The basaltic host rocks of the VQC facies are moderately to intensely altered and have a distinctive dark bluish-green or greenish-grey groundmass (Figure 5.14). The magnetic susceptibility of these rocks is uniformly very low; most values are < 50 x 10^{-5} SI units (Figure 5.4 and Appendix 3). The alteration mineral assemblage is dominated by quartz veins and breccias that cut across the chloritised groundmass. Relict plagioclase phenocrysts (albitised) are variably preserved, but most are partly replaced with very fine-grained, mottled or streaky chlorite. Fine- to medium-grained pyrite and epidote also occur as disseminated crystals or massive aggregates (mostly < 10 mm in diameter) in the altered groundmass and hydrothermal veins, although they are not ubiquitous (Figure 5.15 and 5.16). Minor, late-stage prehnite veins (1–5 mm-wide) rarely cut across quartz and pyrite veinlets. Primary igneous features, such as pillow basalt morphologies and porphyritic textures, are mostly overprinted and obscured by the hydrothermal assemblages, although relict primary structures are preserved in some less intensely altered enclaves (especially in zones of low fracture intensity).

Quartz is the most diagnostic secondary mineral in the VQC facies, and its widespread occurrence is largely responsible for the distinctive outcrop style. Quartz veins and massively altered groundmass domains are mostly pale and milky, although surface staining (oxidation) is common. Ovoid vughs and irregular-shaped vein cavities are also abundant (mostly < 1 cm across, but some up to 1–3 cm), and many are lined with fine- to medium-grained euhedral crystals (Figure 5.17). Quartz occurs in three distinctive textural forms:

i. Patchy zones of massive quartz alteration;

ii. Discrete, major quartz veins; and

iii. Irregular quartz veinlet arrays (stockworks).

Patchy zones of massive quartz alteration

Domains of massive quartz alteration commonly overprint and replace the primary basaltic groundmass (Figure 5.18). These irregular, semi-pervasive to pervasive quartz zones vary widely in size and shape; they include abundant 5–20 mm-wide patches, and outcrop domains ~ 80 to 100 cm-across (with a spectrum of intermediate sizes between these extremes). Subangular to very angular fragments of chlorite-altered wall rock (basalt) commonly occur in massive, quartz-rich patches (Figure 5.19). Most fragments are 2–5 mm-across (up to ~ 15–20 mm) and, where abundant, they commonly impart a distinctive brecciated texture.

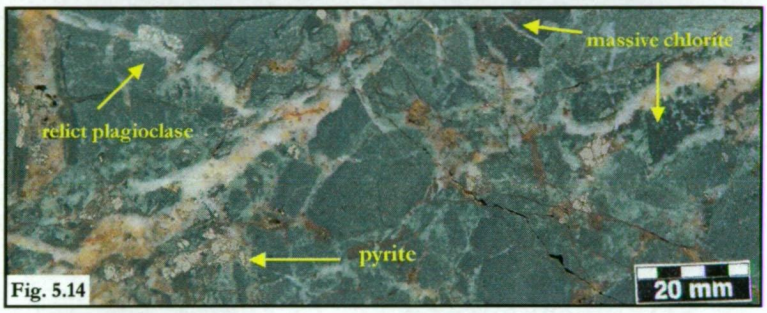

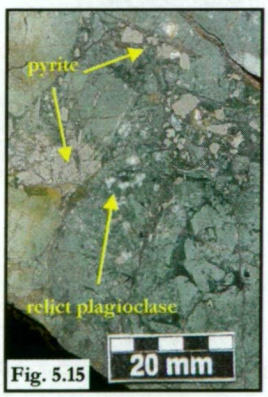

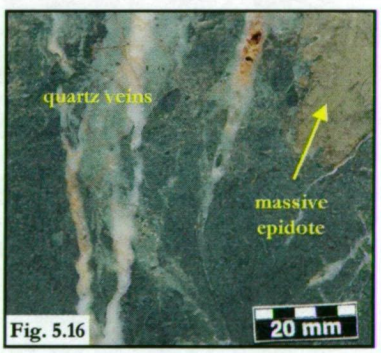

Figure 5.13: Central outcrop zone of the vein and breccia, quartz-chlorite (VQC) alteration facies at East Mt Martin (Site 2C). The VQC facies rocks are prominently exposed, in contrast to the eroded host rocks that surround the outcrop. The narrow valley (left of view) coincides with the strike of the Major Lake Fault Zone (Figure 5.12).

Figure 5.14: Narrow, irregular quartz veins and fine- to medium-grained pyrite are abundant in the chloritised groundmass of this altered dolerite. The massive, dark greenish-black chlorite patches and variable oxidation (staining) of quartz veins are also typical features of the vein and breccia, quartz-chlorite facies (sample MCQ-222 from the Lusitania Bay escarpment, Site 2D).

Figure 5.15: Subhedral pyrite crystals have partly replaced the intensely altered basaltic groundmass in this sample from the vein and breccia, quartz-chlorite alteration facies. Pyrite occurs mainly as medium- to coarse-grained, massive intergrowths or isolated crystals. Although chlorite and epidote alteration is widespread, pale plagioclase grains commonly occur as relict phenocrysts in the groundmass (sample MCQ-208 from Lusitania Bay, Site 2D).

Figure 5.16: A strongly altered sample from the sheeted dyke complex at Lusitania Bay (Site 2D). The fine-grained, bluish-green groundmass is intensely chloritised and massive epidote patches, narrow quartz veinlets, and minor disseminated pyrite are common (sample MCQ-229).

Discrete, major quartz veins

Discrete quartz veins 5–10 mm-wide (average) are very abundant at all outcrop sites of the VQC facies (Figure 5.20). These veins are well defined anastomosing structures that commonly have narrow off-shoots and multiple branching segments. Most veins randomly pinch and swell along-strike, and some thicker segments comprise 20–50 mm-wide quartz-rich 'blows'. Similar to the massive alteration patches, many wider vein segments also host angular breccia fragments of altered basalt.

Irregular quartz veinlet arrays (stockworks)

Interconnected networks of fine quartz veinlets are a common component of the VQC facies, although their abundance and intensity varies between each site. Dense veinlet arrays and stockwork zones are widespread in most outcrops, and some have > 100 veinlets/m^2. Individual veinlets are mostly curvi-planar and < 5 mm-wide, although veinlet thickness typically varies along-strike (Figure 5.21). Veinlet continuity is also highly variable, and many narrow dendritic branches have abrupt terminations in the surrounding wall rock.

Narrow, focussed quartz vein (NQV) facies

The quartz-rich mineral assemblage and hydrothermal textures of the narrow, focussed quartz vein (NQV) facies have many similarities with the VQC facies. The NQV facies is also strongly focussed within structural conduits; all outcrops are subparallel zones with similar physical features, mineral compositions, and magnetic susceptibilities (Figure 5.4) as the VQC facies. However, several major differences warrant the distinct facies classifications presented here. The NQV facies does not have an intimate spatial relationship with the Major Lake Fault, and the five known outcrops (Sites 2E, 2F, 2G, 2H, and 2J; Figure 5.1 and Table 5.2) all occur in the regionally altered footwall block of the MLFZ, i.e., the SBSD and the Zone BVI extrusive domains (Figure 5.1). In addition, the scale and spatial dimensions of NQV facies outcrops are commonly an order of magnitude less than the exposed alteration zones of the VQC facies (Table 5.2). The NQV facies also has a more diverse range of structural hosts (conduits); these include brittle faults and fractures, and discrete dyke margins (Figure 5.22).

Quartz veins, wall rock breccias (chloritised basalt fragments in quartz cement), and irregular domains of massive quartz alteration are the diagnostic features of the NQV facies. Discrete major veins (Figure 5.17) and fine quartz stockwork arrays (Figure 5.20) have similar characteristics as those previously described for the VQC facies. Minor epidote veinlets (~ 1–2 mm-wide) are also associated with quartz alteration in the NQV facies. Very fine-grained pyrite is sparsely disseminated in some quartz veins and altered basalt fragments, although most sulfide minerals are now strongly oxidised (weathered).

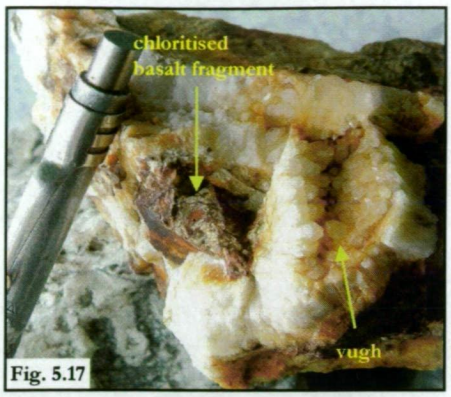

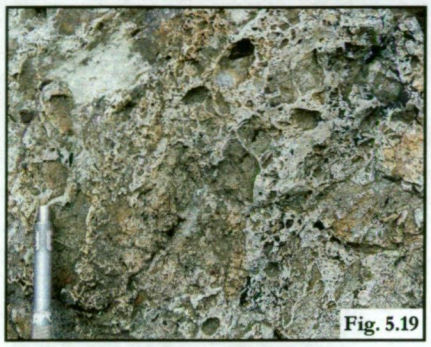

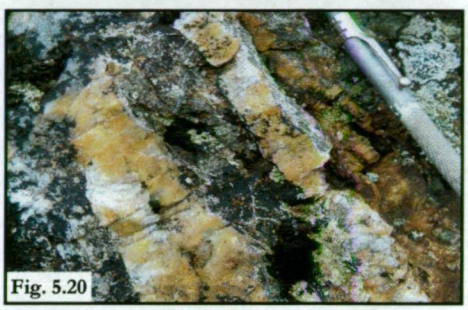

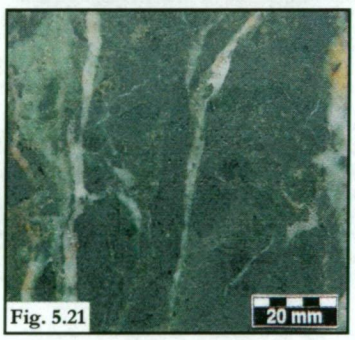

Figure 5.17: Elongated, crystal-lined cavities are common in quartz veins and massive alteration patches from the vein and breccia, quartz-chlorite (VQC) facies and the narrow, focussed quartz vein (NQV) facies. In this sample, a strongly chlorite-altered breccia fragment of basaltic wall-rock occurs near a vuggy cavity in quartz cement (sample MCQ-261 from Tio south, Site 2F).

Figure 5.18: Massive quartz alteration pervasively overprints the basaltic groundmass in this outcrop of the vein and breccia, quartz-chlorite (VQC) facies at East Mt Martin (Site 2C). This ~ 30 cm-wide zone also hosts angular breccia fragments and is cross-cut by late-stage quartz veins.

Figure 5.19: Massive, quartz-altered pillow basalt from the Sandell Bay escarpment (Site 2J) contains abundant breccia fragments of chloritised wall rock. Many basaltic fragments are eroded from the quartz matrix, resulting in the distinctive honeycomb-textured weathering surface shown here.

Figure 5.20: Steeply dipping, subparallel quartz veins in strongly altered pillow basalt at Major Lake south (Site 2H). These discrete major veins show many features typically associated with both the vein and breccia, quartz-chlorite facies (VQC), and the narrow, focussed, quartz vein facies (NQV); narrow, crystal-lined vughs and oxidation staining are especially prominent.

Figure 5.21: Thin, irregular quartz veinlets cut across the chlorite and epidote altered groundmass of this dolerite sample. Typical features of the vein and breccia, quartz-chlorite alteration facies include the discontinuous, branching veinlet arrays, along-strike variations in vein widths, and sharp vein terminations in the groundmass (sample MCQ-229 from Lusitania Bay, Site 2D).

Figure 5.22: A prominent outcrop of the narrow, focussed quartz vein alteration facies at Tio east (Site 2G) on the central plateau. A 50–70 cm-wide zone with abundant massive and veined quartz occurs in a small-scale fault that cuts across the regional pillow basalt package (the Zone BVI association). This subplanar alteration zone strikes NNW and dips 75° W (view looking south).

The orientation of quartz veins from the different outcrop sites of the NQV and VQC facies closely correlates with the dominant trend of their (local) host structures (Figure 5.23 and Table 5.2). Most quartz veins in the VQC facies at Sandell Bay creek (Site 2A), Major Lake foreshore (Site 2B), East Mt Martin (Site 2C), and the Lusitania Bay escarpment (Site 2D) are moderately to steeply dipping and strike NNW to N. This orientation is similar to the trend of the Major Lake Fault and nearby sheeted dykes in the footwall domain, although many quartz veins are steeper than the moderately dipping intrusive rocks (both discrete and sheeted dykes) (Figure 5.3). An anomalous set of quartz veins from Major Lake foreshore (Site 2B) have the only significant variation from the dominant structural trend. This vein array mainly strikes ENE; dips are moderate to steep and towards the SSE. However, a subordinate group of quartz veins from Site 2B are oriented similar to the MLFZ; thus, the two dominant vein groups at this locality are suborthogonal. Quartz veins in the NQV facies outcrop at Major Lake South (Site 2H, a small-scale alteration zone formed at the margins of a discrete 1 m-wide dyke) also have a similar orientation to their local structural host, i.e., N-strike direction and moderate to steep W dip (Table 5.2 and Figure 5.23).

Foliated, massive chlorite (FMC) facies

Altered rocks from the foliated, massive chlorite (FMC) facies are very susceptible to weathering and only two sites were identified on Macquarie Island. The best exposure occurs at Sandell Bay creek (Site 2A)*, where a 55 m-long and 10 m-wide valley-hosted outcrop coincides with the deeply eroded escarpment (Figure 5.2 and Figure 5.24 - Insert A)❖. Although much of the valley is covered by *in situ* talus and alluvium, active erosion has exposed several relatively fresh outcrops. A detailed overview of altered rocks in the FMC facies is presented here, including their intimate hydrothermal and structural relationships in the central zone of the Major Lake Fault. Highly weathered, clay-rich exposures (probable subcrop?) of altered and deformed FMC facies rocks also occur rarely in the steep fault slope at Major Lake foreshore (Site 2B) (Figure 5.11). However, these low-lying subcrops are extensively covered by soil and scree (very poorly exposed), and are also difficult to access because of the steep terrain; hence, no detailed work was undertaken at this location.

The FMC facies is intimately associated with the ~ 10 m-wide, highly deformed core of the Major Lake Fault Zone (Figure 5.25 - Insert B). This NNW-striking structural corridor mainly consists of intensely fractured fault breccia with a very distinctive and well developed, subparallel foliation (McClay, 1987). Moderate to intense clay and chlorite (?) alteration is widespread in the central fault zone, and variably affects both the fault matrix and breccia fragments (Figure 5.26).

* The other main outcrop zone of the FMC facies occurs at Caroline Cove (Chapter 5.4).

❖ There are three x A2-size field maps referred to in Chapter 5, and these are included in the map pocket at the back of this thesis, i.e., Figure 5.24 – Insert A, Figure 5.25 – Insert B, and Figure 5.58 – Insert C.

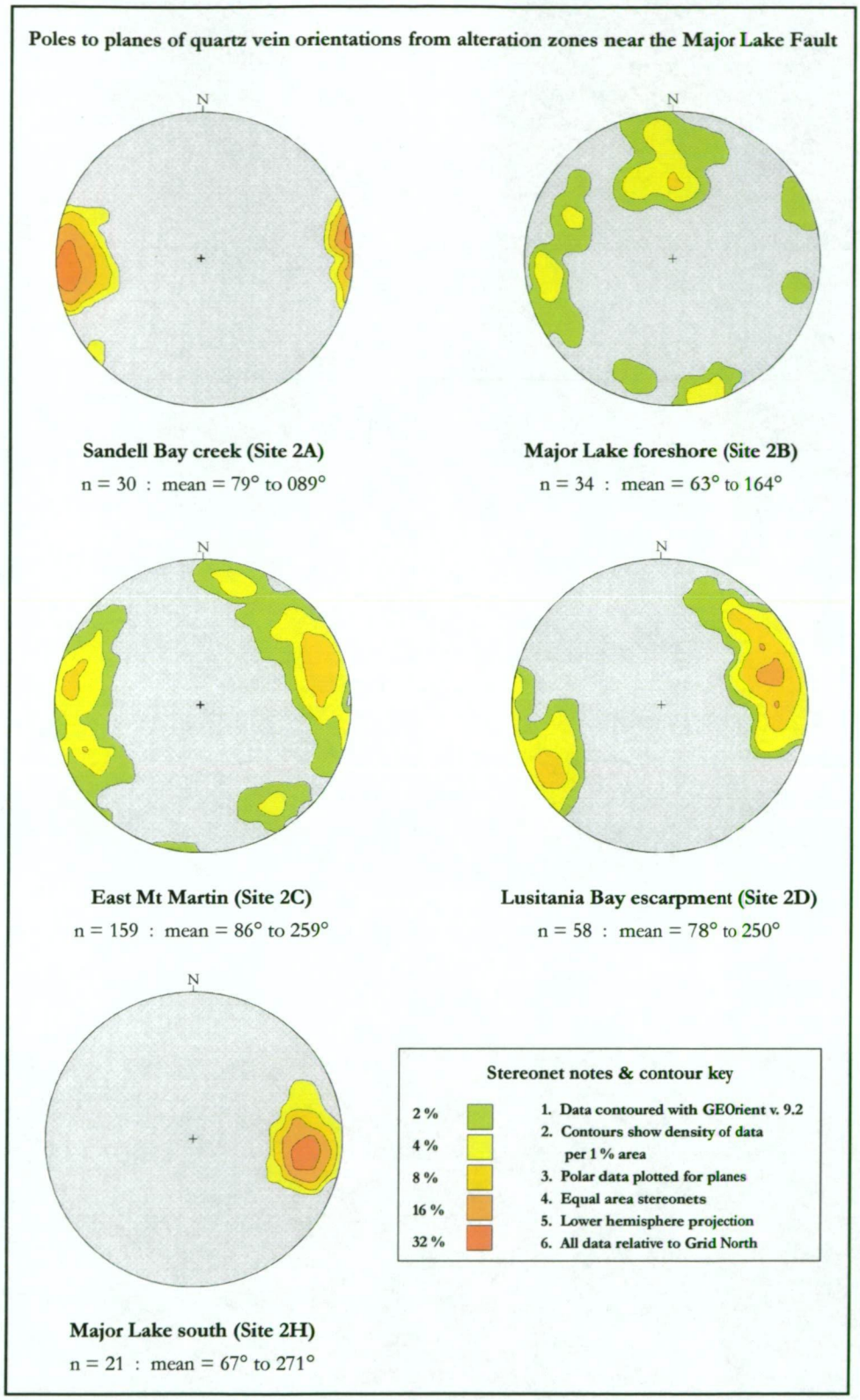

Figure 5.23: Contoured stereographic projections of quartz veins (poles to planes) from discrete sites of focussed hydrothermal alteration in the Major Lake – Mt Martin district. The four sites on the Major Lake Fault Zone (Sites 2A to 2D) host the vein and breccia, quartz-chlorite (VQC) alteration facies, whereas the narrow, focussed quartz vein (NQV) alteration facies occurs at Major Lake south (site 2H). Most quartz veins are steeply E- or W-dipping and strike NNW to N; the only exception are the group of ENE-striking veins from the Major Lake foreshore (site 2B), which are suborthogonal to the dominant vein trend (most dip S).

Narrow clay-rich seams (closely associated with the pervasive structural fabric) are especially common in the FMC facies, and many have well preserved slickenlines and fault plane striations. The finely foliated, fault zone breccia of the FMC facies comprises elongated and irregular wall rock fragments (most are < 30 mm in diameter, with an average size of ~ 2–10 mm) in very fine-grained clay gouge matrix. The altered and highly fractured wall rock fragments are subangular to angular and most have dark greenish-black, very fine- to fine-grained basaltic groundmass. Fine-grained pyrite is also sparsely disseminated in the chloritised fault zone matrix, and forms rare wispy veinlets.

The dominant orientation of the brecciated fault zone fragments varies along-strike in the outcropping valley section (Figure 5.25 - Insert B). However, most foliated fragments are moderately to steeply dipping and subparallel to the Major Lake Fault Zone, mainly striking NNW to NNE. A subordinate set of subvertical, foliated breccia fragments strikes E to SE, and are locally abundant along several 3–5 m-long sections that are parallel to the MLFZ (see the contoured stereonet data in Figure 5.25 - Insert B). Narrow seams of dark greenish-black, clay-rich gouge also occur in the foliated matrix; these are commonly subparallel to the orientation of the Major Lake Fault.

The FMC facies also hosts many moderately to steeply dipping veins and veinlets (contoured stereonet data in Figure 5.25 - Insert B). Most are 2–5 mm-wide (up to ~ 10 mm) and have pale greenish-white prehnite-rich cement. Prehnite is massive and fine-grained, and some thicker vein segments contain small crystal-lined vughs (< 2 mm-wide) and fragments of dark greenish-black wall rock (strongly altered). Individual vein segments are commonly subplanar, although many have anastomosing projections and contain multiple off-shoots (veinlets) that obliquely branch away from the main strand. Prehnite-rich veins clearly post-date clay and chlorite alteration (evidenced by the presence of altered breccia fragments in the prehnite cement) but, similar to the fault zone matrix, most are finely brecciated subparallel to the main foliation (Figure 5.27).

Although most rocks in the FMC facies are finely brecciated, the exposed core of the Major Lake Fault Zone (MLFZ) contains fractured wall rocks that lack the distinctive foliated appearance. These irregular and blocky outcrop fragments consist of dark grey-green, clay- and chlorite-altered basalt (similar to the fault breccia, e.g., Figure 5.28), and most are cross-cut by numerous small faults and fractures. However, two anomalously large (~ 2–4 m-long) 'exotic' rock fragments also outcrop prominently in the lower-valley section (Figure 5.25 - Insert B and Figure 5.29). These large and highly fractured blocks lack the typical clay and chlorite alteration assemblages and finely foliated breccia common throughout the MLFZ. Instead, they have a well preserved primary igneous texture comprising weakly altered plagioclase phenocrysts and minor altered olivine pseudomorphs (moderately porphyritic rocks) in slightly oxidised, prehnite-veined groundmass (brownish-grey). The 'exotic' basalt blocks are significantly more prominent (less eroded) than the surrounding foliated fault zone outcrop. Shallow to moderately SE-dipping

dextral faults and NW-striking reverse faults bound the large rock fragments, and brittle faults and fractures dissect their non-foliated interiors (Figure 5.29). Angular basalt fragments with similar alteration mineral assemblages (i.e., relatively weakly regional alteration assemblages) are also sparsely distributed in the fault zone. These smaller blocks range from < 10–100 mm across, and have an average size of 20–50 mm.

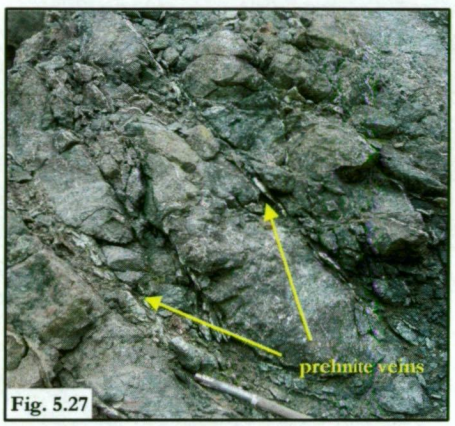

Figure 5.26: At Sandell Bay creek (site 2A) moderately to strongly altered basalt of the foliated, massive chlorite (FMC) alteration facies occurs in the central deformation zone of the Major Lake Fault. The FMC facies rocks are highly fractured and many have a characteristic foliation trend. Angular, elongated breccia fragments occur commonly in the fine clay-gouge matrix, and striated faults are also abundant.

Figure 5.27: Narrow veinlets of pale, massive prehnite commonly cut across the highly fractured wall-rocks of the foliated, massive chlorite facies in the Major Lake Fault Zone. Similar to altered basalt in the main fault-zone, many prehnite veins are also finely brecciated and foliated by discrete late-stage (post-hydrothermal) faults and fracture zones.

Figure 5.28: Deformation intensity is heterogeneous in the central corridor of the Major Lake Fault Zone, and many outcrops of the foliated, massive chlorite (FMC) alteration facies are not finely brecciated. The fractured but non-foliated blocks of altered FMC basalt shown here outcrop in the lower south wall of the Sandell Bay creek (site 2A), and are surrounded by foliated clay-gouge. The brecciated fault matrix is very susceptible to erosion; it outcrops less prominently in the creek valley than coherent basalt blocks.

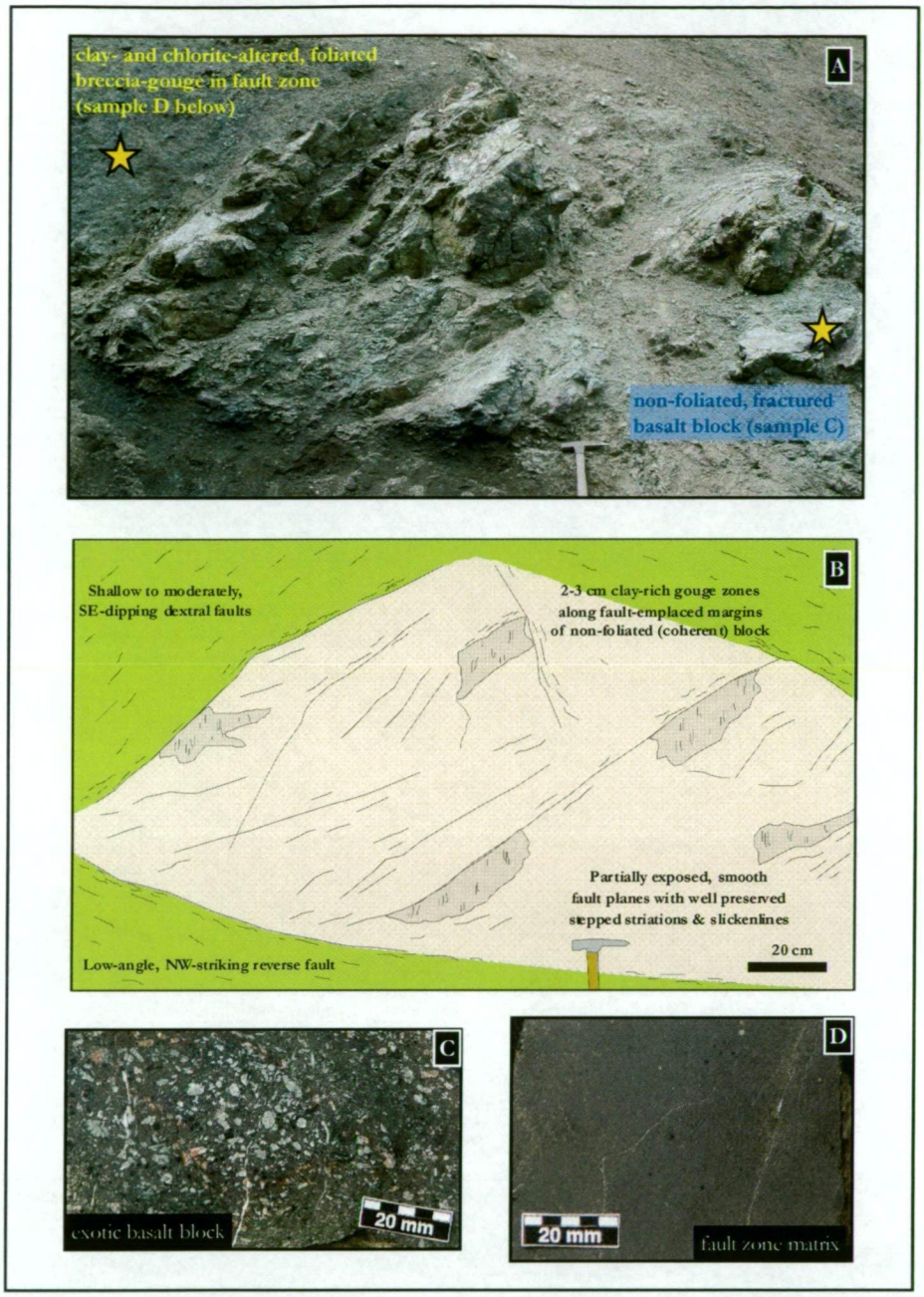

Figure 5.29: Outcrop photograph (A) and interpretative sketch (B) of an 'exotic' basalt block exposed at Sandell Bay creek (Site 2A, refer to Figure 5.25 – Insert B for location). This large breccia fragment occurs in the central deformation zone of the Major Lake Fault, and is completely surrounded by finely foliated and pervasively clay- and chlorite-altered fault matrix (typical of the foliated, massive chlorite (FMC) facies). The 'exotic' basalt block is relatively less altered than the surrounding fault zone matrix, and there are many significant textural and mineral differences between the two rock types, e.g., distinct variations in the abundance and type of igneous phenocrysts, and the alteration mineral assemblages (as shown in the comparative hand-sample photographs in C and D). Although the 'exotic' block is highly fractured, the basalt is relatively coherent and lacks the fine foliation of the breccia-gouge zone. This large rock fragment is emplaced in the central deformation corridor of the Major Lake Fault Zone along well defined NE-striking dextral faults and NW-striking reverse faults. Most fault margins are highly fractured and have gouge seams and matrix-dominated breccia zones; however, they lack fault-specific hydrothermal assemblages and veins. Unusual geological relationships as shown here provide clear evidence that the Major Lake Fault Zone has a complex evolutionary history involving multiple stages of hydrothermal, magmatic, and tectonic activity (refer to accompanying text for further discussion).

The magnetic susceptibility of many coherent wall rock fragments in the FMC facies (such as the large, non-foliated outcrop blocks shown in Figure 5.29) contrasts significantly with the regionally altered footwall rocks (i.e., the upper greenschist to lower amphibolite facies rocks of the Sandell Bay Sheeted Dyke Swarm) and the fault-proximal rocks of the vein and breccia, quartz-chlorite facies. Most non-foliated FMC rock fragments have relatively high magnetic susceptibilities of 500–2000 x 10^{-5} SI units (Figure 5.4), indicating that primary Ti-magnetite in the basaltic groundmass is relatively pristine, and that many of these rocks are not pervasively altered. Intense chlorite alteration (e.g., in the basaltic groundmass of the VQC facies) is typically associated with very low magnetic susceptibility values, due to the widespread destruction (alteration) of igneous-derived Ti-magnetite. The relatively high magnetic susceptibility of many FMC facies rocks is similar to values obtained for weakly altered pillow basalt (Zone BIV domain) situated north-east of the Major Lake Fault Zone (Figure 5.4). These comparable magnetic signatures provide evidence to suggest that the central deformation zone of the Major Lake Fault (the valley-hosted exposure of highly fractured, brecciated, and foliated FMC facies rocks) mainly formed by tectonic disruption of the hangingwall pillow basalt package, i.e., deformation mostly affected the Zone BIV volcanic rocks. Furthermore, this hydrothermal – structural relationship may also indicate that the alteration processes which formed the FMC facies may have overprinted pre-existing regional alteration assemblages (zeolite grade) in the Zone BVa hangingwall package.

Importantly, the foliated, massive chlorite facies also contains other 'exotic' rock fragments within its brecciated fault zone matrix, although these are less prominent than the plagioclase-phyric basalt blocks (described above). Of special significance are small, angular fragments of quartz-veined basalt typical of the VQC alteration facies. These 10–30 mm-wide fragments are sporadically distributed in the brecciated matrix of the FMC facies, and are most abundant near prominent enclaves of VQC facies alteration in the adjacent footwall. The presence of these altered rock fragments has critical implications for the genetic relationship and relative timing of the juxtaposed FMC and VQC facies, and suggests that they have formed during temporally distinct hydrothermal and structural episodes. The significance of these relationships and their genetic associations are further discussed in Chapter 5.6, although the crucial point here is that the formation of the VQC facies clearly pre-dated the FMC alteration assemblage.

Brittle structural discontinuities are an important component of the FMC facies; they reflect the intimate spatial association and genetic relationship with the Major Lake Fault Zone. Discrete faults of variable size and fracture intensity are abundant in the foliated breccia matrix and in the non-foliated outcrop blocks (all fault zone alteration styles). Individual faults are moderately to steeply dipping, and structural styles and orientations vary along different segments of the MLFZ (Figure 5.25 - Insert B). Based on fault kinematics (as recorded from structural indicators such as clay and chlorite slickenlines), four distinct fault groups are recognised at Sandell Bay creek (Site 2A; Table 5.3).

Table 5.3: Summary of fault groups associated with the foliated, massive chlorite alteration facies in the Major Lake Fault Zone.

Fault type	Number of faults measured	% of total faults in the MLFZ	Mean orientation	Mean slickenline orientation	Comments
Dextral to dextral-oblique	33	28 %	43° to 143°	01° to 057°	There are three main fault orientation groups, with the dominant group comprising moderately, SE-dipping faults. The secondary fault groups are (respectively) moderately and steeply, S- to SW-dipping, and moderately NW-dipping. Dextral faults are also relatively early (commonly cross-cut by other faults), and many are associated with prehnite veins.
Sinistral to sinistral-oblique	31	26 %	63° to 290°	11° to 024°	Most are moderate to steep, WNW- to NW-dipping faults. A minor group of steep to very-steep, NE- or SW-dipping faults also occur. Thick breccia-gouge seams are common.
Reverse to reverse-oblique	31	26 %	47° to 085°	53° to 072°	Moderately ENE- to E-dipping faults are common, although a subsidiary set of steep S- to SW-dipping faults also occurs. Most of the oblique-slip component is dextral. Many reverse faults clearly pre-date the other fault orientations; they are commonly overprinted.
Normal to normal-oblique	24	20 %	79° to 041°	72° to 031°	A tightly constrained group of steep to very steep, NE- or SW-dipping faults. Most normal faults post-date the reverse and dextral fault groups, although variations occur.

Notes:
1. The fault orientation data is shown here as dip and dip direction and striation data is shown as amount of plunge and trend (converted using GeoCalculator software from fault plane pitch angles measured in the field).
2. Contoured stereonet projections of these data are shown in Figure 5.30.
3. These data were recorded from the 55 m-long creek valley transect undertaken in the Major Lake Fault Zone. The along-strike distribution of fault orientations is presented in Figure 5.25 – Insert B.

Dextral to dextral-oblique faults are most abundant in the core of the MLFZ (28 %), although reverse and sinistral faults are also relatively common (both account for 26 % of total faults; Table 5.3). Contoured stereonet projections of the structural data (poles to fault planes) show two main suborthogonal orientations (Figure 5.30). These trends are broadly similar to the breccia foliations in the Major Lake Fault Zone (refer to stereonets in Figure 5.25 - Insert B); relatively early NE- to SE-striking faults (mostly dextral- and sinistral-oblique faults) are overprinted by faults that are mostly subparallel to the NW–NNW strike of the MLFZ (especially for steeply dipping normal- and sinistral-oblique faults). Comparable structural orientations also link the late prehnite vein stage of the FMC facies (Figure 5.25 - Insert B) with the dextral to dextral-oblique fault group.

Several cross-cutting and overprinting structural relationships occur in the FMC facies, attesting to the complex, multi-stage tectonic evolution of the Major Lake Fault Zone. Although relative timing relationships between discrete fault groups are difficult to ascertain (e.g., commonly obscured by soil or scree, or lack direct outcrop interaction), several consistent associations are recognised. In general, reverse- and dextral-oblique faults are relatively early structures that pre-date most normal and sinistral faults. These relationships are not consistent for all outcrop sections however, and notable variations occur, e.g., some normal faults are cross-cut by sinistral faults. The normal and dextral faults are also more closely associated with discrete veins (e.g., prehnite), and sinistral faults commonly have the most extensive (thickest) clay-gouge seams (although breccia and gouge zones are commonly associated with each fault group).

Detailed mapping of the FMC facies in the Sandell Bay creek also identified a previously unknown structural component of the Major Lake Fault Zone. At the mid-escarpment level (~ 100 m above sea-level) a steep ESE-dipping fault cuts across and displaces the Major Lake Fault (Figure 5.25 - Insert B and Figure 5.31). This high-angle structure is well defined by a 20–50 cm-wide zone comprising brecciated wall rock fragments in clay gouge matrix. Prominent striations are common on discrete clay seams and indicate mostly dextral to dextral-oblique movement along shallow S- to SSW-plunging slickenlines. Hydrothermal veining and fault zone alteration is not intimately associated with this NNE-striking cross-fault. Although the total amount of offset is unknown, the MLFZ (and associated VQC and FMC facies rocks) is not exposed further down-slope along its projected NNW trend, or on the nearby Sandell Bay beach (Figure 5.32). Instead, the lower escarpment slopes host a tightly packed sequence of pillow basalt variably intruded by dolerite dykes (discrete, steeply dipping dykes and not part of the Sandell Bay Dyke Swarm). The host rocks, structural features, and alteration assemblages in the outcropping lower slope are significantly different from those in the upper escarpment. These relationships clearly indicate that the NNE-striking fault is a major terminating margin of the MLFZ (also the VQC and FMC facies). Furthermore, the absence of focussed hydrothermal assemblages suggests that the NNE fault is unlikely to represent an active transfer structure during formation of the MLFZ, i.e., it probably formed during uplift tectonism.

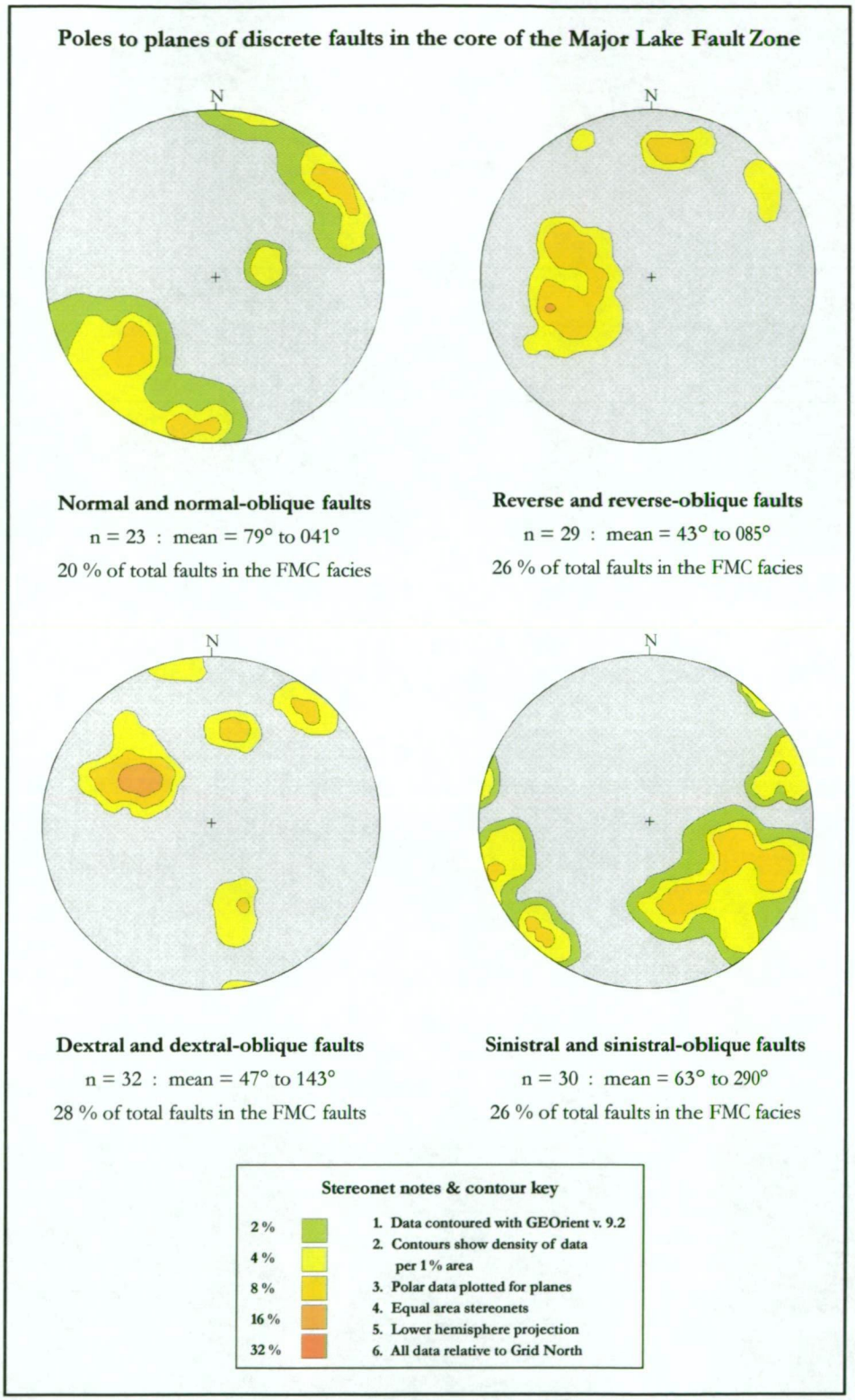

Figure 5.30: Contoured stereographic projections (poles to planes) of the main fault groups identified from the foliated, massive chlorite (FMC) alteration facies. The four structural associations shown here occur in approximately equal abundance (~ 20 to 25 % each), although the preferred orientation of each group is distinctive. All data were collected from the 55 m-long valley-hosted outcrop at Sandell Bay creek (Site 2A), which coincides with the only known exposure of the Major Lake Fault Zones central deformation corridor.

Figure 5.31: The escarpment valley at Sandell Bay creek (site 2A) coincides with the Major Lake Fault Zone (MLFZ) and its associated alteration facies. In this view of the southern valley wall (~ 100 m above sea-level) the strongly altered rocks of the foliated, massive chlorite facies (hosted in the MLFZ) are cross-cut by a steeply dipping, NNE-striking breccia-gouge fault. This fault has displaced the MLFZ and the FMC facies (amount of off-set unknown), and a coherent pillow basalt package that lacks intense fault-zone alteration and structural deformation occurs further down-slope.

Figure 5.32: The NNE-striking cross-fault that terminates the Major Lake Fault Zone (MLFZ) occurs mid-way down the steep west coast escarpment. The MLFZ, and the altered rocks of the vein and breccia, quartz-chlorite facies and the foliated, massive chlorite facies only occur in the upper section of the slope.

Major Lake Fault Zone summary

Chapter 5.3 has focussed on the structurally controlled alteration facies associated with the Major Lake Fault Zone, the most significant spreading-related fault investigated during this study. To provide the initial context for this structural system I outlined the spatial distribution of the Major Lake Fault Zone (MLFZ) and the key study locations, and then presented the main geological characteristics of the local footwall and hangingwall rocks. However, the main purpose of Chapter 5.3 was to describe the outcrop and hand-specimen characteristics of focussed alteration facies associated with the MLFZ (the VQC and FMC facies), and also the smaller-scale alteration assemblages hosted in the regional footwall rocks, i.e., the NQV facies in the Sandell Bay Sheeted Dyke Swarm and the Zone BVI volcanic rock domain. Some genetic interpretations have also been briefly canvassed here, although important geological, structural, and hydrothermal relationships are further discussed in Chapter 5.6.

5.4. Altered rocks from the Caroline Cove Fault Zone

Geographic distribution and regional context

The Caroline Cove region (Site 3A), situated at the far south-western end of Macquarie Island (Figure 5.33), hosts a very distinctive association of altered basaltic rocks. Three focussed alteration facies occur here; the massive and veined, chlorite-quartz-pyrite (CQP) facies, the foliated, massive chlorite (FMC) facies, and the pervasive, Fe-oxyhydroxide overprint (PFO) facies (Table 5.1). These moderately to intensely altered rocks are variably exposed in the lower reaches of the Caroline Creek valley and several nearby foreshore cuttings (Figure 5.34).

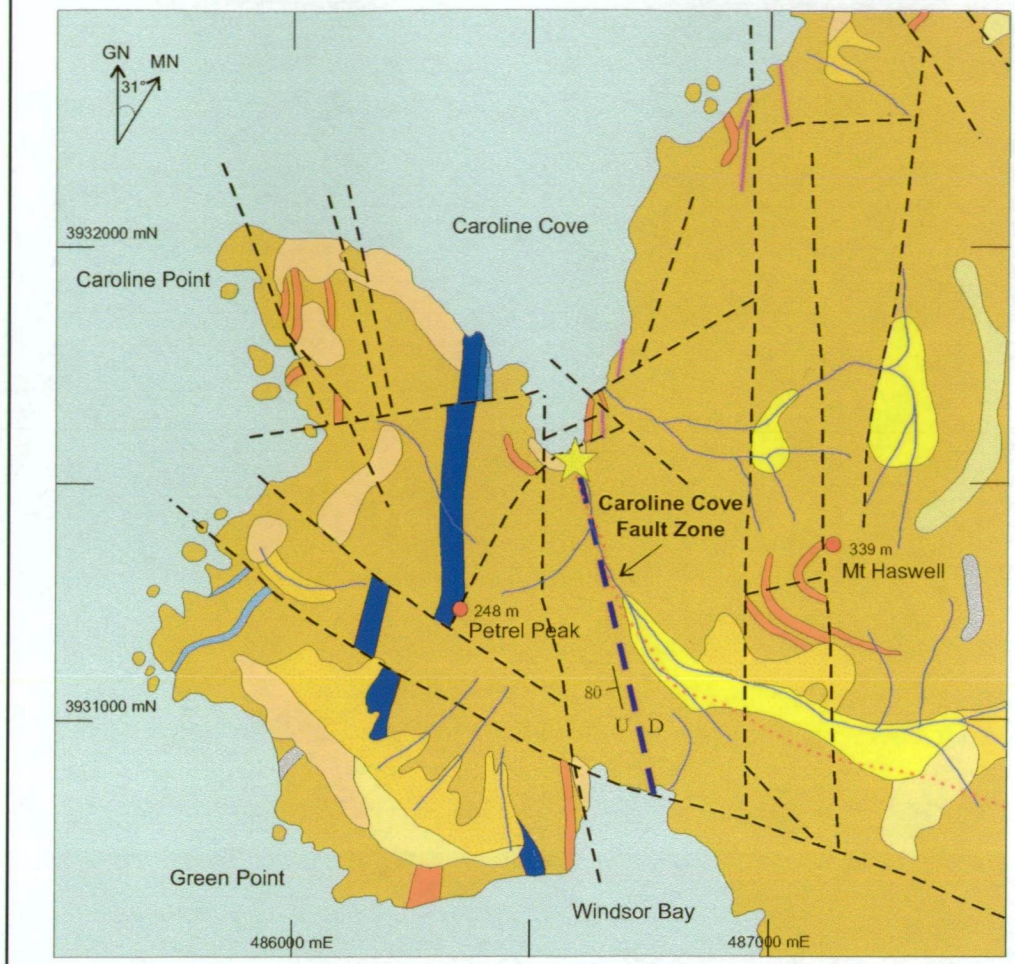

Geology of the Caroline Cove region

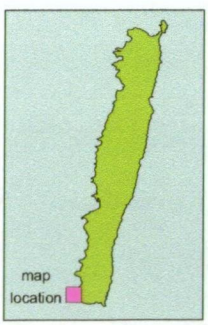

Scale 1:16,000

0 meters 500

Projection: UTM Zone 57 S
Datum: WGS-84
Contours: Not shown

This map is modified from map sheet 7 in the 1:10,000 Macquarie Island map series produced by Mineral Resources of Tasmania (1998). Geological data is based on field mapping by Ben Goscombe and John Everard (Tasmanian Geological Survey). Most faults are interpreted from topographic features (lineaments) evident on airborne photographs and satellite imagery. Hence, the direction and magnitude of displacement is largely unknown for most faults shown here.

Legend

Aeolian sands	Mudstone	Discrete dykes
Alluvium	Sandstone	Fault (interpreted)
Beach deposits	Conglomerate	Study site (3A)
Colluvium	Volcanic breccia	Creek
Palaeo-beach deposits	Pillow basalt	Spot height
Scree slope deposits	Massive flow basalt	Walking track

Figure 5.33: Geology map of the Caroline Cove region showing the location of the Caroline Cove Fault Zone and the main study area (Site 3A, refer to Figure 5.34 for detailed site geology). The terrain is very rugged around the coastline and on the plateau, and pillow basalts from the Zone BVI extrusive domain (Hurd Point association) are widespread in the local area.

Geology of Caroline Cove (Site 3A)

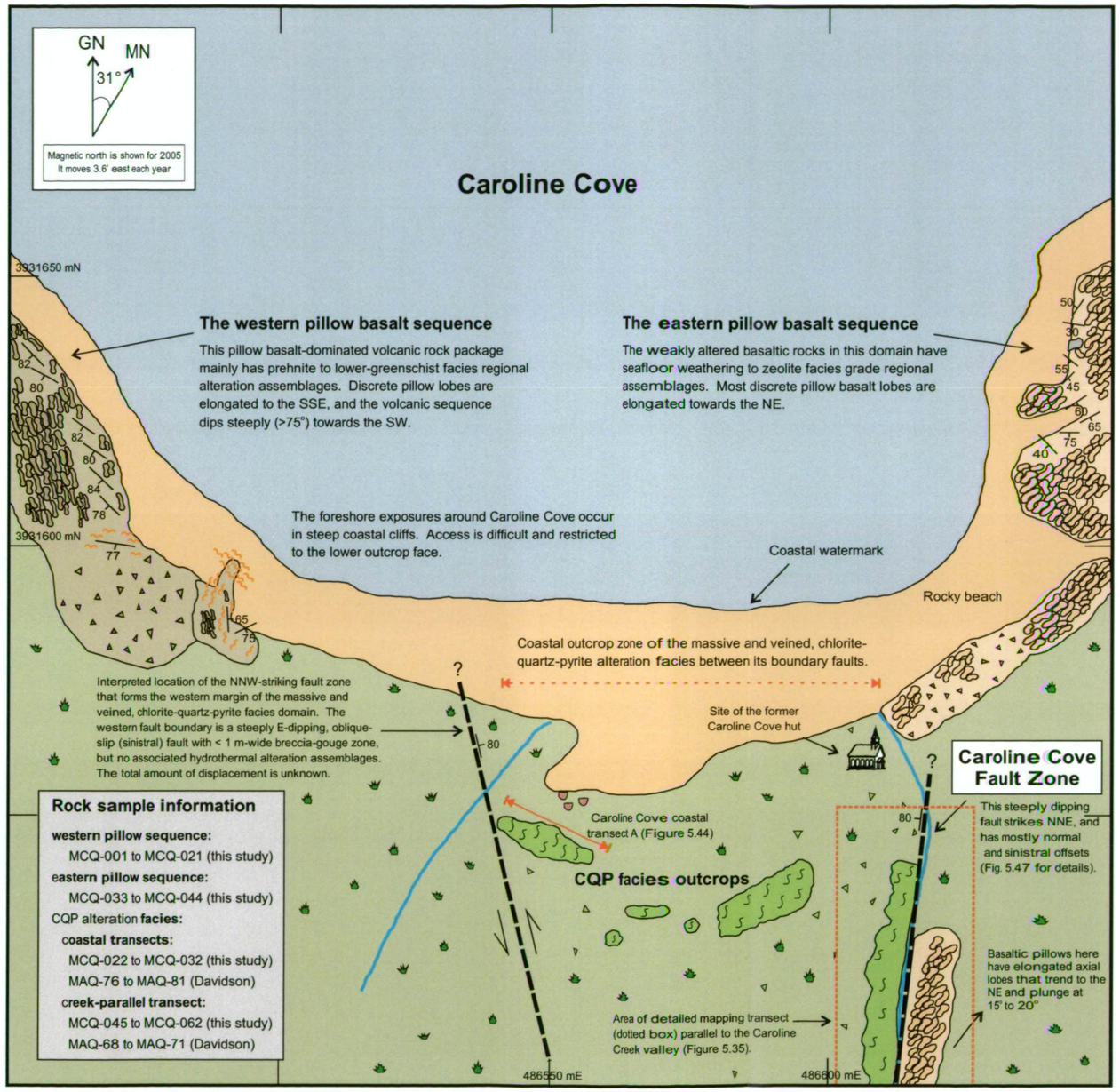

Legend

- Altered basalt with distinctive massive and veined chlorite-quartz-pyrite facies mineral assemblages and textures - outcrop & scree
- Western pillow basalt sequence - outcrop & scree
- Eastern pillow basalt sequence - outcrop & scree
- Dolerite dyke
- Prehnite veins
- Orientation of minor outcrop fault
- Interpreted fault trend
- Vegetation cover - mostly coastal tussock
- Rocky beach and shoreline
- Creek
- Tri-pots (archaeological relic)

Scale 1 : 1000

0 meters 50

Projection: UTM Zone 57 S
Datum: WGS-84
Contours: Not shown
Survey control: Garmin E-trex GPS unit
Mapping & drafting: Steven Lewis

Note:
Rock and mineral samples studied from the Caroline Cove district were collected during this project, and also during fieldwork carried out by Dr Garry Davidson in 1998 (unpublished data, also stored at the Centre for Ore Deposit Research at the University of Tasmania). Refer to Appendix 2 for further sample details.

Figure 5.34: Outcrop geology plan of the Caroline Cove foreshore showing the location of the fault-bound domain of the massive and veined, chlorite-quartz-pyrite (CQP) alteration facies. The strongly altered rocks in the CQP domain outcrop between the western and eastern pillow basalt sequences. The main deformation corridor of the Caroline Cove Fault Zone coincides with the narrow confines of the Caroline Creek valley, and several outcrops of the foliated, massive chlorite facies and the pervasive, Fe-oxyhydroxide overprint facies are well exposed in the steep valley walls (not shown here, refer to Figure 5.35 and Figure 5.47. The hydrothermal mineral assemblages and textures vary significantly between each focussed alteration facies, and there is also considerable variation in the regional alteration assemblages that occur in the western and eastern pillow basalt sequences (refer to further explanations in the text).

Outcrops in the Caroline Creek valley occur within a ~ 200 m-long section upstream of the beach (Figure 5.35), whereas the coastal outcrops form an ~ 80 m-wide zone parallel to the foreshore. Rock exposures are commonly steep and unstable, and most are also partly obscured by vegetation, organic-rich soils, and unconsolidated debris. The narrow creek valley is especially prone to major landslips, and these frequently erode and modify the outcrops. In addition, extensive weathering and oxidation imparts a brownish-red surface stain on many rocks.

The massive and veined, chlorite-quartz-pyrite (CQP) facies is the most widespread and diagnostic alteration facies at Caroline Cove. These intensely altered pillow basalts occupy a discrete structural domain in the central Caroline Cove embayment (Figure 5.34). This anomalous alteration zone is entirely fault-bound; it forms an elongated wedge juxtaposed between weakly altered pillow basalts. These adjacent volcanic rock domains (Zone BVI) have relatively low grade secondary mineral assemblages (recharge-related) and lack focussed alteration zones. Although most faulted domain boundaries are covered by vegetation and soil, the main deformation corridor of the eastern CQP facies margin (termed here the Caroline Cove Fault Zone or CCFZ) is partly exposed in several sections of the lower Caroline Creek valley (Figure 5.35). Sporadic valley-bound segments of the CCFZ host the only known sites of the FMC and PFO facies in the local area.

Host rocks of the Caroline Cove Fault Zone

Caroline Cove is situated in the Hurd Point association of the BVI extrusive domain (Goscombe and Everard, 2001). Reconnaissance examination of the coastal outcrops showed that the main focussed alteration zone (which hosts the CQP facies) is faulted against low (alteration) grade volcanic rock packages that consist of abundant pillow basalts, minor hyaloclastites, and thin sedimentary rock horizons (relatively rare). The host rocks, which completely surround the CQP facies block, are here termed (respectively) the western and eastern pillow basalt sequences (Figure 5.34). These small, localised rock domains have not previously been classified. Discrete intrusive rocks are uncommon in the area, and sheeted dyke complexes are absent. Detailed site mapping further showed significant differences in mineral compositions, outcrop attributes, and structural features between the western and eastern rock packages (Figure 5.36).

The western pillow basalt sequence

The western coastal exposures at Caroline Cove consist of a conformable sequence of tightly packed pillow basalt. Most individual pillows are elongated lobes ~ 1–2 m long and 50–80 cm in diameter. Pillow long-axes are mainly oriented SSE, and the entire volcanic rock package dips steeply SW (> 75°) (with volcanic layering, or 'pseudo-bedding', defined by the most pronounced flattened pillow plane). Thin selvages (mostly < 10 mm) of dark greenish-black basaltic glass (altered) surround the discrete pillow lobes, and many inter-pillow zones contain angular fragments of brecciated basalt (commonly 10–50 mm across).

Geology of the Caroline Cove Fault Zone

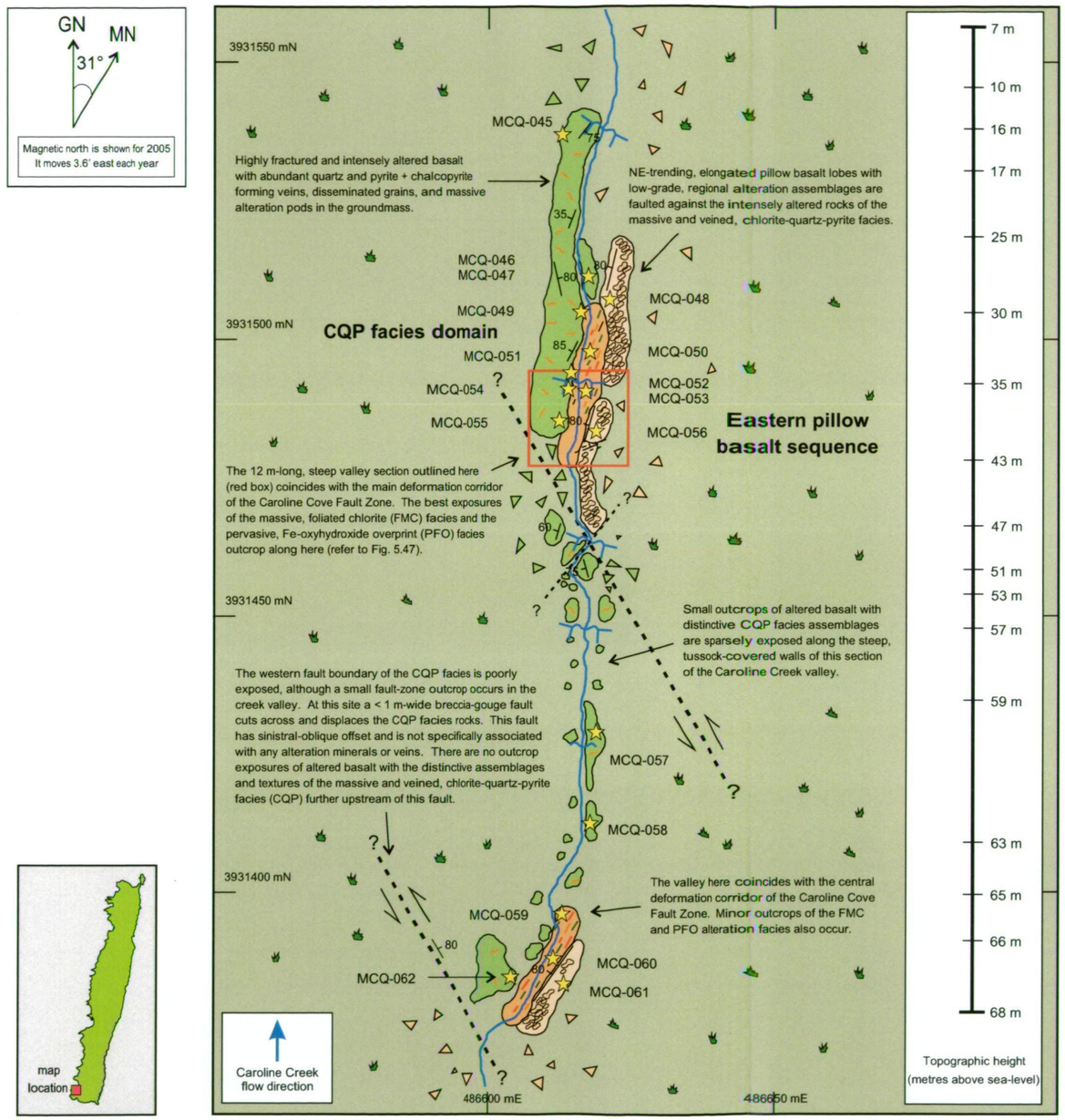

Legend

- Altered basalt with distinctive massive and veined, chlorite-quartz-pyrite alteration facies assemblages and textures - outcrop & scree
- Eastern pillow basalt sequence - outcrop & scree
- Main deformation zone of the Caroline Cove Fault, with sporadic along-strike exposures of the massive, foliated chlorite facies, and the pervasive, Fe-oxyhydroxide overprint facies
- Quartz veins
- Minor outcrop fault (oriented) — 40
- Interpreted fault (off-setting altered outcrop zones)
- Vegetation cover - mostly coastal tussock
- Caroline Creek
- Small waterfall
- Rock sample
- Sample number — MCQ-061

Scale 1 : 1000

0 meters 50

Projection: UTM Zone 57 S
Datum: WGS-84
Survey control: Garmin E-trex GPS unit
Height survey: Barigo digital altimeter
Mapping & drafting: Steven Lewis

The 180 m-long, north-trending segment of the lower Caroline Creek shown here occurs in a very steep and narrow valley. Outcrops are sporadically exposed and commonly obscured by vegetation, soil, and alluvial cover. Access is difficult and mainly restricted to the creek bed and lower-most valley walls due to the highly weathered and unstable exposures (refer to Figure 2.15 for a photographic view and Figure 5.34 for the traverse location in the valley). Since this mapping work was undertaken several episodes of mass-wasting and erosion (land-slips) have significantly modified the *in situ* exposures.

Figure 5.35: Outcrop geology and sample location plan for the lower section of the Caroline Creek (Site 3A, refer to Figure 5.34 for creek location relative to the foreshore). The Caroline Cove Fault Zone (CCFZ) outcrops at several key sites within the confines of the 180 m-long, narrow creek valley shown here. The 1–2 m-wide main deformation corridor of the CCFZ consists of highly faulted and fractured basalt and hosts the only local outcrops of the foliated, massive chlorite alteration facies, and the pervasive, Fe-oxyhydroxide overprint facies. The Caroline Cove Fault Zone also forms the boundary between the intensely altered rocks of the massive and veined, chlorite-quartz-pyrite alteration facies (the outcrop domain to the west), and the low-grade, regionally altered eastern pillow basalt sequence (eastern wall) with seafloor weathering to zeolite facies grade assemblages.

Pillow basalts in the western sequence are sparsely to moderately porphyritic (5–10 % phenocrysts), and have dark purplish-brown to brownish-grey aphanitic groundmass (Figure 5.36). Plagioclase, the most abundant phenocryst, forms pale, medium- to coarse-grained crystals with distinctive tabular or lath-like shapes. The basaltic rocks are also sparsely vesicular, and primary vughs are most abundant near aphyric pillow rims. Vesicles are commonly infilled by fine-grained secondary minerals such as pale calcite and prehnite, and soft greenish-brown clays.

Small-scale faults and fractures with 10–30 cm-wide deformation zones are common in the western pillow basalt sequence. These brittle, curvi-planar faults preferentially form in glassy, inter-pillow selvages; most lack significant displacement (< 1 m offset). Fault zones dip steeply SW and are commonly associated with subparallel prehnite-rich vein arrays and minor hydrothermal breccias (Figure 5.36). The discontinuous and irregular veins are mainly 1–5 mm-thick, although some vein widths vary up to ~ 15 mm along-strike. Veins are infilled by massive, fine-grained prehnite and minor calcite, and most proximal wall rocks are partially bleached (Figure 5.36).

The magnetic susceptibility of the rocks in the western basalt sequence varies from ~ 200–1000 x 10^{-5} SI units; average values are 800–900 x 10^{-5} SI units (Figure 5.37). Rocks with the lowest magnetic susceptibilities (< 200 x 10^{-5} SI units) typically occur in the inter-pillow selvages and veined faults. The low magnetic signature of fault zone rocks probably reflects relatively increased alteration intensity and widespread destruction (alteration) of primary Ti-magnetite in the igneous groundmass.

The eastern pillow basalt sequence

The coastal exposures east of the Caroline Cove Fault Zone are also dominated by a faulted package of extrusive rocks that mainly consist of pillow basalt, minor basalt flows, and matrix-rich breccias (Figure 5.36). Discrete, 1.0–1.5 m elongate pillow lobes trend consistently NE (suborthogonal to the western sequence), and most plunge at ~ 5°–20°. Thin selvages of altered volcanic glass surround individual pillows, and 10–30 mm pods of green and pinkish-red sedimentary ooze (siliceous material) occur in some inter-pillow zones (the sedimentary oozes are more common here than the western basalt sequence).

Basaltic rocks in the eastern sequence are aphyric to sparsely plagioclase-phyric and have brownish-grey or dark grey aphanitic groundmass. Subrounded amygdules (1–2mm diameter) occur sporadically in pillow rims, and most are infilled with soft greenish-black clays. Eastern sequence basalts have high to very high magnetic susceptibilities that commonly range from 2000–3000 x 10^{-5} SI units (Figure 5.37). These elevated magnetic signatures are significantly greater than all other rocks in the Caroline Cove district, and indicate that primary Ti-magnetite is relatively pristine.

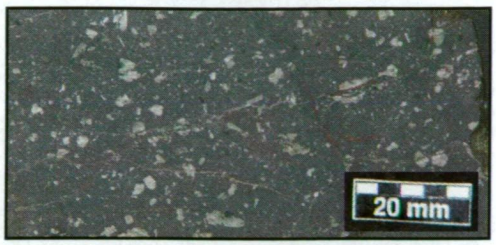

Sparsely plagioclase-phyric basalt from the western pillow basalt sequence at Caroline Cove (MCQ-004). Many igneous grains are streaked or mottled by pale greenish alteration minerals (clays); these are mostly absent from plagioclase crystals in rocks that occur in the eastern pillow basalt sequence.

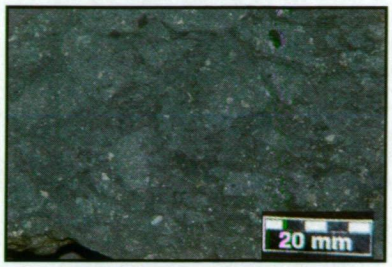

Weakly altered hyaloclastite from the eastern pillow basalt sequence. This rock consists of relatively fresh, subangular to angular basalt fragments in a dark matrix of altered volcanic glass (MCQ-038).

This small-scale, brittle fault zone occurs in the western pillow basalt sequence exposed around the Caroline Cove foreshore. The fault, which contains many narrow prehnite veinlets (subparallel), preferentially deforms the glassy matrix that separates individual pillow lobes.

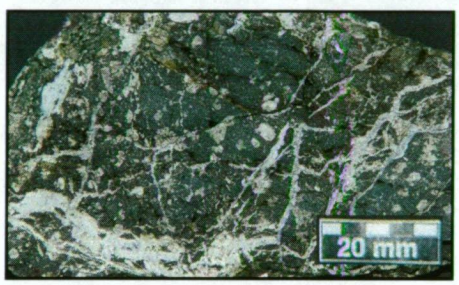

Western sequence pillow basalt from a small, local fault zone at Caroline Cove (shown opposite). The fine, irregular veinlets that cut across the bleached groundmass are prehnite-rich (sample MCQ-021).

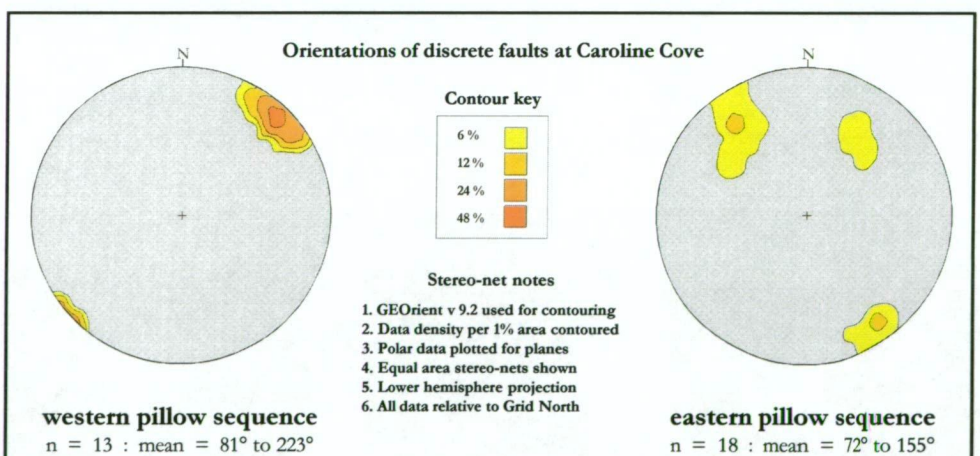

Contoured stereographic projections (poles to planes) of small-scale brittle faults and fracture zones (discrete structures) from the western and eastern pillow basalt domains in the Caroline Cove area.

Figure 5.36: Common hand-specimen and outcrop features in the western and eastern pillow basalt sequences at Caroline Cove. Significant variations in the primary igneous compositions, and the regional alteration assemblages and textures, are recognised for these different host rock domains. The contoured stereonets also show that most discrete faults have different orientations from each separate association, which further suggests that the western and eastern pillow basalt domains have evolved under different magmatic, structural, and hydrothermal conditions.

Figure 5.37: Frequency histogram of magnetic susceptibility data from upper crustal rocks in the Caroline Cove region.

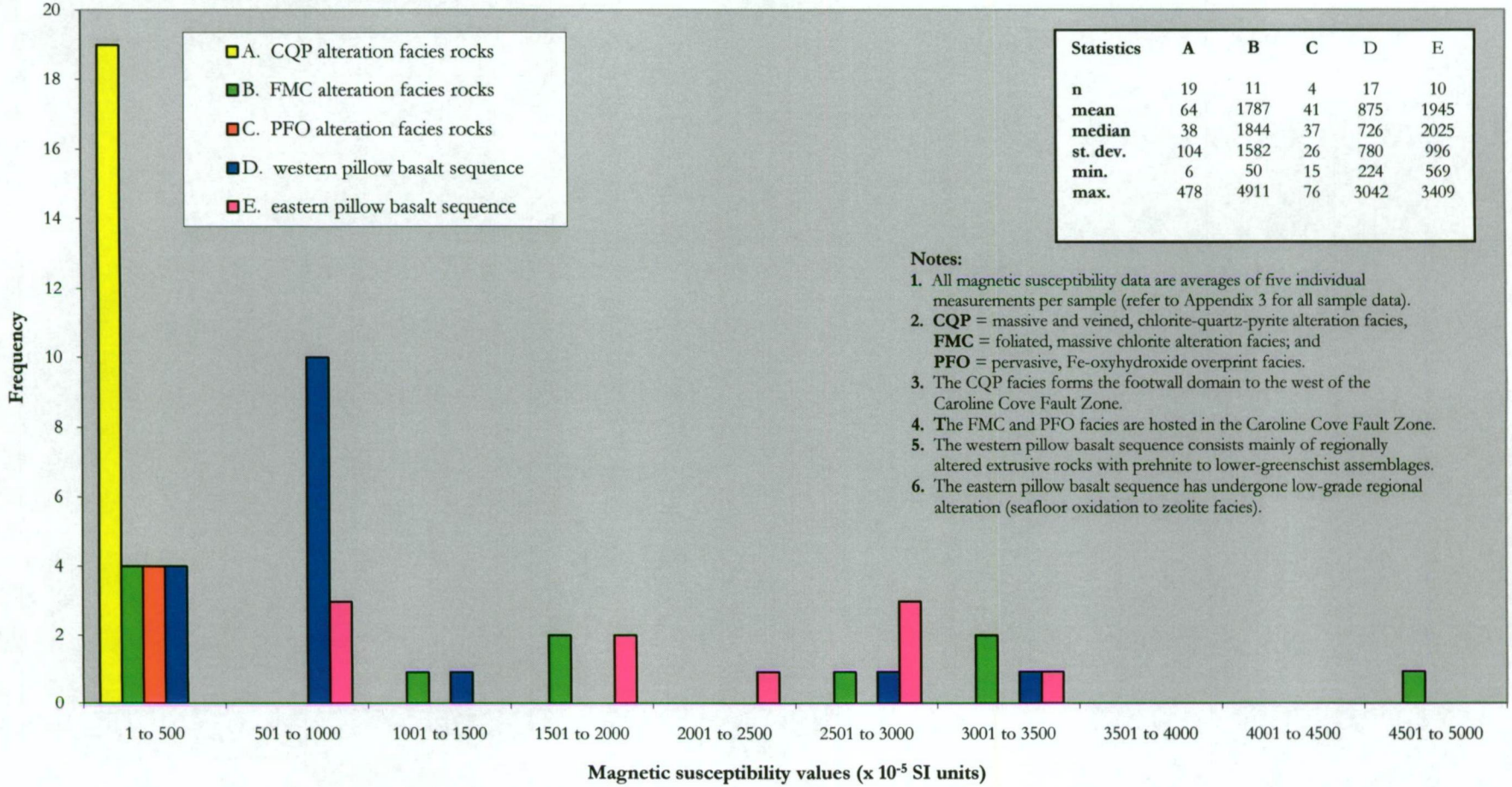

Statistics	A	B	C	D	E
n	19	11	4	17	10
mean	64	1787	41	875	1945
median	38	1844	37	726	2025
st. dev.	104	1582	26	780	996
min.	6	50	15	224	569
max.	478	4911	76	3042	3409

Notes:

1. All magnetic susceptibility data are averages of five individual measurements per sample (refer to Appendix 3 for all sample data).
2. **CQP** = massive and veined, chlorite-quartz-pyrite alteration facies, **FMC** = foliated, massive chlorite alteration facies; and **PFO** = pervasive, Fe-oxyhydroxide overprint facies.
3. The CQP facies forms the footwall domain to the west of the Caroline Cove Fault Zone.
4. The FMC and PFO facies are hosted in the Caroline Cove Fault Zone.
5. The western pillow basalt sequence consists mainly of regionally altered extrusive rocks with prehnite to lower-greenschist assemblages.
6. The eastern pillow basalt sequence has undergone low-grade regional alteration (seafloor oxidation to zeolite facies).

Small-scale faults with brittle deformation zones < 50 cm-wide and minimal displacement occur sporadically in the eastern pillow basalt sequence. However, unlike the western sequence, most faults strike NE and have moderate to steep NW- and SE-directed dips (Figure 5.36). Narrow vein arrays with pale, fine-grained calcite and zeolite cements infill many of the fault zones, and are typically surrounded by thin selvages of altered wall rock. The magnetic susceptibility of fault zone basalt is commonly < 1000 x 10^{-5} SI units, reflecting increased alteration intensity within these structural conduits.

Geological and hydrothermal characteristics of alteration facies from the Caroline Cove Fault Zone

The Caroline Cove Fault Zone (CCFZ) hosts some of the most intensely altered and anomalous volcanic rocks on Macquarie Island; the fault-bound, massive and veined chlorite-quartz-pyrite (CQP) facies is particularly distinctive. Two 10–15 m-long, creek-bed segments of the CCFZ also provide the only local exposures of the foliated, massive chlorite (FMC) facies and the pervasive, Fe-oxyhydroxide overprint (PFO) facies (Figure 5.35). The following section documents the main outcrop and hand-specimen characteristics of each focussed alteration facies, and also summarises important structural features of the Caroline Cove Fault Zone (particularly its intimate relationship with the FMC facies). To complement this section, the structural architecture and FMC facies characteristics are compared for the Major Lake and Caroline Cove Fault Zones in Chapter 5.6. In addition, the alteration paragenesis and hydrothermal textures of each fault zone assemblage in the Caroline Cove district are presented in Chapter 6.

Massive and veined, chlorite-quartz-pyrite (CQP) facies

The massive and veined, chlorite-quartz-pyrite (CQP) facies is the most abundant of the three focussed alteration facies in the Caroline Cove area. Basaltic rocks in the CQP domain are strongly altered and have very distinctive grey-green or bluish-grey aphanitic groundmass, i.e., semi-pervasive chlorite alteration. The intensity of groundmass alteration is relatively consistent at most exposures. Massive, dark greenish-black chlorite commonly forms thin veinlets (< 2 mm), irregular patches of variable size and shape, and mottled or streaked groundmass zones (Figure 5.38). Primary volcanic features are poorly preserved due to intense hydrothermal alteration and structural disruption; vague, relict pillow lobes or hyaloclastite textures are evident only in rare outcrops. Some plagioclase laths are partly preserved, although most phenocrysts are extensively corroded and have indistinct crystal shapes because of widespread chloritisation. Massive chlorite also forms pseudomorphs after rare olivine crystals (completely replaced) and commonly infills amygdules. Intense chlorite alteration also destroys most primary groundmass Ti-magnetite, and CQP facies basalts have very low to low magnetic susceptibility values (most are < 50 x 10^{-5} SI units; Figure 5.37).

Fine- to medium-grained, milky quartz is widespread in the CQP facies and forms fine stringer-style veinlets, thicker curvi-planar veins, or massive alteration pods. Most veins are < 1–5 mm wide, although thickness commonly varies along-strike in discrete vein strands and many 10–20 mm segments occur (also rare 50–70 mm veins) (Figure 5.39). Dense, subparallel veinlet arrays are abundant in some outcrops and most are associated with steeply dipping faults. Thick vein segments (> 10 mm) and massive quartz pods commonly contain crystal-lined vughs (5–10 mm in diameter) and angular fragments of the chlorite-altered wall rock. Jigsaw-fit breccias are especially abundant in massive quartz enclaves (Figure 5.40), ranging in size from small groundmass patches < 5 cm in diameter to irregular-shaped blocks 50–100 cm-wide (uncommon). Many large-diameter quartz-rich domains are spatially related (proximal) to brittle faults and fracture zones. Minor accessory minerals in quartz cement include fine-grained aggregates of epidote (Figure 5.41) and pale barite crystals that infill vuggy cavities.

The third diagnostic alteration mineral of the CQP facies is pyrite (± chalcopyrite). Fine- to coarse-grained pyrite comprises ~ 5–20 % of the alteration mineral assemblage, and has multiple textural forms. Isolated groundmass crystals (mostly fine-grained) or small pyrite aggregates (< 0.5–3 mm-across) are widely disseminated in the chloritised groundmass (Figure 5.38 and 5.42). Wispy, discontinuous pyrite veinlets also cross-cut the altered groundmass and many of these form highly distinctive anastomosing strands 0.5–1.0 mm-wide. In contrast, the most spectacular form of pyrite mineralisation is closely associated with quartz (± epidote). Medium- and coarse-grained pyrite crystals are commonly hosted in discrete quartz veins, quartz-cemented breccias, and massive (irregular) alteration pods (Figure 5.39–5.41). The subhedral to euhedral pyrite grains occur as isolated or intergrown crystal aggregates in many central vein segments, and narrow, discontinuous pyrite selvages were also noted along some quartz vein margins. Massive, fine-grained chalcopyrite (and rare sphalerite) occurs in some quartz-pyrite veins; partial to complete overgrowths commonly mantle earlier-formed pyrite in these vein segments.

Moderately to steeply dipping brittle faults and tectonic breccia zones commonly cut across altered basaltic rocks in the CQP facies. Matrix-dominated breccias (~ 50–100 mm-wide) are infilled with gritty clay-gouge and contain fragments of strongly chlorite- or quartz-altered (and veined) basalt (Figure 5.43). Fault zone breccia fragments vary widely in size and shape, but most are subangular to very angular wall rock particles < 10 mm-across. Discrete faults are planar to curvi-planar structures that commonly preserve delicate slickenlines and clay-gouge striations. Typically, faults and breccia zones are highly oxidised and mostly obscured by soil and scree. A detailed sample collection transect along a 20 m-wide coastal outcrop from the CQP domain highlighted many common features of this alteration facies; steeply dipping faults, indistinct and poorly defined pillow basalt lobes, and veins or groundmass enclaves of massive quartz (± epidote) are all abundant (Figure 5.34 and 5.44).

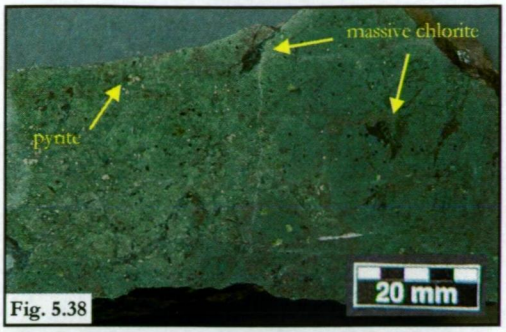

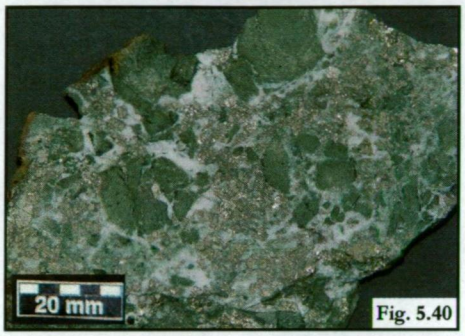

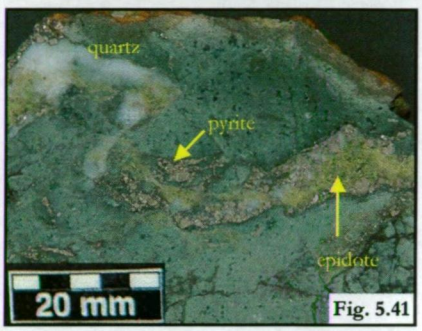

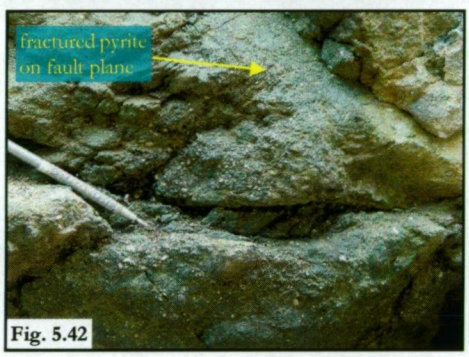

Figure 5.38: Intensely altered pillow basalt from the massive and veined, chlorite-quartz-pyrite (CQP) facies at Caroline Cove. The fine-grained igneous groundmass is extensively chloritised and irregular patches and mottled zones of massive, dark greenish-black chlorite are also abundant. Minor fine- to medium-grained pyrite and epidote are widely disseminated in the altered groundmass. This sample (MCQ-032) has low magnetic susceptibility, which is typical of the CQP alteration facies.

Figure 5.39: Vuggy, moderately oxidised quartz veins cut sharply across the intensely chlorite-altered groundmass of this massive and veined, chlorite-quartz-pyrite facies basalt. Central quartz vein segments commonly contain medium-grained pyrite and intergrown sulfide aggregates (pyrite ± chalcopyrite). Very fine- to fine-grained pyrite is sparsely disseminated in the altered groundmass surrounding the veins, and mottled zones of massive chlorite also occur (sample MCQ-030).

Figure 5.40: Jigsaw-fit breccias are a distinctive component of the massive and veined, chlorite-quartz-pyrite (CQP) alteration facies, and these rocks commonly outcrop in the lower Caroline Creek valley. Angular fragments of chlorite-altered basalt and crystalline aggregates of fine- to coarse-grained pyrite are abundant, and pale, milky quartz forms the breccia cement (sample MCQ-057).

Figure 5.41: Massive, fine-grained quartz and epidote are complexly intergrown with abundant pyrite in this anastomosing vein. Epidote is a minor but widespread component of the CQP alteration facies and mainly occurs in quartz-pyrite veins or massive groundmass patches (sample MCQ-031).

Figure 5.42: Medium- and coarse-grained pyrite is widely disseminated within the intensely altered basaltic groundmass of the massive and veined, chlorite-quartz-pyrite facies. This outcrop, in the western wall of the Caroline Creek valley, has abundant cubic pyrite grains and intergrown sulfide aggregates (pyrite + chalcopyrite) exposed on a steep fault plane. Post-hydrothermal faulting (neotectonic) has fractured and cleaved many of the discrete pyrite crystals shown here.

Figure 5.43: Steeply dipping breccia-gouge fault zones commonly cut across the altered pillow basalt of the massive and veined, chlorite-quartz-pyrite facies in the Caroline Creek valley. The matrix-dominated breccia zones, which commonly have a well developed subparallel foliation, host angular wall rock and vein fragments in gritty clay-gouge.

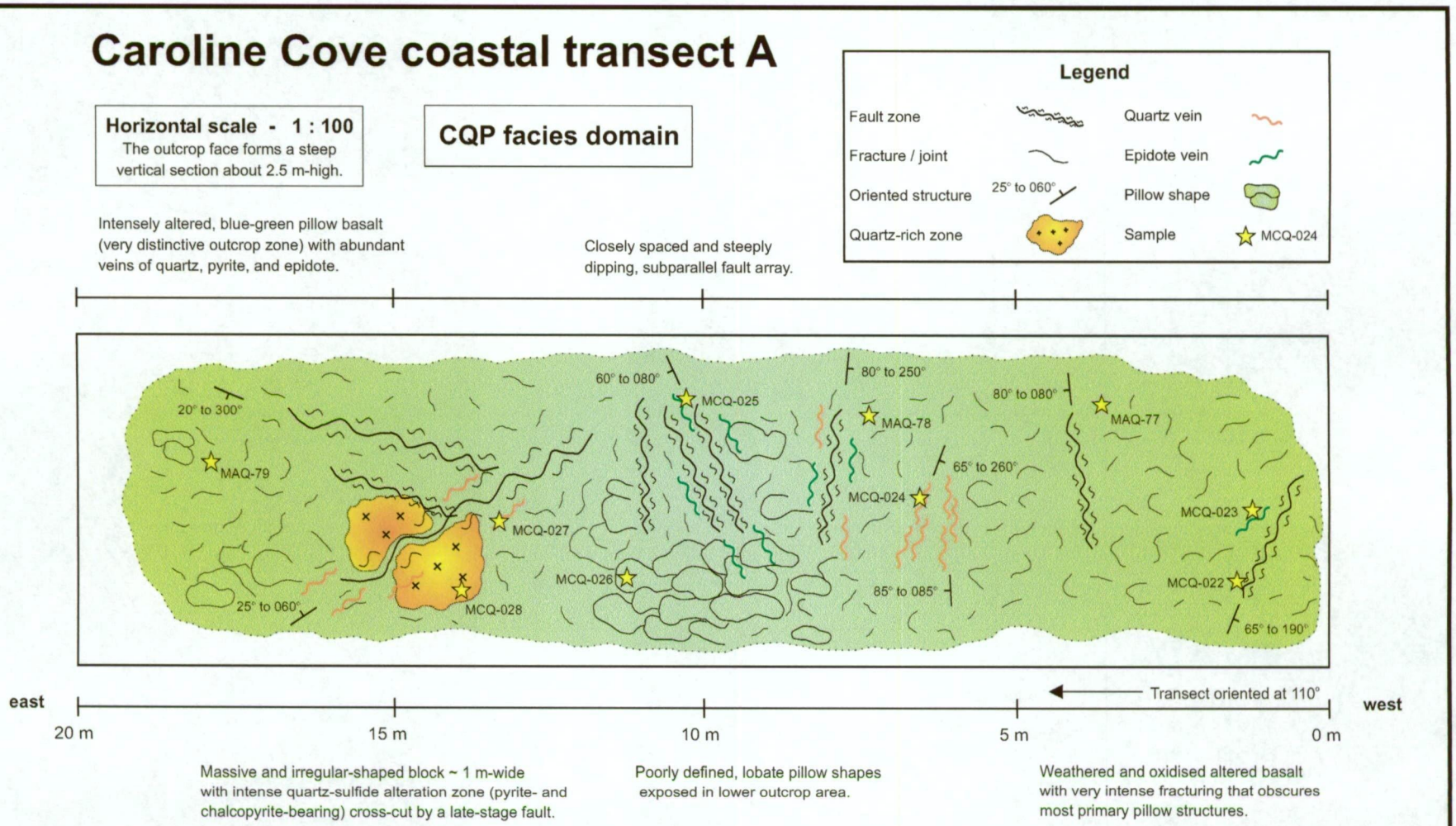

Figure 5.44: Schematic representation of a 20 m-long coastal exposure in the massive and veined, chlorite-quartz-pyrite alteration facies domain at Caroline Cove (refer to Figure 5.34 for location details). This view shows many of the characteristic outcrop features associated with the intensely altered pillow basalt, such as the high abundance of steeply dipping faults, irregular fractures, and various types of veined and massive alteration zones. Rock and mineral sample locations are also shown on this diagram. Rock specimens collected during this study and by G. J. Davidson in 1998 (unpublished data); refer to Appendix 2 for further details.

The massive and veined, chlorite-quartz-pyrite facies is entirely fault-bound at Caroline Cove; it outcrops within a wedge-shaped segment (~ 8 km^2 total area) in the central (on-land) section of the embayment. Apart from several 10–15 m-long segments of the eastern boundary (which are relatively well exposed in the Caroline Creek valley), the margins of the CQP facies domain are obscured by soil or vegetation. The only exposure of the western CQP fault boundary is a small (< 2 m-wide) soil-covered outcrop in the Caroline Creek valley, situated about 200 m upstream of the foreshore (Figure 5.35). The western fault margin is a steeply dipping breccia-gouge zone that strikes NNW and has rare fault striations that indicate sinistral-oblique offset. The fault clearly terminates the CQP facies domain (i.e., there are no further CQP facies outcrops further upstream), and lacks a specific alteration zone. Instead, this sinistral-oblique fault contains breccia fragments and clay-gouge, and is thus interpreted as a late-stage, post-hydrothermal (uplift-related) structure.

Foliated, massive chlorite (FMC) facies

Outcrops of the foliated, massive chlorite (FMC) facies at Caroline Cove occur only in the brittle deformation core of the Caroline Cove Fault Zone (CCFZ). The intimate spatial relationship between the central fault zone and the strongly chlorite-altered rocks is similar to the FMC facies association in the Major Lake Fault (previously described from the Sandell Bay creek site in Chapter 5.3). The alteration mineral assemblages and textural features of the FMC facies at Caroline Cove share many of the same characteristics as the outcrop occurrence hosted by the Major Lake Fault. However, significant differences in the spatial distribution of the alteration facies and the structural architecture of each fault were identified during mapping. The main features of the FMC facies in the CCFZ are summarised below.

The FMC facies is sporadically exposed along several segments (< 15 m-long) of the lower Caroline Creek (Figure 5.35). Within the deeply incised valley the creek bed coincides with the central deformation corridor of the Caroline Cove Fault Zone, juxtaposing the intensely altered footwall block (i.e., the CQP facies rocks to the west) against the low grade and regionally altered eastern pillow basalt sequence (the hangingwall). The brittle and highly fractured, 1–2 m-wide Caroline Fault strikes N to NNE and dips steeply W (< 75°) (Figure 5.45); subvertical discontinuities and brecciated clay-gouge faults are abundant in the creek-hosted outcrop. Brecciated fault zones host abundant subangular to angular wall rock fragments (~ 1–5 mm diameter) in the gouge matrix. Larger breccia fragments (10–50 mm across) are less common, and most are blocky, irregular, and lack penetrative foliation.

Moderate to strong, clay and chlorite alteration along small-scale structures is characteristic of the FMC facies; most fault planes, gouge seams, and brecciated fault zones are infilled with soft and pliable, dark greenish-black phyllosilicate minerals. Discrete fault planes have well developed slickenlines, and narrow clay- and chlorite-rich seams (< 5 mm-wide) commonly separate fractured wall rock fragments (Figure 5.46). An important interpretative point (with implications

for the evolution and timing of hydrothermal alteration in the CCFZ) is that clay and chlorite seams associated with the FMC facies are distinct from widespread groundmass chlorite associated with the CQP facies (footwall domain). Thus, different hydrothermal textures, spatial distributions, and alteration mineral associations attest to multiple phyllosilicate-forming (alteration) stages in the Caroline Cove region.

Figure 5.45: This steep W-dipping fault plane forms a 12 m-long segment of the eastern valley wall in the lower reaches of the Caroline Creek (~ 75 m upstream of the beach). The fault plane is part of the Caroline Cove Fault Zone (CCFZ), which here cuts across the weakly altered (regional) eastern pillow basalt sequence. On the opposite side of the eroded valley, which here coincides with the central deformation corridor of the CCFZ, the footwall outcrop consists of intensely altered basalts that comprise part of the massive and veined, chlorite-quartz-pyrite (CQP) facies.

Figure 5.46: A brittle zone of highly fractured eastern pillow sequence basalt is exposed in the central deformation corridor of the Caroline Cove Fault. Subparallel and steep W-dipping faults and fractures have narrow breccia-gouge seams and strong clay and chlorite alteration (slickenlines). The coherent basalt fragments lack pervasive alteration, and most retain highly elevated magnetic susceptibility. These rocks contrast markedly with the pervasively chlorite-altered basalts in the adjacent CQP facies domain (footwall block). This view shows the eastern valley wall of the Caroline Creek valley about 50 m upstream of the coastal foreshore.

Brecciated rock fragments in the Caroline Cove Fault Zone, all variably affected by FMC facies alteration, are derived from both the proximal footwall and hangingwall. Fragments of relatively low grade, regionally altered basalt from the eastern pillow sequence are most abundant, and comprise 70–80 % of the fractured fault zone (Figure 5.46). Despite intense clay and chlorite alteration along discrete fault planes and clay gouge seams, most eastern pillow basalt fragments in the Caroline Cove Fault Zone are not pervasively altered, i.e., similar to the non-pervasive alteration that occurs in the core of the Major Lake Fault Zone. The fine-grained basaltic groundmass is relatively weakly altered (regional alteration assemblages) and rock fragments commonly retain their primary mineral compositions, volcanic textures, and characteristic high to very high magnetic signatures (commonly > 1500 x 10^{-5} SI units; Figure 5.37). In contrast, brecciated rock fragments derived from the CQP facies are less abundant and mainly occur near the western valley wall of the Caroline Cove Fault Zone, i.e., within ~ 1 m of their source domain. These rocks have typical CQP facies assemblages and hydrothermal textures, such as chlorite-quartz-pyrite-epidote veins, massive and disseminated sulfides, and irregular quartz-rich blocks. The juxtaposition of fractured rock fragments in the CCFZ, which are clearly derived

from separate and very distinctive hydrothermal assemblages (both focussed and regional alteration facies), provides further interpretative evidence that the FMC facies post-dates formation of the main chlorite-forming (+ quartz + pyrite) alteration stage (CQP facies).

A detailed mapping transect was undertaken along a well exposed 12 m-long section of the Caroline Creek valley to further elucidate the structural architecture of the Caroline Cove Fault Zone, and its relationship to the FMC alteration facies (Figure 5.47). Most discrete faults and brittle fractures strike N to NNE and have moderate to steep dips (many dip > 70° to the W or E), consistent with the dominant trend of the CCFZ (refer to contoured stereonet data on Figure 5.47). Narrow, elongated slickenlines indicate predominantly oblique-normal slip, although some NW-dipping faults steeply cut across the main structural trend; these have sinistral to sinistral-oblique displacement. Fault planes also preserve evidence for structural reactivation and multiple tectonic episodes, with late-stage clay striations associated with the FMC facies overprinting earlier fault plane growth fibres (quartz or chlorite). Kinematic indicators on reactivated faults indicate predominantly oblique-slip movement although ~ 10 % of faults preserve evidence of reverse displacement (refer to contoured stereonet data on Figure 5.47).

The close spatial association of the Caroline Cove Fault Zone with the CQP and FMC alteration facies provides good evidence that this fault initially formed as a seafloor-spreading structure. Abundant quartz and sulfide minerals in the CQP alteration assemblages are consistent with hydrothermal conditions that occur in the on-axis environment (Chapter 4). An extensional tectonic setting is also supported by the early-formed, steep normal-oblique faults recognised in the central deformation corridor of the CCFZ. However, the abundance of reactivated and cross-cutting faults with oblique-slip kinematics (mostly sinistral) suggests that the fault has remained active during neotectonic uplift and transpression. Most late-stage faults have breccia-gouge seams that lack intimate alteration assemblages (i.e., they are not associated with hydrothermally derived minerals), which further suggests they formed post-spreading and are not related to late-stage oblique-spreading transfer structures (as these may have provided conduits for seafloor hydrothermal fluids).

Pervasive, Fe-oxyhydroxide overprint (PFO) facies

The Caroline Cove Fault Zone is the structural host for multiple occurrences (~ 8–10 discrete zones) of the pervasive, Fe-oxyhydroxide overprint (PFO) facies. Patchy outcrops of the PFO facies are restricted to the central fault corridor of the CCFZ (similar to the FMC facies) and occur sporadically along-strike in the Caroline Creek valley (Figure 5.47). The PFO facies mainly forms elongated fault-parallel pods ~ 1–2 m-long and < 1 m-wide. These altered outcrops are very distinctive and typically occur as mottled, purplish-brown and brownish-red enclaves (irregular size and shape) superimposed on the earlier-formed FMC and CQP facies (Figure 5.48).

Detailed geology and structure of the Caroline Cove Fault Zone

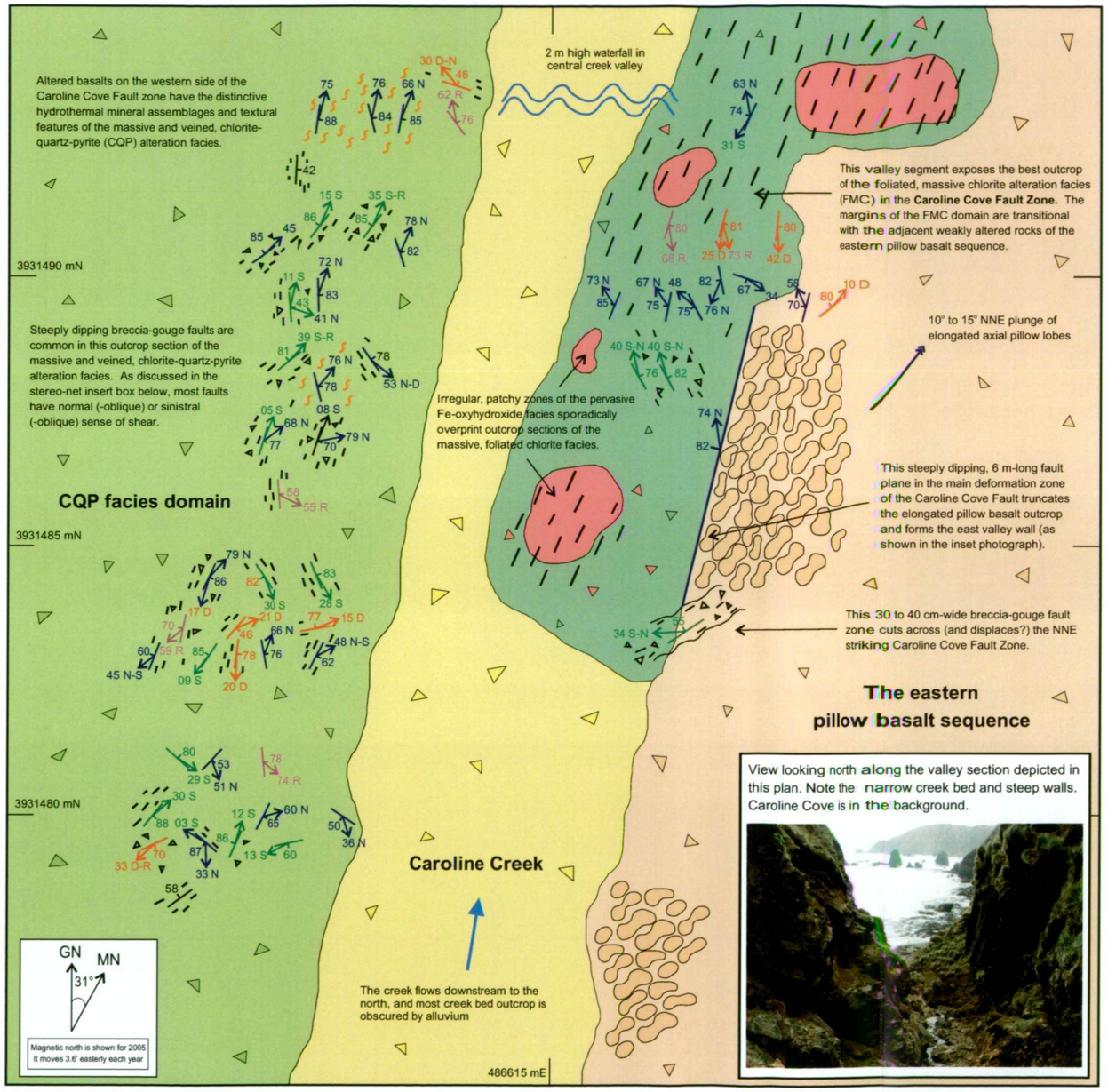

Legend

- Altered basalt with massive and veined, chlorite-quartz-pyrite facies (CQP) assemblages - outcrop and scree
- Altered basalt with foliated, massive chlorite facies (FMC) assemblages - outcrop and scree
- Altered basalt with pervasive, Fe-oxyhydroxide overprint facies (PFO) assemblages - outcrop and scree
- Eastern pillow basalt sequence - outcrop zone with elongated pillow lobes and scree
- Creek bed alluvium and slope-wash debris
- Oriented outcrop fault with trend and plunge of fault plane striations shown (arrow with letter symbol)
  - blue = normal and normal-oblique faults (N)
  - green = sinistral and sinistral-oblique faults (S)
  - red = dextral and dextral-oblique faults (D)
  - purple = reverse and reverse-oblique faults (R)
- Highly fractured, breccia-gouge zone associated with discrete oriented fault (same colour scheme as above)
- Oriented trend-lines for the dominant fracture direction in the Caroline Cove Fault Zone - most are subvertical
- Oriented quartz veins in the CQP alteration facies

0 meters 5

N-S scale 1 : 100

E-W scale x 2.5

Projection: UTM Zone 57 S
Datum: WGS-84
Contours: Not shown
Survey control: Garmin E-trex GPS & tape and compass
Mapping & drafting: Steven Lewis
Note: Although a plan view is depicted here, the east and west valley walls are actually very steep (as shown in the inset photograph).

Poles to planes of faults in the CCFZ

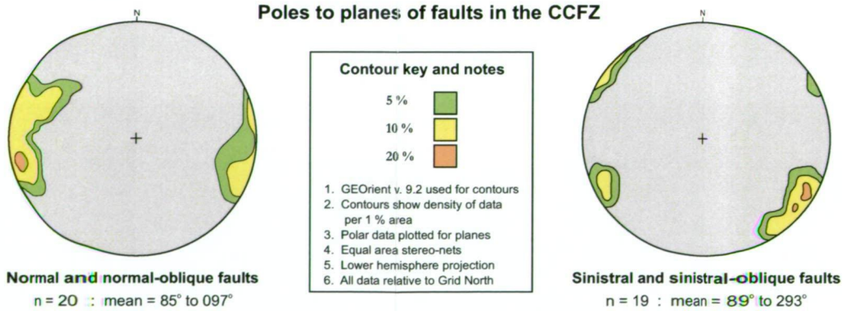

Normal and normal-oblique faults
n = 20 : mean = 85° to 097°

Sinistral and sinistral-oblique faults
n = 19 : mean = 89° to 293°

Contoured stereographic projections (poles to planes) of discrete faults in the CCFZ, showing the most common fault types that occur in and near the main deformation zone (based on sense of shear criteria). More than 75 % of all recorded faults preserve kinematic evidence for either normal (-oblique) or sinistral (-oblique) movement (minor dextral and reverse faults also occur (~ 10 % each) but are not shown here). The normal faults are steeply dipping and mostly subparallel with the NNW- to NNE-strike of the main fault zone. The sinistral faults are also steeply dipping but form two suborthogonal fault groups, although most sinistral faults are also subparallel to the Caroline Cove Fault Zone (NNE- to NE-strike).

Figure 5.47: Detailed plan view of the alteration facies distribution and structural geology at the best outcrop exposure of the Caroline Cove Fault Zone (Site 3A, refer to Figure 5.35 for traverse location). The steep Caroline Creek valley coincides with the 1.0 to 1.5 m-wide main deformation zone of the fault, and most outcrops are highly fractured and contain abundant breccia-gouge zones. The western valley wall mainly consists of strongly altered basalt of the massive and veined, chlorite-quartz-pyrite alteration facies (CQP); in contrast, the opposite valley wall hosts weakly altered pillow basalt of the eastern sequence domain. An elongated outcrop zone of the foliated, massive chlorite alteration facies (FMC) occurs mainly in the creek bed, and these altered basaltic rocks have a ~ 1 m-wide transitional zone with the adjacent eastern pillow basalt sequence. The FMC outcrop exposure is also partly overprinted by several patchy and irregular zones of the pervasive Fe-oxyhydroxide facies (PFO).

Massive, pervasively altered patches of brownish-red Fe-oxyhydroxide minerals (e.g., goethite?) have overprinted pre-existing Fe-bearing phases, including relict igneous minerals (e.g., clinopyroxene) and early-stage hydrothermal minerals such as chlorite and pyrite. Extensive degradation of primary Ti-magnetite in the altered groundmass is confirmed by the very low magnetic susceptibility of oxidised rocks in the PFO facies, with average values ~ 50 x 10^{-5} SI units (Figure 5.37). Irregular patches of brownish-red oxidation minerals also infill and overprint earlier-formed vein and vugh cements in the basaltic groundmass.

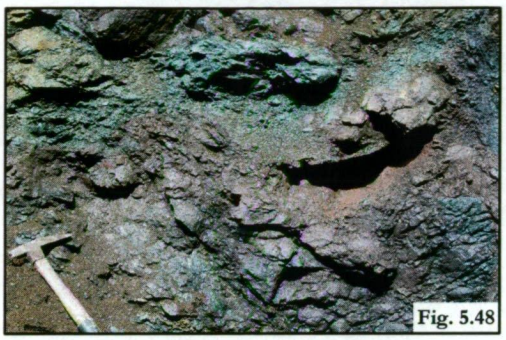
Fig. 5.48

Fig. 5.49

Figure 5.48: Irregular patchy zones with mottled, purplish-red staining occur sporadically along-strike in the Caroline Cove Fault. These alteration zones are typical of the pervasive, Fe-oxyhydroxide overprint (PFO) facies and are superimposed on earlier formed hydrothermal assemblages. The PFO alteration facies only occurs in the central deformation corridor of the Caroline Cove Fault Zone.

Figure 5.49: A reddish-brown, concentric oxidation halo overprints chlorite alteration in the groundmass of this fine-grained basalt from the Caroline Cove Fault Zone. Intense oxidation of Fe-rich groundmass minerals (both primary and secondary phases) occurs adjacent to narrow rock discontinuities, which have acted as small-scale, focussed fluid conduits. The unoxidised chlorite-rich patch in the centre of the hand-specimen (sample MCQ-060) represents a relict core, and provides evidence to interpret progressive alteration along a pervasive oxidation 'front'.

The most intensely oxidised PFO facies basalts occur near narrow discontinuities in the wall rock. Concentrically zoned haloes are characteristic textural features, and many preserve irregular-shaped cores of non-oxidised groundmass (commonly chlorite-altered) pervasively enveloped by oxidised alteration selvages (Figure 5.49). The unoxidised core zones are typically < 50 mm across and have sharp and well defined boundaries within the enclosing selvage. Groundmass oxidation intensity commonly increases every 5–10 mm away from the relict core, i.e., progressive transitional oxidation effects emanating from the original discontinuity (fluid conduit). Concentrically zoned oxidation halos in the PFO facies have many similarities with strongly oxidised seafloor basalts documented from other global localities, e.g., Alt et al. (1996), Talbi and Honnorez (2003), Schramm (2004), and probably formed under similar 'open' hydrothermal conditions (oxidised). The characteristic PFO facies zonation texture is here interpreted as evidence for late-stage oxidised fluid flow, i.e., a pervasive 'oxidation front'. These fluids were channelled in highly permeable brittle fractures at a range of scales, with the Caroline Cove Fault Zone locally representing the largest scale (and the main fluid conduit), and the various cm- to mm-sized wall rock fractures being smaller-scale structural zones.

Caroline Cove Fault Zone summary

Chapter 5.4 has presented the main geological and hydrothermal characteristics of three focussed alteration facies (and their proximal host rocks) identified in the Caroline Cove area (Site 3A). Two of these facies are uniquely associated with the Caroline Cove Fault Zone (i.e., the massive and veined, chlorite-quartz-pyrite (CQP) facies and the pervasive, Fe-oxyhydroxide overprint (PFO) facies), and the foliated, massive chlorite (FMC) facies (initially described from the Major Lake Fault) also occurs here (albeit on a smaller-scale). These field descriptions have highlighted some of the important geological variations between the Caroline Cove and Major Lake Fault Zones (Chapter 5.3), and provided evidence for different hydrothermal conditions and structural regimes. However, the presence of similar alteration minerals and hydrothermal textures within these key diagnostic assemblages (e.g., abundant massive and veined, quartz and chlorite in both the VQC and CQP facies), and the occurrence of the FMC facies at both locations, suggests that these major fault systems may share some evolutionary links. A comprehensive summary and comparison of these alteration assemblages are presented in Chapter 5.6, to further evaluate the geology, structure, and hydrothermal conditions of the Caroline Cove and Major Lake Faults.

5.5. Altered rocks from the Sellick Bay Fault Zone

Geographic distribution and regional context

The Sellick Bay Fault Zone (SBFZ) was investigated as part of this study because it has a similar orientation to the Major Lake Fault and was thus considered a likely structural host for the vein and breccia, quartz-chlorite (VQC) facies and the foliated, massive chlorite (FMC) facies*. However, detailed fieldwork showed that the SBFZ is uniquely associated with the vein-dominated, prehnite-zeolite (VPZ) facies, and has many significant differences from the Major Lake Fault (and also the Caroline Cove Fault). In particular, the quartz-chlorite-sulfide-bearing assemblages typical of the focussed alteration facies from Major Lake and Caroline Cove are absent from the Sellick Bay district.

Regional reconnaissance mapping discovered that the Sellick Bay Fault Zone is only exposed in the steep upper escarpment slope overlooking the southern end of Sellick Bay (Site 1A; Figure 5.50). At this site, located ~ 600 m north of Mt Waite, a narrow creek valley (< 20 m-wide) coincides with the NW- to NNW-striking Sellick Bay Fault Zone. Six prominent outcrops occur within a ~ 200 m-long and 50 m-wide sublinear zone surrounded by *in situ* scree and weathered rock debris. Further down-slope the SBFZ is concealed by unconsolidated basaltic talus, and no outcrops of VPZ facies rocks occur on the exposed coastline (~ 700 m further west) or the adjacent plateau (which is extensively eroded and mostly covered by a thick soil profile).

* In addition, relatively little attention had previously been focussed on the Sellick Bay Fault, and many of its geological characteristics were unknown e.g., its hydrothermal features.

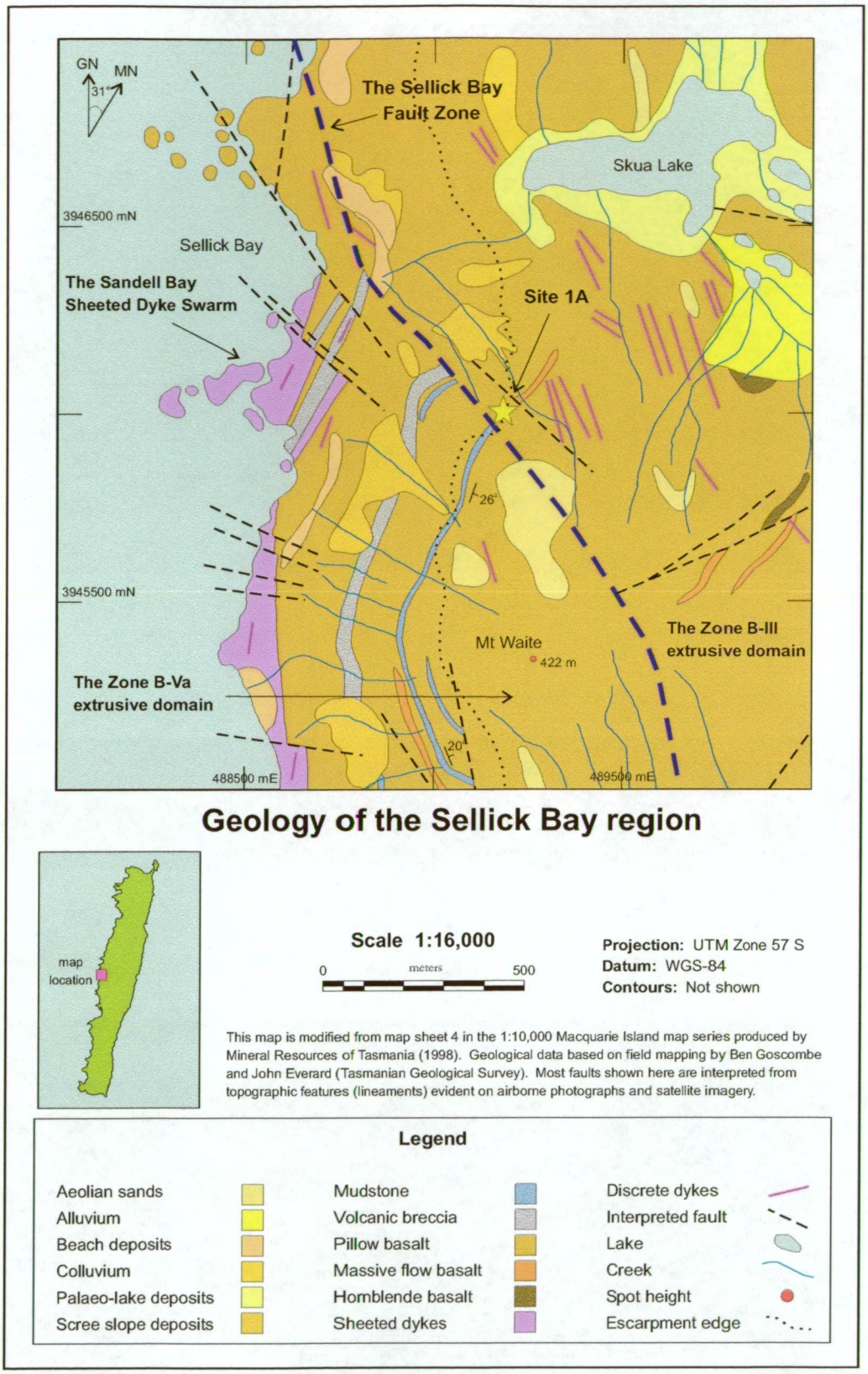

Figure 5.50: Geology map of the Sellick Bay region showing the location of the Sellick Bay Fault Zone and the main study site investigated during this project (Site 1A). The Zone BVa and BIII pillow basalt domains are separated by the SBFZ, although the main deformation zone of the fault is rarely exposed. In addition, most basaltic rock outcrops are restricted to the coastline or the steep escarpment. The northernmost occurrence of the Sandell Bay Sheeted Dyke Swarm occurs along the Sellick Bay foreshore. Note the abundance of discrete NNW-striking dykes near Site 1A in Zone BIII, and the moderately E-dipping package of thin sedimentary and volcaniclastic rock horizons in the escarpment slopes (Zone Bva).

Goscombe and Everard (2001) described the Sellick Bay Fault Zone as the most significant neotectonic fault on Macquarie Island because of its relatively broad deformation halo (> 50 m-wide) and extensive strike length (> 4 km). They interpreted the Sellick Bay Fault Zone as a major strike-slip (dextral) fault that formed during transpression and uplift, i.e., during their interpreted D3 tectonic stage (Goscombe and Everard, 2001). They also suggested that the SBFZ represents an important geological boundary that forms the northern margin of the Zone BVa and BVI extrusive rock domains, and is also the main terminating structure of the Sandell Bay Sheeted Dyke Swarm. Goscombe and Everard (2001) further suggested that major differences in the regional metamorphic grade and the stratigraphic level (depth of the host rock sequence) occur across the SBFZ, and these variations are explicitly shown on their geological maps (Goscombe and Everard, 2001). My detailed site mapping in the Sellick Bay escarpment mostly supports the geological observations and regional interpretations proposed by Goscombe and Everard (2001). However, recognition of the vein-dominated, prehnite-zeolite facies, and its close spatial association with the Sellick Bay Fault Zone, provides strong evidence for a primary, spreading-related structural origin, and further suggests that it was a significant hydrothermal fluid conduit in the upper ocean crust.

Host rocks of the Sellick Bay Fault Zone

The Sellick Bay Fault Zone is hosted in a thick package of predominantly volcanic rocks that contains abundant pillow basalt (Figure 5.50). Minor basaltic flows and matrix-rich hyaloclastites also occur, and steeply dipping dolerite dykes sporadically intrude the volcanic rock sequence (thirty-two discrete dykes occur in a ~ 500 m^2 area centred about the main outcrop site). Thin (most are < 1 m), discontinuous horizons of fine-grained, reddish-brown mudstone and greenish-grey sandstone are interbedded with the extrusive sequence, and provide useful marker horizons in the volcanic stratigraphy.

Volcanic rocks

The pillow basalt package in the Sellick Bay escarpment forms a thick (at least 400 m) and conformable volcanic pile. Individual pillow shapes, separated by narrow glass-rich selvages, are mainly elongate or partly rounded lobes ~ 1–2 m-long and 0.5–1.0 m in diameter. The long axis of most pillow basalts trends consistently NE and plunges at 35°–45°, although minor structural variations occur in fault-bound segments north of the main Sellick Bay site (Figure 5.51 and Figure 5.52). Large-diameter pillows (> 2 m-wide) with irregular, bulbous shapes occur in several outcrops of transitional pillowed and massive basalt (Figure 5.53).

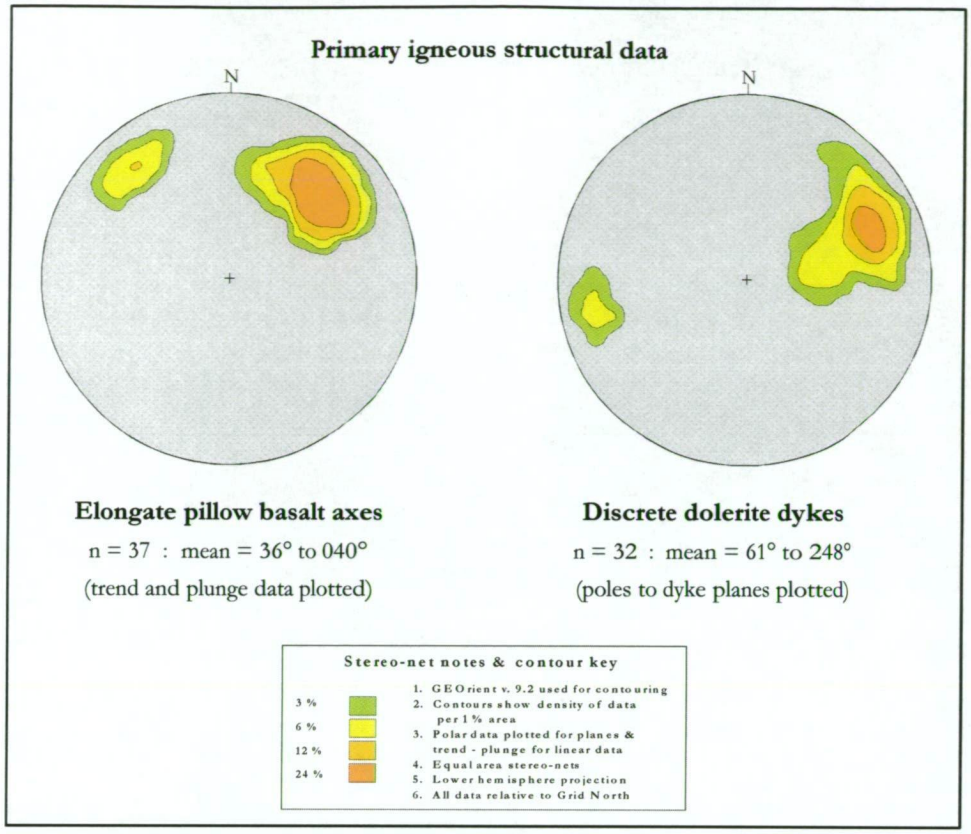

Figure 5.51: Contoured stereographic projections of the orientation of primary igneous structures in the regional host rock package (upper escarpment) of the Sellick Bay Fault Zone (SBFZ). Most elongated pillow basalt axes trend NNE and have shallow to moderate plunges. However, outcrop exposures to the north of the SBFZ have a more diverse range of structural orientations and include a subordinate group of fault-bound pillow basalts that have relatively shallow NW-plunges. Discrete dykes throughout the entire region are mostly orthogonal to the orientation of volcanic 'bedding' (striking NW to NNW), although consistent variations in the amount of dip occur between the northern domain (moderate to steep dips in Zone BIII) and the southern domain (shallow to moderate dips in Zone BVa).

Most regional pillow basalt is sparsely to moderately porphyritic (5–10 % plagioclase and rare olivine phenocrysts), although several large-diameter pillow and massive units (flows) contain ~ 15–20 % coarse-grained plagioclase. Tabular and lath-like plagioclase crystals (mostly 2–20 mm-long) are randomly oriented in the dark purplish-grey groundmass. The aphanitic groundmass of many basaltic rocks is moderately to strongly oxidised, and contains irregular-shaped patches and domains of semi-pervasive, brownish-red staining (Fe-rich oxidation) (Figure 5.54). Strongly oxidised basaltic rocks commonly occur adjacent to minor faults or less altered dykes, and provide good examples of localised wall rock alteration controlled by small-scale structural zones. The oxidised basalts are more widespread in the extrusive package to the north of the Sellick Bay Fault Zone, i.e., within the Zone BIII domain of Goscombe and Everard (2001).

Vesicles are common in most pillow basalts (comprising ~ 1–2 % of the total rock), and are especially abundant in outermost pillow rims. Amygdules are mainly infilled with radiating masses of fine-grained zeolites, and these pale subrounded spots post-date oxidised groundmass alteration (Figure 5.54). Narrow zeolite veinlets also occur sporadically in the basaltic rocks, especially in semi-pervasively to pervasively altered groundmass patches and small-scale faults.

The alteration mineral assemblages that occur in vughs, veins, and the groundmass of most basaltic rocks, indicate relatively low-grade regional (non-discharge) alteration under oxidising ('seafloor weathering') or zeolite facies conditions (Griffin, 1982).

Massive basaltic units (coherent flows) outcrop prominently at several sites near the Sellick Bay Fault Zone, and their primary mineralogy and groundmass textures are similar to the surrounding pillow basalts. However, massive flows form relatively prominent outcrops compared to volcanic rock packages dominated by pillow basalts (and hyaloclastites), as the flow units are relatively more resistant to weathering and erosion. Well developed columnar jointing is also common, and most massive flows are blocky, angular, and highly fractured (Figure 5.55). Reddish-brown, Fe-rich alteration and groundmass oxidation is restricted to irregular patches and zones adjacent to small structural discontinuities or intrusive margins.

Matrix-dominated hyaloclastites are a minor but distinctive component of the Sellick Bay host rock sequence. They form thin (~ 1–2 m) and discontinuous horizons in the extrusive rock domain, and most are surrounded by pillow basalt. Dark greenish-black, clay-altered volcanic glass comprises the primary breccia matrix. Clasts consist mainly of plagioclase-phyric basalt and include small, partially spalled pillow fragments (most are < 20 cm across) and subangular to angular, coherent basalt (Figure 5.56). Pervasive hyaloclastite alteration is widespread, manifested in the glassy matrix as discrete streaks and mottled patches of fine-grained, dark green or reddish-brown hydrothermal minerals (various clay and Fe-oxyhydroxide mineral phases), and pale zeolite veinlets.

Detailed mapping along the Sellick Bay escarpment recognised important geological differences between the volcanic rock packages that occur to the north and south of the Sellick Bay Fault Zone. These variations provide good evidence to support Goscombe and Everard's (2001) interpretation of the Sellick Bay Fault Zone being the main geological boundary between the Zone BIII (north) and Zone BVa (south) extrusive domains. Although most of the rocks in the Sellick Bay escarpment were formed by volcanic processes (i.e., seafloor lava eruptions), consistent geological variations occur either side of the Sellick Bay Fault Zone, e.g., the type and abundance of volcanic rocks, and their structural orientations and regional alteration assemblages. The main host rock variations include:

i. The volcanic rocks that occur in the Zone BIII domain are considerably more diverse than those from Zone BVa (which is dominated by pillow basalts). Coherent massive flows, hyaloclastites, and discrete extrusive layers with upper-most large diameter pillow lobes (transitional with massive flows) are relatively abundant and geographically widespread north of the SBFZ (i.e., within the Zone BIII domain), but are comparatively rare in Zone BVa (south of the SBFZ);


Fig. 5.52

Fig. 5.53

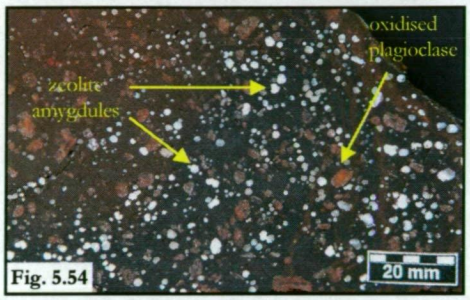

Fig. 5.54

Fig. 5.55

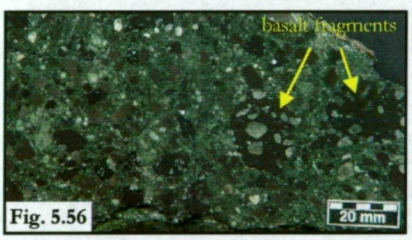

Fig. 5.56

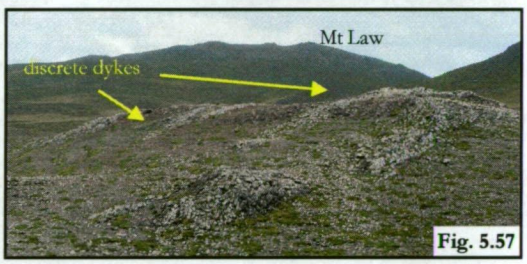

Fig. 5.57

Figure 5.52: Elongate pillow basalt lobes, situated in the west coast escarpment near the Sellick Bay Fault Zone (Site 1A), plunge at ~ 40° towards the NE. Most discrete pillow shapes are variably disaggregated, although several extensive outcrop sections (> 20 m-high) occur in the steep, talus-strewn slopes. These rocks have low-grade, regional alteration assemblages consistent with seafloor oxidation to zeolite facies conditions.

Figure 5.53: Basaltic units dominated by large-diameter pillows (> 2 m-across) are commonly transitional with overlying massive flows near the Sellick Bay Fault Zone. These relatively coherent rocks, which are more resistant to erosion and weathering than nearby pillow basalts, form prominent outcrops in the escarpment slope.

Figure 5.54: A highly vesicular pillow basalt from the upper escarpment north of the SBFZ. The selectively pervasive oxidation assemblages shown here (Fe-rich regional alteration) commonly occur near small-scale structural conduits (e.g., dyke margins) where they variably overprint the aphanitic groundmass and many plagioclase phenocrysts. Most vesicles are infilled with pale zeolite minerals that post-date groundmass oxidation (sample MCQ-289).

Figure 5.55: Vertical columnar joints are well developed in coherent basalt flow units in the Sellick Bay escarpment. This massive, jointed basalt flow overlies a brittle hyaloclastite zone; typically, the extrusive boundary is sharp and forms a prominent outcrop feature.

Figure 5.56: Hyaloclastite-rich zones occur sporadically in the volcanic rock package near the Sellick Bay Fault Zone. The relatively fresh, matrix-dominated breccia shown here (sample MCQ-305) consists mainly of pale and dark green volcanic glass (altered), and also contains several 10–30 mm-wide fragments of crystal-rich (plagioclase-phyric) basalt.

Figure 5.57: Steeply dipping dolerite dykes ~ 2–3 m-wide have intruded the pillow basalt package on the west coast plateau (~ 200 m south of Skua Lake). The subparallel, NNW-striking dykes typically form prominent outcrops as they are less susceptible to erosion than the surrounding volcanic rocks. This view looks towards the SE from the central Sellick Bay upper escarpment rim; the distant horizon is dominated by Mt Law's 310 m-high peak.

ii. Primary igneous structures have a greater range of orientations in the northern domain (Zone BIII), whereas pillow axes trend more consistently in the Zone BVa rock association (Figure 5.51). In addition, although most dykes have similar NW- to NNW-strike throughout the entire Sellick Bay district, most dykes north of the SBFZ have steeper dips than those in the southern domain (commonly 40°–60° greater amount of dip in Zone BIII). Discrete dykes north of the SBFZ are also consistently wider (~ 1.5–2 m-wide on average) than dykes south from Zone BVa (most of these are < 1 m-wide); and

iii. The regional alteration assemblages north of the Sellick Bay Fault Zone (Zone BIII) are dominated by fine-grained, reddish-brown minerals (late-stage, Fe-rich oxidation assemblages) and pale zeolites (these are especially common infilling vesicles and as vein cement). These mineral assemblages are widespread in the northern escarpment slopes and are commonly associated with small-scale structural conduits. Consistent overprinting relationships suggest that they formed from multiple episodes of regional hydrothermal activity (Figure 5.54). In contrast, the basaltic domain south of the SBFZ (Zone BVa) lacks significant oxidation-bearing assemblages, zeolite veins, and small structural zones with focussed regional alteration. The alteration assemblages in Zone BVa mainly consist of very fine-grained minerals (clay-rich?) disseminated in weakly altered basaltic groundmass (regional, recharge-style alteration).

Discrete dykes

The Sellick Bay escarpment exposes a volcanic-dominated sequence, and is locally devoid of sheeted dykes. The nearest sheeted dyke complex forms part of the upper crust transition zone that juxtaposes the Sandell Bay Sheeted Dyke Swarm (SBSD) and the Zone BVa volcanic domain (Davidson et al., 2004). These transition zone dykes are exposed about 500 m to the west of the Sellick Bay Fault Zone, where they outcrop along Macquarie Island's western coastline (Figure 5.50). Assuming that the volcanic sequence in the escarpment is tilted (on average) ~ 30° E*, and that no major neotectonic displacement has significantly disrupted the underlying rock package (in the escarpment section), then Site 1A is stratigraphically separated from the nearest sheeted dyke complex by a conformable volcanic pile at least 400 m thick.

Despite the absence of sheeted dykes near the Sellick Bay Fault Zone many isolated dykes have intruded the local volcanic rock package. Discrete dykes are massive and blocky, commonly forming prominent exposures (positive relief) in the escarpment slope and adjacent plateau; these contrast markedly with the more eroded pillow basalt outcrops (Figure 5.57). Dykes vary from < 50 cm to ~ 4 m-wide, and most are 1–2 m-across. Discrete dykes have slightly irregular margins, and most have preferentially intruded along less resistant inter-pillow selvages. Chilled, aphanitic

* The average amount of crustal tilt estimated here is consistent with my structural data, and the regional geological mapping work undertaken by Goscombe and Everard (2001) and Davidson et al. (2004).

dyke margins commonly envelop fine- to medium-grained phenocryst-bearing interiors. Many dyke margins are also sparsely vesicular; the 1–2 mm-wide, subrounded amygdules are mainly infilled with dark greenish-black clay minerals or pale, subradiating zeolite aggregates. The presence of vesicles in discrete dykes is here interpreted as evidence that dykes intruded into relatively high levels of the ocean crust, e.g., probably < 200 m below seafloor (McPhie et al., 1993).

Individual dykes near the SBFZ cut across the moderately E-dipping pillow sequence at a high-angle (suborthogonal) and consistently dip 50°–70° W to SW (Figure 5.51). The orientation of dykes both north and south of the SBFZ is similar, and their average strike is ~ 25°–35° W of the majority trend for the Sandell Bay Sheeted Dyke Swarm (SBSD) (Davidson et al., 2004). The dykes in the SBSD also have steeper dips than most discrete dykes (by ~ 10°–15°). These consistent structural variations may indicate that local dykes near Site 1A are not genetically related to the SBSD; they likely formed during separate and temporally distinct magmatic episodes.

Geological and hydrothermal features of alteration facies from the Sellick Bay Fault Zone

The Sellick Bay Fault Zone forms a 50–60 m-wide, NW- to NNW-striking structural corridor that cuts across the extrusive rock sequence in the Sellick Bay escarpment (Site 1A; Figure 5.58 - Insert C). The basaltic rocks have undergone moderate to strong brittle deformation (fracturing) and hydrothermal alteration; their secondary mineral assemblages, hydrothermal textures, and structural attributes are diagnostic of the vein-dominated, prehnite-zeolite alteration (VPZ) facies. These altered rocks occur in the main deformation corridor of the Sellick Bay Fault Zone (SBFZ), although they also outcrop sporadically in an adjacent ~ 100 m-wide transition zone to the north, i.e., transitional with Zone BIII (Figure 5.58 - Insert C). The northern extension is less intensely altered and deformed than the SBFZ, although discrete faults and hydrothermally derived assemblages are relatively more abundant than in other outcrop sections of the upper escarpment. In comparison, the spatial distribution of the VPZ facies is more sharply restricted (not transitional?) at the southern margin of the SBFZ, resulting in an intact outcrop sequence of regionally altered pillow basalts < 10 m away from the main deformation and alteration zone. Unfortunately, the along-strike distribution of the VPZ facies is unknown, as outcrops are only exposed in the ~ 200 m-long section of the upper escarpment. Despite regional reconnaissance along the projected fault trend (north and south of Site 1A), no other exposures of the Sellick Bay Fault Zone were identified (due to extensive soil cover on the plateau, and abundant unconsolidated talus further down-slope).

Vein-dominated, prehnite-zeolite (VPZ) facies

The vein-dominated, prehnite-zeolite (VPZ) facies consists of four main hydrothermal components. These characteristic phases are widespread in the Sellick Bay Fault Zone (SBFZ),

although most are heterogeneously distributed and preferentially associated with small-scale faults and breccias. Unlike the diagnostic alteration facies of the Major Lake Fault (the VQC and FMC facies) and the Caroline Cove Fault (the CQP and FMC facies), the VPZ facies lacks quartz, chlorite, and sulfide minerals. Instead, the hydrothermal components are dominated by:

i. Thick prehnite-bearing veins;

ii. Intense networks of zeolite- and prehnite-rich veinlets in minor faults and fractures;

iii. Massive, prehnite-dominated alteration pods; and

iv. Semi-pervasive to pervasive alteration of the primary basaltic groundmass and phenocrysts (plagioclase and olivine). Alteration minerals in the groundmass mainly comprise prehnite + zeolites + pumpellyite + clays + Fe-oxyhydroxide minerals.

Thick prehnite veins

Thick, curvi-planar to planar veins (> 10 mm-wide) consisting mainly of massive prehnite are a diagnostic component of the VPZ facies (Figure 5.59). These pale, single or multi-phase veins have sharp and well defined margins with their surrounding host rocks (Figure 5.60). Discrete vein segments typically have good outcrop continuity, and strike lengths are commonly > 50 m, i.e., vein continuity is limited by outcrop extent. The thickness of individual veins commonly varies along-strike from 20–40 mm, and some short segments have localised 'blows' up to ~ 100 mm-wide. Most thick prehnite veins strike consistently W to NW and dip steeply (subvertical) towards the SW or N (Figure 5.61).

Major outcrop veins in the VPZ facies are pale green to greyish-white and mainly contain massive, crystalline prehnite (± pumpellyite). Mottled, irregular patches of reddish-brown cement (Fe-oxyhydroxide minerals) are common along the outer margins of many vein segments. Vuggy cavities (< 20 mm diameter) are sparsely distributed throughout the cement (Figure 5.60), and some thicker veins also contain small angular fragments of altered basalt. Wall rock alteration selvages 50–100 mm-wide envelop many major vein segments, although they are not ubiquitous. Intensely altered vein selvages are characterised by multi-phase mineral envelopes that pervasively overprint the surrounding wall rock (Figure 5.62). These compositionally distinct selvages are (respectively) brownish-red and pale to dark green, and mainly consist of very fine-grained crystalline (intergrowths?) of prehnite + pumpellyite + clay minerals + Fe-oxyhydroxide minerals (Figure 5.63; refer to Chapter 6.3 for further details on the vein mineralogy and paragenetic relationships).

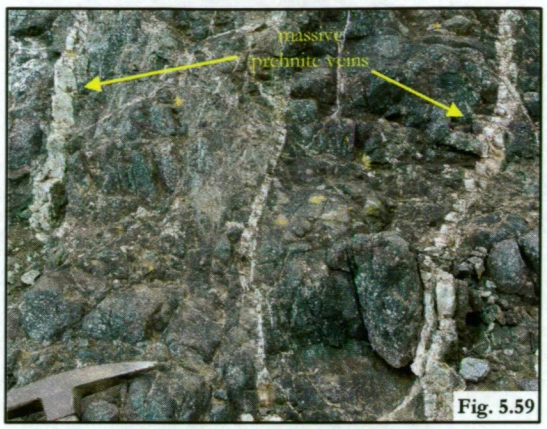

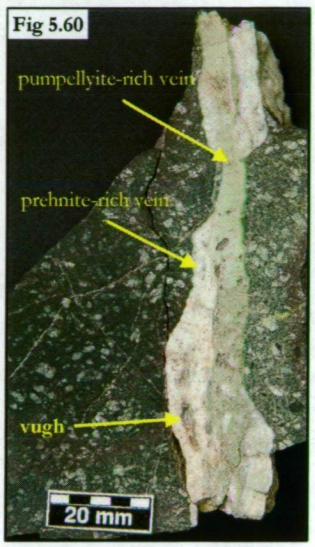

Figure 5.59: Massive, steeply dipping veins (> 10 mm-wide) are a diagnostic component of the vein-dominated, prehnite-zeolite alteration facies. Most thick veins are cemented with pale, fine-grained prehnite (± pumpellyite) and have sharp contacts with the surrounding basaltic host-rocks. The veins shown here intrude moderately altered flow basalt, and are well exposed in the north bank of the Sellick Bay creek (site 1A).

Figure 5.60: This multi-phase prehnite and pumpellyite vein has well defined margins that cut across the crystal-rich basalt groundmass. The crack-seal vein texture shown here indicates temporally distinct vein-forming stages, with the pale green pumpellyite vein post-dating the white prehnite vein. Both veins are massive, sparsely vuggy, and lack vein-specific alteration selvages in the surrounding host-rock (sample MCQ-285).

Intense zeolite-prehnite veinlet networks

Subparallel veinlet arrays are commonly associated with localised, small-scale (0.5–1.0 m-wide) brittle faults in the vein-dominated, prehnite-zeolite facies (Figure 5.64). Fault-hosted veinlets are irregular and discontinuous, and many have multiple dendritic branches and low- to moderate-angle offshoots (Figure 5.65). Thickness and continuity are highly variable along-strike, but most veinlets are < 10 mm-wide (2–5 mm average). Pale greyish-white to white zeolite minerals and minor prehnite comprises the hydrothermal cement and mainly occurs as finely intergrown aggregates. The basaltic groundmass (brittle-fractured fault zone rock) is also semi-pervasively replaced; very fine-grained, dark grey-green clays or reddish-brown Fe-oxyhydroxide minerals are abundant in most small fault zones (Figure 5.64).

Most veins (major and minor) in the Sellick Bay Fault Zone are steeply dipping and consistently strike W to NW; the dominant trend of the thick prehnite veins is about 15°–20° W of the SBFZ, and up to 35° W for the veinlet arrays (Figure 5.61). The wider data scatter associated with the narrow veinlets (compared to the major veins) probably reflects the irregular nature of these stockwork arrays, especially the abundance of finely branched veinlet networks and discontinuous offshoots. These anomalous veinlet characteristics may also account for the ~ 15° discrepancy with the mean orientation (dip direction) of the thick prehnite veins (Figure 5.61). Given their spatial, textural, and compositional affinities it seems likely that the major prehnite

veins are genetically related to the veinlet stockworks, and probably formed under similar hydrothermal and tectonic conditions. However, the consistent strike variation between the SBFZ (striking at ~ 310°–320°) and the prehnite and zeolite veins (striking at ~ 270°–290°) may indicate they formed under different stress regimes. This also provides evidence to suggest that the vein-forming hydrothermal stage is temporally distinct from the main (or most recent?) stage of tectonic activity that formed most structural components in the Sellick Bay Fault Zone, i.e., most SBFZ structures formed during neotectonic activity (post-spreading).

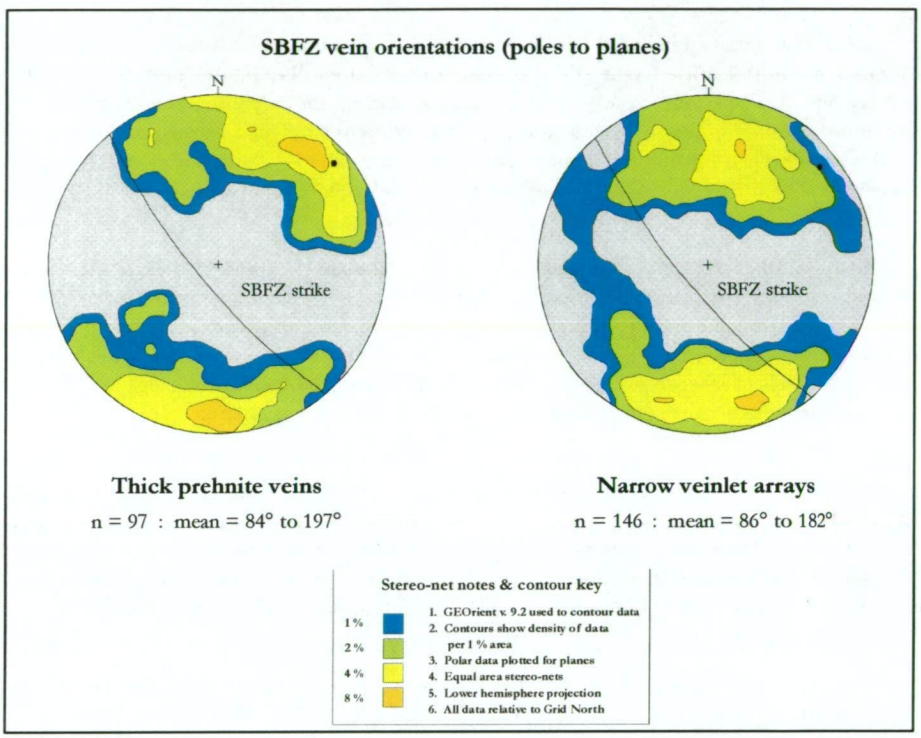

Figure 5.61: Contoured stereographic projections (poles to planes) of major and minor veins from the vein-dominated, prehnite-zeolite (VPZ) facies. The orientation of the Sellick Bay Fault Zone (SBFZ), which hosts the VPZ facies, is shown by the great circle overlay and cross-pole (solid black dot). The thick prehnite veins form a relatively well constrained dataset that mostly strike subparallel to the SBFZ. In contrast, the majority strike of narrow veinlet arrays are about 25°–35° W of the main structural trend (SBFZ) and have more diverse orientations, although the average amount of dip is similar.

Many veinlet arrays in the VPZ facies domain are structurally disrupted by highly fractured gouge and breccia zones (Figure 5.66). Brittle deformation structures are dominated by relatively small-scale fractures and joints (~ 10–20 mm-wide), and extend to larger, discrete faults (1–3 m across) with a spectrum of other tectonic discontinuities between these extremes. The breccia-gouge zones are finely foliated (subparallel) and structurally overprint the earlier-formed vein networks (Figure 5.67), further suggesting that most fracturing in the SBFZ post-dated the formation of hydrothermal veins. Fault breccias typically consist of small, elongated fragments of altered wall rock and vein cement (most < 20 mm across) in friable clay-gouge matrix. Brecciated fragments are angular to very angular and most are variably stained reddish-brown or pale green due to strong groundmass alteration (Figure 5.67).

Figure 5.62: A 10–20 cm-wide alteration selvage envelops the pale, massive prehnite vein that cuts across this pillow basalt outcrop. Many thick vein segments in the Sellick Bay Fault Zone (SBFZ) are surrounded by similar alteration haloes in the proximal wall-rocks. In this view, a narrow, reddish-brown selvage of Fe-oxyhydroxide minerals mantles the vein margins, and is further enclosed by a wider pumpellyite-dominated (pale green) alteration zone.

Figure 5.63: This intensely altered flow basalt is typical of many rocks that outcrop in the vein-dominated, prehnite-zeolite facies (VPZ) domain in the Sellick Bay Fault Zone (SBFZ) (Site 1A). Very fine- to fine-grained pumpellyite, prehnite, and minor clay minerals selectively replace most primary igneous phases, and impart a distinctive mottled texture in the altered groundmass. Pervasive pumpellyite alteration occurs in small (5–10 mm-wide) vein halos that enclose several of the narrow white prehnite veinlets shown here (sample MCQ-295).

Figure 5.64: Small-scale brecciated fault zones < 1 m-wide are common in the Sellick Bay Fault Zone, and many are spatially associated with highly fractured, subparallel vein arrays. Veins and veinlets are irregular and discontinuous, and most are cemented with pale, fine-grained zeolite minerals and prehnite. The local wall-rocks (pillow basalt) are moderately to strongly altered and consist of intergrown Fe-oxyhydroxide minerals (red-brown staining) and dark green to pale greenish-white crystal aggregates of prehnite + pumpellyite.

Figure 5.65: A subparallel array of zeolite veinlets cuts across the strongly altered groundmass of this pillow basalt from the Sellick Bay Fault Zone (SBFZ). These fine, anastomosing strands are characteristic of intense zeolite veinlet networks associated with the VPZ alteration facies. Textural evidence suggests that most zeolite veinlets post-date the widespread groundmass alteration, and formed relatively late in the hydrothermal paragenesis (sample MCQ-273).

Figure 5.66: This flow basalt unit, situated in the northern bank of the Sellick Bay creek (Site 1A), is cross-cut by a high intensity network of prehnite and zeolite veins. Typical of most outcrops in the Sellick Bay Fault Zone, the wall-rocks have undergone extensive brittle deformation and are highly fractured. Steeply dipping faults and joints are abundant, and the suborthogonal fracture-set disrupts the vein networks and their associated alteration selvages.

Figure 5.67: A typical finely foliated (subparallel) breccia-gouge fault from the Sellick Bay Fault Zone (SBFZ). The local deformation halo of this fault is < 1 m-wide and contains abundant, elongated wall-rock fragments (most < 20 mm) in gritty clay matrix. The breccia fragments mainly consist of moderately to strongly altered basalt (local wall-rock material) and pale zeolite vein segments. Small-scale brittle faults such as this are common in the SBFZ, and provide good evidence that the hydrothermal alteration assemblages formed prior to the main brittle deformation stage.

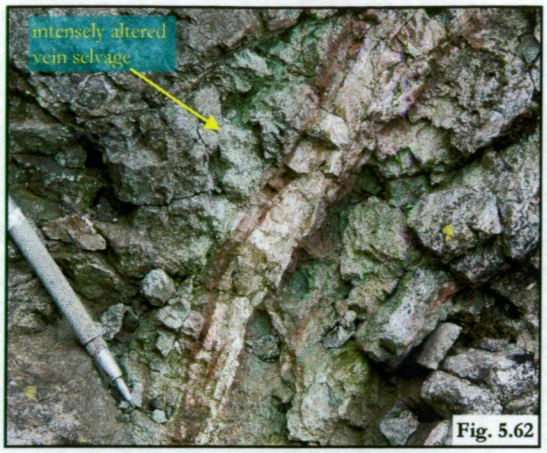

Fig. 5.62

Fig. 5.63


Fig. 5.64

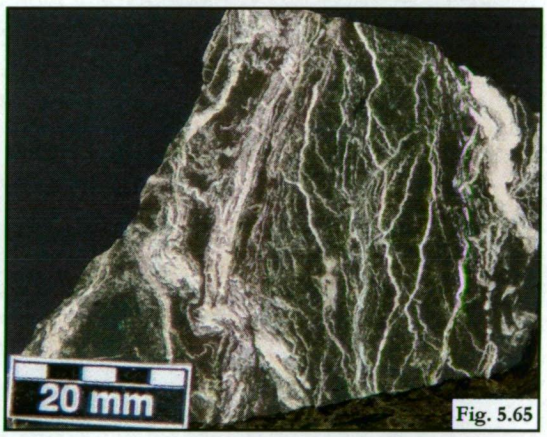

Fig. 5.65


Fig. 5.66


Fig. 5.67

Massive prehnite-rich alteration pods

Complex alteration pods dominated by massive prehnite partly replace many pillow basalt outcrops in the VPZ facies domain (Site 1A). These hydrothermally derived enclaves have compositions and textures that are similar to the thick prehnite veins and their proximal alteration selvages. The alteration pods mainly consist of very fine- to fine-grained intergrowths of pale greenish-white prehnite, dark green pumpellyite, and reddish-brown Fe-oxyhydroxide minerals (Figure 5.68). Small vughs and cavities are also common in the hydrothermal cement, and many are lined with fine- to medium-grained crystals.

Massive, prehnite-rich zones in the pillow basalt package have two main textural styles. Commonly, individual pillow cores are partly to completely replaced by subrounded alteration pods (Figure 5.69). Altered pillow cores have complex and irregular margins and vary widely in size, but most are 80–120 mm across. Massive alteration patches also partly replace glass-rich inter-pillow selvages and zones of hyaloclastite matrix. Most of the altered inter-pillow selvages are < 30 mm-wide, although larger wedge-shaped zones (up to 50–70 mm-across) occur in thicker inter-pillow segments adjacent to intersecting pillow lobe axes (Figure 5.70).

Semi-pervasive to pervasive groundmass alteration

The intensity of groundmass alteration in the VPZ facies ranges from moderate to very strong. Wall rock alteration is spatially heterogeneous and strongly dependant on permeability, with hyaloclastite zones commonly more intensely altered than surrounding pillow and coherent basalt. Intensely altered hyaloclastite matrix consists of a complex, multi-component assemblage of intergrown, fine-grained alteration minerals. Mottled patches of dark brownish-red (Fe-oxyhydroxide) and greenish-black (clay) hydrothermal material are widespread, and pale prehnite and zeolite veinlets irregularly cut across many altered hyaloclastites (Figure 5.71). Coherent basalt fragments hosted in the matrix are typically less altered than the surrounding volcanic glass, and many retain vestiges of their primary igneous textures e.g., plagioclase phenocrysts are still recognisable.

Small-scale faults (< 1 m-wide) and some primary volcanic structures (e.g., the margins of coherent basalt flow units) are also sites of locally intense groundmass alteration; their close spatial association provides further evidence of the intimate genetic relationship between hydrothermal alteration and 'oceanic' discontinuities. Groundmass alteration domains adjacent to permeable conduits have variable sizes and shapes, and are dominated by semi-pervasive to pervasive oxidation assemblages, e.g., locally intense patches of reddish-brown Fe-oxyhydroxide minerals (Figure 5.72). The intensity and distribution of alteration patches around rock discontinuities (conduits) is generally proportional to the size of the host structure (i.e., wider faults host larger and more extensive alteration zones), which probably reflects greater fluid volumes and more intense water–rock reactions.

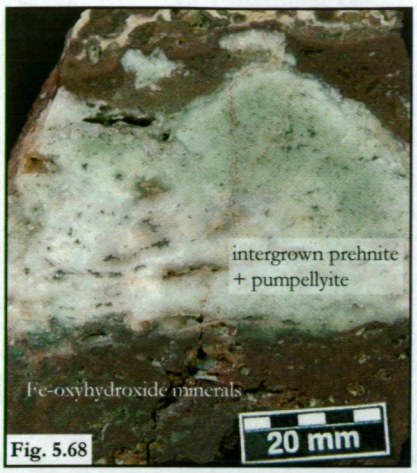

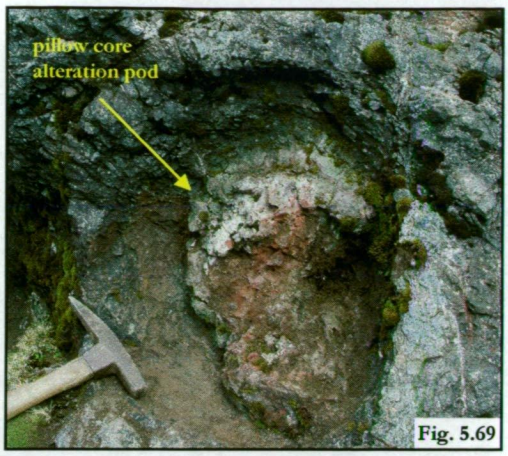

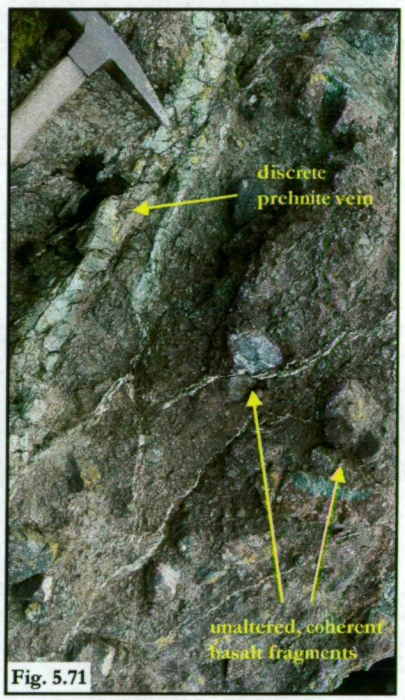

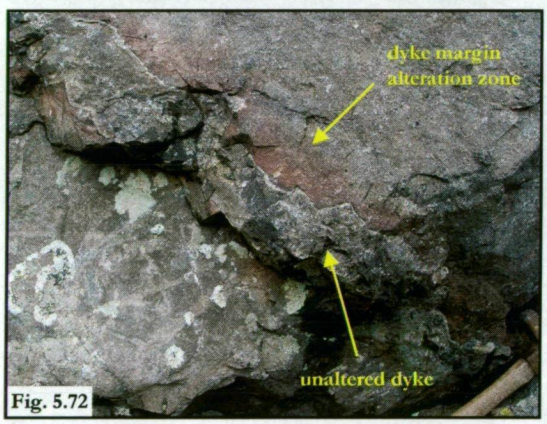

Figure 5.68: Cross-section view of a massive alteration pod from the inner core of a discrete pillow basalt lobe. The primary groundmass is pervasively altered and replaced by a complexly, intergrown assemblage of secondary minerals. The pale, greenish-white central segment is slightly vuggy and mainly consists of very fine-grained prehnite + pumpellyite. The core is enclosed by a strongly oxidised, Fe-rich groundmass alteration assemblage (sample MCQ-281).

Figure 5.69: A massive, subrounded alteration pod with an inner core of Fe-oxyhydroxide minerals enveloped by concentrically zoned and intergrown prehnite + pumpellyite + clay minerals. Altered pillow cores are a common component of the vein-dominated, prehnite-zeolite facies but rarely occur outside of the highly deformed and altered Sellick Bay Fault Zone.

Figure 5.70: Pale, prehnite-rich cement occupies many inter-pillow selvages in the pillow basalt sequence hosted in the Sellick Bay Fault Zone. This view shows wedge-shaped enclaves of massive alteration replacing glass-rich, inter-pillow axial margins ~ 10-20 cm-wide.

Figure 5.71: Intensely altered hyaloclastite is sporadically exposed in the central Sellick Bay Fault Zone. The highly permeable, glass-rich matrix shown here is pervasively altered and cross-cut by abundant prehnite and zeolite veins. However, coherent basalt fragments remain relatively unaltered, and commonly retain primary textural features, e.g., plagioclase phenocrysts.

Figure 5.72: A narrow dyke with irregular but well defined margins has intruded a flow basalt unit in the upper Sellick Bay escarpment (Site 1A). A ~ 10 cm-wide, reddish-brown alteration selvage (oxidised zone) is well developed in the host-rock groundmass, but is absent from the dyke.

Basalt and discrete dykes associated with the VPZ alteration facies, including rocks from veined and strongly altered fault conduits, mostly have low to moderate magnetic susceptibilities. Depending on the intensity of hydrothermal alteration, magnetic susceptibility commonly ranges from < 500–1500 x 10^{-5} SI units (Figure 5.73). Intensely prehnite-altered rocks (massive pods and vein-dominated zones) generally have the lowest magnetic signatures (most are < 500 x 10^{-5} SI units), indicating that primary igneous Ti-magnetite is mostly altered. In contrast, many regionally altered basalts (seafloor oxidation to zeolite facies grade) in the surrounding escarpment are highly magnetic (average values ~ 1300 x 10^{-5} SI units, Figure 5.73), although there is considerable overlap between the less altered VPZ facies rocks and many regionally altered basalt units. Thus, differences in magnetic susceptibility do not discriminate the VPZ facies basalts from their precursor rocks as effectively as the magnetic variations that differentiate the VQC and CQP facies (respectively) within the Major Lake and Caroline Cove districts.

Sellick Bay Fault Zone summary

The Sellick Bay Fault Zone is the only major fault system investigated during this project that hosts the vein-dominated, prehnite-zeolite (VPZ) alteration facies. The geographic distribution, host rock package, and hydrothermally derived components of the VPZ facies were outlined in Chapter 5.5. Many of these distinctive geological and hydrothermal features differ markedly from those associated with the Major Lake and Caroline Cove Faults. Significant contrasts provided by the unique mineral assemblages and textures of the VPZ facies suggest major variations in hydrothermal parameters and alteration processes, e.g., temperatures, fluid compositions, and the timing and intensity of fluid–rock interactions (relative to the hydrothermal systems that were active in the Major Lake and Caroline Cove Fault Zones). Based upon the detailed field observations and data previously outlined in this chapter, the following Discussion (Chapter 5.6) further explores the variability of the geological environments and hydrothermal regimes associated with the three major fault zones.

5.6. Discussion, synthesis and conclusions

The final component of Chapter 5 provides in-depth analysis and interpretation of important geological themes identified from fieldwork at the Major Lake, Caroline Cove, and Sellick Bay Fault Zones. This section addresses many of the critical issues relating to the interplay between the relict magmatic, tectonic, and hydrothermal systems that were active within these major upper crustal faults. Particular emphasis is given to:

i. Summarising the main geological and hydrothermal features associated with the Major Lake, Caroline Cove, and Sellick Bay Fault Zones;

Figure 5.73: Frequency histogram of magnetic susceptibility data from upper crustal rocks in the Sellick Bay region.

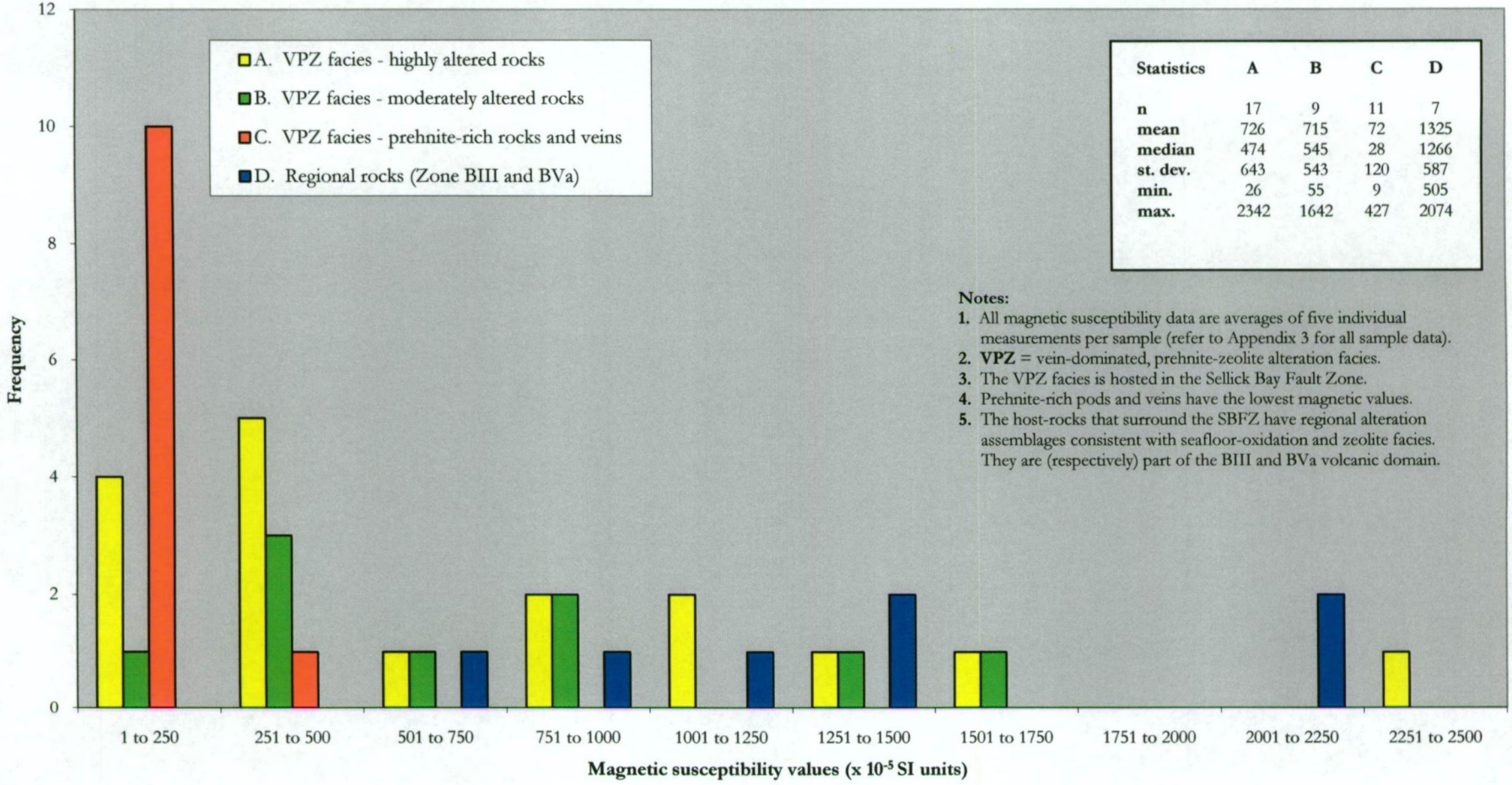

Statistics	A	B	C	D
n	17	9	11	7
mean	726	715	72	1325
median	474	545	28	1266
st. dev.	643	543	120	587
min.	26	55	9	505
max.	2342	1642	427	2074

Notes:

1. All magnetic susceptibility data are averages of five individual measurements per sample (refer to Appendix 3 for all sample data).
2. **VPZ** = vein-dominated, prehnite-zeolite alteration facies.
3. The VPZ facies is hosted in the Sellick Bay Fault Zone.
4. Prehnite-rich pods and veins have the lowest magnetic values.
5. The host-rocks that surround the SBFZ have regional alteration assemblages consistent with seafloor-oxidation and zeolite facies. They are (respectively) part of the BIII and BVa volcanic domain.

ii. Providing an initial interpretation of the hydrothermal conditions which formed the focussed alteration facies identified during this project;

iii. Evaluating the spatial distribution of alteration zones along the Major Lake Fault, especially their apparent segmentation pattern;

iv. Estimating and comparing the likely crustal depths (subseafloor) at which the main fault zone facies may have formed;

v. Highlighting the inherent heterogeneity of the focussed alteration assemblages;

vi. Outlining the most significant magmatic – structural – and hydrothermal relationships identified from field mapping and outcrop studies, and assessing the genetic implications of these geological associations; and

vii. Discussing the main geological themes that remain ambiguous or poorly understood following my detailed field-based investigation.

Summary of the geological and hydrothermal characteristics of focussed alteration facies on Macquarie Island

The Major Lake, Caroline Cove, and Sellick Bay Fault Zones are significant upper crustal discontinuities in the Macquarie Island ophiolite (Table 5.4). Each fault transects the entire width of the island (on-land strike lengths vary from ~ 1–4 km), and their projected orientations are closely correlated with offshore lineaments (spreading fabric) identified from marine geophysical surveys (Massell et al., 2000; Daczko et al., 2003). These NW- to NNE-striking faults each form important and well defined geological boundaries that juxtapose different rock types and regional (hydrothermal) alteration domains, e.g., the Major Lake Fault separates the upper greenschist facies rocks of the Sandell Bay Sheeted Dyke Swarm from the Zone BVa extrusive domain (zeolite grade). The lithological units that surround each fault mainly consist of diverse extrusive rocks (dominated by pillow basalt) and minor transition-zone sheeted dyke complexes; all are typical of the upper ocean crust.

Although fault zone rocks are poorly exposed along-strike, key outcrop sites preserve the intensely fractured cores of each major fault system. A spectrum of hydrothermal assemblages and abundant discrete faults, fracture networks, and breccia-gouge seams provides clear evidence for the complex evolution of these highly deformed fault corridors. Structural attributes and hydrothermal relationships indicate that each fault initially formed during slow-spreading crustal extension at the Proto-Macquarie Spreading Ridge. Widespread geological evidence further suggests that the fault zones remained focal points for prolonged tectonism; reactivated fault and fracture networks, intensely re-brecciated alteration zones and various late-stage structures that cross-cut, overprint, or displace original fault segments all attest to multiple tectonic stages.

Table 5.4: Comparison of the geological and hydrothermal attributes of major upper crustal fault zones investigated on Macquarie Island.

Structural system	Main outcrop locations and study sites	Fault zone orientation	Estimated fault zone length (on-land)	Width of main deformation zone	Alteration facies	Rocks in the footwall	Rocks in the hangingwall	Main structural trends
The Major Lake Fault Zone	There are 4 main outcrop sites on the central plateau and escarpment slopes of south-central Macquarie Island (Sites 2A to 2D).	The fault zone mostly strikes NW to NNW.	~ 4 km strike extent from the east coast at Lusitania Bay across the plateau to the west coast at Sandell Bay. Probably extends off-shore.	The main deformation zone at the Sandell Bay creek exposure is 10 to 20 m-wide. Other sites are poorly exposed but probably < 10 m-wide.	**1. The vein and breccia, quartz-chlorite (VQC) facies;** 2. The foliated, massive chlorite (FMC) facies; and 3. The narrow, focussed quartz vein (NQV) facies (in the proximal footwall domain).	Upper-greenschist to lower-amphibolite facies dolerite dykes and transition zone pillow basalt of the Sandell Bay Sheeted Dyke Swarm and the Zone BVI volcanic rock domain.	Low grade (oxidised and zeolite facies) pillow basalts of the Zone BVa and BIV volcanic rock domains. Discrete dykes and minor hyaloclastites also occur.	Relatively early, steep NE- to SE-striking dextral-oblique and reverse faults are cross-cut by abundant NNW- to NNE-striking faults and fractures. Most of the late discontinuities are subparallel with the Major Lake Fault Zone.
The Caroline Cove Fault Zone	A single main outcrop location (with multiple foreshore and creek valley exposures) occurs at Caroline Cove, on the far south-west coastline of Macquarie Island.	The fault strikes NNW to NNE, although most creek exposures are oriented N to NNE.	~ 1 km on-land strike from Windsor Bay to Caroline Cove.	The main deformation zone in the Caroline Creek valley is 1–2 m-wide. The estimated maximum width is probably < 5 m.	**1. The massive and veined, chlorite-quartz-pyrite (CQP) facies;** 2. The foliated, massive chlorite (FMC) facies; and 3. The pervasive, Fe-oxyhydroxide overprint (PFO) facies.	The western pillow sequence; mainly comprising elongated pillow basalt with prehnite and lower- greenschist facies regional alteration assemblages.	The eastern pillow sequence; mainly comprising weakly altered (seafloor oxidation facies) pillow basalt. These rocks are highly magnetic.	Mainly steep, N- to NNE-striking faults, fractures, and breccia zones with normal or oblique-slip kinematics (commonly sinistral). Minor NNW-striking faults also occur, and these cut across the dominant orientation.
The Sellick Bay Fault Zone	A single main outcrop site occurs in the upper escarpment at Sellick Bay, on Macquarie Island's central west coast.	The fault zone mainly strikes NW to NNW.	~ 4 km strike length (estimated), extending from the west coast escarpment at Sellick Bay towards the south-east.	The NW-striking zone of intense deformation and alteration occurs in a 50 m-wide outcrop zone.	**1. The vein-dominated, prehnite-zeolite (VPZ) facies.**	Mainly pillow basalt with rare discrete dykes; most have zeolite grade regional alteration assemblages.	Regionally oxidised and zeolite-altered pillow and massive flow basalt, hyaloclastite, and minor dolerite dykes.	Steeply dipping, NW- to NNW-striking faults are most common; many have dextral sense of shear.

Note:
1. The diagnostic alteration facies of each fault zone is highlighted in bold.

The initial phase of structural activity associated with each fault probably involved episodic periods of deformation and displacement during (mainly) tectonic-induced seafloor spreading (Daczko et al., 2003; Rivizzigno and Karson, 2004). As discussed in Chapter 4.2, various stages (commonly cyclic) and processes (tectonic- and magmatic-induced) of extension are typical of modern slow-spreading mid-ocean ridges, e.g., the mid-Atlantic Ridge and Southwest Indian Ridge. Episodic spreading accommodated by multiple extensional processes may be especially favoured by the inherent tectonic and magmatic characteristics of anomalously slow and obliquely-spreading ridges, as interpreted for the Proto-Macquarie Spreading Ridge (Rivizzigno, 2002).*

Further structural modification of each major fault system continued as the Indo-Australian–Pacific plate margin evolved into the present dextral transcurrent system (Goscombe and Everard, 2001). Abundant, late-stage clay-gouge faults and breccia zones, most of which specifically lack high temperature alteration minerals, have dominantly strike-slip and oblique-slip kinematic indicators. These structural and hydrothermal relationships provide clear evidence that neotectonic faulting (uplift-related) post-dated the peak hydrothermal conditions, and probably modified the distribution, abundance, and geological associations of many earlier-formed (on-axis) alteration zones (including focussed assemblages and regional domains).

Some of the most compelling evidence for the spreading-related origin of the Major Lake, Caroline Cove, and Sellick Bay Fault Zones is their spatial affinities with localised hydrothermal assemblages. My field study led to the recognition of six distinctive alteration facies that are uniquely associated with these major faults. Altered fault zone basalts have significantly different mineral assemblages and hydrothermal textures from those in the surrounding regional alteration domains, which were interpreted by Griffin (1982) to have formed during seawater-dominated recharge. The geographic distribution and physical attributes (e.g., outcrop dimensions and structural orientations) of the focussed alteration zones are also closely allied to the strike of their host structure. Thus, the multi-faceted association between these structural zones and altered rocks provides evidence that the major discontinuities were highly permeable conduits in the ocean crust. Seafloor hydrothermal fluids were preferentially channelled in the structural breaks, and intense water–rock reactions formed their characteristic alteration minerals (locally abundant but spatially restricted). Hydrothermal conditions in the fault conduits (e.g., fluid temperatures, pressures, and compositions) were clearly anomalous compared to those in the more widespread zones of seawater recharge.

The three major fault zones each host a unique and highly distinctive hydrothermal assemblage that consists of between one and three individual alteration facies (Table 5.4). A diagnostic, multi-component (mineral) facies characterises each fault; some facies are also associated with

* Although, as discussed in Chapter 3.9, inconsistent data and interpretations for each (main) tectonic model proposed for Macquarie Island's formation means that the localised spreading ridge environment (e.g., a ridge-transform intersection or an oblique accommodation zone) currently remains enigmatic, and the source of continuing speculation.

more than one structural host, e.g., the foliated, massive chlorite facies occurs in both the Major Lake and Caroline Cove Fault Zones. The spatial distribution, alteration intensity, and physical features of different alteration facies also vary significantly between faults (Figure 5.74). Moderate to intense wall rock alteration, abundant veins and breccias, and minor enclaves of massive mineralisation are characteristic features of the focussed alteration zones. Cross-cutting and overprinting relationships between different mineral assemblages (representing distinct temporal stages of vein formation and wall rock alteration) also occur within each discrete facies and between different (but spatially related) facies (Figure 5.74); these relationships imply disequilibrium conditions and multiple episodes of hydrothermal activity

Preliminary interpretation of hydrothermal conditions and processes

The Major Lake and Caroline Cove Fault Zones

The field scheme used to classify each hydrothermal facies is based on the significant alteration mineral assemblages and hydrothermal textures, and the intensity and extent of the alteration zones, i.e., their spatial association, regional distribution, and stratigraphic relationships (Gifkins et al., 2005). These criteria clearly differentiated each facies, and provided an effective and consistent framework to identify the alteration zones in the field. However, several diagnostic alteration facies share similar traits, and these provide evidence for common hydrothermal processes and conditions between different faults. In particular, the alteration minerals of the diagnostic facies from the Major Lake Fault (VQC facies) and the Caroline Cove Fault (CQP facies) are dominated by quartz, chlorite, and pyrite (Table 5.5 and Figure 5.74). Discrete veins and quartz-cemented breccias are abundant, and the basaltic wall rocks are semi-pervasively to pervasively chloritised. These focussed alteration facies also share similarities with spatially restricted alteration zones documented from many ophiolite terranes (e.g., Zierenberg et al., 1988; Haymon et al., 1989; Richards et al., 1989) and oceanic ridges (Ridley et al., 1994; Martin and Lowell, 2000; Teagle and Alt, 2004) (and other references cited in Chapter 4.4).

Reference to, and comparison with, previous studies of focussed alteration zones (in other ocean crust and ophiolite settings) provide an initial method of interpreting the hydrothermal systems that formed the quartz- + chlorite- + sulfide-bearing assemblages at Major Lake and Caroline Cove. These characteristic mineral assemblages and textural attributes are commonly interpreted to evolve from high temperature fluids associated with hydrothermal discharge in the axial environment, e.g., Delaney et al. (1987), Saccocia and Gillis (1995), Gillis et al. (2001). Water–rock ratios are significantly greater than those in the surrounding rocks (which are less fractured and have lower permeability), and fluid compositions are highly evolved relative to their seawater precursor. Various studies have shown that upflow fluids are hotter (~ 250°–350° C), more acidic, and contain greater concentrations of dissolved metals and sulfur than off-axis (recharge-related) oceanic hydrothermal fluids (Hannington et al., 1995a; Honnorez, 2003).

The structural association and spatial distribution of focussed, fault-zone alteration facies

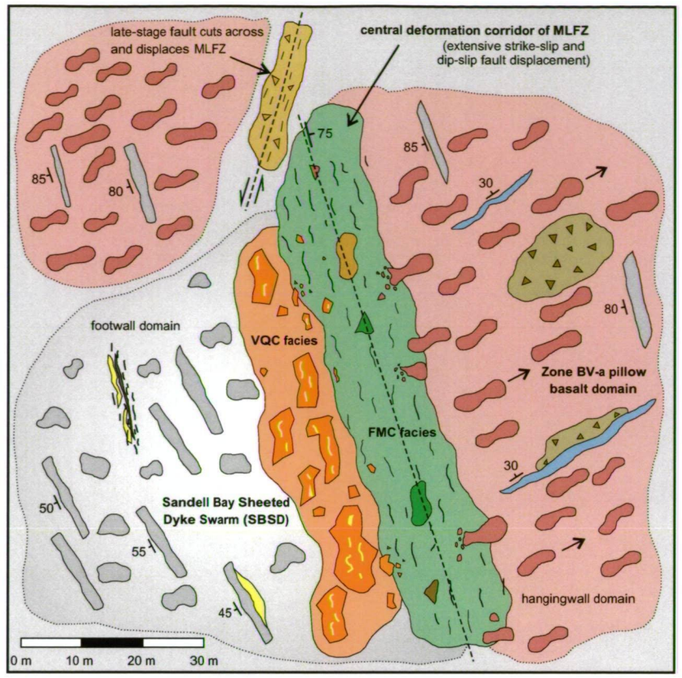

The Major Lake Fault Zone

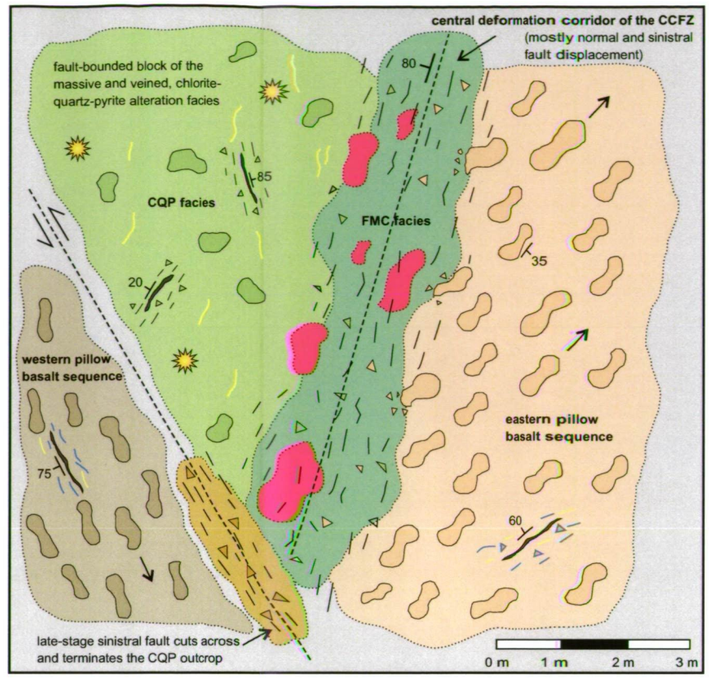

The Caroline Cove Fault Zone

Notes

1. These diagrams schematically depict the three fault systems investigated during this project, based upon geological information obtained during detailed outcrop mapping of the key sites. All of the diagrams are oriented towards grid north and are shown at approximate scale (although the scale varies for each fault-zone).

2. These diagrams clearly show the consistent and intimate relationship between the focussed alteration facies and their structural hosts. All of the focussed alteration facies occur in an elongated zone that is parallel to the major fault system.

3. The Major Lake and Caroline Cove Fault Zones host multiple alteration facies, providing good evidence for episodic hydrothermal circulation. The peak hydrothermal stage formed very distinctive mineral assemblages that are characterised by quartz, chlorite, epidote, and sulfide minerals. The parent fluids are interpreted as high-temperature and chemically evolved; they were probably associated with the discharge (upflow) stage of an on-axis hydrothermal system.

4. The alteration facies hosted in the Sellick Bay Fault Zone significantly contrasts with those at Major Lake and Caroline Cove. The strongly altered fault zone contains relatively low-temperature alteration assemblages that are broadly similar to those in the surrounding host-rocks. The Sellick Bay Fault Zone is thus interpreted as a primary seafloor conduit for recharge-related hydrothermal fluids (probably seawater-dominated).

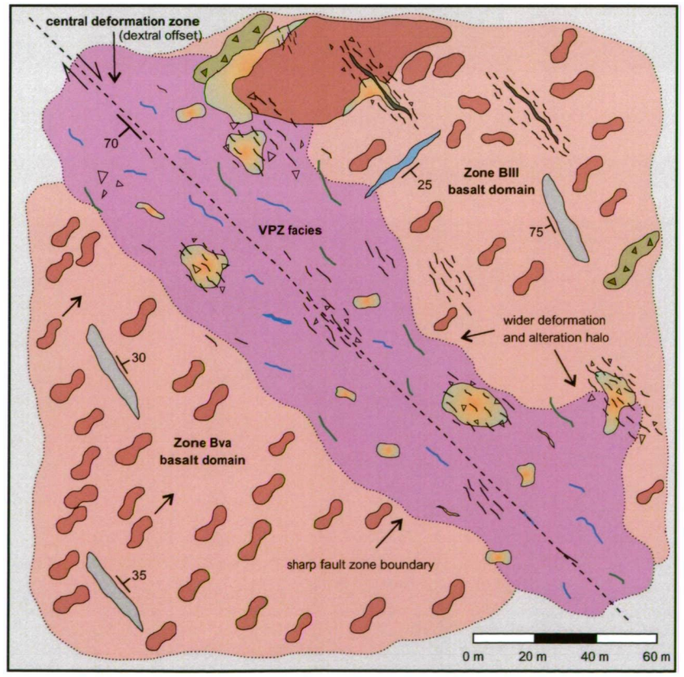

The Sellick Bay Fault Zone

Legend

Focussed alteration zones

- Vein and breccia, quartz-chlorite (VQC) facies
- Foliated, massive chlorite (FMC) facies
- Massive and veined, chlorite-quartz-pyrite (CQP) facies
- Narrow, focussed quartz vein (NQV) facies
- Pervasive, Fe-oxyhydroxide overprint (PFO) facies
- Vein-dominated, prehnite-zeolite (VPZ) facies

Regional alteration zones

- Low intensity seafloor oxidation facies
- High intensity oxidation and zeolite facies
- Prehnite to lower-greenschist facies
- Mid- to upper-greenschist facies

Late-stage strike-slip fault zone - abundant breccia and gouge but no fault-specific alteration

- Elongate pillow basalt (with trend)
- Pillow basalt (trend not determined)
- Massive flow basalt layer
- Hyaloclastite-rich zone
- Dolerite dyke
- Sedimentary rock layer
- Massive sulfide alteration zone
- Massive prehnite-rich alteration zone
- Quartz veins
- Prehnite veins
- Regional fault zone
- Oriented fractures
- Breccia fragments
- Strike and dip symbols

GN MN 31°

Magnetic north is shown for 2005. It moves 3.6' east each year

Figure 5.74: Schematic plan view diagrams showing the spatial distribution and structural architecture of the focussed alteration facies defined during this study. These diagrams summarise and compare the facies associations of each fault zone investigated during this project, and particularly highlight the unique association between altered fault zone rocks and their structural hosts (fluid conduits). All of the faults contain moderately to intensely altered upper crustal rocks that have significantly different alteration mineral assemblages, hydrothermal textures, and outcrop features from the relatively low-grade, regional alteration assemblages that occur in the surrounding volcanic-dominated wall rocks.

Table 5.5: Comparison of the main geological features associated with the diagnostic alteration facies in the Major Lake and Caroline Cove Faults.

Vein and breccia, quartz-chlorite (VQC) facies (Major Lake Fault)	Massive and veined, chlorite-quartz-pyrite (CQP) facies (Caroline Cove Fault)
Recognised from four main outcrop sites on the south-central plateau and the upper escarpment slopes at Lusitania Bay (east coast) and Sandell Bay (west coast) (Sites 2A to 2D).	A single occurrence in the central segment of the Caroline Cove embayment, with multiple outcrops exposed in steep coastal foreshore and creek valley segments.
Hosted in regionally altered (greenschist facies) sheeted dolerite dykes and transition zone pillow basalts of the Sandell Bay Sheeted Dyke Swarm and the Zone BVI volcanic domain	Hosted in an extrusive rock-dominated package of pillow basalt and minor hyaloclastite; rare discrete dykes have also intruded the sequence. The regional alteration assemblages are relatively low grade, typified by widespread zeolites and minor prehnite.
Outcrops occur adjacent to the Major Lake Fault Zone and form relatively resistant exposures that significantly contrast (positive relief) with the surrounding host rocks. Altered outcrop zones are elongate and fault-parallel, although their spatial dimensions vary between sites.	Occurs in a relatively large and fault-bound outcrop wedge (~ 8 km^2), with the Caroline Cove Fault Zone forming the eastern boundary of the alteration zone.
The intensity and spatial distribution of alteration within each outcrop zone is very heterogeneous.	Groundmass alteration is consistently strong in the main zone of altered basalt.
Abundant veined and massive quartz alteration is the most characteristic feature. Major veins have preferred orientations subparallel to the Major Lake Fault Zone. Quartz-rich hydrothermal cements commonly contain angular, brecciated fragments of strongly chlorite-altered basaltic wall rocks. Minor pyrite occurs as fine-grained disseminated crystals and veinlets.	Strong chlorite-alteration of basaltic wall rocks is characteristic and widespread throughout the main zone. Quartz, epidote, and sulfide minerals (pyrite ± chalcopyrite) are common and form massive pod-like zones or complex vein arrays. Some spectacular massive sulfides also occur.
Minor epidote occurs in some quartz veins, and late-stage prehnite veins rarely cut across quartz-altered zones.	Minor barite occurs in the chlorite-quartz paragenesis, and late-stage prehnite and calcite veins cut across the pre-existing chlorite alteration in the groundmass.
The VQC facies is partly overprinted in the Major Lake Fault Zone by the foliated, massive chlorite (FMC) facies.	The CQP facies is partly overprinted in the Caroline Cove Fault Zone by the foliated, massive chlorite (FMC) facies, and the pervasive, Fe-oxyhydroxide overprint (PFO) alteration facies.

Interpretative note:
Based on their characteristic alteration mineral assemblages, hydrothermal textures, and close spatial association with major crustal fault zones, both of these diagnostic alteration facies are interpreted to have formed from high temperature, chemically evolved hydrothermal fluids associated with the discharge phase of an on-axis hydrothermal system. The main facies differences outlined here probably reflect variations in crustal depth and the relative influence (abundance) of entrained seawater that mixed with the hydrothermal fluid in the upper crust. These factors would promote slightly different physico-chemical conditions in the hydrothermal system and thus affect the type, abundance, and distribution of alteration minerals.

These anomalous hydrothermal conditions produce distinctive alteration domains in the upper crust (sheeted dykes and extrusive rocks) characterised by abundant veins and breccias, massive sulfide mineralisation, and pervasively altered wall rocks. The mineral assemblages formed under these hydrothermal conditions are typified by abundant quartz + chlorite + sulfides; thus, they are very similar to the diagnostic alteration facies in the Major Lake and Caroline Cove Faults. Therefore, the mineral assemblages and hydrothermal textures of the VQC and CQP facies, combined with their spatially restricted (fault focussed) distribution, provide good evidence to interpret a strong genetic association with the discharge phase of the oceanic hydrothermal system. In particular, high temperature and chemically reactive fluids, enriched in Si, S, and metals, are implicated in the formation of these altered fault zone rocks.

The Sellick Bay Fault Zone

The moderate to strong alteration intensity, widespread spatial distribution (> 50 m-wide fault-hosted zone), and significant textural contrasts with the surrounding wall rocks all suggest that the Sellick Bay Fault Zone was a highly permeable fluid conduit in the ocean crust. However, unlike the alteration zones along the Major Lake and Caroline Cove Faults, the vein-dominated, prehnite-zeolite (VPZ) facies at Sellick Bay is dominated by relatively low temperature hydrothermal minerals, e.g., most zeolites form at temperatures < 100°–150° C (Chipera and Apps, 2001). The VPZ facies lacks the main alteration minerals and hydrothermal assemblages that typically form in ridge-axis upflow zones; instead, prehnite, zeolites, and Fe-oxyhydroxides are the most common secondary minerals. The absence of quartz, chlorite, and sulfide minerals indicates that hydrothermal conditions (e.g., fluid compositions) and alteration reactions were considerably different in the Sellick Bay Fault Zone (compared to conditions in the Major Lake and Caroline Cove Faults). The relatively low temperature mineral assemblages of the VPZ facies have broad similarities with the regional alteration facies (recharge-related) that occur widely in the surrounding volcanic rocks. Although the scale and intensity of VPZ facies alteration is considerably greater than the alteration effects in the nearby host rocks (Zone BIII and BVa), the hydrothermal mineral assemblages and textural attributes are comparable. Furthermore, the most intensely altered regional (host rock) assemblages are also strongly focussed along structural conduits, albeit at a much smaller scale than the Sellick Bay Fault Zone, e.g., the margins of discrete dykes and minor faults. The geological similarities between the VPZ facies and surrounding regionally altered rocks, combined with significant mineral and textural contrasts with the main hydrothermal assemblages at Major Lake and Caroline Cove, suggests that the Sellick Bay Fault Zone was unlikely to have been a site of high temperature fluid upflow. Rather, this major structural conduit may have provided a highly permeable crustal pathway for recharge-related fluids (i.e., relatively low temperature fluids with dominantly seawater-like compositions) in an off-axis (ridge-flank?) setting, or during periods of low hydrothermal flux at the Proto-Macquarie Spreading Ridge.

Along-strike segmentation of focussed alteration facies

Along-strike (fault-parallel) variations in spatial distribution and alteration intensity, and their causative mechanisms, are difficult to evaluate for several reasons. Considerable geological evidence (previously documented in Chapter 5) indicates that the structural architecture of many major faults has been extensively modified by post-hydrothermal displacement and reactivation. For example, the Major Lake Fault Zone is cross-cut and displaced at Sandell Bay creek (along with its intimate hydrothermal assemblages) by a brecciated (but unaltered) dextral-oblique fault (interpreted to have formed during neotectonic activity). In addition to causing widespread deformation and a diverse range of fault styles and orientations (Figure 5.25 – Insert B), late-stage structural activity has also changed the spatial distribution of the focussed alteration facies (both along- and across-strike). Assessing the magnitude of post-hydrothermal changes and reconstructing the original facies architecture is further hampered by extensive weathering and erosion along each fault zone and the physical isolation of the key sites. The fault hosted assemblages are commonly obscured by soil and debris, and only occur as sporadic outcrops which are not continuously developed along-strike. The alteration facies associated with the Caroline Cove and Sellick Bay Fault Zones, for example, are restricted to single localities where the preservation and exposure of the altered rocks is favoured by the local topography. Reconnaissance mapping along the projected fault zone orientation failed to locate other distal outcrops. However, multiple scree-covered areas along-strike of the projected Sellick Bay Fault Zone consist of abundant angular rock fragments that have many similar features to the vein-dominated, prehnite-zeolite (VPZ) facies. These localised debris occurrences (scattered across areas < 200 m^2) suggest that other segments of the Sellick Bay Fault Zone, now largely eroded and covered by overburden, may host similar zones of VPZ facies alteration. However, given their highly dispersed nature and the total absence of *in situ* outcrop, these sites are not readily amenable to further mapping or detailed studies.

Despite the impediments outlined above, the Major Lake Fault Zone provides a limited opportunity to evaluate along-strike (fault-parallel) variations in the alteration facies architecture. The vein and breccia, quartz-chlorite facies, diagnostic of the Major Lake Fault Zone, is relatively resistant to weathering and is the sole focussed alteration zone that outcrops on the central plateau. In contrast, the foliated, massive chlorite (FMC) facies, which is intimately associated with the highly deformed and poorly exposed core of the Major Lake Fault, only occurs at Sandell Bay creek (Site 2A; Figure 5.74). Thus, it is not possible to further evaluate or interpret the along-strike distribution of the FMC facies, or any spatial variations in alteration intensity that may occur along the Major Lake Fault, e.g., is it continuously developed or segmented at semi-regular intervals along-strike (?)

The four main outcrops of the vein and breccia, quartz-chlorite (VQC) facies are segmented at intervals of ~ 750–1500 m along the Major Lake Fault Zone (Figure 5.1). The mineral assemblages and hydrothermal textures are similar at each site, although the outcrop dimensions (Table 5.2) and the relative abundances of some minerals vary, e.g., sulfide minerals are more widespread at Lusitania Bay (Site 2D). These site-specific characteristics show no obvious systematic or consistent variations

along-strike, and are interpreted to reflect local geological or hydrothermal heterogeneities rather than any pattern of broader (regional) segmentation along the fault, i.e., the obvious site-by-site variations are probably unrelated to along-strike differences in crustal depth during focussed hydrothermal flow. The Major Lake Fault Zone is not exposed between the four outcrop sites; hence, the spatial distribution of the VQC facies is unknown between the discrete alteration zones. However, the absence of remnant outcrops or angular quartz-rich scree fields on the projected fault trend suggests that the VQC alteration zones are not continuously developed along-strike. Instead, the localised occurrence of discrete sites with well defined spatial and geographic limits (Table 5.2) provides evidence for along-strike segmentation of the parent hydrothermal system. However, because of the relatively sporadic along-strike exposure and extensive overburden, the full geographic extent of the VQC facies, and the nature of any transitional assemblages that may occur between discrete sites, currently remains unknown and speculative.

Along-strike segmentation of axial hydrothermal systems, and their focussed alteration zones, has been documented from the mid-Atlantic Ridge (German and Parson, 1998) and the East Pacific Rise (Haymon and White, 2004) (Chapter 4.4). Hydrothermal segmentation occurs across a wide scalar range (e.g., 3rd- and 4th-order ridge segments) and is mostly controlled by the interaction of subseafloor magmatic and tectonic features, e.g., segregated axial melt lens and the structural architecture of rift valley faults (Haymon and White, 2004). Tivey and Johnson (2002) described segmented zones of low magnetisation at the Endeavour and High Rise hydrothermal fields on the northern Juan de Fuca ridge. These form narrow, pipe-like bodies which are consistently spaced ~ 200 m-apart along the axial valley. The pipe-like magnetic lows are interpreted as zones of hydrothermal upflow that contain intensely altered basaltic crust (Tivey and Johnson, 2002). In this example, fine-scale segmentation of the discharge system is thought to be influenced by obliquely intersecting basement faults and across-axis (ridge-normal) zones of hydrothermal flow (Tivey and Johnson, 2002).

Major structural discontinuities provide important focal mechanisms that strongly influence the location of hydrothermal discharge sites in the ocean crust (Alt, 1995). Highly fractured and permeable fault intersections, commonly with multiple cross-cutting orientations, are especially effective conduits for localising rapid fluid upflow. Detailed studies of the structural architecture underlying the active TAG mound (perhaps the best known *in situ* example of a modern hydrothermal upflow system) have suggested that the relatively narrow fluid discharge zone (subseafloor) is focussed by the intersection of active, axis-parallel faults with another set of obliquely oriented (and earlier-formed) discontinuities (Kleinrock and Humphris, 1996; Kleinrock et al., 1996). Segmented fault intersections similar to those at the TAG mound and Juan de Fuca Ridge (Tivey and Johnson, 2002) form important structural breaks in the ocean crust that may facilitate rapid and effective discharge of hydrothermal fluids. Consequently, segmented zones of highly altered basalt, genetically associated with these discontinuities, would likely be spaced at relatively consistent intervals along the main axis-parallel faults.

Intersecting basement structures provide a possible mechanism to explain apparent along-strike segmentation of the vein and breccia, quartz-chlorite (VQC) facies in the Major Lake Fault. Many of the focussed VQC facies zones, which are here interpreted as localised and structurally controlled sites of hydrothermal upflow, are spaced along-strike at intervals of ~ 750 m (Figure 5.1)*. This relatively consistent segmentation pattern implies that processes of hydrothermal flow and wall rock interaction within the MLFZ were heterogeneous, i.e., hydrothermal parameters varied significantly at different segments of the fault. Discrete basement structures that obliquely transect the main structural corridor (e.g., pre-existing fault and fracture networks) may have influenced the along-strike distribution of the VQC facies. Limited geological evidence supports this hypothesis, especially the occurrence of abundant suborthogonal fracture networks that cut across the NNW trend of the MLFZ (as noted at Sandell Bay creek (Site 2A), refer to the detailed structural transect shown in Figure 5.25 – Insert B). Obliquely intersecting quartz veins at Major Lake foreshore (Site 2B) (Figure 5.23) also provide evidence that cross-cutting structures may have influenced fault-parallel segmentation of the VQC facies, particularly as local vein orientations are strongly influenced by the dominant structural trends, i.e., quartz veins consistently strike subparallel to the orientation of the main fault zone (Figure 5.23). There is also no compelling field evidence to support alternative models of hydrothermal segmentation. For example, the VQC facies zones are not spatially associated with localised volcanic activity or high intensity dyke swarms, which may have provided potential heat sources to initiate and sustain small-scale (and spatially segmented) hydrothermal upflow.

Despite the observations and results arising from my field study, many enigmatic questions remain about the nature of along-strike variations in fault focussed hydrothermal upflow systems and their alteration facies. Field observations and data indicate that the VQC facies is structurally segmented along the Major Lake Fault, and that these localised sites of hydrothermal discharge may have been influenced by intersecting basement structures. However, definitive evidence of the range of geological factors that may have controlled the pattern of segmentation is elusive, and is further complicated by the effects of post-hydrothermal faulting (displacement) and extensive overburden. Important questions remain unresolved on the absolute spatial extent and distribution of the segmented alteration zones in the Major Lake Fault (both along- and across-strike), and the characteristics of any transitional assemblages that may link the hydrothermal facies identified during this project, e.g., the nature of the boundary between the VQC and FMC facies.

Estimates of crustal depth during focussed fluid flow and wall rock alteration in major fault systems

Multiple lines of evidence suggest that the Major Lake and Caroline Cove Fault Zones were originally significant seafloor discontinuities (on-axis) at the Proto-Macquarie Spreading Ridge.

* Sites 2A, 2B, and 2C are spaced at intervals of ~ 750 m along the fault (Figure 5.1). Site 2D occurs about 1500 m away from Site 2C, i.e., double the interval spacing of the other sites. Despite extensive reconnaissance work, no intermediate outcrop site was located between 2C and 2D, although it may have been removed by erosion or neotectonic activity.

These faults were highly permeable crustal pathways at the relict spreading ridge, and preferentially channelled high temperature, chemically evolved fluids associated with hydrothermal upflow, i.e., the discharge phase of oceanic hydrothermal systems. As previously discussed, both fault zones have alteration mineral assemblages and hydrothermally derived textures that are typical of upflow zones. However, important differences characterise the diagnostic alteration facies of each fault (i.e., the VQC and CQP facies), and these imply that the hydrothermal conditions and alteration processes in the underlying stockworks were locally variable.

Previous studies of hydrothermal upflow zones in modern oceanic settingsand ophiolite terranes have shown that many alteration assemblages and facies associations correspond to different crustal depths, e.g., investigations undertaken at the Galapagos Fossil Hydrothermal Field (Ridley et al., 1994) and the Bent Hill Massive Sulfide Deposit (Teagle and Alt, 2004). Subhorizontal zonation (vertical profiles) of alteration facies in the fractured basement beneath the TAG mound is also well documented from ocean drilling programs, e.g., Tivey et al. (1995), Alt and Teagle (1998), Humphris and Tivey (2000). The main hydrothermal features are similar to those documented in the stockworks of ophiolite-hosted massive sulfide bodies, such as the Turner-Albright deposit in the Josephine ophiolite (Zierenberg et al., 1988), and the Cyprus-type deposits of Troodos (Constantinou, 1980). Depth-related facies variations largely reflect the complex and multi-stage evolution of the parent hydrothermal system, and the ephemeral nature of hydrothermal activity, e.g., periods of vigorous discharge versus less active stages of fluid upflow. Temporal and spatial variations in fluid compositions (which commonly reflect different mixing proportions of entrained seawater and evolved hydrothermal fluid), and variable water–rock reactions (the main process affecting mineral precipitation), are important factors that lead to the formation of different alteration zones at specific crustal levels (Honnorez, 2003).

Prior to interpreting crustal depth in the Major Lake and Caroline Cove Fault Zones from (potentially) analogous hydrothermal systems, geological evidence at the main field sites can be used to provide broad and complementary guidelines. Important geological evidence that helps to constrain the formative depths of the VQC and CQP facies includes:

i. The local host rocks, which are typical of the upper ocean crust, were mostly formed during volcanic eruptions on the relict seafloor. Plutonic rocks from the deep crust and upper mantle are not spatially associated with the major faults of central and southern Macquarie Island (although gabbros and various ultramafic rocks commonly occur in the island's northern quarter). Locally, the deepest (exposed) crustal levels correlate with the uppermost transitional package of sheeted dykes and pillow basalts that outcrop in the footwall block of the Major Lake Fault. The Sellick Bay Fault Zone occurs at a significantly higher stratigraphic level above the sheeted dyke complex, with a calculated 400 m-thick (minimum) volcanic pile separating it from the underlying Sandell Bay Sheeted Dyke Swarm (its co-magmatic feeder zone, as discussed by Davidson et al., 2004). Abundant pillow

basalts (intercalated with minor sedimentary rock layers), coupled with the rarity of discrete intrusive rocks and the local absence of sheeted dykes, also suggest that the Caroline Cove region occurs at a relatively high crustal level within its extrusive rock package. In general, the abundance of volcanic host rocks locally associated with each fault zone constrains their likely stratigraphic position within the upper 500 m of the ocean crust (with reference to the standard crustal section, e.g. Figure 4.1);

ii. The igneous minerals in the volcanic wall rocks surrounding each fault zone have been variably affected by hydrothermal processes during regional alteration, e.g., partly to completely replaced by alteration minerals. This widespread style of alteration is associated with the recharge phase of seafloor hydrothermal systems, and the different alteration assemblages can be broadly correlated with variations in crustal depth. Griffin (1982) identified five regional alteration facies in upper crustal rocks on Macquarie Island (Chapter 3.6), ranging from the uppermost seafloor weathering facies (dominated by low temperature and strongly oxidised mineral assemblages) to lower-amphibolite metamorphic grades in the roots of some sheeted dyke complexes. Regional alteration assemblages in volcanic rocks that surround the Major Lake, Caroline Cove, and Sellick Bay Fault Zones mainly range from seafloor weathering (oxidised) to lower-greenschist facies (Figure 5.74). Thus, the main alteration assemblages are consistent with estimated depths for the local volcanic rocks ranging from < 200 m below seafloor (oxidation zone), up to a maximum crustal depth of ~ 1000 m for the greenschist facies (Griffin, 1982); and

iii. The focussed alteration zones are clearly fault-hosted and have formed during subseafloor hydrothermal replacement, veining, and brecciation of the surrounding basaltic wall rocks. There is no direct evidence on Macquarie Island for seafloor hydrothermal vent deposits, such as massive sulfide mounds or chimney-like edifices. By analogy with other oceanic hydrothermal systems previously discussed (Chapter 4.4), upflow fluids channeled within the Major Lake and Caroline Cove Faults may have (potentially) vented at the palaeo-seafloor, formed various styles of exhalative mineralisation, and then been subsequently removed or displaced by erosion, weathering, or post-hydrothermal faulting (or any combination of these processes). However, because of the lack of evidence for relict seafloor deposits, the ultimate fate of high temperature upflow fluids that formed the fault-hosted assemblages remains speculative.

Geological evidence in and around each major fault system constrains the depth of focussed hydrothermal alteration from just below the level of the palaeo-seafloor (but not directly venting at the crust–water interface) to a maximum crustal depth of < 1 km. However, this relatively broad range may be further restricted by reference to the diagnostic alteration facies in the Major Lake and Caroline Cove Fault Zones. As previously discussed, the vein and breccia, quartz-chlorite (VQC) facies (Major Lake) and the massive and veined, chlorite-quartz-pyrite (CQP) facies (Caroline Cove)

are both interpreted to have formed during focussed hydrothermal upflow. Their dominant mineral assemblages, and associated hydrothermal textures, closely correlate with similar features from different crustal levels of other oceanic upflow zones, such as the TAG mound (Alt and Teagle, 1998).

The spatial distribution of alteration zones underlying the TAG mound is here used to model and interpret relative crustal depths during peak hydrothermal discharge in the Major Lake and Caroline Cove Faults, i.e., the fluid events that formed the VQC and CQP facies. Several ocean drilling programs of the TAG stockwork have shown that the active seafloor edifice is underlain by highly fractured basement (~ 150–200 m-thick and ~ 100 m-wide) consisting mainly of altered (variable intensity) mid-ocean ridge basalts (Honnorez et al., 1998; Humphris et al., 1998). The approximate formation depths for the VQC facies at Major Lake, and the CQP facies at Caroline Cove, can be broadly estimated by comparison with the internal structure and alteration features of the TAG mound (Figure 5.75). However, although the overall basis for this correlation seems geologically valid, some caution must be exercised in applying and interpreting these estimated conditions. This particularly applies to absolute (or direct) depth comparisons between TAG and Macquarie Island, because both the VQC and CQP alteration zones (and hence their parent hydrothermal systems) have considerably smaller dimensions (area and volume) than the TAG mound (Table 5.2). In addition, although several different alteration zones are recognised in the fault conduit underlying TAG, there is scant geological information to interpret the nature of transitional alteration assemblages and depth variations between the main outcrops from the Major Lake and Caroline Cove Fault Zones (as previously mentioned).

Several fundamental differences between the VQC and CQP alteration facies are here used to interpret variations in their relative crustal depths during hydrothermal alteration. These differences consistently indicate that the CQP facies formed at a relatively higher crustal level than the VQC facies, i.e., closer to the palaeo-seafloor. The most important facies variations that support this interpretation are:

i. Sulfide minerals such as pyrite and chalcopyrite, which form massive pods, veins, breccia cements, and disseminated grains, are considerably more abundant in the CQP facies, whereas quartz is predominant in the VQC alteration zones;

ii. The alteration paragenesis of the CQP facies contains barite, but barite is noticeably absent from the VQC facies. This significant difference may reflect the greater influence and abundance of unevolved seawater entrained within the upper crust at Caroline Cove;

iii. The CQP facies is closely associated with, and partly overprinted by, the pervasive, Fe-oxyhydroxide (PFO) facies (absent from the Major Lake Fault Zone), which is interpreted to reflect late-stage (post-discharge) oxidised fluid flow in the upper crust; and

iv. The alteration domain associated with the CQP facies is considerably broader and more extensive (both along- and across-strike) than the relatively narrow and focussed alteration zones of the VQC facies. This may correspond to 'flaring' of the hydrothermal system closer to the seafloor, with fluid flow being more focussed (narrower zones) at deeper crustal levels.

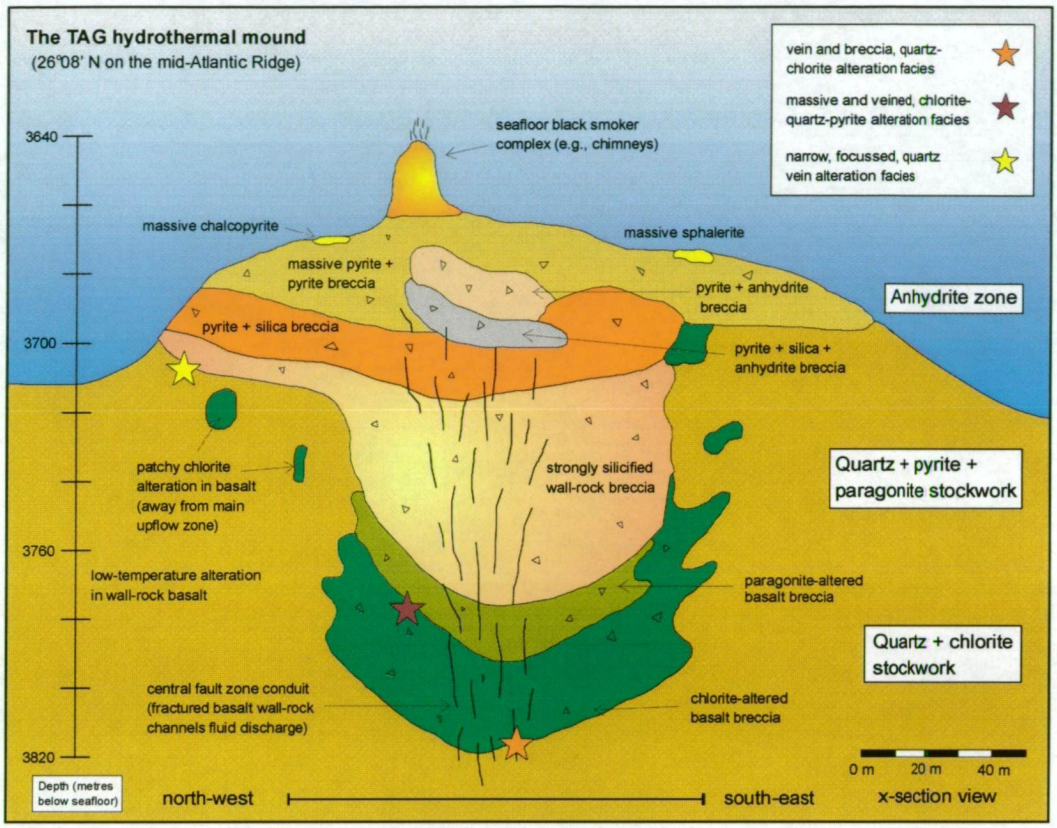

Figure 5.75: An interpreted NW to SE cross-section showing the internal structure beneath the TAG hydrothermal mound. Of particular interest is the spatial distribution (zonation) of hydrothermally altered basalts within the fractured feeder system (stockwork zone). Based upon their characteristic mineral assemblages and textures, the interpreted crustal position of the main alteration facies from Major Lake (the VQC facies) and Caroline Cove (the CQP facies) are also shown here (relative to the TAG system). Important compositional, textural, and spatial variations between the VQC and the CQP facies (outlined in the accompanying text) suggest that they formed at slightly different crustal levels within their respective upflow zones. The NQV facies is not intimately associated with major crustal structures, but occurs in small-scale conduits in the footwall domain of the Major Lake Fault (all NQV sites are < 1.5 km from the MLFZ). The geographic distribution, relatively small outcrop size, and abundance of quartz all suggest that the NQV facies formed at a higher crustal level and was relatively distal from the main upflow zone (modified after Alt and Teagle, 1998; Humphris and Tivey, 2000).

Despite the important variations that characterise the CQP and VQC facies, both alteration assemblages contain extensive chlorite. Widespread chlorite alteration is largely confined to the lower levels of the TAG upflow zone, with chloritised wall rock fragments most common at crustal depths > 100 m below seafloor (Humphris and Tivey, 2000). Chlorite-rich assemblages are comparatively rare in altered rocks which form closer to the seafloor; these levels are largely dominated by various sulfide minerals, quartz, and anhydrite (Figure 5.75). Thus, notwithstanding the differences previously outlined, the presence of abundant chlorite in the altered rocks of both the VQC and CQP facies suggests that they both formed at lower stockwork levels in the discharge

zone. In relatively large and long-lived hydrothermal systems such as TAG the lower stockwork likely corresponds to depths of ~ 100–150 m below the seafloor. However, as previously discussed, these absolute depths may not be directly applicable to the Major Lake and Caroline Cove systems because of their comparatively restricted hydrothermal systems (both spatially and temporally).

The narrow, focussed quartz vein (NQV) facies occurs in the proximal footwall domain of the Major Lake Fault and is not closely linked to the main deformation corridor. The NQV facies is, however, interpreted to have formed from structurally controlled fluid flow associated with hydrothermal discharge. The local structural conduits include narrow fault and fracture zones, and discrete dyke margins in the Sandell Bay Sheeted Dyke Swarm (Table 5.2). The relatively small size of all NQV alteration zones attests to significantly smaller fluid volumes than the VQC and CQP facies, and rapid but short-lived episodes (highly transient) of hydrothermal flow. Several lines of geological evidence, such as the abundance of hydrothermal quartz and the limited spatial dimensions of their alteration zones, suggest that the NQV facies formed at relatively higher crustal levels and were distal from the main upflow conduit (Figure 5.75). The depth interpretation for the NQV sites is also consistent with their local geological setting (i.e., most of the NQV alteration zones are hosted in pillow basalts), and the close relationship between local structural features.

Finally, it is difficult to directly compare the vein-dominated, prehnite-zeolite (VPZ) facies from the Sellick Bay Fault Zone with the TAG hydrothermal system. Their respective alteration assemblages and hydrothermal textures are considerably different, and these variations limit the application of the TAG analogy for estimating crustal depths. As previously discussed, the VPZ facies is not interpreted to have formed from high temperature fluids associated with hydrothermal upflow. Abundant, relatively low temperature alteration minerals (e.g., zeolites and prehnite) are more closely allied to the regional alteration assemblages in the surrounding host rocks. Hydrothermal alteration in the Sellick Bay Fault Zone probably occurred following the peak axial discharge phase that formed the VQC and CQP facies. This interpretation is, however, difficult to substantiate because the VPZ facies does not directly interact with the Major Lake or Caroline Cove Faults; it is also not spatially or genetically associated with other focussed hydrothermal facies. Most geological evidence suggests that the parent hydrothermal system of the VPZ facies was restricted to the uppermost 100–150 m of the permeable ocean crust. Within this crustal zone relatively low temperature, oxidising conditions occur because of the open hydrothermal regime, and the abundance of cold and relatively unevolved seawater (Gillis and Robinson, 1990). These conditions probably favour the evolution of non-discharge alteration assemblages similar to those in the Sellick Bay Fault Zone.

Alteration heterogeneity in the ocean crust

Fundamentally different mineral assemblages, hydrothermal textures, and outcrop attributes clearly differentiate the six focussed alteration facies and emphasise their major variations. However, all hydrothermal assemblages on Macquarie Island (including regional and focussed zones) share an important and very distinctive characteristic; **alteration heterogeneity**. A variety of facies

parameters, including the intensity, distribution, and mineral paragenesis of discrete alteration zones, are significantly heterogeneous within their host rock domains. These fundamental variations exist across a wide range of scales (i.e., at the hand-, outcrop-, and district-scale), and are manifested as a spectrum of hydrothermal features. Alteration heterogeneity is particularly characterised by the close spatial association between intense alteration zones and discrete faults, and the highly variable preservation of primary igneous textures and structures in most outcrops, e.g., plagioclase phenocrysts, individual pillow basalt lobes, and the intrusive margins of sheeted dykes. Heterogeneous alteration assemblages have also been widely documented from modern oceanic settings (Gillis and Thompson, 1993; Ridley et al., 1994) and ancient ophiolites (Alexander et al., 1993; Bickle et al., 1998), suggesting that it is a common and fundamental characteristic of hydrothermal processes in the ocean crust.

One of the most important controls on alteration heterogeneity is the permeability of the host rock or structural conduit (Harper, 1999). Permeability is a critical factor because it primarily governs the duration and extent of water–rock interaction (Alt, 1999). The most permeable crustal zones provide effective and very efficient conduits for focussed fluid flow at elevated water-rock ratios. These conditions are conducive to the formation of intensely altered wall rocks, extensive vein and breccia networks, and massive alteration enclaves. Focussed hydrothermal flow occurs at many scales and involves both structural (e.g., faults and fractures) and lithological conduits, e.g., the margins of discrete dykes and permeable pillow basalt or hyaloclastite layers. Major structural breaks in the crust (e.g., rift axis faults) are particular focal points for large-scale hydrothermal systems, as they commonly provide pathways for high temperature and chemically evolved hydrothermal fluids, i.e., focussed discharge zones with high degrees of fluid–rock disequilibrium. An intimate association of intensely altered rocks with zones of structurally enhanced permeability was consistently observed in the Major Lake, Caroline Cove, and Sellick Bay Fault Zones. These geological relationships provide strong supportive evidence for the genetic links between crustal permeability and alteration heterogeneity.

Evidence for the interaction of hydrothermal – magmatic – and tectonic processes in upper crustal faults

The Major Lake, Caroline Cove, and Sellick Bay Fault Zones are major structural systems that host many highly distinctive geological features on Macquarie Island. Detailed outcrop mapping has provided important evidence to interpret the complex fault zone histories, and has clearly indicated that multiple stages of magmatic, tectonic, and hydrothermal activity have affected each structural system. The prolonged and episodic interaction of these various crust-forming processes resulted in the spectrum of geological and hydrothermal components that now characterise these faults. Several of the most critical relationships, and their important evolutionary implications, are outlined below.

Magmatic – hydrothermal relationships

The igneous rock packages that locally surround each fault zone (i.e., the various footwall and hangingwall basaltic and sheeted dyke domains) are interpreted to have formed during temporally distinct magmatic events. Consistent geological relationships observed during fieldwork, combined with previous whole-rock geochemical studies on Macquarie Island (e.g., Kamenetsky et al., 2000; Davidson et al., 2004), provide evidence for the episodic nature of local magmatic activity. As discussed in Chapter 4.2, ephemeral magmatism is common at slow-spreading ridges because most lack a steady-state axial melt lens; hence, many magmatic features and relationships observed in the Macquarie Island fault zones may be typical of slow-spreading ocean crust*. Important geological evidence indicative of different magmatic phases includes:

i. The presence of unconformable 'stratigraphic' boundaries that separate volcanic rock units with distinct lithological and outcrop characteristics. The well preserved contact between hyaloclastite and overlying pillow basalt in the hangingwall block (Zone BVa) of the Major Lake Fault (Figure 5.24 – Insert A), sporadically marked by a thin sedimentary rock horizon, provides good evidence to interpret episodic volcanic activity;

ii. Multiple generations of intrusive rocks within sheeted dyke complexes. Distinct textural contrasts (e.g., chilled dyke margins and different phenocryst populations), combined with variations in the orientation of mutually intrusive dykes, indicate that sheeted dyke domains were formed during prolonged (and possibly episodic?) magmatic events; and

iii. Variations in the orientation of discrete dykes that intruded different volcanic rock domains, some with oblique cross-cutting relationships. These variations occur both within individual lithologic domains and between separate crustal blocks, and further show that temporally distinct extrusive and intrusive events have occurred.

In addition to the geological relationships outlined above, further evidence for multiple magmatic events is derived from geochemical studies of volcanic rock domains. Previous investigations have used distinctive trace element signatures to interpret genetic links between some sheeted dyke complexes and proximal extrusive rocks, i.e., stratigraphically related. For example, Davidson et al. (2004) showed that, on the basis of similar Nb/Y and Ti/Zr ratios, the Sandell Bay Sheeted Dyke Swarm is co-magmatic with the overlying Zone BVa basaltic domain (these units respectively represent the footwall and hangingwall blocks of the Major Lake Fault). However, these volcanic rock associations have significantly different trace element compositions from other basalts in central and southern Macquarie Island, such as the older (underlying) basaltic packages from Zone BVb and Zone BVI (although these latter units are genetically related to each other) (Goscombe and Everard,

* Although, as also discussed in Chapter 4.2, slow-spreading ridges typically have very heterogeneous crustal profiles and hydrothermal systems. This inherent variability cautions against the widespread use of generalised models. However, the unusual features mentioned here certainly seem more likely to be associated with slow-spreading ridges, rather than intermediate- or fast-spreading systems.

2001; Davidson et al., 2004). The characteristic geochemical variations likely reflect different melt sources, and hence different magmatic episodes, during the evolution of the slow- and obliquely-spreading Proto-Macquarie Ridge. Evidence of lithologic domain variations from whole-rock geochemical data obtained during this project is presented and further discussed in Chapter 7.

Robust magmatic activity is an important mechanism that drives hydrothermal circulation in the ocean crust. Discrete magmatic (dyking) events may generate vigorous hydrothermal cells and promote active, high temperature fluid discharge (Wilcock and Delaney, 1996). Although hydrothermal systems at slow-spreading ridges commonly wax and wane over a prolonged time frame*, most distinct episodes of high heat flux are closely associated with magmatic events (Chapter 4.4). Thus, the presence of high temperature, discharge-style alteration assemblages in the Major Lake (VQC facies) and Caroline Cove (CQP facies) Fault Zones suggests that their parent hydrothermal cells may be related to an energetic magmatic event.

Most geological features and relationships from the Major Lake and Caroline Cove Faults indicate that the formation of their diagnostic (high temperature) alteration facies post-dated the main stage of magmatic activity that formed the surrounding volcanic rocks and sheeted dykes. There is no compelling field-based evidence to interpret synchronous magmatic-hydrothermal activity in the local fault zone environment, i.e., the NW- to N-striking seafloor grabens proposed by Rivizzigno and Karson (2004). Unaltered dykes or late-stage extrusive rocks do not directly interact (e.g., cross-cut or overlie) with the zones of intensely altered fault-hosted assemblages, indicating that late-stage (post-hydrothermal discharge) eruptions were not preferentially focussed within the major fault corridors. The distinct absence of intimate magmatic-hydrothermal interactions suggests that relatively distal magmatic activity (i.e., not localised along interpreted fault zone grabens) promoted the high temperature hydrothermal upflow systems. These (speculative) magmatic events may have been focussed at deeper crustal levels (and never reached the seafloor?), or on different segments of the oblique-spreading ridge system, producing extrusive rocks at other parts of the regional oceanic crust, e.g., possibly along linked segments of an extensional fault array?

Limited geological evidence in the vicinity of each fault zone provides further support for the interpretation of cyclic magmatic and hydrothermal stages. At multiple locations in the Sandell Bay Sheeted Dyke Swarm (e.g., 200 m south-east of the Major Lake Fault Zone at Sandell Bay creek) sinuous micro-dykes (1–2 cm-wide) cut across and terminate discrete prehnite-rich veinlets (Figure 5.76). In the Zone BIII (north of the Sellick Bay Fault Zone) and Zone BVa volcanic rock associations (north of the Major Lake Fault), several strongly oxidised pillow basalt and hyaloclastite outcrops are intruded by late-stage dykes (discrete intrusions) that lack similar alteration assemblages, implying that intrusion of these dykes locally post-dated hydrothermal activity (Figure 5.77). Cross-cutting dykes and alteration zones provide evidence for multiple and transient episodes of igneous

* This is because they may also be driven by thermal fluxes derived from deeper sources (e.g., prolonged thermal output from the cooling and contraction of lower crust and upper mantle rocks), or possibly by exothermic alteration reactions (Chapter 4.4).

and hydrothermal activity which may have been regionally extensive. Furthermore, these geological relationships also suggest that local dyke events may have driven episodes of rapid hydrothermal upflow that formed the fault-specific, focussed alteration zones.

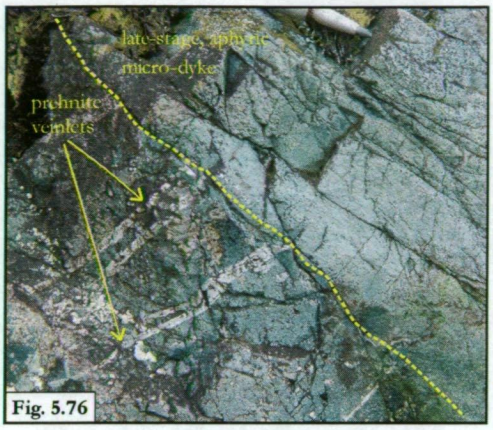

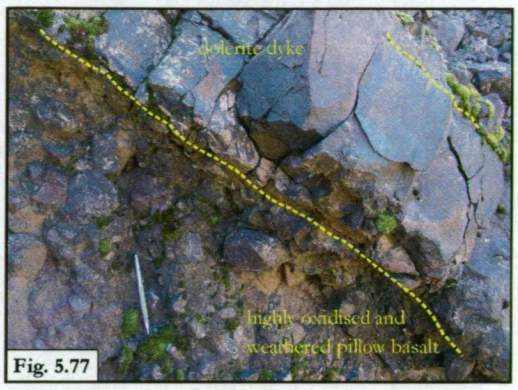

Figure 5.76: Pale and narrow, prehnite-rich veinlets in the Sandell Bay Sheeted Dyke Swarm are cross-cut by a very fine-grained, greenish-blue dolerite micro-dyke. Although not widespread, these relatively late-stage intrusive rocks provide good evidence for episodic cycles of alternating magmatic and hydrothermal activity. This locality occurs in the upper west coast escarpment above south Sandell Bay and is situated about 200 m south of the Major Lake Fault Zone.

Figure 5.77: A moderately dipping, late-stage discrete dyke has intruded strongly altered and oxidised pillow basalts in the hangingwall package of the Zone BVa domain. The dyke is only weakly altered and is interpreted to have intruded the extrusive rocks after the main stage of hydrothermal activity. This outcrop is situated in a steep and highly eroded creek valley near Waterfall Bay on Macquarie Island's east coast, and occurs north of the Major Lake Fault Zone.

Structural – hydrothermal relationships

Detailed structural mapping along well exposed segments of the Major Lake, Caroline Cove, and Sellick Bay Fault Zones documented a variety of discrete faults, fractures, and breccia zones. Normal, strike-slip (mostly dextral), and oblique-slip faults are abundant in these highly deformed structural corridors, although their distribution, size, and intensity vary considerably between faults. Many small-scale, individual discontinuities host subparallel arrays of hydrothermally derived veins, or have a spatial association with pervasively altered wall rocks; these intimate relationships provide good evidence for their spreading-related origins, i.e., they acted as hydrothermal fluid conduits at the relict spreading ridge. However, the formation of many discontinuities in the major fault zones post-dated peak hydrothermal activity, and these are not interpreted as extensional seafloor structures. Locally unaltered faults (i.e., lacking specific alteration assemblages) commonly have extensive breccia-gouge zones, and many also cross-cut, overprint, or displace hydrothermally derived assemblages and other (early) spreading-related structures. The spectrum of fault types and the variety of structural – hydrothermal relationships that occur in the Major Lake, Caroline Cove, and Sellick Bay Faults indicates that each has undergone multiple stages of structural disruption and hydrothermal alteration. Their complex structural histories reflect the progressive change in the regional tectonic environment, as the Indo-Australian – Pacific plate margin evolved from an extensional seafloor ridge to a dextral transcurrent system (Goscombe and Everard, 2001).

Many geological features and structural relationships provide clear evidence that extensive faulting and tectonic deformation post-dated the peak hydrothermal phase. According to Rivizzigno and Karson (2004), the NW- to N-striking accommodation structures were sites for on-going episodes of structural activity at or near the spreading ridge (Chapter 3.9). Sporadic phases of tectonic deformation are interpreted to have affected the major fault zones as extension at the plate margin was superseded by transpression and uplift (Goscombe and Everard, 2001). Local disparities in the styles of (recharge-related) alteration within the lithologic domains juxtaposed by the Major Lake and Caroline Cove Faults (Figure 5.74) suggests that extensive displacement (seafloor faulting) has rearranged the original facies architecture prior to (or possibly synchronous with) formation of the late-stage FMC and PFO facies. The growth of new hydrothermal minerals in the volcanic rock packages surrounding each fault zone (albeit representing relatively low temperature clay-rich and oxidised assemblages) indicates that these crustal sections were still within the seafloor environment during this structural activity (late extensional regime?), and that faulting must have occurred prior to uplift and subaerial exposure of Macquarie Island. This interpretation is further supported by the lack of high temperature alteration assemblages from the adjacent hangingwall rocks (e.g., Zone BIV and BV domains at Major Lake), and is broadly consistent with the model proposed by Daczko et al. (2003) for late-stage seafloor hydrothermal circulation.

A consistent set of hydrothermally derived features indicates that the foliated, massive chlorite (FMC) facies is genetically related to synchronous (or near-synchronous) tectonic activity in the Major Lake and Caroline Cove Fault Zones. This phase of structural activity clearly post-dated the discharge-style alteration that formed the diagnostic quartz- + chlorite- + sulfide-bearing assemblages at each location (evidenced by the lack of altered VQC facies rocks from the hangingwall of the Major Lake Fault Zone). Narrow, elongated slickenlines associated with the FMC facies are common on discrete clay-rich seams or thin vein margins in the main deformation corridor of the Major Lake and Caroline Cove Faults. Many breccia-bearing discontinuities also contain fragments derived from the pre-existing high temperature alteration assemblages, e.g., angular and highly fractured fragments of CQP facies basalt occur in the main deformation zone of the Caroline Cove Fault and are juxtaposed and overprinted by the late-stage FMC assemblage. In addition, the proximal hangingwall domains at Sandell Bay creek (Zone BVa domain) and Caroline Cove (the eastern pillow basalt sequence' both consist of (relatively) weakly altered basaltic rocks that have zeolite and seafloor oxidation mineral assemblages (formed during regional hydrothermal recharge). The hangingwall rocks at both sites are markedly different from those in the adjacent footwall (e.g., the Sandell Bay Sheeted Dyke Swarm), particularly as they specifically lack the quartz-, chlorite-, sulfide-bearing alteration assemblages. The combination of geological and structural features cited here provides strong evidence for multiple hydrothermal activity (fault zone focussed and regional-style hydrothermal systems), interspersed with temporally distinct episodes of on- or near-axis structural deformation.

The Major Lake, Caroline Cove, and Sellick Bay Fault Zones also have many geological features and relationships which indicate that extensive tectonic activity also post-dated hydrothermal fluid circulation. Abundant breccia- and gouge-bearing zones in each fault corridor, which lack specific and spatially related alteration assemblages, are interpreted to have formed during uplift-related tectonism (post-extension) at the Indo-Australian – Pacific plate margin (neotectonic activity). For example, the strongly altered and veined rocks of the CQP and FMC facies in the Caroline Cove Fault Zone are cross-cut, displaced, and brecciated by many low- to moderate-angle, oblique-slip and strike-slip faults. Furthermore, the CQP facies domain is completely fault bound, and the gouge-bearing western fault boundary is devoid of focussed alteration assemblages. Massive prehnite-rich pods and intense zeolite vein arrays in the Sellick Bay Fault Zone are likewise affected by post-hydrothermal tectonism; many discrete alteration zones are finely brecciated and contain abundant elongated and foliated (subparallel) fragments. At Sandell Bay creek, the well exposed valley section of the Major Lake Fault Zone is displaced and terminated at the mid-escarpment level by a dextral-oblique fault that has a 20–50 cm wide clay-gouge breccia zone. This late-stage, cross-cutting structural break is also devoid of localised hydrothermal assemblages and is interpreted as an uplift-related structure (neotectonic). Multiple, overprinting fault plane striations and brecciated faults that lack hydrothermal veins are also common in the Major Lake Fault Zone (Figure 5.25 – Insert B), and these provide further evidence of post-extension deformation. The diverse range of heterogeneous structures that occur in the major fault zones reflect significant structural modification and disruption in the post-hydrothermal (uplift-related) tectonic environment, and the superposition of these effects on earlier-formed (oceanic) structures and altered rocks.

Uncertain geological attributes and relationships in major fault zones

To conclude this chapter, it is worthwhile to outline some of the important geological ambiguities that remain despite my detailed fieldwork. A diverse range of structural, magmatic, and hydrothermal features and relationships have been documented and interpreted for the Major Lake, Caroline Cove, and Sellick Bay Fault Zones. These attest to the multi-stage evolution of the major NW- to NNE-striking discontinuities, and the complex interactions of the various processes which have helped to shape their present architecture and facies distribution. However, some critical evolutionary details from each fault zone remain poorly understood, particularly relating to the genetic relationships between fundamental magmatic–tectonic–hydrothermal processes. These ambiguities have mainly resulted from the relatively poor along-strike exposure of each fault, and the variable (alluded to but largely undetermined) effects of neotectonic faulting and (post-spreading) structural disruption. In addition, as geological observations and data collection were mainly limited to the six key outcrop sites, broader (regional-scale) interpretations of the major fault zones were also limited.

Below, I have nominated the four main uncertainties arising from the detailed field study of the geology, structure, and alteration characteristics of the Major Lake, Caroline Cove, and Sellick Bay Fault Zones. These issues are further considered and discussed in Chapter 9, when other

mineralogical, geochemical, and isotopic constraints (the focus of the next three data presentation chapters) are integrated with the field data.

The following topics remain geologically ambiguous:

i. Determining and assessing the complete (actual) along-strike facies distribution, and fault-parallel variations in the main alteration parameters (e.g., the size, dimensions, and intensity of the alteration zones), for each major fault system. This is especially problematic for the Caroline Cove and Sellick Bay Faults, because the main occurrences of their focussed alteration zones are restricted to single localities (with total exposed fault segments < 30 m- and < 50 m-long, respectively). Although the alteration zones along the Major Lake Fault outcrop at four key sites, fundamental questions also remain unresolved regarding the nature of transitional assemblages between each site, and the apparent fault-parallel segmentation of the VQC facies. These problems are particularly difficult to evaluate because fault segments between discrete alteration zones are not exposed. The lack of outcrop also hampers assessment of the spatial distribution of the foliated, massive chlorite (FMC) facies, e.g., is it segmented or continuously developed along-strike in the MLFZ? A comprehensive understanding of the along-strike facies distribution would provide important information on the spatial extent of the different alteration zones and the nature of any transitional alteration assemblages that may exist. These data would also provide better interpretive constraints on the size and relative influence of the hydrothermal systems in each fault, and further assist with interpreting crustal depths during alteration (and, by implication, the structural architecture of the host fault zone);

ii. Related to the above point, it is also difficult to determine the structural or lithological factors that may have controlled (localised) formation of the vein and breccia, quartz-chlorite (VQC) facies at specific sites along the Major Lake Fault Zone. Although the observed segmentation of the VQC facies outcrops is likely controlled by the basement structural architecture (as previously discussed), it may simply reflect a post-hydrothermal artifact related to erosion, weathering, or neotectonic activity. This is difficult to satisfactorily evaluate because of incomplete fault zone exposures, although the lack of quartz-rich scree along the projected fault trend does provide support for the segmentation hypothesis. However, there is certainly no unequivocal field evidence to support the interpretation of intersecting basement structures localised at the four VQC facies sites. Although I presented a plausible geological explanation (previously in this discussion section) for the development of along-strike segmentation, it was based on relatively minor and speculative structural data. It is hoped that recent ground magnetic surveys conducted by researchers at the University of Tasmania may provide useful geophysical data to better constrain the structural architecture in the vicinity of the major faults. Unfortunately, these

data are still undergoing initial processing and evaluation, and are unlikely to be available prior to early-2006;

iii. Determining the timing of different hydrothermal phases relative to regional-scale block tilting of lithologic domains (volcanic rocks and sheeted dykes) in central and southern Macquarie Island. The geological attributes and relationships in many fault zones have clearly indicated that multiple stages of hydrothermal alteration and structural activity occurred. However, it is very difficult to determine if structural disruption within each fault zone is related to regional block tilting that occurred at or near the palaeo-spreading ridge*, or if it represents spatially restricted (localised) tectonic activity, i.e., essentially restricted to the interpreted seafloor accommodation zones. Understanding the distribution and timing of regional structural activity would provide important information to assist with interpreting the stratigraphic and facies architecture of each fault zone at different stages of hydrothermal activity, e.g., were the volcanic rocks relatively flat-lying or were they regionally tilted at low to moderate angles during different hydrothermal stages (?); and, finally

iv. Determining the relative timing of the volcanic activity which formed the hangingwall pillow basalts (Zone BIV and BVa) at the Major Lake Fault Zone, and its temporal relationship with the various episodes of localised structural and hydrothermal activity. This important theme is directly related to the geological model proposed by Rivizzigno and Karson (2004), which interpreted the NW- to NNE-striking faults investigated here as accommodation zones which segmented the oblique-spreading Proto-Macquarie Spreading Ridge (Chapter 3.9). These workers suggested that the fault zones formed elongated seafloor depressions (small grabens) and were focal points for localised magmatic, hydrothermal, and tectonic activity. Several geological characteristics and relationships documented at the key outcrop sites suggest that volcanic activity which formed the hangingwall rocks post-dated the main stage of hydrothermal upflow, i.e., the formation of the VQC facies. These important features, which provide evidence to support the model of localised magmatic, structural, and hydrothermal processes along the NW- to N-striking fault zones, include:

- The absence of intensely altered vein and breccia, quartz-chlorite (VQC) facies rocks from the local hangingwall block, i.e., there are no VQC facies rocks that occur north of the MLFZ within the Zone BIV and Zone BVa domains;

- The abundance of weakly altered (regional zeolite facies) pillow basalts in the hangingwall block, which contrasts markedly with the regional greenschist-dominated

* Evidence for regional structural tilting is mainly implied by the consistent 20°–30° eastward dip of the volcanic rock stratigraphy in the central and southern areas of Macquarie Island, e.g., Goscombe and Everard (2001), Davidson et al. (2004).

assemblages in the footwall sheeted dyke complex and transition zone basalts (Sandell Bay Sheeted Dyke Swarm and Zone BVI domains);

- The suborthogonal orientation of elongate pillow axes relative to the strike of the fault zone (NE-trending pillow axes relative to the NNW-strike of the MLFZ), which may provide evidence of pillow basalt eruptions flowing into an existing seafloor depression (down a fault-bounded graben?); and

- The presence of a local unconformity in the volcanic rock-dominated hangingwall package, attesting to multiple and temporally distinct volcanic events.

It is worth noting however that several of the geological relationships identified above could also have an alternative origin, e.g., they may be genetically linked to structural deformation and widespread tectonism that post-dated all hydrothermal activity. This would imply that the present facies architecture and distribution around the Major Lake Fault Zone has resulted only from neotectonic activity. Although there is abundant evidence for breccia-gouge faults that lack hydrothermal alteration, and are thus interpreted to have formed in the dextral strike-slip (uplift) regime (Goscombe and Everard, 2001), many magmatic – structural – hydrothermal relationships at Major Lake are not solely compatible with a neotectonic origin. For example, the FMC facies (in the core of the MLFZ) has clearly formed in both the footwall and hangingwall blocks that surround the Major Lake Fault Zone. This relationship indicates that the structural juxtaposition of adjacent blocks with significantly different regional alteration assemblages must have pre-dated the formation of the FMC facies. Therefore, although the exact timing and interaction of all volcanic, structural, and hydrothermal processes in the Major Lake Fault Zone cannot be absolutely constrained from field (outcrop) observations, there is compelling evidence to suggest that the current structural architecture and facies distribution has resulted from major crust-forming processes that occurred in both the active spreading (rift axis) and uplift-related (post-spreading) tectonic environments.

Chapter 6. – Microscopic Petrography and Hydrothermal Mineral Chemistry

6.1. Introduction

Detailed micro-analytical studies involving petrographic and electron microprobe techniques are widely used during the investigation of hydrothermally altered rocks in the ocean crust, e.g., Alt et al. (1986), Gillis and Thompson (1993), Laverne et al. (1996), Schramm (2004). These laboratory methods provide important information that cannot be obtained from *in situ* seafloor or field-based (ophiolite) investigations, particularly as altered volcanic rocks are commonly dominated by very fine- and fine-grained hydrothermal minerals. Microscopic petrography is fundamentally required to determine the spectrum of alteration minerals and their precursor igneous phases, the intensity and extent of hydrothermal replacement or recrystallisation, and the common textural styles and inter-mineral relationships. Quantifying the chemical composition of specific alteration minerals (e.g., chlorite) may also help to constrain and interpret critical hydrothermal conditions and fluid–rock reactions, as previously shown by Saccocia and Gillis (1995), and Nimis et al. (2004). Thus, to further characterise and better understand their important hydrothermal components, I conducted a comprehensive micro-analytical study of the focussed alteration facies associated with the Major Lake, Caroline Cove, and Sellick Bay Fault Zones.

Observations, data, and interpretations arising from my petrographic and electron microprobe study are presented in this chapter, and primarily focus on:

i. Confirming the results of previous studies into the nature of regional hydrothermal alteration on Macquarie Island, e.g., Griffin (1982). This involved identifying and comparing the main hydrothermal (and relict igneous) minerals and textures in regionally altered rocks from the island's central and southern regions (Chapter 3.6);

ii. Defining the key hydrothermal textures that commonly occur in focussed alteration assemblages in the Major Lake, Caroline Cove, and Sellick Bay Fault Zones (using the facies classification scheme outlined in Chapter 5);

iii. Describing the spectrum of alteration minerals and inter-mineral associations that specifically occur in each fault zone assemblage;

iv. Using the hydrothermal mineral and textural observations to determine the sequence and relative timing of each discrete alteration stage (i.e., the hydrothermal paragenesis) which formed the multi-component facies;

v. Presenting a brief descriptive overview of the fluid inclusion populations identified in the quartz-bearing assemblages of the vein and breccia, quartz-chlorite (VQC) facies, the massive and veined, chlorite-quartz-pyrite (CQP) facies, and the narrow, focussed quartz vein (NQV) facies;

vi. Characterising the chemical composition of important alteration minerals (e.g., chlorite, plagioclase, and epidote) in the VQC, CQP, and VPZ (vein-dominated, prehnite-zeolite) facies based on new electron microprobe analyses (obtained during this study), and comparing these results with similar studies undertaken on altered oceanic rocks from other global localities; and

vii. Using the mineral composition data to constrain and interpret critical hydrothermal parameters in the Major Lake, Caroline Cove, and Sellick Bay Fault Zones. In particular, extensive analytical and interpretive work was undertaken on hydrothermally derived phyllosilicate minerals such as chlorite; this included evaluating the effectiveness of various chlorite geothermometers.

6.2. Investigative methods

Detailed petrographic examinations (of rock thin-sections) and electron microprobe analyses were used to achieve the objectives of my micro-analytical study. The salient features of these techniques are briefly outlined here, with more rigorous information on operating conditions and instrument parameters provided in Appendix 4 (Table A–4.1). A complete list of microprobe data (major element oxide and cation compositions) is also included in Appendix 4 (Table A–4.2 to A–4.17).

Petrographic analysis

Observations and descriptions of approximately 110 thin-sections were made during this microscopic investigation (Appendix 2). The spectrum of rock types and hydrothermally derived alteration assemblages identified in the field were examined in detail (Chapter 6.3), comprising samples from the six focussed alteration facies (seventy seven discrete rock samples in total) and their regional host rock domains (thirty-three samples). This microscopic study was used to define the alteration paragenesis and the range of textural attributes for each focussed hydrothermal facies, and also aided with genetic interpretations for the Major Lake, Caroline Cove, and Sellick Bay Fault Zones. Careful petrographic work further assisted in planning and implementing my electron microprobe investigation, and provided important constraints for the interpretation of these mineral composition data.

Electron probe micro-analysis

The electron microprobe investigation (Chapter 6.4) quantified the chemical composition of common alteration minerals in rocks from the VQC, CQP, and FMC facies; chlorite, plagioclase,

epidote, Ca-zeolites, and prehnite were primarily studied (Table 6.1). In addition, similar alteration minerals in some of the regionally altered rocks from the Sandell Bay Sheeted Dyke Swarm (Major Lake) and the Zone BVI volcanic rock association (Caroline Cove) were also analysed. The regional microprobe data were further complemented by existing analytical results reported by Griffin (1982) (Appendix 4). The results of my electron microprobe study were used to constrain and interpret hydrothermal conditions and fluid–rock interactions in the Major Lake and Caroline Cove Fault Zones. In addition, electron microprobe analyses also proved useful for identifying enigmatic (unknown) alteration minerals.

6.3. Microscopic alteration petrography

Overview of regional (host rock) alteration features

The petrographic study of regional host rocks surrounding the Major Lake, Caroline Cove, and Sellick Bay Faults was an important (initial) stage in understanding the mineral and textural attributes of the focussed hydrothermal facies. In particular, this work helped to recognise the common effects of widespread regional alteration in the upper crustal rocks*, and thus provided baseline criteria for comparing with the intensely altered fault zone assemblages. The petrographic study also assisted in identifying the primary igneous features of the volcanic and shallow intrusive rock units. Representative basalt and dyke samples from the lithologic domains adjacent to each major fault were examined to determine the style, magnitude, and intensity (grade) of regional alteration. These consisted of twenty rock samples from the Sandell Bay Sheeted Dyke Swarm and Zone BVa volcanic rock domain (the respective footwall and hangingwall of the Major Lake Fault), five samples from the Zone BVI domain (Caroline Cove), and eight samples from Zone BIII and BVa around the Sellick Bay Fault (Appendix 2; Table 6.2). The spectrum of rock types from these regional domains correspond to different levels of the ocean crust profile, interpreted to represent a minimum thickness of ~ 1 km, i.e., from seafloor volcanic rocks to the transition zone package of sheeted dykes and basalts (Goscombe and Everard, 2001). Regional alteration assemblages on Macquarie Island were shown by Griffin (1982) to range from relatively low grade (near-seafloor) oxidised facies in the uppermost volcanic rocks, to greenschist facies assemblages in the lower volcanics and sheeted dyke transition zone (Figure 6.1). Some dolerites in the deeper crustal segment of the sheeted dyke complex also contain hydrothermal minerals which are typical of lower amphibolite grade conditions, such as actinolite and tremolite (Chapter 3.6).

* As discussed in Chapter 3.6, the low- to moderate-grade regional alteration assemblages on Macquarie Island are interpreted to have formed during widespread hydrothermal recharge in the ocean crust, e.g., Griffin (1982).

Table 6.1: Summary of electron microprobe analyses undertaken for focussed and regional alteration facies on Macquarie Island.

Alteration facies	Chlorite	Plagioclase	K-feldspar	Epidote	Amphibole	Zeolite	Prehnite	Pumpellyite
Vein and breccia, quartz-chlorite (VQC) facies	8 samples (used from 3 separate sites (2A, 2B, 2C) for a total of 71 probe analyses (Table A–4.2).	8 samples used from 3 separate field sites (2A, 2B, 2C) for a total of 33 analyses (Table A–4.4).	3 samples used from 3 separate field sites (2A, 2B, 2C) for a total of 6 analyses (Table A–4.6).	n/a	n/a	n/a	n/a	n/a
Sandell Bay Sheeted Dyke Swarm – the regional host domain for the Major Lake Fault Zone	8 samples used from the regional district for a total of 65 analyses (Table A–4.3).	8 samples used from the regional district for a total of 42 analyses (Table A–4.5).	5 samples used from the regional district for a total of 14 analyses (Table A–4.7).	6 samples used from the regional district for a total of 26 analyses (Table A–4.8).	n/a	1 sample (MCQ-319) used for 2 analyses (Table A–4.14).	1 sample (MCQ-319) used for 5 analyses (Table 4.15).	n/a
Foliated, massive chlorite (FMC) facies	2 samples used for 20 analyses (Table A–4.9).	n/a	n/a	n/a	n/a	n/a	n/a	n/a
Massive and veined, chlorite-quartz-pyrite (CQP) facies	6 samples used for a total of 45 analyses (Table A–4.10).	5 samples used for 21 analyses (Table A–4.11).	n/a	4 thin-section samples used for 14 analyses (Table A–4.12).	1 thin-section sample used for 4 analyses (Table A–4.13).	n/a	n/a	n/a
Western pillow basalt sequence – part of the Zone BVI association at Caroline Cove		n/a	n/a	n/a	n/a	2 samples (MCQ-013 and MCQ-021) used for 7 analyses (Table A–4.14).	1 sample (MCQ-013) used for 4 analyses (Table A–4.15).	n/a
Vein-dominated, prehnite-zeolite (VPZ) facies	n/a	n/a	n/a	n/a	n/a	1 sample (MCQ-275) used for 7 analyses (Table A–4.14).	1 sample (MCQ-272) used for 9 analyses (Table A–4.15).	1 sample (MCQ-272) used for 10 analyses (Table a–4.16).

Note:

The complete list of rock samples (thin-sections) analysed with the electron microprobe is shown in Appendix 2. Tables of compositional data are also referenced for different minerals in each facies (shown here in their respective brackets).

Table 6.2: Common secondary minerals and hydrothermal textures associated with regional alteration assemblages in upper crustal rocks surrounding the Major Lake, Caroline Cove, and Sellick Bay Fault Zones.

Fault zone	Footwall domain	Hangingwall domain	Common igneous minerals and textures in primary igneous rocks	Diagnostic alteration minerals and their common inter-mineral associations and relationships	Minor alteration minerals	Common hydrothermal textures	Interpreted regional alteration assemblages
Major Lake Fault	The **Sandell Bay and Waterfall Bay Sheeted Dyke Swarms** and the **Zone BVI extrusive rock domain** (n = 15)		Most dykes have fine- or medium-grained, equigranular textures, and some are also sub-ophitic. Hypocrystalline groundmass is common, and many dykes are sparsely plagioclase-phyric. Minor porphyritic pillow basalt also occurs in the transition zone complexes.	Chlorite and actinolite are common alteration minerals that partly to completely replace primary augite and minor patches of the glassy mesostasis (Figure 6.5). Plagioclase grains are extensively albitised, and many also have patchy chlorite alteration such as intra-grain veinlets or turbid, clay-rich patches. Aggregates of very fine-grained titanite commonly overgrow Ti-magnetite crystals.	Prehnite, quartz, calcite, epidote, and pyrite all occur as very fine- to fine-grained alteration minerals that partly replace groundmass crystals or glass, infill amygdules (mainly in pillow basalt), or form narrow veins. These minerals may be locally abundant but are generally not widespread.	Despite widespread albitisation, many fine- to medium-grained plagioclase crystals retain their primary grain shapes (Figure 6.4). Selectively pervasive alteration of clinopyroxene (moderate to strong) is common. Minor veins cut across the groundmass and many phenocrysts, and rare vesicles, are infilled with single- or multi-phase mineral assemblages (Figure 6.6 and Figure 6.8).	Moderately altered rocks with upper greenschist to lower amphibolite assemblages (actinolite and minor hornblende occur in the deeper dyke sections).
		The **Zone BVa extrusive rock domain** (n = 5)	Sparsely to moderately plagioclase-phyric pillow basalts are common. Most are hypocrystalline and have intersertal groundmass textures. Sub-variolitic and very fine-grained, intergranular groundmass textures also occur in some basalts.	There are three main types of very fine-grained, fibrous clay minerals (smectites), varying from pale or dark green to greenish-brown. Zeolite minerals are also common, mainly forming veins, vuggy infill phases, and partly replacing groundmass glass and igneous crystals (mainly plagioclase phenocrysts and rare olivine).	Sporadic Fe-oxyhydroxide alteration occurs as irregular groundmass patches. Ragged titanite microlites partly to completely overgrow Ti-magnetite (not abundant). Minor calcite occurs in some veins and amygdule cores.	Pervasive, clay-rich alteration is abundant in the primary mesostasis. Most groundmass clinopyroxene and Ti-magnetite is relatively unaltered. Amygdules commonly have multiple, concentric growth rims; these may be texturally distinct (different compositions) from the vugh core.	Weakly altered, seafloor weathering (oxidation) facies to lower zeolite facies regional assemblages.
Caroline Cove Fault	The **western pillow sequence** (local unit in the Zone BVI extrusive rock domain defined during this study) (n = 3)		Sparsely to moderately phyric pillow basalt with intersertal groundmass. Plagioclase is a common phenocryst and also occurs as groundmass laths associated with clinopyroxene (unaltered augite), Ti-magnetite, and volcanic glass. Most rocks are slightly vesicular.	Plagioclase crystals have varying amounts of very fine-grained, smectite-chlorite alteration (Figure 6.2). Abundant smectite-chlorite also pervasively replaces glassy mesostasis and rare olivine crystals (Figure 6.3). Ragged, microlitic titanite grains partly overgrow primary Ti-magnetite.	Fibrous, very fine-grained smectite-chlorite and other clay minerals (various brownish-green and green phases) infill vughs and form narrow veins. Minor zeolites (laumontite and analcite), and late-stage prehnite and calcite veins are locally abundant in some small-scale faults.	Extensive smectite-chlorite alteration occurs in disseminated patches, along many grain cracks and cleavages (Figure 6.2), and near microlitic melt and glass inclusions. Minor veining and amygdule infill phases also occur.	Weak to moderate intensity alteration, mainly zeolite or prehnite facies assemblages, but locally also some lower greenschist facies zones.
		The **eastern pillow sequence** (local unit in the Zone BVI extrusive rock domain defined during this study) (n = 2)	Aphyric or sparsely phyric pillow basalt with intersertal groundmass. Minor zones of hyaloclastite, and rare discrete dolerite dykes.	Volcanic glass and rare olivine crystals are replaced by very fine-grained, fibrous green or greenish-brown clay minerals (Figure 6.4).	Calcite, pyrite, and zeolite (phillipsite) alteration of rare olivine crystals. Minor phillipsite and calcite also forms irregular veins (Figure 6.7) and infills vughs.	Selective groundmass alteration (e.g., primary glass) and minor irregular veining (Figure 6.1). Rare olivine crystals are pseudomorphed by clays.	Relatively weak intensity, seafloor weathering (oxidation) facies
Sellick Bay Fault	The **Zone BVa extrusive rock domain** (n = 4)	The **Zone BIII extrusive rock domain** (n = 4)	Sparsely to moderately plagioclase-phyric pillow basalt, mainly with hypocrystalline groundmass and intersertal to intergranular textures. Most basalt is slightly vesicular. Minor coherent basalt flows, dykes, and hyaloclastites also occur.	Very fine-grained, fibrous clay-rich alteration (smectite) is common in the groundmass and some phenocrysts. Clay alteration in turbid patches or along thin cleavage planes is common in plagioclase. Rare olivine crystals are completely pseudomorphed, and irregular Fe-oxyhydroxide alteration occurs in locally abundant patches.	Zeolite minerals (intergrown aggregates of natrolite, thomsonite, and mesolite in varying abundances) and calcite occur as discrete veins and also infills vughs.	Pervasive clay alteration of groundmass glass and infill of primary vesicles.	Weak to moderate intensity, oxidation to lower zeolite facies regional alteration.

Notes:

1. Regional alteration characteristics presented here are based mainly on petrographic observations made during my petrographic study. Refer to Chapter 3 and 5 for further geological information on the footwall and hangingwall domains, e.g., Figure 3.4.
2. The alteration nomenclature proposed by Griffin (1982) for upper crustal rocks on Macquarie Island was used to interpret the regional alteration assemblages for the main rock associations.
3. The number of thin-section samples observed for each domain is shown in brackets, i.e., n = 15 for the Sandell Bay Sheeted Dyke Swarm.

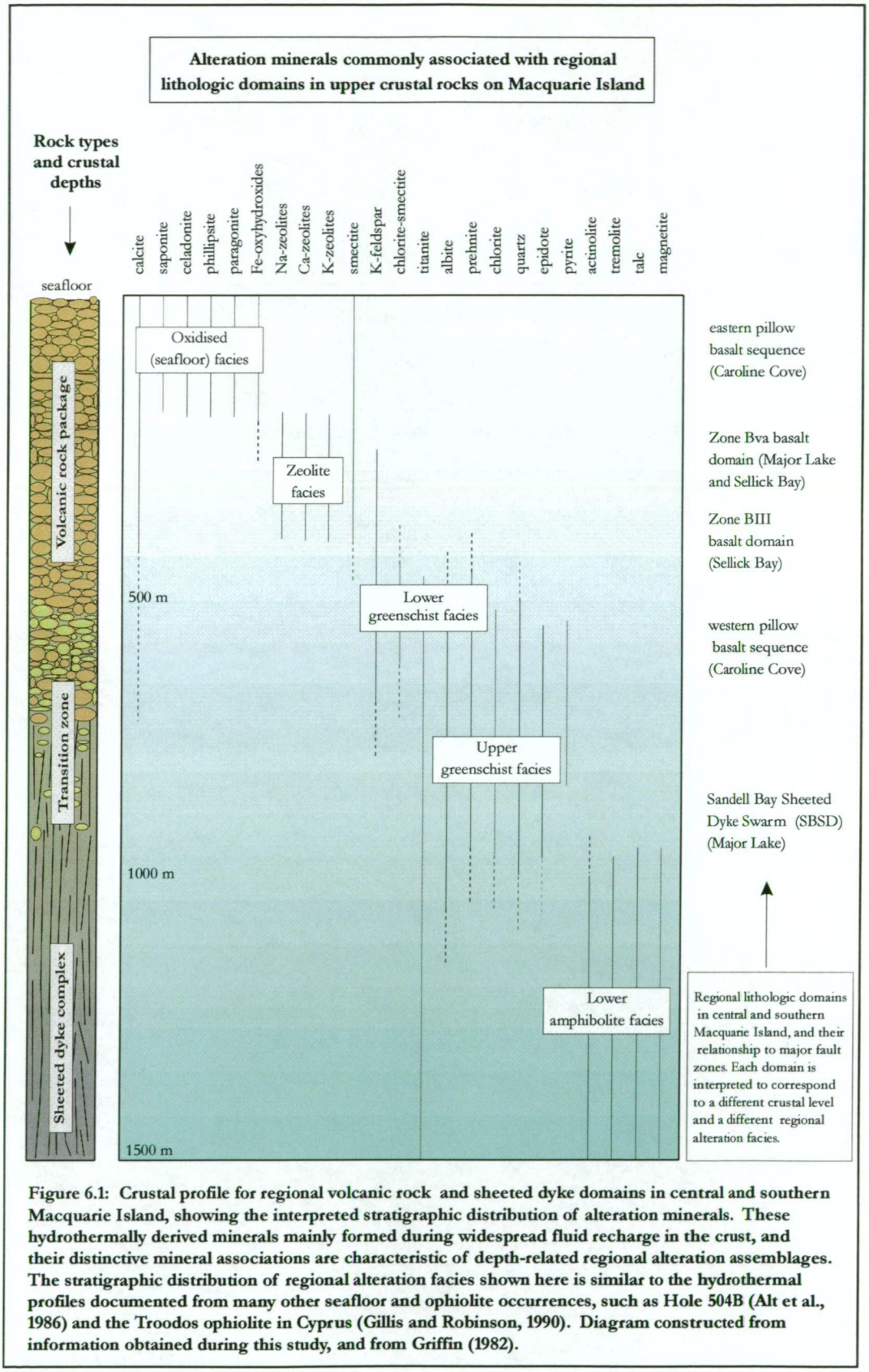

Figure 6.1: Crustal profile for regional volcanic rock and sheeted dyke domains in central and southern Macquarie Island, showing the interpreted stratigraphic distribution of alteration minerals. These hydrothermally derived minerals mainly formed during widespread fluid recharge in the crust, and their distinctive mineral associations are characteristic of depth-related regional alteration assemblages. The stratigraphic distribution of regional alteration facies shown here is similar to the hydrothermal profiles documented from many other seafloor and ophiolite occurrences, such as Hole 504B (Alt et al., 1986) and the Troodos ophiolite in Cyprus (Gillis and Robinson, 1990). Diagram constructed from information obtained during this study, and from Griffin (1982).

My petrographic investigation of the fault-proximal host rock domains confirmed the research findings of Griffin (1982), which recognised that basalts and dykes in central and southern Macquarie Island do not contain wholly pristine igneous mineral assemblages (Table 6.2). All of the regional rocks consist of variable proportions of primary igneous minerals and secondary alteration minerals. These disequilibrium assemblages, and their common textural habits and inter-mineral relationships, clearly indicate that most upper crustal rocks on Macquarie Island were affected by hydrothermal alteration during semi-pervasive fluid–rock interaction (Figure 6.1). Although it is beyond the scope of my research project to reconstruct or revaluate the seminal work of Griffin (1982), it is appropriate to outline the main petrographic features of the regional alteration assemblages (as determined during my petrographic study). The distribution and relationship of these broad hydrothermal regions to zones of focussed alteration in the Major Lake, Caroline Cove, and Sellick Bay Faults, are further discussed in Chapter 9. In addition, the final synthesis chapter also compares and contrasts the characteristics of the regional (and focussed) alteration domains on Macquarie Island with other ocean crust examples.

In summary, important petrographic features associated with regional (host rock domain) alteration assemblages near the Major Lake, Caroline Cove, and Sellick Bay Faults are:

i. The effects of regional alteration are very heterogeneous, and have resulted in diverse mineral assemblages, textural features, and alteration intensities; a spectrum of these characteristics commonly occurs within individual thin-sections. The distribution of regional alteration domains proposed by Griffin (1982) (Chapter 3.6) is broadly supported by my study, although Griffin's classification scheme oversimplifies the complex spatial patterns and small-scale variations inherent in each domain. Similar to the focussed alteration assemblages, the most intensely altered regional rocks are intimately associated with local faults, fractures, and other zones of enhanced permeability (primary conduits), such as discrete dyke margins;

ii. Igneous rock textures are commonly well preserved in all of the regional alteration domains. For example, magmatic-derived plagioclase phenocrysts may be partly or completely altered (variably replaced) to secondary minerals such as smectite or paragonite, but the primary grain shapes are largely unaffected. The *in situ* preservation of delicate (igneous) groundmass textures and primary volcanic structures (e.g., vesicles) suggests that hydrothermal processes associated with regional alteration did not involve dynamic recrystallisation or intense deformation;

iii. Ca-rich igneous plagioclase, ranging in composition from anorthite to labradorite, is the main type of phenocryst in most regional basaltic rocks, and commonly has distinctive alteration textures. Typically, these medium- to coarse-grained plagioclase crystals are more intensely altered than the surrounding groundmass laths. The intensity of plagioclase alteration also varies significantly between discrete domains, closely reflecting

variations in the overall regional alteration grade. Relatively pristine crystals affected only by minor and sporadic clay alteration (very fine-grained 'speckled' patches) are common in rocks from the low grade seafloor weathering and oxidation facies (Figure 6.2). However, in geographic regions dominated by relatively higher grade alteration assemblages (e.g., lower greenschist domains), plagioclase crystals are partly or completely replaced by extensive turbid patches and irregular aggregates of microlitic and very fine-grained alteration minerals. For example, basalt-hosted phenocrysts in the prehnite and lower greenschist facies domains commonly have multi-phase alteration assemblages and diverse hydrothermal textures. Narrow ($\leq$ 10–20 μm-wide) and irregular smectite-rich veinlets are particularly distinctive, and commonly occur along internal grain fractures or cleavage planes (Figure 6.3);

iv. The igneous phases which are most susceptible to the effects of hydrothermal alteration are volcanic glass, which is a common component of the interstitial (groundmass) mesostasis in many extrusive rocks and some shallow-level dykes, and rare phenocrysts of olivine. None of the (thin-section) samples examined during my petrographic study contained pristine glass or olivine; recognition of their previous existence in these rocks was based solely on characteristic groundmass relationships, and distinctive (partly preserved) primary habits and shapes (Figure 6.2 and Figure 6.4). These findings are consistent with the earlier work of Griffin (1982), who only recognised fresh (unaltered) magnesian olivine crystals ($Fo_{89.5-85.1}$) in eight basalts on the entire island. Volcanic glass and olivine are commonly replaced by very fine-grained, brownish-green to green phyllosilicate minerals (the precise mineral species varies depending on the alteration grade, but smectite and mixed chlorite-smectite are most abundant). Other minor alteration minerals that may partly replace olivine crystals include calcite, epidote, and prehnite (Figure 6.5);

v. Clinopyroxene (augite) is mainly a fine-grained groundmass mineral in regional basalts, although partly resorbed phenocrysts (xenocrysts?) occur rarely in rocks from some domains, e.g., in the western pillow basalt sequence at Caroline Cove. Augite is typically the least altered igneous mineral in the volcanic rocks, and most grains observed during this study are relatively pristine. The main exception occurs in deeper segments of the Sandell Bay Sheeted Dyke Swarm, where fine- to medium-grained augite (common groundmass phase) is strongly altered to chlorite and amphibole (mainly actinolite and magnesio-hornblende with Si^{IV} = 7.0–7.4, Davidson et al., 2004). These fine-grained, fibrous amphibole minerals commonly form greenish-brown (slightly pleochroic), 'beard-like' overgrowths around the margins of individual clinopyroxene grains (Figure 6.6);

vi. Primary rock cavities (vesicles) are widespread throughout all of the extrusive rock domains, and most are infilled by hydrothermally derived minerals (Figure 6.7). Vugh infill phases are typically dominated by a single type of very fine- or fine-grained hydrothermal mineral, which corresponds to the most abundant (and diagnostic) alteration phase specific to each regional domain. For example, calcite is a common infill phase in rocks affected by relatively low grade alteration typical of the uppermost volcanic section (Griffin's so-called 'seafloor weathering' facies), whereas phyllosilicate minerals such as smectite and chlorite are more abundant in the lower greenschist assemblages interpreted to have formed at deeper crustal levels (Figure 6.5);

vii. Veins are a minor but distinctive component of most regional alteration assemblages, and mainly form in rocks which are cross-cut by small-scale faults and fractures. However, extensively developed vein networks are uncommon; most form narrow (~ 2–5 mm-wide) and isolated strands which irregularly cut across igneous groundmass and phenocryst minerals (Figure 6.8). Veins are typically dominated by compositionally uniform hydrothermal cements, although the main vein mineral in each domain varies depending upon the regional alteration grade (similar to the compositional variations noted for the vuggy infill phases). Moderate to strong veining comprises the most texturally destructive feature of the regional alteration assemblages, although it is comparatively rare; and, finally

viii. The most common and diagnostic hydrothermal minerals in each regional domain have multiple textural forms and inter-mineral associations (Figure 6.9). Cross-cutting vein relationships, concentrically infilled (multi-phase) vughs, and coexisting disequilibrium replacement assemblages (commonly occurring in the same igneous crystal) all provide good evidence for multiple stages of fluid–rock interaction and hydrothermal alteration. These features suggest that regional hydrothermal processes (recharge-related) were relatively long-lived and consistent throughout Macquarie Island's upper crust, albeit with system-wide variations (temporal and spatial) in the magnitude, intensity, and extent of critical fluid–rock processes and hydrothermal parameters (as previously mentioned, the characteristics of the various regional alteration assemblages around Macquarie Island's major fault zones are further discussed and interpreted in Chapter 9).

Figure 6.2: Typical igneous groundmass textures in weakly altered hypocrystalline basalt from the eastern pillow sequence at Caroline Cove (the hangingwall block of the Caroline Cove Fault Zone). This sparsely phyric basalt is dominated by very fine- to fine-grained plagioclase and clinopyroxene and, typical of most basaltic rocks in this domain, these groundmass minerals are relatively pristine. However, the glassy mesostasis is pervasively altered and replaced by irregular patches of greenish-brown clay (mainly smectite). The regional alteration assemblage shown here is characteristic of Griffin's (1982) low intensity seafloor weathering and oxidation facies (sample MCQ-050 in PPL).

Figure 6.3: The medium-grained plagioclase phenocrysts shown here have a variety of alteration styles, including narrow intra-grain veinlets and irregularly shaped turbid patches. The alteration mineral assemblage is dominated by microlitic to very fine-grained clays (smectite-chlorite), which are well developed along multiple cleavage planes and near some small glassy inclusions. The secondary minerals and hydrothermal textures of this moderately phyric basalt are typical of lower greenschist facies conditions in the western pillow basalt sequence at Caroline Cove (sample MCQ-014 in PPL).

Figure 6.4: Olivine phenocrysts are relatively rare in basaltic rocks on Macquarie Island. Those which do occur are intensely altered, although their primary crystal shapes are commonly well preserved, i.e., pseudomorphic replacement. The medium-grained olivine pseudomorph shown here is replaced by intergrown aggregates of pale brown and green smectite-chlorite, and minor opaque minerals (iddingsite?). The colourless, elongated crystal above the altered olivine is relatively pristine augite, typical of most clinopyroxene in the western pillow basalt sequence at Caroline Cove (sample MCQ-014 in PPL).

Figure 6.5: Regional greenschist facies alteration occurs commonly in rocks from the Sandell Bay Sheeted Dyke Swarm (SBSD). This sample from the upper Sandell Bay escarpment shows chlorite + epidote replacing a medium-grained olivine phenocryst (upper left). Chlorite has also infilled a small rounded vugh adjacent to the subhedral plagioclase crystal (a shallow-level dyke?) and replaced many other fine-grained minerals in the groundmass. The pale plagioclase grain is mainly altered to chlorite along intra-grain cleavages and irregular crystal fractures (sample MCQ-348 in PPL).

Figure 6.6: Fine-grained clinopyroxene is strongly altered in the groundmass of this dolerite from the Sandell Bay Sheeted Dyke Swarm at Major Lake foreshore (Site 2B). Finely fibrous aggregates of greenish-brown amphibole (mainly actinolite) have replaced most of the igneous-derived augite. An irregular patch of pale green, massive chlorite occurs near the right of view, and most of the elongate groundmass laths have Na-rich compositions (albite altered plagioclase). These mineral assemblages are typical of regional alteration in most sheeted dyke complexes on Macquarie Island (sample MCQ-324 in PPL).

Figure 6.7: Small, subrounded vesicles occur sporadically in hypocrystalline rocks (dolerite) from the uppermost levels of the Sandell Bay Sheeted Dyke Swarm. Multiple generations of pale green and greenish-brown chlorite have infilled this vuggy cavity, and these are post-dated by the narrow, slightly sinuous K-feldspar veinlet that cuts sharply across the core. K-feldspar is only a relatively minor alteration phase in the SBSD (sample MCQ-324 in PPL).

Figure 6.8: Irregular but well defined vein networks cut across weakly altered, hypocrystalline basalt in several small fault zones in the eastern pillow sequence at Caroline Cove. The pale vein minerals here consist of massive, very fine-grained Ca-rich zeolites (low relief) which are intergrown with fine to medium-grained, platy calcite crystals. Veins commonly contain subangular fragments of brecciated basalt, but most lack well defined alteration selvages in the adjacent wall rocks (sample MCQ-034 in PPL).

Figure 6.9: Multiple episodes of hydrothermal alteration have affected transition zone pillow basalts in the Lusitania Bay escarpment (sample MCQ-392 in PPL). In this sample, the glassy mesostasis is pervasively altered to chlorite, and many plagioclase phenocrysts and groundmass minerals also have extensive turbid patches and fine veinlet alteration. Very fine-grained chlorite infills the small, ovoid vugh which occurs near the strand of disseminated pyrite crystals. The early-formed alteration minerals are cross-cut by a thin veinlet filled with Ca-rich zeolites such as thomsonite.

Photomicrographs of common hydrothermal minerals and textures associated with regional alteration assemblages on Macquarie Island.

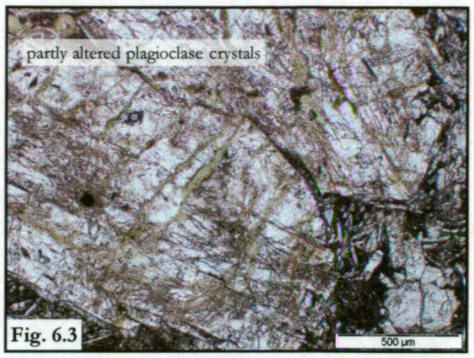

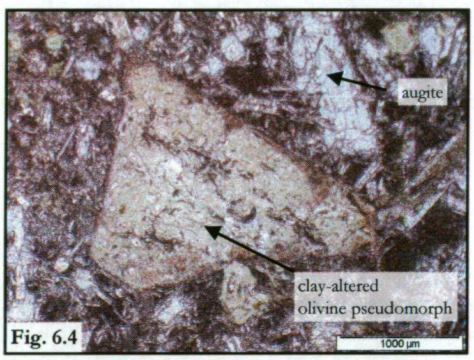

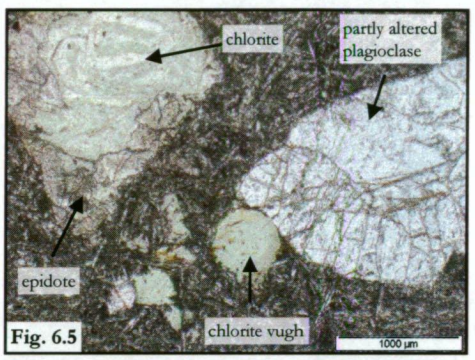

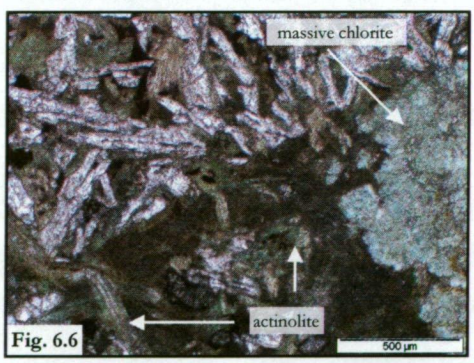

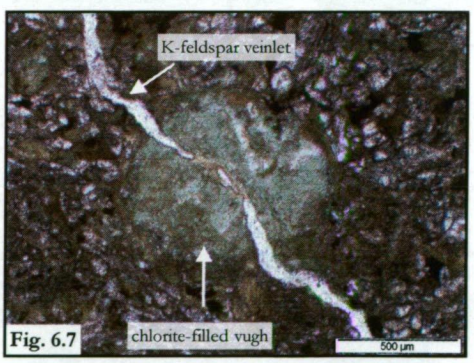

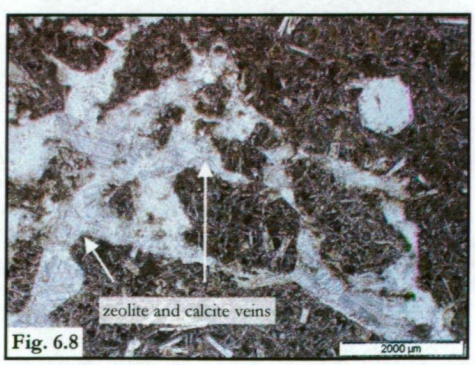

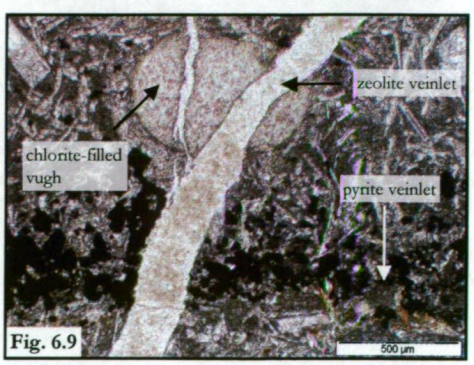

Hydrothermal textures and alteration styles in the fault hosted (focussed) alteration facies

The focussed alteration facies identified in this study each contain a characteristic group of hydrothermally derived minerals (Table 6.3). These multi-component alteration assemblages coexist with varying proportions of igneous minerals in the fault zone rocks; visual estimates suggest that the primary compositions are commonly 70–100 % recrystallised and replaced. The most abundant hydrothermal minerals associated with each focussed alteration facies occur in multiple textural forms, and the range of diverse styles are typically evident within a single thin-section. Although the type, abundance, and distribution of the alteration mineral suite differ significantly between separate fault zones, four distinctive textural styles were consistently recognised (irrespective of specific facies). These are similar to the common spectrum of hydrothermal textures described from previous petrographic studies of altered oceanic rocks, e.g., Ishizuka, 1989; Alt et al., 1996; Talbi and Honnorez, 2003; Schramm, 2004; Teagle and Alt, 2004.

The main hydrothermal textures identified within altered basalts and dolerites from the Major Lake, Caroline Cove, and Sellick Bay Fault Zones are:

i. Primary igneous minerals are partly to completely replaced by secondary alteration minerals;

ii. Irregularly shaped patches of volcanic glass in the primary mesostasis of hypocrystalline rocks are completely replaced by secondary alteration minerals;

iii. Most primary rock cavities and voids (such as vesicles) are completely infilled by single- or multi-phase hydrothermal mineral assemblages (amygdules); and

iv. Well defined veins, veinlets, and breccias filled with a variety of different hydrothermal cements cut across primary groundmass patches and igneous-derived crystals.

Replacement of igneous minerals

Volcanic rocks affected by focussed hydrothermal alteration are mainly hypocrystalline pillow basalts with aphyric to moderately phyric textures and intersertal groundmass (commonly sub-variolitic) (Figure 6.10). The sheeted dolerite dykes are fine- to medium-grained rocks that contain sparse plagioclase phenocrysts; some also have typical sub-ophitic groundmass textures. Primary igneous phases in these rocks are dominated by groundmass plagioclase and clinopyroxene (augite), with minor Ti-magnetite and interstitial glass. Plagioclase is the most common phenocryst (Figure 6.10 and Figure 6.11), although crystals of olivine, clinopyroxene, and spinel also occur (rarely).

Table 6.3: Alteration minerals and hydrothermal textures associated with fault zone alteration facies on Macquarie Island.

Alteration facies	Macro-alteration minerals	Micro-alteration minerals	Common hydrothermal textures	Igneous - alteration associations
Vein and breccia, quartz-chlorite (VQC) facies (n = 34)	quartz + chlorite ± epidote ± pyrite	Na-rich plagioclase (albite) + titanite + leucoxene ± amphibole (actinolite) ± chalcopyrite ± calcite ± Ca-zeolites ± Fe-hydroxides and clay minerals	• abundant quartz veins and massive alteration zones of varying thickness and intensity; • quartz-cemented breccias with angular, chlorite-altered wall rock fragments; and • late-stage oxidised clay overprint (veinlets and patches).	plagioclase → albite, chlorite, epidote; augite → chlorite, actinolite; Ti-magnetite → titanite, epidote, leucoxene; and (olivine and glass) → chlorite.
Massive and veined, chlorite-quartz-pyrite (CQP) facies (n = 16)	chlorite + quartz + pyrite ± chalcopyrite ± epidote ± barite	Na-rich plagioclase (albite) + titanite + leucoxene + oxidised clays (saponite) ± amphibole (actinolite) ± sphalerite ± calcite ± zeolites (analcite and laumontite)	• extensive chlorite alteration is widespread in basaltic groundmass and also infills many veins and vughs; • massive and veined quartz – pyrite – chalcopyrite, commonly with hydrothermal breccias; and • minor late-stage veins infilled with calcite, zeolites, and Fe-rich clays.	plagioclase → albite, chlorite, epidote; augite → chlorite, actinolite; Ti-magnetite → titanite, epidote, leucoxene; and (olivine and glass) → chlorite, epidote, pyrite.
Vein-dominated, prehnite-zeolite (VPZ) facies (n = 17)	prehnite + zeolite minerals (laumontite) + Fe-oxyhydroxides	pumpellyite + smectite (clay) + titanite ± calcite	• thick prehnite veins, many with selvages; • intense veinlet arrays with abundant zeolites (mainly laumontite) and Fe-oxyhydroxides; and • complex, intergrown massive alteration pods replace pillow basalt cores and inter-pillow glass.	(plagioclase, augite, olivine, glass) → smectite, prehnite, zeolite, pumpellyite (variable assemblages depending on rock location and alteration intensity).
Foliated, massive chlorite (FMC) facies (n = 4)	clay-chlorite minerals ± prehnite	microscopic study identified mixed-layer smectite and smectite-chlorite assemblages	• irregular, wispy and discontinuous veinlets and small patches of foliated clay-chlorite commonly surround weakly altered basalt fragments; and • late-stage prehnite veins.	Weakly altered basalt fragments have low-grade, seafloor oxidation facies assemblages.
Pervasive, Fe-oxyhydroxide overprint (PFO) facies (n = 3)	Fe-oxyhydroxide minerals		• late-stage, pervasive oxidation overprint of Fe-rich igneous and hydrothermal minerals, commonly with well preserved halo textures.	(augite, Ti-magnetite, chlorite, pyrite) → Fe-oxyhydroxide minerals.
Narrow, focussed quartz vein alteration (NQV) facies (n = 3)	quartz + chlorite ± epidote ± pyrite	titanite + albitised plagioclase	• narrow zones of strongly focussed quartz-rich alteration.	Similar to the VQC facies assemblage.

Note:

The number of thin-sections observed for each alteration facies is shown in brackets, e.g., n = 34 for the VQC facies.

Focussed hydrothermal alteration has variably affected the igneous-derived assemblages. Many primary minerals are extensively replaced (> 90 % alteration) in strong and intensely altered groundmass domains, destroying much of the original (igneous) rock fabric (Figure 6.12). Irregularly shaped patches of less altered basaltic groundmass occur sporadically throughout the intensely altered zones (heterogeneous alteration effects), and some groundmass minerals (especially augite) have undergone relatively weak selective pervasive alteration. Primary groundmass textures (typically defined by the widespread occurrence of very fine- to fine-grained plagioclase laths) are commonly well preserved *in situ*, even in rocks affected by moderate to strong hydrothermal alteration. Back-scattered electron microscopy (pilot study results only) showed that the primary compositions of many igneous-derived plagioclase laths (Ca-rich), particularly their crystal cores, are highly modified by Na-rich metasomatism, i.e., albite alteration, although relict patches and rims of Ca-rich plagioclase may coexist (Figure 6.13).

In most fault zone rocks, the primary igneous phenocrysts are more intensely altered than the surrounding groundmass minerals. Medium- to coarse-grained crystals are commonly completely replaced by alteration phases, resulting in well preserved plagioclase pseudomorphs in many focussed alteration assemblages, e.g., the vein-dominated, prehnite-zeolite (VPZ) facies (Figure 6.14). Plagioclase phenocrysts typically have multiple alteration styles (affecting both their mineral compositions and textures); many coexist within discrete grains. Depending on the specific alteration facies, plagioclase crystals may be selectively replaced by microlitic phyllosilicate minerals such as chlorite and smectite, various zeolite minerals (e.g., laumontite), and prehnite or pumpellyite (Table 6.3). In many crystals, hydrothermal alteration initially occurred along narrow intra-grain cracks (< 0.1 mm-wide) and cleavage planes, forming complex stringer-like networks and inter-connected veinlet trails (Figure 6.15 and Figure 6.16). Irregularly shaped patches of turbid alteration, mainly comprising aggregates of microlitic phyllosilicate minerals, are also abundant, especially in altered phenocryst cores and adjacent to igneous-derived crystal inclusions, e.g., minute glass and melt inclusions in plagioclase. In general, plagioclase crystals in most rocks affected by focussed hydrothermal alteration are heterogeneous pseudomorphs which now consist of variable proportions of relict igneous plagioclase (Ca-rich compositions), hydrothermally derived plagioclase (Na-rich), and microlitic or very fine-grained secondary alteration minerals such as chlorite, epidote, and prehnite (Figure 6.17).

Olivine phenocrysts are a minor primary component of some basaltic rocks on Macquarie Island. In many fault zone assemblages, rare olivine is extensively altered and completely replaced by chlorite (± calcite, pyrite, and Fe-oxyhydroxides); however, most are perfectly pseudomorphed and retain their distinctive euhedral crystal shape (Figure 6.17).

Figure 6.10: Primary igneous textures are well preserved in this pillow basalt from the narrow, focussed quartz vein (NQV) facies, with abundant fine- to medium-grained plagioclase crystals in the glass-rich (hypocrystalline) groundmass. Despite excellent preservation of relict volcanic textures, very fine- to fine-grained alteration minerals such as chlorite, quartz, titanite, albite, and pyrite are widespread, partly to completely replacing many primary igneous crystals (sample MCQ-404 in PPL; NQV facies from Major Lake south, Site 2H).

Figure 6.11: Fine- to medium-grained plagioclase is common in volcanic rocks on Macquarie Island. The elongate plagioclase laths in this moderately phyric basalt are surrounded by dark and pervasively altered (intersertal) groundmass patches. Plagioclase is strongly albite-altered (Na-rich), and larger crystals commonly have a very turbid appearance due to microlitic chlorite and epidote (sample MCQ-031 in PPL; CQP facies from Caroline Cove, Site 3A).

Figure 6.12: Intense chlorite and quartz alteration has overprinted the primary basaltic groundmass and destroyed most igneous textures in this basalt. Pervasive alteration and widespread textural destruction in volcanic rocks mainly occurs in the focussed hydrothermal facies associated with the Major Lake (VQC) and Caroline Cove (CQP) Faults. In this view, quartz mostly forms pale, irregularly shaped patches or fine, discontinuous veinlets, whereas chlorite has pervasively altered groundmass plagioclase, augite, and interstitial mesostasis (glass). Very fine- to fine-grained pyrite, titanite, leucoxene, and epidote) also occurs in the altered groundmass (sample MCQ-071 in PPL, VQC facies from Major Lake foreshore, Site 2B).

Figure 6.13: A back-scattered electron (BSE) image of typical basaltic groundmass affected by intense VQC facies alteration. Randomly oriented, fine-grained plagioclase laths are abundant in the groundmass, and most are extensively albite-altered (Na-enrichment). These alteration effects are highlighted in this image by distinct variations in brightness; most plagioclase laths have narrow marginal rims of relict Ca-rich plagioclase (pale grey tone) that surround strongly Na-altered cores (darker grey). Irregularly shaped patches of very fine-grained titanite, leucoxene, and epidote (bright white grains) are sporadically disseminated in the groundmass, and these complexly intergrown aggregates have mainly replaced primary Ti-magnetite crystals (BSE image of sample MCQ-071; Major Lake foreshore, Site 2B).

Figure 6.14: This photomicrograph shows medium-grained plagioclase phenocrysts in basaltic groundmass near the margins of a pale prehnite vein. The primary euhedral crystal shapes are well preserved, but plagioclase is pervasively altered and replaced by very fine-grained pumpellyite + prehnite, i.e., pseudomorphic alteration. Acicular grains of pumpellyite are particularly abundant and commonly form intra-grain networks that randomly dissect their relict crystal host. Pumpellyite (+ minor prehnite and smectite) also occurs widely in the groundmass, forming a well defined alteration selvage adjacent to the vein (sample MCQ-272 in PPL, VPZ facies from Sellick Bay escarpment, Site 1A).

Figure 6.15: Relict igneous textures in many of the altered fault zone rocks are commonly obscured (partly to completely) by hydrothermally derived minerals (in contrast to most regionally altered rocks). This medium-grained plagioclase phenocryst is extensively altered and replaced by abundant chlorite and albite. Minor quartz, pyrite, and microlitic opaque phases (pyrite?) also occur sporadically in the altered crystal. Chlorite is especially abundant and mainly forms fine, intra-grain veinlets along irregular fractures or cleavage planes (sample MCQ-375 in PPL, VQC facies from Lusitania Bay escarpment, Site 2D).

Figure 6.16: Alteration intensity is very heterogeneous in the VPZ facies from the Sellick Bay Fault Zone. For example, contrast the well preserved plagioclase phenocryst and hypocrystalline groundmass shown here with the pervasively altered basaltic groundmass in Figure 6.14. This medium-grained plagioclase crystal is affected by relatively low intensity alteration; patchy zones and veinlets of greenish smectite occur mainly on cleavage and fracture planes, and the igneous plagioclase composition (Ca-rich) is largely unaltered. In addition, although the glassy mesostasis is pervasively replaced by pale green smectite, the main groundmass minerals (plagioclase, augite and Ti-magnetite) are relatively pristine (sample MCQ-290 in PPL, VPZ facies from Sellick Bay escarpment, Site 1A).

Figure 6.17: Despite moderate to strong alteration in this VQC facies basalt, the primary crystal shapes of these plagioclase and olivine grains are well preserved. However, olivine is extensively chlorite-altered (pseudomorphed), and also partly overprinted by pale and irregular patches and veinlets of quartz. Irregular zones and veinlets of greenish chlorite occur commonly in the coarse-grained plagioclase crystal, and its original Ca-rich composition is now mostly altered to albite (sample MCQ-208 in PPL, VQC facies from Lusitania Bay, Site 2D).

Photomicrographs of igneous phenocryst and groundmass textures associated with focussed hydrothermal alteration facies on Macquarie Island.

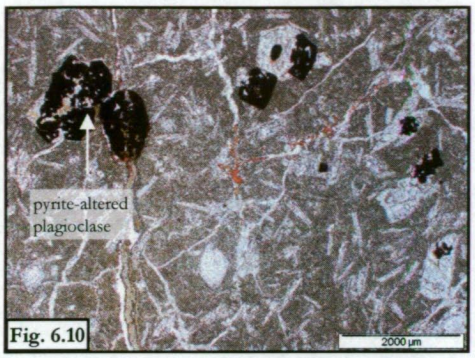

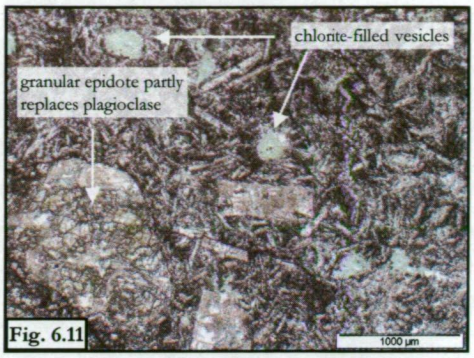

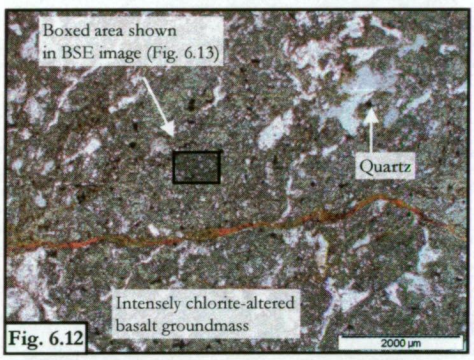

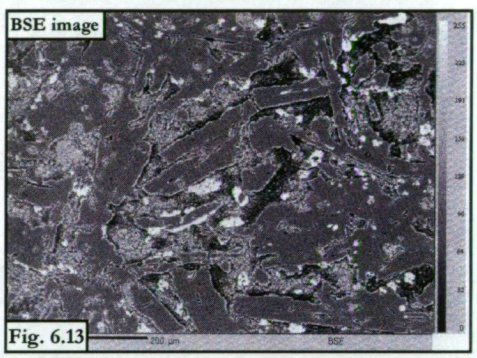

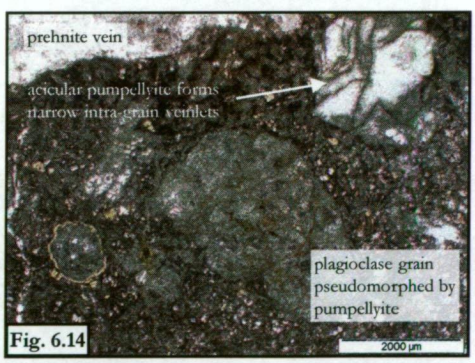

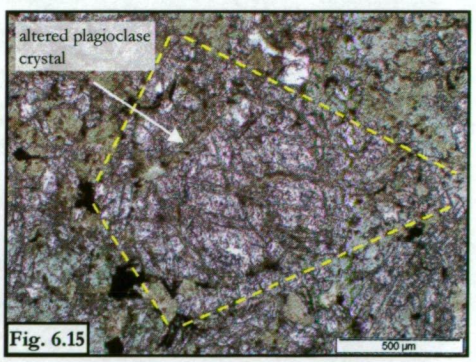

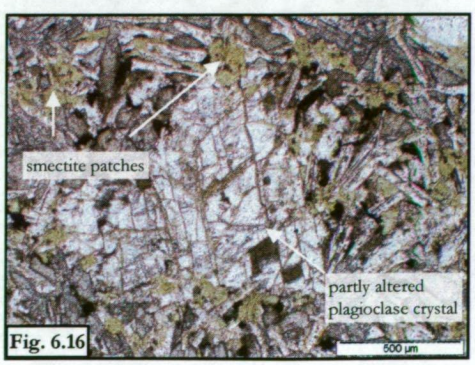

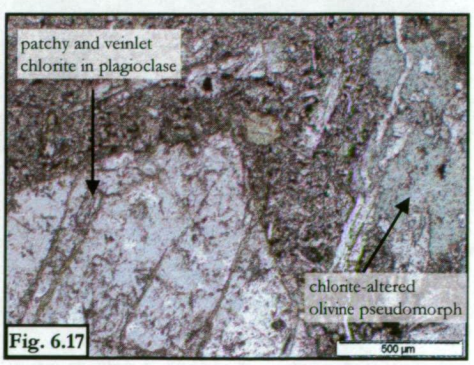

Clinopyroxene (also rare) is generally the least altered igneous mineral, although widespread replacement of groundmass clinopyroxene (augite) by chlorite and secondary amphiboles, such as actinolite, occurs in the diagnostic alteration facies of the Major Lake and Caroline Cove Fault Zones (respectively, the VQC and CQP alteration facies). Very fine- to fine-grained, Ti-rich magnetite is also common throughout the groundmass of most basaltic rocks; most of these primary oxides are strongly altered and replaced by ragged, intergrown aggregates of microlitic titanite, leucoxene, epidote, and chlorite (Godber, 2003).

Replacement of the glassy mesostasis

The aphanitic groundmass of most extrusive rocks and some dolerites (including some from the Sandell Bay Sheeted Dyke Swarm) contains abundant volcanic glass, i.e., they are hypocrystalline rocks. The glassy mesostasis partly to completely envelops discrete igneous crystals (both phenocryst and groundmass phases), forming small (< 0.5–1 mm-across) and irregularly shaped interstitial matrix domains which are widespread throughout many rocks, i.e., typical intersertal textures. However, volcanic glass is highly susceptible to hydrothermal alteration, and practically all (> 99 %) glass-rich groundmass patches are pervasively altered in the fault zone rocks that I observed (Figure 6.12 and Figure 6.16). Volcanic glass is mainly replaced by complexly intergrown aggregates of microlitic or very fine-grained, greenish phyllosilicate minerals, e.g., intergrown chlorite and chlorite-smectite mixtures. The widespread distribution and abundance of these minute hydrothermal minerals is the main cause of the distinctive greenish tinge in the VQC and CQP facies (Figure 6.12). Glass-rich groundmass patches may also be replaced by minor pyrite and epidote, or massive Fe-oxyhydroxides and zeolites, especially in the VPZ facies from the Sellick Bay Fault.

Infill of voids and formation of amygdules

Most pillow basalts on Macquarie Island, and some massive basaltic flows and discrete dykes, are slightly or moderately vesicular (commonly ~ 1–3 % of the rock composition, Chapter 3 and 5). Vesicles are typically < 1mm-wide (many are < 0.5 mm) and have rounded, subrounded, or partly elongated shapes. These primary rock cavities are most abundant in the basaltic groundmass of uppermost pillow rims (relative to the pillow core) and, as such, provide reliable criteria for assessing the younging direction (way-up).

Basalt hosted vesicles in the focussed alteration zones are infilled by a variety of hydrothermal minerals. These amygdules contain both mono- and multi-phase (coexisting) assemblages, and most of the infill minerals form intergrown aggregates of microlitic or very fine-grained crystals (Figure 6.18). Chlorite, prehnite, and various zeolite species (e.g., thomsonite and natrolite) are the most abundant hydrothermal minerals (depending on the specific facies), and fine-grained, platy alteration phases such as epidote and calcite also occur in some assemblages, e.g., the VPZ facies in the Sellick Bay Fault (Figure 6.18 and Figure 6.19).

Photomicrographs of vugh textures associated with focussed hydrothermal alteration facies on Macquarie Island.

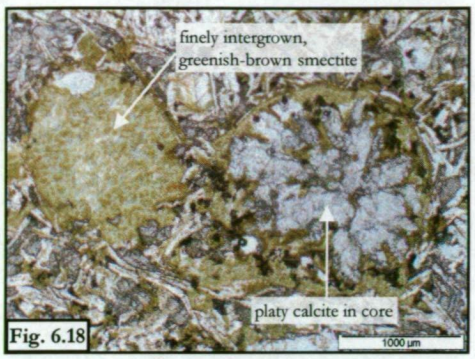

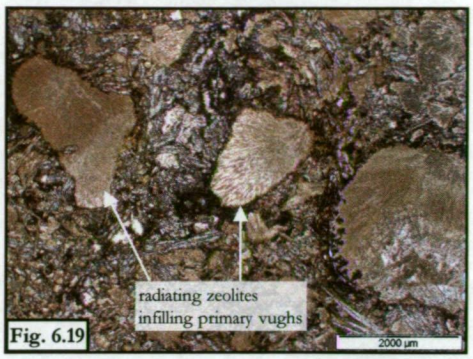

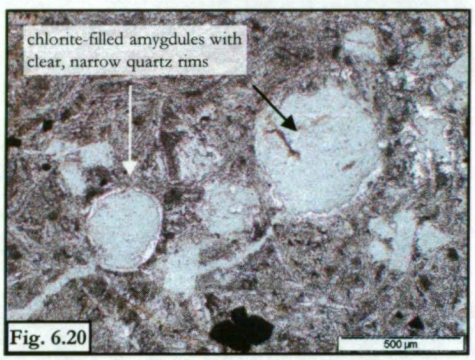

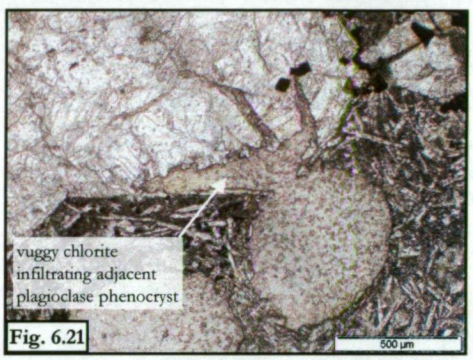

Figure 6.18: The small, subrounded vughs shown here are mostly infilled with greenish-brown smectite and pale calcite. The amygdule on the right is dominated by an aggregate of pale calcite crystals, and has a narrow outer rim of intergrown smectite and disseminated Fe-oxyhydroxide grains (opaque phases). In contrast, the vesicle on the left hosts finely sheeted smectite aggregates; similar greenish clay minerals have also pervasively altered nearby patches of glass in the groundmass (sample MCQ-282 in PPL; VPZ facies basalt from the Sellick Bay escarpment, Site 1A).

Figure 6.19: These relatively large and irregularly shaped vesicles are infilled with subradiating aggregates of finely intergrown Ca- and Na-rich zeolite minerals, dominated by thomsonite, mesolite, and natrolite. The amygdule cement, and most other igneous and alteration minerals in the surrounding basaltic groundmass, is also moderately to strongly oxidised, imparting a distinctive and widespread reddish-brown stain throughout the field-of-view (sample MCQ-292 in PPL; VPZ facies basalt from the Sellick Bay escarpment, Site 1A).

Figure 6.20: Evidence for multiple episodes of hydrothermal activity occurs in each of the focussed alteration facies on Macquarie Island. The subrounded vesicles shown here are mainly filled with massive, very fine-grained chlorite that formed during a relatively early hydrothermal event. Narrow rims of clear, crystalline quartz partly to completely envelop the chlorite-filled cores, providing clear evidence of subsequent fluid–rock interaction. Pale green chlorite is also abundant in the intersertal groundmass, where it has pervasively replaced the mesostasis and most of the very fine- to medium-grained plagioclase and olivine crystals (sample MCQ-062 in PPL; CQP facies basalt from Caroline Cove, Site 3A).

Figure 6.21: Vesicles in the hypocrystalline groundmass of this transition zone basalt are mainly infilled with pale brownish-green chlorite, a common alteration mineral in the vein and breccia, quartz-chlorite (VQC) facies. The finely intergrown chlorite aggregate in the central amygdule has breached the outer rim of its host vesicle and partly invaded the nearby plagioclase crystal; alteration is especially well developed along internal fractures and cleavage planes. Turbid patches of microlitic clay minerals also occur widely in this albitised plagioclase grain (sample MCQ-392 in PPL; VQC facies basalt from the Lusitania Bay escarpment, Site 2D).

Many amygdules are lined by narrow rims that partly to completely enclose massive or subradiating crystalline cores (Figure 6.20); these relationships provide compelling textural evidence to interpret distinct episodes of hydrothermal precipitation. Multiple, concentrically grown amygdule rims are also characteristic of many alteration facies, with different minerals formed in the cores and rims readily identified by distinct variations in colour and fine-scale textures (Figure 6.20). Some vuggy infill minerals have partly breached the outer boundary of their host cavity and infiltrated adjacent phenocryst or groundmass phases (Figure 6.21).

Formation of veins and breccias

Veins and breccias are distinctive textural features in each focussed alteration facies, although their abundance and composition vary for different fault assemblages. The intensity and spatial distribution of hydrothermal veining is also very heterogeneous, and the three diagnostic fault zone facies (i.e., the VQC facies from Major Lake, the CQP facies from Caroline Cove, and the VPZ facies from Sellick Bay) each consist of multiple generations of cross-cutting veins with compositionally diverse cements. Distinctive vein attributes provide fundamental criteria for classifying the main alteration facies, and are also critical for defining their relative paragenetic stages, e.g., providing evidence for temporal variations based on cross-cutting relationships.

Individual vein segments commonly have well defined margins that sharply transect the altered groundmass of their basaltic host rocks. However, many vein strands are highly irregular and discontinuous; high-angle off-shoots, sharp terminations, and narrow dendritic branches are abundant, especially in quartz-dominated assemblages such as the VQC and NQV facies in the Major Lake district (Figure 6.22). Subparallel vein networks consisting of discrete major veins and subsidiary veinlets also occur in many focussed alteration zones, e.g., the VPZ facies in the Sellick Bay Fault (Figure 6.23). Most vein arrays form interconnected 'stringer'-like systems which are dominated by single-phase hydrothermal cements; these include quartz or chlorite in the VQC facies, and prehnite or zeolites in the VPZ facies.

Vein-specific, wall rock alteration haloes or selvages are not commonly associated with the focussed hydrothermal zones, except around some prehnite-rich veins in the VPZ facies (Figure 6.24). In many rock samples, discrete igneous minerals which are cross-cut by veins (such as medium- and coarse-grained plagioclase phenocrysts) have no obvious vein-related alteration textures or significantly increased alteration intensities (relative to other nearby grains that are not cut by veins).

Separate vein phases comprised of different hydrothermal cements typically have oblique (high-angle) cross-cutting relationships, providing clear evidence for multiple and temporally distinct vein-forming stages (Figure 6.25). In contrast, angular intersections between compositionally similar veins are comparatively rare. Some multi-component veins also consist of irregularly shaped and discontinuous 'layers' which formed subparallel to the main trend. In these veins,

different hydrothermal cements occur in the vein core and along the vein margins (e.g., quartz veins partly overprinting earlier-formed chlorite veins), suggesting that evolving fluids (temporally distinct stages) may have exploited similar host rock pathways during the prolonged hydrothermal evolution of each fault system (Figure 6.26).

Many fault zone vein arrays contain abundant angular fragments which impart distinctive brecciated textures in the host cement (Figure 6.27). Hydrothermal breccias are especially common in quartz-bearing veins, and they represent diagnostic features of the VQC facies (Major Lake Fault) and the CQP facies at Caroline Cove. Vein hosted breccia fragments mainly consist of minute hydrothermal minerals and crystalline particles (these minerals are commonly different from the main vein cement), and strongly chloritised fragments of basalt. The microlitic to very fine-grained crystal inclusions may be sporadically disseminated in the vein cement, concentrated in discrete crystal aggregates, or variably clustered at the vein–wall rock interface. Common inter-mineral vein associations include pyrite, chlorite, and epidote with quartz veins (VQC and NQV facies), and pumpellyite with prehnite (VPZ facies; Figure 6.28).

Altered (strongly chloritised) wall rocks hosted in quartz veins from the VQC and CQP facies range from highly fractured and disaggregated particles to relatively intact (coherent) fragments with well preserved igneous textures (Figure 6.29). Most lithic fragments are angular to very angular and are interpreted to have been derived from proximal basalts, i.e., rocks immediately adjacent to the vein arrays. The VQC and CQP breccias lack physical evidence that would typically be expected if the vein particles were mobilised in their parent hydrothermal fluids, such as partly rounded fragment edges or elongated particle trails. The textural attributes of these fragments contrast with those reported by Delaney et al. (1987) for hydrothermal breccias from the MARK area (mid-Atlantic Ridge). Rapid and turbulent fluid flow regimes were implied at MARK by the occurrence of partly rounded, pebble-like fragments hosted in quartz veins. Fluid flow rates were estimated at > 1 m/s, and were interpreted as sufficiently vigorous to have transported discrete breccia fragments (Delaney et al., 1987). Davidson et al. (2004) also discussed partly rounded and altered (pyritic) lithic fragments in hydrothermal veins from the Double Point area on Macquarie Island's west coast (~ 1–2 km north of the VQC facies zones at Sandell Bay and Major Lake, Figure 5.1). The fragments described by Davidson et al. (2004) are coated by concentrically banded rinds of very fine-grained chlorite, which attest to turbulent hydrothermal fluid conditions and possible particle transportation by the fluid. The absence of similar breccia textures from the Major Lake and Caroline Cove Faults suggests that local fluids may not have attained such rapid velocities or turbulent conditions as reported elsewhere.

Figure 6.22: Well defined, suborthogonal quartz veins cut sharply across this strongly altered basalt from the vein and breccia, quartz-chlorite (VQC) facies. Quartz veining clearly post-dated the extensive chlorite-dominated groundmass alteration, and many veins host angular and disaggregated fragments derived from nearby wall rocks. Consistent textural evidence indicates that most quartz veins formed during a single hydrothermal stage, i.e., cross-cutting relationships are uncommon. Vein-proximal selvages are also absent in the groundmass, typical of most quartz-rich alteration zones in the VQC facies (sample MCQ-153 in PPL; VQC facies basalt from Sandell Bay creek, Site 2A).

Figure 6.23: Intensely developed subparallel veinlet arrays are common in the main deformation zone of the Sellick Bay Fault, and are a diagnostic component of the vein-dominated, prehnite-zeolite (VPZ) facies. Most of the wavy veinlets shown here are filled with very fine-grained zeolite minerals; tabular crystals of laumontite (Ca-rich zeolite) are especially common. The extensive veinlet networks have severely disrupted the primary rock fabric, partly to completely destroying many igneous minerals and textures (sample MCQ-276 in PPL; VPZ facies from the Sellick Bay escarpment, Site 1A).

Figure 6.24: Distinctive alteration selvages of variable width envelop many prehnite veins in the vein-dominated, prehnite-zeolite (VPZ) facies. In this view, pervasive pumpellyite + prehnite alteration has affected the dark, hypocrystalline groundmass adjacent to the prehnite vein; most igneous minerals and textures are obliterated in the vein halo. The intergrown mosaic of prehnite crystals comprising the vein cement are typically clear and colourless, but have a bright birefringence spectrum in XPL (sample MCQ-272 in XPL; VPZ facies basalt from the Sellick Bay escarpment, Site 1A).

Figure 6.25: Cross-cutting relationships between different vein stages are common in the focussed alteration facies on Macquarie Island and provide good evidence for multiple stages of hydrothermal activity. In this photomicrograph, subparallel Fe-oxyhydroxide veinlets (opaque) are cross-cut and slightly off-set by late zeolite veins (mostly cemented with Ca-rich laumontite). The veins typically have irregular but well defined margins that significantly disrupt primary volcanic textures; most of the surrounding groundmass is also extensively replaced by similar alteration minerals (sample MCQ-176 in PPL; VPZ facies basalt from the Sellick Bay escarpment, Site 1A).

Figure 6.26: Some veins in the CQP facies have distinctive overprinting textures, suggesting that multiple stages of hydrothermal flow were likely focussed along similar fluid pathways. In this view, ragged fragments from an early-formed, massive chlorite vein are sporadically distributed in the pale cement of late-stage quartz. The quartz vein has sharp but slightly irregular margins that cut across the strongly chlorite-altered igneous groundmass, although relict igneous textures are well preserved in this basalt away from the vein margins (sample MCQ-058 in PPL; CQP facies basalt from Caroline Cove, Site 3A).

Figure 6.27: Quartz-cemented hydrothermal breccias contain abundant wall rock fragments, disaggregated lithic particles, various microlitic to fine-grained crystals (e.g., chlorite), and minute fluid inclusions (mostly < 10 μm). These vein-hosted components impart a very turbid appearance which commonly clouds the hydrothermal cement. The pervasively altered groundmass of the basaltic wall rocks are intensely chloritised (green), and also contain minor fine- to medium-grained pyrite (anhedral opaque crystals) and ragged quartz patches (sample MCQ-375 in PPL; VQC facies basalt from Lusitania Bay escarpment, Site 2D).

Figure 6.28: Discrete prehnite veins commonly contain trellis-like arrays (veinlet networks) or irregularly intergrown aggregates of very fine-grained pumpellyite. Acicular, greenish-brown crystals (slightly pleochroic) of pumpellyite markedly contrast with the surrounding colourless prehnite cement. Pumpellyite is commonly associated with prehnite in the VPZ facies (Sellick Bay Fault), although the intimate mineral association is not ubiquitous and single-phase prehnite veins also transect some volcanic rocks (sample MCQ-279 in PPL; VPZ facies basalt from the Sellick Bay escarpment, Site 1A).

Figure 6.29: Angular fragments of brecciated basalt occur in most thick quartz veins or massive alteration zones in the VQC facies. Quartz hosted rock fragments commonly retain their primary volcanic textures (such as relict plagioclase laths), although most igneous minerals are strongly altered to chlorite; minor albite, quartz, epidote, titanite, leucoxene, and pyrite also occur in the groundmass. Several irregularly shaped patches of massive chlorite occur in this altered basalt fragment, and minute particles of disaggregated wall rock and various crystal fragments are also widely distributed throughout the clear hydrothermal cement (sample MCQ-373 in PPL, Lusitania Bay escarpment, Site 2D).

Photomicrographs of vein-related textures associated with focussed hydrothermal alteration facies on Macquarie Island

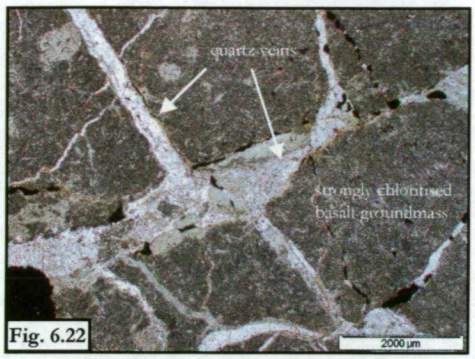

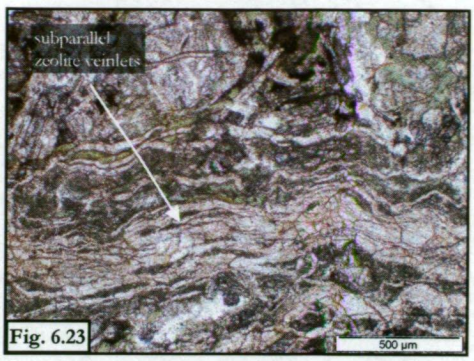

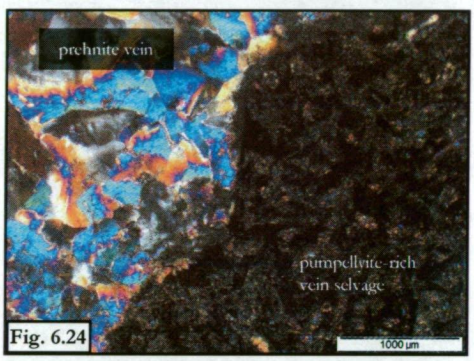

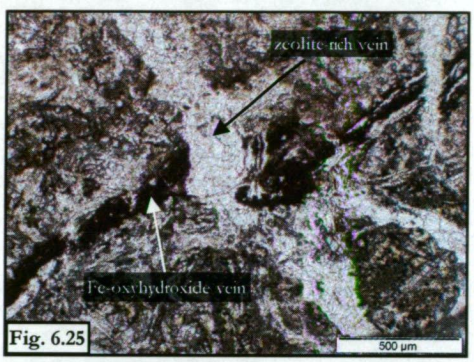

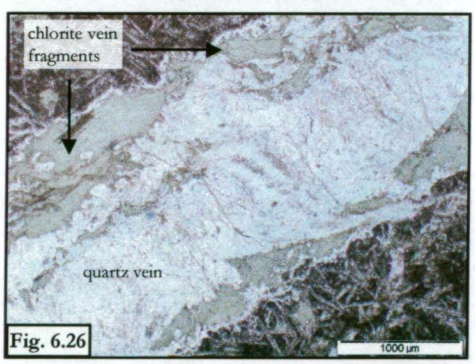

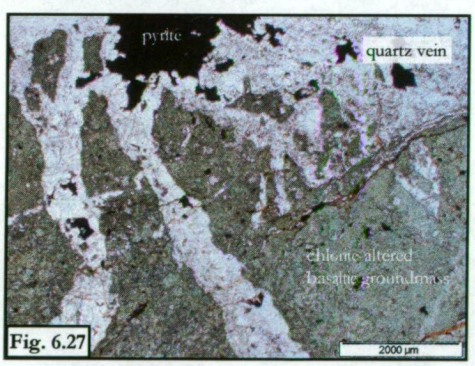

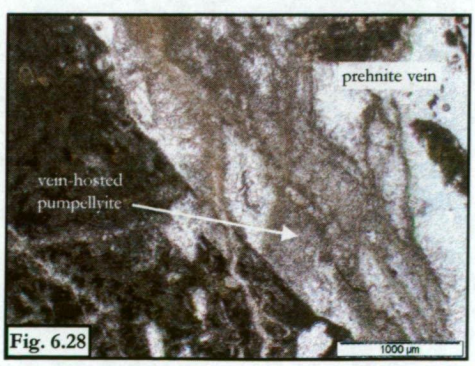

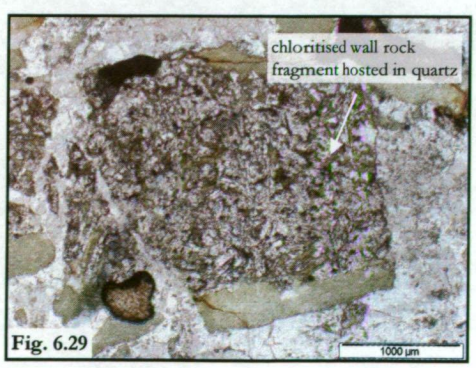

Paragenetic stages in the focussed hydrothermal facies

The results of my petrographic study showed that the focussed alteration facies represent disequilibrium mineral assemblages that formed during several hydrothermal events. Evidence of temporally distinct hydrothermal stages is provided by consistent mineral associations and textural features, particularly cross-cutting vein phases, selectively replaced phenocrysts, and concentrically filled amygdules with compositionally variable cements. Significant hydrothermal relationships were summarised from multiple petrographic observations*, and this information helped to define a characteristic paragenesis for each facies. The paragenetic nomenclature used herein is based on the dominant mineral species and main hydrothermal textures associated with discrete alteration stages. The diagnostic hydrothermal assemblages from the Major Lake (VQC facies), Caroline Cove (CQP facies), and Sellick Bay Faults (VPZ facies) each consist of a multi-component paragenesis, typically comprising four or five distinct stages. In contrast, the subordinate alteration facies (spatially restricted) in the Major Lake and Caroline Cove Fault Zones (i.e., the FMC and PFO facies) represent relatively simple paragenetic systems (one or two stages).

The vein and breccia, quartz-chlorite facies (VQC) and the narrow, focussed quartz-vein facies (NQV)

The mineral assemblages, hydrothermal textures, and paragenetic stages of the vein and breccia, quartz-chlorite (VQC) facies and the narrow, focussed quartz vein (NQV) facies are very similar. Their main differences (and hence the reasons for their demarcation) relate to field-based criteria such as distinctive outcrop attributes (e.g., the distribution, appearance, and spatial extent of their respective alteration zones), and the relationship with their respective structural hosts (Chapter 5.3). Thus, for the purposes of this petrographic discussion, it is appropriate to group the VQC and NQV facies.

Detailed petrographic observations of representative samples from the VQC and NQV facies helped to define four main stages in the alteration sequence (Figure 6.30). These are:

Stage I – Extensive alteration of primary phenocryst and groundmass phases in basalts and dolerites, characterised by widespread hydrothermal chlorite;

Stage II – Formation of quartz-dominated vein and breccia networks which are closely associated with minor epidote and pyrite;

Stage III – Minor calcite, zeolite, and prehnite alteration in veinlets and vughs; and

* None of the individual samples (thin-sections) observed during my petrographic study contained evidence for the complete spectrum of hydrothermal stages in each facies. Thus, each paragenetic sequence is derived from a composite of multiple sample observations.

VQC facies - Major Lake Fault Zone

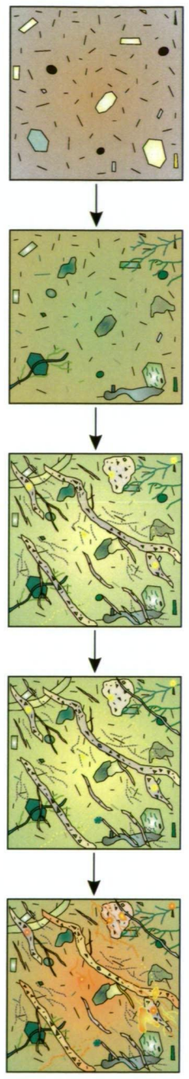

Pristine basalt - unaltered protolith

* hypocrystalline basalt with abundant plagioclase laths
* common intersertal groundmass textures
* medium- to coarse-grained plagioclase crystals
* rare olivine and augite phenocrysts
* sporadic vesicles in groundmass

Stage I - Chlorite-dominated groundmass alteration

* extensive chlorite alteration in selective and pervasive domains
* distinctive green groundmass
* irregularly shaped massive alteration domains widespread
* massive chlorite patches and veinlets in crystal pseudomorphs
* chlorite-filled vesicles and vughs
* minor albite, titanite, leucoxene, epidote, and pyrite

Stage II - Quartz-bearing veins and breccias (+ minor epidote and pyrite)

* thick quartz veins, narrow veinlets, and stockwork zones
* hydrothermal breccias with wall rock fragments in quartz
* massive quartz patches + minor massive epidote and pyrite
* rare narrow epidote veins and veinlets
* disseminated pyrite in thin veinlets and groundmass

Stage III - Minor calcite, zeolite, and prehnite alteration in veinlets and vughs

* rare zeolite veinlets cut across groundmass
* minor clay minerals partially rim amygdules
* calcite infills drusy vein cavities
* minor prehnite veinlets

Stage IV - Late-stage oxidised alteration

* variably oxidised pyrite, irregularly shaped patches
* distinctive rusty orange tint in groundmass
* heterogeneous intensity and distribution
* quartz pods and veins also stained

CQP facies - Caroline Cove Fault Zone

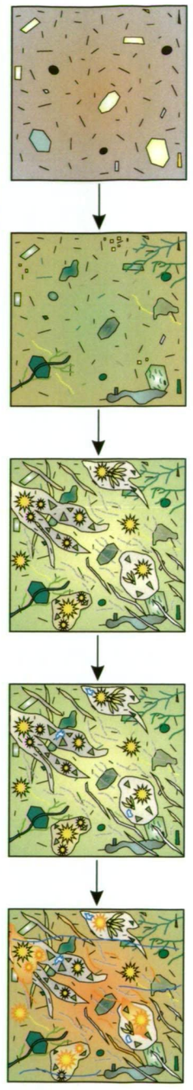

Pristine basalt - unaltered protolith

* hypocrystalline basalt with abundant plagioclase laths
* intersertal groundmass textures common
* medium- to coarse-grained plagioclase crystals
* rare olivine and augite phenocrysts
* sporadic small, subrounded vesicles

Stage I - Widespread chlorite alteration in basaltic groundmass

* widespread groundmass chlorite patches
* patchy and veinlet plagioclase alteration
* selectively replaced olivine pseudomorphs
* chlorite-filled amygdules
* minor disseminated and veinlet, fine-grained pyrite
* minor albite, titanite, leucoxene, and epidote in groundmass

Stage II - Quartz-rich veins and breccias with abundant sulfide minerals and epidote

* extensive quartz alteration in veins and massive patches
* wall rock breccia fragments and crystals in quartz cement
* abundant medium- to coarse-grained pyrite in quartz
* massive and vein epidote intergrown with quartz
* fine-grained pyrite common in groundmass
* minor chalcopyrite in quartz cement

Stage III - Minor barite replacement and infill of quartz cement

* sporadic barite in quartz veins
* barite infills vuggy quartz cavities
* minor barite also replaces some vein hosted crystals

Stage IV and V - Formation of sporadic late-stage veins

* minor late-stage calcite veins
* oxidised stringer networks and massive sulfide clusters
* pyrite partially oxidised, varying intensity and distribution
* common orange-red staining in quartz veins

VPZ facies - Sellick Bay Fault Zone

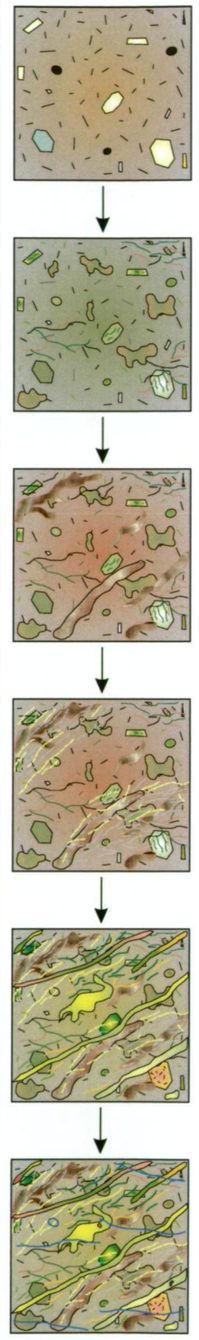

Pristine basalt - unaltered protolith

* hypocrystalline basalt
* intersertal groundmass texture
* medium to coarse plagioclase
* rare olivine and augite crystals
* sporadic vesicles

Stage I - Selectively pervasive, smectite-rich groundmass alteration

* very fine-grained smectite alteration in groundmass
* selectively pervasive, with glass and olivine strongly altered
* primary vesicles commonly infilled
* partial plagioclase alteration in patches and veinlets

Stage II - Diffuse Fe-oxyhydroxide alteration

* Fe-rich oxyhydroxide minerals abundant
* mostly forming diffuse veins in groundmass
* skeletal, web-like appearance
* primary textures moderately to strongly disrupted

Stage III - Formation of extensive zeolite vein and veinlet networks

* subparallel zones with intensely developed veins and veinlets
* inter-connected stockwork arrays
* pale, massive hydrothermal vein cement
* dominantly Ca-rich zeolites, e.g., laumontite
* extensively overprints the Fe-oxyhydroxide alteration

Stage IV - Massive and veined prehnite and pumpellyite alteration

* thick discrete prehnite veins
* massive groundmass domains
* plagioclase pseudomorphs common
* minor pumpellyite intergrown with prehnite
* intense vein selvages common in groundmass

Stage V - Minor calcite and late-stage clay minerals in veinlets and vughs

* calcite dominated alteration stage
* mainly narrow veinlets, not extensively developed
* rare infill of drusy vein cavities
* minor late-stage clay minerals

Legend

Unaltered groundmass (+ laths)	Groundmass chloritisation	Major quartz veins	Groundmass smectite overprint
Phenocrysts - plagioclase and olivine	Chlorite-altered crystals	Quartz veinlets (stringers)	Massive smectite patch
Primary vesicles (unfilled)	Chlorite-filled amygdules	Massive sulfide clusters	Discrete smectite vein
Prehnite altered groundmass	Chlorite-cemented veins	Sulfide veins and veinlets	Smectite altered crystals
Thick prehnite vein	Massive chlorite patches	Epidote veins and clusters	Smectite filled vesicles
Massive prehnite alteration patch	Disseminated pyrite	Barite in quartz	Fe-oxyhydroxide groundmass
Prehnite-pumpellyite pseudomorph	Groundmass silicification	Partially oxidised groundmass	Diffuse Fe-oxyhydroxide vein
Minor zeolite or calcite veins	Massive quartz alteration	Oxidised quartz and sulfides	Zeolite veins

Figure 6.30: Schematic diagrams showing the main alteration stages involved in the formation of diagnostic hydrothermal assemblages in the Major Lake (VQC), Caroline Cove (CQP), and the Sellick Bay (VPZ) Fault Zones. As depicted here, the contemporary mineral assemblages (final stage) represent multiple stages of hydrothermal activity which have significantly overprinted and altered the original basaltic protolith.

Stage IV – Late-stage oxidised alteration, which has partially overprinted some earlier-formed minerals such as pyrite and chlorite.

Stage I – Chlorite-dominated groundmass alteration

The igneous phenocryst and groundmass minerals in basaltic rocks from the VQC and NQV facies are moderately to intensely altered, and the multi-phase alteration assemblages are characterised by abundant early-formed chlorite. Chlorite is widespread in all VQC and NQV alteration zones, and its common occurrence primarily imparts the distinctive bluish-green to dark green groundmass (Figure 6.31). Consistent textural relationships between the altered wall rocks and discordant vein and breccia networks clearly indicate that most chlorite alteration pre-dated the formation of widespread quartz veins (Stage II). Chlorite compositions were verified during my complementary electron microprobe study, which showed that most grains are trioctahedral chlorites of the clinochlore (Mg-rich) and chamosite (Fe-rich) series (further discussed in Chapter 6.4). These analyses were undertaken on chlorite samples with variable textural forms and inter-mineral relationships, collected from multiple site locations (Table 6.1).

Early-formed chlorites are typically very fine-grained (most discrete crystals are < 10–20 μm-diameter) and mainly occur as intergrown, felted aggregates of fibrous, sheeted, or platy micro-crystals. Stage I chlorites have diverse textural styles, occurring commonly as amygdule infill material (some with multiple, concentrically zoned rims), discrete veinlets, and along narrow cracks and cleavage planes in plagioclase phenocrysts (Figure 6.32 and Figure 6.33). Chlorite is a common alteration product in hypocrystalline basalts (in the VQC and NQV zones) where it forms massive, amorphous patches after volcanic glass, and partly to completely replaces groundmass minerals such as plagioclase and augite (Figure 6.34). Primary (igneous-derived) groundmass textures are poorly preserved in zones of strong to intense chlorite alteration, i.e., intense chloritisation is texturally destructive. However, alteration intensity is significantly heterogeneous in the VQC and NQV facies and partial igneous relicts also commonly occur, e.g., tabular phenocryst shapes may be preserved (Figure 6.35). In some basalts, small (< 20 μm-diameter), chlorite-altered grains are partly replaced by acicular intergrowths of brownish-green actinolite, although these relationships are not widespread.

Albite, pyrite, epidote, titanite, and leucoxene are key alteration phases associated with the chlorite-dominated stage, although they are relatively less abundant and have fewer textural modes than chlorite. Most relict plagioclase (e.g., pale, irregularly shaped patches in groundmass laths and phenocrysts) is strongly albite-altered from its original magmatic composition (Ca-rich), especially discrete crystal cores and intra-grain cracks or cleavage planes (Figure 6.13)*. Very fine- to fine-grained pyrite crystals are also sporadically disseminated throughout the altered VQC and NQV facies basalts. These groundmass hosted pyrites mainly form discrete anhedral

* Plagioclase compositions for altered rocks from the VQC and NQV facies are further discussed in Chapter 6.4, based on the results of my electron microprobe study.

grains or small crystal clusters (most < 1 mm-wide), and most are associated with massive chlorite patches or albitised plagioclase laths. Rare wispy, stringer-like veinlets (< 0.5 mm-wide) also discontinuously transect some altered groundmass domains.

Primary Ti-magnetite crystals in the groundmass of most VQC and NQV facies basalts are partly to completely mantled (overgrown and replaced) by ragged aggregates of microlitic and very fine-grained alteration minerals. The abundance and distribution of these high-relief crystal clusters, which mainly consist of complexly intergrown titanite, leucoxene, and epidote, is directly proportional to the intensity of chlorite alteration. For example, strongly to intensely chloritised groundmass domains commonly have a distinctive 'spotted' appearance (highly turbid) due to the widespread abundance of these small (commonly < 50 μm-diameter) crystal aggregates (Figure 6.31 and 6.35).

Stage II – Quartz-bearing veins and breccias (+ minor epidote and pyrite alteration)

Quartz veins, breccias, and massive patches of pervasive groundmass alteration are key diagnostic components of the VQC and NQV facies, occurring extensively at each site in the Major Lake district (Site 2A to 2D). Epidote and pyrite are relatively minor phases which are closely associated (spatially and texturally) with quartz alteration, comprising ~ 10–15 % of this paragenetic stage (estimated from visual observations). Limited textural evidence indicates that the formation of epidote (and possibly pyrite) initially pre-dated quartz (Figure 6.36), although consistent inter-mineral relationships suggest mostly concurrent (and on-going) precipitation of these phases throughout Stage II, e.g., crystals of epidote and pyrite are commonly intergrown with quartz and hosted in discrete veins and breccias (Figure 6.37 and 6.38).

Complex quartz stockworks are well developed at each VQC facies site along the Major Lake Fault (Site 2A to 2D). Subparallel veins of massive quartz and associated 'stringer' networks (e.g., dendritic off-shoots and irregular, web-like veinlet arrays) cut irregularly across the chloritised basaltic groundmass in these zones (Figure 6.39 and Figure 6.40). Most veins > 10–20 mm-wide are oriented subparallel to the strike of their main structural host (the Major Lake Fault for each VQC site, and various small-scale local structures for the NQV facies), whereas narrow veins and veinlets trend more randomly. In thin-section, veins are typically sharp and well defined, and most lack proximal alteration selvages or wall rock haloes (Figure 6.36 and Figure 6.40).

Figure 6.31: Very fine-grained chlorite is a diagnostic component of the VQC and NQV facies and is largely responsible for the distinctive green groundmass that commonly occurs in altered fault zone rocks (basalts and dolerites). This photomicrograph shows many characteristic features associated with intense chlorite alteration (Stage I) in the VQC facies. Massive and irregularly shaped patches of intergrown chlorite have variably overprinted the volcanic-derived mesostasis and many igneous crystals (e.g., plagioclase), and also infilled most rock cavities (vughs) (sample MCQ-108 in PPL, Sandell Bay creek, Site 2A).

Figure 6.32: Hydrothermally derived chlorite is widespread in the VQC facies and exists in diverse textural forms. Turbid patches and intra-grain veinlets are abundant in many partially altered grains of plagioclase, and most olivine phenocrysts (rare) are completely replaced, i.e., pseudomorphed. The basaltic groundmass shown here is also strongly chloritised (semi-pervasive greenish tinge), and several subrounded vughs are infilled with massive chlorite. Minor patches and veinlets of quartz alteration also commonly occur in this rock (sample MCQ-208 in PPL, Lusitania Bay escarpment, Site 2D).

Figure 6.33: This coarse-grained plagioclase crystal shows some of the common alteration effects associated with partial chloritisation. Narrow, discontinuous veinlets form mainly along internal zones of weakness in the crystal structure, such as cleavage and fracture planes. The phenocryst is also clouded by aggregates of microlitic chlorite (very fine disseminated alteration) which occur widely throughout the grain. In addition to extensive chlorite alteration, colourless patches of relict plagioclase (originally Ca-rich) are now mostly altered to albite (Na-rich) (sample MCQ-373 in PPL, Lusitania Bay escarpment, Site 2D).

Figure 6.34: Augite is a rare phenocryst phase in some volcanic rocks on Macquarie Island. Most augite crystals affected by VQC facies alteration are extensively replaced by massive chlorite (pseudomorphs) although, as shown here, pristine remnants of the primary crystal may coexist, i.e., distinctive disequilibrium assemblages. Clinopyroxene is generally the primary igneous mineral which is most resistant to the effects of intense hydrothermal alteration in the VQC facies (sample MCQ-155 in PPL, Sandell Bay creek, Site 2A).

Figure 6.35: Strong to intense hydrothermal alteration in the VQC facies significantly modifies the primary composition and texture of most basaltic wall rocks hosted in the Major Lake Fault Zone. Abundant groundmass chlorite has intensely overprinted the primary igneous fabric in this example, although partially corroded phenocryst relicts (especially tabular plagioclase crystals) are commonly preserved in many fault zone basalts (sample MCQ-375 in PPL, Lusitania Bay escarpment, Site 2D).

Figure 6.36: Veins of massive epidote (Stage II) are a minor but distinctive component of the hydrothermal mineral assemblage in the VQC and NQV facies. This slightly pleochroic, yellowish-green epidote vein is sharply cut by the more extensive quartz stockwork at the Major Lake south field locality (Site 2H). Textural relationships such as this show that some epidote (mainly in discrete veins) pre-dated the formation of widespread quartz in Stage II of the VQC facies. Typical of most Stage II assemblages, the epidote and quartz veins both have well defined boundaries and lack marginal alteration haloes in adjacent wall rocks (sample MCQ-404 in PPL).

Figure 6.37: Irregularly shaped groundmass patches of fine- to medium-grained epidote occur sporadically in strongly altered rocks from the VQC facies. The massively intergrown aggregate of birefringent epidote shown here is typical of many altered groundmass domains associated with Stage II of the VQC facies paragenesis. In contrast to the mineral relationships shown in Figure 6.36, this epidote cluster is intimately associated (intergrown) with massive quartz, providing clear evidence for the co-precipitation of quartz and epidote in Stage II of the VQC facies (sample MCQ-210 in XPL, Lusitania Bay escarpment, Site 2D).

Figure 6.38: A cluster of fine- to medium-grained pyrite crystals are hosted in this narrow quartz vein from the focussed zone of VQC facies alteration at Sandell Bay creek (Site 2A). These subhedral to euhedral sulfide grains have well developed cubic crystal habits and are compositionally uniform, although irregular surface pitting and fracturing is widespread. Similar to epidote, pyrite is commonly intergrown with quartz cement in many veins and massive alteration pods in the VQC and NQV facies (sample MCQ-153 in reflected light).

Photomicrographs of common alteration minerals and textures associated with Stage I and II of the vein and breccia, quartz-chlorite (VQC) facies and the narrow, focussed quartz vein (NQV) facies.

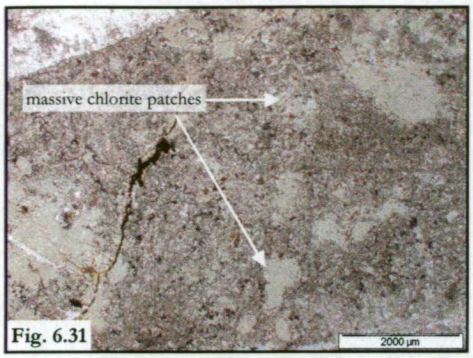

Fig. 6.31

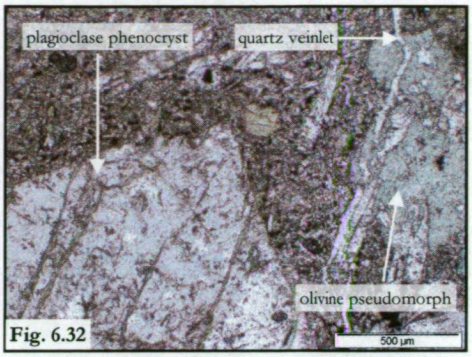

Fig. 6.32

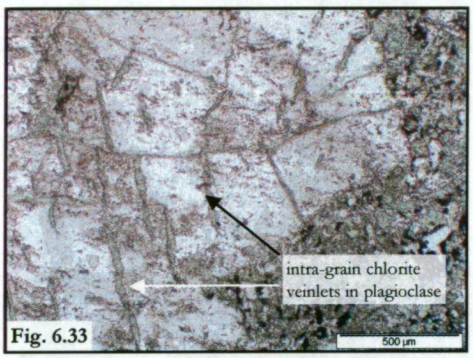

Fig. 6.33

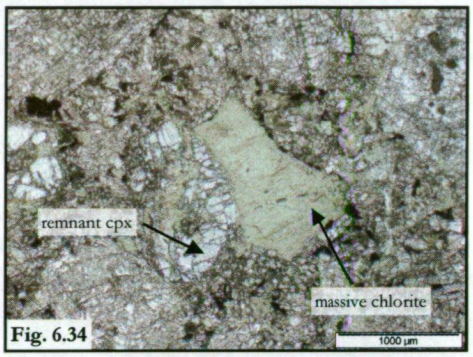

Fig. 6.34

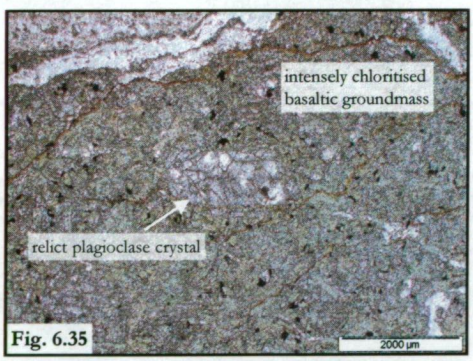

Fig. 6.35

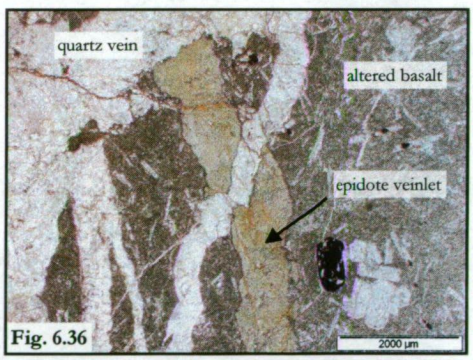

Fig. 6.36

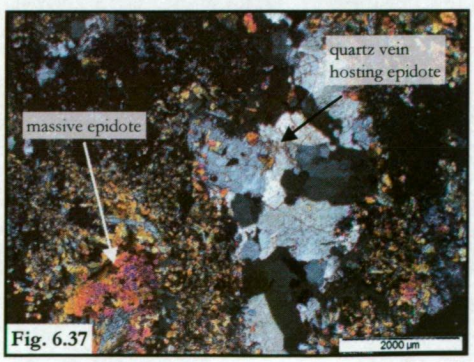

Fig. 6.37

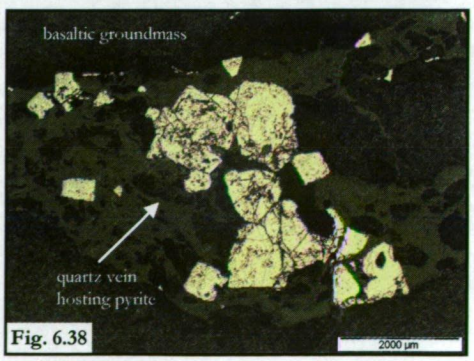

Fig. 6.38

Irregularly intergrown crystals of fine- to medium-grained anhedral quartz comprise most vein segments, and these commonly have consertal textures. Some veins consist of elongated quartz crystals (anhedral and subhedral grains) which are suborthogonal to the main vein strike direction, i.e., forming distinctive comb-textures (Figure 6.41). The central segments of thicker veins (generally > 5 mm) may also contain small vuggy cavities lined with prismatic quartz crystals.

Most vein hosted quartz crystals are highly turbid due to the presence of abundant inclusions. Quartz hosted inclusions comprise a diverse range of hydrothermally derived grains, small fragments and particles of altered basalt (wall rocks), and various trails, clusters, and arrays of minute fluid inclusions. Fluid inclusions trapped in some quartz crystals form distinctive growth zones that partly mimic prismatic grain shapes, and multiple inclusion-rich layers also occur (fluid inclusions are further discussed at the end of Chapter 6.3). Microlitic chlorite is the most abundant type of crystal inclusion hosted in quartz cement. These grains are texturally distinct from groundmass chlorites in the surrounding wall rocks (Stage I), and typically form vermicular or spiral-like aggregates sporadically distributed throughout their host vein segments (Figure 6.42). The elongate crystalline spirals consist of multiple fibrous intergrowths, and most discrete chlorite crystals are 20–50 μm-long (Figure 6.43). These microlitic grains are texturally similar to chlorites hosted in quartz veins and hydrothermal breccias recovered from the mid-Atlantic ridge and the East Pacific Rise (Delaney et al., 1987; Saccocia and Gillis, 1995). Their characteristic textures and mineral associations imply that they are cogenetic with Stage II quartz, i.e., formation of the quartz hosted chlorites post-dated Stage I chloritisation (Chapter 6.4).

In addition to crystal inclusions, many quartz veins and massive alteration zones contain subangular to angular fragments derived from the surrounding basaltic wall rocks (Figure 6.44 and 6.45). Brecciated lithic fragments, which commonly contain Stage I alteration assemblages (i.e., chlorite-dominated), are widely and randomly distributed throughout their host cements, and may form distinctive jigsaw-fit breccias. The margins of many vein hosted fragments are extensively disaggregated, and fragmented debris partly mantles the coherent remnants.

Massive 'speckled' quartz alteration also occurs in the groundmass of some VQC and NQV facies basalts, although it is much less common than major quartz veins and fine stockwork arrays (only ~ 5–10 % of Stage II). Sporadic domains of 'speckled' quartz form small (most < 5 mm-wide) and irregularly shaped zones in the basaltic groundmass, or distinctive vein-like channels 10–50 mm-wide (Figure 6.46). These diffusely flooded patches comprise granular (crystalline) quartz mosaics and have a distinctive 'speckled' or saccharine texture. The primary igneous fabric is commonly obliterated in these intensely quartz altered domains, although remnant fragments of chloritised wall rock may locally occur.

Figure 6.39: Extensive quartz vein arrays and inter-connected stockwork zones are diagnostic components of the VQC and NQV facies. The colourless quartz veins shown here overprint earlier-formed chlorite veinlets and the strongly chloritised basaltic groundmass (formed during Stage I of the paragenesis). Irregularly shaped fragments of massive vein chlorite are sporadically hosted in the quartz cement, and many narrow chlorite tendrils are also variably affected by late-stage quartz alteration, e.g., partly incorporated or disaggregated (sample MCQ-153 in PPL, Sandell Bay creek, Site 2A).

Figure 6.40: Overprinting relationships between temporally distinct quartz vein stages are not commonly observed in rock samples from the VQC and NQV facies. Indeed, most quartz vein stockworks and discrete veins are interpreted to have formed during a single (main) hydrothermal event (Stage II). However, minor quartz vein relationships, such as the obliquely cross-cutting vein arrays shown here, suggest limited temporal (progressive) evolution of the Stage II hydrothermal system occurred at some sites along the Major Lake Fault (sample MCQ-311 in PPL, Major Lake foreshore, Site 2B).

Figure 6.41: The patchwork mosaic of intergrown quartz crystals shown here is typical of discrete Stage II veins in the VQC and NQV facies. Very fine- to medium-grained quartz is abundant, and many crystals have elongate or prismatic shapes which are oriented suborthogonal to the main vein strike. The slight turbid appearance marking some pale quartz grains is caused by minute crystals, degraded fluid inclusions, or disaggregated wall rock fragments in the hydrothermal cement (sample MCQ-261 in XPL, Tio south, Site 2F).

Figure 6.42: Crystalline aggregates of microlitic chlorite are intergrown with many quartz veins in Stage II of the VQC facies. These small and irregular clusters have a distinctive textural form that differs significantly from massive chlorite alteration in the basaltic groundmass (Stage I). For example, contrast the vein hosted chlorites shown here with the intra-grain veinlets and sporadic alteration patches in the adjacent plagioclase crystal (sample MCQ-208 in PPL, Lusitania Bay escarpment, Site 2D).

Figure 6.43: Detailed microscopic view of an intergrown chlorite aggregate hosted in Stage II quartz from the VQC facies at Lusitania Bay (Site 2D). These fibrous crystals of microlitic or very fine-grained chlorite clearly show the spiral and 'worm-like' (vermicular) textural forms that characterise this quartz-chlorite assemblage. These distinctive hydrothermal chlorites are interpreted to have formed during the main stage of quartz veining (Stage II) in the VQC and NQV facies (sample MCQ-373 in PPL).

Figure 6.44: Hydrothermally derived breccias are a characteristic component of the VQC and NQV facies, and are especially common in thick quartz vein segments and massive alteration domains (Stage II). Most quartz-hosted breccia fragments are subhedral to euhedral pyrite grains of various size (fine- to coarse-grained), and disaggregated particles or massive chlorite-altered fragments derived from adjacent basaltic wall rocks (sample MCQ-208 in PPL, Lusitania Bay escarpment, Site 2D).

Figure 6.45: A variety of angular to very angular rock and vein fragments are hosted in the crystalline cement of this VQC facies quartz vein. The vein hosted material mainly comprises disaggregated fragments of irregularly shaped massive chlorite (pre-existing alteration phase) and strongly altered wall rocks. Typical of most vein relationships in the VQC facies, evolution of the quartz-dominated stage clearly post-dated widespread groundmass alteration (sample MCQ-072 in PPL, Major Lake foreshore, Site 2B).

Figure 6.46: Diffuse groundmass zones of 'speckled' quartz represent a relatively early phase of quartz alteration in the VQC facies, i.e., they pre-dated formation of most discrete quartz veins and stockwork arrays. The quartz-rich groundmass domains shown here are strongly recrystallised and texturally distinct from chlorite altered wall rocks, although many also contain disaggregated fragments of altered basalt. 'Speckled' quartz zones are not as common or well defined as most quartz veins in the VQC and NQV facies, and most also lack associated sulfide minerals and epidote (sample MCQ-155 in PPL, Sandell Bay creek, Site 2A).

Photomicrographs of common alteration minerals and hydrothermal textures associated with the quartz-dominated stage (Stage II) of the vein and breccia, quartz-chlorite (VQC) facies and the narrow, focussed quartz vein (NQV) facies.

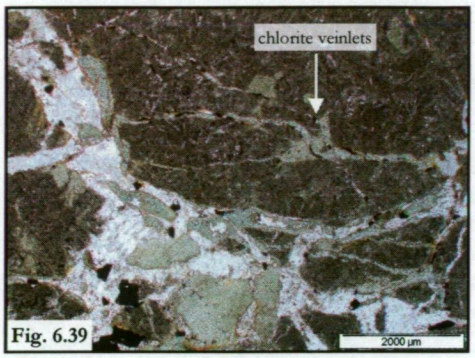

Fig. 6.39

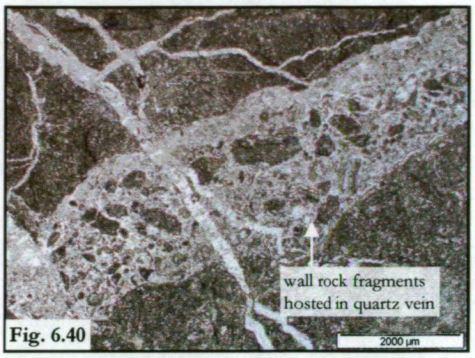

Fig. 6.40

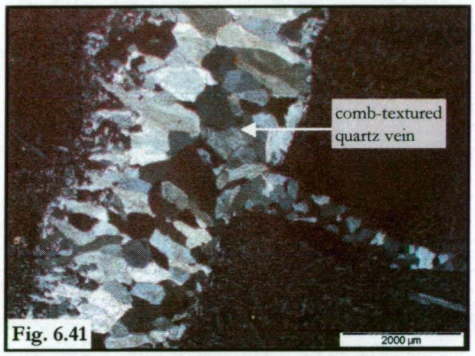

Fig. 6.41

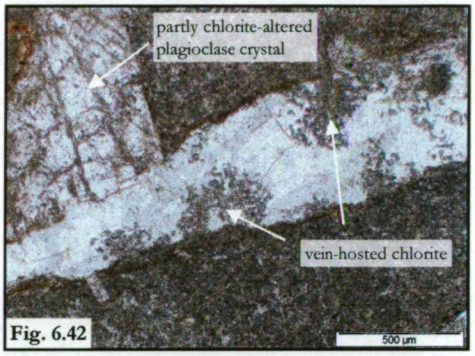

Fig. 6.42

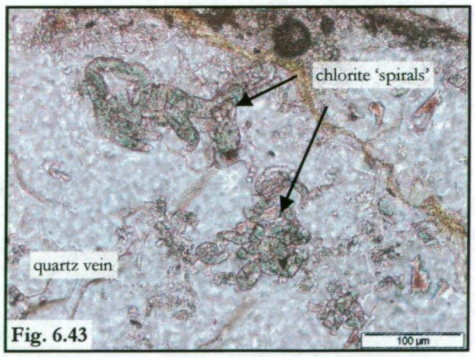

Fig. 6.43

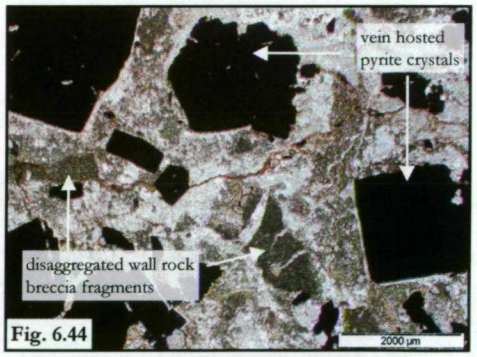

Fig. 6.44

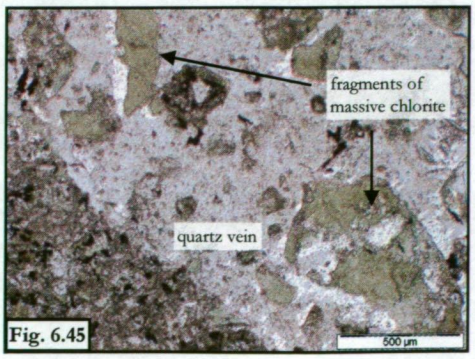

Fig. 6.45

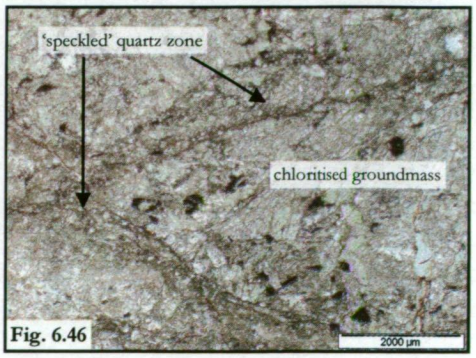

Fig. 6.46

Minor alteration minerals associated with hydrothermal quartz in Stage II veins and breccias are epidote and pyrite. Yellowish-green epidote veins and massive alteration patches consist of fine- to medium-grained crystals with distinctive granular or bladed habit. Zones of massive and veined epidote lack proximal alteration haloes or wall rock selvages (similar to quartz), although fine-grained crystal clusters may be locally abundant in semi-pervasive alteration domains (Figure 6.37). Microlitic and very fine-grained epidote crystals also form irregular crystal aggregates which have partly replaced some plagioclase phenocrysts.

Pyrite is the most abundant sulfide mineral in Stage II of the VQC and NQV facies, although it rarely comprises > 5 % of these quartz-rich assemblages. Traces of chalcopyrite (< 1 %) also occur at the Lusitania Bay escarpment (Site 2D), mainly as massive overgrowths that partly to completely surround earlier-formed pyrite crystals. Fine- to medium-grained pyrite (~ 5–30 mm in diameter) is commonly intergrown with quartz veins and breccias, forming isolated crystals or small intergrown aggregates (Figure 6.38 and Figure 6.44). Most vein hosted pyrites are subhedral grains with partial cubic shapes, and their close relationship with widespread quartz alteration (on a spatial, textural, and inferred genetic basis) clearly differentiates these sulfide grains from rare pyrite crystals that sporadically occur in chloritised groundmass (Stage I).

Stage III – Minor calcite, zeolite, and prehnite alteration in veinlets and vughs

Late-stage veinlets and vughs cemented with relatively low temperature hydrothermal minerals such as calcite, prehnite, and zeolite occur sporadically in the VQC and NQV facies. In particular, minor zeolite veinlets (most filled with analcite) cut randomly across earlier-formed zones of chlorite and quartz alteration (Figure 6.47). Rare drusy vughs in some quartz veins (most < 1–2 mm-wide) may also be filled with platy calcite or massive prehnite (fine-grained). In addition, some VQC facies amygdules have thin rims of smectite (~ 1–5 μm-thick) that partly to completely enclose chlorite- and quartz-rich cores. Isolated vughs filled with early-formed chlorite (Stage I) may also be partly replaced with intergrown aggregates of fibrous or bladed zeolites (particularly analcite and laumontite), or clusters of very fine-grained anhedral calcite.

Stage IV – Late-stage, oxidised alteration

Many Fe-bearing alteration minerals in the VQC and NQV facies (and rare partial igneous relicts such as augite) are affected by weak to moderate oxidation. Minor oxidation represents the final paragenetic stage, and the effects are commonly manifested as widespread orange-brown staining throughout the earlier-formed groundmass and vein-stage assemblages. These late-stage alteration features are clearly evident both macroscopically (i.e., *in situ* outcrop and hand-sample specimens) and in thin-section (Figure 6.48). Oxidised minerals are opaque or partly translucent, and include reddish-brown to orange-red Fe-hydroxides, Fe-oxyhydroxides, and Fe-rich (oxidised) clay minerals. Pyrite is the most intensely oxidised mineral, and many proximal groundmass domains or quartz veins (adjacent to oxidised pyrites) are also affected by the

oxidised alteration assemblages. Oxidised pyrite crystals are variably overprinted by irregular, web-like veinlets. Commonly, these are most intensely developed around grain margins, and relict sulfide-rich cores may be preserved in some oxidised pyrites. However, because the late oxidation stage is heterogeneously developed in the VQC and NQV facies, many pyrite crystals are completely oxidised (no relict sulfide material), especially the very fine-grained groundmass crystals (Stage I). The oxidised alteration assemblages are widely developed at each VQC facies site on the Major Lake Fault, although distinct variations in alteration intensity (distribution patterns) are spatially unrelated to the Major Lake Fault Zone.

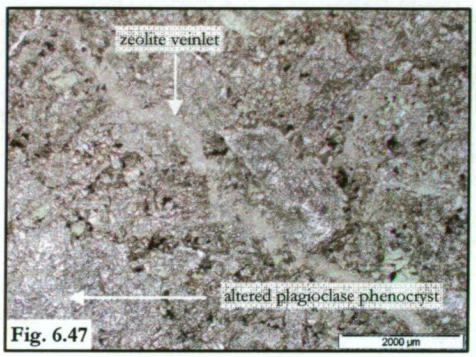

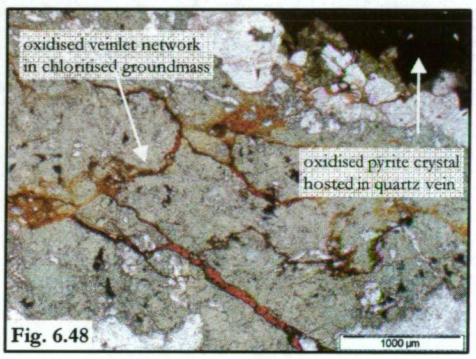

Figure 6.47: The formation of relatively low temperature alteration minerals such as zeolite and prehnite post-dated the main chlorite and quartz stages in the VQC facies. In this view, a narrow turbid veinlet filled with intergrown zeolite minerals (mainly isotropic analcite) cuts across the strongly chloritised groundmass of a typical hypocrystalline pillow basalt (sample MCQ-155 in PPL, Sandell Bay creek, Site 2A).

Figure 6.48: Strongly oxidised veinlet arrays, which mainly consist of reddish-brown and orange-brown Fe-rich hydroxide and oxyhydroxide minerals, represent the final paragenetic stage of the VQC and NQV facies (Stage IV). These irregular, trellis-like networks commonly transect the altered basaltic groundmass and zones or veins of massive quartz alteration. Many veinlet strands initially nucleated from vein hosted pyrite crystals, and most of these grains are strongly oxidised and partly to completely replaced by the oxidised phases (sample MCQ-375 in PPL, Lusitania Bay escarpment, Site 2D).

The massive and veined, chlorite-quartz-pyrite facies (CQP)

The five-stage paragenesis of the massive and veined, chlorite-quartz-pyrite (CQP) facies shares much with the VQC and NQV facies, e.g., strong to intense chlorite alteration and widespread quartz veins and breccias. However, in addition to significant field-based differences (Chapter 5.4), there are also petrographic motivations for separate classifications. In particular, the CQP facies is more sulfide-rich, and some quartz veins contain minor barite. To avoid repetition, this section focusses (in detail) only on the petrographic features of these key facies variations.

The multi-component CQP facies paragenesis (Figure 6.30) comprises:

Stage I – Extensive alteration (commonly pervasive) of primary phenocryst and groundmass minerals in basaltic rocks, characterised by widespread hydrothermal chlorite;

Stage II – Formation of quartz-dominated vein and breccia networks which host abundant sulfide minerals (mainly pyrite and chalcopyrite) and epidote;

Stage III – Minor barite alteration, which partly replaces or infills small cavities in quartz-cemented veins and breccias;

Stage IV – Late-stage calcite, zeolite, and prehnite alteration in veinlets and vughs; and

Stage V – Oxidised alteration, which has partially overprinted some earlier-formed minerals such as pyrite and chlorite.

Stage I – Widespread chlorite alteration in basaltic groundmass

The petrographic features associated with selectively pervasive groundmass alteration in the CQP facies are similar to those previously described for the Major Lake district (refer to the previous descriptions of the VQC and NQV facies for details). Common alteration minerals and hydrothermal textures associated with Stage I of the CQP facies are illustrated in Figure 6.49–6.52.

Stage II – Quartz-rich veins and breccias with abundant sulfide minerals and epidote

Fine- to coarse-grained sulfide minerals are widespread in the CQP facies and represent a diagnostic component of most altered basalts at Caroline Cove. Pyrite and chalcopyrite are the main sulfide phases, commonly comprising 10–20 % of the hydrothermal assemblage (locally up to ~ 30–40 % in some sulfide-rich enclaves). Similar to the VQC facies most sulfides are intimately associated with massive and veined quartz, although pyrite and chalcopyrite are significantly more enriched in the Caroline Cove district (relative to the Major Lake Fault). The petrographic features of Stage II quartz alteration are very similar to those previously described for the VQC and NQV facies. For example, veins cut sharply across the altered wall rocks and predominantly consist of intergrown fine- to medium-grained quartz crystal mosaics (Figure 6.53–6.56).*

Two distinct types of pyrite are associated with the CQP facies; very fine- to fine-grained pyrite occurs widely throughout the chloritised groundmass, whereas medium- to coarse-grained pyrite is mainly hosted in quartz (Figure 6.57). Fine, disseminated pyrite alteration consists of 0.2–0.5 mm-diameter grains with anhedral or partial cubic shapes. These may be discrete and isolated crystals or (more commonly) occur in small crystal aggregates or irregularly shaped domains in the altered groundmass. Some groundmass pyrite also forms narrow and discontinuous veinlets (< 1–2 mm-wide) which overprint the primary igneous rock fabric. In places, these ribbon-like veinlets are cross-cut by thin veins of massive chlorite and quartz, suggesting that some groundmass pyrite may have initially formed during early Stage I alteration, i.e., pre-dated formation of the coarser-grained quartz-hosted sulfides (Figure 6.58).

* As for the previous chlorite-rich alteration stage (Stage I), please refer back to petrographic descriptions presented in the VQC and NQV facies section for the main hydrothermal textures associated with quartz veins and breccias in the CQP facies.

Figure 6.49: Early-stage chlorite alteration is widespread throughout the groundmass of this hypocrystalline basalt from the CQP facies at Caroline Cove (Site 3A). Chlorite has pervasively altered the glassy mesostasis and variably replaced most fine-grained plagioclase laths and anhedral augite crystals in the intersertal groundmass. Sheeted chlorite also occurs in discontinuous veinlets, which have overprinted well preserved volcanic textures in the basaltic groundmass, and a subrounded vesicle (sample MCQ-054 in PPL, Caroline Cove, Site 3A).

Figure 6.50: Basaltic rocks in the CQP facies have pale or dark bluish-green to green groundmass caused by widespread chlorite alteration. In this photomicrograph intense chloritisation has affected most igneous crystals and volcanic glass, and chlorite also infills most of the small vuggy cavity in the centre of view. Relict plagioclase laths are strongly albite-altered and some are partly replaced by irregular patches of quartz (clear patches in the groundmass). Most of the disseminated opaque grains shown here are very fine crystals of Ti-magnetite; these are also strongly altered and replaced by ragged clusters of microlitic titanite, leucoxene, and epidote (sample MCQ-027 in PPL, Caroline Cove, Site 3A).

Figure 6.51: Massive fibrous chlorite forms narrow (~ 1–2 mm-wide) and wispy veinlets that cut across many basaltic rocks at Caroline Cove. The subparallel array of spidery green tendrils shown here are typical of many chlorite veinlets in the CQP facies. In particular, note their characteristic along-strike thickness variations and multiple dendritic off-shoots (sample MCQ-032 in PPL).

Figure 6.52: Clinopyroxene (mainly augite) is a rare phenocryst mineral in the basaltic rocks affected by CQP facies alteration at Caroline Cove. Where present, moderate to strong chlorite alteration has typically replaced most augite crystals, although irregularly shaped relict patches are partly preserved among the massive chlorite aggregates. Acicular clusters of very fine-grained actinolite (yellowish-green) also occur (sporadically) around the altered margins of some chlorite altered augite grains (sample MCQ-032 in PPL, Caroline Cove, Site 3A).

Figure 6.53: A well developed quartz stockwork cuts sharply across the texturally well preserved groundmass of this CQP facies basalt from Caroline Cove (Site 3A). The colourless vein cement consists mainly of fine- or medium-grained quartz crystals, and also contains minor pyrite (opaque grains) and fragments of altered wall rock or earlier-formed veins, e.g., massive chlorite. Most thick vein segments are oriented subparallel, but narrow dendritic off-shoots and inter-connected veinlets are commonly oblique to the main vein trend (sample MCQ-027 in PPL).

Figure 6.54: Stage II quartz veins in the CQP facies have commonly overprinted and re-opened pre-existing chlorite veinlets, suggesting that multiple stages of hydrothermal activity were focussed along similar fluid conduits. Ragged vein fragments of massive chlorite (Stage I) are abundant in the pale quartz cement shown here, and have a wide variety of sizes and irregular shapes (sample MCQ-058 in PPL, Caroline Cove, Site 3A).

Figure 6.55: Irregular groundmass domains of 'speckled' quartz alteration (Stage II) occur sporadically in strongly chloritised basalts from the CQP facies (similar to the VQC facies). These patchy groundmass zones consist of crystalline aggregates of very fine- to fine-grained anhedral quartz and have a distinctive saccharine texture. 'Speckled' quartz zones have commonly overprinted and destroyed primary groundmass minerals and textures (igneous rock fabric), and may have also partly incorporated earlier-formed alteration phases such as Stage I chlorite (sample MCQ-030 in PPL, Caroline Cove, Site 3A).

Figure 6.56: Many subhedral quartz grains in this Stage II vein segment are partially clouded by abundant fluid inclusions. Several discrete crystals have well defined fluid inclusion growth zones which mimic the prismatic grain habit and provide good evidence of their primary hydrothermal origin. However, relatively few quartz hosted fluid inclusions remain intact; most are extensively disrupted (i.e., necked or leaked), which probably reflects persistent tectonic activity in the Caroline Cove Fault following the main hydrothermal stages (sample MCQ-047 in PPL, Caroline Cove).

Photomicrographs of common alteration minerals and textures associated with Stage I and II of the massive and veined, chlorite-quartz-pyrite (CQP) facies in the Caroline Cove district.

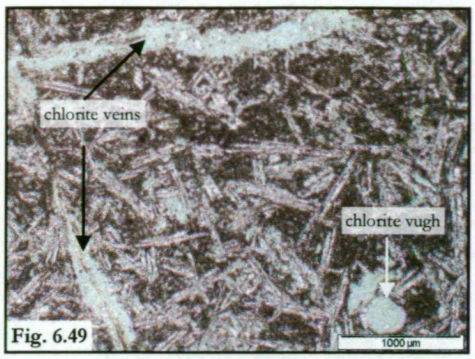

Fig. 6.49

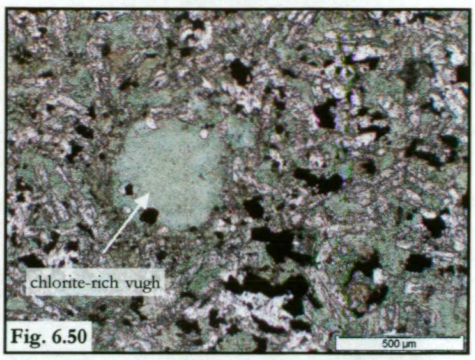

Fig. 6.50

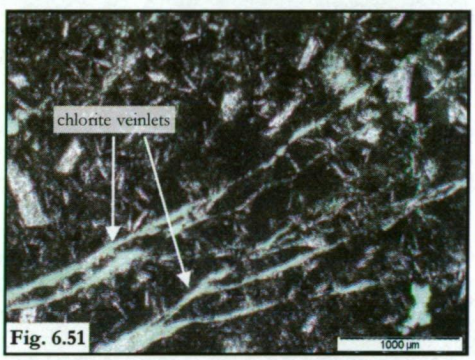

Fig. 6.51

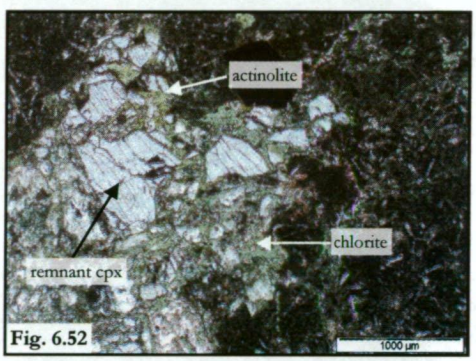

Fig. 6.52

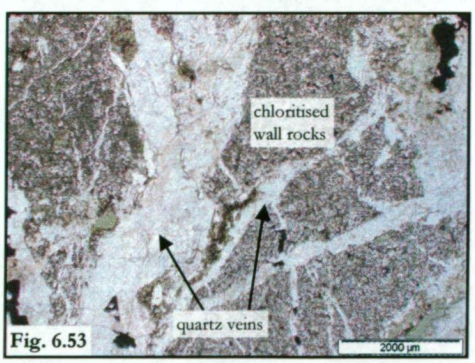

Fig. 6.53

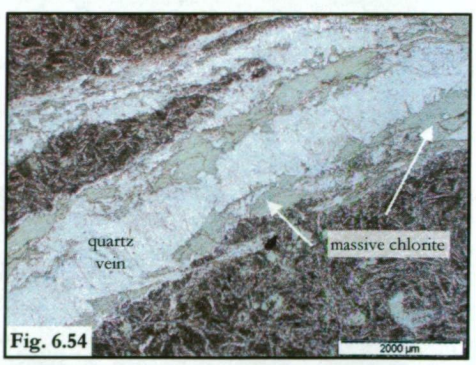

Fig. 6.54

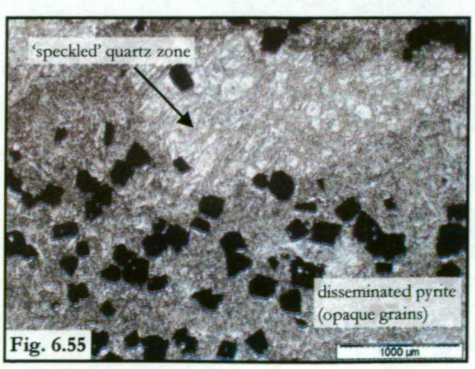

Fig. 6.55

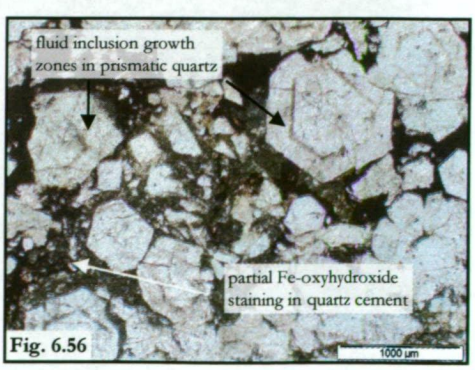

Fig. 6.56

Subhedral to euhedral, cubic pyrite crystals are widespread in quartz-rich alteration zones (Figure 6.59 and 6.60). Discrete pyrite grains are mainly 0.5–2 mm-in diameter, although significantly coarser pyrite (5–10 mm) sporadically occurs in the CQP facies and may form spectacular sulfide-rich aggregates up to 20 cm-across. Stage II pyrites are massive and compositionally homogeneous; crystal inclusions or textural variations are uncommon, e.g., there are no obvious petrographic differences between grain cores and rims. However, many vein-hosted pyrite crystals are moderately to strongly brecciated, and transected by extensive networks of brittle fractures (hairlines). Widespread fracturing has also partly disaggregated and structurally disrupted many pyrite grains, especially along discrete crystal margins (Figure 6.60).

Chalcopyrite is less abundant than pyrite in the CQP facies, although it locally dominates some quartz stockworks and massively altered groundmass enclaves. Chalcopyrite mainly forms intergrown clusters ~ 10–50 mm-wide which consist of anhedral aggregates of fine- or medium-grained crystals. Irregular overgrowths of chalcopyrite consistently mantle earlier-formed pyrite crystals, and may also host small and isolated fragments of brecciated pyrite (Figure 6.61). Some chalcopyrite grains contain blebs of massive and homogeneous sphalerite < 0.2 mm-wide (inclusions?), although these are not very abundant. In addition, minor covellite forms narrow and discontinuous rims that may partially line the margins of discrete chalcopyrite grains; these probably developed during late-stage oxidation or weathering.

Fine- to medium-grained, yellowish-green epidote (slightly pleochroic) is commonly associated with quartz-hosted sulfides. Subradiating aggregates of elongated epidote crystals occur in many vein segments or massive alteration pods, and these may be intergrown with discrete crystals or small aggregates of pyrite (Figure 6.62). However, pyrite is generally less abundant in quartz veins which also contain widespread epidote (relative to other CQP facies veins in which epidote is rare). Crystalline epidote laths mostly occur in central quartz vein segments (vein cores), and are commonly isolated from the adjacent wall rock, i.e., epidote clusters rarely occur in direct physical contact with the surrounding basaltic groundmass. However, aggregates of anhedral epidote may form small and irregular-shaped patches (sporadically) in the altered groundmass. These mainly consist of granular crystal mosaics with very fine- to fine-grained anhedral epidote; most are not intimately associated with sulfide minerals.

Stage III – Minor barite replacement and infill of quartz cement

Barite is a relatively minor alteration mineral in the CQP facies (< 2–3 % of the total assemblage), although it does represent a key paragenetic component and one of the major mineralogical differences with the VQC and NQV facies*.

* Barite was not observed in any thin-section samples during my petrographic study of the VQC and NQV facies from the Major Lake district.

Figure 6.57: Sulfide minerals such as pyrite and chalcopyrite are an important component of the CQP facies assemblage (Stage II). This view shows the two main textural styles of pyrite, which may have formed during separate hydrothermal stages. Very fine-grained pyrite is sporadically disseminated in the altered basaltic groundmass. In contrast, abundant fine- to coarse-grained pyrite is commonly hosted in massive quartz veins and breccias. These consistent mineral associations suggest that formation of groundmass pyrite largely pre-dated the vein hosted sulfides (sample MCQ-031 in reflected light, Caroline Cove, Site 3A).

Figure 6.58: A narrow veinlet of disseminated pyrite grains is transected and partly off-set by discontinuous veinlets of massive chlorite and irregular quartz. Although not commonly observed, these inter-vein relationships suggest that the formation of some groundmass hosted pyrite may have pre-dated widespread chlorite alteration (Stage I assemblage). Note that, despite the semi-pervasive groundmass alteration and abundance of disruptive veinlets, the primary intersertal texture (volcanic-derived) is well preserved in this basalt, typical of most CQP facies alteration (sample MCQ-054 in PPL, Caroline Cove, Site 3A).

Figure 6.59: Thick veins and massive patches of hydrothermal quartz in Stage II of the CQP facies commonly contain angular breccia fragments. Most are derived from proximal basaltic wall rocks which, although extensively disaggregated and strongly chloritised, commonly have well preserved relict igneous textures. Medium- to coarse-grained, cubic pyrite is also common in many quartz veins (the opaque mineral phases shown here). Microlitic crystals (especially of chlorite and epidote) and remnant fluid inclusions are also widespread in some quartz veins, further contributing to the distinctive brecciated texture (sample MCQ-057 in PPL, Caroline Cove, Site 3A).

Figure 6.60: This massive cluster of fine- to coarse-grained cubic pyrite is exclusively hosted in hydrothermally derived quartz (Stage II). Many discrete sulfide grains display extensive brittle fracturing, which is a characteristic feature of vein hosted pyrite grains in the CQP facies. Most pyrite is compositionally homogeneous and rarely contains inclusions of other sulfide minerals (sporadic traces of sphalerite only). These sulfides are also relatively pristine, apart from partial oxidation effects observed at the margins of some crystals (sample MCQ-031 in reflected light, Caroline Cove, Site 3A).

Figure 6.61: The coarse-grained, cubic pyrite crystal shown here is completely enclosed within massive and relatively late-stage chalcopyrite (Stage II). These sulfide phases are common components of the CQP facies assemblage, and typically form massive crystalline aggregates and discrete veins or stringer-like networks. Abundant micro-fractures in the pyrite grain are a common facies attribute, and likely reflect the prolonged tectonic history of the nearby transpressional Macquarie Ridge Complex (sample MCQ-027 in reflected light, Caroline Cove, Site 3A).

Figure 6.62: Clusters of elongate epidote crystals are commonly intergrown with pyrite and quartz in Stage II veins of the CQP facies. The subradiating epidote aggregate shown here consists of fine- to medium-grained, pale greenish-yellow (slightly pleochroic) epidote. Typical of most epidote at Caroline Cove (Site 3A), these bladed crystals are hosted within the central core of a massive quartz vein (sample MCQ-055 in PPL).

Figure 6.63: Barite comprises a minor but important component of the alteration assemblage in the CQP facies (Stage III). It mainly occurs as a vuggy infill phase in quartz vein cavities (e.g., it completely fills the drusy quartz vugh shown here), or partly envelops some vein hosted pyrite grains. Barite grains are distinguished by their high optical relief, well developed cleavage, and abundant secondary fluid inclusion trails, most of which are leaked (sample MCQ-057 in PPL, Caroline Cove, Site 3A).

Figure 6.64: Similar to altered rocks in the VQC facies (Major Lake Fault Zone), late-stage oxidation (weathering-related?) has variably affected the basaltic rocks at Caroline Cove. Narrow and irregular veinlets filled with dark orange or reddish-brown Fe-oxide and Fe-hydroxide minerals have overprinted earlier-formed alteration phases in many veins and groundmass domains throughout the CQP facies. The oxidised assemblages associated with Stage V of the CQP facies are most intensely developed around pre-existing pyrite grains and intergrown sulfide clusters, and many of these earlier-formed alteration minerals (Stage II) are completely replaced (sample MCQ-062 in PPL, Caroline Cove, Site 3A).

Photomicrographs of important alteration mineral relationships in Stage II, III, and V of the massive and veined, chlorite-quartz-pyrite (CQP) facies in the Caroline Cove area.

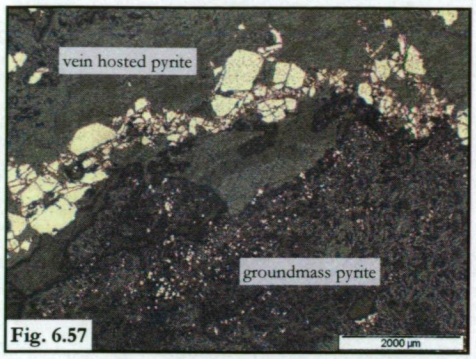

Fig. 6.57

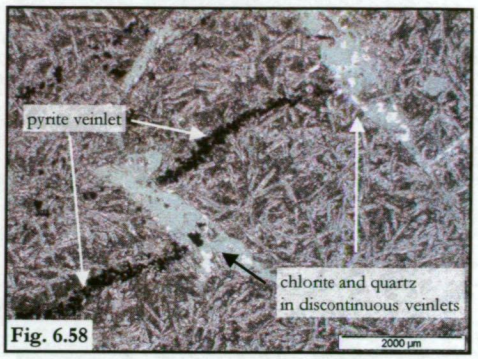

Fig. 6.58

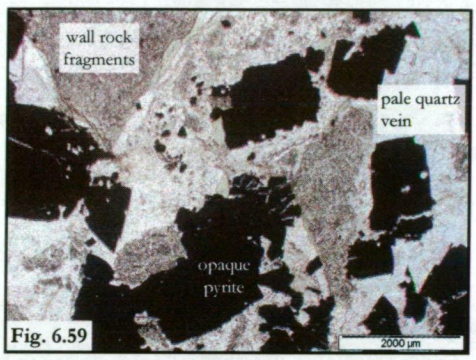

Fig. 6.59

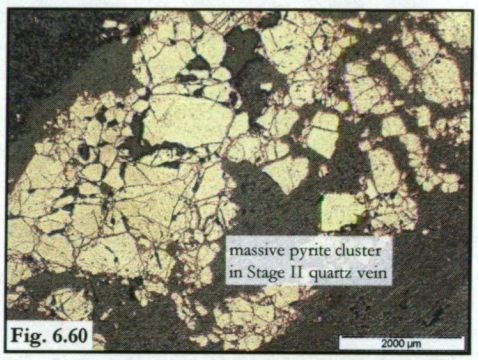

Fig. 6.60

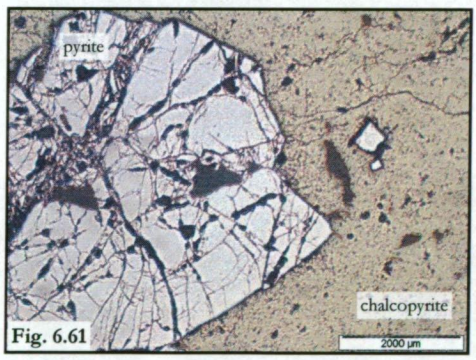

Fig. 6.61

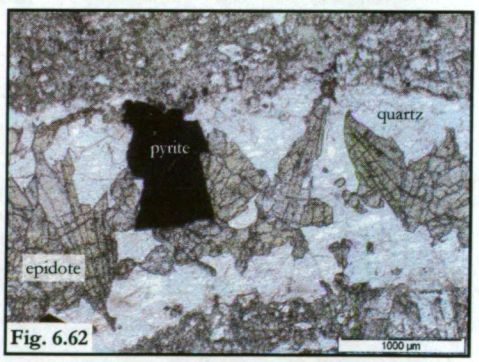

Fig. 6.62

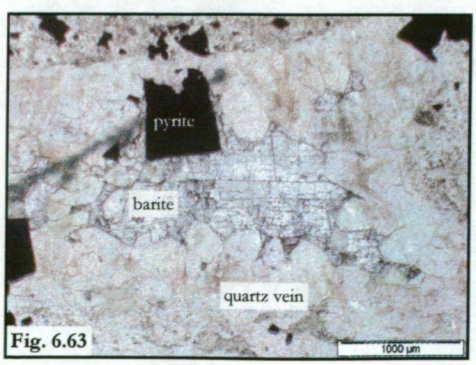

Fig. 6.63

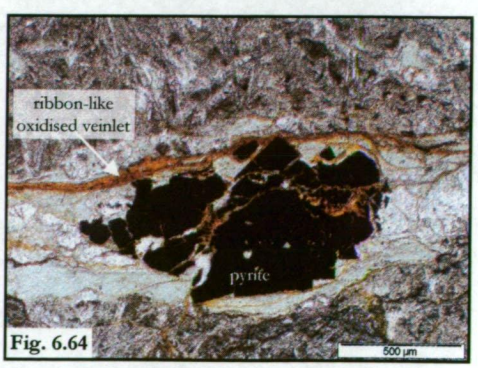

Fig. 6.64

Very fine- or fine-grained barite is intimately associated with hydrothermally derived quartz, and mainly occurs in discrete vein cores where it infills small (~ 1-2 mm) crystal-lined vughs (Figure 6.63). Barite also partially surrounds some quartz-hosted pyrite grains (marginal overgrowths on discrete crystals or aggregates), although there is no evidence that barite replaces earlier-formed sulfides.

Most barite grains have angular or very angular crystal shapes, which mainly reflect their common occurrence as late-stage vugh infill. Fluid inclusion trails occur in some barite grains, typically forming subparallel arrays and inter-connected secondary networks (fluid inclusions are further discussed at the end of the paragenesis section). Unfortunately, the relatively minor amount of barite observed in the CQP facies samples is insufficient to conduct further geochemical work, such as determining sulfur isotope compositions.

Stage IV and V – Formation of sporadic late-stage veins

Alteration minerals associated with the final stages of the CQP paragenesis are volumetrically subordinate (significantly less abundant) to the earlier-formed assemblages, representing < 1 % of the hydrothermal assemblage. The abundance, distribution and inter-mineral relationships in Stage Iv and V are also broadly similar to those from the VQC and NQV facies. For example, narrow, discontinuous veinlets of calcite, prehnite, or zeolite (~ 0.5–2 mm-wide) cut across or partly replace pre-existing groundmass and vein phase minerals in Stage IV. Wispy, sinuous veinlets (< 0.5 mm-wide) or irregularly shaped patches dominated by strongly oxidised, brownish-red alteration minerals (e.g., Fe-hydroxides and Fe-oxyhydroxides) represent the final paragenetic stage (Figure 6.64).

The vein-dominated, prehnite-zeolite facies (VPZ)

The main alteration minerals in the vein-dominated, prehnite-zeolite (VPZ) facies are significantly different from the hydrothermal assemblages in the VQC, NQV, and CQP facies. In particular, quartz, pyrite, and epidote are absent from the VPZ facies and relatively low temperature minerals such as prehnite, pumpellyite, and various zeolite species (e.g., laumontite) predominate. However, many textural attributes are similar; for example, intensive subparallel vein arrays and selectively pervasive wall rock alteration are characteristic of the VPZ facies.

Five key stages are recognised in the VPZ facies paragenesis (Figure 6.30):

Stage I – Selectively pervasive alteration of igneous phenocryst and groundmass minerals in the basaltic host rocks, characterised by widespread smectite (clay alteration);

Stage II – Diffuse Fe-oxyhydroxide alteration;

Stage III – Formation of extensive zeolite vein and veinlet arrays;

Stage IV – Massive and veined, prehnite and pumpellyite alteration; and

Stage V – Sporadic calcite and clay minerals cementing veins and vughs

Stage I – Selectively pervasive, smectite-rich groundmass alteration

Basaltic wall rocks in the VPZ facies at Sellick Bay contain abundant hydrothermally derived clay minerals which formed early in the alteration paragenesis. Reconnaissance microprobe analyses identified Fe- and Mg-rich smectite as the most abundant type, although detailed compositional data was not acquired. Minor colour and textural variations suggest that several compositionally different species occur, although no consistent over-printing or cross-cutting relationships were observed, i.e., no specific temporal evolution recognised for clay alteration. Most early-formed smectites are very fine-grained crystals (< 10–20 μm) which form intergrown sheeted aggregates or subradiating clusters, and typically vary from pale yellowish-green to darker brownish-green.

Many primary magmatic minerals are partly to completely replaced by early smectite alteration in the VPZ facies. However, the intensity of alteration may vary considerably within individual samples (thin-sections), and the primary igneous rock fabric is commonly preserved *in situ*, i.e., alteration does not significantly affect the relict texture. Irregularly shaped, turbid patches and narrow vein-like tendrils of smectite occur in plagioclase, affecting both fine-grained groundmass laths and medium- to coarse-grained crystals (Figure 6.65). Rare olivine phenocrysts are completely altered and replaced by massively intergrown smectite, although their distinctive grain shapes are well preserved, i.e., pseudomorphic replacement. In comparison, anhedral clinopyroxene grains are relatively unaltered in the groundmass, except in narrow but pervasively recrystallised vein selvages. Volcanic glass in the primary basaltic mesostasis is also intensely altered, with practically all interstitial groundmass patches completely replaced by very fine grained, greenish-brown smectite (Figure 6.64). The common occurrence of massive smectite replacing glassy mesostasis provides evidence of the selectively pervasive nature of Stage I alteration in the VPZ facies.

Minor secondary minerals associated with Stage I alteration include titanite, leucoxene, calcite, and laumontite. Ragged, anhedral clusters of microlitic titanite and leucoxene are most abundant (after smectite), and are widely disseminated in the altered groundmass of many basalts. Most intergrown titanite-leucoxene aggregates partly to completely envelop or overgrow very fine-or fine-grained crystals of Ti-magnetite. However, the intensity of titanite-leucoxene alteration is highly variable in many samples, and relatively pristine Ti-magnetite crystals are commonly preserved. The heterogeneity of demagnetisation (observed petrographically) helps to explain the greater range of magnetic susceptibility values obtained for altered basalts in the VPZ facies (relative to those from the Major Lake and Caroline Cove Faults, e.g., compare the magnetic susceptibility histogram shown in Figure 5.73 to those in Figure 5.4 and 5.37).

Small (< 2 mm-wide), subrounded to rounded vesicles occur in most VPZ facies basalts, typically comprising ~ 2–3 % of the groundmass fabric. Relative to the surrounding regional alteration domains (Zone BIII and BVa, Chapter 5), amygdules in the VPZ facies are infilled with more diverse hydrothermal minerals. Many amygdules have multi-component infill assemblages which consist of varying proportions of smectite, calcite, and zeolites. Complexly intergrown aggregates of very fine-grained smectite most commonly occur in vughs, and these are texturally and compositionally similar to proximal clay-altered patches in the surrounding groundmass (Figure 6.66). In some amygdules, multiple smectite-filled rims (mostly < 0.2 mm-wide) may line the outermost margins of the vesicle, partly to completely enveloping massive cores of fine-grained zeolite or calcite.

Stage II – Diffuse Fe-oxyhydroxide alteration

Massive, opaque or dark reddish-brown Fe-rich oxyhydroxide minerals are a common component of the VPZ paragenesis. Preliminary electron microprobe analyses confirmed the hydrous, Fe-rich nature of these hydrothermal phases, although the precise mineral species could not be determined. However, these VPZ facies minerals have many textural and compositional similarities with Fe-oxyhydroxides described from other studies of altered oceanic crust, e.g., Laverne et al. (1996); Schramm (2004), which provides evidence to support the Stage II mineral classification used here

Stage II Fe-oxyhydroxide minerals are widespread in the VPZ facies and form massive groundmass domains of irregular size and shape. Diffuse, subplanar veinlet arrays are also abundant, commonly transecting, overprinting, and partially incorporating pre-existing minerals from the groundmass (both relict igneous and hydrothermally derived phases). These dendritic Fe-oxyhydroxide arrays are oriented both subparallel and oblique to the trend of other veins in the VPZ facies, such as zeolite or prehnite veins from Stage III and Stage IV (respectively). Some amygdules also have narrow rims of moderate to strong Fe-oxyhydroxide alteration that surround clay-filled interiors (Figure 6.66).

Patches of basaltic groundmass dominated by Fe-oxyhydroxide alteration have distinctive skeletal textures. In areas of the most strongly oxidised groundmass, primary magmatic minerals are extensively disrupted (partly to completely incorporated or disaggregated), and scant remnants of the relict igneous fabric are preserved (Figure 6.67). Individual vein strands vary from < 1 mm to ~ 5 mm-wide, but Fe-oxyhydroxide alteration mainly comprises diffuse groundmass domains up to several centimetres thick. In many of these irregularly shaped enclaves discrete crystals of very fine- to fine-grained clinopyroxene are well preserved and relatively unaltered, although most other primary igneous minerals are extensively oxidised. This unusual groundmass texture is a highly distinctive and diagnostic petrographic (microscopic) feature of Stage II alteration in the VPZ facies (Figure 6.67).

Stage III – Formation of extensive zeolite vein and veinlet networks

Zeolite veins are abundant in the VPZ facies, forming inter-connected arrays that intensely disrupt the primary basaltic groundmass (minerals and textures) and many earlier-formed alteration minerals (Figure 6.68). The intricate zeolite-cemented networks consist of discrete veins and veinlets which irregularly cut across fragmented domains throughout their altered host rocks. Thicker vein segments (> 1 mm-wide) are oriented subparallel to the dominant structural trend (the NW-striking Sellick Bay Fault Zone), although oblique veinlet off-shoots and high-angle dendritic strands are relatively abundant (Figure 6.69). Individual veinlets are thin (average vein widths are ~ 0.5–2.0 mm) and moderately sinuous, and most have well defined (sharp) boundaries with the surrounding groundmass. Discrete veins within broader stockwork arrays are commonly separated by narrow, elongated segments or fragmented particles of altered wall rock. Most igneous minerals within these ribbon-like basaltic strands are extensively altered and texturally disrupted, except for relict granules of augite (as previously described, Figure 6.67).

Zeolite veins and veinlets in Stage III of the VPZ facies mainly consist of interlocking crystalline mosaics. Discrete crystals commonly range from 0.1–0.3 mm-wide, with maximum grain diameters ~ 1 mm. Most zeolite veins are compositionally uniform; they consist of pale, blocky or tabular crystals with well developed (orthogonal) cleavages. The crystal habit and grain appearance is typical of laumontite (Griffin, 1982), and the widespread occurrence of this Ca-rich zeolite was confirmed during my reconnaissance electron microprobe study (Chapter 6.4).

Stage IV – Massive and veined, prehnite and pumpellyite alteration

Discrete veins and groundmass pods cemented with massive prehnite are key diagnostic components of the VPZ facies, and occur throughout the Sellick Bay Fault Zone. Consistent hydrothermal textures and inter-mineral relationships indicate that most prehnite formed relatively late in the paragenetic sequence (Figure 6.70), e.g., it clearly post-dated the evolution of the main smectite- and Fe-oxyhydroxide stages (Stage I and II respectively). However, limited textural evidence, such as minor zeolite veinlets cut by prehnite, suggests that the on-set of prehnite alteration was likely transitional with waning hydrothermal activity associated with the preceding zeolite-rich stage.

Stage IV prehnite alteration occurs in diverse textural modes. Selectively pervasive replacement of primary igneous minerals (Figure 6.71) and partial or complete infill of vuggy cavities are common, although massive, subplanar veins are clearly the most distinctive hydrothermal feature. Individual prehnite veins are generally thicker (commonly > 10 mm) and regionally more abundant in the Sellick Bay Fault Zone than (mostly) earlier-formed zeolite veins (Stage III), although local variations may occur (Figure 6.70). Prehnite veins typically comprise interlocking crystalline mosaics which mainly host very fine to fine anhedral grains, commonly < 0.5 mm-long. The very fine- to fine-grained nature of some vein hosted prehnite crystals appear

to have formed by dynamic recrystallisation; originally coarser prehnite grains may have reduced in size due to post-hydrothermal tectonic activity in the Sellick Bay Fault. Medium-grained crystals are preserved in some vein interiors (up to ~ 2–3 mm-diameter), and may sporadically rim drusy cavities formed in the prehnite cement (Figure 6.72). Both vein and groundmass prehnite has low relief and bright birefringence, and most grains are uniformly clear and colourless, i.e., free of turbidity caused by microlitic alteration minerals or abundant inclusions.

Many prehnite veins are enveloped by intense alteration selvages (genetically related) which have pervasively infiltrated the proximal basaltic wall rocks. These vein haloes, which are compositionally and texturally similar to massively altered pillow cores (Chapter 5.5), are dominated by microlitic or very fine-grained pumpellyite crystals (<0.5 mm-long) intergrown with prehnite. Pumpellyite is moderately pleochroic (pale green to green), and most grains have distinctive elongate to acicular crystal habits. Individual grains commonly occur in irregularly shaped, felted aggregates or small subradiating masses ~ 1–2 mm-wide. Intergrown clusters of pumpellyite mantle some groundmass zones dominated by widespread Fe-oxyhydroxide alteration, consistent with these earlier alteration assemblages having acted as nucleation sites for pumpellyite crystallisation. Strong to intense pumpellyite alteration has overprinted and partly or completely destroyed many igneous textures and primary rock fabrics, including groundmass crystals of clinopyroxene which are generally unaffected by other styles of VPZ alteration, e.g., recall that pristine augite commonly occurs in zones of intense Fe-oxyhydroxide alteration. Pumpellyite may also form narrow, trellis-like veinlets or small crystal aggregates in some prehnite veins, or prehnite-altered plagioclase crystals (Figure 6.71). Prehnite and pumpellyite compositions were verified during my reconnaissance microprobe study (Chapter 6.4); most are geochemically similar to grains reported from other ophiolites, e.g., the Del Puerto ophiolite (Evarts and Schiffman, 1983)

Stage V – Minor calcite and late-stage clay minerals in veinlets and vughs

The formation of minor, late-stage alteration minerals post-dated the main hydrothermal activity in the VPZ facies. Calcite is the main component of the Stage V assemblage, and mainly occurs as narrow and isolated veinlets or massive patches which infill small cavities in earlier-formed vughs (mainly in prehnite-cemented veins, Figure 6.72). Some smectite-filled amygdules, typical of the Stage I assemblage, are also partly to completely enclosed by narrow rims of late-stage brownish-green clay which are thought to have formed during Stage V.

Figure 6.65: Sheet-like aggregates of intergrown yellowish-green smectite are characteristic of Stage I alteration in the VPZ facies. This photomicrograph shows different textural forms of smectite alteration which commonly affect igneous minerals and patches of mesostasis in the host rocks. Massive smectite alteration is sporadically disseminated in the groundmass (mainly replacing volcanic glass), and turbid zones or thin veinlets of smectite commonly occur in partly altered plagioclase crystals (sample MCQ-271 in PPL, Sellick Bay, Site 1A).

Figure 6.66: Many basaltic rocks in the Sellick Bay district are moderately vesicular, and most vughs are pervasively infilled by early-stage clay minerals. Clay-rich amygdules are commonly < 2 mm-wide and mainly consist of finely sheeted smectite. The central vesicle in this photomicrograph is surrounded by a strongly oxidised halo (opaque Fe-oxyhydroxide minerals) which has selectively overprinted much of the intersertal groundmass (sample MCQ-271 in PPL, Sellick Bay, Site 1A).

Figure 6.67: Diffuse Fe-oxyhydroxide alteration commonly replaces the primary groundmass and early-formed clay minerals (Stage I) in basaltic rocks from the VPZ facies. These dark reddish-brown or opaque alteration patches and veinlets significantly obscure most igneous minerals and textures. However, as shown here, fine-grained crystals of relict augite are mostly unaffected by the oxidised assemblages. Many anhedral grains of pristine augite (colourless) are enveloped by massive, web-like Fe-oxyhydroxides (opaques); these have selectively overprinted most other groundmass phases (sample MCQ-176 in PPL, Sellick Bay escarpment, Site 1A).

Figure 6.68: Multiple zeolite veins (Stage III) cut sharply across early-formed clay- and Fe-rich alteration assemblages in this VPZ facies basalt. The smectite-altered olivine pseudomorph in the centre of this photomicrograph is significantly disrupted and disaggregated by the zeolite vein, and fragments of massive smectite are incorporated throughout the hydrothermal vein cement. Blocky crystals of fine-grained laumontite comprise most of these veins, although minor thomsonite and analcite also occur (sample MCQ-273 in PPL, Sellick Bay escarpment, Site 1A).

Figure 6.69: Intensely developed subparallel vein arrays and irregularly shaped patches of zeolite alteration are diagnostic components of groundmass alteration in the VPZ facies. This view shows many common features associated with the Stage III zeolite-rich assemblages, including along-strike variations in vein thickness and randomly anastomosing veinlet strands. Multiple, cross-cutting intersections clearly indicate that zeolite alteration post-dated the evolution of diffuse Fe-oxyhydroxide alteration (Stage II) in the VPZ paragenesis (sample MCQ-176 in PPL, Sellick Bay escarpment, Site 1A).

Figure 6.70: A narrow prehnite veinlet cuts obliquely across a patch of earlier-formed zeolite alteration in the groundmass of this basalt from the Sellick Bay Fault Zone (Site 1A). The margins of the colourless prehnite vein are lined with very fine anhedral grains, whereas the inner vein core contains more diverse crystals of varying size and shape. Discrete prehnite veins commonly overprint other alteration phases in the VPZ facies, and these consistent cross-cutting relationships indicate that prehnite formed relatively late in the paragenesis (sample MCQ-273 in PPL, Sellick Bay escarpment, Site 1A).

Figure 6.71: The euhedral plagioclase phenocryst in the centre of this view is completely pseudomorphed by crystalline prehnite and pumpellyite associated with Stage IV of the VPZ facies. Prehnite also occurs sporadically in nearby groundmass patches, and is mostly fine-grained, clear and colourless. Yellowish-green needles of pumpellyite mainly form trellis-like networks that have transected the pseudomorphed grain, although some massive alteration zones pervasively overprint parts of the primary crystal (sample MCQ-272 in PPL, Sellick Bay escarpment, Site 1A).

Figure 6.72: An intergrown crystalline mosaic of highly birefringent, fine-grained prehnite infills this vein from a pillow basalt sample in the Sellick Bay Fault Zone. A subrounded vein cavity is fringed by slightly larger prehnite grains and is completely infilled by massive calcite, which represents the final paragenetic phase of the VPZ facies (Stage V). Unlike many massive prehnite veins this segment lacks proximal alteration selvages, and relatively unaltered clinopyroxene occurs < 1 mm from the vein margin (sample MCQ-295 in XPL).

Photomicrographs of common alteration minerals and textures associated with the vein-dominated, prehnite-zeolite (VPZ) facies in the Sellick Bay Fault Zone.

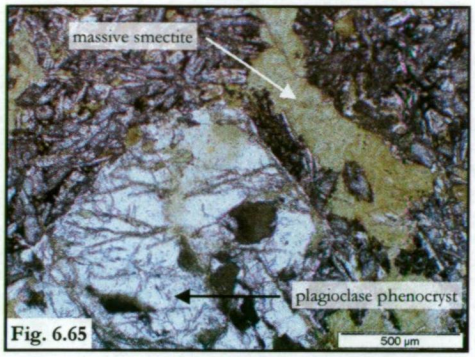

Fig. 6.65

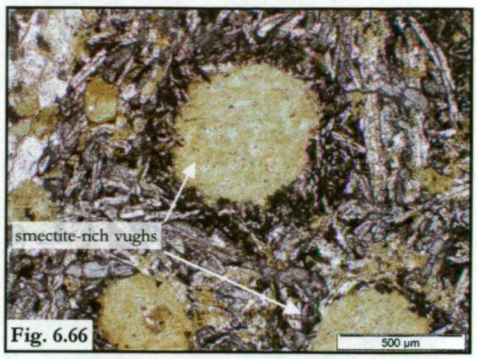

Fig. 6.66

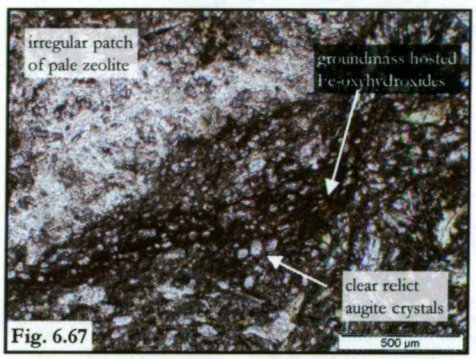

Fig. 6.67

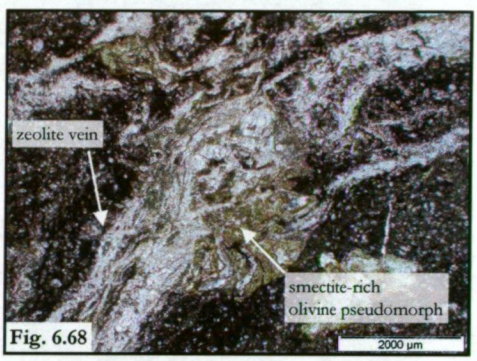

Fig. 6.68

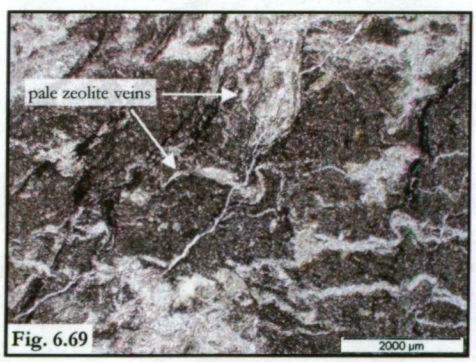

Fig. 6.69

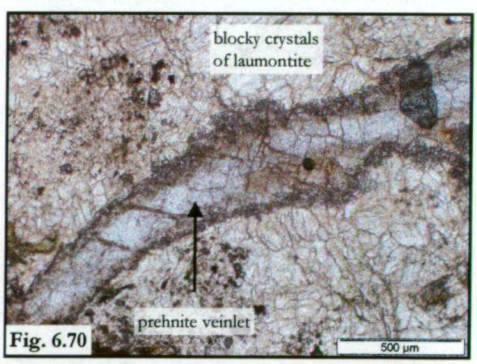

Fig. 6.70

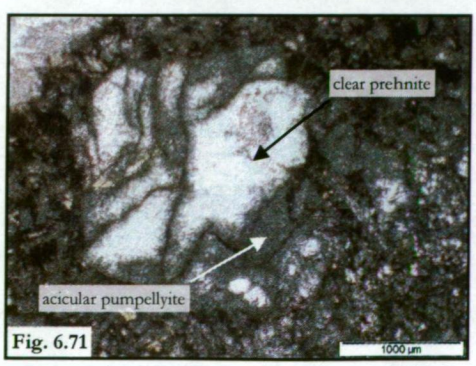

Fig. 6.71

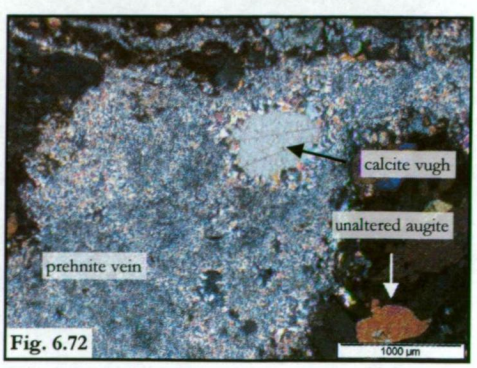

Fig. 6.72

The foliated, massive chlorite facies (FMC)

The foliated, massive chlorite (FMC) facies only occurs in the central deformation corridor of the Major Lake and Caroline Cove Fault Zones. Most of the *in situ* outcrops are poorly preserved*, and the actual spatial distribution and intimate fault zone relationships of the FMC facies are not well understood, especially along the Major Lake Fault (Chapter 5.3). Initially, the FMC facies was classified and described based on its main outcrop features. Subsequent petrographic and electron microprobe work on selected rock samples (outlined in this section and in Chapter 6.4) showed that the mineral identified as 'chlorite' during fieldwork (which comprises the most abundant and diagnostic hydrothermal component of the FMC facies) is predominantly a compositionally mixed smectite-chlorite phase. However, despite this subtle mineral variation, I elected to continue with the existing FMC facies nomenclature for the sake of consistency and continuity.

The FMC facies is characterised by very finely intergrown crystals of hydrothermally derived smectite-chlorite (Chapter 6.4). Most clay minerals in the FMC facies range from dark brownish-green to green, and commonly form delicate sheeted crystalline aggregates (Figure 6.73). Thin spidery veinlets (most < 1–2 mm-wide) and inter-connected web-like networks (fragmental breccias) are diagnostic textures in the FMC facies; many are partly foliated and have very fine-grained growth fibres elongated suborthogonal to the vein walls (Figure 6.74). Narrow and irregular veinlets of prehnite also occur sporadically in the FMC facies. Consistent cross-cutting relationships and the absence of distinct foliations indicate that prehnite formation post-dated the clay-rich veins. Some smectite-rich veins and breccias have partly to completely overprinted pre-existing alteration minerals and textures formed during earlier stages of focussed hydrothermal activity, such as the quartz-rich VQC facies. In addition, many rock fragments in the FMC zone contain regional alteration assemblages typical of relatively low grade zeolite conditions, i.e., these breccia fragments are unaffected by clay-filled veins typical of the FMC facies (Figure 6.75 and 6.76). Thus, the distribution and intensity of smectite-chlorite alteration in the FMC facies is significantly heterogeneous (even at microscopic scale), and many textural and compositional relicts of earlier-formed hydrothermal (and igneous) minerals are preserved throughout the central deformation zones of the Major Lake and Caroline Cove Faults (host sites for the FMC facies).

* As previously explained, altered rocks in the FMC facies are highly deformed and very fragile, and most outcrops are extensively weathered and eroded (Chapter 5.3 and 5.4)

Photomicrographs of common hydrothermal minerals and textures in the foliated, massive chlorite (FMC) facies from the Major Lake and Caroline Cove Fault Zones

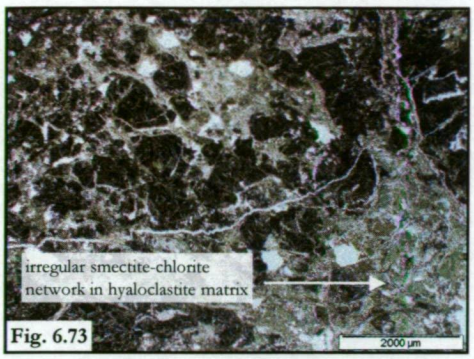

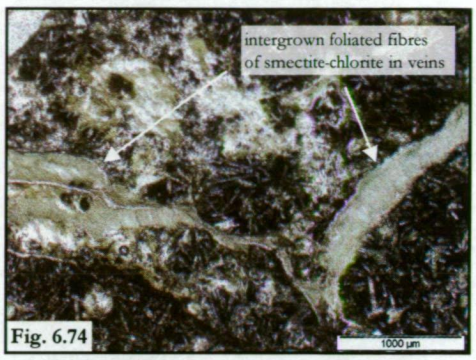

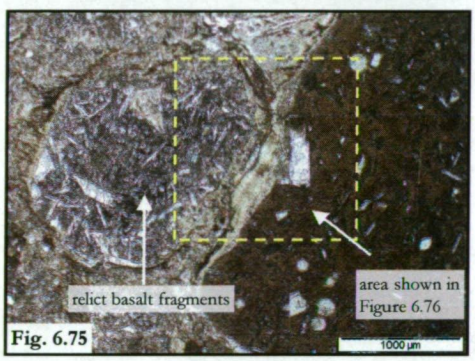

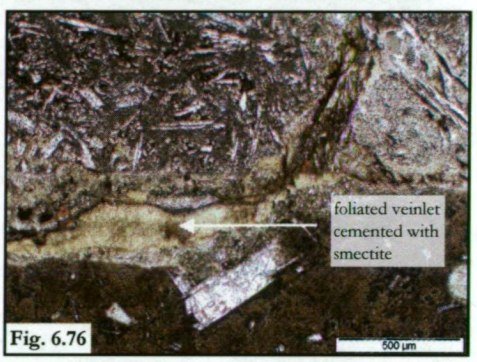

Figure 6.73: Irregular alteration patches and fine stringer-like veins are well developed in the glassy groundmass of this hyaloclastite from the Major Lake Fault Zone at Sandell Bay creek (Site 2A). The complex network of green smectite-rich clay minerals shown here is typical of the non-pervasive alteration style associated with the FMC facies. Relict fragments of igneous-derived material comprise the brecciated dark brown fragments which are randomly enveloped by the smectite-rich alteration network (sample MCQ-173 in PPL).

Figure 6.74: Pale brownish-green to green veinlets cemented with intergrown aggregates of very fine-grained smectite-chlorite cut across this basaltic rock from the Major Lake Fault Zone. Extensive clear patches in many smectite veins attest to the fragile nature of these alteration minerals, as much of the original cement was unavoidably removed during thin-sectioning. This view also highlights the finely foliated and sheeted textures that commonly occur in smectite-rich veins associated with the FMC facies (sample MCQ-173 in PPL, Site 2A).

Figure 6.75: The very fine-grained smectite-rich veinlet shown here has preferentially formed around the glassy margins of proximal breccia fragments in a fault hosted hyaloclastite from the Caroline Cove Fault. The adjacent rock fragments lack pervasive smectite alteration, and also have significantly different primary groundmass textures. Clearly, smectite alteration is not pervasively developed in these FMC facies rocks, as the brecciated fragments contain relatively pristine igneous mineral assemblages (sample MCQ-053 in PPL).

Figure 6.76: An enlarged view of the area highlighted in Figure 6.75, showing a segment of the narrow smectite veinlet that separates adjacent rock fragments in this FMC facies hyaloclastite. The brownish-green veinlet comprises very fine-grained aggregates of fibrous smectite-chlorite which are delicately intergrown and have a distinctive subparallel foliation. Similar clay-rich veinlets commonly form narrow slickenlines along discrete cleavage planes in many fractured basalts from the central deformation zone of the Caroline Cove Fault (sample MCQ-053 in PPL, Caroline Cove, Site 3A).

The pervasive Fe-oxyhydroxide overprint facies (PFO)

The pervasive, Fe-oxyhydroxide overprint (PFO) facies exclusively occurs in the central zone of the Caroline Cove Fault (Chapter 5.4). This strongly oxidised hydrothermal assemblage is variably superimposed on basaltic fragments affected by earlier-formed CQP and FMC facies alteration. In addition, the PFO facies has also overprinted (fault hosted) breccia fragments derived from the adjacent hangingwall domain, i.e., the eastern pillow basalt sequence. However, the PFO facies has a relatively sporadic and restricted spatial distribution along-strike (variably developed) and is not as abundant as either the CQP or FMC facies.

Brownish-red or orange-brown Fe-bearing oxyhydroxide minerals (translucent and opaque phases) are diagnostic of the PFO facies. Intense oxidation has selectively overprinted pre-existing Fe-rich alteration minerals such as chlorite and pyrite (associated with the earlier-formed CQP and FMC facies), and has also affected relict Fe-bearing igneous minerals such as augite (although igneous remnants are much less abundant than alteration minerals in these rocks). Most amygdules in the PFO facies, which have typically been infilled by Fe-rich clays such as smectite, and many earlier-formed vein assemblages are also moderately to strongly 'dusted' with very fine-grained oxidised minerals.

In comparison, relict plagioclase laths and irregularly shaped patches of early groundmass quartz (associated with the CQP facies) remain relatively pristine or are only weakly replaced (partial alteration) by oxidised assemblages. The highly selective nature of PFO facies alteration reflects varying concentrations of Fe in the precursor minerals. It is also worth noting here that the intensity, distribution, and composition of the PFO assemblages are significantly different from the partially oxidised vein networks that comprise the final alteration stage of the CQP facies*.

Wall rock oxidation haloes are the most distinctive outcrop feature of the PFO facies, and many are also well preserved in sample thin-sections. Typically, the PFO haloes comprise unoxidised and texturally distinct basaltic interiors which are completely enveloped by concentric oxidation selvages of variable size and shape (Figure 6.77). Oxidation intensity progressively increases away from the relict cores, most of which are demarcated by sharp and well defined boundaries. The most intensely oxidised groundmass commonly occurs near narrow structural discontinuities, considered to represent primary conduits that facilitated circulation of the oxidised fluids. Igneous and hydrothermally derived Fe-bearing minerals in the intensely oxidised groundmass of the outer haloes are pervasively altered and replaced by various reddish-brown Fe-oxyhydroxide minerals (Figure 6.78).

However, the oxidation effects of the PFO facies relatively diminish with proximity towards the central halo core, and partial remnants of the pre-existing igneous or earlier-formed alteration

* Recall from the earlier description of the CQP facies paragenesis that the partly oxidised assemblage comprising Stage V is highly selective and mainly localised around pre-existing sulfide grains, i.e., non-pervasive alteration.

assemblages (e.g., chlorite and pyrite from the CQP facies) may occur in the weakly oxidised interiors. Most primary basaltic textures, such as fine-grained, interlocking plagioclase laths and rounded vesicles, are well preserved in rocks affected by the oxidised assemblages of the PFO facies, i.e., not texturally destructive (Figure 6.78).

Along several segments of the central Caroline Cove Fault Zone, pyrite grains and crystal aggregates hosted in quartz (a common CQP facies mineral association) are commonly affected by PFO facies alteration. In many of these domains, pyrite is extensively replaced by dark reddish-brown or opaque Fe-oxyhydroxide minerals, commonly forming completely oxidised and pseudomorphed grains. However, some irregularly shaped pyritic remnants are partially and sporadically preserved in the oxidised groundmass, attesting to the non-pervasive nature and variable intensity of PFO facies alteration. Vein hosted Fe-oxyhydroxides in PFO facies rocks commonly form irregular skeletal networks that overprint and obscure the earlier-formed hydrothermal cements, especially quartz veins with abundant wall rock fragments and disaggregated particles (Figure 6.79). Most of these massive, trellis-like arrays nucleated from strongly oxidised grains of vein hosted pyrite (Figure 6.80). Many quartz vein segments are extensively overprinted by the opaque Fe-oxyhydroxide webs, although relict quartz crystals may be preserved. This distinctive vein overprint texture is a diagnostic feature of the PFO facies.

Fluid inclusions: A brief overview

The quartz-rich hydrothermal stages of the VQC, NQV, and CQP facies contain abundant fluid inclusions. However, only a small percentage of fluid inclusions originally trapped in the quartz cement are now preserved intact (estimated at < 5 %). Various post-trapping processes (e.g., previous and on-going structural activity) have severely disrupted the fluid inclusion population and commonly resulted in their partial or complete destruction due to necking and leaking. The lack of well preserved fluid inclusions limited the application of detailed analytical techniques, and no micro-thermometry or compositional analyses (e.g., proton-induced X-ray emission or laser Raman spectroscopy) were undertaken during this project. However, a summary of the salient features observed from sporadic remnants of the fluid inclusion population is presented below.

The composition (mostly assumed) and textural appearance of preserved fluid inclusions (quartz-hosted) is remarkably uniform throughout the VQC, NQV, and CQP facies. Quartz veins in these alteration assemblages contain sublinear trails, clusters, and aggregates of fluid inclusions (or their degraded remnants), although their abundance varies for different samples and locations.

Photomicrographs of hydrothermal assemblages and textural features in the pervasive, Fe-oxyhydroxide overprint (PFO) facies from the Caroline Cove Fault

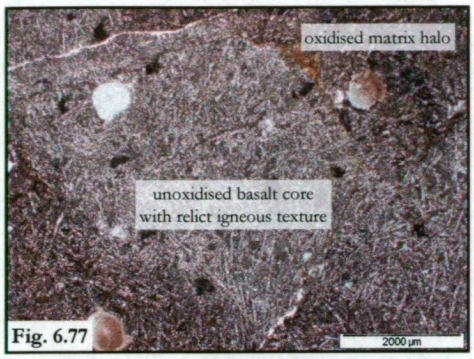

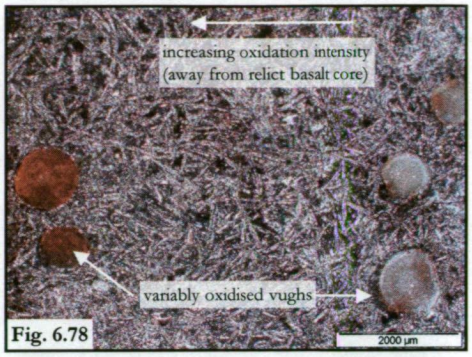

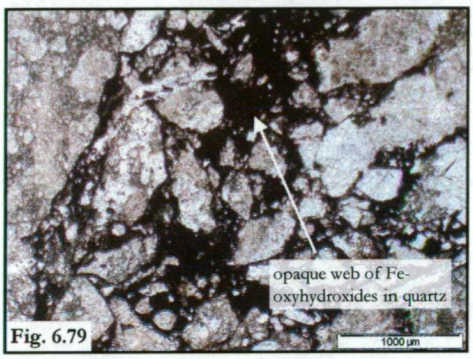

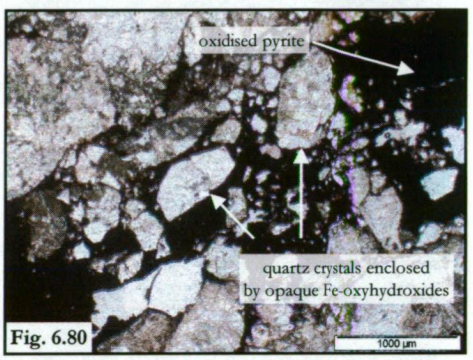

Figure 6.77: Well defined alteration haloes are a characteristic texture in the PFO facies. In zones of strong groundmass alteration, reddish-brown oxidation assemblages have significantly affected the igneous minerals, early-formed alteration phases, and infilled amygdules. Sharp groundmass boundaries clearly demarcate the limits of hydrothermal fluid ingress, with the unoxidised basalt cores enveloped by pervasive oxidation 'fronts' that progressively vary in intensity away from the remnant interiors (sample MCQ-060 in PPL, Caroline Cove, Site 3A).

Figure 6.78: This vesicular, hypocrystalline pillow basalt is typical of volcanic rocks in the PFO facies at Caroline Cove (Site 3A). Alteration intensity increases with distance from the relict pillow basalt core (unoxidised), and the most intense groundmass alteration occurs adjacent to small rock discontinuities, i.e., zones along which oxidised fluids were preferentially channelled in the rock. This diagnostic hydrothermal texture provides good evidence to interpret the existence of progressive oxidation fronts in the PFO facies (sample MCQ-060 in PPL).

Figure 6.79: A web-like array of massive Fe-oxyhydroxides (opaque phases) has partly overprinted this massive quartz vein (originally part of the CQP facies). Similar reddish-brown overgrowths occur sporadically throughout the main deformation corridor of the Caroline Cove Fault (Chapter 5.4), and these oxidised phases variably affect the earlier-formed quartz-rich assemblages. Typical of the PFO facies, the oxidised vein network shown here is heterogeneously developed in its host quartz vein (CQP Stage II). Many discrete quartz crystals are partly to completely enveloped by the opaque web, but remnant grains which are essentially unaffected by oxidation also occur (sample MCQ-047 in PPL).

Figure 6.80: The massive, skeletal network of opaque Fe-oxyhydroxides in this photomicrograph has nucleated from a cluster of vein hosted pyrite grains in pillow basalt which was originally part of the CQP facies. The strongly oxidised Fe-rich assemblage has extensively invaded the quartz-vein and preferentially altered brecciated wall rock fragments and minute particles of disaggregated basalt throughout the hydrothermal cement (sample MCQ-047 in PPL, Caroline Cove, Site 3A).

Preserved fluid inclusions are typically elliptical or rounded (Figure 6.81); most are < 5 μm in diameter, although rare 10–20 μm fluid inclusions do occur. Fluid inclusions > 10 μm-wide have more diverse subangular and elongated shapes, and may form isolated occurrences in their host crystal (interpreted primary origin). Commonly, the best preserved fluid inclusions occur adjacent to vein-hosted sulfide crystals (medium- or coarse-grained) or wall rock particles, suggesting that these breccia fragments have partially shielded proximal fluid inclusions during episodes of tectonic activity.

Clear, liquid-dominated fluid inclusions are most abundant in quartz veins; these represent typical single-phase Type I fluid inclusions (Roedder, 1984). Some liquid-rich fluid inclusions contain small vapour bubbles (relatively high vapour to liquid ratios), although distinctive, vapour-rich fluid inclusions (Type II) are very rare (< 2 % of the fluid inclusion population). During this preliminary study there were no Type III or Type IV fluid inclusions recognised, i.e., none of the observed fluid inclusions contain daughter minerals or CO_2-rich vapour.

A wide variety of fluid inclusion trails and clusters occur in quartz veins from the VQC, NQV, and CQP facies, with intra-granular and trans-granular arrays being most abundant. Partial concentric growth zones (single or multiple strands) also exist in some subhedral or euhedral quartz grains, and these mimic the prismatic shape of their host crystals (Figure 6.82). Many fluid inclusions are intimately associated with hairline micro-fractures that transect multiple grain boundaries, and these sublinear or slightly sinuous trails clearly post-date the formation of their host crystals. The spectrum of fluid inclusion arrays suggests that the quartz-hosted population comprises a combination of primary, secondary, and pseudo-secondary fluid inclusions (Roedder, 1984).

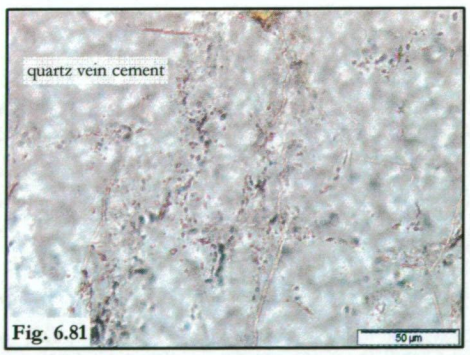

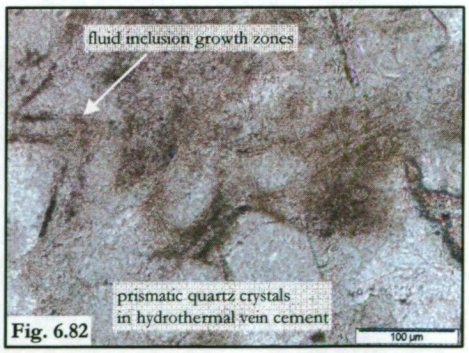

Figure 6.81: Quartz hosted fluid inclusions commonly occur in the VQC facies; most are small (< 5 μm-wide), subrounded and liquid-rich (Type I). Individual quartz crystals in this vein are cross-cut by a sublinear array of typical Type I fluid inclusions which are interpreted to have post-dated their host vein, i.e., formed during a later evolutionary stage (sample MCQ-373 in PPL, Lusitania Bay, Site 2D).

Figure 6.82: Minute fluid inclusions occur abundantly in the hydrothermal cement of this VQC facies quartz vein from Major Lake foreshore (Site 2B). Several fine-grained prismatic quartz crystals host multiple fluid inclusion growth zones, providing unequivocal evidence for their primary hydrothermal origin. However, despite the widespread abundance of quartz hosted fluid inclusions in the VQC facies, on-going tectonism (post-hydrothermal) has significantly disrupted most primary fluid inclusions and caused extensive necking and leaking of their interiors; hence, relatively few remain intact (sample MCQ-311 in PPL).

6.4. The chemical composition of hydrothermal silicate minerals

Overview

Hydrothermally derived minerals from altered fault zone rocks on Macquarie Island were analysed by electron microprobe ('probe') at the University of Tasmania (refer to Appendix 4.2 for operating conditions and instrument parameters). Representative samples were selected from each structural system, although the study mainly focussed on the Major Lake and Caroline Cove Faults (Table 6.1). Most probe analyses were of chlorite and inter-layered chlorite-smectite minerals, although minor compositional data for plagioclase, epidote, amphiboles, zeolites, prehnite, and pumpellyite was also obtained (Appendix 4, Table A–4.2 to A–4.17).

Very fine- to fine-grained phyllosilicate minerals (chiefly chlorite and clay minerals) are diagnostic components of most focussed alteration facies on Macquarie Island; determining their major element compositions and classifying the different mineral species was a major focus of my microprobe investigation. Previous research on altered oceanic (and ophiolitic) basalts has shown that the chemical composition of the main hydrothermal silicates may vary considerably, e.g., Alt et al., 1996; Bettison-Varga et al., 1991; Gillis and Thompson, 1993; Teagle and Alt, 2004 (Figure 6.83). Diverse phyllosilicate minerals include smectite, celadonite, paragonite, talc, chlorite, and various inter-layered clays, e.g., mixed chlorite-smectite. This mineralogical spectrum partly reflects variations in whole-rock igneous compositions and magmatic mineral assemblages, i.e., localised precursor (mineral grains) alteration sites within the rock. However, the formation of different hydrothermal minerals is also significantly influenced by important physicochemical fluid parameters; in particular, the fluid temperature, aqueous composition, and the extent and intensity of water–rock interaction all play an important role (Shikazono and Kawahata, 1987). Thus, by characterising mineral compositions in the focussed alteration facies on Macquarie Island (especially the different phyllosilicate minerals), I obtained useful data to help further interpret critical hydrothermal conditions and processes.

Alteration minerals from the vein and breccia, quartz-chlorite facies and the Sandell Bay Sheeted Dyke Swarm (Major Lake Fault Zone)

Mineral composition data (chlorite, plagioclase, and K-feldspar) for the vein and breccia, quartz-chlorite (VQC) facies was obtained from eight individual samples (polished thin-sections) collected from Sandell Bay creek (Site 2A), Major Lake foreshore (Site 2B), and East Mt Martin (Site 2C) (Table 6.1)*. Similar alteration minerals (+ epidote, zeolite, and prehnite) were also analysed in eight other samples from the Sandell Bay Sheeted Dyke Swarm (regional domain in the Major Lake district). During this study, particular care was taken to ensure that different textural forms of chlorite in the VQC facies were analysed; these included vuggy infill phases,

* Throughout this chapter, the number of grain analyses is shown for each alteration mineral in each facies using the following nomenclature, e.g., VQC chlorite (n = 71).

massive alteration patches, 'spiral-like' crystals hosted in quartz cement, and irregular pseudomorphs (mostly replacing igneous plagioclase and olivine).

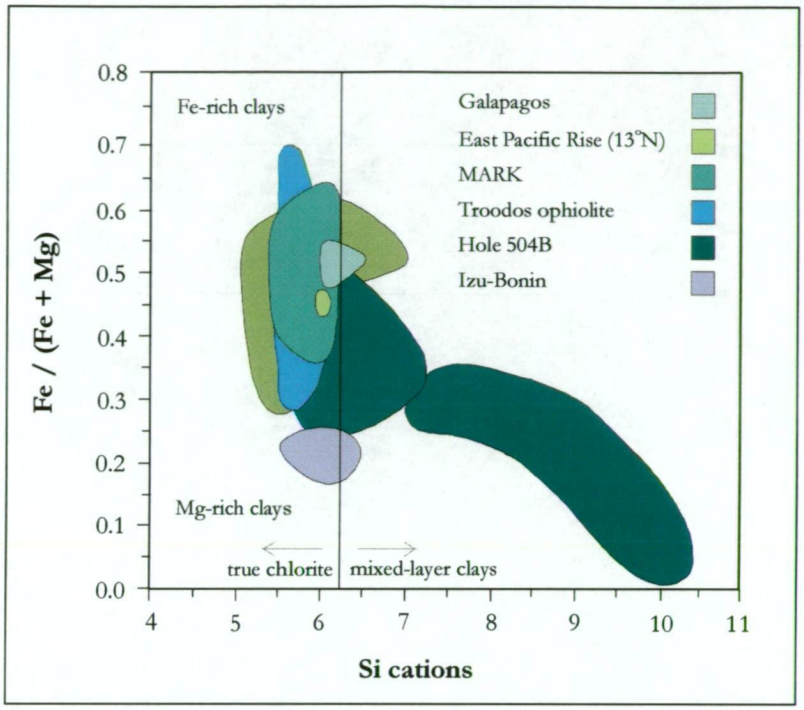

Figure 6.83: Compositional fields for hydrothermally derived phyllosilicate minerals in basaltic rocks from the modern seafloor and the Troodos ophiolite (Cyprus). Most alteration minerals are Mg-rich (Fe # < 0.5) and may be classified as either 'true' chlorites or mixed-layer clay minerals (chlorite-smectite) depending on the number of Si cations. However, some Fe-rich chlorites occur in rocks associated with discharge-related (upflow) hydrothermal fluids, e.g., the Kane Fracture Zone on the mid-Atlantic Ridge (MARK) (diagram modified after Teagle and Alt, 2004; various sources of compositional data are cited within).

Chlorite

Chlorite compositions (Table A–4.2) were recalculated from electron microprobe analyses on the basis of 28 anhydrous oxygens and classified using the nomenclature of Hey (1954). Although the Hey classification scheme is now considered obsolete by some workers (e.g., Nimis et al., 2004), its widespread application in previous studies makes it useful for comparing mineral chemistry data. The distinction between chlorite and mixed-layer chlorite-smectite is based on relative cation abundances of Si and inter-layered species (Ca + Na + K) (Gillis and Thompson, 1993). 'True' chlorite contains < 6.25 Si cations and the sum of Ca + Na + K is nominally < 0.3 (Bettison and Schiffman, 1988; Gillis et al., 2001). In contrast, mixed-layer chlorite-clay minerals (e.g., smectite or talc) have > 6.25 Si cations; however, determining the precise inter-layered species requires x-ray diffraction (not undertaken during my investigation).

Most phyllosilicates in the VQC facies (n = 71) are trioctahedral chlorites of the clinochlore (Mg-rich) – chamosite (Fe-rich) series (Bayliss, 1975). Compositions plot mainly within the pychnochlorite or brunsvigite fields on the Hey diagram (Figure 6.84), and are well correlated with chlorite compositions from oceanic basalts at other seafloor (upflow-related) localities, e.g.,

the Kane Fracture Zone (mid-Atlantic Ridge) and the East Galapagos Rift (Figure 6.83). A lone phyllosilicate analysed during this study has > 6.25 Si cations and is thus not a 'true' chlorite (plots within Hey's diabinite field).

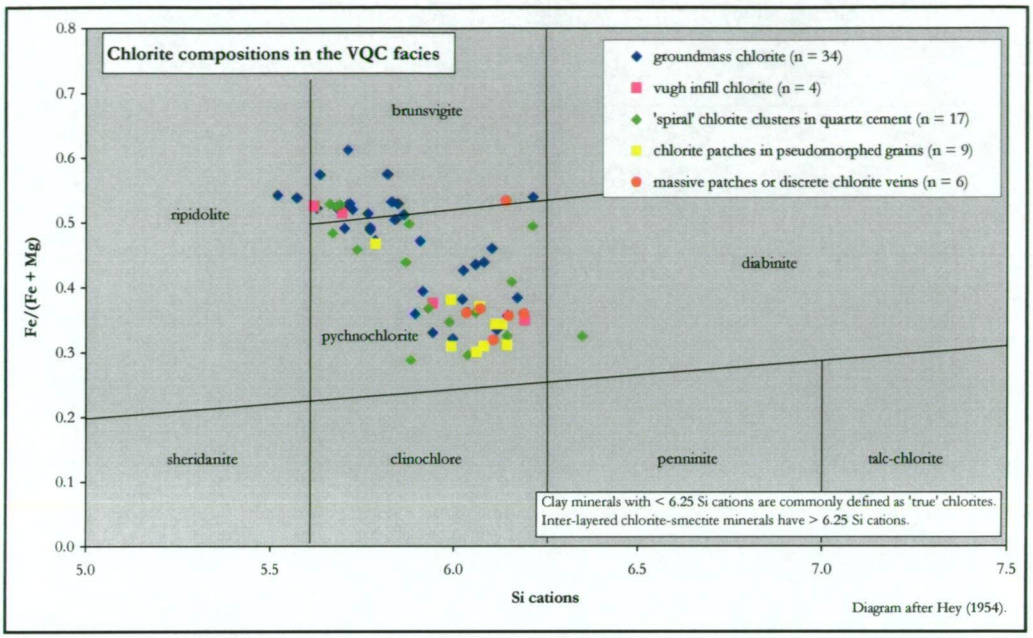

Figure 6.84: A modified Hey classification plot for hydrothermal chlorites in the vein and breccia, quartz-chlorite (VQC) facies. These compositional data are derived from samples collected at the Sandell Bay creek, Major Lake foreshore, and East Mt Martin field sites, and are grouped relative to the five main textural forms. Groundmass and quartz hosted chlorites have the most diverse compositions, although this may simply reflect a greater number of analyses relative to the other types.

The Fe #* of VQC facies chlorite ranges from 0.29 to 0.64. There is a general trend of increasing Si with decreasing Fe #, coupled with Fe + Al substitution for Mg + Si. The main geochemical characteristics are similar to those described for basalt hosted chlorites (oceanic) from Middle Valley on the Juan de Fuca Ridge (Teagle and Alt, 2004), and from the Ivanovka region (ophiolitic) of western Russia (Nimis et al., 2004). Chlorite grains in the altered basaltic groundmass of the VQC facies, and 'spiral'-like grains in quartz cement, span the widest range of Fe compositions (although relatively more microprobe analyses were made of these textural forms). Many groundmass and vein hosted grains are strongly enriched in Fe (Fe # > 0.5) relative to Mg-rich chlorites from typical ocean crust, e.g., in Hole 504B (Figure 6.83). In contrast, chlorite formed in altered crystals of plagioclase and olivine is mostly Mg-rich and has a more restricted range of Fe #'s (mostly 0.3 to 0.4). These are also broadly similar to chlorite aggregates which infill primary vesicles (vuggy chlorite) and form massive alteration patches or discrete veins, i.e., pychnochlorite compositions, with Fe #'s < 0.5 (Figure 6.84).

The concentration of MnO in VQC facies chlorite ranges from 0.35 to 1.74 wt. %, with an average of 0.81 wt % for all textural forms (Figure 6.85). These compositions are considerably

* Fe # = Fe / (Fe + Mg) and Mg # = Mg / (Mg + Fe) based on mineral cation data.

enriched relative to most other chlorites in the ocean crust, e.g., ~ 0.1–0.3 wt. % MnO is the average value for seafloor- and ophiolite-hosted chlorites, e.g., Alt et al. (1986); Laverne et al. (1995). However, Mn-rich chlorites have previously been identified in some oceanic rocks, especially from zones of stockwork sulfide mineralisation in the volcanic rock to sheeted dyke transition zone. For example, the Mn content of chlorites hosted in transition zone rocks drilled at Hole 504B ranges up to ~ 0.8–1.0 wt. %, Alt et al. (1985) (the implications of these elevated Mn contents are further considered in the discussion section of Chapter 6.4) Irrespective of MnO content and grain texture, most chlorites contain < 0.2 wt. % TiO_2 and have negligible amounts of CaO and other alkali elements (Na_2O and K_2O commonly below detection limits), further confirming the predominance of 'true' chlorites in altered VQC facies rocks.

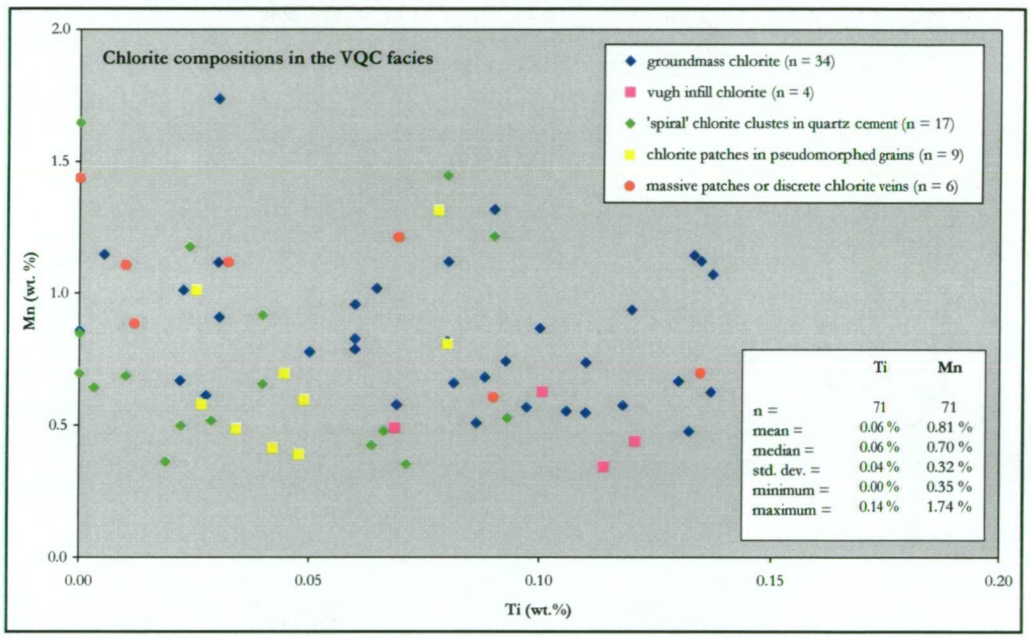

Figure 6.85: Irrespective of textural form, most VQC facies chlorites are moderately to strongly enriched in Mn relative to chlorites from other altered oceanic rocks. In fact, chlorites with > 1 wt. % MnO have rarely been reported from previous seafloor or ophiolite studies, suggesting that hydrothermal chlorites in the VQC facies are compositionally distinct and relatively unusual.

Chlorites in the regionally altered Sandell Bay Sheeted Dyke Swarm (n = 65) have a relatively restricted compositional range that partly overlaps with the VQC facies (Figure 6.86, Table A–4.3). These compositions also compare closely with analytical data reported by Griffin for chlorites hosted by other sheeted dyke complexes on Macquarie Island (Table A–4.17). However, unlike the VQC facies, SBSD chlorites are not strongly enriched in Fe (the average Fe # is 0.34). Most grains are classified as pychnochlorite, although three vuggy infill grains contain > 6.25 Si cations and may represent a mixed-layer chlorite-clay mineral such as diabinite. Several of these vuggy phyllosilicate minerals also contain slightly elevated levels of Ca + Na + K, further suggesting that they are not 'true' chlorites. Most of the SBSD chlorites have significantly less Mn than phyllosilicates from the VQC facies (the average MnO content of SBSD chlorite is 0.3 wt. %).

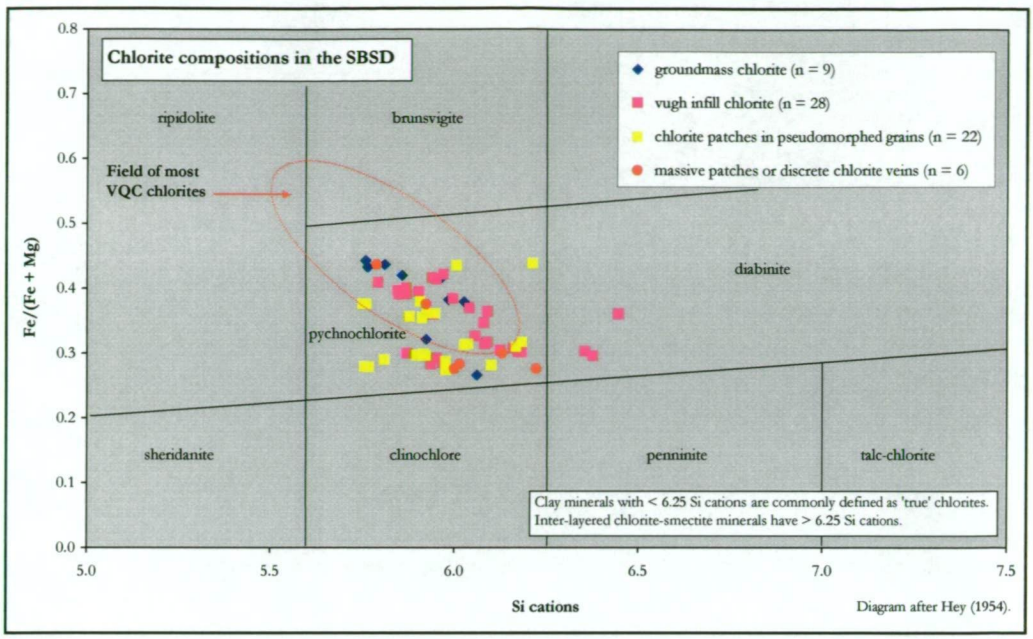

Figure 6.86: A modified Hey classification plot for hydrothermal chlorite from the Sandell Bay Sheeted Dyke Swarm (SBSD). The transition zone pillow basalts and sheeted dykes in this regional domain are mainly affected by widespread greenschist facies alteration. In contrast to the VQC facies, most chlorites here are Mg-rich (pychnochlorite) and show no obvious or well defined relationships between textural form and chemical composition.

Plagioclase and K-feldspar

Plagioclase commonly occurs as phenocrysts and groundmass laths in altered basalts and dykes from the VQC facies (n = 33) and the SBSD (n = 42). This electron microprobe study provided unequivocal evidence to support my petrographic observations (e.g., regarding the extent and intensity of alteration), and clearly indicated that most VQC facies plagioclase is strongly altered from its original magmatic composition (Table A–4.4). Griffin (1982) showed that igneous plagioclase in Macquarie Island basalt is Ca-rich (compositions mainly vary from An_{50} to An_{90}, i.e., labradorite to anorthite, and many grains are zoned), and has average Fe concentrations of 0.4–0.8 wt %. Some plagioclase crystals hosted in relatively less altered (regional) rocks from the SBSD have mostly retained their igneous-derived (Ca-rich) signatures (Table A–4.5), although the spectrum of SBSD compositions (anorthite contents) is quite broad and extends towards the albite field (Figure 6.87). In contrast, nearly all of the VQC facies plagioclase is highly enriched in Na (albite); most grains have compositions < An_{10}, clearly implying extensive (pervasive) hydrothermal alteration. Albitisation of igneous plagioclase has been widely reported from other studies of altered oceanic and ophiolitic basalts, and the range of VQC and SBSD plagioclase compositions are consistent with these previous data, e.g., Evarts and Schiffman (1983); Ishizuka (1989); Gillis and Thompson (1993); Alt et al. (1998).

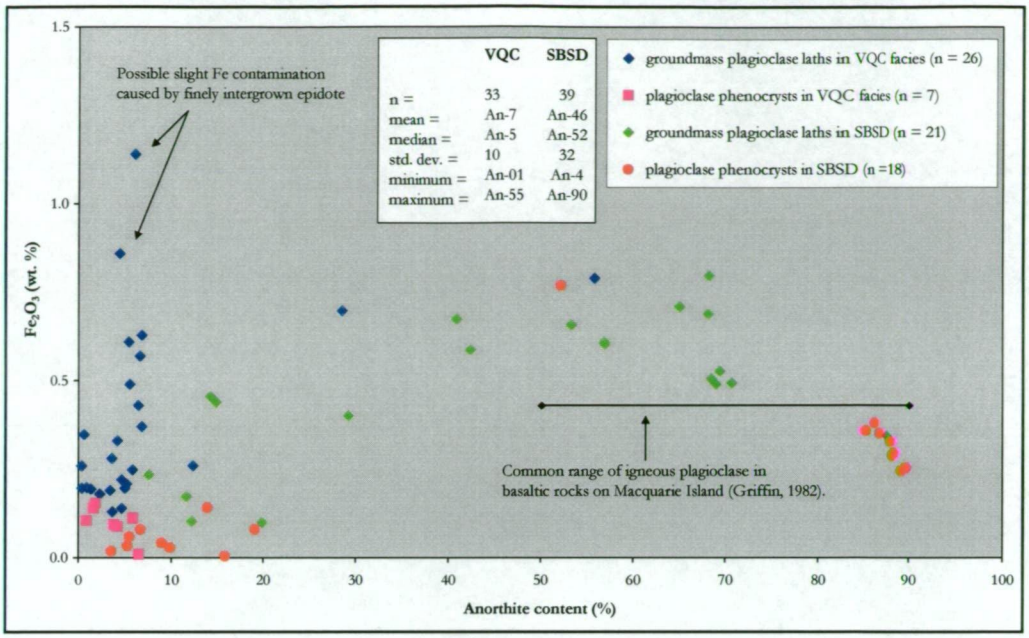

Figure 6.87: Hydrothermally altered plagioclase compositions from the Major Lake district, shown as a function of anorthite content and the abundance of Fe^{3+} in the crystal structure. Groundmass laths and phenocrysts in the vein and breccia, quartz-chlorite (VQC) facies are strongly enriched in Na, reflecting extensive albitisation during intense fluid–rock interaction in the Major Lake Fault Zone (discharge fluids). Plagioclase hosted in the Sandell Bay Sheeted Dyke Swarm (SBSD) is variably altered and spans a wider range of anorthite compositions, e.g., many crystals have retained their original Ca-bearing compositions and relatively elevated levels of Fe enrichment (igneous-derived).

Albite alteration is coupled with moderate Fe depletion in many plagioclase grains from the VQC facies. Most Na-rich crystals and laths contain < 0.3–0.5 wt. % Fe_2O_3, whereas Ca-rich plagioclase in the SBSD is relatively Fe-rich and commonly has > 0.5 wt. % Fe_2O_3. Anomalous Fe concentrations in several albite crystals from the East Mt Martin site (> 1 wt. % Fe_2O_3) are probably caused by slight contamination resulting from very finely intergrown epidote or chlorite (Figure 6.87). The concentrations of most other elements in VQC and SBSD plagioclase are insignificant, and mostly below detection limits, e.g., SrO and BaO.

Hydrothermally derived K-feldspar is a minor component in regionally altered rocks from the SBSD (n = 14), and occurs rarely in the VQC facies (n = 6; Table A–4.6 and A–4.7). Similar to plagioclase, K-feldspar alteration has diverse textural styles including narrow veinlets (< 2–3 mm-wide), discrete rims around vesicles, and irregularly shaped patches which have partly replaced primary plagioclase. The concentration of K_2O is relatively uniform in samples from the SBSD, and ranges from 15–17 wt. %. VQC facies K-feldspar have more variable compositions (~ 2–16 wt. %) which predominantly reflect slight to moderate levels of K enrichment in Na-altered plagioclase. Many K-feldspars in the Major Lake district are also enriched in Ba, with ~ 36 % of all SBSD analyses containing > 0.5 wt. % BaO (up to maximum levels of 1.4 wt. %). In comparison, concentrations of Na_2O, MgO, and SrO are relatively uniform and mostly insignificant (< 0.3 wt. %).

Epidote

Electron microprobe analyses of epidote (n = 26) focussed on samples from the Sandell Bay Sheeted Dyke Swarm (SBSD), as epidote is not abundant in the VQC facies (Chapter 6.3). Epidote structural formulae were calculated on the basis of 25 oxygen atoms, and assumed all Fe as Fe^{3+} (Table A–4.8). The pistacite content* of SBSD epidote is relatively uniform and varies from 0.20 to 0.30, with a mean of 0.25. These restricted compositions are similar to epidote analyses from many other greenschist facies rocks in the ocean crust, e.g., Evarts and Schiffman (1983); Ishizuka (1989); Gillis et al. (2001). However, the pistacite values are considerably less than those reported by Saccocia and Gillis (1995) for breccia hosted epidote (Type II) from the Kane Fracture Zone (mid-Atlantic Ridge) and the Hess Deep (East Pacific Rise); these mainly vary from ~ 0.6 to 1.0. In common with other hydrothermal epidote occurrences (e.g., Alt et al., 1986), microprobe data from the SBSD also have a well correlated 1:1 substitution trend of Fe^{3+} for octahedral Al. In addition, concentrations of other major elements are relatively homogeneous, e.g., CaO mostly ranges from 22.5–23.5 wt. % and average Fe_2O_3 is ~ 12 wt. % (Figure 6.88).

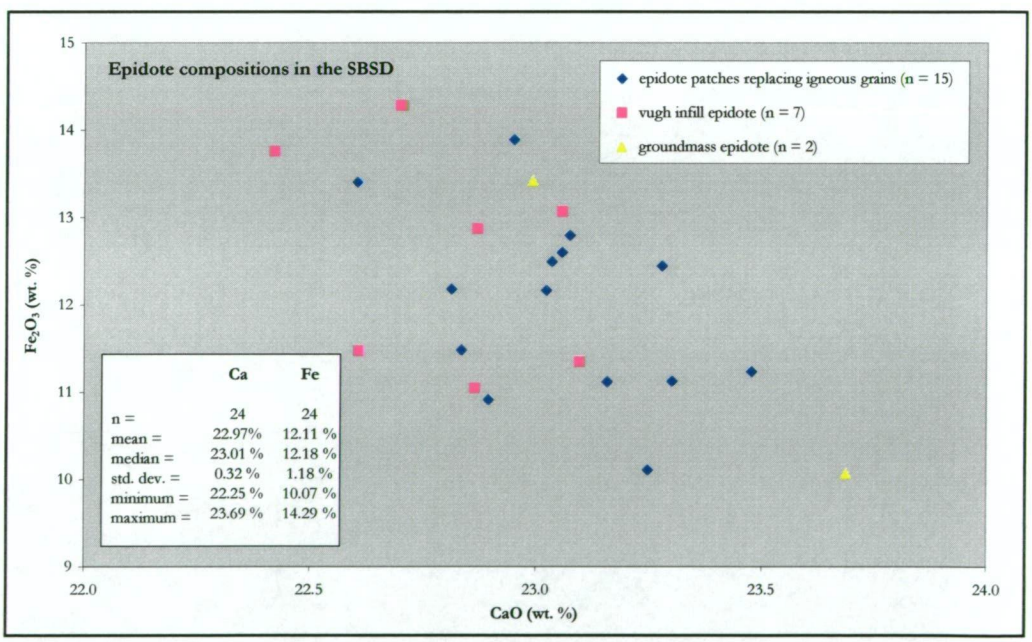

Figure 6.88: Ca versus Fe abundance for hydrothermally derived epidote from the Sandell Bay Sheeted Dyke Swarm. The Ca content of most epidote forms a relatively narrow and well defined range that corresponds with mean Fe levels ~ 12 wt. %. These relatively homogeneous compositions are similar to other epidote analyses reported from altered oceanic basalts, e.g., epidote in Hole 504B.

* pistacite content = $Fe^{3+} / (Fe^{3+} + Al^{VI})$

Alteration minerals from the foliated, massive chlorite facies in the Major Lake Fault Zone

Clay minerals

Mixed-layer clay minerals in two rock samples (n = 20) of the foliated, massive chlorite (FMC) facies from Sandell Bay creek (Major Lake Fault) were analysed with the electron microprobe (Table A–4.9). Compositions were determined for various textural forms, including partly altered groundmass patches, pseudomorphed olivine phenocrysts, and vuggy infill phases*. In contrast to trioctahedral chlorites in the VQC facies and the SBSD, clay minerals in the FMC facies are relatively enriched in silica (30–39 wt. % SiO_2), having > 6.25 Si cations per unit formula (Figure 6.89). Most analytical data plot within the diabinite field on the Hey diagram, which suggests that they are probably mixed-layer smectite-chlorite phases rather than true 'chlorites' (as previously mentioned in Chapter 6.3). Two compositionally distinct groups (also evident on the Hey diagram) correspond to different rock samples rather than any obvious or consistent textural variations.

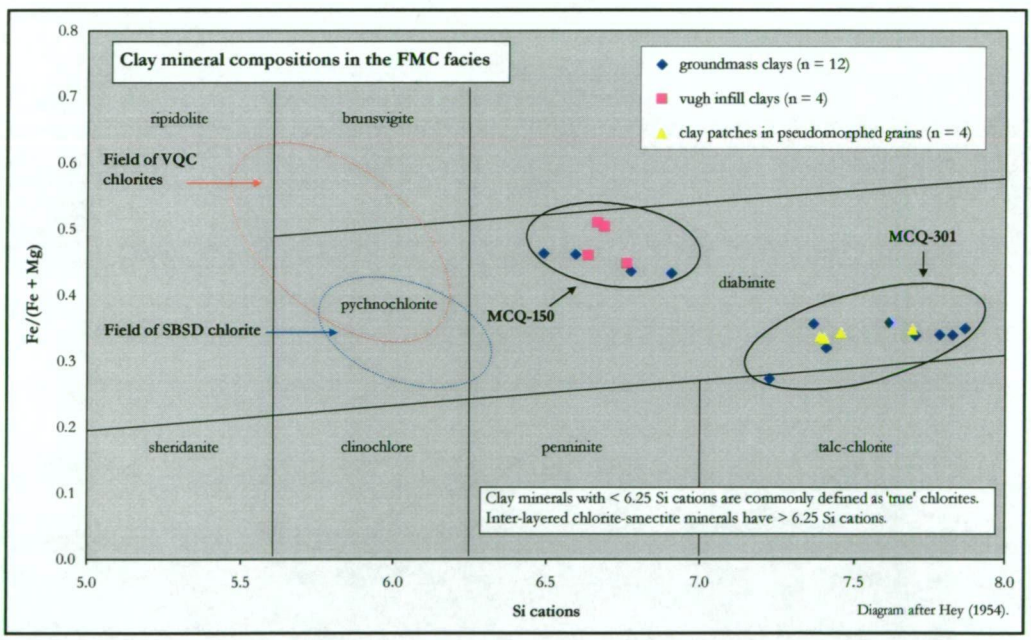

Figure 6.89: A modified Hey diagram for hydrothermally derived clay minerals in the foliated, massive chlorite (FMC) facies at Sandell Bay creek (Site 2A). All analyses have > 6.25 Si cations, and are thus likely to represent mixed-layer chlorite-smectite minerals (diabinite) rather than 'true' chlorites. Distinct data groups reflect two different rock samples, and are unrelated to textural variations. These phyllosilicate compositions are considerably different from chlorites in the VQC facies and the SBSD.

The Fe # of clay minerals in the FMC facies ranges from 0.27–0.51, although most clays are characteristically Mg-rich, i.e., mean Fe # = 0.39 (Figure 6.89). CaO abundance varies from 0.3 to 1.4 wt. %, with an average of 0.8 wt. %. These represent relatively enriched CaO compositions compared to phyllosilicates in the VQC facies and the SBSD, which probably

* Note that, unless stated otherwise, mineral formulae calculations and nomenclature are similar to those previously stated for similar minerals analysed from other facies, e.g., these clay mineral analyses were calculated on the basis of 28 oxygens and classified using the Hey terminology (similar to the VQC and SBSD chlorites).

reflects the greater abundance of inter-layered cationic species (Ca^{2+} + Na^{+} + K^{+}) in the crystal structure of these mixed smectite-chlorite minerals. The amount of MnO is relatively homogeneous in all clays analysed from the FMC facies (mean = 0.2 wt %), further contrasting with the VQC facies chlorite (relatively Mn-rich). Abundances of TiO_2, Na_2O, and K_2O in diabinite are negligible and rarely exceed 0.1 wt %.

There were no microprobe analyses undertaken on FMC facies samples from the Caroline Cove Fault Zone. However, Daczko et al. (2003) reported variable illite-smectite clay mineral mixtures (XRD analyses) from the Caroline Cove region, as well as other phyllosilicate minerals such as true chlorite and minor amounts of muscovite. Presumably, the mixed-layer clay minerals analysed by Daczko et al. (2003) were obtained from FMC facies rocks, whereas true chlorites and muscovite were likely sampled from the CQP facies block (although these authors give no detailed spatial information on sample locations). In general, clay compositions reported from the FMC facies (my study and other data) are also consistent with mixed-layer phyllosilicate minerals from other oceanic environments, e.g., clays reported from Hole 504B (Figure 6.83).

Alteration minerals from the massive and veined, chlorite-quartz-pyrite facies in the Caroline Cove Fault Zone

Mineral composition data (chlorite, plagioclase, epidote, and amphiboles) for the massive and veined, chlorite-quartz-pyrite (CQP) facies was obtained from eight Caroline Cove rock samples (Table 6.1), with similar study objectives as those previously outlined for the Major Lake district.

Chlorite

Very fine-grained chlorite is common in basaltic rocks from the CQP facies, and this microprobe study primarily focussed on determining these mineral compositions (n = 46). Chlorites in the CQP facies are moderately to strongly Mg-rich (clinochlore); the Fe # ranges between 0.18–0.42 and the mean and median = 0.33. Most analysed grains contain < 6.25 Si cations and have correspondingly low abundances of inter-layered cationic species such as Ca^{2+}, Na^{+}, and K^{+} (all typically < 0.2 wt. %). These data indicate that the CQP facies contains mainly 'true' trioctahedral chlorites of the pychnochlorite sub-group (Figure 6.90). However, the spectrum of microprobe data partially overlaps with the mixed-layer chlorite-smectite field (> 6.25 Si cations) and ~ 9 % of these phyllosilicates are classified as either diabinite or penninite (Figure 6.90). Compared to the VQC facies data, chlorite compositions in the CQP facies are more restricted and homogeneous, and lack strong Fe-enrichment. The Fe / Mg ratio compares most closely with chlorites from the uppermost (volcanic rock) alteration zone intersected by Hole 504B (with mean Fe # ~ 0.3 for the 0–300 m-deep crustal section, Alt et al., 1986), but is significantly different from basalt hosted chlorites in many other hydrothermal discharge systems (Figure 6.83). Chlorites in the CQP facies are also moderately enriched in Mn (mean ~ 0.6 wt

%, Figure 6.91) relative to typical ocean crust (mainly < 0.3 wt % MnO), although the average Mn content is lower than that of VQC facies chlorite.

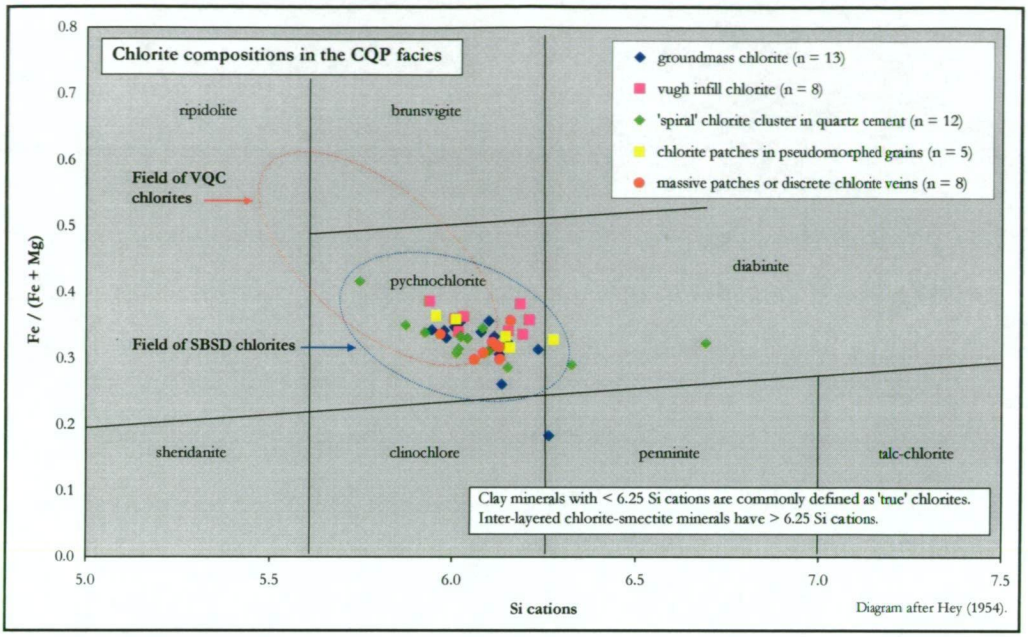

Figure 6.90: A modified Hey diagram for hydrothermal clay minerals hosted in the massive and veined chlorite-quartz-pyrite facies at Caroline Cove. Most clays are Mg-rich chlorites (pychnochlorite) that form a relatively tight data cluster and have no consistent relationship between chemical composition and textural form.

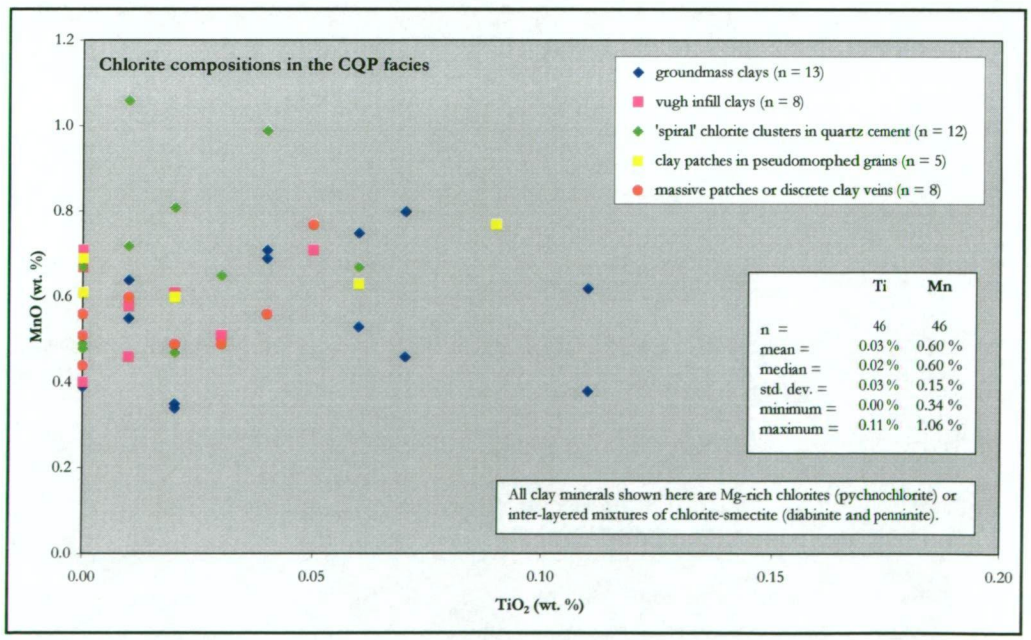

Figure 6.91: Mn concentrations in chlorites from the CQP facies are slightly to moderately enriched compared to most altered oceanic basalts (commonly 0.1–0.3 wt. % MnO). However, the mean MnO composition is less than that of chlorite hosted in the VQC facies. Most chlorites contain relatively insignificant levels of Ti, although several analyses in the raw dataset were omitted from this plot because their enriched TiO_2 concentrations (> 0.3 wt. %) were thought to reflect contamination from finely intergrown aggregates of titanite and leucoxene.

Multiple analyses were performed on the five main textural forms of chlorite identified in the CQP facies. Compositional data was collected for groundmass alteration phases, vesicle cements, quartz hosted crystal aggregates, partial grain pseudomorphs, and massive chlorite patches (Figure 6.90). Chlorite associated with vughs and quartz-cemented veins ('spiral'-type) are slightly more Fe-rich than altered groundmass or massive patches, although there are no well defined or consistent compositional groups, i.e., considerable data overlap. In general, these microprobe data provide no consistent evidence for any correlation between chlorite compositions and different textural forms.

Plagioclase

Plagioclase compositions were analysed from five samples of CQP facies basalt (n = 21), with mineral formulae calculated on the basis of 8 oxygen atoms (Table A–4.11). Irrespective of textural form, these grains are strongly enriched in Na (albitised) relative to magmatic plagioclase (> An_{50}); the common compositional range is An_0 to An_{20} (Figure 6.92).

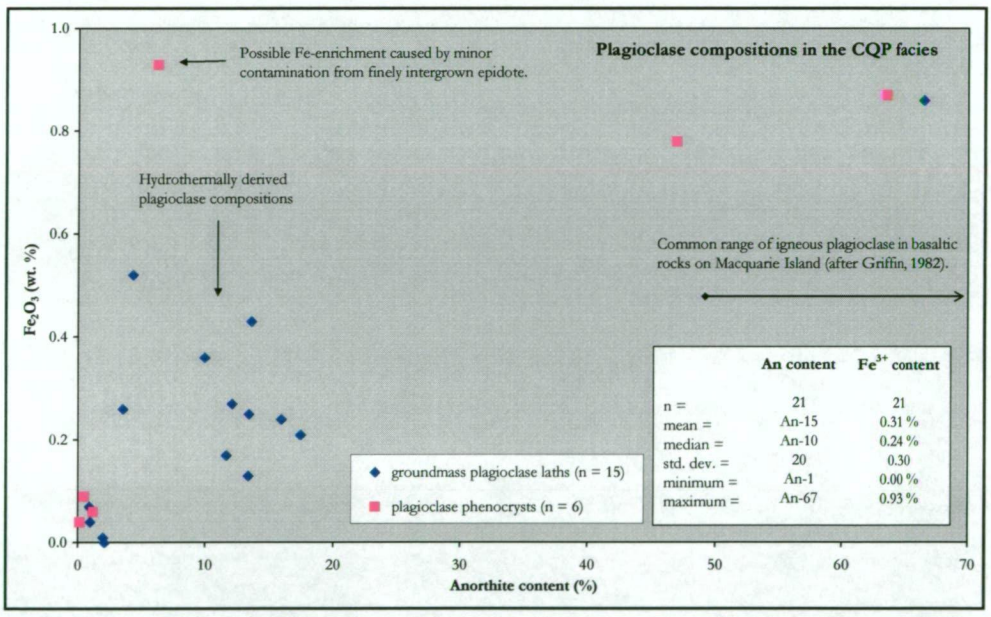

Figure 6.92: Hydrothermal plagioclase compositions from CQP facies rocks in the Caroline Cove area, plotted as a function of anorthite content and Fe^{3+} abundance. Extensive Na-rich alteration (albitisation) has affected most plagioclase, although primary crystal shapes are commonly well preserved. Intense albitisation is also associated with decreased Fe concentrations, typical of many altered oceanic basalts.

Similar to the alteration effects noted for the VQC facies, strong albitisation is coupled with slight Fe depletion, e.g., most CQP facies albite contains < 0.50 wt. % Fe_2O_3 (mean = 0.31 wt. %). However, the intensity and distribution of Na-enrichment and Fe-depletion is not homogeneous, and many irregularly shaped patches and narrow crystal rims (both phenocrysts and groundmass laths) have remnants of their primary igneous compositions, i.e., they remain partly Ca-rich (An_{40} to An_{70}). Altered plagioclase contains insignificant levels of K (< 0.2 wt. %) and, unlike many rocks from the Major Lake Fault, hydrothermally derived K-feldspar was not

identified in the CQP facies. Other minor elements such as Mg, Sr, Ba, and Ti are also relatively insignificant components of CQP facies plagioclase, commonly occurring below detection limits (Table A–4.11).

Epidote

Epidote is a common component of the CQP facies, and is considerably enriched (in abundance) relative to other focussed alteration assemblages on Macquarie Island (Chapter 6.3). Groundmass and vein hosted epidote analysed during this electron microprobe study (n = 14; Table A–4.12) showed relatively homogeneous pistacite compositions ranging from 0.21–0.29, with a median of 0.26 (Figure 6.93).

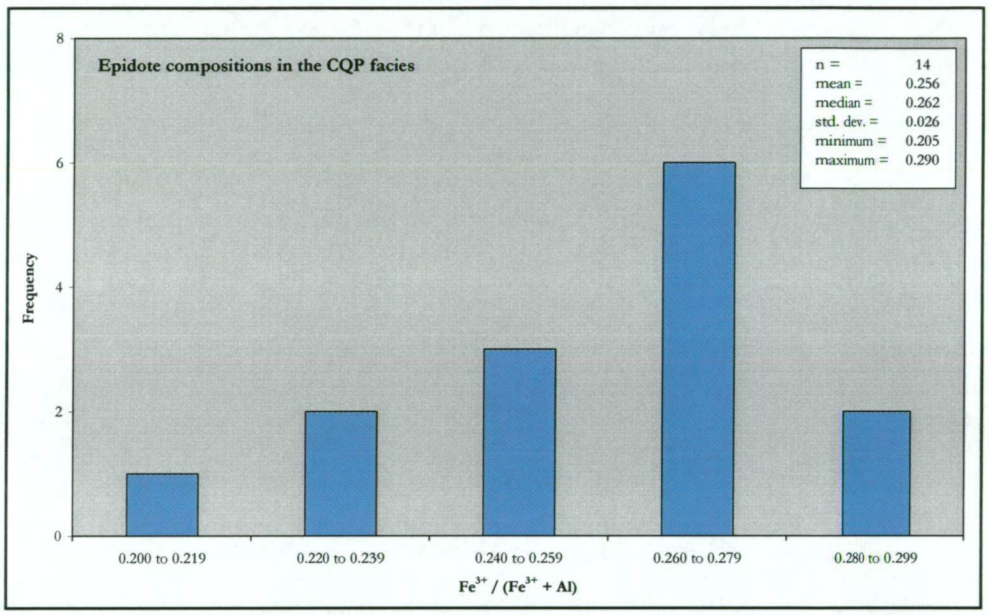

Figure 6.93: Frequency distribution plot for the Fe / (Fe + Al) ratio (pistacite content) of epidote from the CQP facies at Caroline Cove. The narrow compositional spectrum is very similar to other epidote analyses reported from Macquarie Island, and suggests that the hydrothermal conditions and processes which formed epidote were relatively homogeneous for both fault zone and regional assemblages.

There is also a strong coupled relationship between Fe and Al. Fe^{3+} has commonly substituted for octahedral Al in these crystal lattices, and most analytical data plot along a well correlated 1:1 substitution line (Figure 6.94). Minor differences in epidote compositions appear unrelated to textural variations, i.e., vein and groundmass epidote do not have significantly different compositions. The restricted compositional spectrum in the CQP facies is similar to epidote from the Sandell Bay Sheeted Dyke Swarm, and is also well correlated with other epidote compositions from Macquarie Island reported by Griffin (1982)*. These relatively homogeneous compositions indicate that there are no significant differences between epidotes

* The pistacite content of Macquarie Island epidote analysed by Griffin (1982) ranged from 0.13 to 0.29 and averaged 0.25. Griffin's epidote samples were collected mainly from the regionally altered pillow basalt domains at a number of locations across the island, including Soucek Bay and Unity Point (refer to Appendix 4, section E of Griffin's 1982 PhD thesis for further details).

from fault hosted and regional alteration domains, and may imply that hydrothermal conditions and processes were broadly similar.

Amphiboles

Amphibole minerals occur sporadically in some altered CQP facies rocks, mainly forming very fine-grained crystals which have partly replaced irregularly shaped patches of earlier-formed groundmass chlorite. Many amphibole analyses undertaken during this study were rejected because the compositional data indicated probable mixed (contaminated) mineral assemblages comprising variable abundances of chlorite and amphibole, i.e., finely intergrown aggregates. Consequently only four amphibole compositions are reported here (Table A–4.13).

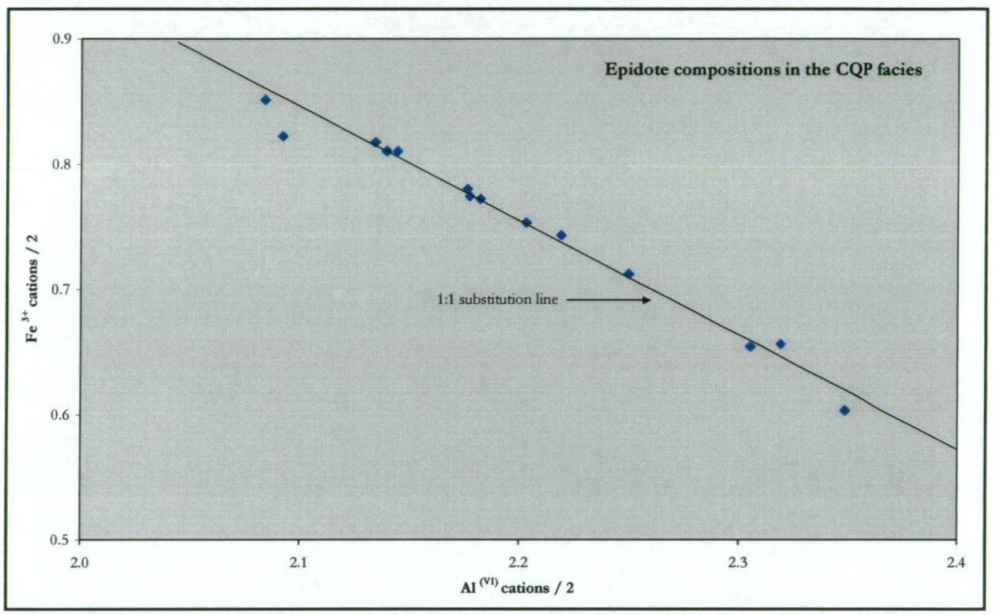

Figure 6.94: Molar substitution plot of Fe^{3+} vs. octahedral Al for hydrothermal epidote in the CQP facies. The analytical data have a strong negative correlation which indicates common 1:1 substitution of Fe for Al, a common feature of hydrothermally derived epidote hosted in altered oceanic rocks.

These mineral compositions were calculated on the basis of 23 oxygens and assumed all Fe as FeO. All amphiboles in the CQP facies have > 7.5 Si cations, indicating actinolite (Mg # > 0.5 for three samples) or ferro-actinolite (Mg # < 0.5 for one sample) compositions (Figure 6.95). The CaO content ranges from 9.7–11.1 wt % and three samples also have > 1 wt. % MnO. Other major components such as TiO_2, Na_2O, and K_2O occur at relatively insignificant concentrations (< 0.2 wt. %). These compositions are within the range of analytical data reported by Griffin (1982) for actinolite hosted in various sheeted dyke complexes on Macquarie Island, but have relatively enriched Si contents compared to magnesio- and actinolitic-hornblende compositions reported by Davidson et al. (2004), e.g., $Si^{IV} = 7.0 – 7.4$; n = 8.

Alteration minerals from the vein-dominated, prehnite-zeolite facies in the Sellick Bay Fault Zone

Mineral chemistry data for Ca-rich zeolites, prehnite, and pumpellyite was obtained from two rock samples (polished thin-sections) from the vein-dominated, prehnite-zeolite (VPZ) facies (Table 6.1). This part of the electron microprobe study effectively amounted to a reconnaissance investigation primarily designed to identify enigmatic alteration minerals (e.g., pumpellyite) and characterise the zeolite-bearing vein assemblages. Thus, only a relatively limited amount of compositional data was collected for the VPZ facies, i.e., considerably less than the VQC and CQP facies.

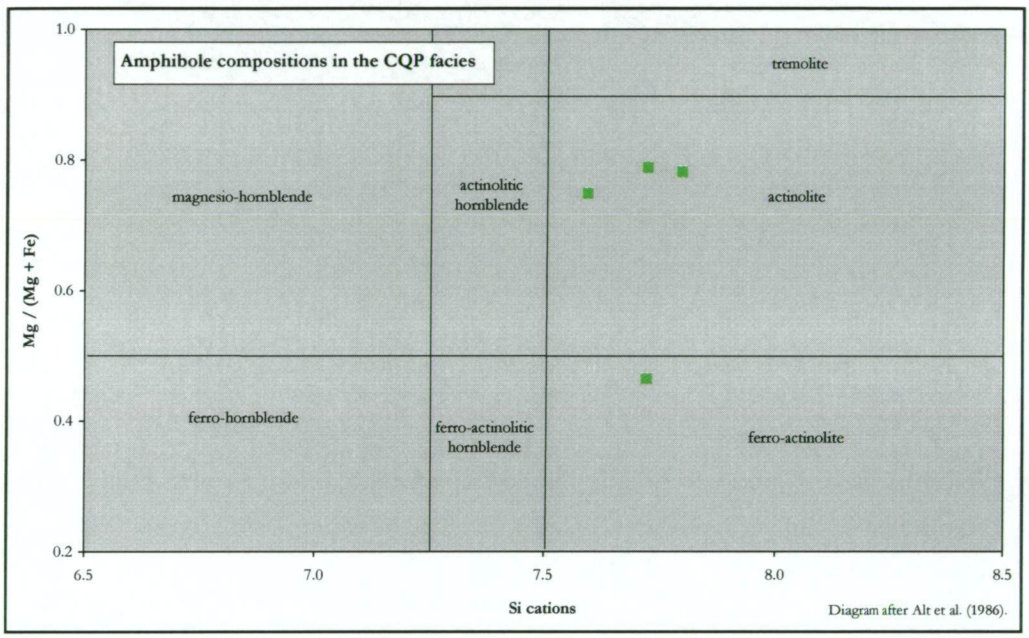

Figure 6.95: Actinolite is the main amphibole mineral in the CQP facies at Caroline Cove. It occurs sporadically throughout the altered basaltic groundmass, and most is finely intergrown with irregularly shaped patches and aggregates of sheeted chlorite.

Zeolite minerals

Zeolite vein compositions for sample MCQ-275 (n = 7) were calculated on the basis of 72 oxygen atoms, with all Fe assumed as Fe^{2+} (FeO). These analyses indicated that Ca-rich laumontite is the dominant zeolite species in the VPZ facies (Table A–4.14), consistent with the petrographic evidence, e.g., crystal habits and textures. Vein hosted laumontites have relatively homogeneous compositions, with CaO comprising ~ 11–12 wt. % and Al_2O_3 ~ 21–22 wt. %. Alkali elements such as Na and K are uniformly low (< 1 wt. % for their respective oxide forms), and the concentrations of TiO_2, FeO, and MnO are commonly below detection limits. Laumontite in the VPZ facies is compositionally similar to previous analytical data for Ca-zeolites from Macquarie Island (Griffin, 1982), and also compares favourably with laumontite analyses reported from Hole 504B (Alt et al., 1986; Ishizuka, 1989).

For comparative purposes, vein hosted zeolites (n = 9) were analysed from several regional alteration domains on Macquarie Island (Table 6.1). These included the western pillow basalt sequence at Caroline Cove, and the Sandell Bay Sheeted Dyke Swarm near Major Lake foreshore (Site 2B). Most regional zeolites are compositionally similar to those from the VPZ facies (dominantly laumontite), although minor Na-bearing zeolite minerals such as thomsonite and analcite were also identified (Table A–4.14). Zeolite compositions in regionally altered basalts on Macquarie Island were rigorously investigated by Griffin (1982), and interested readers are referred to this work for more substantive information.

Prehnite

Groundmass and vein hosted prehnite is a diagnostic component of the VPZ alteration assemblage, and also occurs widely throughout some regional domains on Macquarie Island (Griffin, 1982). During this electron microprobe study, prehnite was analysed in discrete rock samples from the VPZ facies (n = 10), the Sandell Bay Sheeted Dyke Swarm (n = 5), and the western pillow basalt sequence at Caroline Cove (n = 4). Mineral formulae were calculated on 22 oxygen atoms, and assumed total Fe as Fe_2O_3 (Table A–4.15).

Prehnites in the VPZ facies have relatively homogeneous compositions, e.g., CaO ranges from 25–27 wt. % and most Fe_2O_3 from 2.5–5.5 wt % (Table A–4.15). The Fe / (Fe + Al^{VI}) ratio varies from 0.13 to 0.34, with the mean = 0.21 (Figure 6.96). The abundance of Fe in prehnite is negatively correlated with Al, indicating that Fe^{3+} substitutes for octahedral Al in the crystal lattice. The uniform concentrations of CaO, Fe_2O_3, and Al_2O_3 in VPZ facies prehnite are broadly consistent with nineteen analyses reported by Griffin (1982). Elements such as Ti, Mn, Mg, Na, and K are relatively insignificant components of VPZ facies prehnite, and their respective oxide forms comprise < 0.1 wt. % of most analyses (Table A–4.15).

The compositions of other prehnite grains (regional domains) determined during this project are not as uniform as the analytical data from the VPZ facies. Although most CaO compositions are similar (CaO = 25–27 wt. %), the concentrations of Fe_2O_3 and Al_2O_3 are distinctly more variable (Table A–4.15). Prehnites from the Sandell Bay Sheeted Dyke Swarm are particularly Fe-poor; some vein hosted grains contain < 1 wt. % Fe_2O_3 and have correspondingly low Fe / (Fe + Al) ratios of < 0.05 (Figure 6.96). Prehnite veins from the western pillow basalt sequence at Caroline Cove have a broader range of Fe and Al compositions than the VPZ facies, and several grains are relatively enriched in Fe_2O_3(up to 7.71 wt. %). As for the VPZ facies, other elemental components occur in negligible amounts. These consistent compositional variations (especially for Fe) suggest that hydrothermal conditions and processes associated with the formation of prehnite are considerably more heterogeneous across broad regional domains, relative to focussed structural zones.

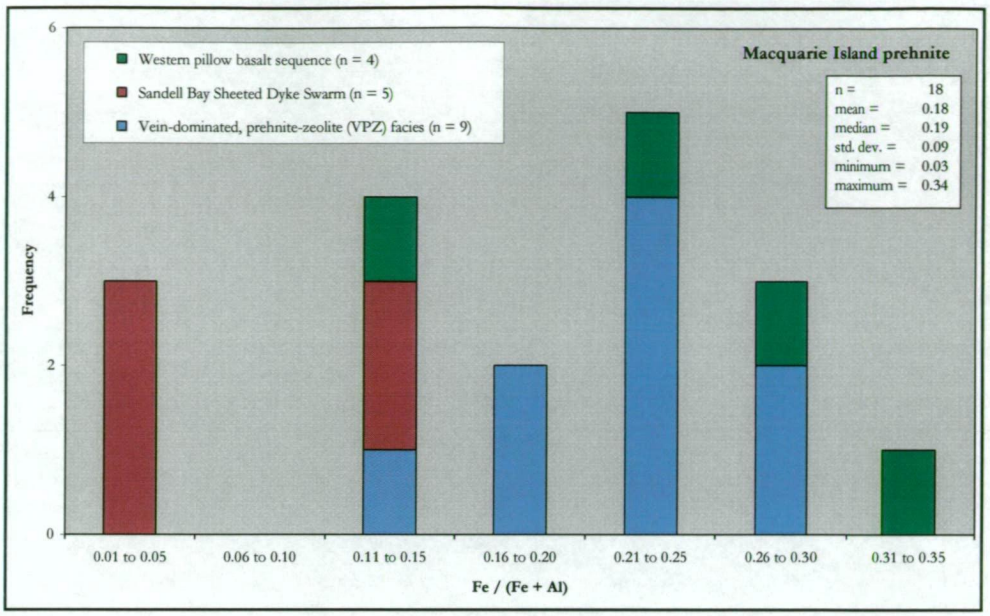

Figure 6.96: Frequency histogram for the Fe / (Fe + Al) ratio of hydrothermal prehnite hosted in focussed and regional alteration zones on Macquarie Island. Prehnite veins in the Sandell Bay Sheeted Dyke Swarm are relatively Fe-poor compared to those from Sellick Bay and Caroline Cove. The statistical information shown here is for all prehnite analyses from this study.

Pumpellyite

Pumpellyite is a relatively rare alteration mineral in oceanic rocks and, prior to this study, it had not previously been identified on Macquarie Island, e.g., Griffin (1982); Goscombe and Everard (2001). Few investigations have reported pumpellyite as a major component of seafloor hydrothermal systems (e.g., Mevel, 1981), although it has been more commonly noted from some ophiolites, e.g., the Jurassic Del Puerto ophiolite in central California (Evarts and Schiffman, 1983). During this study pumpellyite was identified as a minor (but significant) component of the VPZ facies from the Sellick Bay Fault Zone. It is commonly intergrown with prehnite (Chapter 6.3), and mainly occurs as a vein, groundmass, or phenocryst hosted phase in some intensely altered basalts, e.g., discrete selvages around massive prehnite veins.

Ten spot analyses were undertaken on vein and groundmass pumpellyite crystals from altered VPZ facies basalt (Table A–4.16). Mineral formulae were calculated following the method of Coombs et al. (1976), which assumes sixteen cations and total Fe as FeO (Fe^{2+}). Most pumpellyite in the VPZ facies is compositionally homogeneous, with total Si cations close to the ideal six atoms per formula unit. Concentrations of the main elemental components are very similar, with CaO comprising ~ 21.5–22.5 wt. % and FeO ranging from 6.5–8.5 wt. %. Al_2O_3 has the most variation, comprising ~ 21–25 wt. %. The similarity of Fe / (Fe + Al) ratios (Figure 6.97) and the absence of correlated trends between Fe and Al suggests that, unlike pumpellyite in the Del Puerto ophiolite, there no substantial substitution of Fe for Al (Evarts and Schiffman, 1983). Slight antithetic relationships link Mg (~ 1–3 wt. %) and Fe compositions in several grains, possibly indicating limited substitution between these elements; however, the

trends are not consistent for all analyses. Concentrations of other elements such as Mn, Ti, Na, and K are relatively insignificant in VPZ facies pumpellyite, e.g., MnO comprises < 0.3 wt. %, and TiO_2, Na_2O, and K_2O mainly occur below detection limits (< 0.1 wt. %).

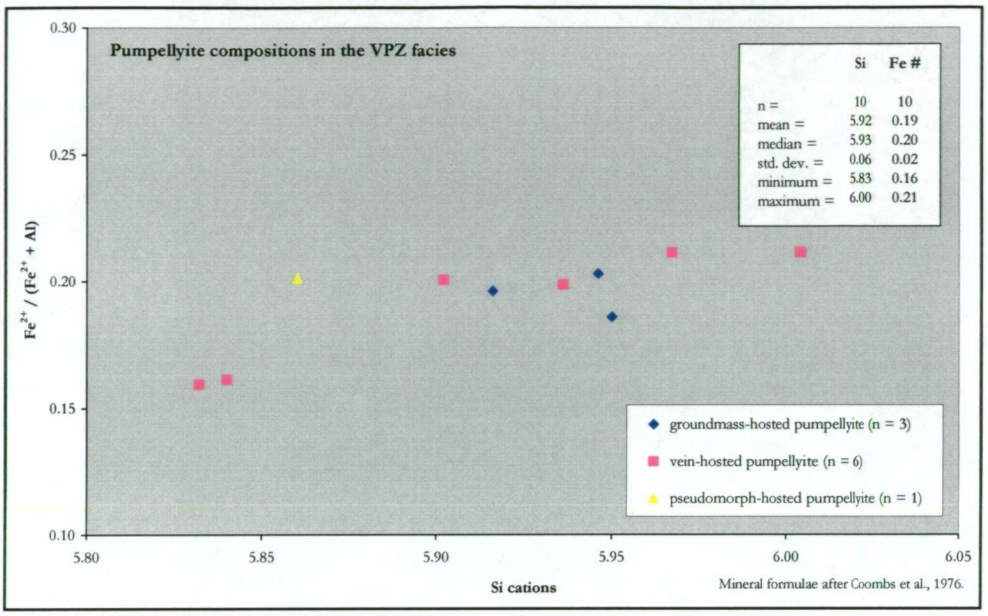

Figure 6.97: The vein-dominated, prehnite-zeolite facies in the Sandell Bay Fault Zone commonly hosts very fine-grained pumpellyite which is characterised by a restricted range of Fe / (.Fe + Al) values. The relatively homogeneous chemical compositions are similar for each of the main textural forms of pumpellyite, and are consistent with pumpellyite analyses from the Del Puerto ophiolite in California (Evarts and Schiffman, 1983).

Discussion and analysis: Geochemistry of alteration minerals

Overview

Phyllosilicate minerals rich in Fe and Mg are commonly formed during the interaction of hydrothermal fluids and basaltic rocks in the upper oceanic crust. Diverse clay mineral species are stable across the broad temperature range of subseafloor environments (~ 50° to 400° C at < 0.5 kbar), although smectite, chlorite, and various inter-layered clays are most abundant (Bevins et al., 1991). The dominant mafic phyllosilicate mineral generally varies as a function of crustal depth; relatively low temperature clays such as saponite are most abundant in the upper volcanic rock package (e.g., 0–500 m crustal depth in the well documented section of Hole 504B; Alt et al., 1986) whereas mixed-layer smectite-chlorite and chlorite become progressively more common in the underlying transition zone to sheeted dyke complex. These depth-related compositional variations mainly reflect the consistent downward increase in temperature (broad-scale recharge pattern) which characterises the oceanic hydrothermal system (Chapter 4).

Previous research into alteration assemblages formed in focussed hydrothermal discharge (upflow) zones has shown that chlorite is typically the most abundant phyllosilicate mineral, e.g., Delaney et al. (1987), Gillis and Robinson (1988), Teagle and Alt (2004). Chlorite is also a common component of many pipe-like alteration bodies in ophiolite terranes, e.g., the Troodos

ophiolite in Cyprus (Richards et al., 1989). These distinctly shaped alteration pipes, which commonly underlie massive sulfide deposits of variable size and shape (e.g., Haymon et al., 1989), are interpreted as relict conduits for structurally controlled hydrothermal fluids. Chlorite associated with altered rocks in modern and ancient discharge zones is characterised by a diverse compositional spectrum. In particular, the ratio of Fe to Mg varies widely, consistent with the solid solution behaviour of chlorite (Saccocia and Seyfried, 1994). Commonly, chlorites formed in altered basalts affected by discharge-style fluids are significantly enriched in Fe, i.e., they commonly have Fe #'s > 0.5 (Figure 6.83). However, despite the expected absence of Mg from evolved hydrothermal fluids (Alt, 1995), Mg-bearing chlorites are also prevalent in some upflow zones, e.g., some parts of the active TAG hydrothermal mound on the mid-Atlantic Ridge (Honnorez et al., 1998). This broad compositional range is significantly more diverse than that of basaltic chlorites formed during regional alteration processes (recharge-related). Chlorites (and other clay minerals) in most regionally altered oceanic rocks are moderately to strongly enriched in Mg, which largely reflects the chemical compositions of their seawater-dominated parent fluids and primary protoliths (Saccocia et al., 1994).

The wide range of basaltic chlorite compositions (Fe # values) associated with hydrothermal upflow zones suggests that the complex evolutionary processes are controlled by multiple fluid and rock parameters. Shikazono and Kawahata (1987), in a study of the hydrothermal ore deposits of the Kuroko district (Japan), attributed the wide compositional range (in chlorites) to variations in fundamental hydrothermal fluid conditions, and to important processes associated with fluid movement and mixing. In particular, the temperature, pressure, pH, and total sulfur content of the fluid, combined with variations in the relative abundances of chemically evolved (Fe-rich) hydrothermal fluids and entrained seawater (Mg-rich), were all considered to influence chlorite compositions. Saccocia and Seyfried (1994) also showed that aqueous chlorite solubility is strongly affected by temperature, pH, and the Fe/Mg ratio of the hydrothermal fluid. Their detailed geochemical modelling suggested that a range of chlorite compositions may result from different physical processes which potentially influence the temperature and composition of hydrothermal fluids (Figure 6.98). Conductive cooling and seawater entrainment were interpreted as especially important evolutionary processes (Saccocia and Seyfried, 1994).

Multiple stages of phyllosilicate mineral precipitation will also directly affect fluid compositions during the life cycle of the hydrothermal system. The dominant alteration reactions and mineral assemblages will vary both temporally and spatially as fluid compositions continue to evolve due to on-going fluid–rock interactions. Compelling evidence for distinct temporal and spatial variations in fluid compositions is provided by multi-stage alteration sequences that occur in many seafloor hydrothermal systems. For example, Humphris and Tivey (2000) described both Fe- and Mg-bearing chlorites from different parts of the TAG mound, which may have formed during different temporal stages (although clear timing relationships were not observed). In many seafloor systems, widespread chloritisation events are followed by subsequent episodes of

silicification and sulfide-rich alteration (e.g., at the Galapagos Ridge, Embley et al., 1988), which further reflect distinct hydrothermal stages with variable fluid compositions, temperatures, and water–rock processes.

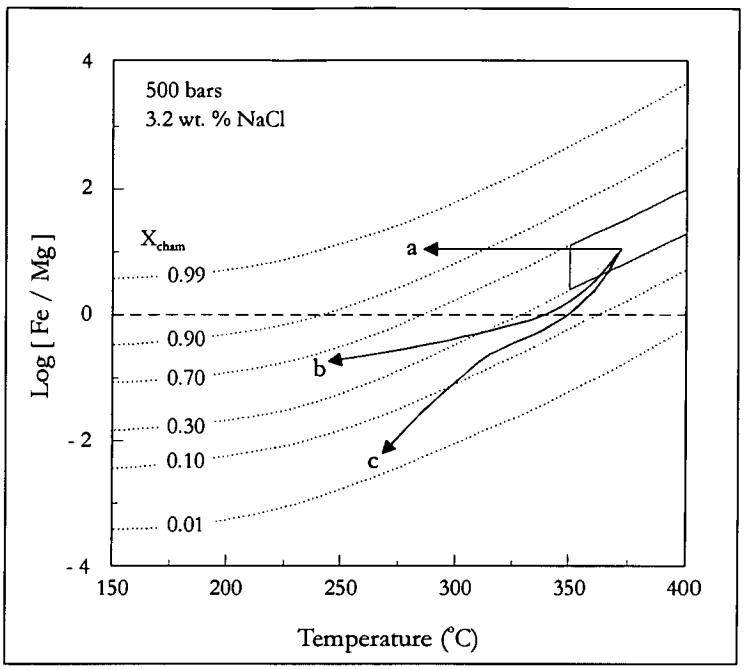

Figure 6.98: The chemical composition of aqueous hydrothermal fluids in equilibrium with chlorite is strongly influenced by the fluid temperature and chlorite composition. This diagram shows how a range of Fe/Mg concentrations may result from different reaction processes in the subseafloor environment. The shaded box represents the expected range of temperatures, aqueous Fe/Mg concentrations, and chlorite compositions in the deep mid-ocean ridge reaction zone. Path (a) shows the change in chlorite composition (X_{cham}) as fluids undergo conductive cooling during hydrothermal upflow. Path (b) depicts the formation of Mg-rich chlorite for small degrees of mixing between evolved hydrothermal fluids (Fe-rich) and seawater (Mg-rich), and the progression to more Fe-rich chlorite with increased mixing. Line (c) shows that Mg-rich chlorite is expected to form during mixing if pyrite equilibrium levels are maintained (diagram modified from Saccocia and Seyfried, 1994).

Chlorite compositions in focussed alteration zones and regional domains on Macquarie Island

Trioctahedral chlorites of the clinochlore (Mg-rich) – chamosite (Fe-rich) series (Bayliss, 1975) are the most abundant phyllosilicate minerals in diagnostic alteration facies at the Major Lake (VQC facies) and Caroline Cove (CQP facies) Fault Zones, and in the Sandell Bay Sheeted Dyke Swarm. These chlorites are texturally diverse, and commonly occur as irregularly shaped patches in altered groundmass minerals and phenocrysts, infilling primary vesicles, and cementing massive veins. In contrast, mixed-layer smectite-chlorite is the characteristic phyllosilicate mineral in the foliated, massive chlorite (FMC) facies, although it also occurs in similar textural habits. The range of chlorite and clay mineral compositions from Macquarie Island (this study) is consistent with the main field of MORB hosted phyllosilicates from other oceanic and ophiolite sites (Figure 6.83).

The chemical composition of many chlorites from focussed alteration zones in the VQC and CQP facies are relatively similar and well correlated, e.g., compare Figure 6.84 with Figure 6.90. However, the compositional range of VQC facies chlorite is more diverse and spans a significantly broader range of Fe /Mg ratios than other chlorites from Macquarie Island (Table 6.4). The VQC facies contains many Fe-rich chlorites (including ripidolite and brunsvigite sub-species), whereas only Mg-bearing chlorites or inter-layered clay minerals (chlorite-smectite) occur in the CQP and FMC facies, and the SBSD (dominantly pychnochlorite compositions). The enriched Fe/Mg chlorite ratios for the VQC facies are similar to those documented from many other focussed upflow zones in oceanic (and ophiolitic) environments, e.g., the Kane Fracture Zone on the mid-Atlantic Ridge (Delaney et al., 1987) and the Oman ophiolite (Haymon et al., 1989). These similarities provide further evidence that hydrothermal systems in the Major Lake Fault were dominated by highly evolved fluids typically associated with active upflow zones, i.e., discharge of high temperature hydrothermal fluids. In comparison, the more uniform and Mg-rich chlorite compositions from the CQP, FMC, and SBSD suggests that less evolved fluids (seawater-dominated?) may have played a more significant role in their evolution.

Table 6.4: Comparison of chlorite Fe #'s for fault zone alteration assemblages on Macquarie Island.

Statistics	VQC facies	CQP facies	FMC facies	SBSD	Griffin (1982) chlorite data
n	71	46	20	65	48
mean	0.43	0.33	0.39	0.35	0.33
median	0.44	0.33	0.36	0.35	0.35
std. dev	0.09	0.04	0.07	0.05	0.08
minimum	0.29	0.18	0.27	0.27	0.08
maximum	0.61	0.42	0.51	0.44	0.45
% of chlorite Fe #'s > 0.5	32 %	0 %	11 %	0 %	0 %

Note: The chlorite compositional data obtained from Griffin (1982) is presented in Table A-4.17. These represent chlorites from several regional greenschist facies domains in central and southern Macquarie Island, such as the Zone BVI Hurd Point association.

Chlorites in the VQC and CQP facies are relatively Mn-rich (their respective means = 0.81 and 0.60 wt. % MnO) compared to most phyllosilicate minerals in altered oceanic crust (typically < 0.2 wt. % MnO). These average Mn contents are also significantly greater than the concentrations in hydrothermally derived chlorites from the Sandell Bay Sheeted Dyke Swarm, which has mean MnO ~ 0.3 wt. %. However, the elevated Mn compositions in the VQC and CQP facies are similar to levels for clay minerals associated with stockwork sulfide mineralisation in the transition zone rocks (basalts and sheeted dykes) of Hole 504B (Figure 6.99). Alt et al. (1986) showed that MnO compositions in hydrothermal phyllosilicates

(including smectites and chlorites) were mostly < 0.2 wt. % throughout the uppermost 1000 m of the ocean crust, apart from a narrow section of the upper transition zone*. Peak MnO concentrations of up to ~ 0.9 wt. % are intimately associated with sulfide alteration between 635–654 mbsf in Hole 504B. The distinctive Mn enrichment at this crustal level was interpreted as evidence for mixing between evolved hydrothermal fluids ascending from deeper crustal levels (likely enriched in Mn), and more oxidised (less evolved) fluids derived from seawater (Alt et al., 1986). Based on the distribution of Mn relative to crustal depth in Hole 504B, elevated Mn contents in VQC and CQP facies chlorites are unlikely to be locally derived or sourced solely from unevolved fluids. Thus, these distinct spatial variations provide further evidence for the genetic influence of deep-seated hydrothermal fluids in fault zones on Macquarie Island. In addition, enriched levels of Mn in the VQC facies (relative to CQP) may indicate comparatively less dilution of the primary Mn signature due to mixing with oxidised fluids, i.e., seawater-dominated fluids played a greater role in the origin of the CQP facies at Caroline Cove.

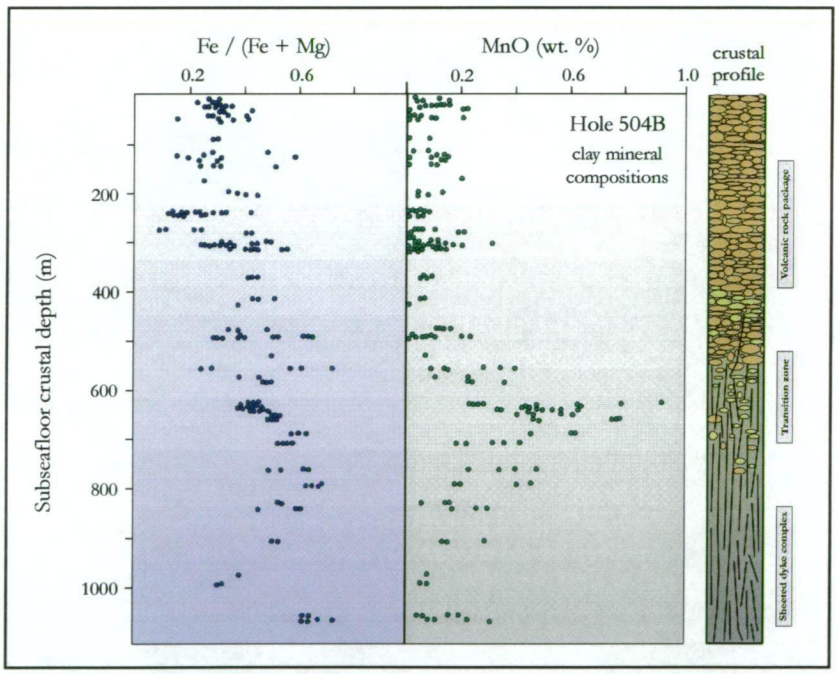

Figure 6.99: Phyllosilicate mineral compositions (mainly saponite and chlorite) in the DSDP Hole 504B section drilled into 5.9-m.y.-old oceanic crust ~ 200 km south of the Costa Rica Rift in the eastern Pacific Ocean. This figure shows variations in Fe # and MnO values for clay minerals relative to crustal depth, and especially highlights the considerable Mn enrichment associated with stockwork sulfide alteration in the dyke to basalt transition zone package. The elevated Mn contents in Hole 504B are similar to chlorite compositions from the VQC and CQP facies on Macquarie Island (diagram modified after Alt et al., 1986).

The Mg-rich chlorites in the CQP facies are well correlated with those in the Sandell Bay Sheeted Dyke Swarm (SBSD), forming overlapping compositional groups on their respective Hey diagrams (Figure 6.90). 'True' chlorites are dominant in both domains (< 6.25 Si cations), although minor mixed-layer clays (Mg-rich diabinite) also occur, i.e., inter-layered clays are more

* Similar depth-related variations in Mn enrichment were also noted for whole-rock compositions in the Hole 504B section by Alt et al. (1986).

abundant than in the VQC facies. These compositional affinities suggest that some physico-chemical conditions (e.g., fluid temperatures and compositions) and fluid–rock interactions were relatively similar, although differences in Mn concentrations (i.e., not enriched in the SBSD) attest to the likely influence of evolved hydrothermal fluids in the Caroline Cove Fault. In comparison, clay minerals in the FMC facies contain > 6.25 Si cations and are classified as mixed-layer phyllosilicates, i.e., there are no 'true' chlorite compositions. Many FMC facies clays also contain a significantly greater proportion of inter-layer cations (primarily Ca^{2+}). These compositional variations suggest that the FMC facies mainly formed from relatively less evolved and low temperature fluids than the VQC and CQP facies, and the SBSD (Kristmannsdottir, 1979).

Consistent geological and mineralogical evidence (Chapter 5 and 6) indicates that the VQC and CQP facies are products of focussed hydrothermal alteration formed in fluid discharge (upflow) zones. However, the chlorite compositional data (this study), together with other mineral assemblage variations, suggests some fundamental differences in their respective hydrothermal systems. A previous wide-ranging study of chlorites in altered breccias from the mid-Atlantic Ridge (Kane Fracture Zone) and the East Pacific Rise (Hess Deep) generated an important insight into the evolution of critical fluid parameters and their related mineral suites (Saccocia and Gillis, 1995). Data and interpretations presented by Saccocia and Gillis (1995) provide a potential analogue to link mineral assemblages with locally specific hydrothermal conditions in the Major Lake and Caroline Cove Fault Zones. Based on variations in the distribution and abundance of different groundmass minerals, Saccocia and Gillis (1995) defined two types of hydrothermal breccias from the Kane Fracture Zone and the Hess Deep (rock samples collected by dredging and submersible operations). Type I breccias are dominated by Fe-chlorite, quartz, minor pyrite, and titanite, whereas the Type II breccias contain Mg-rich chlorite, epidote, quartz, abundant pyrite, and titanite (Saccocia and Gillis, 1995). These respective mineral assemblages are remarkably similar to those in the VQC (Type I analogue) and CQP (Type II analogue) facies on Macquarie Island. Geochemical models of mineral stability relationships in these assemblages indicates that the concentration of H_2S plays a critical role in determining the alteration mineral suite, and particularly influences the composition of the dominant chlorite species, i.e., either Fe- or Mg-rich chlorite (Figure 6.100). Combined with relevant fluid inclusion data (e.g., estimated fluid salinities), and an understanding of active vent fluid chemistry (measured *in situ* at each ridge), the Type I breccias are interpreted to have formed from high salinity (up to 10 wt. % NaCl) and H_2S-depleted fluids, whereas the hydrothermal fluids that formed the Type II breccias were relatively enriched in H_2S but had significantly lower salinities (< 0.1–5.6 wt. % NaCl) (Saccocia and Gillis, 1995).

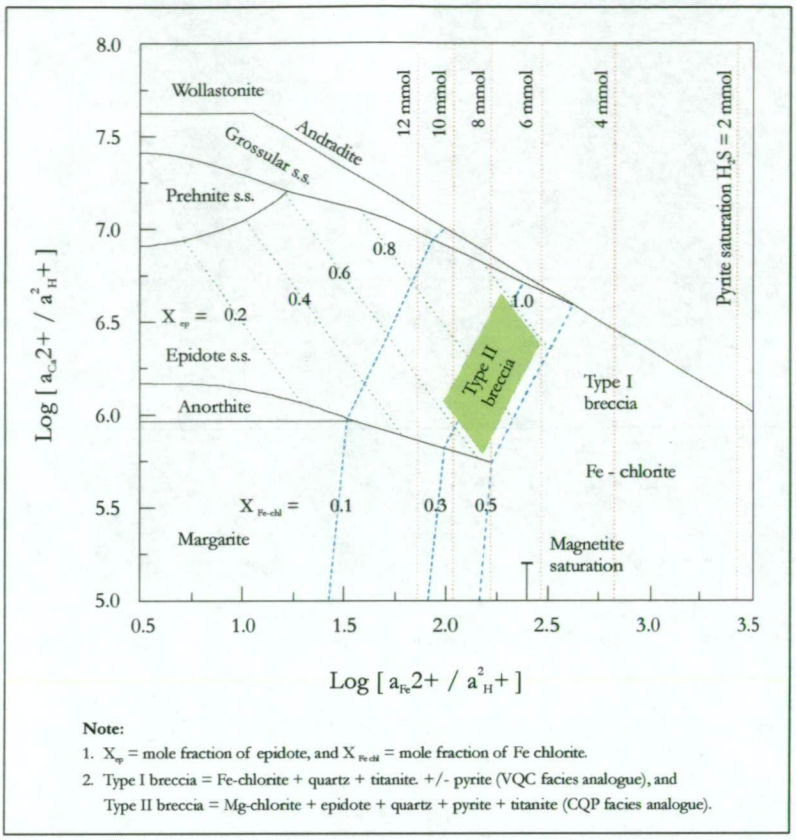

Figure 6.100: Phase diagram for the CaO–FeO–Al_2O_3–Fe_2O_3–SiO_2–H_2O system at 350° C and 0.5 kb (quartz saturation), with oxygen fugacity defined by a dissolved H_2 concentration of 0.1 mmol. The mole fraction of epidote (Xep) in the epidote-clinozoisite solid solution series is shown (dotted green lines), and the chlorite stability field is contoured as a function of chlorite composition. Fe-chlorite is stable at $X_{Fe\text{-}chl} > 0.5$ and pyrite saturation levels (dotted orange lines) are plotted as a function of aqueous (dissolved) H_2S. Increased H_2S shifts the pyrite saturation line from Fe-chlorite formation (i.e., the Type I breccias from the MARK and Hess Deep) into the stability field where epidote co-exists with Mg-rich chlorite ($X_{Fe\text{-}chl} < 0.5$), forming Type II chlorite-bearing breccias. These phase relationships show how variations in critical hydrothermal parameters such as the H_2S concentration can directly influence the alteration mineral assemblage. Analogous aqueous fluid variations may account for the mineral assemblage differences between the vein and breccia, quartz-chlorite (VQC) facies in the Major Lake Fault Zone (Type I assemblage), and the massive and veined, chlorite-quartz-pyrite (CQP) facies at Caroline Cove (Type II assemblage). This diagram reproduced from the work of Saccocia and Gillis (1995), and based on thermodynamic data obtained from Helgeson et al. (1978), Bird et al. (1984), Johnson et al. (1992), Saccocia and Seyfried (1993), and Saccocia and Seyfried (1994).

Research carried out by Saccocia and Gillis (1994), combined with other work by Saccocia and Seyfried (1994) and Saccocia et al. (1994), provides a valid geochemical explanation for the formation of Mg-rich chlorite in zones of hydrothermal fluid upflow, i.e., from parent fluids that have low levels of Mg. Thus, the range of hydrothermal fluid parameters and chlorite-forming processes outlined in Figure 6.100 could account for the presence of Mg-rich chlorite in the CQP facies (Caroline Cove Fault). However, Mg-chlorites may also be precipitated by mixing relatively pristine seawater (Mg-rich), variably entrained within the upper volcanic rock package, with chemically evolved (modified and Fe-bearing) hydrothermal fluids (Teagle and Alt, 2004). Fluid mixing processes leading to the formation of Mg-rich chlorites have been implicated in the formation of altered basalts from other seafloor hydrothermal systems, e.g., massive sulfide stockworks the Galapagos Ridge (Embley et al., 1988), and their ancient ophiolite analogues (Richards et al., 1989). Importantly however, fluid mixing processes are commonly associated

with net gains in whole-rock Mg (Saccocia and Gillis, 1995), which provides a potential means to discriminate between different processes involved in the formation of Mg-chlorite (further discussed in Chapter 7 and Chapter 9).

Chlorite geothermometry

Compositional data obtained from my electron microprobe study was used to calculate precipitation temperatures for chlorite. Chlorite geothermometry is mainly based on observed variations in crystal composition and structure relative to formation temperature, and several empirical- and thermodynamic-based approaches have previously been employed (De Caritat et al., 1993). The main empirical geothermometers, commonly calibrated using temperature data from *in situ* (borehole) measurements in active geothermal fields, rely upon the widely observed correlation between increased levels of tetrahedral Al (Al^{IV}) and fluid temperature (Cathelineau and Nieva, 1985; Cathelineau, 1988). Chlorite geothermometers have been applied in diverse locations and geological environments (e.g., Zimak, 1999; Chang-Bock et al., 2002; Zaccarini et al., 2003), although comparative studies have shown that no individual method performs satisfactorily across the spectrum of hydrothermal conditions and parameters (De Caritat et al., 1993).

Previous studies using location-specific chlorite geothermometers have reported consistent and geologically valid temperatures, e.g., Bevins et al. (1991) showed that the temperature range for chlorites in altered basalts in Wales and North Greenland was compatible with expected formation temperatures from the associated suite of alteration minerals (using the empirical geothermometer devised by Cathelineau and Nieva, 1986; and Cathelineau, 1988). However, other studies have been less successful, with some chlorite-based geothermometers producing diverse and geologically unrealistic temperatures for compositionally similar data (De Caritat et al., 1993). Consequently, the use of chlorite geothermometers as a valid means for estimating precipitation temperatures has been challenged in the scientific literature. Particular problems are associated with chlorites formed in diagenetic environments (< 150°–200° C), where the effects of contamination from mixed-layer clay minerals (metastable assemblages) are difficult to compensate (Shau and Peacor, 1990; Jiang et al., 1994). Chlorites formed in high pressure environments (> 2 kb) are also unlikely to be suitable for geothermometry calculations, because the effects on Al^{IV} substitution (for Si cations) are poorly known for these conditions (Kranidiotis and MacLean, 1987). Thus, due caution is required when evaluating the results of any chlorite geothermometry work, and the estimated temperatures need to be assessed with regard to the geological setting and likely hydrothermal conditions. If possible, chlorite geothermometry should be verified by alternative methods and independent estimates of temperature. This is especially the case if absolute temperature data are required, as the inherent uncertainty of chlorite geothermometry (commonly ±50° C) makes it best suited to assessing relative temperature variations.

This chlorite geothermometry study used compositional data from the VQC, FMC and CQP facies, and the Sandell Bay Sheeted Dyke Swarm. Given the caveats outlined by other workers (e.g., De Caritat et al. 1993 and Jiang et al. 1994), I decided to apply several of the most common empirical techniques (based on the published literature) and compare the results. Bearing in mind the relevant geological context (e.g., the primary subseafloor environment, associated alteration minerals, and likely hydrothermal conditions), this comparative study allowed me to evaluate and select the most appropriate method. The four geothermometry techniques trialled here (Table 6.5) are mainly based on the observation that the Al^{IV} content of chlorite consistently increases with both temperature and Fe #; hence, several of the temperature equations employ a correction factor based on the relationship between Al^{IV} and Fe # to account for these effects (Appendix 4.3).

Table 6.5: Summary of the chlorite geothermometers evaluated for Macquarie Island chlorites.

Authors	Year	Location	Temperature equation	Correction factor
Kranidiotis and MacLean	1987	Phelps Dodge VHMS deposit, Matagami, Quebec	$T = 106 \times Al^{IV}_{corr.} + 18$	$Al^{IV}_{corr.} = Al^{IV} + (0.7 \times Fe\ \#)$
Cathelineau	1988	Los Azufres (Mexico) and Salton Sea (California) geothermal fields	$T = -61.92 + (321.98 \times Al^{IV}$	n/a
Zang and Fyfe	1995	Igarape Bahia gold deposit, Carajas, Brazil	$T = 106.2 \times Al^{IV}_{corr.} + 17.5$	$Al^{IV}_{corr.} = Al^{IV} - 0.88 \times (Fe\ \# - 0.34)$
Xie et al.	1997	Barberton greenstone belt, South Africa	**a.** $T = 321.98 \times [Al^{IV} + 1.33 \times (0.31 - Fe\ \#)] - 61.92$ **b.** $T = 321.98 \times [Al^{IV} - 1.33 \times (Fe\ \# - 0.31)] - 61.92$	**a.** where Fe # < 0.31 **b.** where Fe # > 0.31

The initial trials of the selected geothermometers were undertaken on chlorite compositions from the VQC facies (Appendix 4.3). Given the interpreted origin of the VQC facies and the other alteration minerals associated with chlorite (e.g., quartz, titanite, pyrite etc.), the results of this comparative study indicated that the method of Zang and Fyfe (1995) produced the most consistent and geologically valid temperature estimates (Table 6.6).

Table 6.6: Comparison of chlorite geothermometers applied to the VQC facies data.

Statistics (n=71)	Kranidiotis and MacLean, 1987	Cathelineau, 1988	Zang and Fyfe, 1995	Xie et al., 1997	Modified Zang and Fyfe method (this study)
mean	270° C	605° C	229° C	553° C	237° C
median	264° C	605° C	230° C	554° C	238° C
std. dev.	26° C	63° C	16° C	46° C	15° C
minimum	217° C	470° C	188° C	414° C	188° C
maximum	321° C	737° C	262° C	637° C	266° C

Using the Zang and Fyfe (1995) procedure, chlorite palaeo-temperatures ranged from ~ 190–260° C (the estimated uncertainty of this geothermometer is ± 25° C). In comparison, the geothermometers of Cathelineau (1988) and Xie et al. (1997) commonly yielded temperatures

from ~ 400–700° C, which were considered unrealistic given the geological environment and related evaluation criteria, e.g., associated mineral assemblages. The geothermometer of Kranidiotis and MacLean (1987) provided mean formation temperatures about 40° C higher than those of Zang and Fyfe (1995), and also had a wider temperature range and significantly higher maximum (321° C compared to 262° C).

In an attempt to improve the applicability of the Zang and Fyfe (1995) geothermometer to the Macquarie Island chlorite data, and so enhance the accuracy of the temperature estimates, their original equation was slightly modified. The modification used here is based on a similar method employed by Zang and Fyfe (1995) to alter the Kranidiotis and MacLean (1987) geothermometer and make it more applicable to their local data (from the Igarape Bahia gold deposit in Brazil; notice the similar form of these two equations in Table 6.4). This modification process involved regression analysis of the Al^{IV} and Fe # compositions for chlorites in each alteration facies, so that the required components of the Al^{IV} correction factor (Table 6.4) could be independently obtained for each facies (Figure 6.101).

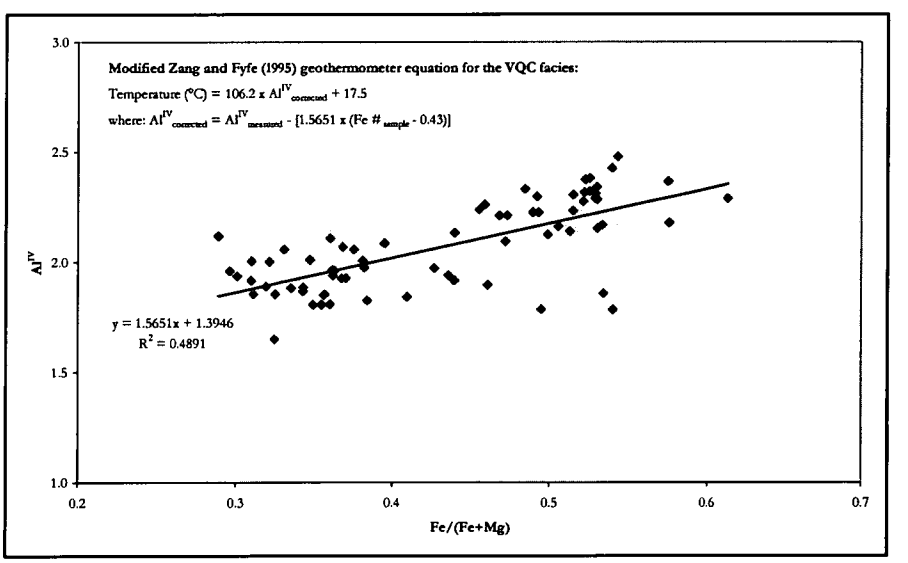

Figure 6.101: Regression analysis of Al^{IV} content vs. Fe # for individual chlorites from the vein and breccia, quartz-chlorite (VQC) facies. The x-intercept of the VQC facies regression line is used in the Al^{IV} correction factor equation (shown above), along with the average Fe # value for VQC facies chlorite (mean Fe # = 0.43 for VQC facies). By undertaking separate regression analyses for each alteration facies (the VQC, CQP, FMC, and SBSD), and combining this information with their average Fe # values (which differ slightly for each), I was able to modify the original Zang and Fyfe (1995) geothermometry equation and make it locally specific for each alteration facies.

Separate regression analyses for the VQC, CQP, FMC, and SBSD provided specific x-intercept values which, when combined with mean chlorite Fe # values for each group, permitted the original Zang and Fyfe (1995) equation to be locally adjusted (Appendix 4.3). In general, the palaeo-temperatures obtained using my modified equations were slightly higher than the corresponding temperatures estimated with the original Zang and Fyfe (1995) method, although most varied by < 10° C. Given its apparent suitability and rigorous use of locally specific constraints (i.e., separate regression line x-intercepts and mean Fe # values), the modified Zang

and Fyfe (1995) geothermometer was independently applied to chlorite data from the VQC, FMC, and CQP facies, and the regional SBSD domain (Appendix 4.3). Frequency histograms and statistics for estimated chlorite palaeo-temperatures are shown in Figure 6.102 to Figure 6.105. The statistical information provides a high degree of confidence in the suitability of the chlorite geothermometer for the VQC and CQP facies and the SBSD, i.e., ~93–95 % analytical precision and very low standard errors (1°–2° C). However, the FMC data are significantly less precise (73 % analytical precision and 6° C standard error), which likely reflects the presence of mixed-layer clay minerals rather than compositionally 'true' chlorites.

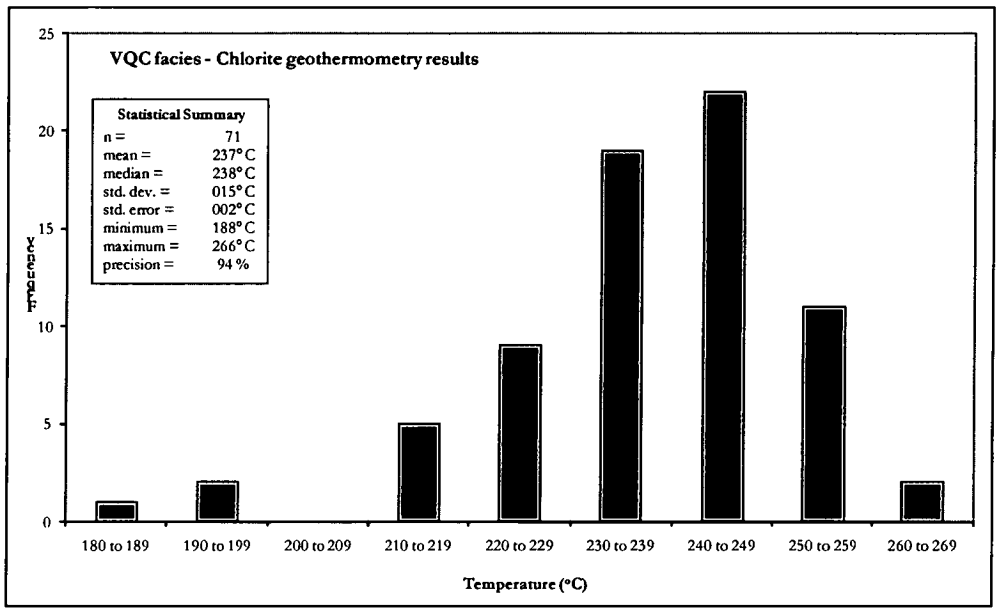

Figure 6.102: Frequency histogram of chlorite formation temperatures estimated for the VQC facies, using facies-specific data in the Zang and Fyfe (1995) geothermometry equation. Analytical precision equates to one standard deviation from the mean (as defined in Rollinson, 1993).

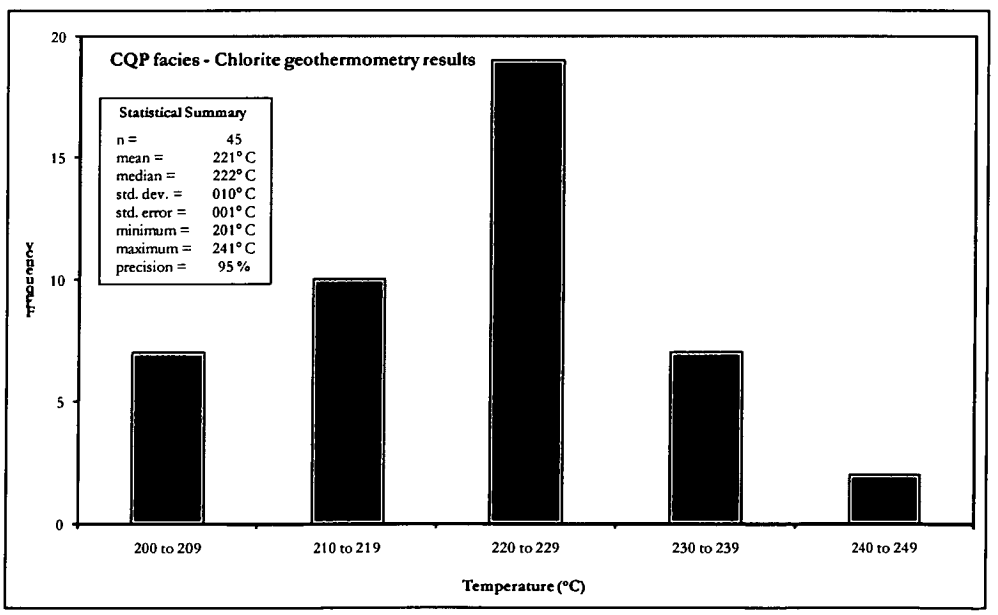

Figure 6.103: Frequency histogram of chlorite formation temperatures estimated for the CQP facies using the modified Zang and Fyfe (1995) geothermometer.

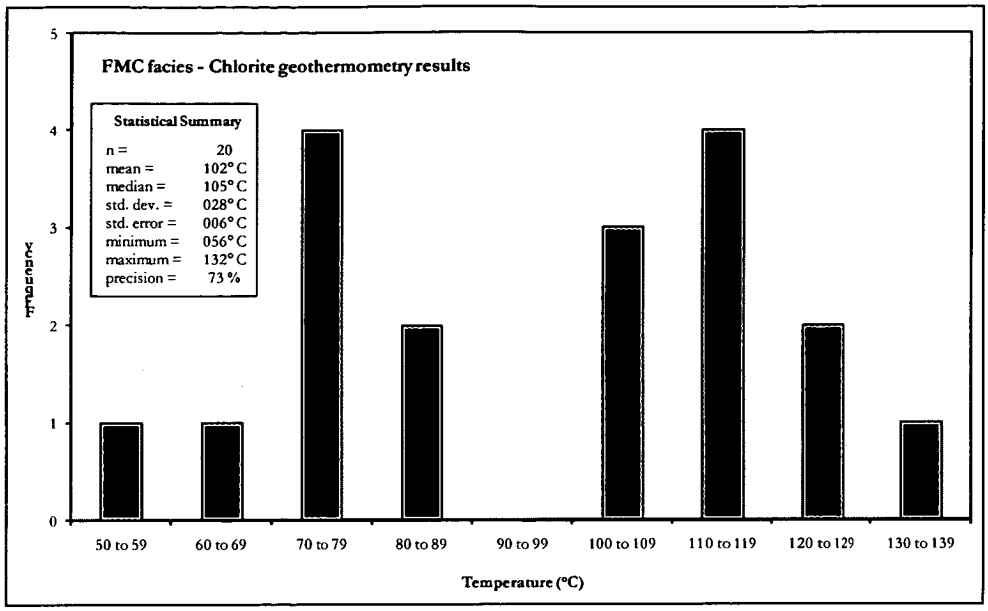

Figure 6.104: Frequency histogram of chlorite formation temperatures for the FMC facies in the Major Lake Fault Zone. These temperatures were calculated using facies specific data for the x-intercept value and mean Fe # for the Al^{IV} correction factor in the Zang and Fyfe (1995) geothermometer.

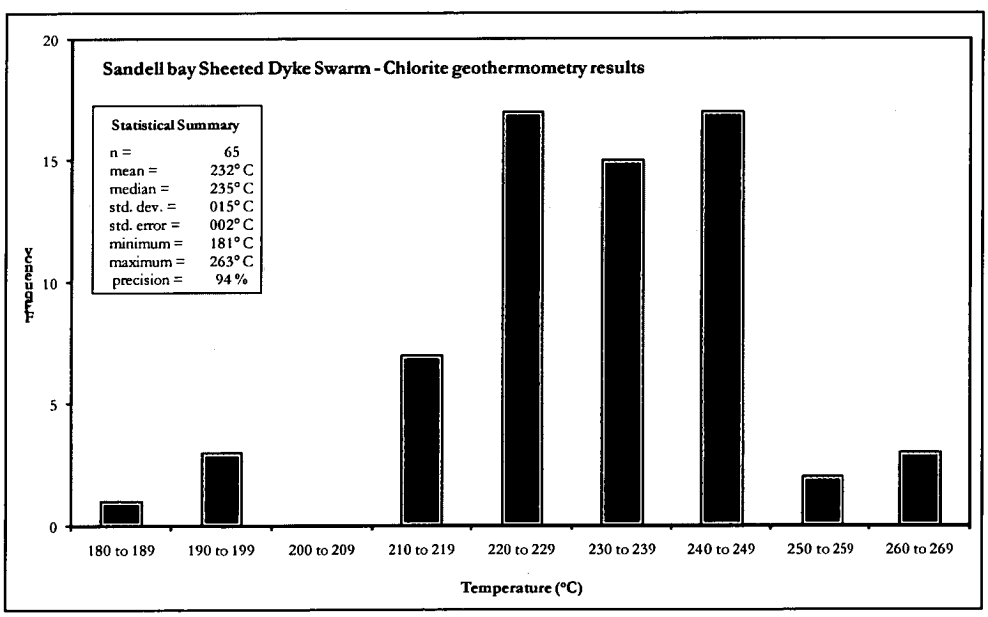

Figure 6.105: Frequency histogram of chlorite formation temperatures from the regionally altered Sandell Bay Sheeted Dyke Swarm domain. These temperatures were calculated using the modified Zang and Fyfe (1995) geothermometer.

In summary, the results of my geothermometry study indicated that:

i. The calculated formation temperatures for chlorites in the VQC and CQP facies are relatively well constrained and occur within the expected stability range for the subseafloor hydrothermal environment. Most VQC facies chlorite (~ 85 %) formed at 220°–260° C (mean = 237° C), whereas formation temperatures are consistently ~ 15–20° C lower for the CQP facies, with ~ 95 % of these chlorites ranging from 200°–240° C (mean = 221° C). These estimated temperatures are largely consistent with previous

studies which have shown that chlorite is typically the dominant phyllosilicate mineral in hydrothermal systems at temperatures of 200°–240° C (Kristmannsdottir, 1979; Cathelineau, 1988). In most hydrothermal environments chlorite is stable up to ~ 275° C, with amphibole minerals (such as actinolite) dominant at higher temperatures, especially > 300° C (Bird et al., 1984; Schiffman and Fridleifsson, 1991). The calculated VQC and CQP facies temperatures are also consistent with the mid to lower range of fluid temperatures independently measured from other mid-ocean ridge discharge systems, e.g., by *in situ* measurements of active vent fluids and fluid inclusions in hydrothermal precipitates (de Ronde, 1995; Scott, 1997; Kelley and Fruh-Green, 2000). Thus, the estimated palaeo-temperatures for the VQC and CQP facies are considered geologically valid (within error of the geothermometry technique), and representative of local hydrothermal conditions during the precipitation of chlorite in the Major Lake and Caroline Cove Fault Zones;

ii. There are no well defined correlations between formation temperatures and chlorite textures (of which five main forms exist; Chapter 6.3) in either the VQC or CQP facies. When plotted against the percentage of 'pure' chlorite (using the method of Bettison and Schiffman, 1988)*, the different textural styles form a consistent and overlapping group with no obvious trends or patterns (Figure 6.106 and 6.107). Although the groundmass and quartz hosted chlorite phases typically span the widest range of temperatures and compositions, this is most likely to represent a statistical anomaly, i.e., these dominant styles were subjected to the most number of discrete analyses. Hence, this study has provided no evidence that different chlorite styles are associated with discrete temperature intervals, suggesting that hydrothermal conditions are unlikely to be an important control on textural forms. However, the results of the chlorite compositional study (Bettison and Schiffman, 1988) have clearly supported the Hey diagram classification, and recognised that most chlorites in the VQC and CQP facies have high levels of purity, i.e., mostly < 10 % smectite clay contamination;

iii. Chlorites from the regionally altered Sandell Bay Sheeted Dyke Swarm (SBSD) mainly formed over a similar temperature range as the VQC and CQP facies. Most SBSD chlorites (86 %) precipitated from their parental fluids between 210°–250° C (mean = 232° C), suggesting that regional hydrothermal conditions in this part of the sheeted dyke section were mostly analogous to those associated with early-stage alteration (i.e., Stage I chloritisation) in the focussed fault zone assemblages. The SBSD temperature range is also consistent with chlorite stability work for other hydrothermal systems (outlined above), including previous interpretations of regional (recharge-related) fluid–

* As further explained in Appendix 4.3, the percentage of inter-layered clay contamination in the chlorite crystal structure can be expressed as a ratio between two end-member compositions, ie., 'pure' chlorite = 100 % chlorite, and 'pure' saponite = 0 % chlorite.

rock interactions on Macquarie Island, e.g., Cocker et al. (1982), Griffin (1982), Alt et al. (2003). The lowest palaeo-temperatures in the SBSD (< 200° C) mainly correspond to narrow chlorite rims which developed around the margins of discrete vughs (Figure 6.108). This evidence suggests that some vuggy chlorite rims in the SBSD likely formed from lower temperature fluids which probably post-dated the peak hydrothermal activity associated with higher temperature chlorites;

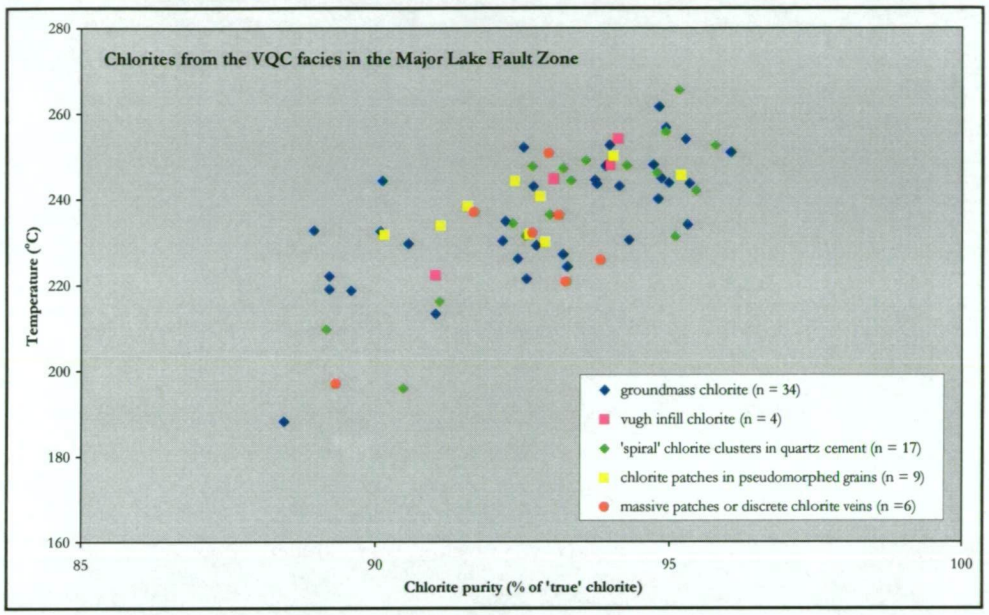

Figure 6.106: Calculated palaeo-temperatures for the vein and breccia, quartz-chlorite (VQC) facies show that most chlorites formed in the range from 220–260° C. Temperatures are plotted relative to the calculated % of 'pure' chlorite (using the method of Bettison and Schiffman, 1988), which provides a measure of the amount of inter-layered smectite (contamination) in the chlorite structure.

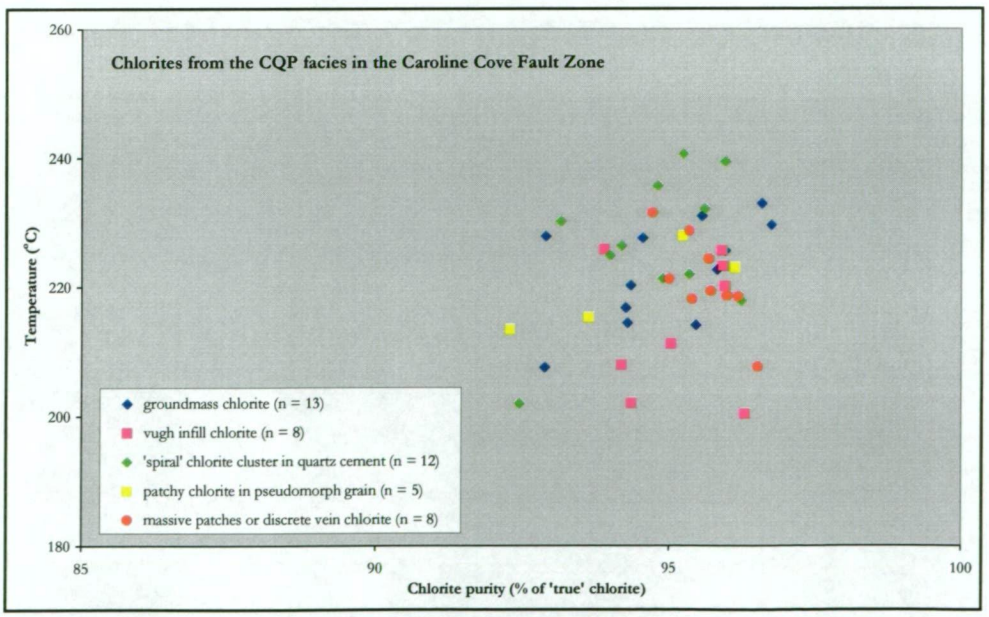

Figure 6.107: Plot of chlorite formation temperatures (derived from the modified Zang and Fyfe geothermometer) vs. the % of pure chlorite for the massive and veined, chlorite-quartz-pyrite (CQP) facies at Caroline Cove.

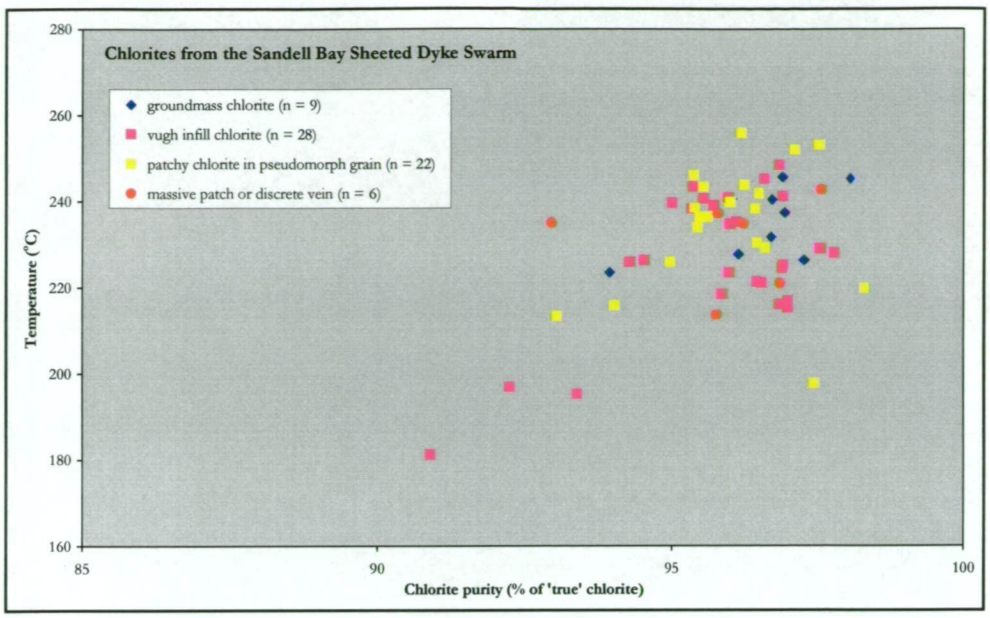

Figure 6.108: Plot of chlorite palaeo-temperatures relative to textural form and estimated chlorite % for the Sandell Bay Sheeted Dyke Swarm, showing the typical positive correlation between high formation temperatures and chlorite purity (as defined by Bettison and Schiffman, 1988). Most chlorites have high purity and form a well constrained group, although several chlorite rims around small vughs formed at lower temperatures, i.e., they have a greater proportion of smectite contamination.

iv. The mixed-layer smectite-chlorite minerals of the FMC facies were formed at significantly lower temperatures than chlorites from the VQC and CQP facies, and the Sandell Bay Sheeted Dyke Swarm. These data mostly define two discrete palaeo-temperature groups that range (respectively) from 50°–90° C and 100–130° C (Figure 6.104). The mean temperature for all clays in the FMC facies is 102° C, with a single anomalous maximum value (probably a partially contaminated sample?) of 171° C. There are no obvious texture-related compositional variations, although this may be influenced by less microprobe data. Lower palaeo-temperature estimates for the FMC facies were generally expected prior to the geothermometry study because of the absence of 'true' chlorites (Hey diagram definition; Figure 6.89). Smectite-rich inter-layered clays are commonly the main phyllosilicate mineral which occurs in altered basaltic rocks which have not experienced hydrothermal conditions > ~ 200° C (Kristmannsdottir, 1979). Thus, lower palaeo-temperatures in the FMC facies provide further evidence to interpret fundamentally different hydrothermal conditions from those which formed the VQC and CQP facies. Furthermore, this interpretation is consistent with previously reported geologic (Chapter 5) and petrographic variations (Chapter 6.3), most of which clearly indicate that the FMC facies post-dated the earlier phase of quartz + chlorite + sulfide bearing alteration which now dominates the fault focussed assemblages at Major Lake and Caroline Cove; and, finally

v. Chlorite geothermometry was one of two methods that I used during this investigation to derive palaeo-temperatures for focussed hydrothermal facies on Macquarie Island.

Oxygen isotope data from quartz vein separates provided an independent geothermometry technique for both the VQC and CQP facies (albeit mostly associated with a different stage of the alteration paragenesis, Chapter 6.3), and the results of this complementary analytical work are outlined and further discussed in Chapter 8. Although the calculated chlorite formation temperatures are relatively well constrained and consistent with the interpreted geologic environments (i.e., subseafloor upflow zones and regional hydrothermal systems), due caution is still required when interpreting and applying these temperature data (De Caritat et al., 1993). Ideally, independent methods for estimating hydrothermal fluid temperatures (such as fluid inclusion microthermometry) should be undertaken to verify the results and provide a more rigorous test of the geothermometric methods. However, although the calculated chlorite temperatures have inherent uncertainties and may not represent absolute values, the relative temperature ranges and mean values provide another useful technique for discriminating the different assemblages and, particularly, for interpreting facies-specific differences related to evolutionary variations in the physico-chemical conditions and alteration processes of each hydrothermal system.

Interpretation of mineral assemblages in the vein-dominated, prehnite-zeolite (VPZ) facies

The hydrothermal minerals which characterise the VPZ facies differ significantly from those associated with altered rocks in the Major Lake and Caroline Cove Faults. In particular, the absence of quartz and sulfide minerals, coupled with the widespread abundance of laumontite, prehnite, and minor pumpellyite, implies fundamentally different hydrothermal conditions, fluid compositions, and water–rock interactions. The main mineral phases in the VPZ facies imply relatively low grade metamorphic conditions, and are typical of many sub-greenschist facies assemblages, e.g., zeolite facies (Carr et al., 1999). The bulk mineral chemistry suggests that hydrothermal fluids were especially rich in Ca (with variable Fe contents), but had relatively low levels of Si (not quartz saturated) and H_2S (compared to the Major Lake and Caroline Cove Fault Zones). Low concentrations of CO_2 in the VPZ fluids are also implied by the abundance of zeolites and prehnite, and the relative dearth of carbonate minerals, e.g., altered basalts with similar prehnite and pumpellyite dominated assemblages in the Flin Flon district of Canada were shown to have fluid X_{CO2} levels <0.005 (Digel and Gordon, 1995).

Although only limited compositional data was obtained for alteration minerals in the VPZ facies, these analyses provide broad constraints for interpreting some aspects of the relict hydrothermal system in the Sellick Bay Fault Zone. For instance, experimental studies (which have also been independently verified, e.g., by measured borehole temperatures in geothermal systems) have shown that laumontite from low pressure environments (typical of seafloor hydrothermal systems) typically forms at temperatures < 200° C, e.g., Liou (1971), Cho et al. (1987). Sub-200°

C fluids are also suggested by the absence of epidote from these rocks (lower temperature stability ~ 200° C, Schiffman and Liou, 1983), and the presence of Fe-rich prehnite and pumpellyite. Fe^{3+} is preferentially partitioned into epidote relative to both prehnite and pumpellyite, so the relatively Fe-rich compositions of these diagnostic VPZ facies minerals may indicate that they formed below the minimum temperature at which epidote is stable (Harper, 1995). Prehnite and pumpellyite may form over a relatively wide range of hydrothermal conditions, with temperatures of 100°–300° C and pressures of < 0.1–0.95 GPa cited for pumpellyite, and 170°–320° C and < 0.45 GPa for prehnite, depending on individual mineral activities (Beiersdorfer and Day, 1995; Carr et al., 1999). However, most experimental and theoretical studies, coupled with mineral observations form active geothermal fields, suggest that coexisting prehnite and pumpellyite assemblages in altered mafic rocks formed under low pressure conditions (< 2 kbar), with temperatures ~ 250° C ± 50° C (Frey et al., 1991). Unfortunately, there is little consensus in the literature on how compositional differences in prehnite and pumpellyite are related to variations in physico-chemical fluid parameters. Various mineralogical studies have produced conflicting results in altered basaltic rocks from different localities. In particular, the Fe / (Fe + Al) ratio of prehnite and pumpellyite has been shown to both decrease and increase with increasing metamorphic grade, or remain essentially unchanged, i.e., highly inconsistent (Beiersdorfer and Day, 1995). My microprobe study has shown that prehnite in the Sellick Bay Fault Zone is Fe-rich relative to prehnite from the regionally altered Sandell Bay Sheeted Dyke Swarm. These compositional variations suggest that fluids associated with broad-scale (regional) hydrothermal systems may be Fe-depleted compared to structurally focussed alteration zones, at least in upper crustal rocks on Macquarie Island.

6.5. Conclusions

The detailed petrographic and electron microprobe study that I conducted has provided important new insights into the nature of alteration minerals and hydrothermal styles associated with the Major Lake, Caroline Cove, and Sellick Bay Fault Zones. Many distinctive textural and compositional features of these fine-grained mineral assemblages were documented and interpreted during this investigative phase (this work was largely beyond the scope of the field-based study). In summary, the most significant outcomes arising from my petrographic and microprobe investigation are:

i. The host rock domains which surround the Major Lake, Caroline Cove, and Sellick Bay Fault Zones are variably affected by low to moderate grade hydrothermal alteration. Confirming Griffin's (1982) work on Macquarie Island's regional alteration characteristics, the hydrothermal mineral assemblages are most typical of the oxidised (near-seafloor) facies, zeolite facies, and greenschist facies (depending on the actual crustal block). The primary igneous minerals have been variably altered during fluid–

rock interactions (i.e., very selective alteration, ranging from partial and sporadic effects to complete grain pseudomorphs), and relict primary textures are well preserved *in situ*;

ii. The structurally focussed alteration facies associated with the Major Lake, Caroline Cove, and Sellick Bay Faults each comprise multi-component and multi-stage mineral assemblages. Strong to intense recrystallisation and replacement of the primary magmatic minerals occurs widely throughout these facies, although the distribution and intensity of hydrothermal alteration is very heterogeneous (micro and macroscopic scales). The hydrothermal assemblages are dominated by very fine- to fine-grained alteration minerals, and these commonly form pervasive alteration domains of irregular size and shape within the facies host rocks;

iii. Although the type and distribution of alteration minerals varies between the six focussed hydrothermal facies, they each share four dominant textural styles. Igneous minerals (both crystal and groundmass phases) are selectively or pervasively replaced; most patches of volcanic glass in the igneous mesostasis are pervasively replaced; voids, vughs, and other primary rock cavities are completely infilled (many with multiple mineral components); and veins, veinlets, and hydrothermally derived breccias are abundant and spatially widespread. Typically, discrete veins and intense vein stockworks represent the most distinctive textural components of each fault zone facies;

iv. Consistent cross-cutting, overprinting, and replacement relationships exist between the main mineral components of the diagnostic facies associated with the Major Lake (VQC), Caroline Cove (CQP), and Sellick Bay (VPZ) Faults. The characteristic inter-mineral associations indicate that four (VQC and CQP facies) or five (VPZ facies) temporally distinct hydrothermal stages have formed these assemblages;

v. The bulk mineralogy of the VQC and CQP facies are broadly similar, although subtle variations in the abundance and specific composition of these hydrothermal assemblages differentiates the Major Lake and Caroline Cove Faults. The VQC facies is dominated by quartz and Fe-rich chlorite, and contains subordinate amounts of pyrite, epidote, albite, and titanite. In comparison, the CQP facies is characterised by Mg-rich chlorite and quartz, and pyrite, chalcopyrite and epidote are considerably more abundant and spatially widespread. In addition, albite and titanite occur commonly in the CQP facies, and late-stage barite is also an important component. The final alteration stages recognised in both the VQC and CQP facies involved minor (partial) oxidation and staining of the earlier-formed minerals, especially Fe-rich phases such as pyrite;

vi. The VPZ facies in the Sellick Bay Fault Zone has a markedly different suite of alteration minerals from those in the VQC and CQP facies. In particular, this focussed hydrothermal facies lacks quartz, chlorite, and sulfide minerals; abundant Ca-zeolites (laumontite), prehnite, pumpellyite, and Fe-oxyhydroxide minerals predominate. However, many characteristic textural styles and petrographic features are similar, and the multi-stage VPZ facies also has extensive and well developed hydrothermal veins and breccias. Major differences in the composition of the alteration assemblages implies that critical hydrothermal fluid conditions, processes, and water–rock interactions varied significantly between the major fault systems;

vii. The FMC and PFO facies are spatially restricted late-stage hydrothermal assemblages which occur only in the central deformation corridor of the Major Lake (FMC only) and Caroline Cove Faults (both FMC and PFO facies). These highly focussed alteration zones have a less diverse mineral assemblage; mixed layer smectite-chlorite clays are dominant in the FMC facies, whereas Fe-rich oxides and hydroxides are the main components of the PFO facies. However, each of these contains very distinctive textural features, which have partially overprinted some of the earlier-formed alteration assemblages. The FMC facies is characterised by narrow and distinctly foliated clay-cemented veins and breccias, whereas the PFO facies has well developed oxidation haloes that progressively decrease in intensity away from their primary fluid pathways. Relict, unoxidised basaltic cores are commonly encircled by these progressive oxidation 'fronts';

viii. Fluid inclusions are poorly preserved in hydrothermal cements (mainly quartz) associated with altered rocks in the Major Lake, Caroline Cove, and Sellick Bay Faults. Small, subrounded to rounded Type I (liquid-rich) fluid inclusions are most common, although extensive necking and leaking has occurred due to on-going tectonic disruption in each fault system. The remnant population includes primary, secondary, and pseudo-secondary fluid inclusions;

ix. Electron microprobe analyses mainly focussed on the very fine- to fine-grained phyllosilicate minerals (mainly chlorites) that comprise major components of the VQC and CQP facies. Chlorites in the VQC facies are compositionally diverse (pychnochlorite, brunsvigite, and ripidolite sub-species), and many are distinctly Fe-rich. In comparison, chlorites in the CQP facies are Mg-rich (pychnochlorites), and many are compositionally similar to chlorites from the regionally altered Sandell Bay Sheeted Dyke Swarm (SBSD). However, chlorites in both fault zone facies are significantly enriched in Mn relative to typical ocean crust (i.e., regional lithologic domains such as the SBSD); several VQC facies chlorites contain > 1 wt. % MnO, which marks them as some of the most Mn-rich varieties ever documented in altered oceanic basalts. The

phyllosilicate minerals in the FMC facies are not 'true' chlorites, but mixed smectite-chlorite clays with Mg-rich (and relatively Mn-poor) compositions. Inter-facies variations in chlorite chemistry (e.g., their Fe #'s and Mn contents) suggest distinct differences in the nature of their parent hydrothermal systems and processes, including fluid conditions and water–rock interactions. For example, the presence of Mg-bearing chlorites (CQP) in contrast to Fe-rich compositions (VQC) provides evidence to interpret more extensive input and mixing between compositionally distinct end-member fluids, and particularly implies that entrained (crustal) seawater may have played a critical role in their evolution;

x. Following evaluation of chlorite geothermometric techniques, the Zang and Fyfe (1995) geothermometer (modified using facies-specific compositional data) was selected to derive estimated formation temperatures for chlorites in the VQC, CQP, and FMC facies, and the Sandell Bay Sheeted Dyke Swarm (SBSD). The geothermometry results showed that the VQC facies chlorites formed at slightly higher average temperatures than the CQP facies, with respective means = 237° C and 221° C (commonly ± 20° C range). These temperatures are considerably greater than those in the FMC facies clays (mean = 102° C), but relatively similar to the chlorite temperatures obtained for the SBSD (mean = 232° C);

xi. There are no consistent correlations or groupings which link the five different textural forms of chlorite in the VQC and CQP facies rocks (i.e., groundmass, quartz-hosted, vugh infill, partial phenocryst alteration, and massive veins or patches of chlorite) with specific mineral compositions or formation temperatures; and

xii. The main alteration minerals in the VPZ facies have fairly homogeneous compositions. Many minerals in these Ca-rich assemblages, such as prehnite and pumpellyite, contain relatively high levels of Fe compared to similar mineral occurrences in other oceanic and ophiolitic environments. Prehnite in the VPZ facies is particularly Fe-rich compared to prehnite from the Sandell Bay Sheeted Dyke Swarm.